AOP ID and Title:

AOP 483: Deposition of Energy Leading to Learning and Memory Impairment
Short Title: Deposition of Energy Leading to Learning and Memory Impairment

Graphical Representation

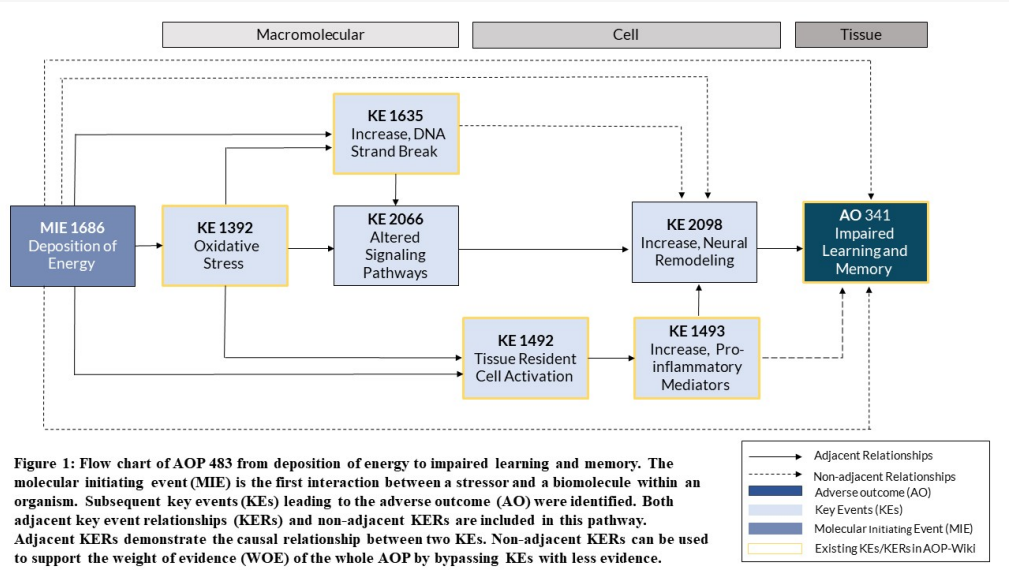

Figure 1: Flow chart of AOP 483 from deposition of energy to impaired learning and memory. The molecular initiating event (MIE) is the first interaction between a stressor and a biomolecule within an organism. Subsequent key events (KEs) leading to the adverse outcome (AO) were identified. Both adjacent key event relationships (KERs) and non-adjacent KERs are included in this pathway. Adjacent KERs demonstrate the causal relationship between two KEs. Non-adjacent KERs can be used to support the weight of evidence (WOE) of the whole AOP by bypassing KEs with less evidence.

Authors

Ahmad Sleiman[1], Kathleen Miller[2], Danicia Flores[3], Jaqueline Kuan[3], Kaitlyn Altwasser[3], Benjamin Smith[3], Tatiana Kozbenko[3], Robyn Hocking[3], Carole Yauk[4], Ruth Wilkins[3], Vinita Chauhan[3]

(1) Institut de Radioprotection et de Sûreté Nucléaire, St. Paul Lez Durance, Provence, France

(2) National Institute of Aerospace, Hampton, Virginia, USA

(3) Consumer and Clinical Radiation Protection Bureau, Environmental and Radiation Health Sciences Directorate, Health Canada, Ottawa, Ontario, Canada

(4) Department of Biology, University of Ottawa, Ottawa, Ontario, Canada

Consultants

Scott Wood[1], Janice Huff[2], Christelle-Adam Guillermin[3], Nobuyuki Hamada[4]

(1) NASA Johnson Space Center, Houston, Texas, USA

(2) NASA Langley Research Center, Hampton, Virginia, USA

(3) Institut de Radioprotection et de Sûreté Nucléaire, St. Paul Lez Durance, Provence, France

(4) Biology and Environmental Chemistry Division, Sustainable System Research Laboratory, Central Research Institute of Electric Power Industry (CRIEPI), Tokyo, Japan

Status

Author status	OECD status	OECD project	SAAOP status
Open for citation & comment			

Abstract

An adverse outcome pathway (AOP) is described from the molecular initiating event (MIE) of deposition of energy to the adverse outcome (AO) of learning and memory impairment. This AOP uses well-understood mechanistic events that encompass oxidative stress, DNA damage, tissue resident cell activation, altered signaling pathways, neuroinflammation, and their interactions, leading to

eventual neural remodeling. The empirical evidence to support this AOP is primarily derived from studies that utilize ionizing radiation stressors relevant to space travel and radiotherapy treatments. Following deposition of energy (MIE, KE#1686), the adjacent key events are oxidative stress (KE#1392), tissue resident cell activation (KE#1492) and increased DNA strand breaks (KE#1635). Uncontrolled radical production within the cell has an adjacent connection with increased DNA strand breaks (KE#1635), altered signaling pathways (KE#2066) and tissue resident cell activation (KE#1492). Tissue resident cell activation has an adjacent connection to increased proinflammatory mediators (KE#1493). Prolonged neuroinflammation and altered signaling pathways have adjacent connections with neural remodeling (KE#2098) and subsequently learning and memory impairment (AO, KE#341). The AOP also includes multiple non-adjacent connections between key events. The overall evidence for this AOP is moderate. Despite multiple knowledge gaps that are present, the evidence demonstrates a high-level of biological plausibility. The quantitative understanding is low as there is high uncertainty in the quantitative predictions between the KEs. This AOP has wide applicability and is particularly relevant to exposures from long-duration space flight and medical exposures using radiation therapy.

Background

Understanding the impact of ionizing radiation on non cancer outcomes of the central nervous system (CNS) is essential as there are many possibilities for exposure including from medical procedures and occupational settings (e.g. astronuats). Various studies have reported cognitive deficits after high-doses of radiation from radiotherapy treatments, though there is a reported individual variability in human cohorts (Greene-Schloesser et al., 2012; Katsura et al., 2021; Turnquist et al., 2020). In preclinical animal models, studies suggest that even low-to-moderate doses of ionizing radiation from heavy ions can cause structural and functional impairments to the CNS including reductions in neurogenesis, changes in dendritic properties, activation of glial cells, and neuronal remodeling (Cekanaviciute et al., 2018; Kiffer et al., 2019b). However, how key changes in structural and functional properties of the CNS from ionizing radiation exposure are related to changes in cognitive function have yet to be delineated. Furthermore, preclinical studies also suggest that ionizing radiation may impact two major cognitive processes: learning and memory. Learning is the ability to create new associative or non-associative relationships and memory is the ability to recall sensory, short-term or long-term information (Desai et al., 2022, Kiffer et al., 2019b). Both learning and memory involve multiple brain areas including the hippocampal region, as well as the amygdala, the prefrontal cortex and the basal ganglia (Cucinotta et al., 2014; Desai et al., 2022; NCRP Commentary, 2016). Thus far, direct pathways linking radiation to key cellular and molecular events leading to an AO of impaired learning and memory have not been established. This AOP can serve as a starting pathway for expansion to other cognitive disorders and CNS diseases from an MIE of deposition of energy.

Summary of the AOP

Events

Molecular Initiating Events (MIE), Key Events (KE), Adverse Outcomes (AO)

Sequence	Type	Event ID	Title	Short name
	MIE	1686	Deposition of Energy	Energy Deposition
	KE	1392	Oxidative Stress	Oxidative Stress
	KE	2066	Altered Signaling Pathways	Altered Signaling
	KE	1492	Tissue resident cell activation	Tissue resident cell activation
	KE	2097	Increase, Pro-Inflammatory Mediators	Increase, Pro-Inflammatory Mediators
	KE	2098	Increase, Neural Remodeling	Increase, Neural Remodeling
	KE	1635	Increase, DNA strand breaks	Increase, DNA strand breaks
	AO	341	Impairment, Learning and memory	Impairment, Learning and memory

Key Event Relationships

Upstream Event	Relationship Type	Downstream Event	Evidence	Quantitative Understanding
Deposition of Energy	adjacent	Oxidative Stress	High	Moderate
Deposition of Energy	adjacent	Tissue resident cell activation	Moderate	Moderate
Oxidative Stress	adjacent	Altered Signaling Pathways	High	Low
Oxidative Stress	adjacent	Tissue resident cell activation	Moderate	Low
		Increase, Pro-Inflammatory		

Upstream Event	Relationship Type	Downstream Event	Evidence	Quantitative Understanding
Tissue resident cell activation	adjacent	Mediators	Moderate	Low
Increase, Pro-Inflammatory Mediators	adjacent	Increase, Neural Remodeling	Moderate	Low
Increase, Neural Remodeling	adjacent	Impairment, Learning and memory	Moderate	Low
Altered Signaling Pathways	adjacent	Increase, Neural Remodeling	Moderate	Low
Increase, DNA strand breaks	adjacent	Increase, Neural Remodeling	Moderate	Low
Oxidative Stress	adjacent	Increase, DNA strand breaks	Moderate	Moderate
Deposition of Energy	adjacent	Increase, DNA strand breaks	High	High
Increase, DNA strand breaks	adjacent	Altered Signaling Pathways	Moderate	Low
Deposition of Energy	non-adjacent	Increase, Neural Remodeling	Moderate	Low
Deposition of Energy	non-adjacent	Impairment, Learning and memory	Moderate	Low
Increase, Pro-Inflammatory Mediators	non-adjacent	Impairment, Learning and memory	Moderate	Low

Stressors

Name	Evidence
Ionizing Radiation	

Overall Assessment of the AOP

Summary of evidence (KE & KER relationships and evidence)

This AOP was derived from data that investigates the CNS of humans, animals and cellular models following exposure to ionizing radiation. Stressors in the present pathway include a range of doses (low (<0.1 Gy) to high (>1 Gy) doses), dose rates and radiation qualities (low-LET and high-LET) with an emphasis on low-to-moderate (0.1-1 Gy) dose heavy-ion studies relevant to space travel. The goal of this AOP is to model the connectivity of the MIE of deposition of energy through the cellular and biological KEs that lead to the AO of impaired learning and memory. The KEs chosen for this AOP had strong biological plaucibility with available empirical evidence, however, other KEs may be added later to incorporate new mechanisms and AOs into its broader network. The pathway is applicable to multiple stressors of deposition of energy including radiation exposure from space travel and radiotherapy.

Biological Plausibility

The overall biological plausibility in this AOP is high. The KERs in the AOP have either moderate or high evidence for mechanistic relationships between the upstream and downstream KEs. The KEs are well-studied, and an understanding of the structural and functional linkages are well-established.

This AOP is initiated with deposition of energy. Deposition of energy can damage DNA via direct mechanisms, by which the electrons ionize DNA molecules themselves, or via indirect mechanisms, by which the ionization of water produces hydroxyl radicals that can damage DNA bases causing DNA strand breaks (Nikjoo et al., 2016; Wilkinson et al., 2023) or directly upregulating enzymes involved in reactive oxygen and nitrogen species (RONS) production (i.e., catalase) (de Jager, Cockrell and Du Plessis, 2017). Both reactive oxygen species (ROS) as well as reactive nitrogen species (RNS) (Ahmadi et al., 2022; Karimi et al., 2017; Slezak et al., 2015; Tahimic & Globus, 2017; Wang et al., 2019a) may be produced after deposition of energy. If RONS cannot be eliminated quickly and efficiently by the cell's defense system, oxidative stress ensues (Balasubramanian, 2000; Ganea & Harding, 2006; Karimi et al., 2017). Within the brain, oxidative stress can lead to the activation of microglial cells (Fishman et al., 2009; Schnegg et al., 2012; Zhang et al., 2017) and astrocytes (Daverey & Agrawal, 2016; Wang et al., 2017). These cells then release pro-inflammatory mediators and initiate antioxidant defenses (Lee, Cha & Lee, 2021; Simpson & Oliver, 2020). However, if the antioxidant capacity is overwhelmed, chronic inflammation may result.

Oxidative stress can also lead to altered signaling pathways. Directly, ROS causes oxidation of amino acid residues resulting in conformational changes, protein expansion, and protein degradation. This can cause changes in the activity and level of signaling proteins (Ping et al., 2020; Li et al., 2013). Oxidation of key functional amino acids can also alter the activity of signaling proteins, resulting in downstream alterations in signaling pathways (Ping et al., 2020; Schmidt-Ullrich et al., 2000; Valerie et al., 2007; Lehtinen & Bonni, 2006; Ramalingam & Kim, 2012). DNA strand breaks from oxidative damage can activate DNA damage response signaling and modify the expression of other signaling proteins (Ping et al., 2020; Nagane et al., 2021; Schmidt-Ullrich et al., 2000; Valerie et al., 2007).

Both increased pro-inflammatory mediators and altered signaling pathways can lead to neural remodeling. Various pro-

inflammatory cytokines can affect neural remodeling, the most common being IL-1β, TNF-α, IL-6 and IFN-γ. During an inflammatory response, these cytokines act on different receptors to initiate several signaling pathways to induce neuronal degeneration, apoptosis or to propagate further pro-inflammatory responses (Mousa & Bakhiet, 2013; Prieto & Cotman, 2018). These signaling pathways include, but are not limited to PI3K/Akt pathways, MAPK pathways, senescence signaling, and apoptosis pathways. The PI3K/Akt and MAPK pathways are involved in many processes in neurons, including cell survival, morphology, proliferation, differentiation, and synaptic activity (Davis and Laroche, 2006; Falcicchia et al., 2020; Long et al., 2021; Mazzucchelli and Brambilla, 2000; Mielke and Herdegen, 2000; Nebreda and Porras, 2000; Rai et al., 2019; Rodgers and Theibert, 2002; Sherrin, Blank, and Todorovic, 2011). The apoptosis pathway influences cell number, while senescence signaling can influence the regenerative potential of the cell and therefore, neurogenesis (Betlazar et al., 2016; McHugh and Gil, 2018; Mielke and Herdegen, 2000). Disruptions to components of these pathways will lead to neuronal remodeling, which includes alterations in both morphological properties and functional properties of the neurons (Betlazar et al., 2016; Davis and Laroche, 2006; Mazzucchelli and Brambilla, 2000; Nebreda and Porras, 2000). However, the biological changes that follow perturbation of these pathways is not understood in every context and cell type, making the biological plausibility for this relationship moderate (Nebreda and Porras, 2000). Decreased morphological properties of neurons, including reductions in dendritic complexities and spine densities, as well as altered functional properties of neurons including altered synaptic signaling and neurogenesis, has been associated with learning and memory impairment (Bálentová & Adamkov, 2020; Hladik & Tapio, 2016; Monje & Palmer, 2003; Romanella et al., 2020; Tomé et al., 2015).

Empirical Support (Temporal, Dose, and Incidence Concordance)

This AOP demonstrates moderate empirical evidence to support the modified Bradford Hill criteria. Overall, many studies demonstrated that upstream KEs occurred at lower or the same doses and at earlier or the same times as downstream KEs. There were some inconsistencies where the KEs were only measured at one dose or time. The evidence collected was gathered from various studies using in vitro and in vivo rat, mice, rabbit, squirrel, bovine and human models. Various stressors were applied, including UV, UVB, UVA, gamma ray, X-ray, protons, alpha particle, neutron, and heavy ion irradiation.

Regarding time concordance, deposition of energy occurs immediately following irradiation, and downstream events will always occur at a later time-point. DNA damage occurs within nanoseconds of deposition of energy with DNA strand breaks measured from seconds to minutes later and altered signaling measured minutes to days later (Acharya et al., 2010; Antonelli et al., 2015; Mosconi et al., 2011; Rogakou et al., 1999; Rothkamm and Lo, 2003; Sabirzhanov et al., 2020; Zhang et al., 2017). Rapid increases in ROS (Limoli et al., 2004; Giedzinski et al., 2005; Suman et al., 2013) and activation of microglia and astrocytes have been observed within hours of irradiation and can persist for 12 months (Kyrkanides et al., 1999; Hwang et al., 2006; Suman et al., 2013). For tissue resident cell activation and increase in pro-inflammatory mediators, studies generally show that these events occur at a similar time frame (Parihar et al., 2018; Liu et al., 2010; Dong et al., 2015; Lee et al., 2010; Zhou et al., 2017). The alteration of signaling pathways is a molecular-level KE like oxidative stress, and both can occur concurrently (Xu et al., 2019), although increased ROS levels can be initiated significantly before altered signaling pathways (Suman et al., 2013). Neural remodeling has been observed at various time points from hours to months after exposure to a stressor, and its upstream KEs (altered signaling and increased pro-inflammatory mediators) generally appear earlier (Kanzawa et al., 2006; Limoli et al., 2004; Pius-Sadowska et al., 2016) or at similar times, respectively (Zonis et al., 2015; Wong et al., 2004, Green et al., 2012; Ryan et al., 2013; Vallieres et al., 2002). In response to irradiation, impaired learning and memory is typically observed at similar time-points of neural remodeling due to the timing of measurements (Raber et al., 2004; Parihar et al., 2016; Madsen et al., 2003; Winocur et al., 2006; Rola et al., 2004).

Regarding dose concordance, multiple studies also demonstrate that the upstream KEs occur at lower or the same doses as downstream KEs as energy is deposited immediately at any dose of radiation. Some studies report a linear-dose-dependent increases in DNA strand breaks for a large range of doses (Antonelli et al., 2015; Hamada et al, 2006; Rübe et al., 2008). In addition, neural precursor cells irradiated with protons at 1, 2, 5 and 10 Gy showed a dose-dependent increase in ROS levels (Giedzinski et al., 2005). In another study, activation of microglia and astrocytes were seen at doses as low as 5 cGy that persisted to 30 cGy (Parihar et al., 2018). However, dose concordance is not consistently observed across studies, which can be attributed to differences in experimental design. Some studies also only measured the key events at one dose, which presented further inconsistencies.

Few studies showed incidence concordance where the upstream KE demonstrated a greater change than the downstream KE following a stressor. Not all KERs displayed an incident-concordant relationship, but for those that did, only a small proportion of the empirical evidence supported this relationship. For example, mice exposed to 2 Gy of gamma irradiation showed increases of pro-apoptotic markers p53 and BAX by 8.4- and 2.3-fold, respectively. A 0.6-fold decrease in Bcl-2 (anti-apoptotic marker) was also observed, and gamma rays cause a decrease in cortical thickness by 0.9-fold (Suman et al., 2013).

Uncertainties, Inconsistencies, and Data Gaps

There are a few inconsistencies in this AOP. Some studies show sex-specific changes in the KEs. For example, two studies reported that tissue resident cell activation was not affected in female mice after 0.3 and 0.5 Gy of radiation (Krukowski et al., 2018a; Parihar et al., 2020) while a separate study showed that only female mice had activated cells after 2 Gy (Raber et al., 2019). Another study reported a greater radiation-induced reduction in neurogenesis in male mice compared with female mice (Kalm et al., 2013). More research is necessary to identify if these results are sex-specific or due to other modulating factors.

There have been some inconsistencies reported in the KER Deposition of Energy (KE#1686) to Increase DNA Strand Breaks (KE#1635). For example, dose-rates and radiation quality may influence dose-response relationships (Brooks et al., 2016, Sutherland et al., 2000; Nikjoo et al., 2001; Jorge et al., 2012). More research is necessary to understand the impact low-doses of ionizing radiation exposure on DNA damage as some studies report low-dose exposures may invoke protection against

spontaneous genomic damage (as reviewed by ICRP (2007) and UNSCEAR (2008)).

Anatomical location of change in the KEs may impact its response. For example, in response to ionizing radiation, changes occurred in hippocampal dendritic spines CA1 subregion of hippocampus but not in the dorsal dentate gyrus (Kiffer et al., 2019a).

Changes in KEs and the AO may be dose and stressor specific when assessed using animal models. For example, cue feared conditioning, a measure of learning and memory had different responses in mice at 0.2 Gy vs. 1 Gy of 28Si exposure (Whoolery et al., 2017). Also in mice, object memory was impaired after 0.1 or 0.25 Gy 16O exposure and social novelty learning was impaired after 0.25 Gy 16O exposure, but neither dose impaired short-term spatial memory (Kiffer et al., 2019a).

Changes in signaling pathways may provide inconsistent outcomes in neural remodeling. For example, the p38 pathway is involved in many, often opposing, biological processes (Nebreda and Porras, 2000). Furthermore, the MAPK pathways can exhibit varied responses after exposure to oxidative stress (Azimzadeh et al., 2015).

Many studies do not report direct measures of oxidative stress. As free radicals are quickly scavenged, the quantitative understanding of this relationship can be inconsistent, due to varied response of antioxidant enzymes across experimental conditions and time measurements. This has led to some inconsistencies within the KERs. For example, in contrast to other studies demonstrating an increase in oxidative stress following deposition of energy, neutron radiation decreased malondialdehyde, a product of oxidative stress (Chen et al., 2021).

Finally, many of the KERs do not include studies in humans. More research could be done to observe these relationships in human models.

There were multiple challenges present in the development of this AOP which identified gaps in the data. The majority of the evidence for this AOP is extracted from preclinical animal and cellular models. Therefore, the low availability of human studies presents a challenge as translation of the animal and cellular models to humans is difficult due to differences in physiology, methods and measurements. In addition, although both age and sex are listed as modulating factors, there is more research necessary to elucidate the interaction between age and sex on the KEs, particularly how these factors may modulate the causal connectivity of the relationships and the AO. Direct comparisons between studies were also difficult due to differences in model, radiation quality, dose, dose rate and endpoint which led to some inconsistencies. Many studies reported limited dose ranges or time-points and often measured a single KE, limiting evidence for direct KERs. The current AOP has low quantitative evidence supporting the KERs, however, this AOP can be expanded with experiments that further exemplify the level of dose- and time-concordance across multiple endpoints. This will improve the quantitative understanding of the relationships which can then support the development of risk models and tools for mitigating risk.

Domain of Applicability

Life Stage Applicability

Life Stage	Evidence
All life stages	High

Taxonomic Applicability

Term	Scientific Term	Evidence	Links
human	Homo sapiens	Moderate	NCBI
mouse	Mus musculus	High	NCBI
rat	Rattus norvegicus	High	NCBI
rabbit	Oryctolagus cuniculus	Low	NCBI
dog	Canis lupus familiaris	Low	NCBI
pigs	Sus scrofa	Low	NCBI
cow	Bos taurus	Low	NCBI

Sex Applicability

Sex	Evidence
Unspecific	High
Male	Moderate
Female	Low

This AOP is relevant to vertebrates, such as humans, mice, rats. The taxonomic evidence supporting the AOP comes from the use of human (Homo sapiens), human-derived cell line, beagle dog (Canis lupus familiaris), rat (Rattus orvegicus), and mouse (Mus musculus) studies. Across all species, most available data was derived from adult and adolescent models with a moderate to high level of evidence compared to less available data from preadolescent models. Many of the KEs demonstrated moderate to high evidence for males and low evidence for females. In multiple KEs, sex was unspecified.

Essentiality of the Key Events

Overall, the KEs in this AOP demonstrate moderate essentiality. Essentiality is demonstrated when upstream KEs are blocked or inhibited eliciting a change in the downstream KE.

Essentiality of the Deposition of Energy (MIE, KE#1686)

- Deposition of energy is difficult to test for essentiality as deposition of energy is a physical stressor and cannot be blocked/decreased using chemicals. Since deposited energy initiates events immediately, the removal of deposited energy, a physical stressor, also supports the essentiality of the key event. Studies that do not deposit energy are observed to have no downstream effects.

Essentiality of Oxidative Stress (KE#1392)

- The effect of antioxidants on altered signaling pathways (KE#2066)
- Antioxidants including Melandrii Herba extract, N-acetyl-L-cysteine (NAC), gallocatechin gallate/epigallocatechin-3-gallate, Cornus officinalis (CC) and fermented CC (FCC), L-165041, fucoxanthin, and edaravone were shown to decrease phosphorylation of MAPKs such as ERK1/2, JNK1/2 and p38 after exposure to radiation, H2O2 or lipopolysaccharide (LPS) (Lee et al., 2017; Deng et al., 2012; Park et al., 2021; Tian et al., 2020; Schnegg et al., 2012; Zhao et al., 2017; Zhao et al., 2013; El-Missiry et al., 2018).
- The effects of antioxidants on tissue resident cell activation (KE#1492)
- Antioxidants including Kukoamine A (KuA) and curcumin were found to reduce levels of microglia and astrocyte activation (Zhang et al. 2017; Daverey & Agrawal, 2016; Wang et al., 2017).
- The effect of knocking out a ROS-producing enzyme
- A knockout model of mitochondrial superoxide dismutase 2 (SOD2) resulted in an increase in reactivity of microglial cells (Fishman et. al 2009).

Essentiality of Increase, DNA Strand Breaks (KE#1635)

- The effects of blocking DNA strand breaks on altered signaling (KE#2066)
- Treatment with mesenchymal stem cell-conditioned medium (MSC-CM) reduced γ-H2AX, decreased the levels of p53, Bax, cleaved caspase 3 and increased the levels of Bcl-2 in HT22 cells irradiated with 10 Gy of X-rays (Huang et al., 2021).
- The inhibition of microRNA (miR)-711 decreased levels of DNA damage markers, p-ATM, p-ATR and γ-H2AX, and decreased signaling molecules including p-p53, p21 and cleaved caspase 3 (Sabirzhanov et al., 2020).
- The effects of blocking DNA strand breaks on neural remodeling (KE#2098)
- Treatment of HT22 hippocampal neuronal cells with minocycline inhibited the expression of γ-H2AX and the p-ATM/ATM ratio as well as reduced apoptosis following X-ray exposure (Zhang et al., 2017). Similarly, MSC-CM reduced the expression of γ-H2AX and reduced apoptosis, reversing the changes induced by X-ray radiation (Huang et al., 2021).
- Lithium chloride was also shown to reduce γ-H2AX levels and increase proliferation in neural stem cells irradiated with 60Co gamma rays (Zanni et al., 2015).

Essentiality of Altered Signaling Pathways (KE#2066)

- The effects of modulating cell signaling on neural remodeling (KE#2098)
- Knockout models of key molecules in the MAPK pathways and apoptotic pathway reduced apoptotic activity and restored neuron numbers induced by simulated ischemic stroke or radiation (Tian et al., 2020; Chow, Li and Wong, 2000; Limoli et al., 2004).
- Inhibition of key signaling molecules involved in the MAPK pathways and the PI3K/Akt pathway restored neural stem cell numbers, neuronal differentiation, and neuronal structure induced by radiation (Eom et al., 2016; Kanzawa et al., 2006; Zhang et al. 2018)

Essentiality of Tissue Resident Cell Activation (KE#1492)

- The effects of modulating cell activation on pro-inflammatory mediators (KE#1493)
- Drugs including tamoxifen, retinoic acid, N-acetyl-L-cysteine (NAC), SP 600125 (SP), a specific c-jun kinase inhibitor, and NS-398, a microglial activator attenuated the activation of tissue-resident cells and consequently reduced the levels of pro-inflammatory mediators (Liu et al., 2010; van Neerven et al., 2010; Komatsu et al., 2017; Ramanan, 2008; Kyrkanides et al., 2002).

Essentiality of Pro-Inflammatory Mediators (KE#1493)

- The effects of modulating pro-inflammatory mediators on neural remodeling (KE#2098)
- Treatments including MW-151, a selective inhibitor of pro-inflammatory cytokine production, KuA, and histamine restored neurogenic signaling, hippocampal apoptosis, and neuronal complexity (Jenrow et al., 2013; Zhang et al., 2017; Saraiva et al., 2019).
- Multiple studies use cytokine receptor antagonists or knock-out key receptors to block the effects of IL-1β, TNF-α, and CCL2, which preserves neuron survival (Green et al., 2012; Ryan et al., 2013; Wu et al., 2012; Chen and Palmer, 2013). Complement component 3 (C3) knockout models also caused increased synaptic number, reduced neuron loss and ameliorated synaptic morphology impairment (Shi et al., 2017).
- The effects of modulating pro-inflammatory mediators on learning and memory impairment (AO, KE#341)
- Anti-inflammatory drugs or hormones including MW-151, a selective inhibitor of pro-inflammatory cytokine production, lidocaine, an anesthetic with anti-inflammatory properties, ethyl-eicosapentaenoate (E-EPA) and 1-[(4-nitrophenyl)sulfonyl]-4-phenylpiperazine (NSPP), both of which are anti-inflammatory drugs and α-Melanocyte stimulating hormone (α-MSH), which antagonizes the effects of pro-inflammatory cytokines, have rescued the impairments seen in learning and memory (Bhat et al., 2020; Gonzalez et al., 2009; Jenrow et al., 2013; Taepavarapruk & Song, 2010; Tan et al., 2014).

Essentiality of Neural Remodeling (KE#2098)

No identified studies describe essentiality of neural remodeling as it cannot be blocked / decreased using chemicals.

Weight of Evidence Summary

1. Support for Biological Plausibility of KERs	Defining Question	High (Strong)	Moderate	Low (Weak)
	Is there a mechanistic relationship between KEup and KEdown consistent with established biological knowledge?	Extensive understanding of the KER based on extensive previous documentation and broad acceptance; Established mechanistic basis	KER is plausible based on analogy to accepted biological relationships, but scientific understanding is not completely established	There is empirical support for statistical association between KEs, but the structural or functional relationship between them is not understood
Deposition of Energy (MIE, KE#1686) → Oxidative Stress (KE#1392)	**High** There is high evidence surrounding the biological plausibility of deposition of energy leading to increased oxidative stress. When energy reaches a cell, it reacts with water and organic materials to produce ROS. Oxidative stress occurs when antioxidant systems cannot eliminate ROS.			
Deposition of Energy (MIE, KE#1686) → Tissue Resident Cell Activation (KE#1492)	**High** There is high evidence surrounding biological plausibility of deposition of energy leading to tissue resident cell activation. It is well understood that deposition of radiation energy leads to a recruitment of immune cells within the local tissue which can induce an immune and inflammatory response, characterized by the recruitment and activation of local macrophages in the brain.			
Oxidative Stress (KE#1392) → Increase, DNA Strand Breaks (KE#1635)	**High** There is high evidence surrounding biological plausibility of oxidative stress leading to DNA strand breaks. Oxidative stress can induce DNA damage by oxidizing or deleting DNA bases leading to strand breaks.			
Increase, DNA Strand Breaks (KE#1635) → Altered Signaling Pathways (KE#2066)	**High** There is high evidence surrounding biological plausibility of increased DNA strand breaks to altered signaling pathways. DNA strand breaks induce DNA damage responses which result in the induction of various signaling pathways.			
Oxidative Stress (KE#1392) → Tissue	**Moderate** There is moderate evidence surrounding biological plausibility of increased oxidative stress leading to tissue resident			

Resident Cell Activation (KE#1492)	cell activation. Increases in oxidative stress elicits activation of microglial cells and astrocytes in the brain. Activated microglia and astrocytes release pro-inflammatory mediators and promote antioxidant defenses. Feedforward and feedback loops of RONS and inflammatory pathways make the direct link between oxidative stress and microglial cell or astrocyte activation difficult to discern.
Oxidative Stress (KE#1392) → Altered Signaling Pathways (KE#2066)	**High** There is high evidence surrounding the biological plausibility of increased oxidative stress to altered signaling pathways. Oxidative stress can lead to altered signaling pathways both directly and indirectly. Directly, oxidative stress conditions can lead to oxidation of amino acid residues. This causes conformational changes, protein expansion, and protein degradation, leading to changes in the activity and level of signaling proteins that result in downstream alterations in signaling pathways. Indirectly, oxidative stress can damage DNA causing changes in the expression of signaling proteins as well as the activation of DNA damage response signaling.
Altered Signaling Pathways (KE#2066) → Increase, Neural Remodeling (KE#2098)	**Moderate** There is moderate evidence surrounding biological plausibility of altered signaling pathways to neural remodeling. Neural remodeling is controlled by signaling pathways in the brain, including PI3K/Akt pathway, MAPK pathways, senescence pathways, and apoptosis pathways. The PI3K/Akt and MAPK pathways are involved in many processes in neurons, including cell survival, morphology, proliferation, differentiation, and synaptic activity. The apoptosis pathway influences cell numbers, while the senescence pathway can influence neurogenesis. Disruptions to components of these pathways will lead to neural remodeling in a relationship that is structurally well-understood. However, the biological changes that follow perturbation of these pathways is not understood in every context and cell type.
Tissue Resident Cell Activation (KE#1492) → Increase, Pro-inflammatory Mediators (KE#2097)	**High** There is high evidence surrounding biological plausibility of tissue resident activation to increase in pro-inflammatory mediators. In the brain, activated astrocytes and microglia undergo gliosis and proliferate, releasing pro-inflammatory mediators and production of cytokines. This response is normal after exposure to pathogens, but prolonged activation can prolong the inflammatory response. Cytokines and chemokines can also increase the permeability of the blood-brain barrier, further increasing pro-inflammatory mediator levels.
Increase, Pro-inflammatory Mediators (KE#2097) → Increase, Neural Remodeling (KE#2098)	**Moderate** There is moderate evidence surrounding the biological plausibility of increased pro-inflammatory mediators to neural remodeling. There are various pro-inflammatory cytokines that can affect neuronal integrity an inflammatory response and these cytokines act on different receptors to initiate several signaling pathways to induce neuronal degeneration, apoptosis or to propagate pro-inflammatory responses. However, the exact mechanistic relationship remains to be elucidated due to the complexity of cytokine cascading events.
Increase, Neural Remodeling (KE#2098) → Impairment, Learning and Memory (AO, KE#341)	**Moderate** There is moderate evidence surrounding biological plausibility of neural remodeling leading to impaired learning and memory. Evidence of neural remodeling, such as reductions in spine density, reduced adult neurogenesis and impaired neuronal networks are associated with cognitive impairments, as evident from studies in multiple different species.
Deposition of Energy (MIE, KE# 1686) → Increase, Neural Remodeling (KE#2098)	**Moderate** There is moderate evidence surrounding biological plausibility of deposition of energy to neural remodeling. Irradiation induces oxidative stress and neuroinflammation, which alter neuronal integrity. Many reviews examine the radiation-induced neuronal damage and identify correlation with oxidative stress and neuroinflammatory mechanisms.
Deposition of Energy (MIE, KE#1686) → Impairment, Learning and Memory (AO, KE#341)	**High** There is high evidence surrounding biological plausibility of deposition of energy to impaired learning and memory. Energy deposition in the form of ionizing radiation can result in behavioural changes and impairments in learning and memory. Under normal conditions, diminished cognitive functions is influenced by aging or can occur if there is a predisposition to neurodegenerative diseases such as Alzheimer's, however, exposure to ionizing radiation may accelerate risk for age-related cognitive decline.
Deposition of Energy (MIE, KE#1686) →	**High**

Increase, DNA Strand Breaks (KE#1635)	There is high evidence surrounding biological plausibility of deposition of energy to DNA strand breaks. Direct DNA damage can occur after deposition of energy by direct oxidation of the DNA. Indirect DNA damage from deposition of energy can also occur via generation of ROS that can subsequently oxidize and damage DNA.
Increase, DNA Strand Breaks (KE#1635) → Increase, Neural Remodeling (KE#2098)	**Moderate** There is moderate evidence surrounding biological plausibility of increased DNA strand breaks to increase, neural remodeling. DNA strand breaks may initiate apoptotic signaling and impact synaptic activity, neural plasticity, differentiation, and proliferation.
Pro-inflammatory Mediators (KE#2097) → Impairment, Learning and Memory (AO, KE#341)	**Moderate** There is moderate support for the biological plausibility of the key event relationship between pro-inflammatory mediators to impaired learning and memory. In a neuroinflammatory response, pro-inflammatory mediators including cytokines induce physiological and/or structural changes within the brain that can ultimately lead to impaired learning and memory. The exact mechanistic relationship is still unclear due to the complexity of cytokine cascading events.

	Defining Question	**High (Strong)**	**Moderate**	**Low (Weak)**
Review of the Empirical support for each KER	Does KEupstream occur at lower doses and earlier time points than KEdownstream; is the incidence or frequency of KEupstream greater than that for KEdownstream for the same dose of tested stressor?	There is a dependent change in both events following exposure to a wide range of specific stressors (extensive evidence for temporal, dose-response and incidence concordance) and no or few data gaps or conflicting data.	There is demonstrated dependent change in both events following exposure to a small number of specific stressors and some evidence inconsistent with the expected pattern that can be explained by factors such as experimental design, technical considerations, differences among laboratories, etc	There are limited or no studies reporting dependent change in both events following exposure to a specific stressor (i.e., endpoints never measured in the same study or not at all), and/or lacking evidence of temporal or dose-response concordance, or identification of significant inconsistencies in empirical support across taxa and species that don't align with the expected pattern for the hypothesised AOP

Deposition of Energy (MIE, KE#1686) → Oxidative Stress (KE#1392)	**High** Ample evidence from in vitro and in vivo rat, mice, rabbit, squirrel, bovine and human models support time and dose response effects related to deposition of energy from various ionizing radiation sources leading to an increase in oxidative stress.
Deposition of Energy (MIE, KE#1686) → Tissue Resident Cell Activation (KE#1492)	**Moderate** With increasing dose of ionizing radiation, there are increasing amounts of resident tissue activation in both astrocytes and microglial cells. Multiple studies show dose-response and time-response effects with both high and low dose studies, as well as time ranges from hours to months, though additional studies at low-doses would improve empirical support.
Oxidative Stress (KE#1392) → Increase, DNA Strand Breaks (KE#1635)	**Moderate** Empirical evidence from in vivo and in vitro studies demonstrates increased DNA strand breaks from oxidative stress. Multiple studies show dose-response effects, though time response effects are difficult to monitor for both KEs.
Increase, DNA Strand Breaks (KE#1635) → Altered Signaling Pathways	**Moderate** A few studies demonstrate dose-concordance, and multiple studies demonstrate time-concordance for this relationship. DNA strand breaks were observed prior to altered signaling pathways.

(KE#2066)	
Oxidative Stress (KE#1392) → Tissue Resident Cell Activation (KE#1492)	**Moderate** The literature demonstrates that an increase in the level of stressor related to oxidative stress results in an increase in cellular activation of microglial cells or astrocytes and this relationship is consistent between studies. However, dose and time concordance are unclear as there is limited data that describes oxidative stress occurring at lower doses or before tissue resident cell activation.
Oxidative Stress (KE#1392) → Altered Signaling Pathways (KE#2066)	**Moderate** Many studies demonstrate dose-concordance, and few demonstrate time-concordance for this relationship. Oxidative stress was often observed at lower, or the same doses as altered signaling and sometimes also at earlier times as altered signaling. However, only a few specific stressors are used in this KER and inconsistencies are present, likely due to different experimental designs.
Altered Signaling Pathways (KE#2066) Increase, Neural Remodeling (KE#2098)	**Moderate** Many studies demonstrate dose-concordance in multiple signaling pathways. Studies have also shown that signaling pathways are altered before neural remodeling is observed. However, inconsistent changes in signaling pathways may be due to the context-dependence of signaling pathways as they can have different biological processes.
Tissue Resident Cell Activation (KE#1492) → Increase, Pro-inflammatory Mediators (KE#2097)	**Moderate** Studies consistently observed changes in astrocyte and microglial activation at lower or the same dose as increased pro-inflammatory mediators and many studies also found changes in astrocyte and microglial activation earlier or at the same time as increased pro-inflammatory mediators. However, inconsistencies could be due to differences in experimental conditions.
Increase, Pro-inflammatory Mediators (KE#2097) → Increase, Neural Remodeling (KE#2098)	**Moderate** There are multiple studies that show time-concordance, though studies on dose-concordance are lacking. Studies suggest that pro-inflammatory mediators are increased before neural remodeling occurs, reporting changes as early as 3 hours and persisting as long as 3 months. However, additional studies describing dose-concordance would improve empirical support.
Increase, Neural Remodeling (KE#2098) → Impairment, Learning and Memory (AO, KE#341)	**Moderate** Multiple studies suggest dose- and time-response effects of deposited energy leading to neural remodeling and impaired learning and memory. However, additional studies at low doses would improve empirical support. Also, discrepancies in the data may be due to experimental set up and type of exposure from the stressor.
Deposition of Energy (MIE, KE#1686) → Increase, Neural Remodeling (KE#2098)	**Moderate** Multiple studies suggest dose- and time-response effects of deposition of energy to neuronal remodeling. Studies report changes at very low doses. However, responses may be dependent on exposure type. Also, additional studies describing time-concordance would improve empirical support.
Deposition of Energy (MIE, KE#1686) → Impairment,	**Moderate** Various studies show that ionizing radiation can lead to impairments in learning and memory in a dose and time

Learning and Memory (AO, KE#341)	dependent manner. Although the impairment to learning and memory is well-studied across various doses and over multiple time points, studies often do not show impaired learning and memory with every cognitive test used, contributing to inconsistency in the relationship.
Deposition of Energy (MIE, KE#1686) → Increase, DNA Strand Breaks (KE#1635)	**High** There is ample empirical evidence demonstrating the relationship between deposition of energy and increase, DNA strand breaks. Multiple studies in various models show both dose-concordance and time-concordance.
Increase, DNA Strand Breaks (KE#1635) → Increase, Neural Remodeling (KE#2098)	**Moderate** Multiple studies demonstrate that increased DNA strand breaks lead to increased neural remodeling. However, additional studies describing both dose-concordance and time-concordance would improve empirical support.
Increase, Pro-inflammatory Mediators (KE#2097) → Impairment, Learning and Memory (AO, KE#341)	**Moderate** Evidence shows that pro-inflammatory mediators increase at lower or the same stressor doses than impaired learning. Also, pro-inflammatory mediators increase before impaired learning and memory is observed. Significant inconsistencies in empirical support across taxa and species that do not align with the expected pattern have not been identified.

Support for Essentiality of KEs	**Defining Question**	**High (Strong)**	**Moderate**	**Low (Weak)**
	Are downstream KEs and/or the AO prevented if an upstream KE is blocked?	Direct evidence from specifically designed experimental studies illustrating essentiality for at least one of the important KEs	Indirect evidence that sufficient modification of an expected modulating factor attenuates or augments a KE	No or contradictory experimental evidence of the essentiality of any of the KEs

MIE, KE#1686: Deposition of energy	**Moderate** Deposition of energy is difficult to test for essentiality as deposition of energy is a physical stressor and cannot be blocked/decreased using chemicals. In the absence of energy deposition or presence of shielding as demonstrated there should be no alterations to the relevant downstream KE.
KE#1392: Oxidative stress	**Moderate** Treatments with antioxidants, which reduce oxidative stress, attenuate downstream microglial activation and DNA strand breaks.
KE#1635: Increase, DNA Strand Breaks	**Moderate** Prevention of DNA strand breaks, for example treatment with mesenchymal stem cell-conditioned medium or minocycline, has restored altered signaling and neural remodeling.
KE#2066: Altered Signaling Pathways	**Moderate** Knockout models or inhibition of key signaling molecules, have all been shown to influence the effects of signaling pathways on neural remodeling through the attenuation of stressor-induced changes in neuronal morphology and growth. The KE has also been shown to be modulated by sex and exercise.
KE#1492: Tissue Resident Cell Activation	**Moderate** For example, the attenuation of the activation of tissue-resident cells and consequent reduction in pro-inflammatory mediators has been reported using multiple drugs.
KE#2097: Increase, Pro-inflammatory Mediators	**Moderate** Treatments with anti-inflammatory drugs, antioxidants or hormones have influenced the effects of pro-inflammatory mediators and improved neuronal structure and function. Anti-inflammatory drugs have also influenced the effects of pro-inflammatory mediators and rescued the impairments seen in learning and memory.
	Moderate

KE#2098: Neural Remodeling	No identified studies describe essentiality of neural remodeling as it cannot be blocked / decreased using chemicals.

Quantitative Consideration

Overall quantitative understanding for the KERs in the AOP is low. Despite evidence supporting the KERs, there is limited understanding of the trends of the relationships between KEs. In the KERs of this AOP, there are positive relationships between the KEs (i.e., an increase in the upstream KE elicits a change in the downstream KE); however, the trends and shapes of the relationships are not well established due to differences in experimental parameters, such as model, radiation type, doses, dose rate, and time of measurements. The measures of the KEs cannot be precisely predicted based on relevant measures of the other KEs in the KER and the quantitative descriptions does not account for all known modulating factors and feedback or feedforward mechanisms.

Considerations for Potential Applications of the AOP (optional)

This AOP was developed to bring together mechanistic knowledge in the area of impairments in learning and memory from exposure to radiation. It includes studies from multiple species at multiple life stages and radiation exposures that contain different doses, dose-rates, and radiation qualities. Relevant studies have been selected, consolidated, and reported using the framework.

There are multiple considerations for potential applications of the AOP. Since exposure to radiation can occur in humans from multiple events, including occupational settings, accidental exposures, nuclear events, radiotherapy treatment and space travel, understanding its impact on CNS structure and function is essential. This AOP outlines a biological framework for the connection between the MIE and AO. It can be expanded to other pathophysiologies of the CNS. The qualitaive information presented within each KER can be used to inform on risk-model strategies, countermeasure development, and identification of gaps in the evidence base where more research is necessary. Importantly, this AOP is a dynamic document so it can be modified as new evidence emerges.

References

Acharya, M. M. et al. (2010), "Consequences of ionizing radiation-induced damage in human neural stem cells", Free Radical Biology and Medicine, Vol. 49/12, Pergamon, https://doi.org/10.1016/j.freeradbiomed.2010.08.021.

Ahmadi, M. et al. (2022), “Early responses to low-dose ionizing radiation in cellular lens epithelial models”, Radiation research, Vol. 197/1, Radiation Research Society, Bozeman, https://doi.org/10.1667/RADE-20-00284.1

Antonelli, A.F. et al. (2015), "Induction and Repair of DNA DSB as Revealed by H2AX Phosphorylation Foci in Human Fibroblasts Exposed to Low- and High-LET Radiation: Relationship with Early and Delayed Reproductive Cell Death", Radiation Research, Vol 183/4, BioOne, Washington, httrps://doi.org/10.1667/RR13855.1.

Azimzadeh, O. et al. (2015), "Integrative proteomics and targeted transcriptomics analyses in cardiac endothelial cells unravel mechanisms of long-term radiation-induced vascular dysfunction", Journal of Proteome Research, Vol. 14/2, American Chemical Society, Washington, https://doi.org/10.1021/pr501141b

Balasubramanian, D (2000), “Ultraviolet radiation and cataract”, Journal of ocular pharmacology and therapeutics, Vol. 16/3, Mary Ann Liebert Inc., Larchmont, https://doi.org/10.1089/jop.2000.16.285.

Bálentová, S. and M. Adamkov. (2020), "Pathological changes in the central nervous system following exposure to ionizing radiation", Physiological Research, Czech Academy of Sciences, https://doi.org/10.33549/PHYSIOLRES.934309.

Barrientos, R. M. et al. (2009), "Time course of hippocampal IL-1 β and memory consolidation impairments in aging rats following peripheral infection", Brain, Behavior, and Immunity, Vol. 23/1, Elsevier, Amsterdam, https://doi.org/10.1016/j.bbi.2008.07.002.

Barrientos, R. M. et al. (2012), "Aging-related changes in neuroimmune-endocrine function: Implications for hippocampal-dependent cognition", Hormones and Behavior, Vol. 62/3, Elsevier, Amsterdam, https://doi.org/10.1016/j.yhbeh.2012.02.010.

Belkacémi, Y. et al. (2001), “Lens epithelial cell protection by aminothiol WR-1065 and anetholedithiolethione from ionizing radiation”, International journal of cancer, Vol. 96, John Wiley & Sons, Ltd., Hoboken, https://doi.org/10.1002/ijc.10346.

Betlazar, C. et al. (2016), "The impact of high and low dose ionising radiation on the central nervous system", Redox Biology, Vol. 9, Elsevier, Amsterdam, https://doi.org/10.1016/j.redox.2016.08.002.

Bhat, K. et al. (2020), "1-[(4-Nitrophenyl)sulfonyl]-4-phenylpiperazine treatment after brain irradiation preserves cognitive function in mice", Neuro-Oncology, Vol. 22/10, Oxford University Press, Oxford, https://doi.org/10.1093/neuonc/noaa095.

Brooks, A.L., D.G. Hoel & R.J. Preston (2016), "The role of dose rate in radiation cancer risk: evaluating the effect of dose rate at the molecular, cellular and tissue levels using key events in critical pathways following exposure to low LET radiation.", International Journal of Radiation Biology, Vol. 92/8, Taylor & Francis, London, doi:10.1080/09553002.2016.1186301.

Casciati, A. et al. (2016), "Age-related effects of X-ray irradiation on mouse hippocampus", Oncotarget, Vol. 7/19,

https://doi.org/10.18632/oncotarget.8575.

Cekanaviciute, E., S. Rosi and S. V. Costes. (2018), "Central nervous system responses to simulated galactic cosmic rays", International Journal of Molecular Sciences, Multidisciplinary Digital Publishing Institute (MDPI) AG, Basel, https://doi.org/10.3390/ijms19113669.

Chen, Z. and T. D. Palmer. (2013), "Differential roles of TNFR1 and TNFR2 signaling in adult hippocampal neurogenesis", Brain, Behavior, and Immunity, Vol. 30, Elsevier Inc., Amsterdam, https://doi.org/10.1016/j.bbi.2013.01.083.

Chen, Y. et al. (2021), “Effects of neutron radiation on Nrf2-regulated antioxidant defense systems in rat lens”, Experimental and therapeutic medicine, Vol. 21/4, Spandidos Publishing Ltd, Athens, https://doi.org/10.3892/etm.2021.9765.

Chitchumroonchokchai, C. et al. (2004), “Xanthophylls and α-tocopherol decrease UVB-induced lipid peroxidation and stress signaling in human lens epithelial cells”, The Journal of Nutrition, Vol. 134/12, American Society for Nutritional Sciences, Bethesda, https://doi.org/10.1093/jn/134.12.3225.

Chow, B. M., Y.-Q. Li and C. S. Wong. (2000), "Radiation-induced apoptosis in the adult central nervous system is p53-dependent", Cell Death & Differentiation, Vol. 7/8, Springer Nature, https://doi.org/10.1038/sj.cdd.4400704.

Cucinotta, F. A. et al. (2014), "Space radiation risks to the central nervous system", Life Sciences in Space Research, Vol. 2, Elsevier Ltd, Amsterdam, https://doi.org/10.1016/j.lssr.2014.06.003.

Daverey, A. and S. K. Agrawal. (2016), "Curcumin alleviates oxidative stress and mitochondrial dysfunction in astrocytes", Neuroscience, Vol. 333, https://doi.org/10.1016/j.neuroscience.2016.07.012.

Davis, S. and S. Laroche. (2006), "Mitogen-activated protein kinase/extracellular regulated kinase signalling and memory stabilization: a review", Genes, Brain and Behavior, Vol. 5, Wiley, https://doi.org/10.1111/j.1601-183X.2006.00230.x.

de Jager, T. L., A. E. Cockrell, S. S. Du Plessis (2017), “Ultraviolet Light Induced Generation of Reactive Oxygen Species”, in: Ultraviolet Light in Human Health, Diseases and Environment, vol 996. Springer Cham, https://doi.org/10.1007/978-3-319-56017-5_2.

Demir, E. et al. (2020), “Nigella sativa oil and thymoquinone reduce oxidative stress in the brain tissue of rats exposed to total head irradiation”, International journal of radiation biology, Vol. 96/2, Informa, London, https://doi.org/10.1080/09553002.2020.1683636.

Deng, Z. et al. (2012), "Radiation-Induced c-Jun Activation Depends on MEK1-ERK1/2 Signaling Pathway in Microglial Cells", (I. Ulasov, Ed.) PLoS ONE, Vol. 7/5, https://doi.org/10.1371/journal.pone.0036739.

Desai, R. I. et al. (2022), "Impact of spaceflight stressors on behavior and cognition: A molecular, neurochemical, and neurobiological perspective", Neuroscience & Biobehavioral Reviews, Vol. 138, Elsevier, Amsterdam, https://doi.org/10.1016/j.neubiorev.2022.104676.

Dong, X. et al. (2015), "Relationship between irradiation-induced neuro-inflammatory environments and impaired cognitive function in the developing brain of mice", International Journal of Radiation Biology, Vol. 91/3, Informa Healthcare, London, https://doi.org/10.3109/09553002.2014.988895.

El-Missiry, M. A. et al. (2018), "Neuroprotective effect of epigallocatechin-3-gallate (EGCG) on radiation-induced damage and apoptosis in the rat hippocampus", International Journal of Radiation Biology, Vol. 94/9, https://doi.org/10.1080/09553002.2018.1492755.

Eom, H. S. et al. (2015), "Ionizing radiation induces neuronal differentiation of Neuro-2a cells via PI3-kinase and p53-dependent pathways", International Journal of Radiation Biology, Vol. 91/7, Informa, London, https://doi.org/10.3109/09553002.2015.1029595.

Falcicchia, C. et al. (2020), "Involvement of p38 MAPK in Synaptic Function and Dysfunction", International Journal of Molecular Sciences, Vol. 21/16, MDPI, Basel, https://doi.org/10.3390/ijms21165624.

Fatma, N. et al. (2005), “Impaired homeostasis and phenotypic abnormalities in Prdx6-/- mice lens epithelial cells by reactive oxygen species: Increased expression and activation of TGFβ”, Cell death and differentiation, Vol. 12, Nature Portfolio, London, https://doi.org/10.1038/sj.cdd.4401597.

Fishman, K. et al. (2009), "Radiation-induced reductions in neurogenesis are ameliorated in mice deficient in CuZnSOD or MnSOD", Free Radical Biology and Medicine, Vol. 47/10, https://doi.org/10.1016/j.freeradbiomed.2009.08.016.

Fletcher, A. E (2010), “Free radicals, antioxidants and eye diseases: evidence from epidemiological studies on cataract and age-related macular degeneration”, Ophthalmic Research, Vol. 44, Karger International, Basel, https://doi.org/10.1159/000316476.

Ganea, E. and J. J. Harding (2006), “Glutathione-related enzymes and the eye”, Current eye research, Vol. 31/1, Informa, London, https://doi.org/10.1080/02713680500477347.

Giedzinski, E. et al. (2005), “Efficient production of reactive oxygen species in neural precursor cells after exposure to 250 MeV protons”, Radiation research, Vol. 164/4, Radiation Research Society, Bozeman, https://doi.org/10.1667/rr3369.1.

Gonzalez, P. V. et al. (2009), "Memory impairment induced by IL-1β is reversed by α-MSH through central melanocortin-4

receptors", Brain, Behavior, and Immunity, Vol. 23/6, Elsevier, Amsterdam, https://doi.org/10.1016/j.bbi.2009.03.001.

Green, H. F. et al. (2012), "A role for interleukin-1β in determining the lineage fate of embryonic rat hippocampal neural precursor cells", Molecular and Cellular Neuroscience, Vol. 49/3, Elsevier Inc., Amsterdam, https://doi.org/10.1016/j.mcn.2012.01.001.

Greene-Schloesser, D. et al. (2012), "Radiation-induced brain injury: A review", Frontiers in Oncology, Vol. 2, Frontiers, Lausanne, https://doi.org/10.3389/fonc.2012.00073.

Hanslik, K. L., K. M. Marino and T. K. Ulland. (2021), "Modulation of Glial Function in Health, Aging, and Neurodegenerative Disease", Frontiers in Cellular Neuroscience, Vol. 15, https://doi.org/10.3389/fncel.2021.718324.

Hamada, N. et al. (2006), “Histone H2AX phosphorylation in normal human cells irradiated with focused ultrasoft X rays: evidence for chromatin movement during repair”, Radiation Research, Vol. 166/1, Radiation Research Society, United States, https://doi.org/10.1667/RR3577.1

Hladik, D. and S. Tapio. (2016), "Effects of ionizing radiation on the mammalian brain", Mutation Research - Reviews in Mutation Research, Vol. 770, Elsevier B.V., Amsterdam, https://doi.org/10.1016/j.mrrev.2016.08.003.

Huang, Y. et al. (2021), "Mesenchymal Stem Cell-Conditioned Medium Protects Hippocampal Neurons From Radiation Damage by Suppressing Oxidative Stress and Apoptosis", Dose-Response, Vol. 19/1, SAGE publications, https://doi.org/10.1177/1559325820984944.

Hua, H. et al. (2019), “Protective effects of lanosterol synthase up-regulation in UV-B-induced oxidative stress”, Frontiers in pharmacology, Vol. 10, Frontiers Media SA, Lausanne, https://doi.org/10.3389/fphar.2019.00947.

Hunsberger, H. C. et al. (2019), "The role of APOE4 in Alzheimer’s disease: strategies for future therapeutic interventions", Neuronal Signaling, Vol. 3/2, Portland Press, London, https://doi.org/10.1042/NS20180203.

Hwang, S. Y. et al. (2006), "Ionizing radiation induces astrocyte gliosis through microglia activation", Neurobiology of Disease, Vol. 21/3, Academic Press, https://doi.org/10.1016/j.nbd.2005.08.006.

International commission on Radiological Protection (ICRP). (2007), “The 2007 recommendations of the International Commission on Radiological Protection.”, Ann ICRP 37, ICRP Publication 103.

Ismail, A. F. and S. M. El-Sonbaty (2016), “Fermentation enhances Ginkgo biloba protective role on γ-irradiation induced neuroinflammatory gene expression and stress hormones in rat brain”, Journal of photochemistry and photobiology. B, Biology, Vol. 158, Elsevier, Amsterdam, https://doi.org/10.1016/j.jphotobiol.2016.02.039.

Jenrow, K. A. et al. (2013), "Selective Inhibition of Microglia-Mediated Neuroinflammation Mitigates Radiation-Induced Cognitive Impairment", Radiation Research, Vol. 179/5, BioOne, https://doi.org/10.1667/RR3026.1.

Ji, J. et al. (2014), "Forced running exercise attenuates hippocampal neurogenesis impairment and the neurocognitive deficits induced by whole-brain irradiation via the BDNF-mediated pathway", Biochemical and Biophysical Research Communications, Vol. 443/2, Elsevier, Amsterdam, https://doi.org/10.1016/j.bbrc.2013.12.031.

Jiang, Q. et al. (2006), “UV radiation down-regulates Dsg-2 via Rac/NADPH oxidase-mediated generation of ROS in human lens epithelial cells”, International Journal of Molecular Medicine, Vol. 18/2, Spandidos Publishing Ltd, Athens, https://doi.org/10.3892/ijmm.18.2.381.

Serment-Guerrero, J. et al. (2012), "Evidence of DNA double strand breaks formation in Escherichia coli bacteria exposed to alpha particles of different LET assessed by the SOS response", Applied Radiation and Isotopes, Vol. 71, Elsevier, Amsterdam, https://doi.org/10.1016/j.apradiso.2012.05.007.

Kalm, M., K. Roughton and K. Blomgren. (2013), "Lipopolysaccharide sensitized male and female juvenile brains to ionizing radiation", Cell Death & Disease, Vol. 4/12, https://doi.org/10.1038/cddis.2013.482.

Kang, L. et al. (2020), “Ganoderic acid A protects lens epithelial cells from UVB irradiation and delays lens opacity”, Chinese journal of natural medicines, Vol. 18/12, Elsevier, Amsterdam, https://doi.org/10.1016/S1875-5364(20)60037-1.

Kanzawa, T. et al. (2006), "Ionizing radiation induces apoptosis and inhibits neuronal differentiation in rat neural stem cells via the c-Jun NH2-terminal kinase (JNK) pathway", Oncogene, Vol. 25/26, Springer Nature, https://doi.org/10.1038/sj.onc.1209414.

Karimi, N. et al. (2017), “Radioprotective effect of hesperidin on reducing oxidative stress in the lens tissue of rats”, International Journal of Pharmaceutical Investigation, Vol. 7/3, Phcog Net, Bengaluru, https://doi.org/10.4103/jphi.JPHI_60_17.

Katsura, M. et al. (2021), "Recognizing Radiation-induced Changes in the Central Nervous System: Where to Look and What to Look For", RadioGraphics, Vol. 41/1, https://doi.org/10.1148/rg.2021200064.

Kiffer, F. et al. (2019a), "Late Effects of 16O-Particle Radiation on Female Social and Cognitive Behavior and Hippocampal Physiology", Radiation Research, Vol. 191/3, BioOne, Washington, https://doi.org/10.1667/RR15092.1.

Kiffer, F., M. Boerma and A. Allen. (2019b), "Behavioral effects of space radiation: A comprehensive review of animal studies", Life Sciences in Space Research, Vol. 21, Elsevier, Amsterdam, https://doi.org/10.1016/j.lssr.2019.02.004.

Komatsu, W. et al. (2017), “Nasunin inhibits the lipopolysaccharide-induced pro-inflammatory mediator production in RAW264 mouse macrophages by suppressing ROS-mediated activation of PI3 K/Akt/NF-κB and p38 signaling pathways”, Bioscience, Biotechnology, and Biochemistry, Vol. 81/10, Elsevier, https://doi.org/10.1080/09168451.2017.1362973

Kozbenko, T. et al. (2022), "Deploying elements of scoping review methods for adverse outcome pathway development: a space travel case example", International Journal of Radiation Biology, Vol. 98/12, https://doi.org/10.1080/09553002.2022.2110306.

Krukowski, K. et al. (2018a), "Female mice are protected from space radiation-induced maladaptive responses", Brain, Behavior, and Immunity, Vol. 74, Academic Press Inc., https://doi.org/10.1016/j.bbi.2018.08.008.

Kyrkanides, S. et al. (1999), "TNFα and IL-1β mediate intercellular adhesion molecule-1 induction via microglia-astrocyte interaction in CNS radiation injury", Journal of Neuroimmunology, Vol. 95/1–2, Elsevier, Amsterdam, https://doi.org/10.1016/S0165-5728(98)00270-7.

Kyrkanides, S. et al. (2002), "Cyclooxygenase-2 modulates brain inflammation-related gene expression in central nervous system radiation injury", Molecular Brain Research, Vol. 104/2, Elsevier, https://doi.org/10.1016/S0169-328X(02)00353-4.

Lee, W. H. et al. (2010), "Irradiation induces regionally specific alterations in pro-inflammatory environments in rat brain", International Journal of Radiation Biology, Vol. 86/2, Informa, London, https://doi.org/10.3109/09553000903419346.

Lee, K., A. Lee and I. Choi. (2017), "Melandrii Herba Extract Attenuates H2O2-Induced Neurotoxicity in Human Neuroblastoma SH-SY5Y Cells and Scopolamine-Induced Memory Impairment in Mice", Molecules, Vol. 22/10, MDPI, Basel, https://doi.org/10.3390/molecules22101646.

Lee, K. H., M. Cha and B. H. Lee. (2021), "Crosstalk between Neuron and Glial Cells in Oxidative Injury and Neuroprotection", International Journal of Molecular Sciences, Vol. 22/24, https://doi.org/10.3390/ijms222413315.

Lehtinen, M. and A. Bonni. (2006), "Modeling Oxidative Stress in the Central Nervous System", Current Molecular Medicine, Vol. 6/8, https://doi.org/10.2174/156652406779010786.

Li, J. et al. (2013), "Oxidative Stress and Neurodegenerative Disorders", International Journal of Molecular Sciences, Vol. 14/12, https://doi.org/10.3390/ijms141224438.

Liguori, I. et al. (2018), "Oxidative stress, aging, and diseases", Clinical Interventions in Aging, Vol.13, https://doi.org/10.2147/CIA.S158513.

Limoli, C. L. et al. (2004), “Radiation response of neural precursor cells: linking cellular sensitivity to cell cycle checkpoints, apoptosis and oxidative stress”, Radiation research, Vol. 161/1, Radiation Research Society, Bozeman, https://doi.org/10.1667/rr3112.

Limoli, C. L. et al. (2007), “Redox changes induced in hippocampal precursor cells by heavy ion irradiation”, Radiation and environmental biophysics, Vol. 46/2, Springer, London, https://doi.org/10.1007/s00411-006-0077-9.

Liu, J. L. et al. (2010), "Tamoxifen alleviates irradiation-induced brain injury by attenuating microglial inflammatory response in vitro and in vivo", Brain Research, Vol. 1316, Elsevier B.V., https://doi.org/10.1016/j.brainres.2009.12.055.

Long, H.-Z. et al. (2021), "PI3K/AKT Signal Pathway: A Target of Natural Products in the Prevention and Treatment of Alzheimer’s Disease and Parkinson’s Disease", Frontiers in Pharmacology, Vol. 12, Frontiers, https://doi.org/10.3389/fphar.2021.648636.

Madsen, T. M. et al. (2003), "Arrested neuronal proliferation and impaired hippocampal function following fractionated brain irradiation in the adult rat", Neuroscience, Vol. 119/3, Elsevier Ltd, https://doi.org/10.1016/S0306-4522(03)00199-4.

Manda, K. et al. (2007a), “Melatonin attenuates radiation-induced learning deficit and brain oxidative stress in mice”, Acta neurobiologiae experimentalis, Vol. 67/1, Nencki Institute of Experimental Biology, Warsaw, pp. 63 –70.

Manda, K. et al. (2007b), "Radiation-induced cognitive dysfunction and cerebellar oxidative stress in mice: Protective effect of α-lipoic acid", Behavioural Brain Research, Vol. 177/1, Elsevier, Amsterdam, https://doi.org/10.1016/j.bbr.2006.11.013.

Manda, K., M. Ueno and K. Anzai (2008), “Memory impairment, oxidative damage and apoptosis induced by space radiation: ameliorative potential of alpha-lipoic acid”, Behavioural brain research, Vol. 187/2, Elsevier, Amsterdam, https://doi.org/10.1016/j.bbr.2007.09.033.

Mazzucchelli, C. and R. Brambilla. (2000), "Ras-related and MAPK signalling in neuronal plasticity and memory formation", Cellular and Molecular Life Sciences, Vol. 57/4, Springer Nature, https://doi.org/10.1007/PL00000722.

McHugh, D. and J. Gil. (2018), "Senescence and aging: Causes, consequences, and therapeutic avenues", Journal of Cell Biology, Vol. 217/1, Rockefeller University Press, New York, https://doi.org/10.1083/jcb.201708092.

Mielke, K. and T. Herdegen. (2000), "JNK and p38 stresskinases — degenerative effectors of signal-transduction-cascades in the nervous system", Progress in Neurobiology, Vol. 61/1, Elsevier, Amsterdam, https://doi.org/10.1016/S0301-0082(99)00042-8.

Mosconi, M. et al. (2011), "53BP1 and MDC1 foci formation in HT-1080 cells for low- and high-LET microbeam irradiations", Radiation and Environmental Biophysics, Vol. 50/3, Springer Nature, Berlin, https://doi.org/10.1007/s00411-011-0366-9.

Monje, M. L. and T. Palmer. (2003), "Radiation injury and neurogenesis", Current Opinion in Neurology, Vol. 16/2, Ovid Technologies (Wolters Kluwer Health), https://doi.org/10.1097/01.wco.0000063772.81810.b7.

Mousa, A. and M. Bakhiet. (2013), "Role of Cytokine Signaling during Nervous System Development", International Journal of Molecular Sciences, Vol. 14/7, MDPI, Basel, https://doi.org/10.3390/ijms140713931.

Nagane, M. et al. (2021), "DNA damage response in vascular endothelial senescence: Implication for radiation-induced cardiovascular diseases", Journal of Radiation Research, Vol. 62/4, Oxford University Press, Oxford, https://doi.org/10.1093/jrr/rrab032

National Council on Radiation Protection and Measures (NCRP). (2016). Commentary No. 25 – Potential for central nervous system effects from radiation exposure during space activities phase I: Overview.

Nikjoo, H. et al. (2001), "Computational approach for determining the spectrum of DNA damage induced by ionizing radiation.", Radiation Research, Vol. 156/5 Pt 2, BioOne, Washington, https://doi.org/10.1667/0033-7587(2001)156[0577:cafdts]2.0.co;2

Nikjoo, H. et al. (2016), "Radiation track, DNA damage and response—a review", Reports on Progress in Physics, Vol. 79/11, IOP Publishing, Bristol, https://doi.org/10.1088/0034-4885/79/11/116601.

Nebreda, A. R. and A. Porras. (2000), "p38 MAP kinases: beyond the stress response", Trends in Biochemical Sciences, Vol. 25/6, Elsevier, Amsterdam, https://doi.org/10.1016/S0968-0004(00)01595-4.

Parihar, V. K. et al. (2016), "Cosmic radiation exposure and persistent cognitive dysfunction", Scientific Reports, Vol. 6/1, Nature Publishing Group, https://doi.org/10.1038/srep34774.

Parihar, V. K. et al. (2018), "Persistent nature of alterations in cognition and neuronal circuit excitability after exposure to simulated cosmic radiation in mice", Experimental Neurology, Vol. 305, Elsevier B.V., https://doi.org/10.1016/j.expneurol.2018.03.009.

Parihar, V. K. et al. (2020), "Sex-Specific Cognitive Deficits Following Space Radiation Exposure", Frontiers in behavioral neuroscience, Vol. 14, Frontiers, https://doi.org/10.3389/fnbeh.2020.535885.

Park, D. H. et al. (2021), "Neuroprotective Effect of Gallocatechin Gallate on Glutamate-Induced Oxidative Stress in Hippocampal HT22 Cells", Molecules, Vol. 26/5, MDPI, Basel, https://doi.org/10.3390/molecules26051387.

Patterson, S. L. (2015), "Immune dysregulation and cognitive vulnerability in the aging brain: Interactions of microglia, IL-1β, BDNF and synaptic plasticity", Neuropharmacology, Vol. 96, Elsevier B.V., https://doi.org/10.1016/j.neuropharm.2014.12.020.

Ping, Z. et al. (2020), "Oxidative Stress in Radiation-Induced Cardiotoxicity", Oxidative Medicine and Cellular Longevity, Vol. 2020, Hindawi, London, https://doi.org/10.1155/2020/3579143

Pius-Sadowska, E. et al. (2016), "Alteration of Selected Neurotrophic Factors and their Receptor Expression in Mouse Brain Response to Whole-Brain Irradiation", Radiation Research, Vol. 186/5, BioOne, https://doi.org/10.1667/RR14457.1.

Prieto, G. A. and C. W. Cotman. (2017), "Cytokines and cytokine networks target neurons to modulate long-term potentiation", Cytokine & Growth Factor Reviews, Vol. 34, Elsevier, Amsterdam, https://doi.org/10.1016/j.cytogfr.2017.03.005.

Raber, J. et al. (2004), "Radiation-induced cognitive impairments are associated with changes in indicators of hippocampal neurogenesis", Radiation Research, Vol. 162/1, Allen Press, https://doi.org/10.1667/RR3206.

Raber, J. et al. (2019), "Combined Effects of Three High-Energy Charged Particle Beams Important for Space Flight on Brain, Behavioral and Cognitive Endpoints in B6D2F1 Female and Male Mice", Frontiers in physiology, Vol. 10, Frontiers, https://doi.org/10.3389/fphys.2019.00179.

Rai, S. N. et al. (2019), "The Role of PI3K/Akt and ERK in Neurodegenerative Disorders", Neurotoxicity Research, Vol. 35/3, Elsevier, Amsterdam, https://doi.org/10.1007/s12640-019-0003-y.

Ramalingam, M. and S.-J. Kim. (2012), "Reactive oxygen/nitrogen species and their functional correlations in neurodegenerative diseases", Journal of Neural Transmission, Vol. 119/8, Springer Nature, Berlin, https://doi.org/10.1007/s00702-011-0758-7.

Ramanan, S. et al. (2008), "PPARα ligands inhibit radiation-induced microglial inflammatory responses by negatively regulating NF-κB and AP-1 pathways", Free Radical Biology and Medicine, Vol. 45/12, Elsevier B.V., https://doi.org/10.1016/j.freeradbiomed.2008.09.002.

Rodgers, E. E. and A. B. Theibert. (2002), "Functions of PI 3-kinase in development of the nervous system", International Journal of Developmental Neuroscience, Vol. 20/3–5, Wiley, https://doi.org/10.1016/S0736-5748(02)00047-3.

Rogakou, E. P. et al. (1999), "Megabase Chromatin Domains Involved in DNA Double-Strand Breaks in Vivo", Journal of Cell Biology, Vol. 146/5, Rockefeller University Press, New York, https://doi.org/10.1083/jcb.146.5.905.

Rola, R. et al. (2004), "Radiation-induced impairment of hippocampal neurogenesis is associated with cognitive deficits in young mice", Experimental Neurology, Vol. 188/2, Academic Press Inc., https://doi.org/10.1016/j.expneurol.2004.05.005.

Romanella, S. M. et al. (2020), "Noninvasive Brain Stimulation & Space Exploration: Opportunities and Challenges",

Neuroscience & Biobehavioral Reviews, Vol. 119, https://doi.org/10.1016/j.neubiorev.2020.09.005.

Rothkamm, K. and M. Löbrich. (2003), "Evidence for a lack of DNA double-strand break repair in human cells exposed to very low x-ray doses", Proceedings of the National Academy of Sciences, Vol. 100/9, National Academy of Sciences, https://doi.org/10.1073/pnas.0830918100.

Rübe, C. E. et al. (2008), "DNA Double-Strand Break Repair of Blood Lymphocytes and Normal Tissues Analysed in a Preclinical Mouse Model: Implications for Radiosensitivity Testing", Clinical Cancer Research, Vol. 14/20, American Association for Cancer Research, Washington, https://doi.org/10.1158/1078-0432.CCR-07-5147.

Ryan, S. M. et al. (2013), "Negative regulation of TLX by IL-1β correlates with an inhibition of adult hippocampal neural precursor cell proliferation", Brain, Behavior, and Immunity, Vol. 33, Elsevier, Amsterdam, https://doi.org/10.1016/j.bbi.2013.03.005.

Sabirzhanov, B. et al. (2020), "Irradiation-Induced Upregulation of miR-711 Inhibits DNA Repair and Promotes Neurodegeneration Pathways", International Journal of Molecular Sciences, Vol. 21/15, Multidisciplinary Digital Publishing Institute (MDPI) AG, Basel, https://doi.org/10.3390/ijms21155239.

Saraiva, C. et al. (2019), "Histamine modulates hippocampal inflammation and neurogenesis in adult mice", Scientific Reports, Vol. 9/1, Springer Nature, Berlin, https://doi.org/10.1038/s41598-019-44816-w.

Schmidt-Ullrich, R. K. et al. (2000), "Signal transduction and cellular radiation responses.", Radiation research, Vol. 153/3, BioOne, https://doi.org/10.1667/0033-7587(2000)153[0245:stacrr]2.0.co;2

Schnegg, C. I. et al. (2012), "PPARδ prevents radiation-induced proinflammatory responses in microglia via transrepression of NF-κB and inhibition of the PKCα/MEK1/2/ERK1/2/AP-1 pathway", Free Radical Biology and Medicine, Vol. 52/9, Pergamon, https://doi.org/10.1016/J.FREERADBIOMED.2012.02.032.

Sherrin, T., T. Blank and C. Todorovic. (2011), "c-Jun N-terminal kinases in memory and synaptic plasticity", Reviews in the Neurosciences, Vol. 22/4, De Gruyter, https://doi.org/10.1515/rns.2011.032.

Shi, Q. et al. (2017), "Complement C3 deficiency protects against neurodegeneration in aged plaque-rich APP/PS1 mice", Science Translational Medicine, Vol. 9/392, American Association for the Advancement of Science, Washington, https://doi.org/10.1126/scitranslmed.aaf6295.

Simpson, D. S. A. and P. L. Oliver. (2020), "ROS Generation in Microglia: Understanding Oxidative Stress and Inflammation in Neurodegenerative Disease", Antioxidants, Vol. 9/8, https://doi.org/10.3390/antiox9080743.

Slezak, J. et al. (2017), “Potential markers and metabolic processes involved in the mechanism of radiation-induced heart injury”, Canadian journal of physiology and pharmacology, Vol. 95/10, Canadian Science Publishing, Ottawa, https://doi.org/10.1139/cjpp-2017-0121.

Sutherland, B. M. et al. (2000), "Clustered DNA damages induced in isolated DNA and in human cells by low doses of ionizing radiation", Proceedings of the National Academy of Sciences, Vol. 97/1, National Academy of Sciences, https://doi.org/10.1073/pnas.97.1.103.

Suman, S. et al. (2013), “Therapeutic and space radiation exposure of mouse brain causes impaired DNA repair response and premature senescence by chronic oxidant production”, Aging, Vol. 5/8, Impact Journals, Orchard Park, https://doi.org/10.18632/aging.100587.

Taepavarapruk, P. and C. Song. (2010), "Reductions of acetylcholine release and nerve growth factor expression are correlated with memory impairment induced by interleukin-1β administrations: effects of omega-3 fatty acid EPA treatment", Journal of Neurochemistry, Vol. 112/4, Wiley https://doi.org/10.1111/j.1471-4159.2009.06524.x.

Tan, H. et al. (2014), "Critical role of inflammatory cytokines in impairing biochemical processes for learning and memory after surgery in rats", Journal of Neuroinflammation, Vol. 11/1, Springer Nature, https://doi.org/10.1186/1742-2094-11-93.

Tian, R. et al. (2020), "miR-137 prevents inflammatory response, oxidative stress, neuronal injury and cognitive impairment via blockade of Src-mediated MAPK signaling pathway in ischemic stroke", Aging, Vol. 12/11, https://doi.org/10.18632/aging.103301.

Tomé, W. A. et al. (2015), "Hippocampal-dependent neurocognitive impairment following cranial irradiation observed in pre-clinical models: current knowledge and possible future directions", The British Journal of Radiobiology, Vol. 89/1057, British Institute of Radiology, https://doi.org/10.1259/bjr.20150762.

Turnquist, C., B. T. Harris and C. C. Harris. (2020), "Radiation-induced brain injury: current concepts and therapeutic strategies targeting neuroinflammation", Neuro-Oncology Advances, Vol. 2/1, Oxford University Press, Oxford, https://doi.org/10.1093/noajnl/vdaa057.

United Nations Scientific Committee on the Effects of Atomic Radiation (UNSCEAR). (2008), “Sources and effects of ionizing radiation”, UNSCEAR 2008 Report, Vol 1, UN Publications.

Valerie, K. et al. (2007), "Radiation-induced cell signaling: inside-out and outside-in", Molecular Cancer Therapeutics, Vol. 6/3, American Association for Cancer Research, https://doi.org/10.1158/1535-7163.MCT-06-0596

Valliéres, L. et al. (2002), "Reduced hippocampal neurogenesis in adult transgenic mice with chronic astrocytic production of interleukin-6", Journal of Neuroscience, Vol. 22/2, Society for Neuroscience, Washington, https://doi.org/10.1523/jneurosci.22-02-00486.2002.

van Neerven, S. et al. (2010), "Inflammatory cytokine release of astrocytes in vitro is reduced by all-trans retinoic acid", Journal of Neuroimmunology, Vol. 229/1–2, Elsevier B.V., https://doi.org/10.1016/j.jneuroim.2010.08.005.

Wang, Y. L. et al. (2017), "Protective Effect of Curcumin Against Oxidative Stress-Induced Injury in Rats with Parkinson's Disease Through the Wnt/ β-Catenin Signaling Pathway", Cellular Physiology and Biochemistry, Vol. 43/6, https://doi.org/10.1159/000484302.

Wang, H. et al. (2019a), "Radiation-induced heart disease: a review of classification, mechanism and prevention", International Journal of Biological Sciences, Vol. 15/10, Ivyspring International Publisher, Sydney, https://doi.org/10.7150/ijbs.35460.

Whoolery, C. W. et al. (2017), "Whole-body exposure to 28Si-radiation dose-dependently disrupts dentate gyrus neurogenesis and proliferation in the short term and new neuron survival and contextual fear conditioning in the long term", Radiation Research, Vol. 188/5, Radiation Research Society, https://doi.org/10.1667/RR14797.1.

Wilkinson, B., Hill, M.A., and Parsons, J.L. (2023), "The Cellular Response to Complex DNA Damage Induced by Ionising Radiation" International Journal of Molecular Sciences Vol. 24/4920, Multidisciplinary Digital Publishing Institute (MDPI) AG, Basel, http://doi.org/10.3390/ijms24054920.

Winocur, G. et al. (2006), "Inhibition of neurogenesis interferes with hippocampus-dependent memory function", Hippocampus, Vol. 16/3, https://doi.org/10.1002/HIPO.20163.

Wong, G., Y. Goldshmit and A. M. Turnley. (2004), "Interferon-γ but not TNFα promotes neuronal differentiation and neurite outgrowth of murine adult neural stem cells", Experimental Neurology, Vol. 187/1, Elsevier, Amsterdam, https://doi.org/10.1016/j.expneurol.2004.01.009.

Wu, M. D. et al. (2012), "Adult murine hippocampal neurogenesis is inhibited by sustained IL-1β and not rescued by voluntary running", Brain, Behavior, and Immunity, Vol. 26/2, Elsevier Inc., Amsterdam, https://doi.org/10.1016/j.bbi.2011.09.012.

Xu, B. et al. (2019), "Oxidation Stress-Mediated MAPK Signaling Pathway Activation Induces Neuronal Loss in the CA1 and CA3 Regions of the Hippocampus of Mice Following Chronic Cold Exposure", Brain Sciences, Vol. 9/10, MDPI, Basel, https://doi.org/10.3390/brainsci9100273.

Yang, H. et al. (2020), "Cytoprotective role of humanin in lens epithelial cell oxidative stress-induced injury", Molecular medicine reports, Vol. 22/2, Spandidos Publishing Ltd, Athens, https://doi.org/10.3892/mmr.2020.11202.

Zanni, G. et al. (2015), "Lithium increases proliferation of hippocampal neural stem/progenitor cells and rescues irradiation-induced cell cycle arrest in vitro", Oncotarget, Vol. 6/35, https://doi.org/10.18632/oncotarget.5191.

Zhang, L. et al. (2017), "The inhibitory effect of minocycline on radiation-induced neuronal apoptosis via AMPKα1 signaling-mediated autophagy", Scientific Reports, Vol. 7/1, Springer Nature, Berlin, https://doi.org/10.1038/s41598-017-16693-8.

Zhang, Y. et al. (2017), "Kukoamine A Prevents Radiation-Induced Neuroinflammation and Preserves Hippocampal Neurogenesis in Rats by Inhibiting Activation of NF-κB and AP-1", Neurotoxicity Research, Vol. 31/2, https://doi.org/10.1007/s12640-016-9679-4.

Zhang, Q. et al. (2018), "The effect of brain-derived neurotrophic factor on radiation-induced neuron architecture impairment is associated with the NFATc4/3 pathway", Brain Research, Vol. 1681, Elsevier, Amsterdam, https://doi.org/10.1016/j.brainres.2017.12.032.

Zhao, Z.-Y. et al. (2013), "Edaravone Protects HT22 Neurons from H 2 O 2 -induced Apoptosis by Inhibiting the MAPK Signaling Pathway", CNS Neuroscience & Therapeutics, Vol. 19/3, John Wiley & Sons, Hoboken, https://doi.org/10.1111/cns.12044.

Zhao, D. et al. (2017), "Anti-Neuroinflammatory Effects of Fucoxanthin via Inhibition of Akt/NF-κB and MAPKs/AP-1 Pathways and Activation of PKA/CREB Pathway in Lipopolysaccharide-Activated BV-2 Microglial Cells", Neurochemical Research, Vol. 42/2, Springer Nature, Berlin, https://doi.org/10.1007/s11064-016-2123-6.

Zhou, K. et al. (2017), "Radiation induces progenitor cell death, microglia activation, and blood-brain barrier damage in the juvenile rat cerebellum", Scientific Reports, Vol. 7, Springer Nature, London, https://doi.org/10.1038/srep46181.

Zhu, Y. et al. (2012), "APOE genotype alters glial activation and loss of synaptic markers in mice", Glia, Vol. 60/4, John Wiley & Sons, Inc., Hoboken, https://doi.org/10.1002/glia.22289.

Zigman, S. et al. (1995), "Damage to cultured lens epithelial cells of squirrels and rabbits by UV-A (99.9%) plus UV-B (0.1%) radiation and alpha tocopherol protection", Molecular and cellular biochemistry, Vol. 143, Springer, London, https://doi.org/10.1007/BF00925924.

Zonis, S. et al. (2015), "Chronic intestinal inflammation alters hippocampal neurogenesis", Journal of Neuroinflammation, Vol. 12/1, Springer Nature, Berlin, https://doi.org/10.1186/s12974-015-0281-0.

Appendix 1

List of MIEs in this AOP

Event: 1686: Deposition of Energy

Short Name: Energy Deposition

AOPs Including This Key Event

AOP ID and Name	Event Type
Aop:272 - Deposition of energy leading to lung cancer	MolecularInitiatingEvent
Aop:432 - Deposition of Energy by Ionizing Radiation leading to Acute Myeloid Leukemia	MolecularInitiatingEvent
Aop:386 - Deposition of ionizing energy leading to population decline via inhibition of photosynthesis	MolecularInitiatingEvent
Aop:387 - Deposition of ionising energy leading to population decline via mitochondrial dysfunction	MolecularInitiatingEvent
Aop:388 - Deposition of ionising energy leading to population decline via programmed cell death	MolecularInitiatingEvent
Aop:435 - Deposition of ionising energy leads to population decline via pollen abnormal	MolecularInitiatingEvent
Aop:216 - Deposition of energy leading to population decline via DNA strand breaks and follicular atresia	MolecularInitiatingEvent
Aop:238 - Deposition of energy leading to population decline via DNA strand breaks and oocyte apoptosis	MolecularInitiatingEvent
Aop:311 - Deposition of energy leading to population decline via DNA oxidation and oocyte apoptosis	MolecularInitiatingEvent
Aop:299 - Deposition of energy leading to population decline via DNA oxidation and follicular atresia	MolecularInitiatingEvent
Aop:441 - Ionizing radiation-induced DNA damage leads to microcephaly via apoptosis and premature cell differentiation	MolecularInitiatingEvent
Aop:444 - Ionizing radiation leads to reduced reproduction in Eisenia fetida via reduced spermatogenesis and cocoon hatchability	MolecularInitiatingEvent
Aop:470 - Deposition of energy leads to vascular remodeling	MolecularInitiatingEvent
Aop:473 - Energy deposition from internalized Ra-226 decay lower oxygen binding capacity of hemocyanin	MolecularInitiatingEvent
Aop:478 - Deposition of energy leading to occurrence of cataracts	MolecularInitiatingEvent
Aop:482 - Deposition of energy leading to occurrence of bone loss	MolecularInitiatingEvent
Aop:483 - Deposition of Energy Leading to Learning and Memory Impairment	MolecularInitiatingEvent

Stressors

Name
Ionizing Radiation

Biological Context

Level of Biological Organization
Molecular

Evidence for Perturbation by Stressor

Overview for Molecular Initiating Event

It is well documented that ionizing radiation((eg. X-rays, gamma, photons, alpha, beta, neutrons, heavy ions) leads to energy deposition on the atoms and molecules of the substrate. Many studies, have demonstrated that the type of radiation and distance from source has an impact on the pattern of energy deposition (Alloni, et al. 2014). High linear energy transfer (LET) radiation has been associated with higher-energy deposits (Liamsuwan et al., 2014) that are more densely-packed and cause more complex effects within the particle track (Hada and Georgakilas, 2008; Okayasu, 2012ab; Lorat et al., 2015; Nikitaki et al., 2016) in comparison to low LET radiation. Parameters such as mean lineal energy, dose mean lineal energy, frequency mean specific energy and dose mean specific energy can impact track structure of the traversed energy into a medium (Friedland et al., 2017). The detection of energy deposition by ionizing radiation can be demonstrated with the use of fluorescent nuclear track detectors (FNTDs). FNTDs used in conjunction with fluorescent microscopy, are able to visualize radiation tracks produced by ionizing radiation (Niklas et al., 2013; Kodaira et al., 2015; Sawakuchi and Akselrod, 2016). In addition, these FNTD chips can quantify the LET of primary and secondary radiation tracks up to 0.47 keV/um (Sawakuchi and Akselrod, 2016). This co-visualization of the radiation tracks and the cell markers enable the mapping of the radiation trajectory to specific cellular compartments, and the identification of accrued damage (Niklas et al., 2013; Kodaira et al., 2015). There are no known chemical initiators or prototypes that can mimic the MIE.

Domain of Applicability

Taxonomic Applicability

Term	Scientific Term	Evidence	Links
human	Homo sapiens	Moderate	NCBI
rat	Rattus norvegicus	Moderate	NCBI
mouse	Mus musculus	Moderate	NCBI
nematode	Caenorhabditis elegans	High	NCBI
zebrafish	Danio rerio	High	NCBI
thale-cress	Arabidopsis thaliana	High	NCBI
Scotch pine	Pinus sylvestris	Moderate	NCBI
Daphnia magna	Daphnia magna	High	NCBI
Chlamydomonas reinhardtii	Chlamydomonas reinhardtii	Moderate	NCBI
common brandling worm	eisenia fetida	Moderate	NCBI
Lemna minor	Lemna minor	High	NCBI
Salmo salar	Salmo salar	Low	NCBI

Life Stage Applicability

Life Stage	Evidence
All life stages	High

Sex Applicability

Sex	Evidence
Unspecific	Low

Energy can be deposited into any substrate, both living and non-living; it is independent of age, taxa, sex, or life-stage.

Taxonomic applicability: This MIE is not taxonomically specific.

Life stage applicability: This MIE is not life stage specific.

Sex applicability: This MIE is not sex specific.

Key Event Description

Deposition of energy refers to events where energetic subatomic particles, nuclei, or electromagnetic radiation deposit energy in the media through which they transverse. The energy may either be sufficient (e.g. ionizing radiation) or insufficient (e.g. non-ionizing radiation) to ionize atoms or molecules (Beir et al.,1999).

Ionizing radiation can cause the ejection of electrons from atoms and molecules, thereby resulting in their ionization and the breakage of chemical bonds. The energy of these subatomic particles or electromagnetic waves mostly range from 124 KeV to 5.4 MeV and is dependent on the source and type of radiation (Zyla et al., 2020). To be ionizing the incident radiation must have sufficient energy to free electrons from atomic or molecular electron orbitals. The energy deposited can induce direct and indirect ionization events and this can be via internal (injections, inhalation, or absorption of radionuclides) or external exposure from radiation fields -- this also applies to non-ionizing radiation.

Direct ionization is the principal path where charged particles interact with biological structures such as DNA, proteins or membranes to cause biological damage. Photons, which are electromagnetic waves can also deposit energy to cause direct ionization. Ionization of water, which is a major constituent of tissues and organs, produces free radical and molecular species, which themselves can indirectly damage critical targets such as DNA (Beir et al., 1999; Balagamwala et al., 2013) or alter cellular processes. Given the fundamental nature of energy deposition by radioactive/unstable nuclei, nucleons or elementary particles in

material, this process is universal to all biological contexts.

The spatial structure of ionizing energy deposition along the resulting particle track is represented as linear energy transfer (LET) (Hall and Giaccia, 2018 UNSCEAR, 2020). High LET refers to energy mostly above 10 keV μm^{-1} which produces more complex, dense structural damage than low LET radiation (below 10 keV μm^{-1}). Low-LET particles produce sparse ionization events such as photons (X- and gamma rays), as well as high-energy protons. Low LET radiation travels farther into tissue but deposits smaller amounts of energy, whereas high LET radiation, which includes heavy ions, alpha particles and high-energy neutrons, does not travel as far but deposits larger amounts of energy into tissue at the same absorbed dose. The biological effect of the deposition of energy can be modulated by varying dose and dose rate of exposure, such as acute, chronic, or fractionated exposures (Hall and Giaccia, 2018).

Non-ionizing radiation is electromagnetic waves that does not have enough energy to break bonds and induce ion formation but it can cause molecules to excite and vibrate faster resulting in biological effects. Examples of non-ionizing radiation include radio waves (wavelength: 100 km-1m), microwaves (wavelength: 1m-1mm), infrared radiation (wavelength: 1mm- 1 um), visible light (wavelengths: 400-700 nm), and ultraviolet radiation of longer wavelengths such as UVB (wavelengths: 315-400nm) and UVA (wavelengths: 280-315 nm). UVC radiation (X-X nm) is, in contrast to UVB and UVA, considered to be a type of ionizing radiation.

How it is Measured or Detected

Radiation type	Assay Name	References	Description	OECD Approved Assay
Ionizing radiation	Monte Carlo Simulations (Geant4)	Douglass et al., 2013; Douglass et al. 2012; Zyla et al., 2020	Monte Carlo simulations are based on a computational algorithm that mathematically models the deposition of energy into materials.	No
Ionizing radiation	Fluorescent Nuclear Track Detector (FNTD)	Sawakuchi, 2016; Niklas, 2013; Koaira & Konishi, 2015	FNTDs are biocompatible chips with crystals of aluminium oxide doped with carbon and magnesium; used in conjuction with fluorescent microscopy, these FNTDs allow for the visualization and the linear energy transfer (LET) quantification of tracks produced by the deposition of energy into a material.	No
Ionizing radiation	Tissue equivalent proportional counter (TEPC)	Straume et al, 2015	Measure the LET spectrum and calculate the dose equivalent.	No
Ionizing radiation	alanine dosimeters/NanoDots	Lind et al. 2019; Xie et al., 2022		No
Non-ionizing radiation	UV meters or radiameters	Xie et at., 2020	UVA/UVB (irradiance intensity), UV dosimeters (accumulated irradiance over time), Spectrophoto meter (absorption of UV by a substance or material)	No

References

Balagamwala, E. H. et al. (2013), “Introduction to radiotherapy and standard teletherapy techniques”, *Dev Ophthalmol,* Vol. 52, Karger, Basel, https://doi.org/10.1159/000351045

Beir, V. et al. (1999), “The Mechanistic Basis of Radon-Induced Lung Cancer”, in *Health Risks of Exposure to Radon: BEIR VI*, National Academy Press, Washington, D.C., https://doi.org/10.17226/5499

Douglass, M. et al. (2013), “Monte Carlo investigation of the increased radiation deposition due to gold nanoparticles using kilovoltage and megavoltage photons in a 3D randomized cell model”, *Medical Physics*, Vol. 40/7, American Institute of Physics, College Park, https://doi.org/10.1118/1.4808150

Douglass, M. et al. (2012), “Development of a randomized 3D cell model for Monte Carlo microdosimetry simulations.”, *Medical Physics*, Vol. 39/6, American Institute of Physics, College Park, https://doi.org/10.1118/1.4719963

Hall, E. J. and Giaccia, A.J. (2018), *Radiobiology for the Radiologist*, 8th edition, Wolters Kluwer, Philadelphia.

Kodaira, S. and Konishi, T. (2015), “Co-visualization of DNA damage and ion traversals in live mammalian cells using a fluorescent nuclear track detector.”, *Journal of Radiation Research*, Vol. 56/2, Oxford University Press, Oxford, https://doi.org/10.1093/jrr/rru091

Lind, O.C., D.H. Oughton and Salbu B. (2019), "The NMBU FIGARO low dose irradiation facility", *International Journal of Radiation Biology*, Vol. 95/1, Taylor & Francis, London, https://doi.org/10.1080/09553002.2018.1516906.

Sawakuchi, G.O. and Akselrod, M.S. (2016), “Nanoscale measurements of proton tracks using fluorescent nuclear track detectors.”, *Medical Physics*, Vol. 43/5, American Institute of Physics, College Park, https://doi.org/10.1118/1.4947128

Straume, T. et al. (2015), “Compact Tissue-equivalent Proportional Counter for Deep Space Human Missions.”, *Health physics,* Vol. 109/4, Lippincott Williams & Wilkins, Philadelphia, https://doi.org/10.1097/HP.0000000000000334

Niklas, M. et al. (2013), “Engineering cell-fluorescent ion track hybrid detectors.”, *Radiation Oncology*, Vol. 8/104, BioMed Central, London, https://doi.org/10.1186/1748-717X-8-141

UNSCEAR (2020), *Sources, effects and risks of ionizing radiation*, United Nations.

Xie, Li. et al. (2022), "Ultraviolet B Modulates Gamma Radiation-Induced Stress Responses in Lemna Minor at Multiple Levels of Biological Organisation", *SSRN*, Elsevier, Amsterdam, http://dx.doi.org/10.2139/ssrn.4081705 .

Zyla, P.A. et al. (2020), *Review of particle physics: Progress of Theoretical and Experimental Physics*, 2020 Edition, Oxford University Press, Oxford.

List of Key Events in the AOP

Event: 1392: Oxidative Stress

Short Name: Oxidative Stress

Key Event Component

Process	Object	Action
oxidative stress		increased

AOPs Including This Key Event

AOP ID and Name	Event Type
Aop:220 - Cyp2E1 Activation Leading to Liver Cancer	KeyEvent
Aop:17 - Binding of electrophilic chemicals to SH(thiol)-group of proteins and /or to seleno-proteins involved in protection against oxidative stress during brain development leads to impairment of learning and memory	KeyEvent
Aop:284 - Binding of electrophilic chemicals to SH(thiol)-group of proteins and /or to seleno-proteins involved in protection against oxidative stress leads to chronic kidney disease	KeyEvent
Aop:377 - Dysregulated prolonged Toll Like Receptor 9 (TLR9) activation leading to Multi Organ Failure involving Acute Respiratory Distress Syndrome (ARDS)	KeyEvent
Aop:411 - Oxidative stress Leading to Decreased Lung Function	MolecularInitiatingEvent
Aop:424 - Oxidative stress Leading to Decreased Lung Function via CFTR dysfunction	MolecularInitiatingEvent
Aop:425 - Oxidative Stress Leading to Decreased Lung Function via Decreased FOXJ1	MolecularInitiatingEvent
Aop:429 - A cholesterol/glucose dysmetabolism initiated Tau-driven AOP toward memory loss (AO) in sporadic Alzheimer's Disease with plausible MIE's plug-ins for environmental neurotoxicants	KeyEvent
Aop:437 - Inhibition of mitochondrial electron transport chain (ETC) complexes leading to kidney toxicity	KeyEvent
Aop:452 - Adverse outcome pathway of PM-induced respiratory toxicity	KeyEvent
Aop:464 - Calcium overload in dopaminergic neurons of the substantia nigra leading to parkinsonian motor deficits	KeyEvent
Aop:470 - Deposition of energy leads to vascular remodeling	KeyEvent
Aop:478 - Deposition of energy leading to occurrence of cataracts	KeyEvent
Aop:479 - Mitochondrial complexes inhibition leading to heart failure via increased myocardial oxidative stress	KeyEvent
Aop:481 - AOPs of amorphous silica nanoparticles: ROS-mediated oxidative stress increased respiratory dysfunction and diseases.	KeyEvent
Aop:482 - Deposition of energy leading to occurrence of bone loss	KeyEvent
Aop:483 - Deposition of Energy Leading to Learning and Memory Impairment	KeyEvent

Stressors

Name
Acetaminophen
Chloroform
furan
Platinum
Aluminum
Cadmium
Mercury
Uranium
Arsenic
Silver
Manganese
Nickel
Zinc
nanoparticles

Biological Context

Level of Biological Organization
Molecular

Evidence for Perturbation by Stressor

Platinum

Kruidering et al. (1997) examined the effect of platinum on pig kidneys and found that it was able to induce significant dose-dependant ROS formation within 20 minutes of treatment administration.

Aluminum

In a study of the effects of aluminum treatment on rat kidneys, Al Dera (2016) found that renal GSH, SOD, and GPx levels were significantly lower in the treated groups, while lipid peroxidation levels were significantly increased.

Cadmium

Belyaeva et al. (2012) investigated the effect of cadmium treatment on human kidney cells. They found that cadmium was the most toxic when the sample was treated with 500 µM for 3 hours (Belyaeva et al., 2012). As this study also looked at mercury, it is worth noting that mercury was more toxic than cadmium in both 30-minute and 3-hour exposures at low concentrations (10-100 µM) (Belyaeva et al., 2012).

Wang et al. (2009) conducted a study evaluating the effects of cadmium treatment on rats and found that the treated group showed a significant increase in lipid peroxidation. They also assessed the effects of lead in this study, and found that cadmium can achieve a very similar level of lipid peroxidation at a much lower concentration than lead can, implying that cadmium is a much more toxic metal to the kidney mitochondria than lead is (Wang et al., 2009). They also found that when lead and cadmium were applied together they had an additive effect in increasing lipid peroxidation content in the renal cortex of rats (Wang et al., 2009).

Jozefczak et al. (2015) treated *Arabidopsis thaliana* wildtype, *cad2-1* mutant, and *vtc1-1* mutant plants with cadmium to determine the effects of heavy metal exposure to plant mitochondria in the roots and leaves. They found that total GSH/GSG ratios were significantly increased after cadmium exposure in the leaves of all sample varieties and that GSH content was most significantly decreased for the wildtype plant roots (Jozefczak et al., 2015).

Andjelkovic et al. (2019) also found that renal lipid peroxidation was significantly increased in rats treated with 30 mg/kg of cadmium.

Mercury

Belyaeva et al. (2012) conducted a study which looked at the effects of mercury on human kidney cells, they found that mercury was the most toxic when the sample was treated with 100 µM for 30 minutes.

Buelna-Chontal et al. (2017) investigated the effects of mercury on rat kidneys and found that treated rats had higher lipid peroxidation content and reduced cytochrome c content in their kidneys.

Uranium

In Shaki et al.'s article (2012), they found rat kidney mitochondria treated with uranyl acetate caused increased formation of ROS, increased lipid peroxidation, and decreased GSH content when exposed to 100 µM or more for an hour.

Hao et al. (2014), found that human kidney proximal tubular cells (HK-2 cells) treated with uranyl nitrate for 24 hours with 500 µM showed a 3.5 times increase in ROS production compared to the control. They also found that GSH content was decreased by 50% of the control when the cells were treated with uranyl nitrate (Hao et al., 2014).

Arsenic

Bhadauria and Flora (2007) studied the effects of arsenic treatment on rat kidneys. They found that lipid peroxidation levels were increased by 1.5 times and the GSH/GSSG ratio was decreased significantly (Bhadauria and Flora, 2007).

Kharroubi et al. (2014) also investigated the effect of arsenic treatment on rat kidneys and found that lipid peroxidation was significantly increased, while GSH content was significantly decreased.

In their study of the effects of arsenic treatment on rat kidneys, Turk et al. (2019) found that lipid peroxidation was significantly increased while GSH and GPx renal content were decreased.

Silver

Miyayama et al. (2013) investigated the effects of silver treatment on human bronchial epithelial cells and found that intracellular ROS generation was increased significantly in a dose-dependant manner when treated with 0.01 to 1.0 µM of silver nitrate.

Manganese

Chtourou et al. (2012) investigated the effects of manganese treatment on rat kidneys. They found that manganese treatment caused significant increases in ROS production, lipid peroxidation, urinary H_2O_2 levels, and PCO production. They also found that intracellular GSH content was depleted in the treated group (Chtourou et al., 2012).

Nickel

Tyagi et al. (2011) conducted a study of the effects of nickel treatment on rat kidneys. They found that the treated rats showed a significant increase in kidney lipid peroxidation and a significant decrease in GSH content in the kidney tissue (Tyagi et al., 2011).

Zinc

Yeh et al. (2011) investigated the effects of zinc treatment on rat kidneys and found that treatment with 150 µM or more for 2 weeks or more caused a time- and dose-dependant increase in lipid peroxidation. They also found that renal GSH content was decreased in the rats treated with 150 µM or more for 8 weeks (Yeh et al., 2011).

It should be noted that Hao et al. (2014) found that rat kidneys exposed to lower concentrations of zinc (such as 100 µM) for short time periods (such as 1 day), showed a protective effect against toxicity induced by other heavy metals, including uranium. Soussi, Gargouri, and El Feki (2018) also found that pre-treatment with a low concentration of zinc (10 mg/kg treatment for 15 days) protected the renal cells of rats were from changes in varying oxidative stress markers, such as lipid peroxidation, protein carbonyl, and GPx levels.

nanoparticles

Huerta-García et al. (2014) conducted a study of the effects of titanium nanoparticles on human and rat brain cells. They found that both the human and rat cells showed time-dependant increases in ROS when treated with titanium nanoparticles for 2 to 6 hours (Huerta-García et al., 2014). They also found elevated lipid peroxidation that was induced by the titanium nanoparticle treatment of human and rat cell lines in a time-dependant manner (Huerta-García et al., 2014).

Liu et al. (2010) also investigated the effects of titanium nanoparticles, however they conducted their trials on rat kidney cells. They found that ROS production was significantly increased in a dose dependant manner when treated with 10 to 100 µg/mL of titanium nanoparticles (Liu et al., 2010).

Pan et al. (2009) treated human cervix carcinoma cells with gold nanoparticles (Au1.4MS) and found that intracellular ROS content

in the treated cells increased in a time-dependant manner when treated with 100 µM for 6 to 48 hours. They also compared the treatment with Au1.4MS gold nanoparticles to treatment with Au15MS treatment, which are another size of gold nanoparticle (Pan et al., 2009). The Au15MS nanoparticles were much less toxic than the Au1.4MS gold nanoparticles, even when the Au15MS nanoparticles were applied at a concentration of 1000 µM (Pan et al., 2009). When investigating further markers of oxidative stress, Pan et al. (2009) found that GSH content was greatly decreased in cells treated with gold nanoparticles.

Ferreira et al. (2015) also studied the effects of gold nanoparticles. They exposed rat kidneys to GNPs-10 (10 nm particles) and GNPs-30 (30 nm particles), and found that lipid peroxidation and protein carbonyl content in the rat kidneys treated with GNPs-30 and GNPs-10, respectively, were significantly elevated.

Domain of Applicability

Taxonomic Applicability

Term	Scientific Term	Evidence	Links
rodents	rodents	High	NCBI
Homo sapiens	Homo sapiens	High	NCBI

Life Stage Applicability

Life Stage	Evidence
All life stages	High

Sex Applicability

Sex	Evidence
Mixed	High

Taxonomic applicability: Occurrence of oxidative stress is not species specific.

Life stage applicability: Occurrence of oxidative stress is not life stage specific.

Sex applicability: Occurrence of oxidative stress is not sex specific.

Evidence for perturbation by prototypic stressor: There is evidence of the increase of oxidative stress following perturbation from a variety of stressors including exposure to ionizing radiation and altered gravity (Bai et al., 2020; Ungvari et al., 2013; Zhang et al., 2009).

Key Event Description

Oxidative stress is defined as an imbalance in the production of reactive oxygen species (ROS) and antioxidant defenses. High levels of oxidizing free radicals can be very damaging to cells and molecules within the cell. As a result, the cell has important defense mechanisms to protect itself from ROS. For example, Nrf2 is a transcription factor and master regulator of the oxidative stress response. During periods of oxidative stress, Nrf2-dependent changes in gene expression are important in regaining cellular homeostasis (Nguyen, et al. 2009) and can be used as indicators of the presence of oxidative stress in the cell.

In addition to the directly damaging actions of ROS, cellular oxidative stress also changes cellular activities on a molecular level. Redox sensitive proteins have altered physiology in the presence and absence of ROS, which is caused by the oxidation of sulfhydryls to disulfides (2SH àSS) on neighboring amino acids (Antelmann and Helmann 2011). Importantly Keap1, the negative regulator of Nrf2, is regulated in this manner (Itoh, et al. 2010).

ROS also undermine the mitochondrial defense system from oxidative damage. The antioxidant systems consist of superoxide dismutase, catalase, glutathione peroxidase and glutathione reductase, as well as antioxidants such as α-tocopherol and ubiquinol, or antioxidant vitamins and minerals including vitamin E, C, carotene, lutein, zeaxanthin, selenium, and zinc (Fletcher, 2010). The enzymes, vitamins and minerals catalyze the conversion of ROS to non-toxic molecules such as water and O_2. However, these antioxidant systems are not perfect and endogenous metabolic processes and/or exogenous oxidative influences can trigger cumulative oxidative injuries to the mitochondria, causing a decline in their functionality and efficiency, which further promotes cellular oxidative stress (Balasubramanian, 2000; Ganea & Harding, 2006; Guo et al., 2013; Karimi et al., 2017).

However, an emerging viewpoint suggests that ROS-induced modifications may not be as detrimental as previously thought, but rather contribute to signaling processes (Foyer et al., 2017).

Protection against oxidative stress is relevant for all tissues and organs, although some tissues may be more susceptible. For example, the brain possesses several key physiological features, such as high O2 utilization, high polyunsaturated fatty acids content, presence of autooxidable neurotransmitters, and low antioxidant defenses as compared to other organs, that make it highly susceptible to oxidative stress (Halliwell, 2006; Emerit and al., 2004; Frauenberger et al., 2016).

Sources of ROS Production

Direct Sources: Direct sources involve the deposition of energy onto water molecules, breaking them into active radical species. When ionizing radiation hits water, it breaks it into hydrogen (H*) and hydroxyl (OH*) radicals by destroying its bonds. The hydrogen will create hydroxyperoxyl free radicals (HO_2*) if oxygen is available, which can then react with another of itself to form hydrogen peroxide (H_2O_2) and more O_2 (Elgazzar and Kazem, 2015). Antioxidant mechanisms are also affected by radiation, with catalase (CAT) and peroxidase (POD) levels rising as a result of exposure (Seen et al. 2018; Ahmad et al. 2021).

Indirect Sources: An indirect source of ROS is the mitochondria, which is one of the primary producers in eukaryotic cells (Powers et al., 2008). As much as 2% of the electrons that should be going through the electron transport chain in the mitochondria escape, allowing them an opportunity to interact with surrounding structures. Electron-oxygen reactions result in free radical production, including the formation of hydrogen peroxide (H_2O_2) (Zhao et al., 2019). The electron transport chain, which also creates ROS, is activated by free adenosine diphosphate (ADP), O_2, and inorganic phosphate (P_i) (Hargreaves et al. 2020; Raimondi et al. 2020; Vargas-Mendoza et al. 2021). The first and third complexes of the transport chain are the most relevant to mammalian ROS production (Raimondi et al., 2020). The mitochondria have its own set of DNA and it is a prime target of oxidative damage (Guo et al., 2013). ROS are also produced through nicotinamide adenine dinucleotide phosphate oxidase (NOX) stimulation, an event commenced by angiotensin II, a product/effector of the renin-angiotensin system (Nguyen Dinh Cat et al. 2013; Forrester et al. 2018). Other ROS producers include xanthine oxidase, immune cells (macrophage, neutrophils, monocytes, and eosinophils), phospholipase A_2 (PLA_2), monoamine oxidase (MAO), and carbon-based nanomaterials (Powers et al. 2008; Jacobsen et al. 2008; Vargas-Mendoza et al. 2021).

How it is Measured or Detected

Oxidative Stress. Direct measurement of ROS is difficult because ROS are unstable. The presence of ROS can be assayed indirectly by measurement of cellular antioxidants, or by ROS-dependent cellular damage. Listed below are common methods for detecting the KE, however there may be other comparable methods that are not listed

- Detection of ROS by chemiluminescence (https://www.sciencedirect.com/science/article/abs/pii/S0165993606001683)
- Detection of ROS by chemiluminescence is also described in OECD TG 495 to assess phototoxic potential.
- Glutathione (GSH) depletion. GSH can be measured by assaying the ratio of reduced to oxidized glutathione (GSH:GSSG) using a commercially available kit (e.g., http://www.abcam.com/gshgssg-ratio-detection-assay-kit-fluorometric-green-ab138881.html).
- TBARS. Oxidative damage to lipids can be measured by assaying for lipid peroxidation using TBARS (thiobarbituric acid reactive substances) using a commercially available kit.
- 8-oxo-dG. Oxidative damage to nucleic acids can be assayed by measuring 8-oxo-dG adducts (for which there are a number of ELISA based commercially available kits),or HPLC, described in Chepelev et al. (Chepelev, et al. 2015).

Molecular Biology: Nrf2. Nrf2's transcriptional activity is controlled post-translationally by oxidation of Keap1. Assay for Nrf2 activity include:

- Immunohistochemistry for increases in Nrf2 protein levels and translocation into the nucleus
- Western blot for increased Nrf2 protein levels
- Western blot of cytoplasmic and nuclear fractions to observe translocation of Nrf2 protein from the cytoplasm to the nucleus
- qPCR of Nrf2 target genes (e.g., Nqo1, Hmox-1, Gcl, Gst, Prx, TrxR, Srxn), or by commercially available pathway-based qPCR array (e.g., oxidative stress array from SABiosciences)
- Whole transcriptome profiling by microarray or RNA-seq followed by pathway analysis (in IPA, DAVID, metacore, etc.) for enrichment of the Nrf2 oxidative stress response pathway (e.g., Jackson et al. 2014)
- OECD TG422D describes an ARE-Nrf2 Luciferase test method
- In general, there are a variety of commercially available colorimetric or fluorescent kits for detecting Nrf2 activation

Assay Type & Measured Content	Description	Dose Range Studied	Assay Characteristics (Length / Ease of use/Accuracy)
ROS Formation in the Mitochondria assay (Shaki et al., 2012)	"The mitochondrial ROS measurement was performed flow cytometry using DCFH-DA. Briefly, isolated kidney mitochondria were incubated with UA (0, 50, 100 and 200 µM) in respiration buffer containing (0.32 mM sucrose, 10 mM Tris, 20 mM Mops, 50 µM EGTA, 0.5 mM MgCl2, 0.1 mM KH2PO4 and 5 mM sodium succinate) [32]. In the interval times of 5, 30 and 60 min following the UA addition, a sample was taken and DCFH-DA was added (final concentration, 10 µM) to mitochondria and was then incubated for 10 min. Uranyl acetate-induced ROS generation in isolated kidney mitochondria were determined through the flow cytometry (Partec, Deutschland) equipped with a 488-nm argon ion laser and supplied with the Flomax software and the signals were obtained using a 530-nm bandpass filter (FL-1 channel). Each determination is based on the mean fluorescence intensity of 15,000 counts."	0, 50, 100 and 200 µM of Uranyl Acetate	Long/ Easy High accuracy
Mitochondrial Antioxidant	"GSH content was determined using DTNB as the indicator and spectrophotometer method for the isolated mitochondria. The mitochondrial		

Content Assay Measuring GSH content (Shaki et al., 2012)	fractions (0.5 mg protein/ml) were incubated with various concentrations of uranyl acetate for 1 h at 30 °C and then 0.1 ml of mitochondrial fractions was added into 0.1 mol/l of phosphate buffers and 0.04% DTNB in a total volume of 3.0 ml (pH 7.4). The developed yellow color was read at 412 nm on a spectrophotometer (UV-1601 PC, Shimadzu, Japan). GSH content was expressed as µg/mg protein."	0, 50, 100, or 200 μM Uranyl Acetate	
H_2O_2 Production Assay Measuring H_2O_2 Production in isolated mitochondria (Heyno et al., 2008)	"Effect of $CdCl_2$ and antimycin A (AA) on H_2O_2 production in isolated mitochondria from potato. H_2O_2 production was measured as scopoletin oxidation. Mitochondria were incubated for 30 min in the measuring buffer (see the Materials and Methods) containing 0.5 mM succinate as an electron donor and 0.2 µM mesoxalonitrile 3-chlorophenylhydrazone (CCCP) as an uncoupler, 10 U horseradish peroxidase and 5 µM scopoletin." (	0, 10, 30 μM Cd^{2+} 2 μM antimycin A	
Flow Cytometry ROS & Cell Viability (Kruiderig et al., 1997)	"For determination of ROS, samples taken at the indicated time points were directly transferred to FACScan tubes. Dih123 (10 mM, final concentration) was added and cells were incubated at 37°C in a humidified atmosphere (95% air/5% CO2) for 10 min. At *t* 5 9, propidium iodide (10 mM, final concentration) was added, and cells were analyzed by flow cytometry at 60 ml/min. Nonfluorescent Dih123 is cleaved by ROS to fluorescent R123 and detected by the FL1 detector as described above for Dc (Van de Water 1995)"		Strong/easy medium
DCFH-DA Assay Detection of hydrogen peroxide production (Yuan et al., 2016)	Intracellular ROS production was measured using DCFH-DA as a probe. Hydrogen peroxide oxidizes DCFH to DCF. The probe is hydrolyzed intracellularly to DCFH carboxylate anion. No direct reaction with H_2O_2 to form fluorescent production.	0-400 µM	Long/ Easy High accuracy
H2-DCF-DA Assay Detection of superoxide production (Thiebault et al., 2007)	This dye is a stable nonpolar compound which diffuses readily into the cells and yields H2-DCF. Intracellular OH or ONOO- react with H2-DCF when cells contain peroxides, to form the highly fluorescent compound DCF, which effluxes the cell. Fluorescence intensity of DCF is measured using a fluorescence spectrophotometer.	0–600 µM	Long/ Easy High accuracy
CM-H2DCFDA Assay	**Come back and explain the flow cytometry determination of oxidative stress from Pan et al. (2009)**		

Direct Methods of Measurement

Method of Measurement	References	Description	OECD-Approved Assay
Chemiluminescence	(Lu, C. et al., 2006; Griendling, K. K., et al., 2016)	ROS can induce electron transitions in molecules, leading to electronically excited products. When the electrons transition back to ground state, chemiluminescence is emitted and can be measured. Reagents such as uminol and lucigenin are commonly used to amplify the signal.	No
Spectrophotometry	(Griendling, K. K., et al., 2016)	NO has a short half-life. However, if it has been reduced to nitrite (NO2-), stable azocompounds can be formed via the Griess Reaction, and further measured by spectrophotometry.	No
Direct or Spin Trapping-Based Electron Paramagnetic Resonance	(Griendling, K. K., et al.,	The unpaired electrons (free radicals) found in ROS can be detected with	No

(EPR) Spectroscopy	2016)	EPR, and is known as electron paramagnetic resonance. A variety of spin traps can be used.	
Nitroblue Tetrazolium Assay	(Griendling, K. K., et al., 2016)	The Nitroblue Tetrazolium assay is used to measure $O_2^{\bullet -}$ levels. $O_2^{\bullet -}$ reduces nitroblue tetrazolium (a yellow dye) to formazan (a blue dye), and can be measured at 620 nm.	No
Fluorescence analysis of dihydroethidium (DHE) or Hydrocyans	(Griendling, K. K., et al., 2016)	Fluorescence analysis of DHE is used to measure $O_2^{\bullet -}$ levels. $O_2^{\bullet -}$ is reduced to O2 as DHE is oxidized to 2-hydroxyethidium, and this reaction can be measured by fluorescence. Similarly, hydrocyans can be oxidized by any ROS, and measured via fluorescence.	No
Amplex Red Assay	(Griendling, K. K., et al., 2016)	Fluorescence analysis to measure extramitochondrial or extracellular H_2O_2 levels. In the presence of horseradish peroxidase and H_2O_2, Amplex Red is oxidized to resorufin, a fluorescent molecule measurable by plate reader.	No
Dichlorodihydrofluorescein Diacetate (DCFH-DA)	(Griendling, K. K., et al., 2016)	An indirect fluorescence analysis to measure intracellular H_2O_2 levels. H_2O_2 interacts with peroxidase or heme proteins, which further react with DCFH, oxidizing it to dichlorofluorescein (DCF), a fluorescent product.	No
HyPer Probe	(Griendling, K. K., et al., 2016)	Fluorescent measurement of intracellular H_2O_2 levels. HyPer is a genetically encoded fluorescent sensor that can be used for *in vivo* and *in situ* imaging.	No
Cytochrome c Reduction Assay	(Griendling, K. K., et al., 2016)	The cytochrome c reduction assay is used to measure $O_2^{\bullet -}$ levels. $O_2^{\bullet -}$ is reduced to O2 as ferricytochrome c is oxidized to ferrocytochrome c, and this reaction can be measured by an absorbance increase at 550 nm.	No
Proton-electron double-resonance imagine (PEDRI)	(Griendling, K. K., et al., 2016)	The redox state of tissue is detected through nuclear magnetic resonance/magnetic resonance imaging, with the use of a nitroxide spin probe or biradical molecule.	No
Glutathione (GSH) depletion	(Biesemann, N. et al., 2018)	A downstream target of the Nrf2 pathway is involved in GSH synthesis. As an indication of oxidation status, GSH can be measured by assaying the ratio of reduced to oxidized glutathione (GSH:GSSG) using a commercially available kit (e.g., http://www.abcam.com/gshgssg-ratio-detection-assay-kit-fluorometric-green-ab138881.html).	No
Thiobarbituric acid reactive substances (TBARS)	(Griendling, K. K., et al., 2016)	Oxidative damage to lipids can be measured by assaying for lipid peroxidation with TBARS using a commercially available kit.	No
Protein oxidation (carbonylation)	(Azimzadeh	Can be determined with enzyme	No

Protein oxidation (carbonylation)	(Azimzadeh et al., 2017; Azimzadeh etal., 2015; Ping et al., 2020)	Can be determined with enzyme-linked immunosorbent assay (ELISA) or a commercial assay kit. Protein oxidation can indicate the level of oxidative stress.	No
Seahorse XFp Analyzer	Leung et al. 2018	The Seahorse XFp Analyzer provides information on mitochondrial function, oxidative stress, and metabolic dysfunction of viable cells by measuring respiration (oxygen consumption rate; OCR) and extracellular pH (extracellular acidification rate; ECAR).	No

Molecular Biology: Nrf2. Nrf2's transcriptional activity is controlled post-translationally by oxidation of Keap1. Assays for Nrf2 activity include:

Method of Measurement	References	Description	OECD-Approved Assay
Immunohistochemistry	(Amsen, D., de Visser, K. E., and Town, T., 2009)	Immunohistochemistry for increases in Nrf2 protein levels and translocation into the nucleus	No
Quantitative polymerase chain reaction (qPCR)	(Forlenza et al., 2012)	qPCR of Nrf2 target genes (e.g., Nqo1, Hmox-1, Gcl, Gst, Prx, TrxR, Srxn), or by commercially available pathway-based qPCR array (e.g., oxidative stress array from SABiosciences)	No
Whole transcriptome profiling via microarray or via RNA-seq followed by a pathway analysis	(Jackson, A. F. et al., 2014)	Whole transcriptome profiling by microarray or RNA-seq followed by pathway analysis (in IPA, DAVID, metacore, etc.) for enrichment of the Nrf2 oxidative stress response pathway	No

References

Ahmad, S. et al. (2021), "60Co-γ Radiation Alters Developmental Stages of Zeugodacus cucurbitae (Diptera: Tephritidae) Through Apoptosis Pathways Gene Expression", *Journal Insect Science,* Vol. 21/5, Oxford University Press, Oxford, https://doi.org/10.1093/jisesa/ieab080

Antelmann, H. and J. D. Helmann (2011), "Thiol-based redox switches and gene regulation.", *Antioxidants & Redox Signaling*, Vol. 14/6, Mary Ann Leibert Inc., Larchmont, https://doi.org/10.1089/ars.2010.3400

Amsen, D., de Visser, K. E., and Town, T. (2009), "Approaches to determine expression of inflammatory cytokines", in *Inflammation and Cancer*, Humana Press, Totowa, https://doi.org/10.1007/978-1-59745-447-6_5

Azimzadeh, O. et al. (2015), "Integrative Proteomics and Targeted Transcriptomics Analyses in Cardiac Endothelial Cells Unravel Mechanisms of Long-Term Radiation-Induced Vascular Dysfunction", *Journal of Proteome Research*, Vol. 14/2, American Chemical Society, Washington, https://doi.org/10.1021/pr501141b

Azimzadeh, O. et al. (2017), "Proteome analysis of irradiated endothelial cells reveals persistent alteration in protein degradation and the RhoGDI and NO signalling pathways", *International Journal of Radiation Biology*, Vol. 93/9, Informa, London, https://doi.org/10.1080/09553002.2017.1339332

Azzam, E. I. et al. (2012), "Ionizing radiation-induced metabolic oxidative stress and prolonged cell injury", Cancer Letters, Vol. 327/1-2, Elsevier, Ireland, https://doi.org/10.1016/j.canlet.2011.12.012

Bai, J. et al. (2020), "Irradiation-induced senescence of bone marrow mesenchymal stem cells aggravates osteogenic differentiation dysfunction via paracrine signaling", *American Journal of Physiology - Cell Physiology*, Vol. 318/5, American Physiological Society, Rockville, https://doi.org/10.1152/ajpcell.00520.2019.

Balasubramanian, D (2000), “Ultraviolet radiation and cataract”, *Journal of ocular pharmacology and therapeutics*, Vol. 16/3, Mary Ann Liebert Inc., Larchmont, https://doi.org/10.1089/jop.2000.16.285.

Biesemann, N. et al., (2018), “High Throughput Screening of Mitochondrial Bioenergetics in Human Differentiated Myotubes Identifies Novel Enhancers of Muscle Performance in Aged Mice”, *Scientific Reports,* Vol. 8/1, Nature Portfolio, London, https://doi.org/10.1038/s41598-018-27614-8.

Elgazzar, A. and N. Kazem. (2015), “Chapter 23: Biological effects of ionizing radiation” in *The Pathophysiologic Basis of Nuclear Medicine*, Springer, New York, pp. 540-548

Fletcher, A. E (2010), “Free radicals, antioxidants and eye diseases: evidence from epidemiological studies on cataract and age-related macular degeneration”, *Ophthalmic Research*, Vol. 44, Karger International, Basel, https://doi.org/10.1159/000316476.

Forlenza, M. et al. (2012), “The use of real-time quantitative PCR for the analysis of cytokine mRNA levels” in *Cytokine Protocols,* Springer, New York, https://doi.org/10.1007/978-1-61779-439-1_2

Forrester, S.J. et al. (2018), “Angiotensin II Signal Transduction: An Update on Mechanisms of Physiology and Pathophysiology”, *Physiological Reviews,* Vol. 98/3**,** American Physiological Society, Rockville, https://doi.org/10.1152/physrev.00038.201

Foyer, C. H., A. V. Ruban, and G. Noctor (2017), “Viewing oxidative stress through the lens of oxidative signalling rather than damage”, Biochemical Journal, Vol. 474/6, Portland Press, England, https://doi.org/10.1042/BCJ20160814

Ganea, E. and J. J. Harding (2006), “Glutathione-related enzymes and the eye”, *Current eye research*, Vol. 31/1, Informa, London, https://doi.org/10.1080/02713680500477347.

Griendling, K. K. et al. (2016), “Measurement of reactive oxygen species, reactive nitrogen species, and redox-dependent signaling in the cardiovascular system: a scientific statement from the American Heart Association”, *Circulation research*, Vol. 119/5, Lippincott Williams & Wilkins, Philadelphia, https://doi.org/10.1161/RES.0000000000000110

Guo, C. et al. (2013), “Oxidative stress, mitochondrial damage and neurodegenerative diseases”, *Neural regeneration research*, Vol. 8/21, Publishing House of Neural Regeneration Research, China, https://doi.org/10.3969/j.issn.1673-5374.2013.21.009

Hargreaves, M., and L. L. Spriet (2020), “Skeletal muscle energy metabolism during exercise.”, *Nature Metabolism*, Vol. 2, Nature Portfolio, London, https://doi.org/10.1038/s42255-020-0251-4

Hladik, D. and S. Tapio (2016), “Effects of ionizing radiation on the mammalian brain”, *Mutation Research/Reviews in Mutation Research*, Vol. 770, Elsevier, Amsterdam, https://doi.org/10.1016/j.mrrev.2016.08.003

Itoh, K., J. Mimura and M. Yamamoto (2010), “Discovery of the negative regulator of Nrf2, Keap1: a historical overview”, *Antioxidants & Redox Signaling*, Vol. 13/11, Mary Ann Leibert Inc., Larchmont, https://doi.org/10.1089/ars.2010.3222

Jackson, A.F. et al. (2014), “Case study on the utility of hepatic global gene expression profiling in the risk assessment of the carcinogen furan.”, *Toxicology and Applied Pharmacology,* Vol. 274/11, Elsevier, Amsterdam, https://doi.org/10.1016/j.taap.2013.10.019

Jacobsen, N.R. et al. (2008), “Genotoxicity, cytotoxicity, and reactive oxygen species induced by single-walled carbon nanotubes and C_{60} fullerenes in the FE1-Muta^{TM} Mouse lung epithelial cells”, *Environmental and Molecular Mutagenesis,* Vol. 49/6, John Wiley & Sons, Inc., Hoboken, https://doi.org/10.1002/em.20406

Karimi, N. et al. (2017), “Radioprotective effect of hesperidin on reducing oxidative stress in the lens tissue of rats”, *International Journal of Pharmaceutical Investigation*, Vol. 7/3, Phcog Net, Bengaluru, https://doi.org/10.4103/jphi.JPHI_60_17.

Leung, D.T.H., and Chu, S. (2018), “Measurement of Oxidative Stress: Mitochondrial Function Using the Seahorse System” In: Murthi, P., Vaillancourt, C. (eds) Preeclampsia. Methods in Molecular Biology, vol 1710. Humana Press, New York, NY. https://doi.org/10.1007/978-1-4939-7498-6_22

Lu, C., G. Song, and J. Lin (2006), “Reactive oxygen species and their chemiluminescence-detection methods”, *TrAC Trends in Analytical Chemistry,* Vol. 25/10, Elsevier, Amsterdam, https://doi.org/10.1016/j.trac.2006.07.007

Nguyen Dinh Cat, A. et al. (2013), “Angiotensin II, NADPH oxidase, and redox signaling in the vasculature”, *Antioxidants & redox signaling,* Vol. 19/10**,** Mary Ann Liebert, Larchmont, https://doi.org/10.1089/ars.2012.4641

Ping, Z. et al. (2020), “Oxidative Stress in Radiation-Induced Cardiotoxicity”, *Oxidative Medicine and Cellular Longevity*, Vol. 2020, Hindawi, https://doi.org/10.1155/2020/3579143

Powers, S.K. and M.J. Jackson. (2008), “Exercise-Induced Oxidative Stress: Cellular Mechanisms and Impact on Muscle Force Production”, *Physiological Reviews,* Vol. 88/4**,** American Physiological Society, Rockville, https://doi.org/10.1152/physrev.00031.2007

Raimondi, V., F. Ciccarese and V. Ciminale. (2020), “Oncogenic pathways and the electron transport chain: a dangeROS liason”, *British Journal of Cancer,* Vol. 122/2, Nature Portfolio, London, https://doi.org/10.1038/s41416-019-0651-y

Seen, S. and L. Tong. (2018), “Dry eye disease and oxidative stress”, *Acta Ophthalmologica,* Vol. 96/4**,** John Wiley & Sons, Inc., Hoboken, https://doi.org/10.1111/aos.13526

Ungvari, Z. et al. (2013), “Ionizing Radiation Promotes the Acquisition of a Senescence-Associated Secretory Phenotype and Impairs Angiogenic Capacity in Cerebromicrovascular Endothelial Cells: Role of Increased DNA Damage and Decreased DNA Repair Capacity in Microvascular Radiosensitivity”, *The Journals of Gerontology Series A: Biological Sciences and Medical Sciences*, Vol. 68/12, Oxford University Press, Oxford, https://doi.org/10.1093/gerona/glt057.

Vargas-Mendoza, N. et al. (2021), “Oxidative Stress, Mitochondrial Function and Adaptation to Exercise: New Perspectives in Nutrition”, *Life,* Vol. 11/11, Multidisciplinary Digital Publishing Institute, Basel, https://doi.org/10.3390/life11111269

Wang, H. et al. (2019), “Radiation-induced heart disease: a review of classification, mechanism and prevention”, *International Journal of Biological Sciences,* Vol. 15/10, Ivyspring International Publisher, Sydney, https://doi.org/10.7150/ijbs.35460

Zhang, R. et al. (2009), “Blockade of AT1 receptor partially restores vasoreactivity, NOS expression, and superoxide levels in cerebral and carotid arteries of hindlimb unweighting rats”, *Journal of applied physiology*, Vol. 106/1, American Physiological Society, Rockville, https://doi.org/10.1152/japplphysiol.01278.2007.

Zhao, R. Z. et al. (2019), “Mitochondrial electron transport chain, ROS generation and uncoupling”, *International journal of molecular medicine*, Vol. 44/1, Spandidos Publishing Ltd., Athens, https://doi.org/10.3892/ijmm.2019.4188

Event: 2066: Altered Signaling Pathways

Short Name: Altered Signaling

AOPs Including This Key Event

AOP ID and Name	Event Type
Aop:470 - Deposition of energy leads to vascular remodeling	KeyEvent
Aop:482 - Deposition of energy leading to occurrence of bone loss	KeyEvent
Aop:483 - Deposition of Energy Leading to Learning and Memory Impairment	KeyEvent

Biological Context

Level of Biological Organization

Molecular

Domain of Applicability

Taxonomic Applicability

Term	Scientific Term	Evidence	Links
human	Homo sapiens	Moderate	NCBI
rat	Rattus norvegicus	Moderate	NCBI
mouse	Mus musculus	Moderate	NCBI

Life Stage Applicability

Life Stage	Evidence
All life stages	Moderate

Sex Applicability

Sex	Evidence
Unspecific	Low

Taxonomic applicability: Altered signaling is applicable to all animals as cell signaling occurs among animal cells. This includes vertebrates such as humans, mice and rats (Nair et al., 2019).

Life stage applicability: This key event is not life stage specific.

Sex applicability: This key event is not sex specific.

Evidence for perturbation by a stressor: Multiple studies show that signaling pathways can be disrupted by many types of stressors including ionizing radiation and altered gravity (Cheng et al., 2020; Coleman et al., 2021; Su et al., 2020; Yentrapalli et al., 2013).

Key Event Description

Cells receive, process, and transmit signals to respond to their environment via signaling pathways. Signaling pathways are groups of molecules that work together in a cell to control physiological and metabolic processes. Kinases, for example, are important signaling molecules that can phosphorylate other proteins (Svoboda & Reenstra, 2002). Initiation of signaling pathways is an important component of cellular homeostasis including normal cell development and the response to cellular damage from exposure to external stressors (Esbenshade & Duzic, 2006). Signaling pathways are themselves activated by signals and the same signal can lead to different responses depending on the tissue type (Hamada, et al. 2011; Svoboda & Reenstra, 2002). Examples of signals include the activation of receptors to activate transcriptional targets, induction of receptor-ligand interactions and the initiation of cell-cell contact, or cell-extracellular matrix contact (Hunter, 2000). Many signalling pathways are crucial to intercellular communication via membrane receptors that transduce signals into the cell, while others are activated in an intracellular manner (Svoboda & Reenstra, 2002). Altered signalling (i.e., increase/decrease) can lead to different physiological outcomes, meaning that the directionality of the signaling response, determines the end outcome. For example, increase of the PI3K/Akt/mTOR pathway, which under physiological conditions is responsible for regulating the cell cycle, can lead to increased proliferation and decreased apoptosis. However, a decrease expression of this pathway can lead to an increase in apoptosis and decreased proliferation (Porta et al., 2014; Venkatesulu et al., 2018).

How it is Measured or Detected

Method of Measurement	Reference	Description	OECD Approved Assay
Kinase assays	(Svoboda & Reenstra, 2002)	Block kinase with inhibitors to monitor the activity of a kinase of interest.	No
Cell behaviour assays	(Svoboda & Reenstra, 2002)	Signal transduction events of cells are monitored. Cells are exposed to varying levels of signaling proteins and the resulting actions of a cell are observed (changes in structure, cell shape, matrix binding etc.).	No
Ratiometric or single-wavelength dyes	(Svoboda & Reenstra, 2002)	Detects alterations in signal-transduction activities via monitoring changes in detectable wavelengths.	No
Fluorescence microscopy/spectroscopy	(Oksvold et al., 2002)	Measures cell localization, protein interactions, signal propagation, amplification, and integration in the cell in real-time, or upon stimulation.	Yes
Green Fluorescent Protein (GFP)	(Zaccolo and Pozzan, 2000)	GFP assays act as fluorescent reporters but also as a marker of intracellular signalling events i.e. second messengers Ca2+ and cAMP, or for pH in different various cell compartments	No

Fluorescence Resonance Energy Transfer (FRET)	(Bunt and Wouters, 2017)	Assay helps illuminate the interactions between biological molecules	No
Fluorescence recovery after photobleaching (FRAP)	(Svoboda & Reenstra, 2002)	Determines mobility and diffusion of small molecules.	No
Immunoprecipitation	(Svoboda & Reenstra, 2002)	Involves isolating and concentrating a particular protein from mixed samples to detect changes in signalling molecule activity.	Chromatin immunoprecipitation approved for analyzing histone modifications
Immunohistochemistry	(Kurien et al., 2011; Svoboda & Reenstra, 2002)	Northern, western and southern blotting techniques can be used to visualize signal transduction events. For example, antibodies with recognition epitopes can be used to locate active configurations or phosphorylated proteins within a cell or cell lysate.	No
Reverse transcription-quantitative polymerase chain reaction (RT-qPCR)	(Veremeyko et al., 2012; Alwine et al, 1977)	Measures mRNA expression of the gene of interest.	No
Enzyme-linked immunosorbent assay (ELISA)	(Amsen et al., 2009; Engvall & Perlmann, 1972)	Plate-based assay technique using antibodies to detect presence of a protein in a liquid sample. Can be used to identify presence of a protein of interest especially in when in low concentrations	No

References

Alwine, J. C., D. J. Kemp and G. R. Stark (1977), “Method for detection of specific RNAs in agarose gels by transfer to diazobenzyloxymethyl-paper and hybridization with DNA probes”, *Proceedings of the National Academy of Sciences of the United States of America*, Vol. 74/12, United States National Academy of Sciences, Washington, D.C., https://doi.org/10.1073/pnas.74.12.5350

Amsen, D., de Visser, K. E., and Town, T. (2009), “Approaches to determine expression of inflammatory cytokines”, in *Inflammation and Cancer*, Humana Press, Totowa, https://doi.org/10.1007/978-1-59745-447-6_5

Bunt, G., and F. S. Wouters (2017), “FRET from single to multiplexed signaling events”, *Biophysical reviews*, Vol. 9, Springer, London, https://doi.org/10.1007/s12551-017-0252-z

Cheng, Y. P. et al. (2017), “Acid sphingomyelinase/ceramide regulates carotid intima-media thickness in simulated weightless rats”, *Pflugers Archiv European Journal of Physiology*, Vol. 469, Springer, New York, https://doi.org/10.1007/s00424-017-1969-z

Coleman, M. A. et al. (2015), “Low-dose radiation affects cardiac physiology: gene networks and molecular signaling in cardiomyocytes”, *American Journal of Physiology - Heart and Circulatory Physiology*, Vol. 309/11, American Physiological Society, Rockville, https://doi.org/10.1152/ajpheart.00050.2015

Engvall, E., and P. Perlmann (1972), “Enzyme-Linked Immunosorbent Assay, Elisa”, *The Journal of Immunology*, Vol. 109/1, American Association of Immunologists, Minneapolis, pp. 129-135

Esbenshade, T. A., and E. Duzic (2006), “Overview of signal transduction”, *Current Protocols in Pharmacology*, Vol. 31/1, John Wiley & Sons, Ltd., Hoboken, https://doi.org/10.1002/0471141755.ph0201s31

Hamada, N. et al. (2011), “Signaling pathways underpinning the manifestations of ionizing radiation-induced bystander effects”, *Current Molecular Pharmacology*, Vol. 4/2, Bentham Science Publishers, Sharjah UAE, https://doi.org/10.2174/1874467211104020079

Hunter, T. (2000), “Signaling - 2000 and beyond”, *Cell*, Vol. 100/1, Cell Press, Cambridge, https://doi.org/10.1016/s0092-8674(00)81688-8

Kurien, B. T. et al. (2011), “An overview of Western blotting for determining antibody specificities for immunohistochemistry”, in *Signal Transduction Immunohistochemistry Methods and Protocols*, Springer, London, https://doi.org/10.1007/978-1-61779-024-9_3

Nair, A. et al. (2019), “Conceptual Evolution of Cell Signaling”, *International journal of molecular sciences*, Vol. 20/13, Multidisciplinary Digital Publishing Institute, Basel, https://doi.org/10.3390/ijms20133292

Oksvold, M. P. et al. (2002), “Fluorescent histochemical techniques for analysis of intracellular signaling”, *The Journal of Histochemistry and Cytochemistry*, Vol. 50/3, SAGE Publications, Thousand Oaks, https://doi.org/10.1177/002215540205000301

Porta, C., C. Paglino and A. Mosca (2014), “Targeting PI3K/Akt/mTOR Signaling in Cancer”, *Frontiers in Oncology*, Vol. 4, Frontiers Media SA, Lausanne, https://doi.org/10.3389/fonc.2014.00064

Su, Y. T. et al. (2020), “Acid sphingomyelinase/ceramide mediates structural remodeling of cerebral artery and small mesenteric artery in simulated weightless rats”, *Life Sciences*, Vol. 243, Elsevier, Amsterdam, https://doi.org/10.1016/j.lfs.2019.117253

Svoboda, K. K. and W. R. Reenstra (2002), “Approaches to studying cellular signaling: a primer for morphologists”, *The Anatomical record*, Vol. 269/2, John Wiley & Sons, Ltd., Hoboken, https://doi.org/10.1002/ar.10074

Venkatesulu, B. P. et al. (2018), “Radiation-Induced Endothelial Vascular Injury: A Review of Possible Mechanisms”, *JACC: Basic to Translational Science*, Vol. 3/4, Elsevier, Amsterdam, https://doi.org/10.1016/j.jacbts.2018.01.014

Veremeyko, T. et al. (2012), “Detection of microRNAs in microglia by real-time PCR in normal CNS and during neuroinflammation”, *Journal of Visualized Experiments: JoVE*, Vol. 65, MyJove Corporation, Cambridge, https://doi.org/10.3791/4097

Yentrapalli, R. et al. (2013), “The PI3K/Akt/mTOR pathway is implicated in the premature senescence of primary human endothelial cells exposed to chronic radiation”, *PloS one*, Vol. 8/8, PLOS, San Francisco, https://doi.org/10.1371/journal.pone.0070024

Zaccolo, M. and T. Pozzan (2000), “Imaging signal transduction in living cells with GFP-based probes”, *IUBMB life*, Vol. 49/5, John Wiley & Sons, Ltd., Hoboken, https://doi.org/10.1080/152165400410218

Event: 1492: Tissue resident cell activation

Short Name: Tissue resident cell activation

Key Event Component

Process	Object	Action
cell activation involved in immune response		increased

AOPs Including This Key Event

AOP ID and Name	Event Type
Aop:17 - Binding of electrophilic chemicals to SH(thiol)-group of proteins and /or to seleno-proteins involved in protection against oxidative stress during brain development leads to impairment of learning and memory	KeyEvent
Aop:38 - Protein Alkylation leading to Liver Fibrosis	KeyEvent
Aop:293 - Increased DNA damage leading to increased risk of breast cancer	KeyEvent
Aop:294 - Increased reactive oxygen and nitrogen species (RONS) leading to increased risk of breast cancer	KeyEvent
Aop:483 - Deposition of Energy Leading to Learning and Memory Impairment	KeyEvent

Biological Context

Level of Biological Organization

Cellular
Level of Biological Organization

Domain of Applicability

Taxonomic Applicability

Term	Scientific Term	Evidence	Links
human	Homo sapiens		NCBI
Macaca fascicularis	Macaca fascicularis		NCBI
rat	Rattus norvegicus		NCBI
mouse	Mus musculus		NCBI
zebrafish	Danio rerio		NCBI

Life Stage Applicability

Life Stage	Evidence
All life stages	

Extend to at least invertebrates

Not to plants and not to single-celled organisms

BRAIN:

Tissue resident activation is observed in human, monkey, rat, mouse, and zebrafish, in association with neurodegeneration or following toxicant exposure. Some references (non-exhaustive list) are given below for illustration:

Human: Vennetti et al., 2006

Monkey (Macaca fascicularis): Charleston et al., 1994, 1996

Rat: Little et al., 2012; Zurich et al., 2002; Eskes et al., 2002

Mouse: Liu et al., 2012

Zebrafish: Xu et al., 2014.

LIVER:

Human: Su et al., 2002; Kegel et al., 2015; Boltjes et al.,2014

Rat: Luckey and Peterson,2001

Mouse: Dalton t al., 2009

Life stage applicability: This key event is mainly applicable to all life stages most evidence is derived from adult models (Betlazar et al., 2016; Paladini et al., 2021).

Sex applicability: This key event is not sex specific (Betlazar et al., 2016; Paladini et al., 2021).

Evidence for perturbation by a prototypic stressor: Current literature provides ample evidence of tissue resident cell activation being induced by ionizing radiation (Allen et al., 2020; Krukowski et al., 2018; Parihar et al., 2020; Parihar et al., 2018; Parihar et al., 2016; Poulose et al., 2011; Raber et al., 2019; Sumam et al., 2013).

Key Event Description

Tissue resident cell activation is considered as a hallmark of inflammation irrespective of the tissue type. Strategically placed cells within tissues respond to noxious stimuli, thus regulating the recruitment of neutrophil and the initiation and resolution of inflammation (Kim and Luster, 2015). Examples for these cells are resident immune cells, parenchymal cells, vascular cells, stromal cells, or smooth muscle cells. These cells may be specific for a certain tissue, but they have a common tissue-independent role.

Under healthy conditions there is a homeostatic state, characterized as a generally quiescent cellular milieu. Various danger signals or alarmins that are involved in induction of inflammation like pathogen-associated molecular pattern molecules (PAMPs) and damage-associated molecular pattern molecules (DAMPs) activate these resident cells in affected tissues.

Examples of well-characterized DAMPs (danger signals or alarmins) (Saïd-Sadier and Ojcius, 2012)

DAMPs	Receptors	Outcome of receptor ligation
Extracellular nucleotides (ATP, ADP, adenosine)	PI, P2X and P2Y receptors (ATP, ADP); Al, A2A, A2B and A3 receptors (adenosine)	Dendritic cell (DC) maturation, chemotaxis, secretion of cytokines (IL-1β, IL-18), inflammation
Extracellular heat shock proteins	CD14, CD91, scavenger receptors, TLR4, TLR2, CD40	DC maturation, cytokine induction, DC, migration to lymph nodes
Extracellular HMGB1	RAGE, TLR2, TLR4	Chemotaxis, cytokine induction, DC activation, neutrophil recruitment, inflammation, activation of immune cells
Uric acid crystals	CD14, TLR2, TLR4	DC activation, cytokine induction, neutrophil recruitment, gout induction
Oxidative stress	Intracellular redox-sensitive proteins	Cell death, release of endogenous DAMPs, inflammation
Laminin	Integrins	Neutrophil recruitment, chemotaxis
S100 proteins or calgranulins	RAGE	Neutrophil recruitment, chemotaxis, cytokine secretion, apoptosis
Hyaluronan	TLR2, TLR4, CD44	DC maturation, cytokine production, adjuvant activity

Activation refers to a phenotypic modification of the resident cells that includes alterations in their secretions, activation of biosynthetic pathways, production of pro-inflammatory proteins and lipids, and morphological changes. While these represent a pleiotropic range of responses that can vary with the tissue, there are a number of common markers or signs of activation that are measurable.

Examples of Common markers are

- CD11b
- Iba1
- GFAP
- CD68
- CD86
- Mac-1
- NF-kB
- AP-1
- Jnk
- P38/mapk

These described commonalities allow the use of this KE as a hub KE in the AOP network. However, despite the similarities in the inflammatory process, the type of reactive cells and the molecules triggering their reactivity may be tissue-specific. Therefore, for practical reasons, a tissue specific description of the reactive cells and of the triggering factors is necessary in order to specify in a tissue-specific manner, which cell should be considered and what should be measured.

BRAIN

The most easily detectable feature of brain inflammation or neuroinflammation is activation of microglial cells and astrocytes. It is evidenced by changes in shape, increased expression of certain antigens, and accumulation and proliferation of the glial cells in affected regions (Aschner, 1998; Graeber & Streit, 1990; Monnet-Tschudi et al, 2007; Streit et al, 1999; Kraft and Harry, 2011; Claycomb et al., 2013). Upon stimulation by cytokines, chemokines or inflammogens (e.g. from pathogens or from damaged neurons), both glial cell types activate inflammatory signaling pathways, which result in increased expression and/or release of inflammatory mediators such as cytokines, eicosanoids, and metalloproteinases (Dong & Benveniste, 2001) (cf KE: pro-inflammatory mediators, increased), as well as in the production of reactive oxygen species (ROS) and nitrogen species (RNS) (Brown & Bal-Price, 2003). Different types of activation states are possible for microglia and astrocytes, resulting in pro-inflammatory or anti-inflammatory signaling, and other cellular functions (such as phagocytosis) (Streit et al., 1999; Nakajima and Kohsaka, 2004). Therefore, neuroinflammation can have both neuroprotective/neuroreparative and neurodegenerative consequences (Carson et al., 2006; Monnet-Tschudi et al, 2007; Aguzzi et al., 2013 ; Glass et al., 2010). Under normal physiological conditions, microglial cells survey the nervous system for neuronal integrity (Nimmerjahn et al, 2005) and for invading pathogens (Aloisi, 2001; Kreutzberg, 1995; Kreutzberg, 1996; Rivest, 2009). They are the first type of cell activated (first line of defense), and can subsequently induce astrocyte activation (Falsig, 2008). Two distinct states of microglial activation have been described (Gordon, 2003; Kigerl et al, 2009; Maresz et al, 2008; Mosser & Edwards, 2008; Perego et al; Ponomarev et al, 2005): The M1 state is classically triggered by interferon-gamma and/or other pro-inflammatory cytokines, and this state is characterized by increased expression of integrin alpha M (Itgam) and CD86, as well as the release of pro-inflammatory cytokines (TNF-alpha, IL-1beta, IL-6), and it is mostly associated with neurodegeneration. The M2 state is triggered by IL-4 and IL-13 (Maresz et al, 2008; Perego et al, 2011; Ponomarev et al, 2007) and induces the expression of mannose receptor 1 (MRC1), arginase1 (Arg 1) and Ym1/2; it is involved in repair processes. The activation of astrocytes by microglia-derived cytokines or TLR agonists resembles the microglial M1 state (Falsig 2006). Although classification of the M1/M2 polarization of microglial cells may be considered as a

simplification of authentic microglial reaction states (Ransohoff, 2016), a similar polarization of reactive astrocytes has been described recently Liddlelow et al., 2017): Interleukin-1 alpha (IL-1a), TNF and subcomponent q (C1q) released by activated microglial cells induce A1-reactive astrocytes, which lose the ability to promote neuronal survival, outgrowth, synaptogenesis and phagocytosis and induce the death of neurons and oligodendrocytes.

Regulatory examples using the KE

Measurement of glial fibrillary acidic protein (GFAP) in brain tissue, whose increase is a marker of astrocyte reactivity, is required by the US EPA in rodent toxicity studies for fuel additives (40 CFR 79.67). It has been used on rare occasions for other toxicant evaluations.

LIVER:

Kupffer cells (KCs) are a specialized population of macrophages that reside in the liver; they were first described by Carl Wilhelm von Kupffer (1829–1902) [Haubrich 2004]. KCs constitute 80%-90% of the tissue macrophages in the reticuloendothelial system and account for approximately 15% of the total liver cell population [Bouwens et al., 1986]. They play an important role in normal physiology and homeostasis as well as participating in the acute and chronic responses of the liver to toxic compounds. Activation of KCs results in the release of an array of inflammatory mediators, growth factors, and reactive oxygen species. This activation appears to modulate acute hepatocyte injury as well as chronic liver responses including hepatic cancer. Understanding the role KCs play in these diverse responses is key to understanding mechanisms of liver injury [Roberts et al.,2007]. Besides the release of inflammatory mediators including cytokines, chemokines, lysosomal and proteolytic enzymes KCs are a main source of TGF-β1 (transforming growth factor-beta 1, the most potent profibrogenic cytokine). In addition latent TGF-β1 can be activated by KC-secreted matrix metalloproteinase 9 (MMP-9)[Winwood and Arthur, 1993; Luckey and Peeterson, 2001] through the release of biologically active substances that promote the pathogenic process. Activated KCs also release ROS like superoxide generated by NOX (NADPH oxidase), thus contributing to oxidative stress. Oxidative stress also activates a variety of transcription factors like NF-κB, PPAR-γ leading to an increased gene expression for the production of growth factors, inflammatory cytokines and chemokines. KCs express TNF-α (Tumor Necrosis Factor-alpha), IL-1 (Interleukin-1) and MCP-1 (monocyte-chemoattractant protein-1), all being mitogens and chemoattractants for hepatic stellate cells (HSCs) and induce the expression of PDGF receptors on HSCs which enhances cell proliferation. Expressed TNF-α, TRAIL (TNF-related apoptosis-inducing ligand), and FasL (Fas Ligand) are not only pro-inflammatory active but also capable of inducing death receptor-mediated apoptosis in hepatocytes [Guo and Friedman, 2007; Friedman 2002; Roberts et al., 2007]. Under conditions of oxidative stress macrophages are further activated which leads to a more enhanced inflammatory response that again further activates KCs though cytokines (Interferon gamma (IFNγ), granulocyte macrophage colony-stimulating factor (GM-CSF), TNF-α), bacterial lipopolysaccharides, extracellular matrix proteins, and other chemical mediators [Kolios et al., 2006; Kershenobich Stalnikowitz and Weissbrod 2003].

Besides KCs, the resident hepatic macrophages, infiltrating bone marrow-derived macrophages, originating from circulating monocytes are recruited to the injured liver via chemokine signals. KCs appear essential for sensing tissue injury and initiating inflammatory responses, while infiltrating Ly-6C+ monocyte-derived macrophages are linked to chronic inflammation and fibrogenesis. The profibrotic functions of KCs (HSC activation via paracrine mechanisms) during chronic hepatic injury remain functionally relevant, even if the infiltration of additional inflammatory monocytes is blocked via pharmacological inhibition of the chemokine CCL2 [Baeck et al., 2012; Tacke and Zimmermann, 2014].

KC activation and macrophage recruitment are two separate events and both are necessary for fibrogenesis, but as they occur in parallel, they can be summarised as one KE.

Probably there is a threshold of KC activation and release above which liver damage is induced. Pre-treatment with gadolinium chloride (GdCl), which inhibits KC function, reduced both hepatocyte and sinusoidal epithelial cell injury, as well as decreased the numbers of macrophages appearing in hepatic lesions and inhibited TGF-β1 mRNA expression in macrophages. Experimental inhibition of KC function or depletion of KCs appeared to protect against chemical-induced liver injury [Ide et al.,2005].

How it is Measured or Detected

In General:

Measurement targets are cell surface and intracellular markers; the specific markers may be cell and species-specific.

Available methods include cytometry, immunohistochemistry, gene expression sequencing; western blotting, ELISA, and functional assays.

BRAIN

Neuroinflammation, i.e. the activation of glial cells can be measured by quantification of cellular markers (most commonly), or of released mediators (less common). As multiple activation states exist for the two main cell types involved, it is necessary to measure several markers of neuroinflammation:

1. Microglial activation can be detected based on the increased numbers of labeled microglia per volume element of brain tissue (due to increase of binding sites, proliferation, and immigration of cells) or on morphological changes. A specific microglial marker, used across different species, is CD11b. Alternatively various specific carbohydrate structures can be stained by lectins (e.g. IB4). Beyond that, various well-established antibodies are available to detect microglia in mouse tissue (F4/80), phagocytic microglia in rat tissue (ED1) or more generally microglia across species (Iba1). Transgenic mice are available with

fluorescent proteins under the control of the CD11b promoter to easily quantify microglia without the need for specific stains.
2. The most frequently used astrocyte marker is glial fibrillary acidic protein, GFAP (99% of all studies) (Eng et al., 2000). This protein is highly specific for astrocytes in the brain, and antibodies are available for immunocytochemical detection. In neuroinflamatory brain regions, the stain becomes more prominent, due to an upregulation of the protein, a shape change/proliferation of the cells, and/or better accessibility of the antibody. Various histological quantification approaches can be used. Occasionally, alternative astrocytic markers, such as vimentin of the S100beta protein, have been used for astrocyte staining (Struzynska et al., 2007). Antibodies for complement component 3 (C3), the most characteristic and highly upregulated marker of A1 neurotoxic reactive astrocytes are commercially available.
3. All immunocytochemical methods can also be applied to cell culture models.
4. In patients, microglial accumulation can be monitored by PET imaging, using [11C]-PK 11195 as a microglial marker (Banati et al., 2002).
5. Activation of glial cells can be assessed in tissue or cell culture models also by quantification of sets of M1/M2 phenotype markers. This can for instance be done by PCR quantification, immunocytochemistry, immunoblotting.

- Itgam, CD86 expression as markers of M1 microglial phenotype
- Arg1, MRC1, as markers of M2 microglial phenotype

(for descriptions of techniques, see Falsig 2004; Lund 2006 ; Kuegler 2010; Monnet-Tschudi et al., 2011; Sandström et al., 2014; von Tobel et al., 2014)

LIVER:

Kupffer cell activation can be measured by means of expressed cytokines, e.g. tissue levels of TNF-a [Vajdova et al,2004], IL-6 expression, measured by immunoassays or Elisa (offered by various companies), soluble CD163 [Grønbaek etal., 2012; Møller etal.,2012] or increase in expression of Kupffer cell marker genes such as Lyz, Gzmb, and Il1b, (Genome U34A Array, Affymetrix); [Takahara et al.,2006]

References

Allen, B. D. et al. (2020), "Mitigation of helium irradiation-induced brain injury by microglia depletion", Journal of Neuroinflammation, Vol. 17/1, Nature, https://doi.org/10.1186/s12974-020-01790-9.

Betlazar, C. et al. (2016), "The impact of high and low dose ionising radiation on the central nervous system", Redox Biology, Vol. 9, Elsevier, Amsterdam, https://doi.org/10.1016/j.redox.2016.08.002.

Chan JK, Roth J, Oppenheim JJ, Tracey KJ, Vogl T, Feldmann M, Horwood N, Nanchahal J., Alarmins: awaiting a clinical response. J Clin Invest. 2012 Aug;122(8):2711-9.

Davies LC, Jenkins SJ, Allen JE, Taylor PR, Tissue-resident macrophages, Nat Immunol. 2013 Oct;14(10):986-95.

Escamilla-Tilch M, Filio-Rodríguez G, García-Rocha R, Mancilla-Herrera I, Mitchison NA, Ruiz-Pacheco JA, Sánchez-García FJ, Sandoval-Borrego D, Vázquez-Sánchez EA, The interplay between pathogen-associated and danger-associated molecular patterns: an inflammatory code in cancer? Immunol Cell Biol. 2013 Nov-Dec;91(10):601-10.

Hussell T, Bell TJ, Alveolar macrophages: plasticity in a tissue-specific context, Nat Rev Immunol. 2014 Feb;14(2):81-93.

Kim ND, Luster AD. The role of tissue resident cells in neutrophil recruitment ,Trends Immunol. 2015 Sep;36(9):547-55.

Krukowski, K. et al. (2018), "Female mice are protected from space radiation-induced maladaptive responses", Brain, Behavior, and Immunity, Vol. 74, Academic Press Inc., https://doi.org/10.1016/j.bbi.2018.08.008.

Paladini, M. S. et al. (2021), "Microglia depletion and cognitive functions after brain injury: From trauma to galactic cosmic ray", Neuroscience Letters, Vol. 741, Elsevier, Amsterdam, https://doi.org/10.1016/j.neulet.2020.135462.

Parihar, V. K. et al. (2016), "Cosmic radiation exposure and persistent cognitive dysfunction", Scientific Reports, Vol. 6/June, Nature Publishing Group, https://doi.org/10.1038/srep34774.

Parihar, V. K. et al. (2018), "Persistent nature of alterations in cognition and neuronal circuit excitability after exposure to simulated cosmic radiation in mice", Experimental Neurology, Vol. 305, Academic Press Inc., https://doi.org/10.1016/j.expneurol.2018.03.009.

Parihar, V. K. et al. (2020), "Sex-Specific Cognitive Deficits Following Space Radiation Exposure", Frontiers in behavioral neuroscience, Vol. 14, Frontiers, https://doi.org/10.3389/fnbeh.2020.535885.

Poulose, S. M. et al. (2011), "Exposure to 16O-particle radiation causes aging-like decrements in rats through increased oxidative stress, inflammation and loss of autophagy", Radiation Research, Vol. 176/6, BioOne, https://doi.org/10.1667/RR2605.1.

Raber, J. et al. (2019), "Combined Effects of Three High-Energy Charged Particle Beams Important for Space Flight on Brain, Behavioral and Cognitive Endpoints in B6D2F1 Female and Male Mice", Frontiers in physiology, Vol. 10, Frontiers, https://doi.org/10.3389/fphys.2019.00179.

Saïd-Sadier N, Ojcius DM., Alarmins, inflammasomes and immunity. Biomed J. 2012 Nov-Dec;35(6):437-49.

Schaefer L, Complexity of danger: the diverse nature of damage-associated molecular patterns, J Biol Chem. 2014 Dec 19;289(51):35237-45.

Suman, S. et al. (2013), "Therapeutic and space radiation exposure of mouse brain causes impaired dna repair response and premature senescence by chronic oxidant production", Aging, Vol. 5/8, https://doi.org/10.18632/aging.100587.

BRAIN:

Aschner M (1998) Immune and inflammatory responses in the CNS: modulation by astrocytes. ToxicolLett 103: 283-287

Banati, R. B. (2002). "Visualising microglial activation in vivo." Glia 40: 206-217.

Brown GC, Bal-Price A (2003) Inflammatory neurodegeneration mediated by nitric oxide, glutamate, and mitochondria. Mol Neurobiol 27: 325-355

Charleston JS, Body RL, Bolender RP, Mottet NK, Vahter ME, Burbacher TM. 1996. Changes in the number of astrocytes and microglia in the thalamus of the monkey Macaca fascicularis following long-term subclinical methylmercury exposure. NeuroToxicology 17: 127-138.

Charleston JS, Bolender RP, Mottet NK, Body RL, Vahter ME, Burbacher TM. 1994. Increases in the number of reactive glia in the visual cortex of Macaca fascicularis following subclinical long-term methyl mercury exposure. ToxicolApplPharmacol 129: 196-206.

Dong Y, Benveniste EN (2001) Immune Function of Astrocytes. Glia 36: 180-190

Eng LF, Ghirnikar RS, Lee YL (2000) Glial Fibrillary Acidic Protein: GFAP-Thirty-One Years (1969-2000). NeurochemRes 25: 1439-1451

Eskes C, Honegger P, Juillerat-Jeanneret L, Monnet-Tschudi F. 2002. Microglial reaction induced by noncytotoxic methylmercury treatment leads to neuroprotection via interactions with astrocytes and IL-6 release. Glia 37(1): 43-52.

Falsig J, Latta M, Leist M. Defined inflammatory states in astrocyte cultures correlation with susceptibility towards CD95-driven apoptosis. J Neurochem. 2004 Jan;88(1):181-93.

Falsig J, Pörzgen P, Lund S, Schrattenholz A, Leist M. The inflammatory transcriptome of reactive murine astrocytes and implications for their innate immune function. J Neurochem. 2006 Feb;96(3):893-907.

Falsig J, van Beek J, Hermann C, Leist M. Molecular basis for detection of invading pathogens in the brain. J Neurosci Res. 2008 May 15;86(7):1434-47.

Glass CK, Saijo K, Winner B, Marchetto MC, Gage FH (2010). Mechanisms underlying inflammation in neurodegeneration. Cell. 2010 Mar 19;140(6):918-34.

Gordon S (2003) Alternative activation of macrophages. Nat Rev Immunol 3: 23-35

Graeber MB, Streit WJ (1990) Microglia: immune network in the CNS. Brain Pathol 1: 2-5

Kigerl KA, Gensel JC, Ankeny DP, Alexander JK, Donnelly DJ, Popovich PG (2009) Identification of two distinct macrophage subsets with divergent effects causing either neurotoxicity or regeneration in the injured mouse spinal cord. J Neurosci 29: 13435-13444

Kuegler PB, Zimmer B, Waldmann T, Baudis B, Ilmjärv S, Hescheler J, Gaughwin P, Brundin P, Mundy W, Bal-Price AK, Schrattenholz A, Krause KH, van Thriel C, Rao MS, Kadereit S, Leist M. Markers of murine embryonic and neural stem cells, neurons and astrocytes: reference points for developmental neurotoxicity testing. ALTEX. 2010;27(1):17-42

Kreutzberg GW (1995) Microglia, the first line of defence in brain pathologies. Arzneimttelforsch 45: 357-360

Kreutzberg GW (1996) Microglia : a sensor for pathological events in the CNS. Trends Neurosci 19: 312-318

Liddelow SA, Guttenplan KA, Clarke LE, Bennett FC, Bohlen CJ, Schirmer L, et al. 2017. Neurotoxic reactive astrocytes are induced by activated microglia. Nature 541(7638): 481-487.

Little AR, Miller DB, Li S, Kashon ML, O'Callaghan JP. 2012. Trimethyltin-induced neurotoxicity: gene expression pathway analysis, q-RT-PCR and immunoblotting reveal early effects associated with hippocampal damage and gliosis. Neurotoxicol Teratol 34(1): 72-82.

Liu Y, Hu J, Wu J, Zhu C, Hui Y, Han Y, et al. 2012. alpha7 nicotinic acetylcholine receptor-mediated neuroprotection against dopaminergic neuron loss in an MPTP mouse model via inhibition of astrocyte activation. J Neuroinflammation 9: 98.

Lund S, Christensen KV, Hedtjärn M, Mortensen AL, Hagberg H, Falsig J, Hasseldam H, Schrattenholz A, Pörzgen P, Leist M. The dynamics of the LPS triggered inflammatory response of murine microglia under different culture and in vivo conditions. J Neuroimmunol. 2006 Nov;180(1-2):71-87.

Maresz K, Ponomarev ED, Barteneva N, Tan Y, Mann MK, Dittel BN (2008) IL-13 induces the expression of the alternative activation marker Ym1 in a subset of testicular macrophages. J Reprod Immunol 78: 140-148

Monnet-Tschudi F, Zurich MG, Honegger P (2007) Neurotoxicant-induced inflammatory response in three-dimensional brain cell cultures. Hum Exp Toxicol 26: 339-346

Monnet-Tschudi, F., A. Defaux, et al. (2011). "Methods to assess neuroinflammation." Curr Protoc Toxicol Chapter 12: Unit12 19.

Mosser DM, Edwards JP (2008) Exploring the full spectrum of macrophage activation. Nat Rev Immunol 8: 958-969

Nakajima K, Kohsaka S. 2004. Microglia: Neuroprotective and neurotrophic cells in the central nervous system. Current Drug Targets-Cardiovasc & Haematol Disorders 4: 65-84.

Perego C, Fumagalli S, De Simoni MG (2011) Temporal pattern of expression and colocalization of microglia/macrophage phenotype markers following brain ischemic injury in mice. J Neuroinflammation 8: 174

Ponomarev ED, Maresz K, Tan Y, Dittel BN (2007) CNS-derived interleukin-4 is essential for the regulation of autoimmune inflammation and induces a state of alternative activation in microglial cells. J Neurosci 27: 10714-10721

Ponomarev ED, Shriver LP, Maresz K, Dittel BN (2005) Microglial cell activation and proliferation precedes the onset of CNS autoimmunity. J Neurosci Res 81: 374-389

Ransohoff RM. 2016. A polarizing question: do M1 and M2 microglia exist? Nat Neurosci 19(8): 987-991.

Sandstrom von Tobel, J., D. Zoia, et al. (2014). "Immediate and delayed effects of subchronic Paraquat exposure during an early differentiation stage in 3D-rat brain cell cultures." Toxicol Lett. DOI : 10.1016/j.toxlet.2014.02.001

Struzynska L, Dabrowska-Bouta B, Koza K, Sulkowski G (2007) Inflammation-Like Glial Response in Lead-Exposed Immature Rat Brain. Toxicol Sc 95:156-162

von Tobel, J. S., P. Antinori, et al. (2014). "Repeated exposure to Ochratoxin A generates a neuroinflammatory response, characterized by neurodegenerative M1 microglial phenotype." Neurotoxicology 44C: 61-70.

Venneti S, Lopresti BJ, Wiley CA. 2006. The peripheral benzodiazepine receptor (Translocator protein 18kDa) in microglia: from pathology to imaging. Prog Neurobiol 80(6): 308-322.

Xu DP, Zhang K, Zhang ZJ, Sun YW, Guo BJ, Wang YQ, et al. 2014. A novel tetramethylpyrazine bis-nitrone (TN-2) protects against 6-hydroxyldopamine-induced neurotoxicity via modulation of the NF-kappaB and the PKCalpha/PI3-K/Akt pathways. Neurochem Int 78: 76-85.

Zurich M-G, Eskes C, Honegger P, Bérode M, Monnet-Tschudi F. 2002. Maturation-dependent neurotoxicity of lead aceate in vitro: Implication of glial reactions. J Neurosc Res 70: 108-116.

LIVER:

Baeck, C. et al. (2012), Pharmacological inhibition of the chemokine CCL2 (MCP-1) diminishes liver macrophage infiltration and steatohepatitis in chronic hepatic injury, Gut, vol. 61, no. 3, pp.416–426.

Boltjes, A. et al. (2014), The role of Kupffer cells in hepatitis B and hepatitis C virus infections, J Hepatol, vol. 61, no. 3, pp. 660-671.

Bouwens, L. et al. (1986), Quantitation, tissue distribution and proliferation kinetics of Kupffer cells in normal rat liver, Hepatology, vol. 6, no. 6, pp. 718-722.

Dalton, S.R. et al. (2009), Carbon tetrachloride-induced liver damage in asialoglycoprotein receptor-deficient mice, Biochem Pharmacol, vol. 77, no. 7, pp. 1283-1290.

Friedman, S.L. (2002), Hepatic Fibrosis-Role of Hepatic Stellate Cell Activation, MedGenMed, vol. 4, no. 3, pp. 27.

Grønbaek, H. et al. (2012), Soluble CD163, a marker of Kupffer cell activation, is related to portal hypertension in patients with liver cirrhosis, Aliment Pharmacol Ther, vol 36, no. 2, pp. 173-180.

Guo, J. and S.L. Friedman (2007), Hepatic Fibrogenesis, Semin Liver Dis, vol. 27, no. 4, pp. 413-426.

Haubrich, W.S. (2004), Kupffer of Kupffer cells, Gastroenterology, vol. 127, no. 1, p. 16

Ide, M. et al. (2005), Effects of gadolinium chloride (GdCl(3)) on the appearance of macrophage populations and fibrogenesis in thioacetamide-induced rat hepatic lesions, J. Comp. Path, vol. 133, no. 2-3, pp. 92–102.

Kegel, V. et al. (2015), Subtoxic concentrations of hepatotoxic drugs lead to Kupffer cell activation in a human in vitro liver model: an approach to study DILI, Mediators Inflamm, 2015:640631, http://doi.org/10.1155/2015/640631.

Kershenobich Stalnikowitz, D. and A.B. Weissbrod (2003), Liver Fibrosis and Inflammation. A Review, Annals of Hepatology, vol. 2, no. 4, pp.159-163.

Kolios, G., V. Valatas and E. Kouroumalis (2006), Role of Kupffer Cells in the Pathogenesis of Liver Disease, World J.Gastroenterol, vol. 12, no. 46, pp. 7413-7420.

Luckey, S.W., and D.R. Petersen (2001), Activation of Kupffer cells during the course of carbon tetrachloride-induced liver injury and fibrosis in rats, Exp Mol Pathol, vol. 71, no. 3, pp. 226-240.

Møller, H.J. (2012), Soluble CD163.Scand J Clin Lab Invest, vol. 72, no. 1, pp. 1-13.

Roberts, R.A. et al. (2007), Role of the Kupffer cell in mediating hepatic toxicity and carcinogenesis, Toxicol Sci, vol. 96, no. 1, pp. 2-15.

Su, G.L. et al. (2002), Activation of human and mouse Kupffer cells by lipopolysaccharide is mediated by CD14, Am J Physiol Gastrointest Liver Physiol, vol. 283, no. 3, pp. G640-645.

Tacke, F. and H.W. Zimmermann (2014), Macrophage heterogeneity in liver injury and fibrosis, J Hepatol, vol. 60, no. 5, pp. 1090-1096.

Takahara, T et al. (2006), Gene expression profiles of hepatic cell-type specific marker genes in progression of liver fibrosis, World J Gastroenterol, vol. 12, no. 40, pp. 6473-6499.

Vajdova, K. et al. (2004), Ischemic preconditioning and intermittent clamping improve murine hepatic microcirculation and Kupffer cell function after ischemic injury, Liver Transpl, vol. 10, no. 4, pp. 520–528

Winwood, P.J., and M.J. Arthur (1993), Kupffer cells: their activation and role in animal models of liver injury and human liver disease, Semin Liver Dis, vol. 13, no. 1, pp. 50-59.

Event: 2097: Increase, Pro-Inflammatory Mediators

Short Name: Increase, Pro-Inflammatory Mediators

AOPs Including This Key Event

AOP ID and Name	Event Type
Aop:483 - Deposition of Energy Leading to Learning and Memory Impairment	KeyEvent

Biological Context

Level of Biological Organization

Tissue

Domain of Applicability

Taxonomic Applicability

Term	Scientific Term	Evidence	Links
human	Homo sapiens	Low	NCBI
rat	Rattus norvegicus	Low	NCBI
mouse	Mus musculus	Low	NCBI

Life Stage Applicability

Life Stage	Evidence
Not Otherwise Specified	Moderate

Sex Applicability

Sex	Evidence
Mixed	Moderate

Taxonomic applicability: The inflammatory response and increase of the pro-inflammatory mediators has been observed across species from simple invertebrates such as Daphnia to higher order vertebrates (Weavers & Martin, 2020).

Life stage applicability: This key event is not life stage specific (Kalm et al., 2013; Veeraraghan et al., 2011; Hladik & Tapio, 2016).

Sex applicability: Most studies conducted were on male models, although sex-dependent differences in pro-inflammatory markers have been previously reported (Cekanaviciute et al., 2018; Parihar et al., 2020).

Evidence for perturbation by a prototypic stressor: There is evidence of the increase of pro-inflammatory mediators following perturbation from a variety of stressors including exposure to ionizing radiation. (Abdel-Magied et al., 2019; Cho et al., 2017; Gaber et al., 2003; Ismail et al., 2016; Kim et al. 2002; Lee et al., 2010; Parihar et al., 2018)

Key Event Description

(Adapted from KE 1493 - in blue)

Inflammatory mediators are soluble, diffusible molecules that act locally at the site of tissue damage and infection, and at more distant sites. They can be divided into exogenous and endogenous mediators.

Exogenous mediators of inflammation are bacterial products or toxins like endotoxin or lipopolysaccharides (LPS). Endogenous mediators of inflammation are produced from within the (innate and adaptive) immune system itself, as well as other systems. They can be derived from molecules that are normally present in the plasma in an inactive form, such as peptide fragments of some components of complement, coagulation, and kinin systems. Or they can be released at the site of injury by a number of cell types that either contain them as preformed molecules within storage granules, e.g. histamine, or which can rapidly switch on the machinery required to synthesize the mediators.

This event occurs equally in various tissues and does not require tissue-specific descriptions. Nevertheless, there are some specificities such as the release of glutamate by brain reactive glial cells (Brown & Bal-Price, 2003; Vesce et al., 2007). The differences may rather reside in the type of insult favouring the increased expression and/or release of a specific class of inflammatory mediators, as well the time after the insult reflecting different stages of the inflammatory process. For these reasons, the analyses of the changes of a battery of inflammatory mediators rather than of a single one is a more adequate measurement of this KE.

Table 1: a non-exhaustive list of examples for pro-inflammatory mediators

Classes of inflammatory mediators	Examples
Pro-inflammatory cytokines	TNF- α, Interleukins (IL-1, IL-6, IL-8), Interferons (IFN-γ), chemokines (CXCL, CCL, GRO-α, MCP-1), GM-CSF
Prostaglandins	PGE2
Bioactive peptides	Bradykinin
Vasoactive amines	histamine, serotonin
Reactive oxygen species (ROS)	O2-, H2O2
Reactive nitrogen species (RNS)	NO, iNOS

The increased production of pro-inflammatory mediators can have negative consequences on the parenchymal cells leading even to cell death, as described for TNF-a or peroxynitrite on neurons (Brown and Bal-Price, 2003). Along with TNF-α, IL-1β and IL-6 have been shown to exhibit negative consequences on neurogenesis and neuronal precursor cell proliferation when overexpressed. IFN-γ is also associated with neuronal damage, although it is not as extensively studied compared to TNF-α, IL-1β and IL-6. These cytokines are normally involved in brain homeostasis and maintaining tissue repair following an injury, although it can have negative consequences (Fan & Pang, 2017). In addition, via a feedback loop, they can act on the reactive resident cells thus maintaining or exacerbating their reactive state; and by modifying elements of their signalling pathways, they can favour the M1 phenotypic polarization and the chronicity of the inflammatory process (Taetzsch et al., 2015).

Basically, this event occurs equally in various tissues and does not require tissue-specific descriptions. Nevertheless, there are some specificities such as the release of glutamate by brain reactive glial cells (Brown and Bal-Price, 2003; Vesce et al., 2007). The differences may rather reside in the type of insult favouring the increased expression and/or release of a specific class of inflammatory mediators, as well the time after the insult reflecting different stages of the inflammatory process. For these reasons, the analyses of the changes of a battery of inflammatory mediators rather than of a single one is a more adequate measurement of this KE.

How it is Measured or Detected

Listed below are common methods for detecting the KE, however there may be other comparable methods that are not listed.

Assay	Reference	Description	OECD Approved Assay

• RT-qPCR • Q-PCR	(Veremeyko et al., 2012; Alwine et al, 1977; Forlenza et al., 2012)	Measures mRNA expression of cytokines, chemokines and inflammatory markers	No
Immunoblotting (western blotting)	(Lee et al., 2008)	Uses antibodies specific to proteins of interest, can used to detect presence of pro-inflammatory mediators in samples of cell or tissue lysate	No
Whole blood stimulation assay	(Thurm & Halsey, 2005)	Detects inflammatory cytokines in blood	No
Imaging tests	(Rollins & Miskolci, 2014)	A qualitative technique using a cytokine specific antibodies and fluorophores can be used to visualize expression patterns, subcellular location of the target and protein-protein interactions. Common examples include double immunofluorescence confocal microscopy or other molecular imaging modalities.	No
Flow-cytometry	(Karanikas et al., 2000)	Detects the intracellular cytokines with stimulation.	No
Immunoassays (ex. enzyme-linked immunosorbent assay (ELISA), enzyme-linked immunospot (ELISpot), radioimmunoassay)	(Amsen et al., 2009; Engvall & Perlmann, 1972; Ji & Forsthuber, 2016; Goldsmith, 1975)	Plate based assay technique using antibodies to detect presence of a protein in a liquid sample. Can be used to identify presence of an inflammatory cytokine of interest especially when in low concentrations.	No
Inflammatory cytokine arrays	(Amsen et al., 2009)	Similar to the ELISA, except using a membrane-based rather than plate-based approach. Can be used to measure multiple cytokine targets concurrently.	No
Immunohistochemistry (IHC)	(Amsen et al., 2009; Coons et al., 1942)	Immobilized tissue or cell cultures are stained using antibodies for specificity of ligands of interest. Versions of the assays can be used to visualize localization of inflammatory cytokines.	No

References

Abdel-Magied, N., S. M., Shedid and Ahmed, A. G. (2019), “Mitigating effect of biotin against irradiation-induced cerebral cortical and hippocampal damage in the rat brain tissue”, Environmental Science and Pollution Research, Vol. 26/13, Springer, London, https://doi.org/10.1007/S11356-019-04806-X.

Alwine, J. C., D. J. Kemp and G. R. Stark (1977), “Method for detection of specific RNAs in agarose gels by transfer to diazobenzyloxymethyl-paper and hybridization with DNA probes”, Proceedings of the National Academy of Sciences of the United States of America, Vol. 74/12, United States National Academy of Sciences, Washington, D.C., https://doi.org/10.1073/pnas.74.12.5350

Amsen, D., de Visser, K. E., and Town, T. (2009), “Approaches to determine expression of inflammatory cytokines”, in Inflammation and Cancer, Humana Press, Totowa, https://doi.org/10.1007/978-1-59745-447-6_5

Brown, G. C., and A. Bal-Price (2003), “Inflammatory neurodegeneration mediated by nitric oxide, glutamate, and mitochondria”, Molecular Neurobiology, Vol. 27/3, Springer, London, https://doi.org/10.1385/MN:27:3:325

Cekanaviciute, E., S. Rosi and S. Costes. (2018), "Central Nervous System Responses to Simulated Galactic Cosmic Rays", International Journal of Molecular Sciences, Vol. 19/11, Multidisciplinary Digital Publishing Institute (MDPI) AG, Basel, https://doi.org/10.3390/ijms19113669.

Cho, H. J. et al. (2017), “Role of NADPH Oxidase in Radiation-induced Pro-oxidative and Pro-inflammatory Pathways in Mouse Brain”, International Journal of Radiation Biology, Vol. 93/11, Informa, London, https://doi.org/10.1080/09553002.2017.1377360.

Coons, A. H. et al. (1942), “The Demonstration of Pneumococcal Antigen in Tissues by the Use of Fluorescent Antibody”, The Journal of Immunology, Vol. 45/3, American Association of Immunologists, Minneapolis, pp. 159-169

Engvall, E., and P. Perlmann (1972), “Enzyme-Linked Immunosorbent Assay, Elisa”, The Journal of Immunology, Vol. 109/1, American Association of Immunologists, Minneapolis, pp. 129-135

Fan, L. W. and Y. Pang. (2017), "Dysregulation of neurogenesis by neuroinflammation: Key differences in neurodevelopmental and neurological disorders", Neural Regeneration Research, Vol. 12/3, Wolters Kluwer, Alphen aan den Rijn, https://doi.org/10.4103/1673-5374.202926.

Forlenza, M. et al. (2012), “The use of real-time quantitative PCR for the analysis of cytokine mRNA levels” in Cytokine Protocols, Springer, New York, https://doi.org/10.1007/978-1-61779-439-1_2

Gaber, M. W. et al. (2003), “Differences in ICAM-1 and TNF-alpha expression between large single fraction and fractionated irradiation in mouse brain”, International Journal of Radiation Biology, Vol. 79/5, Informa, London, https://doi.org/10.1080/0955300031000114738.

Goldsmith, S. J. (1975), "Radioimmunoassay: Review of basic principles", Seminars in Nuclear Medicine, Vol. 5/2, https://doi.org/10.1016/S0001-2998(75)80028-6.

Hladik, D. and S. Tapio. (2016), "Effects of ionizing radiation on the mammalian brain", Mutation Research/Reviews in Mutation Research, Vol. 770, Elsevier B. b., Amsterdam, https://doi.org/10.1016/j.mrrev.2016.08.003.

Ismail, A. F. M., A.A.M. Salem and M.M.T. Eassawy (2016), “Modulation of gamma-irradiation and carbon tetrachloride induced oxidative stress in the brain of female rats by flaxseed oil”, Journal of Photochemistry and Photobiology B: Biology, Vol. 161, Elsevier, Amsterdam, https://doi.org/10.1016/J.JPHOTOBIOL.2016.04.031.

Ji, N. and T. G. Forsthuber. (2014), "ELISPOT Techniques" (pp. 63–71), https://doi.org/10.1007/7651_2014_111.

Kalm, M., K. Roughton and K. Blomgren. (2013), "Lipopolysaccharide sensitized male and female juvenile brains to ionizing radiation", Cell Death & Disease, Vol. 4/12, Nature Publishing Group, Berlin, https://doi.org/10.1038/cddis.2013.482.

Karanikas, V. et al. (2000), “Flow cytometric measurement of intracellular cytokines detects immune responses in MUC1 immunotherapy”, Clinical Cancer Research, Vol. 6/3, American Association for Cancer Research, Philadelphia, pp. 829–837

Kim, S. H. et al. (2002), “Expression of TNF-alpha and TGF-beta 1 in the rat brain after a single high-dose irradiation”, Journal of Korean Medical Science, Vol. 17/2, Korean Medical Association, Seoul, https://doi.org/10.3346/JKMS.2002.17.2.242.

Lee, J. W. et al. (2008), “Neuro-inflammation induced by lipopolysaccharide causes cognitive impairment through enhancement of beta-amyloid generation”, Journal of Neuroinflammation, Vol. 5/1, BioMed Central, London, https://doi.org/10.1186/1742-2094-5-37

Lee, W. H. et al. (2010), “Irradiation induces regionally specific alterations in pro-inflammatory environments in rat brain”, International Journal of Radiation Biology, Vol. 86/2, Informa, London, https://doi.org/10.3109/09553000903419346.

Parihar, V. K. et al. (2018), “Persistent nature of alterations in cognition and neuronal circuit excitability after exposure to simulated cosmic radiation in mice”, Experimental Neurology, Vol. 305, Elsevier, Amsterdam, https://doi.org/10.1016/J.EXPNEUROL.2018.03.009.

Parihar, V. K. et al. (2020), "Sex-Specific Cognitive Deficits Following Space Radiation Exposure", Frontiers in Behavioral Neuroscience, Vol. 14, https://doi.org/10.3389/fnbeh.2020.535885.

Rollins, J. and V. Miskolci (2014), “Immunofluorescence and subsequent confocal microscopy of intracellular TNF in human neutrophils” in Cytokines Bioassays, Springer, London, https://doi.org/10.1007/978-1-4939-0928-5_24

Taetzsch, T. et al. (2015), "Redox regulation of NF-κB p50 and M1 polarization in microglia", Glia, Vol. 63/3, John Wiley & Sons, Hoboken, https://doi.org/10.1002/glia.22762.

Thurm, C. W. and J. F. Halsey (2005), “Measurement of Cytokine Production Using Whole Blood”, in Current Protocols in Immunology, John Wiley & Sons, Inc., Hoboken, https://doi.org/10.1002/0471142735.im0718bs66

Veeraraghavan, J. et al. (2011), "Low-dose γ-radiation-induced oxidative stress response in mouse brain and gut: Regulation by NFκB–MnSOD cross-signaling", Mutation Research/Genetic Toxicology and Environmental Mutagenesis, Vol. 718/1–2, Elsevier, Amsterdam, https://doi.org/10.1016/j.mrgentox.2010.10.006.

Veremeyko, T. et al. (2012), “Detection of microRNAs in microglia by real-time PCR in normal CNS and during neuroinflammation”, Journal of Visualized Experiments: JoVE, Vol. 65, MyJove Corporation, Cambridge, https://doi.org/10.3791/4097

Vesce, S. et al. (2007), “Glutamate release from astrocytes in physiological conditions and in neurodegenerative disorders characterized by neuroinflammation”, International Review of Neurobiology, Vol. 82, Elsevier, Amsterdam, https://doi.org/10.1016/S0074-7742(07)82003-4

Weavers, H. and P. Martin (2020), “The cell biology of inflammation: From common traits to remarkable immunological adaptations”, Journal of Cell Biology, Vol. 219, Rockefeller University Press, New York, https://doi.org/10.1083/jcb.202004003

Event: 2098: Increase, Neural Remodeling

Short Name: Increase, Neural Remodeling

AOPs Including This Key Event

AOP ID and Name	Event Type

AOP ID and Name	Event Type
Aop:483 - Deposition of Energy Leading to Learning and Memory Impairment	KeyEvent

Biological Context

Level of Biological Organization

Tissue

Domain of Applicability

Taxonomic Applicability

Term	Scientific Term	Evidence	Links
dog	Canis lupus familiaris	Low	NCBI
rat	Rattus norvegicus	Moderate	NCBI
mouse	Mus musculus	Moderate	NCBI

Life Stage Applicability

Life Stage	Evidence
Juvenile	Low
Adult	Moderate

Sex Applicability

Sex	Evidence
Male	Moderate
Female	Low
Unspecific	Low

Taxonomic applicability: The ability to process complex spatiotemporal information through neuronal networking is a fundamental process underlying the behavior of all higher organisms. The most studied are the neuronal networks of vertebrates such as rodents (Cekanaviciute et al., 2018) and primates (Wang and Arnsten, 2015). https://pubmed.ncbi.nlm.nih.gov/26876924/Invertebrates hold neural circuitries in various degrees of complexity and there are studies describing how neurons are organized into functional networks to generate behaviour (Wong and Wong, 2004; Marder, 1994).

Life stage applicability: This key event is applicable to all life stages, most evidence is derived from studies in adults (Cekanaviciute et al., 2018; Hladik & Tapio, 2016).

Sex applicability: This key event is not sex specific (Hladik & Tapio, 2016).

Evidence for perturbation by a prototypic stressor: Current literature provides ample evidence of neural remodeling being induced by stressors including ionizing radiation (Allen et al., 2015; Cekanaviciute et al., 2018; J. R. Fike et al., 1984; John R. Fike et al., 1988; Hladik & Tapio, 2016; Kiffer et al., 2020; Mizumatsu et al., 2003; Okamoto et al., 2009; Vipan K. Parihar et al., 2016; Vipan K. Parihar; Rola et al., 2005; Tiller-Borcich et al., 1987).

Key Event Description

(Adapted from KE: 618)

Neural remodeling describes abnormal changes in structure and function of the central nervous system (CNS), which occur in the presence of a neuronal input (Chakraborti et al., 2012). However, these connections can also be altered by stressors and stimuli. The neuron is comprised of the cell body, dendrites, axon, and axon terminals (Lodish et al., 2000). Dendritic spines exist in many shapes and sizes, categorized as thin, mushroom, or stubby types (Harris & Stevens, 1989). The presence of immature dendritic spine morphologies and changes in dendritic spine density and structure, including decreases in dendritic branch points, length, and area, are correlated with changes in excitatory synaptic transmission strength (Jandial et al., 2018; Auffret et al., 2009). Dendritic protein synthesis is required for many types of long-term synaptic plasticity (Sutton & Schuman 2006). Changes to the levels of protein synthesis greatly affects neuronal communication. The CNS architecture is also affected by decreases in neurogenesis and increases in neurodegeneration, as dendritic complexity decreases. These events provoke changes in synaptic plasticity and action potential, ultimately leading to the disruption of neuronal signalling (Cekanaviciute et al., 2018).

How it is Measured or Detected

Method of Measurement	References	Description	OECD-Approved Assay
MRI Scan	Jiang et al., 2014	Magnetic resonance imaging (MRI) is an imaging technique used to visualize organs and tissues in the body. MRI can be used to view demyelination.	No
Fluoro-Jade stain	Schmued and Hopkins, 2000	Detects and labels degenerating neurons.	No
3-(4,5-dimethylthiazol-2-yl)-2,5-diphenyl-2H-tetrazolium bromide (MTT) Assay – colorimetric assay used to assess cell metabolic activity based on the reduction of (3-(4,5-dimethylthiazol-2-yl)-2,5-diphenyltetrazolium bromide.	Riss et al., 2004	Cell viability and proliferation assays can be used to measure increased levels of neurodegeneration or decreased levels of neurogenesis.	Yes
Bromodeoxyuridine (BrdU) labeling	Vallieres et al., 2002	Staining method used to identify proliferating cells and measures neurogenesis.	No
SYNPLA	Dore et al., 2020	Synaptic proximity ligation assay (SYNPLA) is a technique that detects learning-induced synaptic plasticity.	No
ELISA	Falsig et al., 2003; Lund et al., 2006; Monnet-Tschudi et al., 2011	The enzyme-linked immunosorbent assay (ELISA) is a technique that detects and quantifies levels of macromolecules such as peptides, proteins, antibodies, and hormones. It can be used to detect specific molecules in neurons that represent loss in integrity such as PSD-95, synapsin 1 or drebrin.	No
Immunoassay/microscopy	Falsig et al., 2003; Lund et al., 2006; Monnet-Tschudi et al., 2011	Various methods that use the specificity of antigen-antibody binding for detection and quantification of target molecules such as PSD-95, synpasin 1, Ki-67 and drebrin.	No
Western Blot	Yang and Mahmood, 2012	Protein identification from a complex mixture after size separation, transfer to solid support and marking target protein. Specific markers include PSD-95, synpasin 1, Ki-67 and drebrin.	No
Golgi-Cox Method	Zaqout and Kaindl, 2016	Visualizes neuronal morphology in vivo.	No
Whole-cell electrophysiology	Hill and Stephens, 2021	Measures intracellular electrical properties by visualizing ionic currents.	No
Terminal deoxynucleotidyl transferase-mediated dUTP nick end-labeling (TUNEL) assay	Kressel and Groscurth, 1994	Apoptosis is detected with the TUNEL method to assay the endonuclease cleavage products by enzymatically end-labeling the DNA strand breaks.	Yes

References

Allen, A. R. et al. (2015), "56Fe Irradiation Alters Spine Density and Dendritic Complexity in the Mouse Hippocampus", Radiation Research, Vol. 184/6, BioOne, Washington, https://doi.org/10.1667/RR14103.1.

Alvarez, M. L. and S. C. Doné. (2014), "SYBR® Green and TaqMan® Quantitative PCR Arrays: Expression Profile of Genes Relevant to a Pathway or a Disease State" (pp. 321–359), Springer Nature, Berlin, https://doi.org/10.1007/978-1-4939-1062-5_27.

Auffret, A. et al. (2009), "Age-Dependent Impairment of Spine Morphology and Synaptic Plasticity in Hippocampal CA1 Neurons of a Presenilin 1 Transgenic Mouse Model of Alzheimer's Disease", Journal of Neuroscience, Vol. 29/32, Society for Neuroscience, Washington, https://doi.org/10.1523/JNEUROSCI.1856-09.2009.

Cekanaviciute, E., S. Rosi and S. V. Costes. (2018), "Central nervous system responses to simulated galactic cosmic rays", International Journal of Molecular Sciences, Vol. 19/11, Multi-Disciplinary Digital Publishing Institute, Basel, https://doi.org/10.3390/ijms19113669.

Chakraborti, A. et al. (2012), "Cranial Irradiation Alters Dendritic Spine Density and Morphology in the Hippocampus", (P.J. Tofilon,

Ed.) PLoS ONE, Vol. 7/7, Public Library of Science, San Francisco, https://doi.org/10.1371/journal.pone.0040844.

Dore, K. et al. (2020), "SYNPLA, a method to identify synapses displaying plasticity after learning", Proceedings of the National Academy of Sciences, Vol. 117/6, Proceedings of the National Academy of Sciences, https://doi.org/10.1073/pnas.1919911117.

Falsig, J., M. Latta and M. Leist. (2003), "Defined inflammatory states in astrocyte cultures: correlation with susceptibility towards CD95-driven apoptosis", Journal of Neurochemistry, Vol. 88/1, John Wiley & Sons, Inc., Hoboken, https://doi.org/10.1111/j.1471-4159.2004.02144.x.

Fike, J. R. et al. (1984), "Computed Tomography Analysis of the Canine Brain: Effects of Hemibrain X Irradiation", Radiation Research, Vol. 99/2, Allen Press, Lawrence, https://doi.org/10.2307/3576373.

Fike, J. R. et al. (1988), "Radiation dose response of normal brain", International Journal of Radiation Oncology, Biology, Physics, Vol. 14/1, Elsevier, Amsterdam, https://doi.org/10.1016/0360-3016(88)90052-1.

Harris, K. and J. Stevens. (1989), "Dendritic spines of CA 1 pyramidal cells in the rat hippocampus: serial electron microscopy with reference to their biophysical characteristics", The Journal of Neuroscience, Vol. 9/8, Society for Neuroscience, Washington, https://doi.org/10.1523/JNEUROSCI.09-08-02982.1989.

Hill, C. L. and G. J. Stephens. (2021), "An Introduction to Patch Clamp Recording" (pp. 1–19), https://doi.org/10.1007/978-1-0716-0818-0_1.

Hladik, D. and S. Tapio. (2016), "Effects of ionizing radiation on the mammalian brain", Mutation Research/Reviews in Mutation Research, Vol. 770, Elsevier B. b., Amsterdam, https://doi.org/10.1016/j.mrrev.2016.08.003.

Kiffer, F. et al. (2020), "Late Effects of 1H + 16O on Short-Term and Object Memory, Hippocampal Dendritic Morphology and Mutagenesis", Frontiers in Behavioral Neuroscience, Vol. 14, Frontiers Media S.A., https://doi.org/10.3389/fnbeh.2020.00096.

Kressel, M. and P. Groscurth (1994), "Distinction of apoptotic and necrotic cell death by in situ labelling of fragmented DNA", Cell and tissue research, Vol. 278/3, Nature, https://doi.org/10.1007/BF00331373.

Kukurba, K. R. and S. B. Montgomery. (2015), "RNA Sequencing and Analysis", Cold Spring Harbor Protocols, Vol. 2015/11, https://doi.org/10.1101/pdb.top084970.

Jandial, R. et al. (2018), "Space–brain: The negative effects of space exposure on the central nervous system", Surgical Neurology International, Vol. 9/1, https://doi.org/10.4103/sni.sni_250_17.

Jiang, X. et al. (2014), "A GSK-3β Inhibitor Protects Against Radiation Necrosis in Mouse Brain", International Journal of Radiation Oncology*Biology*Physics, Vol. 89/4, Elsevier, Amsterdam, https://doi.org/10.1016/j.ijrobp.2014.04.018.

Lodish, H., et al. (2000). Overview of Neuron Structure and Function. https://www.ncbi.nlm.nih.gov/books/NBK21535/

Lund, S. et al. (2006), "The dynamics of the LPS triggered inflammatory response of murine microglia under different culture and in vivo conditions", Journal of Neuroimmunology, Vol. 180/1–2, Elsevier, Amsterdam, https://doi.org/10.1016/j.jneuroim.2006.07.007.

Marder, E. (1994), "Invertebrate Neurobiology: Polymorphic neural networks", Current Biology, Vol. 4/8, Elsevier, Amsterdam, https://doi.org/10.1016/S0960-9822(00)00169-X.

Mizumatsu, S. et al. (2003), "Extreme sensitivity of adult neurogenesis to low doses of X-irradiation", Cancer Research, Vol. 63/14.

Monnet-Tschudi, F. et al. (2011), "Methods to Assess Neuroinflammation", Current Protocols in Toxicology, Vol. 50/1, John Wiley & Sons, Inc., Hoboken, https://doi.org/10.1002/0471140856.tx1219s50.

Okamoto, M. et al. (2009), "Effect of radiation on the development of immature hippocampal neurons in vitro", Radiation Research, Vol. 172/6, BioOne, Washington, https://doi.org/10.1667/RR1741.1.

Parihar, V. K. et al. (2016), "Cosmic radiation exposure and persistent cognitive dysfunction", Scientific Reports, Vol. 6/June, Nature Publishing Group, Berlin, https://doi.org/10.1038/srep34774.

Parihar, V. K. et al. (2015), "What happens to your brain on the way to Mars", Science Advances, Vol. 1/4, American Association for the Advancement of Science, Washington, https://doi.org/10.1126/SCIADV.1400256.

Riss, T. L. et al. (2004), Cell Viability Assays, Assay Guidance Manual, http://www.ncbi.nlm.nih.gov/pubmed/23805433.

Rola, R. et al. (2005), "High-LET radiation induces inflammation and persistent changes in markers of hippocampal neurogenesis", Radiation Research (Volume 164, pp. 556–560), BioOne, Washington, https://doi.org/10.1667/RR3412.1.

Schmued, L. C. and K. J. Hopkins. (2000), "Fluoro-Jade B: a high affinity fluorescent marker for the localization of neuronal degeneration", Brain Research, Vol. 874/2, Elsevier, Amsterdam, https://doi.org/10.1016/S0006-8993(00)02513-0.

Sutton, M. A. and E. M. Schuman. (2006), "Dendritic Protein Synthesis, Synaptic Plasticity, and Memory", Cell, Vol. 127/1, Elsevier, Amsterdam, https://doi.org/10.1016/j.cell.2006.09.014.

Tiller-Borcich, J. K. et al. (1987), "Pathology of Delayed Radiation Brain Damage: An Experimental Canine Model", Radiation

Research, Vol. 110/2, Allen Press, Lawrence, https://doi.org/10.2307/3576896.

Valliéres, L. et al. (2002), "Reduced hippocampal neurogenesis in adult transgenic mice with chronic astrocytic production of interleukin-6", Journal of Neuroscience, Vol. 22/2, Society for Neuroscience, Washington, https://doi.org/10.1523/jneurosci.22-02-00486.2002.

Wang, M. and A. F. T. Arnsten. (2015), "Contribution of NMDA receptors to dorsolateral prefrontal cortical networks in primates", Neuroscience Bulletin, Vol. 31/2, Springer Nature, Berlin, https://doi.org/10.1007/s12264-014-1504-6.

Wong Y.H. and Wong J.T.Y. (2004), Invertebrate Neural Networks, (Y.H. Wong & J.T.Y. Wong, Eds.), S. Karger AG, https://doi.org/10.1159/isbn.978-3-318-01075-6.

Yang, P.-C. and T. Mahmood. (2012), "Western blot: Technique, theory, and trouble shooting", North American Journal of Medical Sciences, Vol. 4/9, Wolters Kluwer, Alphen aan den Rijn, https://doi.org/10.4103/1947-2714.100998.

Zaqout, S. and A. M. Kaindl. (2016), "Golgi-Cox Staining Step by Step", Frontiers in Neuroanatomy, Vol. 10, Frontiers Media, https://doi.org/10.3389/fnana.2016.00038.

Event: 1635: Increase, DNA strand breaks

Short Name: Increase, DNA strand breaks

AOPs Including This Key Event

AOP ID and Name	Event Type
Aop:296 - Oxidative DNA damage leading to chromosomal aberrations and mutations	KeyEvent
Aop:272 - Deposition of energy leading to lung cancer	KeyEvent
Aop:322 - Alkylation of DNA leading to reduced sperm count	KeyEvent
Aop:216 - Deposition of energy leading to population decline via DNA strand breaks and follicular atresia	KeyEvent
Aop:238 - Deposition of energy leading to population decline via DNA strand breaks and oocyte apoptosis	KeyEvent
Aop:478 - Deposition of energy leading to occurrence of cataracts	KeyEvent
Aop:483 - Deposition of Energy Leading to Learning and Memory Impairment	KeyEvent
Aop:470 - Deposition of energy leads to vascular remodeling	KeyEvent

Stressors

Name
Ionizing Radiation
Topoisomerase inhibitors
Radiomimetic compounds

Biological Context

Level of Biological Organization
Molecular

Domain of Applicability

Taxonomic Applicability

Term	Scientific Term	Evidence	Links
human and other cells in culture	human and other cells in culture		NCBI

Life Stage Applicability

Life Stage	Evidence
All life stages	High

Sex Applicability

Sex	Evidence
Unspecific	High

Taxonomic applicability: DNA strand breaks are relevant to all species, including vertebrates such as humans, that contain DNA (Cannan & Pederson, 2016).

Life stage applicability: This key event is not life stage specific as all life stages display strand breaks. However, there is an increase in baseline levels of DNA strand breaks seen in older individuals though it is unknown whether this change due to increased break induction or a greater retention of breaks due to poor repair (White & Vijg, 2016).

Sex applicability: This key event is not sex specific as both sexes display evidence of strand breaks. In some cell types, such as peripheral blood mononuclear cells, males show higher levels of single strand breaks than females (Garm et al., 2012).

Evidence for perturbation by a stressor: There are studies demonstrating that increased DNA strand breaks can result from exposure to multiple stressor types including ionizing & non-ionizing radiation, chemical agents, and oxidizing agents (EPRI, 2014; Hamada, 2014; Cencer et al., 2018; Cannan & Pederson, 2016; Yang et al., 1998).

Key Event Description

DNA strand breaks can occur on a single strand (SSB) or both strands (double strand breaks; DSB). SSBs arise when the phosphate backbone connecting adjacent nucleotides in DNA is broken on one strand. DSBs are generated when both strands are simultaneously broken at sites that are sufficiently close to one another that base-pairing and chromatin structure are insufficient to keep the two DNA ends juxtaposed. As a consequence, the two DNA ends generated by a DSB can physically dissociate from one another, becoming difficult to repair and increasing the chance of inappropriate recombination with other sites in the genome (Jackson, 2002). SSB can turn into DSB if the replication fork stalls at the lesion leading to fork collapse.

Strand breaks are intermediates in various biological events, including DNA repair (e.g., excision repair), V(D)J recombination in developing lymphoid cells and chromatin remodeling in both somatic cells and germ cells. The spectrum of damage can be complex, particularly if the stressor is from large amounts of deposited energy which can result in complex lesions and clustered damage defined as two or more oxidized bases, abasic sites or starnd breaks on opposing DNA strands within a few helical turns. These lesions are more difficult to repair and have been studied in many types of models (Barbieri et al., 2019 and Asaithamby et al., 2011). DSBs and complex lesions are of particular concern, as they are considered the most lethal and deleterious type of DNA lesion. If misrepaired or left unrepaired, DSBs may drive the cell towards genomic instability, apoptosis or tumorigenesis (Beir, 1999).

How it is Measured or Detected

Please refer to the table below for details regarding these and other methodologies for detecting DNA DSBs.

Assay Name	References	Description	OECD Approved Assay
Comet Assay (Single Cell Gel Eletrophoresis - Alkaline)	Collins, 2004; Olive and Banath, 2006; Platel et al., 2011; Nikolova et al., 2017	To detect SSBs or DSBs, single cells are encapsulated in agarose on a slide, lysed, and subjected to gel electrophoresis at an alkaline pH (pH >13); DNA fragments are forced to move, forming a "comet"-like appearance	Yes (No. 489)
Comet Assay (Single Cell Gel Eltrophoresis - Neutral)	Collins, 2014; Olive and Banath, 2006; Anderson and Laubenthal, 2013; Nikolova et al., 2017	To detect DSBs, single cells are encapsulated in agarose on a slide, lysed, and subjected to gel electrophoresis at a neutral pH; DNA fragments, which are not denatured at the neutral pH, are forced to move, forming a "comet"-like appearance	N/A
γ-H2AX Foci Quantification - Flow Cytometry	Rothkamm and Horn, 2009; Bryce et al., 2016	Measurement of γ-H2AX immunostaining in cells by flow cytometry, normalized to total levels of H2AX	N/A
γ-H2AX Foci Quantification - Western Blot	Burma et al., 2001; Revet et al., 2011	Measurement of γ-H2AX immunostaining in cells by Western blotting, normalized to total levels of H2AX	N/A
γ-H2AX Foci Quantification - Microscopy	Redon et al., 2010; Mah et al., 2010; Garcia-Canton et al., 2013	Quantification of γ-H2AX immunostaining by counting γ- H2AX foci visualized with a microscope	N/A
γ-H2AX Foci Detection - ELISA and flow cytometry	Ji et al., 2017; Bryce et al., 2016	Detection of γ-H2AX in cells by ELISA, normalized to total levels of H2AX; γH2AX foci detection can be high-throughput and automated using flow cytometry-based	N/A

		immunodetection.	
Pulsed Field Gel Electrophoresis (PFGE)	Ager et al., 1990; Gardiner et al., 1985; Herschleb et al., 2007; Kawashima et al., 2017	To detect DSBs, cells are embedded and lysed in agarose, and the released DNA undergoes gel electrophoresis in which the direction of the voltage is periodically alternated; Large DNA fragments are thus able to be separated by size	N/A
The TUNEL (Terminal Deoxynucleotidyl Transferase dUTP Nick End Labeling) Assay	Loo, 2011	To detect strand breaks, dUTPs added to the 3'OH end of a strand break by the DNA polymerase terminal deoxynucleotidyl transferase (TdT) are tagged with a fluorescent dye or a reporter enzyme to allow visualization (We note that this method is typically used to measure apoptosis)	N/A
In Vitro DNA Cleavage Assays using Topoisomerase	Nitiss, 2012	Cleavage of DNA can be achieved using purified topoisomerase; DNA strand breaks can then be separated and quantified using gel electrophoresis	N/A
PCR assay	Figueroa-González & Pérez-Plasencia, 2017	Assay of strand breaks through the observation of DNA amplification prevention. Breaks block Taq polymerase, reducing the number of DNA templates, preventing amplification	N/A
Sucrose density gradient centrifuge	Raschke et al. 2009	Division of DNA pieces by density, increased fractionation leads to lower density pieces, with the use of a sucrose cushion	N/A
Alkaline Elution Assay	Kohn, 1991	Cells lysed with detergent-solution, filtered through membrane to remove all but intact DNA	N/A
Unwinding Assay	Nacci et al. 1992	DNA is stored in alkaline solutions with DNA-specific dye and allowed to unwind following removal from tissue, increased strand damage associated with increased unwinding	N/A

References

Ager, D. D. et al. (1990). “Measurement of Radiation- Induced DNA Double-Strand Breaks by Pulsed-Field Gel Electrophoresis.” Radiat Res. 122(2), 181-7.

Anderson, D. & Laubenthal J. (2013), “Analysis of DNA Damage via Single-Cell Electrophoresis. In: Makovets S, editor. DNA Electrophoresis. Totowa.”, NJ: Humana Press. p 209-218.

Asaithamby, A., B. Hu and D.J. Chen. (2011) Unrepaired clustered DNA lesions induce chromosome breakage in human cells. Proc Natl Acad Sci U S A 108(20): 8293-8298 .

Barbieri, S., G. Babini, J. Morini et a l (2019). . Predicting DNA damage foci and their experimental readout with 2D microscopy: a unified approach applied to photon and neutron exposures. Scientific Reports 9(1): 14019

Bryce, S. et al. (2016), “Genotoxic mode of action predictions from a multiplexed flow cytometric assay and a machine learning approach.”, Environ Mol Mutagen. 57:171-189. Doi: 10.1002/em.21996.

Burma, S. et al. (2001), “ATM phosphorylates histone H2AX in response to DNA double-strand breaks.”, J Biol Chem, 276(45): 42462-42467. doi:10.1074/jbc.C100466200

Cannan, W.J. and D.S. Pederson (2016), "Mechanisms and Consequences of Double-Strand DNA Break Formation in Chromatin.", Journal of Cellular Physiology, Vol.231/1, Wiley, New York, https://doi.org/10.1002/jcp.25048.

Cencer, C. et al. (2018), “PARP-1/PAR Activity in Cultured Human Lens Epithelial Cells Exposed to Two Levels of UVB Light”, Photochemistry and Photobiology, Vol.94/1, Wiley-Blackwell, Hoboken, https://doi.org/10.1111/php.12814.

Charlton, E. D. et al. (1989), “Calculation of Initial Yields of Single and Double Stranded Breaks in Cell Nuclei from Electrons, Protons, and Alpha Particles.”, Int. J. Radiat. Biol. 56(1): 1-19. doi: 10.1080/09553008914551141.

Collins, R. A. (2004), “The Comet Assay for DNA Damage and Repair. Molecular Biotechnology.”, Mol Biotechnol. 26(3): 249-61. doi:10.1385/MB:26:3:249

EPRI (2014), Epidemiology and mechanistic effects of radiation on the lens of the eye: Review and scientific appraisal of the literature, EPRI, California.

Figueroa-González, G. and C. Pérez-Plasencia. (2017), “Strategies for the evaluation of DNA damage and repair mechanisms in cancer”, Oncology Letters, Vol.13/6, Spandidos Publications, Athens, https://doi.org/10.3892/ol.2017.6002.

Garcia-Canton, C. et al. (2013), “Assessment of the in vitro p-H2AX assay by High Content Screening asa novel genotoxicity test.”, Mutat Res. 757:158-166. Doi: 10.1016/j.mrgentox.2013.08.002

Gardiner, K. et al. (1986), “Fractionation of Large Mammalian DNA Restriction Fragments Using Vertical Pulsed-Field Gradient Gel Electrophoresis.”, Somatic Cell and Molecular Genetics. 12(2): 185-95.Doi: 10.1007/bf01560665.

Garm, C. et al. (2012), “Age and gender effects on DNA strand break repair in peripheral blood mononuclear cells”, Aging Cell, Vol.12/1, Blackwell Publishing Ltd, Oxford, https://doi.org/10.1111/acel.12019.

Hamada, N. (2014), “What are the intracellular targets and intratissue target cells for radiation effects?”, Radiation research, Vol. 181/1, The Radiation Research Society, Indianapolis, https://doi.org/10.1667/RR13505.1.

Herschleb, J. et al. (2007), “Pulsed-field gel electrophoresis.”, Nat Protoc. 2(3): 677-684. doi:10.1038/nprot.2007.94

Iliakis, G. et al. (2015), “Alternative End-Joining Repair Pathways Are the Ultimate Backup for Abrogated Classical Non-Homologous End-Joining and Homologous Recombination Repair: Implications for the Formation of Chromosome Translocations.”, Mutation Research/Genetic Toxicology and Environmental Mutagenesis. 2(3): 677-84. doi: 10.1038/nprot.2007.94

Jackson, S. (2002). “Sensing and repairing DNA double-strand breaks.”, Carcinogenesis. 23:687-696. Doi:10.1093/carcin/23.5.687.

Ji, J. et al. (2017), “Phosphorylated fraction of H2AX as a measurement for DNA damage in cancer cells and potential applications of a novel assay.”, PLoS One. 12(2): e0171582. doi:10.1371/journal.pone.0171582

Kawashima, Y.(2017), “Detection of DNA double-strand breaks by pulsed-field gel electrophoresis.”, Genes Cells 22:84-93. Doi: 10.1111/gtc.12457.

Khoury, L. et al. (2013), “Validation of high-throughput genotoxicity assay screening using cH2AX in-cell Western assay on HepG2 cells.”, Environ Mol Mutagen, 54:737-746. Doi: 10.1002/em.21817.

Khoury, L. et al. (2016), “Evaluation of four human cell lines with distinct biotransformation properties for genotoxic screening.”, Mutagenesis, 31:83-96. Doi: 10.1093/mutage/gev058.

Kohn, K.W. (1991), “Principles and practice of DNA filter elution”, Pharmacology & Therapeutics, Vol.49/1, Elsevier, Amsterdam, https://doi.org/10.1016/0163-7258(91)90022-E.

Loo, DT. (2011), “In Situ Detection of Apoptosis by the TUNEL Assay: An Overview of Techniques. In: Didenko V, editor. DNA Damage Detection In Situ, Ex Vivo, and In Vivo. Totowa.”, NJ: Humana Press. p 3-13.doi: 10.1007/978-1-60327-409-8_1.

Mah, L. J. et al. (2010), “Quantification of gammaH2AX foci in response to ionising radiation.”, J Vis Exp(38). doi:10.3791/1957.

Nacci, D. et al. (1992), “Application of the DNA alkaline unwinding assay to detect DNA strand breaks in marine bivalves”, Marine Environmental Research, Vol.33/2, Elsevier BV, Amsterdam, https://doi.org/10.1016/0141-1136(92)90134-8.

Nikolova, T., F. et al. (2017), “Genotoxicity testing: Comparison of the γH2AX focus assay with the alkaline and neutral comet assays.”, Mutat Res 822:10-18. Doi: 10.1016/j.mrgentox.2017.07.004.

Nitiss, J. L. et al. (2012), “Topoisomerase assays. ”, Curr Protoc Pharmacol. Chapter 3: Unit 3 3.

OECD. (2014). Test No. 489: “In vivo mammalian alkaline comet assay.” OECD Guideline for the Testing of Chemicals, Section 4 .

Olive, P. L., & Banáth, J. P. (2006), “The comet assay: a method to measure DNA damage in individual cells.”, Nature Protocols. 1(1): 23-29. doi:10.1038/nprot.2006.5.

Platel A. et al. (2011), “Study of oxidative DNA damage in TK6 human lymphoblastoid cells by use of the thymidine kinase gene-mutation assay and the *in vitro* modified comet assay: Determination of No-Observed-Genotoxic-Effect-Levels.”, Mutat Res 726:151-159. Doi: 10.1016/j.mrgentox.2011.09.003.

Raschke, S., J. Guan and G. Iliakis. (2009), “Application of alkaline sucrose gradient centrifugation in the analysis of DNA replication after DNA damage”, Methods in Molecular Biology, Vol.521, Humana Press, Totowa, https://doi.org/10.1007/978-1-60327-815-7_18.

Redon, C. et al. (2010), “The use of gamma-H2AX as a biodosimeter for total-body radiation exposure in non-human primates.”, PLoS One. 5(11): e15544. doi:10.1371/journal.pone.0015544

Revet, I. et al. (2011), “Functional relevance of the histone γH2Ax in the response to DNA damaging agents.” Proc Natl Acad Sci USA.108:8663-8667. Doi: 10.1073/pnas.1105866108

Rogakou, E.P. et al. (1998), “DNA Double-stranded Breaks Induce Histone H2AX Phosphorylation on Serine 139.” , J Biol Chem, 273:5858-5868. Doi: 10.1074/jbc.273.10.5858

Rothkamm, K. & Horn, S. (2009), “γ-H2AX as protein biomarker for radiation exposure.”, Ann Ist Super Sanità, 45(3): 265-71.

White, R.R. and J. Vijg. (2016), “Do DNA Double-Strand Breaks Drive Aging?”, Molecular Cell, Vol.63, Elsevier, Amsterdam,

http://doi.org/10.1016/j.molcel.2016.08.004.

Yang, Y. et al. (1998), “The effect of catalase amplification on immortal lens epithelial cell lines”, Experimental Eye Research, Vol.67/6, Academic Press Inc, Cambridge, https://doi.org/10.1006/exer.1998.0560.

List of Adverse Outcomes in this AOP

Event: 341: Impairment, Learning and memory

Short Name: Impairment, Learning and memory

Key Event Component

Process	Object	Action
learning		decreased
memory		decreased

AOPs Including This Key Event

AOP ID and Name	Event Type
Aop:13 - Chronic binding of antagonist to N-methyl-D-aspartate receptors (NMDARs) during brain development induces impairment of learning and memory abilities	AdverseOutcome
Aop:48 - Binding of agonists to ionotropic glutamate receptors in adult brain causes excitotoxicity that mediates neuronal cell death, contributing to learning and memory impairment.	AdverseOutcome
Aop:54 - Inhibition of Na+/I- symporter (NIS) leads to learning and memory impairment	AdverseOutcome
Aop:77 - Nicotinic acetylcholine receptor activation contributes to abnormal foraging and leads to colony death/failure 1	KeyEvent
Aop:78 - Nicotinic acetylcholine receptor activation contributes to abnormal role change within the worker bee caste leading to colony death failure 1	KeyEvent
Aop:87 - Nicotinic acetylcholine receptor activation contributes to abnormal foraging and leads to colony loss/failure	KeyEvent
Aop:88 - Nicotinic acetylcholine receptor activation contributes to abnormal foraging and leads to colony loss/failure via abnormal role change within caste	KeyEvent
Aop:89 - Nicotinic acetylcholine receptor activation followed by desensitization contributes to abnormal foraging and directly leads to colony loss/failure	KeyEvent
Aop:90 - Nicotinic acetylcholine receptor activation contributes to abnormal roll change within the worker bee caste leading to colony loss/failure 2	KeyEvent
Aop:12 - Chronic binding of antagonist to N-methyl-D-aspartate receptors (NMDARs) during brain development leads to neurodegeneration with impairment in learning and memory in aging	AdverseOutcome
Aop:99 - Histamine (H2) receptor antagonism leading to reduced survival	KeyEvent
Aop:17 - Binding of electrophilic chemicals to SH(thiol)-group of proteins and /or to seleno-proteins involved in protection against oxidative stress during brain development leads to impairment of learning and memory	AdverseOutcome
Aop:442 - Inhibition of voltage gate sodium channels leading to impairment in learning and memory during development	AdverseOutcome
Aop:475 - Binding of chemicals to ionotropic glutamate receptors leads to impairment of learning and memory via loss of drebrin from dendritic spines of neurons	AdverseOutcome
Aop:483 - Deposition of Energy Leading to Learning and Memory Impairment	AdverseOutcome
Aop:490 - Increased glutamate leads to economic burden through reduced IQ and non-cholinergic mechanisms	AdverseOutcome

Biological Context

Level of Biological Organization

Individual

Domain of Applicability

Taxonomic Applicability

Term	Scientific Term	Evidence	Links
human	Homo sapiens	High	NCBI
rat	Rattus norvegicus	High	NCBI
fruit fly	Drosophila melanogaster	High	NCBI
zebrafish	Danio rerio	High	NCBI
gastropods	Physa heterostropha	High	NCBI
mouse	Mus musculus	High	NCBI

Life Stage Applicability

Life Stage	Evidence
During brain development	High
Adult, reproductively mature	High

Sex Applicability

Sex	Evidence
Mixed	High

Basic forms of learning behavior such as habituation have been found in many taxa from worms to humans (Alexander, 1990). More complex cognitive processes such as executive function likely reside only in higher mammalian species such as non-human primates and humans. Recently, larval zebrafish has also been suggested as a model for the study of learning and memory (Roberts et al., 2013).

Life stage applicability: This key event is applicable to various life stages such as during brain development and maturity (Hladik & Tapio, 2016).

Sex applicability: This key event is not sex specific (Cekanaviciute et al., 2018), although sex-dependent cognitive outcomes have been recently ; Parihar et al., 2020).

Evidence for perturbation by a prototypic stressor: Current literature provides ample evidence of impaired learning and memory being induced by ionizing radiation (Cekanaviciute et al., 2018; Hladik & Tapio, 2016).

Key Event Description

Learning can be defined as the process by which new information is acquired to establish knowledge by systematic study or by trial and error (Ono, 2009). Two types of learning are considered in neurobehavioral studies: a) associative learning and b) non-associative learning. Associative learning is based on making associations between different events. In associative learning, a subject learns the relationship among two different stimuli or between the stimulus and the subject's behaviour. On the other hand, non-associative learning can be defined as an alteration in the behavioural response that occurs over time in response to a single type of stimulus. Habituation and sensitization are some examples of non-associative learning.

The memory formation requires acquisition, retention and retrieval of information in the brain, which is characterised by the non-conscious recall of information (Ono, 2009). There are three main categories of memory, including sensory memory, short-term or working memory (up to a few hours) and long-term memory (up to several days or even much longer).

Learning and memory depend upon the coordinated action of different brain regions and neurotransmitter systems constituting functionally integrated neural networks (D'Hooge and DeDeyn, 2001). Among the many brain areas engaged in the acquisition of, or retrieval of, a learned event, the hippocampal-based memory systems have received the most study. For example, the hippocampus has been shown to be critical for spatial-temporal memory, visio-spatial memory, verbal and narrative memory, and episodic and autobiographical memory (Burgess et al., 2000; Vorhees and Williams, 2014). However, there is substantial evidence that fundamental learning and memory functions are not mediated by the hippocampus alone but require a network that includes, in addition to the hippocampus, anterior thalamic nuclei, mammillary bodies cortex, cerebellum and basal ganglia (Aggleton and Brown, 1999; Doya, 2000; Mitchell et al., 2002, Toscano and Guilarte, 2005; Gilbert et al., 2006, 2016). Thus, damage to variety of

brain structures can potentially lead to impairment of learning and memory. The main learning areas and pathways are similar in rodents and primates, including man (Eichenbaum, 2000; Stanton and Spear, 1990).While the prefrontal cortex and frontostriatal neuronal circuits have been identified as the primary sites of higher-order cognition in vertebrates, invertebrates utilize paired mushroom bodies, shown to contain ~300,000 neurons in honey bees (Menzel, 2012; Puig et al., 2014).

For the purposes of this KE (AO), impaired learning and memory is defined as an organism's inability to establish new associative or non-associative relationships, or sensory, short-term or long-term memories which can be measured using different behavioural tests described below.

How it is Measured or Detected

In laboratory animals: in rodents, a variety of tests of learning and memory have been used to probe the integrity of hippocampal function. These include tests of spatial learning like the radial arm maze (RAM), the Barnes maze, Hebb-Williams maze, passive avoidance and Spontaneous alternation and most commonly, the Morris water maze (MWM). Test of novelty such as novel object recognition, and fear based context learning are also sensitive to hippocampal disruption. Finally, trace fear conditioning which incorporates a temporal component upon traditional amygdala-based fear learning engages the hippocampus. A brief description of these tasks follows.

1) RAM, Barnes, MWM, Hebb-Williams maze are examples of spatial tasks, animals are required to learn the location of a food reward (RAM); an escape hole to enter a preferred dark tunnel from a brightly lit open field area (Barnes maze), or a hidden platform submerged below the surface of the water in a large tank of water (MWM) (Vorhees and Williams, 2014). The Hebb-Williams maze measures an animal's problem solving abilities by providing no spatial cues to find the target (Pritchett & Mulder, 2004).

2) Novel Object recognition. This is a simpler task that can be used to probe recognition memory. Two objects are presented to animal in an open field on trial 1, and these are explored. On trial 2, one object is replaced with a novel object and time spent interacting with the novel object is taken evidence of memory retention – I have seen one of these objects before, but not this one (Cohen and Stackman, 2015).

3) Contextual Fear conditioning is a hippocampal based learning task in which animals are placed in a novel environment and allowed to explore for several minutes before delivery of an aversive stimulus, typically a mild foot shock. Upon reintroduction to this same environment in the future (typically 24-48 hours after original training), animals will limit their exploration, the context of this chamber being associated with an aversive event. The degree of suppression of activity after training is taken as evidence of retention, i.e., memory (Curzon et al., 2009).

4) Trace fear conditioning. Standard fear conditioning paradigms require animals to make an association between a neutral conditioning stimulus (CS, a light or a tone) and an aversive stimulus (US, a footshock). The unconditioned response (CR) that is elicited upon delivery of the footshock US is freezing behavior. With repetition of CS/US delivery, the previously neutral stimulus comes to elicit the freezing response. This type of learning is dependent on the amygdala, a brain region associated with, but distinct from the hippocampus. Introducing a brief delay between presentation of the neutral CS and the aversive US, a trace period, requires the engagement of the amygdala and the hippocampus (Shors et al., 2001).

5) Operant Responding. Performance on operant responding reflects the cortex' ability to organize processes (Rabin et al., 2002).

In humans: A variety of standardized learning and memory tests have been developed for human neuropsychological testing, including children (Rohlman et al., 2008). These include episodic autobiographical memory, perceptual motor tests, short and long term memory tests, working memory tasks, word pair recognition memory; object location recognition memory. Some have been incorporated in general tests of intelligence (IQ) such as the Wechsler Adult Intelligence Scale (WAIS) and the Wechsler. Modifications have been made and norms developed for incorporating of tests of learning and memory in children. Examples of some of these tests include:

1) Rey Osterieth Complex Figure test (RCFT) which probes a variety of functions including as visuospatial abilities, memory, attention, planning, and working memory (Shin et al., 2006).

2) Children's Auditory Verbal Learning Test (CAVLT) is a free recall of presented word lists that yields measures of Immediate Memory Span, Level of Learning, Immediate Recall, Delayed Recall, Recognition Accuracy, and Total Intrusions. (Lezak 1994; Talley, 1986).

3) Continuous Visual Memory Test (CVMT) measures visual learning and memory. It is a free recall of presented pictures/objects rather than words but that yields similar measures of Immediate Memory Span, Level of Learning, Immediate Recall, Delayed Recall, Recognition Accuracy, and Total Intrusions. (Lezak, 1984; 1994).

4) Story Recall from Wechsler Memory Scale (WMS) Logical Memory Test Battery, a standardized neurospychological test designed to measure memory functions (Lezak, 1994; Talley, 1986).

5) Autobiographical memory (AM) is the recollection of specific personal events in a multifaceted higher order cognitive process. It includes episodic memory- remembering of past events specific in time and place, in contrast to semantic autobiographical memory is the recollection of personal facts, traits, and general knowledge. Episodic AM is associated with greater activation of the hippocampus and a later and more gradual developmental trajectory. Absence of episodic memory in early life (infantile amnesia) is thought to reflect immature hippocampal function (Herold et al., 2015; Fivush, 2011).

6) Staged Autobiographical Memory Task. In this version of the AM test, children participate in a staged event involving a tour of the hospital, perform a series of tasks (counting footprints in the hall, identifying objects in wall display, buy lunch, watched a video). It is designed to contain unique event happenings, place, time, visual/sensory/perceptual details. Four to five months later, interviews are conducted using Children's Autobiographical Interview and scored according to standardized scheme (Willoughby et al., 2014).

7) Attentional set-shifting (ATSET) task. Measures the ability to relearn cues over various schedules of reinforcement (Heisler et al., 2015).

In Honey Bees: For over 50 years an assay for evaluating olfactory conditioning of the proboscis extension reflex (PER) has been used as a reliable method for evaluating appetitive learning and memory in honey bees (Guirfa and Sandoz, 2012; LaLone et al., 2017). These experiments pair a conditioned stimulus (e.g., an odor) with an unconditioned stimulus (e.g., sucrose) provided immediately afterward, which elicits the proboscis extension (Menzel, 2012). After conditioning, the odor alone will lead to the conditioned PER. This methodology has aided in the elucidation of five types of olfactory memory phases in honey bee, which include early short-term memory, late short-term memory, mid-term memory, early long-term memory, and late long-term memory (Guirfa and Sandoz, 2012). These phases are dependent on the type of conditioned stimulus, the intensity of the unconditioned stimulus, the number of conditioning trials, and the time between trials. Where formation of short-term memory occurs minutes after conditioning and decays within minutes, memory consolidation or stabilization of a memory trace after initial acquisition leads to mid-term memory, which lasts 1 d and is characterized by activity of the cAMP-dependent PKA (Guirfa and Sandoz, 2012). Multiple conditioning trials increase the duration of the memory after learning and coincide with increased Ca2+-calmodulin-dependent PKC activity (Guirfa and Sandoz, 2012). Early long-term memory, where a conditioned response can be evoked days to weeks after conditioning requires translation of existing mRNA, whereas late long-term memory requires de novo gene transcription and can last for weeks (Guirfa andSandoz, 2012)."

Regulatory Significance of the AO

A prime example of impairments in learning and memory as the adverse outcome for regulatory action is developmental lead exposure and IQ function in children (Bellinger, 2012). Most methods are well established in the published literature and many have been engaged to evaluate the effects of developmental thyroid disruption. The US EPA and OECD Developmental Neurotoxicity (DNT) Guidelines (OCSPP 870.6300 or OECD TG 426) as well as OECD TG 443 (OECD, 2018) both require testing of learning and memory (USEPA, 1998; OECD, 2007) advising to use the following tests passive avoidance, delayed-matching-to-position for the adult rat and for the infant rat, olfactory conditioning, Morris water maze, Biel or Cincinnati maze, radial arm maze, T-maze, and acquisition and retention of schedule-controlled behaviour. These DNT Guidelines have been deemed valid to identify developmental neurotoxicity and adverse neurodevelopmental outcomes (Makris et al., 2009).

Also, in the frame of the OECD GD 43 (2008) on reproductive toxicity, learning and memory testing may have potential to be applied in the context of developmental neurotoxicity studies. However, many of the learning and memory tasks used in guideline studies may not readily detect subtle impairments in cognitive function associated with modest degrees of developmental thyroid disruption (Gilbert et al., 2012).

References

Aggleton JP, Brown MW. (1999) Episodic memory, amnesia, and the hippocampal-anterior thalamic axis. Behav Brain Sci. 22: 425-489.

Alexander RD (1990) Epigenetic rules and Darwinian algorithms: The adaptive study of learning and development. Ethology and Sociobiology 11:241-303.

Bellinger DC (2012) A strategy for comparing the contributions of environmental chemicals and other risk factors to neurodevelopment of children. Environ Health Perspect 120:501-507.

Burgess N (2002) The hippocampus, space, and viewpoints in episodic memory. Q J Exp Psychol A 55:1057-1080. Cohen, SJ and Stackman, RW. (2015). Assessing rodent hippocampal involvement in the novel object recognition task. A review. Behav. Brain Res. 285: 105-1176.

Cekanaviciute, E., S. Rosi and S. Costes. (2018), "Central Nervous System Responses to Simulated Galactic Cosmic Rays", International Journal of Molecular Sciences, Vol. 19/11, Multidisciplinary Digital Publishing Institute (MDPI) AG, Basel, https://doi.org/10.3390/ijms19113669.

Cohen, SJ and Stackman, RW. (2015). Assessing rodent hippocampal involvement in the novel object recognition task. A review. Behav. Brain Res. 285: 105-1176.

Curzon P, Rustay NR, Browman KE. Cued and Contextual Fear Conditioning for Rodents. In: Buccafusco JJ, editor. Methods of Behavior Analysis in Neuroscience. 2nd edition. Boca Raton (FL): CRC Press/Taylor & Francis; 2009.

D'Hooge R, De Deyn PP (2001) Applications of the Morris water maze in the study of learning and memory. Brain Res Brain Res Rev 36:60-90.

Doya K. (2000) Complementary roles of basal ganglia and cerebellum in learning and motor control. Curr Opin Neurobiol. 10: 732-739.

Eichenbaum H (2000) A cortical-hippocampal system for declarative memory. Nat Rev Neurosci 1:41-50.

Fivush R. The development of autobiographical memory. Annu Rev Psychol. 2011;62:559-82.

Gilbert ME, Sanchez-Huerta K, Wood C (2016) Mild Thyroid Hormone Insufficiency During Development Compromises Activity-Dependent Neuroplasticity in the Hippocampus of Adult Male Rats. Endocrinology 157:774-787.

Gilbert ME, Rovet J, Chen Z, Koibuchi N. (2012) Developmental thyroid hormone disruption: prevalence, environmental contaminants and neurodevelopmental consequences. Neurotoxicology 33: 842-52.

Gilbert ME, Sui L (2006) Dose-dependent reductions in spatial learning and synaptic function in the dentate gyrus of adult rats following developmental thyroid hormone insufficiency. Brain Res 1069:10-22.

Guirfa, M., Sandoz, J.C., 2012. Invertebrate learning and memory: fifty years of olfactory conditioning of the proboscis extension response in honeybees. Learn. Mem. 19 (2),
54–66.

Herold, C, Lässer, MM, Schmid, LA, Seidl, U, Kong, L, Fellhauer, I, Thomann,PA, Essig, M and Schröder, J. (2015). Neuropsychology, Autobiographical Memory, and Hippocampal Volume in “Younger” and “Older” Patients with Chronic Schizophrenia. Front. Psychiatry, 6: 53.

Hladik, D. and S. Tapio. (2016), "Effects of ionizing radiation on the mammalian brain", Mutation Research/Reviews in Mutation Research, Vol. 770, Elsevier B. b., Amsterdam, https://doi.org/10.1016/j.mrrev.2016.08.003.

Heisler, J. M. et al. (2015), "The Attentional Set Shifting Task: A Measure of Cognitive Flexibility in Mice", Journal of Visualized Experiments, 96, JoVe, Cambridge, https://doi.org/10.3791/51944. Heisler, J. M. et al. (2015), "The Attentional Set Shifting Task: A Measure of Cognitive Flexibility in Mice", Journal of Visualized Experiments, 96, JoVe, Cambridge, https://doi.org/10.3791/51944.

LaLone, C.A., Villeneuve, D.L., Wu-Smart, J., Milsk, R.Y., Sappington, K., Garber, K.V., Housenger, J. and Ankley, G.T., 2017. Weight of evidence evaluation of a network of adverse outcome pathways linking activation of the nicotinic acetylcholine receptor in honey bees to colony death. STOTEN. 584-585, 751-775.

Lezak MD (1984) Neuropsychological assessment in behavioral toxicology--developing techniques and interpretative issues. Scand J Work Environ Health 10 Suppl 1:25-29.

Lezak MD (1994) Domains of behavior from a neuropsychological perspective: the whole story. Nebr Symp Motiv 41:23-55.

Makris SL, Raffaele K, Allen S, Bowers WJ, Hass U, Alleva E, Calamandrei G, Sheets L, Amcoff P, Delrue N, Crofton KM.(2009) A retrospective performance assessment of the developmental neurotoxicity study in support of OECD test guideline 426. Environ Health Perspect. Jan;117(1):17-25.

Menzel, R., 2012. The honeybee as a model for understanding the basis of cognition. Nat. Rev. Neurosci. 13 (11), 758–768.

Mitchell AS, Dalrymple-Alford JC, Christie MA. (2002) Spatial working memory and the brainstem cholinergic innervation to the anterior thalamus. J Neurosci. 22: 1922-1928.

OECD. 2007. OECD guidelines for the testing of chemicals/ section 4: Health effects. Test no. 426: Developmental neurotoxicity study. www.Oecd.Org/dataoecd/20/52/37622194.Pdf [accessed may 21, 2012].

OECD (2008) Nr 43 GUIDANCE DOCUMENT ON MAMMALIAN REPRODUCTIVE TOXICITY TESTING AND ASSESSMENT. ENV/JM/MONO(2008)16

Ono T. (2009) Learning and Memory. Encyclopedia of neuroscience. M D. Binder, N. Hirokawa and U. Windhorst (Eds). Springer-Verlag GmbH Berlin Heidelberg. pp 2129-2137.

Parihar, V. K. et al. (2020), "Sex-Specific Cognitive Deficits Following Space Radiation Exposure", Frontiers in Behavioral Neuroscience, Vol. 14, https://doi.org/10.3389/fnbeh.2020.535885.

Pritchett, K. and G. Mulder. (2004), "Hebb-Williams mazes.", Contemporary topics in laboratory animal science, Vol. 43/5, http://www.ncbi.nlm.nih.gov/pubmed/15461441.

Puig, M.V., Antzoulatos, E.G., Miller, E.K., 2014. Prefrontal dopamine in associative learning and memory. Neuroscience 282, 217–229.

Rabin, B. M. et al. (2002), "Effects of Exposure to 56Fe Particles or Protons on Fixed-ratio Operant Responding in Rats", Journal of Radiation Research, Vol. 43/S, https://doi.org/10.1269/jrr.43.S225.

Roberts AC, Bill BR, Glanzman DL. (2013) Learning and memory in zebrafish larvae. Front Neural Circuits 7: 126.

Rohlman DS, Lucchini R, Anger WK, Bellinger DC, van Thriel C. (2008) Neurobehavioral testing in human risk assessment. Neurotoxicology. 29: 556-567.

Shin, MS, Park, SY, Park, SR, Oeol, SH and Kwon, JS. (2006). Clinical and empirical applications of the Rey-Osterieth complex figure test. Nature Protocols, 1: 892-899.

Shors TJ, Miesegaes G, Beylin A, Zhao M, Rydel T, Gould E (2001) Neurogenesis in the adult is involved in the formation of trace memories. Nature 410:372-376.

Stanton ME, Spear LP (1990) Workshop on the qualitative and quantitative comparability of human and animal developmental neurotoxicity, Work Group I report: comparability of measures of developmental neurotoxicity in humans and laboratory animals. Neurotoxicol Teratol 12:261-267.

Talley, JL. (1986). Memory in learning disabled children: Digit span and eh Rey Auditory verbal learning test. Archives of Clinical Neuropsychology, Elseiver.

Toscano CD, Guilarte TR. (2005) Lead neurotoxicity: From exposure to molecular effects. Brain Res Rev. 49: 529-554.

U.S.EPA. 1998. Health effects guidelines OPPTS 870.6300 developmental neurotoxicity study. EPA Document 712-C-98-239.Office of Prevention Pesticides and Toxic Substances.

Vorhees CV, Williams MT (2014) Assessing spatial learning and memory in rodents. ILAR J 55:310-332.

Willoughby KA, McAndrews MP, Rovet JF. Accuracy of episodic autobiographical memory in children with early thyroid hormone deficiency using a staged event. Dev Cogn Neurosci. 2014 Jul;9:1-11.

Appendix 2

List of Key Event Relationships in the AOP

List of Adjacent Key Event Relationships

Relationship: 2769: Energy Deposition leads to Oxidative Stress

AOPs Referencing Relationship

AOP Name	Adjacency	Weight of Evidence	Quantitative Understanding
Deposition of energy leads to vascular remodeling	adjacent	High	High
Deposition of Energy Leading to Learning and Memory Impairment	adjacent	High	Moderate
Deposition of energy leading to occurrence of bone loss	adjacent	High	Moderate
Deposition of energy leading to occurrence of cataracts	adjacent	High	High

Evidence Supporting Applicability of this Relationship

Taxonomic Applicability

Term	Scientific Term	Evidence	Links
human	Homo sapiens	Moderate	NCBI
mouse	Mus musculus	Moderate	NCBI
rat	Rattus norvegicus	High	NCBI
rabbit	Oryctolagus cuniculus	Low	NCBI

Life Stage Applicability

Life Stage	Evidence
Juvenile	High
Adult	Moderate

Sex Applicability

Sex	Evidence
Male	High
Female	Moderate

Unspecific High

Sex **Evidence**

Most evidence is derived from in vitro studies, predominately using rabbit models. Evidence in humans and mice is moderate, while there is considerable available data using rat models. The relationship is applicable in both sexes, however, males are used more often in animal studies. No studies demonstrate the relationship in preadolescent animals, while adolescent animals were used very often, and adults were used occasionally in in vivo studies.

Key Event Relationship Description

Energy deposited onto biomolecules stochastically in the form on ionizing and non-ionizing radiation can cause direct and indirect molecular-level damage. As energy is deposited in an aqueous solution, water molecules can undergo radiolysis, breaking bonds to produce reactive oxygen species (ROS) (Ahmadi et al., 2021; Karimi et al., 2017) or directly increase function of enzymes involved in ROS generation (i.e. catalaze). Various species of ROS can be generated with differing degrees of biological effects. For example, singlet oxygen, superoxide, and hydroxyl radical are highly unstable, with short half-lives and react close to where they are produced, while species like H_2O_2 are much more stable and membrane permeable, meaning they can travel from the site of production, reacting elsewhere as a much weaker oxidant (Spector, 1990). In addition, enzymes involved in reactive oxygen and nitrogen species (RONS) production can be directly upregulated following the deposition of energy (de Jager, Cockrell and Du Plessis, 2017). Although less common than ROS, reactive nitrogen species (RNS) can also be produced by energy deposition resulting in oxidative stress (Cadet et al., 2012; Tangvarasittichai & Tangvarasittichai, 2019), a state in which the amount of ROS and RNS, collectively known as RONS, overwhelms the cell's antioxidant defense system. This loss in redox homeostasis can lead to oxidative damage to macromolecules including proteins, lipids, and nucleic acids (Schoenfeld et al., 2012; Tangvarasittichai & Tangvarasittichai, 2019; Turner et al., 2002).

Evidence Supporting this KER

Overal weight of evidence: High

Biological Plausibility

A large body of literature supports the linkage between the deposition of energy and oxidative stress. Multiple reviews describe the relationship in the context of ROS production (Marshall, 1985; Balasubramanian, 2000; Jurja et al., 2014), antioxidant depletion (Cabrera et al., 2011; Fletcher, 2010; Ganea & Harding, 2006; Hamada et al., 2014; Spector, 1990; Schoenfeld et al., 2012; Wegener, 1994), and overall oxidative stress (Eaton, 1994, Tangvarasittichai & Tangvarasittichain, 2019). This includes investigations into the mechanism behind the relationship (Ahmadi et al., 2021; Balasubramanian, 2000; Cencer et al., 2018; Eaton, 1994; Fletcher, 2010; Jiang et al., 2006; Jurja et al., 2014; Padgaonkar et al., 2015; Quan et al., 2021; Rong et al., 2019; Slezak et al., 2015; Soloviev & Kizub, 2019; Tian et al., 2017; Tahimic & Globus, 2017; Varma et al., 2011; Venkatesulu et al., 2018; Wang et al., 2019a; Yao et al., 2008; Yao et al., 2009; Zigman et al., 2000).

Water radiolysis is a main source of free radicals. Energy ionizes water and free radicals are produced that combine to create more stable ROS, such as hydrogen peroxide, hydroxide, superoxide, and hydroxyl (Eaton, 1994; Rehman et al., 2016; Tahimic & Globus, 2017; Tian et al., 2017; Varma et al., 2011; Venkatesulu et al., 2018). ROS formation causes ensuing damage to the body, as ~80% of tissues are comprised of water (Wang et al., 2019a). Ionizing radiation (IR) is a source of energy deposition, it can also interact with molecules, such as nitric oxide (NO), to produce less common free radicals, including RNS (Slezak et al., 2015; Tahimic & Globus, 2017; Wang et al., 2019a). Free radicals can diffuse throughout the cell and damage vital cellular components, such as proteins, lipids, and DNA, as well as dysregulate cellular processes, such as cell signalling (Slezak et al., 2015; Tian et al., 2017).

ROS are also commonly produced by nicotinamide adenine dinucleotide phosphate (NADPH) oxidase (NOX). Deposition of energy can activate NOX and induce expression of its catalytic and cytosolic components, resulting in increased intracellular ROS (Soloviev & Kizub, 2019). Intracellular ROS production can also be initiated through the expression of protein kinase C, which in turn activates NOX through phosphorylation of its cytosolic components (Soloviev & Kizub, 2019). Alternatively, ROS are often formed at the electron transport chain (ETC) of the mitochondria, due to IR-induced electron leakage leading to ionization of the surrounding O_2 to become superoxide (Soloviev & Kizub, 2019). Additionally, energy reaching a cell can be absorbed by an unstable molecule, often NADPH, known as a chromophore, which leads to the production of ROS (Balasubramanian, 2000; Cencer et al., 2018; Jiang et al., 2006; Jurja et al., 2014; Padgaonkar et al., 2015; Yao et al., 2009; Zigman et al., 2000).

Energy deposition can also weaken a cell's antioxidant defense system through the depletion of certain antioxidant enzymes, such as superoxide dismutase (SOD) and catalase (CAT). Antioxidants are consumed during the process of neutralizing ROS, so as energy deposition stimulates the formation of ROS it begins to outpace the rate at which antioxidants are replenished; this results in an increased risk of oxidative stress when their concentrations are low (Belkacémi et al., 2001; Giblin et al., 2002; Ji et al., 2014; Kang et al., 2020; Karimi et al., 2017; Padgaonkar et al., 2015; Rogers et al., 2004; Slezak et al., 2015; Tahimic & Globus, 2017; Wang et al., 2019a; Wegener, 1994; Weinreb & Dovrat, 1996; Zhang et al., 2012; Zigman et al., 1995; Zigman et al., 2000). When the amount of ROS overwhelms the antioxidant defense system, the cell will enter oxidative stress leading to macromolecular and cellular damage (Tangvarasittichai & Tangvarasittichai, 2019).

Empirical Evidence

The relationship between energy deposition and oxidative stress is strongly supported by primary research on the effects of IR on ROS and antioxidant levels (Bai et al., 2020; Cervelli et al., 2017; Hatoum et al., 2006; Huang et al., 2018; Huang et al., 2019;

Karam & Radwan, 2019; Kook et al., 2015; Liu et al., 2018; Liu et al., 2019; Mansour, 2013; Philipp et al., 2020; Ramadan et al., 2020; Sharma et al., 2018; Shen et al., 2018; Soltani et al., 2016; Soucy et al., 2010; Soucy et al., 2011; Ungvari et al., 2013; Wang et al., 2016; Wang et al., 2019b; Zhang et al., 2018; Zhang et al., 2020). Of note is that the relationship is demonstrated across studies conducted using various cell types, models and using broad dose-ranges as summarized below. Much evidence is available and described to help discern the quantitative understanding of the relationship, since it is well established.

Dose Concordance

It is well-accepted that any dose of radiation will deposit energy onto matter. Doses as low as 1 cGy support this relationship (Tseung et al., 2014). Following the deposition of energy, markers of oxidative stress are observed in the form of RONS, a change in levels of antioxidants, and oxidative damage to macromolecules. These effects have been shown across various organs/tissues and cell types as described below.

RONS

Cardiovascular tissue:

There is a considerable amount of evidence to support this relationship in cell types and tissues of relevance to the cardiovascular system. Recent studies have shown a linear increase in ROS in human umbilical vein endothelial cells (HUVECs) following 0-5 Gy gamma irradiation (Wang et al., 2019b). HUVECs irradiated with 0.25 Gy X-rays (Cervelli et al., 2017) and 9 Gy 250kV photons (Sharma et al., 2018) show increased ROS. Gamma ray irradiated rats at 5 Gy display increased ROS levels in the aorta (Soucy et al., 2010). A study using cerebromicrovascular endothelial cell (CMVECs) showed a dose-dependent increase in ROS from 0-8 Gy gamma irradiation (Ungvari et al., 2013). Additionally, telomerase-immortalized coronary artery endothelial (TICAE) and telomerase-immortalized microvascular endothelial (TIME) cells irradiated with 0.1 and 5 Gy of X-rays displayed increased ROS production (Ramadan et al., 2020). Gut arterioles of rats showed increased ROS following multiple fractions of 2.5 Gy X-ray rat irradiation (Hatoum et al., 2006). Additionally, rats irradiated with 1 Gy of 56Fe expressed increased ROS levels in the aorta (Soucy et al., 2011).

Brain tissue:

Markers of oxidative stress have also been consistently observed in brain tissue. Human neural stem cells subjected to 1, 2 or 5 Gy gamma rays showed a dose-dependent increase in RONS production (Acharya et al., 2010). A dose-dependent increase in ROS was observed in rat brains following 1-10 Gy gamma rays (Collins-Underwood et al., 2008). Neural precursor cells exposed to 0-10 Gy of X-irradiation showed increased ROS levels (Giedzinski et al., 2005; Limoli et al., 2004). Mice brain tissue displayed increased ROS following proton irradiation (Baluchamy et al., 2012; Giedzinski et al., 2005). Neural processor cells expressed linearly increased ROS levels following doses of 56Fe (Limoli et al., 2007). A dose-dependent increase in RONS was also observed after exposure to 1-15 cGy 56Fe irradiation in mice neural stem/precursor cell (Tseng et al., 2014). Human neural stem cells exposed to 5-100 cGy of various ions demonstrated a dose-dependent increase in RONs (Baulch et al., 2015).

Eye tissue:

The eye is also sensitive to the accumulation of free radicals, in a state of antioxidant decline. It has been shown in human lens epithelial cells (HLECs) and HLE-B3 following gamma irradiation of 0.25 and 0.5 Gy that ROS levels are markedly increased (Ahmadi et al., 2021). Exposure to non-ionizing radiation, such as ultraviolet (UV)-B, has also led to increased ROS in HLECs and mice lenses (Ji et al., 2015; Kubo et al., 2010; Rong et al., 2019; Yang et al., 2020)

Bone tissue:

Rat bone marrow-derived mesenchymal stem cell (bmMSCs) irradiated with 2, 5 and 10 Gy gamma rays and Murine MC3T3-E1 osteoblast cells irradiated with 2, 4, and 8 Gy of X-rays have shown a dose-dependent increase in ROS levels (Bai et al., 2020; Kook et al., 2015). Murine RAW264.7 cells and rat bmMSC irradiated with 2 Gy of gamma rays displayed increased ROS levels (Huang et al., 2019; Huang et al., 2018; hang et al., 2020). Human bone marrow-derived mesenchymal stem cell (hBMMSCs) irradiated with 2 or 8 Gy X-rays showed increased ROS (Liu et al., 2018; Zhang et al., 2018). Similarly, murine MC3T3-E1 osteoblast-like cells irradiated with 6 Gy of X-rays also displayed increased ROS (Wang et al., 2016). Finally, whole-body irradiation of mice with 2 Gy of 31.6 keV/mm LET 12C heavy ions showed increased ROS (Liu et al., 2019)

Antioxidants

Blood:

Workers exposed to X-rays at less than 1 mSv/year for an average of 15 years showed around 20% decreased antioxidant activity

compared to unexposed controls (Klucinski et al., 2008). Similarly, adults exposed to high background irradiation of 260 mSv/year showed about 50% lower antioxidant activity power compared to controls (Attar, Kondolousy and Khansari, 2007).

Cardiovascular tissue:

Heart tissue of rats following gamma irradiation of rats at 5 and 6 Gy resulted in a decrease in antioxidant levels (Karam & Radwan, 2019; Mansour, 2013). Similarly, HUVECs (Soltani, 2016) and TICAE cells (Philipp et al., 2020) irradiated at 2 Gy and 0.25-10 Gy gamma rays, respectively, displayed decreased antioxidant levels. Mice exposed to 18 Gy of X-ray irradiation showed decreased antioxidants in the aorta (Shen et al., 2018).

Brain tissue:

Mice brain tissue following 2, 10 and 50 cGy whole-body gamma irradiation revealed a dose-dependent change in SOD2 activity (Veeraraghan et al., 2011). Mice brain tissue showed decreased glutathione (GSH) and SOD levels following proton irradiation (Baluchamy et al., 2012)

Eye tissue:

Rats exposed to 15 Gy gamma rays demonstrated decreased antioxidants in the lens tissue (Karimi et al, 2017). Neutron irradiation of rats at 3.6 Sv resulted in a decrease in antioxidants in lens (Chen et al., 2021). A few studies found a dose concordance between UV irradiation and decreased antioxidant levels (Hua et al, 2019; Ji et al, 2015; Zigman et al., 2000; Zigman et al, 1995). HLECs following UVB exposure from 300 J/m2 to 14,400 J/m2 in HLECs showed linear decreases in antioxidant activity (Ji et al., 2015). Similarly, HLEC exposed to 4050, 8100 and 12,150 J/m2 found decreased antioxidant levels (Hua et al., 2019). Following UV irradiation of rabbit and squirrel lens epithelial cells (LECs) showed a linear decrease of antioxidant level, CAT (Zigman et al., 2000; Zigman et al., 1995). Mice exposed to UV irradiation found decreased antioxidant levels in lens (Zhang et al., 2012). Similarly, SOD levels decreased following 0.09 mW/cm 2 UVB exposure of HLECs (Kang et al., 2020).

Bone tissue:

Rat bmMSCs irradiated with 2, 5 and 10 Gy gamma rays and Murine MC3T3-E1 osteoblast cells irradiated with 2, 4, and 8 Gy of X-rays showed a dose-dependent decrease in antioxidant levels (Bai et al., 2020; Kook et al., 2015). hBMMSCs irradiated with 8 Gy X-rays also showed a decrease in antioxidant, SOD, levels (Liu et al., 2018).

Oxidative Damage

Cardiovascular tissue:

HUVECs and rat hearts irradiated by gamma rays at 2 and 6 Gy, respectively, resulted in increased levels of oxidative stress markers, such as malondialdehyde (MDA), and thiobarbituric reactive substances (TBARS) (Mansour, 2013; Soltani, 2016).

Brain tissue:

Mice brain tissue were shown to have increased lipid peroxidation (LPO) as determined by MDA measurements, following proton irradiation at 1 and 2 Gy (Baluchamy et al., 2012). Neural precursor cells from rat hippocampus exposed to 0, 1, 5 and 10 Gy of X-irradiation resulted in increased lipid peroxidation (Limoli et al., 2004).

Eye tissue:

Rats exposed to 15 Gy gamma rays demonstrated increased MDA in lens tissue (Karimi et al, 2017). Neutron irradiation of rats at 3.6 Sv resulted in an initial decrease, followed by an increase in MDA in lens (Chen et al., 2021). Following UV irradiation at 300 4050, 8100 and 12,150 J/m2, there was an increase in LPO in in human lens (Chitchumroonchokchai et al, 2004; Hua et al, 2019). Similarly, LPO increased following 0.09 mW/cm 2 UVB exposure of HLECs (Kang et al., 2020).

Time Concordance

It is well-accepted that deposition of energy into matter results in immediate vibrational changes to molecules or ionization events. Deposition of energy is therefore an upstream event to all follow-on latent events like oxidative stress.

RONS

Cardiovascular tissue:

In TICAE and TIME cells, ROS increased at 45 mins after X-ray irradiation (Ramadan et al., 2020). Superoxide and peroxide production were increased 1 day after 2-8 Gy of gamma irradiation in CMVECs (Unvari et al., 2013).

Bone tissue:

hBMMSCs irradiated with X-rays at 2 Gy showed peak ROS production at 2-8h post-irradiation (Zhang et al., 2018). Murine RAW264.7 cells (can undergo osteoclastogenesis) irradiated with 2 Gy of gamma rays showed increased ROS at 2-8h post-irradiation (Huang et al., 2018).

Brain tissue:

In human lymphoblast cells exposed to 2 Gy of X-rays, ROS were increased at various times between 13 and 29 days post-irradiation (Rugo and Schiestl, 2004). RONS were increased in human neural stem cells at 12-48h post-irradiation with 2 and 5 Gy of gamma rays (Acharya et al., 2010). ROS levels were increased in rat neural precursor cells at 6-24h after irradiation with 1-10 Gy of protons (Giedzinksi et al., 2005). Both 56Fe (1.3 Gy) and gamma ray (2 Gy) irradiation of mice increased ROS levels after 2 months post-irradiation in the cerebral cortex (Suman et al., 2013). ROS were also increased 12 months after 56Fe irradiation (Suman et al., 2013). RONS increased as early as 12h post-irradiation continuing to 8 weeks with 2-200 cGy doses of 56Fe irradiation of mouse neural stem/precursor cells (Tseng et al., 2014). The same cell type irradiated with 1 and 5 Gy of 56Fe irradiation showed increased ROS at 6h post-irradiation, with the last increase observed 25 days post-irradiation (Limoli et al., 2004).

Eye tissue:

Mice exposed to 11 Gy of X-rays showed increased ROS at 9 months post-irradiation in lenses (Pendergrass et al., 2010). In human lens cells, ROS were found increased at 1h after 0.25 Gy gamma ray irradiation (Ahmadi et al., 2021), 15 minutes after 30 mJ/cm2 UV radiation (Jiang et al., 2006), 2.5-120 minutes after 0.014 and 0.14 J/cm2 UV radiation (Cencer et al., 2018), and 24h after 30 mJ/cm2 UVB radiation (Yang et al., 2020).

Antioxidants

Cardiovascular tissue:

CAT antioxidant enzyme was decreased in mice aortas as early as 3 days post-irradiation, remaining decreased until 84 days after irradiation with 18 Gy of X-rays (Shen et al., 2018). The antioxidant enzymes peroxiredoxin 5 (PRDX5) and SOD were both shown to have the greatest decrease at 24h after 2 Gy gamma irradiation of TICAE cells (Philipp et al., 2020).

Eye tissue:

Bovine lenses irradiated with 44.8 J/cm2 of UVA radiation showed decreased CAT levels at 48-168h post-irradiation (Weinreb and Dovrat, 1996). UV irradiation of mice at 20.6 kJ/m2 led to decreased GSH at both 1 and 16 months post-irradiation in the lens (Zhang et al., 2012). Bovine lens cells exposed to 10 Gy of X-rays showed decreased levels of the antioxidant GSH at 24 and 120h after exposure (Belkacemi et al., 2001).

Oxidative damage markers

Cardiovascular tissue:

Oxidative damage markers 4-hydroxynonemal (4-HNE) and 3-Nitrotyosine (3-NT) were both significantly increased in the aorta of mice at 3 days post-irradiation, remaining increased until 84 days after irradiation with 18 Gy of X-rays (Shen et al., 2018).

Essentiality

Radiation has been found to induce oxidative stress above background levels. Many studies have shown that lower doses of ionizing radiation resulted in decreased levels in markers of oxidative stress in multiple cell types (Acharya et al., 2010; Ahmadi et

al., 2021; Bai et al., 2020; Baluchamy et al., 2012 Chen et al., 2021; Collins-Underwood et al., 2008; Giedzinski et al., 2005; Kook et al., 2015; Kubo et al., 2010; Philipp et al., 2020; Ramadan et al., 2020; Ungvari et al., 2013; Veeraraghan et al., 2011; Wang et al., 2019b; Zigman et al., 2000; Zigman et al., 1995). The essentiality of deposition of energy can be assessed through the removal of deposited energy, a physical stressor that does not require to be metabolized in order to elicit downstream effects on a biological system. Studies that do not deposit energy are observed to have no downstream effects.

Uncertainties and Inconsistencies

There are several uncertainties and inconsistencies in this KER.

- Chen et al. (2021) found that radiation can have adaptive responses. The study used three neutron radiation doses, 0.4 and 1.2 Sv, and 3.6 Sv. After 0.4 and 1.2 Sv, the activity of antioxidant enzymes GSH and SOD increased, and the concentration of malondialdehyde, a product of oxidative stress, decreased. After 3.6 Sv, the opposite was true.
- While the concentration of most antioxidant enzymes decreases after energy deposition, there is some uncertainty with SOD. Certain papers have found that its concentration decreases with dose (Chen et al., 2021; Hua et al., 2019; Ji et al., 2015; Kang et al., 2020) while others found no difference after irradiation (Rogers et al., 2004; Zigman et al., 1995). Several studies have also found that higher levels of SOD do not increase resistance to UV radiation (Eaton, 1994; Hightower, 1995).
- At 1-week post-irradiation with 10 Gy of 60Co gamma rays, TICAE cells experienced a significant increase in levels of the antioxidant, PRDX5, contrary to the decrease generally seen in antioxidant levels following radiation exposure (Philipp et al., 2020).
- Various studies found an increase in antioxidant SOD levels within the brain after radiation exposure (Acharya et al., 2010; Baluchamy et al., 2012; Baulch et al., 2015; Veeraraghan et al., 2011).

Quantitative Understanding of the Linkage

The table below provides some representative examples of quantitative linkages between the two key events. It was difficult to identify a general trend across all the studies due to differences in experimental design and reporting of the data. All data is statistically significant unless otherwise stated.

Response-response relationship

Dose Concordance

Reference	Experiment Description	Result
Attar, Kondolousy and Khansari, 2007	In vivo. One hundred individuals between 20 and 50 years old in two villages in Iran exposed to background IR at 260 mSv/year had antioxidant levels measured. The control group was from two villages not exposed to the high background radiation. The total antioxidant levels in the blood were determined by the ferric reducing/antioxidant power assay.	The total antioxidant level was significantly reduced from 1187±199 µmol in the control to 686±170 µmol in the exposed group.
Klucinski et al., 2008	In vivo. A group of 14 men and 31 women aged 25–54 years working X-ray equipment (receiving doses of less than 1 mSv/year) for an average of 15.3 years (range of 2-33 years) were compared to a control group for antioxidant activity. Antioxidant activity of SOD, glutathione peroxidase (GSH-Px), and CAT in erythrocytes were measured in U/g of hemoglobin.	All three enzymes showed significantly decreased antioxidant activity in the workers. In the controls (U/g of Hb): • SOD: 1200 ± 300 • GSH-Px: 39 ± 7 • CAT: 300 ± 60 In the workers (U/g of Hb): • SOD: 1000 ± 200 • GSH-Px: 29 ± 4 • CAT: 270 ± 50
	In vitro. Neural precursor cells isolated from rat hippocampi was	At a low dose of 0.25 Gy and 0.5 Gy, relative ROS levels were significantly elevated and showed a linear dose response (from ~1 to

Limoli et al., 2007	exposed to 0.25-5 Gy of 56Fe irradiation at dose rates of 0.5-1.0 Gy/min. ROS were measured 6h post-irradiation.	~2.25 relative ROS levels) until 1 Gy, where it reached its peak (~3 relative ROS levels). At higher doses, the relative ROS levels decreased.
Tseng et al., 2014	In vitro. Neural stem/precursor cells isolated from mouse subventricular and hippocampal dentate subgranular zones were exposed to 1-15 cGy of 56Fe irradiation at dose rates ranging from 5-50 cGy/min. RONS levels were measured.	A dose-dependent and significant rise in RONS levels was detected after 56Fe irradiation. 12 h post-irradiation, a steady rise was observed and reached a 6-fold peak after 15 cGy.
Limoli et al., 2004	In vitro. Neural precursor cells from rat hippocampus were exposed to 0, 1, 5 and 10 Gy of X-irradiation at a dose rate of 4.5 Gy/min. ROS levels were measured. In vivo. MDA was used to quantify oxidative stress.	A dose-dependent increase in ROS levels was seen in the first 12 h post-irradiation, with relative maximums at 12 h after 5 Gy (35% increase) and 24 h after 1 Gy (31% increase). ROS levels measured 1 week after 5 Gy were increased by 180% relative to sham-irradiated controls. MDA levels increased significantly (approximately 1.3-fold) after exposure to 10 Gy.
Collins-Underwood et al., 2008	In vitro. Immortalized rat brain microvascular endothelial cells were exposed to 1-10 Gy of 137Cs-irradiation at a dose rate of 3.91 Gy/min. Intracellular ROS and O2- production were both measured.	Irradiation resulted in a significant dose-dependent increase in intracellular ROS generation from 1-10 Gy. At 5 Gy, there was an approximate 10-fold increase in ROS levels, and at 10 Gy there was an approximate 20-fold increase.
Giedzinski et al., 2005	In vitro. Neural precursor cells were irradiated with 1, 2, 5 and 10 Gy of 250 MeV protons (1.7-1.9 Gy/min) and X-irradiation (4.5 Gy/min). ROS levels were measured.	There was a rapid increase in ROS at 6, 12, 18 and 24h after proton irradiation, with an exception at the 1 Gy 18h point. Most notably, at 6h post-irradiation, a dose-dependent increase in relative ROS levels from 1 to 10 Gy was seen that ranged from 15% (at 1 Gy) to 65% (at 10 Gy). Linear regression analysis showed that at ≤2 Gy, ROS levels increased by 16% per Gy. The linear dose response obtained at 24h showed that proton irradiation increased the relative ROS levels by 3% per Gy.
Veeraraghan et al., 2011	In vivo. Adult mice were exposed to 2, 10 or 50 cGy of whole-body gamma irradiation at 0.81 Gy/min. Brain tissues were harvested 24h post-irradiation. SOD2 levels and activity were measured.	Compared to the controls, the levels of SOD2 expression increased in the brain after 2, 10 and 50 cGy. Analysis revealed a significant and dose-dependent change in SOD2 activity. More specifically, SOD2 activity showed significant increases after 10 (~25% increase above control) and 50 cGy (~60% increase above control), but not 2 cGy.
Baluchamy et al., 2012	In vivo. Male mice were exposed to whole-body irradiation with 250 MeV protons at 0.01, 1 and 2 Gy and the whole brains were dissected out. ROS, LPO, GSH and total SOD were measured.	Dose-dependent increases in ROS levels was observed compared to controls, with a two-fold increase at 2 Gy. A 2.5 to 3-fold increase in LPO levels was also seen at 1 and 2 Gy, respectively, which was directly correlated with the increase in ROS levels. Additionally, results showed a significant reduction in GSH (~70% decrease at 2 Gy) and SOD activities (~2-fold decrease) following irradiation that was dose-dependent.
Acharya et al., 2010	In vitro. Human neural stem cells were subjected to 1, 2 or 5 Gy of gamma irradiation at a dose rate of 2.2 Gy/min. RONS and superoxide levels were determined.	Intracellular RONS levels increased by approximately 1.2 to 1.3-fold compared to sham-irradiated controls and was found to be reasonable dose-responsive. At 12h, levels of superoxide increased 2 and 4-fold compared to control for 2 and 5 Gy, respectively. At 24h and 48h, there was a dose-dependent increase in RONS levels. At 7 days, levels of RONS increased approximately 3 to 7-fold for 2 and 5 Gy, respectively.
Baulch et al., 2015	In vitro. Human neural stem cells were exposed to 5-100 cGy of 16O, 28Si, 48Ti or 56Fe particles (600 MeV) at 10-50 cGy/min. RONS and superoxide levels were	3 days post-irradiation, oxidative stress was found to increase after particle irradiation. Most notably, exposure to 56Fe resulted in a dose-dependent increase with 100% increase in RONS levels at 100 cGy. Dose-dependent increase was also seen in superoxide levels after 56Fe irradiation. At 7 days post-irradiation, 56Fe irradiation induced significantly lower nitric oxide levels by 47% (5 cGy), 55% (25 cGy) and

	determined.	45% (100 cGy).
Bai et al., 2020	In vitro. bmMSCs were taken from 4-week-old, male Sprague-Dawley rats. After extraction, cells were then irradiated with 2, 5, and 10 Gy of 137Cs gamma rays. Intracellular ROS levels and relative mRNA expression of the antioxidants, SOD1, SOD2, and CAT2, were measured to assess the extent of oxidative stress induced by IR.	Cellular ROS levels increased significantly in a dose-dependent manner from 0-10 Gy. Compared to sham-irradiated controls, ROS levels increased by ~15%, ~55%, and ~105% after exposure to 2, 5, and 10 Gy, respectively. Antioxidant mRNA expression decreased in a dose-dependent manner from 0-10 Gy, with significant increases seen at doses 2 Gy for SOD1 and CAT2 and 5 Gy for SOD2. Compared to sham-irradiated controls, SOD1 expression decreased by ~9%, ~18%, and ~27% after exposure to 2, 5, and 10 Gy, respectively. SOD2 expression decreased by ~31% and ~41% after exposure to 5 and 10 Gy, respectively. CAT2 expression decreased by ~15%, ~33%, and ~58% after exposure to 2, 5, and 10 Gy, respectively.
Liu et al., 2018	In vitro. hBMMSCs were irradiated with 8 Gy of X-rays at a rate of 1.24 Gy/min. Intracellular ROS levels and SOD activity were measured to analyze IR-induced oxidative stress.	Compared to sham-irradiated controls, hBMMSCs irradiated with 8 Gy of X-rays experienced a significant increase to intracellular ROS levels. hBMMSCs irradiated with 8 Gy of X-rays experienced a ~46% reduction in SOD activity.
Kook et al., 2015	In vitro. Murine MC3T3-E1 osteoblast cells were irradiated with 2, 4, and 8 Gy of X-rays at a rate of 1.5 Gy/min. Intracellular ROS levels and the activity of antioxidant enzymes, including GSH, SOD, CAT, were measured to assess the extent of oxidative stress induced by IR exposure.	Compared to sham-irradiated controls, irradiated MC3T3-E1 cells experienced a dose-dependent increase in ROS levels, with significant increases at 4 and 8 Gy (~26% and ~38%, respectively). Antioxidant enzyme activity initially increased by a statistically negligible amount from 0-2 Gy and then decreased in a dose-dependent manner from 2-8 Gy. SOD activity decreased significantly at 4 and 8 Gy by ~29% and ~59%, respectively. GSH activity similarly decreased significantly at 4 and 8 Gy by ~30% and ~48%, respectively. CAT activity did not change by a statistically significant amount.
Liu et al., 2019	In vivo. 8–10-week-old, juvenile, female SPF BALB/c mice underwent whole-body irradiation with 2 Gy of 31.6 keV/µm 12C heavy ions at a rate of 1 Gy/min. ROS levels were measured from femoral bone marrow mononuclear cells of the irradiated mice to analyze IR-induced oxidative stress.	Compared to sham-irradiated controls, irradiated mice experienced a ~120% increase in ROS levels.
Zhang et al., 2020	In vitro. Murine RAW264.7 osteoclast precursor cells were irradiated with 2 Gy of 60Co gamma rays at a rate of 0.83 Gy/min. ROS levels were measured to determine the extent of oxidative stress induced by IR exposure.	Compared to sham-irradiated controls, ROS levels in irradiated RAW264.7 cells increased by ~100%.
Wang et al., 2016	In vitro. Murine MC3T3-E1 osteoblast-like cells were irradiated with 6 Gy of X-rays. Intracellular ROS production was measured to assess oxidative stress from IR exposure.	Compared to sham-irradiated controls, Intracellular ROS production increased by ~81%.
Huang et al., 2018	In vitro. Murine RAW264.7 osteoblast-like cells were irradiated with 2 Gy of gamma rays at a rate of 0.83 Gy/min. ROS levels were measured to analyze IR-induced oxidative stress.	Compared to sham-irradiated controls, ROS levels in RAW264.7 cells increased by ~138% by 2 h post-irradiation.
Zhang et al., 2018	In vitro. hBMMSCs were irradiated with 2 Gy of X-rays at a rate of 0.6 Gy/min. Relative ROS concentration was measured to assess the extent of oxidative stress induced by IR.	Compared to sham-irradiated controls, irradiated hBMMSCs experienced a maximum increase of ~90% to ROS levels at 3 h post-irradiation.
Huang et al., 2019	In vitro. Rat bmMSC were irradiated with 2 Gy of 60Co gamma rays at a rate of 0.83	Compared to sham-irradiated controls, ROS levels in irradiated bone marrow stromal cells increased by approximately 2-fold.

Huang et al., 2015	Gy/min. ROS levels were measured to assess IR-induced oxidative stress.	
Soucy et al., 2011	In vivo. 7- to 12-month-old, adult, male Wistar rats underwent whole-body irradiation with 1 Gy of 56Fe heavy ions. ROS production in the aorta was measured along with changes in activity of the ROS-producing enzyme xanthine oxidase (XO) to assess IR-induced oxidative stress.	Compared to sham-irradiated controls, irradiated mice experienced a 74.6% increase in ROS production (from 4.84 to 8.45) and XO activity increased by 36.1% (6.12 to 8.33).
Soucy et al., 2010	In vivo. 4-month-old, adult, male Sprague-Dawley rats underwent whole-body irradiation with 5 Gy of 137Cs gamma rays. Changes in XO activity and ROS production were measured in the aortas of the mice to assess IR-induced oxidative stress.	Compared to sham-irradiated controls, irradiated mice experienced a ~68% increase in ROS production and a ~46% increase in XO activity.
Karam & Radwan, 2019	In vivo. Adult male Albino rats underwent irradiation with 5 Gy of 137Cs gamma rays at a rate of 0.665 cGy/s. Activity levels of the antioxidants, SOD and CAT, present in the heart tissue were measured to assess IR-induced oxidative stress.	Compared to the sham-irradiated controls, SOD and CAT activity decreased by 57% and 43%, respectively, after irradiation.
Cervelli et al., 2017	In vitro. HUVECs were irradiated with 0.25 Gy of X-rays at a rate of 91 mGy/min. ROS production was measured to analyze IR-induced oxidative stress.	Compared to the sham-irradiated controls, irradiated mice experienced a ~171% increase in ROS production (not significant).
Mansour, 2013	In vivo. Male Wistar rats underwent whole-body irradiation with 6 Gy of 137Cs gamma rays at a rate of 0.012 Gy/s. MDA was measured from heart homogenate, along with the antioxidants: SOD, GSH, and GSH-Px.	Compared to sham-irradiated controls, MDA increased by 65.9%. SOD, GSH-Px, and GSH decreased by 33.8%, 42.4%, and 50.0%, respectively.
Soltani, 2016	In vitro. HUVECs were irradiated with 2 Gy of ^{60}Co gamma rays at a dose rate of 0.6 Gy/min. Markers of oxidative stress, including reduced GSH and TBARS, were measured to assess GSH depletion and LPO, respectively.	Compared to non-irradiated controls, sham-irradiated cells experienced a ~28% decrease in GSH and a ~433% increase in TBARS.
Wang et al., 2019b	In vitro. HUVECs were irradiated with 0.2, 0.5, 1, 2, and 5 Gy of 137Cs gamma rays. ROS production was measured to assess IR-induced oxidative stress.	Compared to sham-irradiated controls, ROS production saw a significant, ~32% increase at 5 Gy. While changes to ROS production were insignificant at doses <2 Gy, they followed a linear increase from 0-5 Gy.
Sharma et al., 2018	In vitro. HUVECs were irradiated with 9 Gy of photons. ROS production was measured to determine the effects of IR on oxidative stress.	Compared to sham-irradiated controls, irradiated HUVECs saw a significant, ~133% increase in ROS production.
Hatoum et al., 2006	In vivo. Sprague-Dawley rats were irradiated with 9 fractions of 2.5 Gy of X-rays for a cumulative dose of 22.5 Gy at a rate of 2.43 Gy/min. Production of the ROS	ROS production started increasing compared to the sham-irradiated control after the second dose and peaked at the fifth dose. By the ninth dose, superoxide production increased by 161.4% and peroxide

	superoxide and peroxide in gut arterioles were measured to determine the level of oxidative stress caused by irradiation.	production increased by 171.3%.
Phillip et al., 2020	In vitro. Human TICAE cells were irradiated with 0.25, 0.5, 2, and 10 Gy of 60Co gamma rays at a rate of 0.4 Gy/min. Levels of the antioxidants, SOD1 and PRDX5 were measured to assess oxidative stress from IR exposure.	While SOD1 levels did not follow a dose-dependent pattern. At 2 Gy, SOD1 decreased about 0.5-fold. At 1-week post-irradiation, PRDX5 remained at approximately control levels for doses <2 Gy but increased by ~60% from 2-10 Gy. PRDX5 only decreased at 2 Gy and 24h post-irradiation.
Ramadan et al., 2020	In vitro. Human TICAE/TIME cells were irradiated with 0.1 and 5 Gy of X-rays at a dose rate of 0.5 Gy/min. Intracellular ROS production was measured to determine the extent of IR-induced oxidative stress.	ROS production saw a dose-dependent increase in both TICAE and TIME cells. By 45 mins post-irradiation, 0.1 Gy of IR had induced increases to ROS production of ~3.6-fold and ~8-fold in TICAE and TIME cells, respectively, compared to sham-irradiated controls. 5 Gy of IR caused more significant increases to ROS production of ~18-fold and ~17-fold in TICAE and TIME cells, respectively, compared to sham-irradiated controls.
Shen et al., 2018	In vivo. 8-week-old, female, C57BL/6 mice were irradiated with 18 Gy of X-rays. Levels of the oxidative markers, 4-HNE and 3-NT, and the antioxidants, CAT and heme oxygenase 1 (HO-1) were measured in the aortas of the mice.	Compared to sham-irradiated controls, irradiated mice saw maximum increases of ~1.75-fold on day 14 and ~2.25-fold on day 7 to 4-HNE and 3-NT levels, respectively. While CAT levels decreased up to 0.33-fold on day 7, HO-1 levels increased by ~1.9-fold on day 7.
Ungvari et al., 2013	In vitro. The CMVECs of adult male rats were irradiated with 2, 4, 6, and 8 Gy of 137Cs gamma rays. Production of the reactive oxygen species, peroxide and O2.-, were measured to assess the extent of IR-induced oxidative stress.	Compared to sham-irradiated controls, production of peroxide in CMVECs of irradiated mice 1 day-post exposure increased in a dose-dependent manner from 0-8 Gy, with significant changes observed at doses >4 Gy. At 8 Gy, peroxide production had increased ~3.25-fold. Production of O2.- followed a similar dose-dependent increase with significant observed at doses >6 Gy. At 8 Gy, O2.- production increased ~1.6-fold. 14 days post-exposure, IR-induced changes to ROS production were not significant for either peroxide or O2.- and did not show a dose-dependent pattern. ROS production progressively decreased from 0-4 Gy and then recovered from 6-8 Gy back to control levels.
Ahmadi et al., 2021	In vitro. HLEC and HLE-B3 cells were exposed to 0.1, 0.25 and 0.5 Gy of gamma irradiation at 0.3 and 0.065 Gy/min. Intracellular ROS levels were measured.	In HLE-B3 cells, there were about 7 and 17% ROS-positive cells 1 h after exposure to 0.25 and 0.5 Gy respectively at 0.3 Gy/min. 24 h after exposure there were about 10% ROS-positive cells after 0.5 Gy at 0.3 Gy/min. 1 h after exposure there were about 13 and 17% ROS-positive cells at 0.25 and 0.5 Gy and 0.065 Gy/min. 24 h after exposure there were 8% ROS-positive cells after 0.5 Gy and 0.065 Gy/min. In human lens epithelial cells 1 h after exposure there were about 10 and 19% ROS-positive cells after 0.25 and 0.5 Gy at 0.3 Gy/min. After exposure to 0.5 Gy at 0.065 Gy/min there were about 16 and 9% ROS-positive cells one and 24 h after exposure.
Ji et al, 2015	In vitro. HLECs were exposed to UVB-irradiation (297 nm; 2 W/m2) for 0 – 120 min. Total antioxidative capability (T-AOC), ROS levels, MDA, and SOD were measured at various time points at 5-120 min.	HLECs exposed to 1 W/m2 UVB for 0 - 120 min (representative of dose) showed a gradual increase in ROS levels that began to plateau 105 min post-irradiation at an ROS level 750 000x control.
	In vitro. HLECs were exposed to	MDA activity as a ratio of the control increased about 1.5 at 3.0 W/m2 and about 3 at 4.5 W/m2. SOD activity as a ratio of the control decreased about 0.1 at 1.5 W/m2, 0.2 at W/m2, and 0.3 at 4.5 W/m2.

Hua et al, 2019	4050, 8100 and 12,150 J/m2 of UVB-irradiation at 1.5, 3.0 and 4.5 W/m2. MDA, SOD, GSH-Px, and GSH were measured.	GSH-Px activity as a ratio of the control decreased about 0.02 at 3.0 W/m2 and 0.2 at 4.5 W/m2. GSH activity .as a ratio of the control decreased about 0.2 at 3.0 W/m2 and 0.7 at 4.5 W/m2.
Chen et al, 2021	In vivo. Male rats were irradiated with 0, 0.4, 1.2 and 3.6 Sv of neutron-irradiation at 14, 45 and 131 mSv/h. In rat lenses, MDA, GSH, and SOD, were measured.	MDA concentration decreased by about 1.5 nmol/mg protein at 1.2 Sv and increased by about 7.5 nmol/mg protein relative to the control at 3.6 Sv. GSH concentration increased by about 3.5 µg/mg protein and decreased by about 1 µg/mg protein relative to the control at 3.6 Sv (neutron radiation). SOD activity decreased by about 0.08 U/mg protein relative to the control at 3.6 Sv. It should be noted that Sv is not the correct unit when investigating animals and cultured cells, radiation should have been measured in Gy (ICRU, 1998).
Zigman et al., 2000	In vitro. Rabbit LECs were exposed to 3-12 J/cm2 of UVA-irradiation (300-400 nm range, 350 nm peak). CAT activity was assayed to demonstrate oxidative stress.	Rabbit LECs exposed to 3 – 12 J/cm2 UVA showed an approximately linear decrease in catalase activity (indicative of increased oxidative stress) with the maximum dose displaying a 3.8x decrease.
Chitchumroonchokchai et al, 2004	In vitro. HLECs were exposed to 300 J/m2 of UVB-irradiation at 3 mW/cm2. MDA and HAE were used to measure oxidative stress.	The concentration of MDA and HAE increased by about 900 pmol/mg protein compared to the control after irradiation with 300 J/m2 UVB.
Zigman et al, 1995	In vitro. Rabbit and squirrel LECs were exposed to 6, 9, 12, 15 and 18 J/m2 of UV-irradiation at 3 J/cm2/h (300-400 nm range, 350 nm peak). CAT was used to measure oxidative stress levels.	The CAT activity was 10% of the control activity at 6 J/cm2, and then decreased to 0% of the control activity at 18 J/cm2 (99.9% UV-A and 0.1% UV-B).
Karimi et al, 2017	In vivo. Adult rats were exposed to 15 Gy of gamma 60Co-irradiation at a dose rate of 98.5 cGy/min. In lens tissue, MDA, thiobarbituric acid (TBA), and GSH levels were used to indicate oxidative stress.	MDA concentration increased from 0.37 +/- 0.03 to 1.60 +/- 0.16 nmol/g of lens after irradiation. GSH concentration decreased from 0.99 +/- 0.06 to 0.52 +/- 0.16 µmol/g of lens after exposure.
Rong et al., 2019	In vitro. HLECs were exposed to UVB-irradiation (297 nm; 2 W/m^2 for 10 min). Intracellular H_2O_2 and superoxide levels were measured.	The amount of ROS was measured as the dicholofluoroscein (DCFH-DA) fluorescence density, which increased about 10-fold relative to the control. A similar test but with dihydroethidium (DHE) staining showed a fluorescence density increase of about 3-fold relative to the control.
Kubo et al., 2010	In vitro. Lenses isolated from mice were exposed to 400 or 800 J/m2 of UVB-irradiation. ROS levels were measured.	The ratio of ROS level/survived LECs increased from about 175 to 250% after exposure to 400 and 800 J/m2 UVB respectively.
Kang et al., 2020	In vitro. HLECs were exposed to 0.09 mW/cm2 UVB-irradiation (275-400 nm range, 310 nm peak) for 15 mins. MDA and SOD activity were measured.	MDA activity increased about 30% compared to control after 15 mins of 0.09 mW/cm2 UVB exposure. SOD activity decreased about 50% compared to control under the same conditions.
Yang et al., 2020	In vitro. HLECs were irradiated with 30 mJ/cm2 of UVB-irradiation. ROS levels were determined.	The level of ROS production in HLECs increased approximately 5-fold as determined by 2',7'-dichlorofluorescein diacetate after exposure to 30 mJ/cm2 UVB.
	In vivo. Adult mice were exposed	Decrease in GSH of about 1 and 2 µmol/g wet weight compared to

Zhang et al., 2012	to 20.6 kJ/m2 UV-irradiation (313 nm peak; 1.6 mW/cm2). GSH levels were measured in lens homogenates.	Decrease in GSH of about 1 and 2 µmol/g wet weight compared to control after 1 and 16 months respectively after 20.6 kJ/m2 UV (313 nm peak) at 1.6 mW/cm2.

Time-scale

Time Concordance

Reference	Experiment Description	Result
Tseng et al., 2014	In vitro. Neural stem/precursor cells isolated from mouse subventricular and hippocampal dentate subgranular zones were exposed to 1-200 cGy of 56Fe irradiation at dose rates ranging from 5-50 cGy/min. RONS were measured from 1 to 8 weeks post-irradiation.	Compared to sham-irradiated controls, a trend toward increasing oxidative stress was seen, particularly at 1- and 4-weeks post-irradiation where RONS levels showed dose-responsive increases. The greatest rise was also seen at 10 cGy where relative RONS levels increased ~2-fold from 1 to 4 weeks, ~3-fold from 4 to 6 weeks and ~2 fold from 6 to 8 weeks. RONS were also found increased at doses as low as 2 cGy at 12 and 24h post-irradiation.
Suman et al., 2013	In vivo. Female mice were exposed to either 1.3 Gy of 56Fe irradiation (1 GeV/nucleon; dose rate of 1 Gy/min) or 2 Gy of gamma irradiation (dose rate of 1 Gy/min). ROS were measured in cerebral cortical cells at 2 and 12 months.	ROS levels showed statistically significant increases after 56Fe irradiation at both 2 and 12 months, while gamma irradiation led to an increase at only 2 months. The percent fluorescence intensity of ROS levels for control, gamma irradiated and 56Fe-irradiated were approximately 100, 115 and 140 at 2 months, and 100, 90 and 125 at 12 months, respectively.
Limoli et al., 2004	In vitro. Neural stem/precursor cells isolated from mouse subventricular and hippocampal dentate subgranular zones were exposed to 1 or 5 Gy of 56Fe irradiation at dose rates ranging from 4.5 Gy/min. RONS were measured at various time points until 33 days post-exposure.	ROS levels exhibited statistically significant fluctuations, increasing over the first 12h before dropping at 18h and rising again at 24h. At 5 Gy, ROS levels fluctuated with a peak at 7 days, a decrease at 13 days, an increase at 25 days, and a decrease below control levels at 33 days. At 1 Gy, ROS levels peaked at 25 days and also decreased below control at 33 days.
Gledzinski et al., 2005	In vitro. Neural precursor cells derived from rats were irradiated with 1, 2, 5 and 10 Gy of proton (1.7-1.9 Gy/min). ROS levels were determined at 5-25h post-irradiation.	Proton irradiation led to a rapid rise in ROS levels, with the increase most marked at 6h (approximately 10-70% for 1 and 10 Gy, respectively). The increase in ROS persisted for 24h, mainly for 10 Gy where the ROS levels were around 30% above control at the 12, 18 and 24h mark.
Acharya et al., 2010	In vitro. Human neural stem cells were subjected to 1, 2 or 5 Gy of gamma irradiation at a dose rate of 2.2 Gy/min. RONS and superoxide levels were measured at various time points until 7 days.	Intracellular RONS and superoxide levels showed significant increase from 2- to 4-fold at 12h. At 7 days, levels of RONS increased and were dose-responsive, elevated by ~3- to 7-fold and 3- to 5-fold, respectively, over sham-irradiated controls.
Rugo and Schiestl, 2004	In vitro. Human lymphoblast cell lines (TK6 and TK6 E6) were irradiated with 2 Gy of X-irradiation at a dose rate of 0.72 Gy/min. ROS levels were measured at various time points until 29 days.	In the TK6 E6 clones, there was only a significant ROS increase at day 29 (45.7 DCF fluorescence units). In the TK6 clones, there were significant ROS increases at days 13 (26.0 DCF fluorescence units), 15 (26.3 DCF fluorescence units) and 20 (38.1 DCF fluorescence units), with a strong trend of increased ROS in the treated group at day 25. On day 18, ROS levels decreased in the irradiated group, and there was no significant difference at day 29.
Huang et al., 2018	In vitro. Murine RAW264.7 cells were irradiated with 2 Gy of gamma rays at a rate of 0.83 Gy/min. ROS levels were measured at 2 and 8 h post-irradiation.	ROS levels in irradiated RAW264.7 cells decreased by ~10% from 2 h post-exposure to 8 h post-exposure (from ~138% above control at 2 h to ~98% above control at 8).
Zhang et al., 2018	In vitro. hBMMSCs were irradiated with 2 Gy of X-rays at a rate of 0.6 Gy/min. Relative ROS concentration was measured at 0, 0.5, 2, 3, 6, 8, and 12 h post-irradiation.	ROS levels increased in time dependent manner until a peak of ~90% above control level at 3 h-post irradiation, and then steadily declined back to approximately control levels at 12 h post-irradiation.
Phillip et al., 2020	In vitro. Human TICAE cells were irradiated with 0.25, 0.5, 2, and 10 Gy of 60Co gamma rays at a rate of 400 mGy/min. Levels of the antioxidants, SOD1 and PRDX5 were measured at 4 h, 24 h, 48 h, and 1-week post-irradiation to assess oxidative stress from IR exposure.	SOD1 levels did not follow a time-dependent pattern. However, SOD1 decreased at 2 Gy for every timepoint post-irradiation. While PRDX5 levels stayed at approximately baseline levels for the first two days after exposure to 10 Gy of radiation, levels elevated by ~1.6-fold after 1 week.
Ramadan et	In vitro. Human TICAE/TIME cells were irradiated with 0.1 and 5 Gy of X-rays at a	After irradiation, ROS production saw time-dependent decreases in both TICAE and TIME cells from 45 mins to 3 h post-exposure. ROS

al., 2020	rate of 0.5 Gy/min. Intracellular ROS production was measured at 45 mins, 2 h, and 3 h post-irradiation.	production was elevated at 45 mins but returned to approximately baseline levels at 2 and 3 h.
Shen et al., 2018	In vivo. 8-week-old, female, C57BL/6 mice were irradiated with 18 Gy of X-rays. Levels of the oxidative markers, 4-HNE and 3-NT, and the antioxidants, CAT and heme HO-1 were measured the aortas of the mice at 3, 7, 14, 28, and 84 days post-irradiation.	Significant changes were observed in 4-HNE, 3-NT, CAT, and HO-1 levels of irradiated mice after 3 days. 3-NT and HO-1 levels increased from days 3 to 7 and then progressively decreased, while 4-HNE levels followed the same pattern but with a peak at day 14. CAT levels were at their lowest at day 3 and followed a time dependent increase until day 84.
Ungvari et al., 2013	In vitro. The CMVECs of adult male rats were irradiated with 2, 4, 6, and 8 Gy of 137Cs gamma rays. Production of the reactive oxygen species, peroxide and superoxide, were measured at 1- and 14-days post-irradiation.	ROS production was generally higher at day 1 than day 14, with the difference becoming progressively more significant from 2-8 Gy. Peroxide production was reduced from a ~3.25-fold increase compared to controls at day 1 back to baseline levels at day 14. Superoxide production had a ~1.6-fold increase at day 1 recover to baseline levels at day 14.
Ahmadi et al., 2021	In vitro. HLEC and HLE-B3 cells were exposed to 0.1, 0.25 and 0.5 Gy of gamma irradiation at 0.3 and 0.065 Gy/min. ROS levels were measured.	In human LECs immediately exposed to 0.25 Gy gamma rays, the level of ROS positive cells increased by 5%, relative to control, 1 h post-irradiation.
Jiang et al., 2006	In vitro. HLECs were exposed to UV-irradiation at a wavelength over 290 nm (30 mJ/cm2). ROS levels were measured.	Approximately 10-fold increase in ROS generation 15 mins after exposure to 30 mJ/cm2 UV.
Pendergrass et al., 2010	In vivo. Female mice were irradiated with 11 Gy of X-irradiation at a dose rate of 2 Gy/min. ROS levels in the lenses were used to represent oxidative stress.	9 months after irradiation with 11 Gy X-rays at 2 Gy/min there's 2250% cortical ROS relative to the control. 3 months after there was no significant change.
Belkacemi et al., 2001	In vitro. Bovine lens cells were exposed to 10 Gy of X-irradiation at 2 Gy/min. GSH levels were measured.	The intracellular GSH pool was measured by a decrease of about 15% monobromobimane fluorescence relative to the control 24 h after exposure to 10 Gy X-rays at 2 Gy/min and there was a decrease of about 40% relative to the control by 120 h.
Weinreb and Dovrat, 1996	In vitro. Bovine lenses were irradiated with 22.4 J/cm2 (10 min) and 44.8 J/cm2 (100 min) of UVA-irradiation at 8.5 mW/cm2. CAT levels were determined.	CAT activity decreased from 1.75 (control) to 0.5 U/mg protein at 48-168 h after exposure to 44.8 J/cm2 UV-A.
Cencer et al., 2018	In vitro. HLECs were exposed to 0.014 and 0.14 J/cm^2 of UVB-irradiation at 0.09, 0.9 mW/cm^2 for 2 and 5 min. ROS levels (mainly H_2O_2) were measured.	About 5 min after exposure to both 0.09 and 0.9 mW/cm2 UVB for 2.5 mins there is an increase of about 4 average brightness minus control (densitometric fluorescence scanning for ROS, mostly indicating H_2O_2). About 90 and 120 min after exposure to 0.9 mW/cm^2 the average brightness minus control is about 35 and 20 respectively.
Yang et al., 2020	In vitro. HLECs were irradiated with 30 mJ/cm2 of UVB-irradiation. Intracellular ROS levels were measured.	The level of ROS production in HLECs increased approximately 5-fold as determined by 2',7'-dichlorofluorescein diacetate 24 h after exposure to 30 mJ/cm2 UVB.
Zhang et al.,	In vivo. Adult mice were exposed to 20.6 kJ/m2 UV-irradiation (313 nm peak; 1.6	Decrease in GSH of about 1 and 2 µmol/g wet weight compared to

2012	mW/cm2). GSH levels were measured in lens homogenates.	control after 1 and 16 months respectively after 20.6 kJ/m2 UV (313 nm peak) at 1.6 mW/cm2.

Known modulating factors

Modulating Factors	MF details	Effects on the KER	References
Antioxidants	CAT, GSH-Px, SOD, PRDX, vitamin E, C, carotene, lutein, zeaxanthin, selenium, zinc, alpha-lipoic acid, melatonin, gingko biloba leaf, fermented gingko biloba leaf, Nigella sativa oil, thymoquinone, and ferulic acid	Adding or withholding antioxidants will decrease or increase the level of oxidative stress respectively	Zigman et al., 1995; Belkacémi et al., 2001; Chitchumroonchokchai et al., 2004; Fatma et al., 2005; Jiang et al., 2006; Fletcher, 2010; Karimi et al., 2017; Hua et al., 2019; Kang et al., 2020; Yang et al., 2020; Manda et al., 2008; Limoli et al., 2007; Manda et al., 2007; Taysi et al., 2012; Ismail et al., 2016; Demir et al., 2020; Chen et al., 2021
Age	Increased age	Antioxidant levels are lower and show a greater decrease after radiation in older organisms. This compromises their defense system, resulting in ROS increases and therefore, an increased likelihood of oxidative stress	Marshall, 1985; Spector, 1990; Giblin et al., 2002; Kubo et al., 2010; Pendergrass et al., 2010; Zhang et al., 2012; Hamada et al., 2014; Tangvarasittichai & Tangvarasittichai, 2019
Oxygen	Increased oxygen levels	Higher oxygen concentrations increase sensitivity to ROS	Hightower et al., 1992; Eaton, 1994; Huang et al., 2006; Zhang et al., 2010; Schoenfeld et al., 2012

Known Feedforward/Feedback loops influencing this KER

The relationship between deposition of energy and increased oxidative stress leads to several feedforward loops. Firstly, ROS activates the transforming growth factor beta (TGF)-β, which increases the production of ROS. This process is modulated in normal cells containing PRDX-6, or cells with added MnTBAP, which will both prevent TGF-β from inducing ROS formation (Fatma et al., 2005). Secondly, ROS can damage human mitochondrial DNA (mtDNA), this can then cause changes to the cellular respiration mechanisms, leading to increased ROS production (Turner et al., 2002; Zhang et al., 2010; Tangvarasittichai & Tangvarasittichai, 2019, Ahmadi et al., 2021; Yves, 2000). Some other feedback loops through which deposition of energy causes oxidative stress are discussed by Soloviev & Kizub (2019).

References

Acharya, M. M. et al. (2010), “Consequences of ionizing radiation-induced damage in human neural stem cells”, Free radical biology & medicine, Vol. 49/12, Elsevier, Amsterdam, https://doi.org/10.1016/j.freeradbiomed.2010.08.021.

Ahmadi, M. et al. (2021), “Early responses to low-dose ionizing radiation in cellular lens epithelial models”, Radiation research, Vol. 197/1, Radiation Research Society, Bozeman, https://doi.org/10.1667/RADE-20-00284.1

Attar, M., Y. M. Kondolousy, N. Khansari, (2007), “Effect of High Dose Natural Ionizing Radiation on the Immune System of the Exposed Residents of Ramsar Town, Iran”, Iranian Journal of Allergy, Asthma and Immunology, Vol. 6/2, pp. 73-78.

Bai, J. et al. (2020), “Irradiation-induced senescence of bone marrow mesenchymal stem cells aggravates osteogenic differentiation dysfunction via paracrine signaling”, American Journal of Physiology - Cell Physiology, Vol. 318/5, American Physiological Society, Rockville, https://doi.org/10.1152/ajpcell.00520.2019.

Balasubramanian, D (2000), “Ultraviolet radiation and cataract”, Journal of ocular pharmacology and therapeutics, Vol. 16/3, Mary Ann Liebert Inc., Larchmont, https://doi.org/10.1089/jop.2000.16.285.

Baluchamy, S. et al. (2012), “Reactive oxygen species mediated tissue damage in high energy proton irradiated mouse brain”, Molecular and cellular biochemistry, Vol. 360/1-2, Springer, London, https://doi.org/10.1007/s11010-011-1056-2.

Baulch, J. E. et al. (2015), “Persistent oxidative stress in human neural stem cells exposed to low fluences of charged particles Redox biology, Vol. 5, Elsevier, Amsterdam, https://doi.org/10.1016/j.redox.2015.03.001.

Belkacémi, Y. et al. (2001), “Lens epithelial cell protection by aminothiol WR-1065 and anetholedithiolethione from ionizing radiation”, International journal of cancer, Vol. 96, John Wiley & Sons, Ltd., Hoboken, https://doi.org/10.1002/ijc.10346.

Cabrera M., R. Chihuailaf and F. Wittwer Menge (2011), “Antioxidants and the integrity of ocular tissues”, Veterinary medicine international, Vol. 2011, Hindawi, London, https://doi.org/10.4061/2011/905153.

Cadet, J. et al. (2012), “Oxidatively generated complex DNA damage: tandem and clustered lesions”, Cancer letters, Vol. 327, Elsevier, Amsterdam, https://doi.org/10.1016/j.canlet.2012.04.005.

Cencer, C. et al. (2018), “PARP-1/PAR activity in cultured human lens epithelial cells exposed to tow levels of UVB light”, Photochemistry and photobiology, Vol. 94, John Wiley & Sons, Ltd., Hoboken, https://doi.org/10.1111/php.12814.

Cervelli, T. et al. (2017), “A New Natural Antioxidant Mixture Protects against Oxidative and DNA Damage in Endothelial Cell Exposed to Low-Dose Irradiation”, Oxidative medicine and cellular longevity, Vol. 2017, Hindawi, London, https://doi.org/10.1155/2017/9085947.

Chen, Y. et al. (2021), “Effects of neutron radiation on Nrf2-regulated antioxidant defense systems in rat lens”, Experimental and therapeutic medicine, Vol. 21/4, Spandidos Publishing Ltd, Athens, https://doi.org/10.3892/etm.2021.9765.

Chitchumroonchokchai, C. et al. (2004), “Xanthophylls and α-tocopherol decrease UVB-induced lipid peroxidation and stress signaling in human lens epithelial cells”, The Journal of Nutrition, Vol. 134/12, American Society for Nutritional Sciences, Bethesda, https://doi.org/10.1093/jn/134.12.3225.

Collins-Underwood, J. R. et al. (2008), “NADPH oxidase mediates radiation-induced oxidative stress in rat brain microvascular endothelial cells”, Free radical biology & medicine, Vol. 45/6, Elsevier, Amsterdam, https://doi.org/10.1016/j.freeradbiomed.2008.06.024.

de Jager, T.L., Cockrell, A.E., Du Plessis, S.S. (2017), “Ultraviolet Light Induced Generation of Reactive Oxygen Species”, in Ultraviolet Light in Human Health, Diseases and Environment. Advances in Experimental Medicine and Biology, Springer, Cham, https://doi.org/10.1007/978-3-319-56017-5_2

Demir, E. et al. (2020), “Nigella sativa oil and thymoquinone reduce oxidative stress in the brain tissue of rats exposed to total head irradiation”, International journal of radiation biology, Vol. 96/2, Informa, London, https://doi.org/10.1080/09553002.2020.1683636.

Eaton, J. W. (1994), “UV-mediated cataractogenesis: A radical perspective”, Documenta ophthalmologica, Vol. 88, Springer, London, https://doi.org/10.1007/BF01203677.

Fatma, N. et al. (2005), “Impaired homeostasis and phenotypic abnormalities in Prdx6-/- mice lens epithelial cells by reactive oxygen species: Increased expression and activation of TGFβ”, Cell death and differentiation, Vol. 12, Nature Portfolio, London, https://doi.org/10.1038/sj.cdd.4401597.

Fletcher, A. E (2010), “Free radicals, antioxidants and eye diseases: evidence from epidemiological studies on cataract and age-related macular degeneration”, Ophthalmic Research, Vol. 44, Karger International, Basel, https://doi.org/10.1159/000316476.

Ganea, E. and J. J. Harding (2006), “Glutathione-related enzymes and the eye”, Current eye research, Vol. 31/1, Informa, London, https://doi.org/10.1080/02713680500477347.

Giblin, F. J. et al. (2002), “UVA light in vivo reaches the nucleus of the guinea pig lens and produces deleterious, oxidative effects”, Experimental eye research, Vol. 75/4, Elsevier, Amsterdam, https://doi.org/10.1006/exer.2002.2039.

Giedzinski, E. et al. (2005), “Efficient production of reactive oxygen species in neural precursor cells after exposure to 250 MeV protons”, Radiation research, Vol. 164/4, Radiation Research Society, Bozeman, https://doi.org/10.1667/rr3369.1.

Hamada, N. et al. (2014), “Emerging issues in radiogenic cataracts and cardiovascular disease”, Journal of radiation research, Vol. 55/5, Oxford University Press, Oxford, https://doi.org/10.1093/jrr/rru036.

Hatoum, O. A. et al. (2006), “Radiation induces endothelial dysfunction in murine intestinal arterioles via enhanced production of reactive oxygen species”, Arteriosclerosis, Thrombosis, and Vascular Biology, Vol. 26/2, Lippincot Williams & Wilkins, Philadelphia, https://doi.org/10.1161/01.ATV.0000198399.40584.8C.

Hightower, K. and J. McCready (1992), “Mechanisms involved in cataract development following near-ultraviolet radiation of cultured lenses”, Current eye research, Vol. 11/7, Informa, London, https://doi.org/10.3109/02713689209000741.

Hightower, K. R. (1995), “The role of the lens epithelium in development of UV cataract”, Current eye research, Vol. 14/1, Informa, London, https://doi.org/10.3109/02713689508999916.

Hua, H. et al. (2019), “Protective effects of lanosterol synthase up-regulation in UV-B-induced oxidative stress”, Frontiers in pharmacology, Vol. 10, Frontiers Media SA, Lausanne, https://doi.org/10.3389/fphar.2019.00947.

Huang, L. et al. (2006), “Oxidation-induced changes in human lens epithelial cells 2. Mitochondria and the generation of reactive

oxygen species", Free radical biology & medicine, Vol. 41/6, Elsevier, Amsterdam, https://doi.org/10.1016/j.freeradbiomed.2006.05.023.

Huang, B. et al. (2019), "Amifostine suppresses the side effects of radiation on BMSCs by promoting cell proliferation and reducing ROS production", Stem Cells International, Vol. 2019, Hindawi, London, https://doi.org/10.1155/2019/8749090.

Huang, B. et al. (2018), "Sema3a inhibits the differentiation of raw264.7 cells to osteoclasts under 2gy radiation by reducing inflammation", PLoS ONE, Vol. 13/7, PLOS, San Francisco, https://doi.org/10.1371/journal.pone.0200000.

ICRU (1998), "ICRU report 57: conversion coefficients for use in radiological protection against external radiation", Journal of the ICRU, Vol. 29/2, SAGE Publishing

Ismail, A. F. and S. M. El-Sonbaty (2016), "Fermentation enhances Ginkgo biloba protective role on gamma-irradiation induced neuroinflammatory gene expression and stress hormones in rat brain", Journal of photochemistry and photobiology. B, Biology, Vol. 158, Elsevier, Amsterdam, https://doi.org/10.1016/j.jphotobiol.2016.02.039.

Ji, Y. et al. (2015), "The mechanism of UVB irradiation induced-apoptosis in cataract", Molecular and cellular biochemistry, Vol. 401, Springer, London, https://doi.org/10.1007/s11010-014-2294-x.

Jiang, Q. et al. (2006), "UV radiation down-regulates Dsg-2 via Rac/NADPH oxidase-mediated generation of ROS in human lens epithelial cells", International Journal of Molecular Medicine, Vol. 18/2, Spandidos Publishing Ltd, Athens, https://doi.org/10.3892/ijmm.18.2.381.

Jurja, S. et al. (2014), "Ocular cells and light: harmony or conflict?", Romanian Journal of Morphology & Embryology, Vol. 55/2, Romanian Academy Publishing House, Bucharest, pp. 257–261.

Kang, L. et al. (2020), "Ganoderic acid A protects lens epithelial cells from UVB irradiation and delays lens opacity", Chinese journal of natural medicines, Vol. 18/12, Elsevier, Amsterdam, https://doi.org/10.1016/S1875-5364(20)60037-1.

Karam, H. M. and R. R. Radwan (2019), "Metformin modulates cardiac endothelial dysfunction, oxidative stress and inflammation in irradiated rats: A new perspective of an antidiabetic drug", Clinical and Experimental Pharmacology and Physiology, Vol. 46/12, Wiley-Blackwell, Hoboken, https://doi.org/10.1111/1440-1681.13148.

Karimi, N. et al. (2017), "Radioprotective effect of hesperidin on reducing oxidative stress in the lens tissue of rats", International Journal of Pharmaceutical Investigation, Vol. 7/3, Phcog Net, Bengaluru, https://doi.org/10.4103/jphi.JPHI_60_17.

Kłuciński, P. et al. (2008), "Erythrocyte antioxidant parameters in workers occupationally exposed to low levels of ionizing radiation", Annals of Agricultural and Environmental Medicine, Vol. 15/1, pp. 9-12.

Kook, S. H. et al. (2015), "Irradiation inhibits the maturation and mineralization of osteoblasts via the activation of Nrf2/HO-1 pathway", Molecular and Cellular Biochemistry, Vol. 410/1-2, Springer, London, https://doi.org/10.1007/s11010-015-2559-z.

Kozbenko, T. et al. (2022), "Deploying elements of scoping review methods for adverse outcome pathway development: a space travel case example", International Journal of Radiation Biology, 1–12. https://doi.org/10.1080/09553002.2022.2110306

Kubo, E. et al. (2010), "Protein expression profiling of lens epithelial cells from Prdx6-depleted mice and their vulnerability to UV radiation exposure", American Journal of Physiology, Vol. 298/2, American Physiological Society, Rockville, https://doi.org/10.1152/ajpcell.00336.2009.

Lee, J. et al. (2004), "Reactive oxygen species, aging, and antioxidative nutraceuticals", Comprehensive reviews in food science and food safety, Vol. 3/1, Blackwell Publishing Ltd, Oxford, http://doi.org/10.1111/j.1541-4337.2004.tb00058.x.

Limoli, C. L. et al. (2007), "Redox changes induced in hippocampal precursor cells by heavy ion irradiation", Radiation and environmental biophysics, Vol. 46/2, Springer, London, https://doi.org/10.1007/s00411-006-0077-9.

Limoli, C. L. et al. (2004), "Radiation response of neural precursor cells: linking cellular sensitivity to cell cycle checkpoints, apoptosis and oxidative stress", Radiation research, Vol. 161/1, Radiation Research Society, Bozeman, https://doi.org/10.1667/rr3112.

Liu, F. et al. (2019), "Transcriptional response of murine bone marrow cells to total-body carbon-ion irradiation", Mutation Research - Genetic Toxicology and Environmental Mutagenesis, Vol. 839, Elsevier, Amsterdam, https://doi.org/10.1016/j.mrgentox.2019.01.014.

Liu, Y. et al. (2018), "Protective effects of α2macroglobulin on human bone marrow mesenchymal stem cells in radiation injury", Molecular Medicine Reports, Vol. 18/5, Spandidos Publishing Ltd, Athens, https://doi.org/10.3892/mmr.2018.9449.

Manda, K. et al. (2007), "Melatonin attenuates radiation-induced learning deficit and brain oxidative stress in mice", Acta neurobiologiae experimentalis, Vol. 67/1, Nencki Institute of Experimental Biology, Warsaw, pp. 63 –70.

Manda, K., M. Ueno and K. Anzai (2008), "Memory impairment, oxidative damage and apoptosis induced by space radiation: ameliorative potential of alpha-lipoic acid", Behavioural brain research, Vol. 187/2, Elsevier, Amsterdam, https://doi.org/10.1016/j.bbr.2007.09.033.

Mansour, H. H. (2013), “Protective effect of ginseng against gamma-irradiation-induced oxidative stress and endothelial dysfunction in rats”, EXCLI Journal, Vol. 12, Leibniz Research Centre for Working Environment and Human Factors, Dortmund, pp. 766-777.

Marshall, J. (1985), “Radiation and the ageing eye”, Ophthalmic & physiological optics, Vol. 5, Wiley-Blackwell, Hoboken, https://doi.org.10.1111/j.1475-1313.1985.tb00666.x.

Padgaonkar, V. A. et al. (2015) “Thioredoxin reductase activity may be more important than GSH level in protecting human lens epithelial cells against UVA light”, Photochemistry and photobiology, Vol. 91/2, Wiley-Blackwell, Hoboken, https://doi.org/10.1111/php.12404.

Pendergrass, W. et al. (2010), “X-ray induced cataract is preceded by LEC loss, and coincident with accumulation of cortical DNA, and ROS; similarities with age-related cataracts”, Molecular Vision, Vol. 16, Emory University, Atlanta, pp. 1496-513.

Philipp, J. et al. (2020), “Radiation Response of Human Cardiac Endothelial Cells Reveals a Central Role of the cGAS-STING Pathway in the Development of Inflammation”, Proteomes, Vol. 8/4, Multidisciplinary Digital Publishing Institute, Basel, https://doi.org/10.3390/proteomes8040030.

Quan, Y. et al. (2021), “Connexin hemichannels regulate redox potential via metabolite exchange and protect lens against cellular oxidative damage”, Redox biology, Vol. 46, Elsevier, Amsterdam, https://doi.org/10.1016/j.redox.2021.102102.

Ramadan, R. et al. (2020), “Connexin43 Hemichannel Targeting With TAT-Gap19 Alleviates Radiation-Induced Endothelial Cell Damage”, Frontiers in Pharmacology, Vol. 11, Frontiers Media SA, Lausanne, https://doi.org/10.3389/fphar.2020.00212

Rehman, M. U. et al. (2016), “Comparison of free radicals formation induced by cold atmospheric plasma, ultrasound, and ionizing radiation”, Archives of biochemistry and biophysics, Vol. 605, Elsevier, Amsterdam, https://doi.org/10.1016/j.abb.2016.04.005.

Rogers, C. S. et al. (2004), “The effects of sub-solar levels of UV-A and UV-B on rabbit corneal and lens epithelial cells”, Experimental eye research, Vol. 78, Elsevier, Amsterdam, https://doi.org/10.1016/j.exer.2003.12.011.

Rong, X. et al. (2019), “TRIM69 inhibits cataractogenesis by negatively regulating p53”, Redox biology, Vol. 22, Elsevier, Amsterdam, https://doi.org/10.1016/j.redox.2019.101157.

Rugo, R. E. and R. H. Schiestl (2004), “Increases in oxidative stress in the progeny of X-irradiated cells”, Radiation research, Vol. 162/4, Radiation Research Society, Bozeman, https://doi.org/10.1667/rr3238.

Santos, A. L., S. Sinha, and A. B. Linder (2018), “The good, the bad, and the ugly of ROS: New insights on aging and aging-related diseases from eukaryotic and prokaryotic model organisms”, Oxidative medicine and cellular longevity, Vol. 2018, Hindawi, London, https://doi.org/10.1155/2018/1941285.

Schoenfeld, M. P. et al. (2012), “A hypothesis on biological protection from space radiation through the use of new therapeutic gases as medical counter measures”, Medical gas research, Vol. 2/8, BioMed Central Ltd, London, https://doi.org/10.1186/2045-9912-2-8.

Sharma, U. C. et al. (2018), “Effects of a novel peptide Ac-SDKP in radiation-induced coronary endothelial damage and resting myocardial blood flow”, Cardio-oncology, Vol. 4, BioMed Central Ltd, London, https://doi.org/10.1186/s40959-018-0034-1.

Shen, Y. et al. (2018), “Transplantation of bone marrow mesenchymal stem cells prevents radiation-induced artery injury by suppressing oxidative stress and inflammation”, Oxidative Medicine and Cellular Longevity, Vol. 2018, Hindawi, London, https://doi.org/10.1155/2018/5942916.

Slezak, J. et al. (2017), “Potential markers and metabolic processes involved in the mechanism of radiation-induced heart injury”, Canadian journal of physiology and pharmacology, Vol. 95/10, Canadian Science Publishing, Ottawa, https://doi.org/10.1139/cjpp-2017-0121.

Soloviev, A. I. and I.V. Kizub (2019), “Mechanisms of vascular dysfunction evoked by ionizing radiation and possible targets for its pharmacological correction”, Biochemical pharmacology, Vol. 159, Elsevier, Amsterdam, https://doi.org/10.1016/j.bcp.2018.11.019.

Soltani, B. (2016), “Nanoformulation of curcumin protects HUVEC endothelial cells against ionizing radiation and suppresses their adhesion to monocytes: potential in prevention of radiation-induced atherosclerosis”, Biotechnology Letters, Vol. 38, Springer, London, https://doi.org/10.1007/s10529-016-2189-x.

Soucy, K. G. et al. (2011), “HZE 56Fe-Ion Irradiation Induces Endothelial Dysfunction in Rat Aorta: Role of Xanthine Oxidase”, Radiation Research, Vol. 176/4, Radiation Research Society, Bozeman, https://doi.org/10.1667/RR2598.1.

Soucy, K. G. et al. (2010), “Dietary inhibition of xanthine oxidase attenuates radiation-induced endothelial dysfunction in rat aorta”, Journal of Applied Physiology, Vol. 108/5, American Physiological Society, Rockville, https://doi.org/10.1152/japplphysiol.00946.2009.

Spector, A. (1990), “Oxidation and aspects of ocular pathology”, The CLAO journal, Vol. 16, Contact Lens Association of Ophthalmologists, Colorado, pp. S8-10.

Stohs, S. (1995), “The role of free radicals in toxicity and disease”, Journal of Basic and Clinical Physiology and Pharmacology, Vol. 6/3-4, Walter de Gruyter GmbH, Berlin, pp. 205-228.

Suman, S. et al. (2013), “Therapeutic and space radiation exposure of mouse brain causes impaired DNA repair response and premature senescence by chronic oxidant production”, Aging, Vol. 5/8, Impact Journals, Orchard Park, https://doi.org/10.18632/aging.100587.

Tahimic, C. G. T., and R. K. Globus (2017), “Redox signaling and its impact on skeletal and vascular responses to spaceflight”, International Journal of Molecular Sciences, Vol. 18/10, Multidisciplinary Digital Publishing Institute, Basel, https://doi.org/10.3390/ijms18102153.

Tangvarasittichai, O. and S. Tangvarasittichai (2018), “Oxidative stress, ocular disease and diabetes retinopathy”, Current pharmaceutical design, Vol. 24/40, Bentham Science Publishers, Sharjah, https://doi.org/10.2174/1381612825666190115121531.

Taysi, S. et al. (2012), “Zinc administration modulates radiation-induced oxidative injury in lens of rat”, Pharmacognosy Magazine, Vol. 8/2, https://doi.org/10.4103/0973-1296.103646

Tian, Y. et al. (2017), “The Impact of Oxidative Stress on the Bone System in Response to the Space Special Environment”, International Journal of Molecular Sciences, Vol. 18/10, Multidisciplinary Digital Publishing Institute, Basel, https://doi.org/10.3390/ijms18102132.

Tseng, B. P. et al. (2014), “Functional consequences of radiation-induced oxidative stress in cultured neural stem cells and the brain exposed to charged particle irradiation”, Antioxidants & redox signaling, Vol. 20/9, Mary Ann Leibert Inc., Larchmont, https://doi.org/10.1089/ars.2012.5134.

Turner, N. D. et al. (2002), “Opportunities for nutritional amelioration of radiation-induced cellular damage”, Nutrition, Vol. 18/10, Elsevier Inc, New York, http://doi.org/10.1016/S0899-9007(02)00945-0.

Ungvari, Z. et al. (2013), “Ionizing Radiation Promotes the Acquisition of a Senescence-Associated Secretory Phenotype and Impairs Angiogenic Capacity in Cerebromicrovascular Endothelial Cells: Role of Increased DNA Damage and Decreased DNA Repair Capacity in Microvascular Radiosensitivity”, The Journals of Gerontology Series A: Biological Sciences and Medical Sciences, Vol. 68/12, Oxford University Press, Oxford, https://doi.org/10.1093/gerona/glt057.

Varma, S. D. et al. (2011), “Role of ultraviolet irradiation and oxidative stress in cataract formation-medical prevention by nutritional antioxidants and metabolic agonists”, Eye & contact lens, Vol. 37/4, Lippincot Williams & Wilkins, Philadelphia, https://doi.org/10.1097/ICL.0b013e31821ec4f2.

Venkatesulu, B. P. et al. (2018), “Radiation-Induced Endothelial Vascular Injury: A Review of Possible Mechanisms”, JACC: Basic to Translational Science, Vol. 3/4, Elsevier, Amsterdam, https://doi.org/10.1016/j.jacbts.2018.01.014.

Veeraraghavan, J. et al. (2011), “Low-dose gamma-radiation-induced oxidative stress response in mouse brain and gut: regulation by NFκB-MnSOD cross-signaling”, Mutation research, Vol. 718/1-2, Elsevier, Amsterdam, https://doi.org/10.1016/j.mrgentox.2010.10.006.

Wang, C. et al. (2016), “Protective effects of cerium oxide nanoparticles on MC3T3-E1 osteoblastic cells exposed to X-ray irradiation”, Cellular Physiology and Biochemistry, Vol. 38/4, Karger International, Basel, https://doi.org/10.1159/000443092.

Wang, H. et al. (2019a), “Radiation-induced heart disease: a review of classification, mechanism and prevention”, International Journal of Biological Sciences, Vol. 15/10, Ivyspring International Publisher, Sydney, https://doi.org/10.7150/ijbs.35460.

Wang, H. et al. (2019b), “Gamma Radiation-Induced Disruption of Cellular Junctions in HUVECs Is Mediated through Affecting MAPK/NF-κB Inflammatory Pathways”, Oxidative Medicine and Cellular Longevity, Vol. 2019, Hindawi, London, https://doi.org/10.1155/2019/1486232.

Wegener, A. R. (1994), “In vivo studies on the effect of UV-radiation on the eye lens in animals”, Documenta ophthalmologica, Vol. 88, Springer, London, https://doi.org/10.1007/BF01203676.

Weinreb O. and A. Dovrat (1996), “Transglutaminase involvement in UV-A damage to the eye lens”, Experimental eye research, Vol. 63/5, Elsevier, London, https://doi.org/10.1006/exer.1996.0150.

Yang, H. et al. (2020), “Cytoprotective role of humanin in lens epithelial cell oxidative stress-induced injury”, Molecular medicine reports, Vol. 22/2, Spandidos Publishing Ltd, Athens, https://doi.org/10.3892/mmr.2020.11202.

Yao, K. et al. (2008), “The flavonoid, fisetin, inhibits UV radiation-induced oxidative stress and the activation of NF-κB and MAPK signaling in human lens epithelial cells”, Molecular Vision, Vol. 14, Emory University, Atlanta, pp. 1865-1871.

Yao, J. et al. (2009), “UVB radiation induces human lens epithelial cell migration via NADPH oxidase-mediated generation of reactive oxygen species and up-regulation of matrix metalloproteinases”, International Journal of Molecular Medicine, Vol. 24/2, Spandidos Publishing Ltd, Athens, https://doi.org/10.3892/ijmm_00000218.

Yves, C. (2000), "Oxidative stress and Alzheimer disease", The American Journal of Clinical Nutrition, Vol. 71/2, https://doi.org/10.1093/ajcn/71.2.621s.

Zhang, J. et al. (2012), “Ultraviolet radiation-induced cataract in mice: The effect of age and the potential biochemical mechanism”, Investigative ophthalmology & visual science, Vol. 53, Association for Research in Vision and Ophthalmology, Rockville, https://doi.org/10.1167/iovs.12-10482.

Zhang, L. et al. (2020), “Amifostine inhibited the differentiation of RAW264.7 cells into osteoclasts by reducing the production of ROS under 2 Gy radiation”, Journal of Cellular Biochemistry, Vol. 121/1, John Wiley & Sons, Ltd., Hoboken, https://doi.org/10.1002/jcb.29247.

Zhang, L. et al. (2018), “Astragalus polysaccharide inhibits ionizing radiation-induced bystander effects by regulating MAPK/NF-κB signaling pathway in bone mesenchymal stem cells (BMSCs)”, Medical Science Monitor, Vol. 24, International Scientific Information, Inc., Melville, https://doi.org/10.12659/MSM.909153.

Zigman, S. et al. (2000), “Effects of intermittent UVA exposure on cultured lens epithelial cells”, Current Eye Research, Vol. 20/2, Informa UK Limited, London, https://doi.org/10.1076/0271-3683(200002)2021-DFT095.

Zigman, S. et al. (1995), “Damage to cultured lens epithelial cells of squirrels and rabbits by UV-A (99.9%) plus UV-B (0.1%) radiation and alpha tocopherol protection”, Molecular and cellular biochemistry, Vol. 143, Springer, London, https://doi.org/10.1007/BF00925924.

Relationship: 2832: Energy Deposition leads to Tissue resident cell activation

AOPs Referencing Relationship

AOP Name	Adjacency	Weight of Evidence	Quantitative Understanding
Deposition of Energy Leading to Learning and Memory Impairment	adjacent	Moderate	Moderate

Evidence Supporting Applicability of this Relationship

Taxonomic Applicability

Term	Scientific Term	Evidence	Links
human	Homo sapiens	Low	NCBI
mouse	Mus musculus	Moderate	NCBI
rat	Rattus norvegicus	Moderate	NCBI

Life Stage Applicability

Life Stage	Evidence
All life stages	Moderate

Sex Applicability

Sex	Evidence
Unspecific	Moderate

The domain of applicability is related to any vertebrates and invertebrates with an innate immune system regardless of sex (Beck & Habicht, 1996, Sonetti et al., 1994, Rowley, 1996). The deposition of energy is most detrimental in utero because tissue resident cells and their pro-inflammatory responses can cause permanent tissue damage (Heiervang et al., 2010, McCollough et al., 2007, Kannan et al., 2007).

Key Event Relationship Description

Deposition of energy refers to particles that have sufficient energy to penetrate biological tissue leading to ionization events that can break water molecules and form free radicals. These can damage sensitive macromolecules such as DNA, protein and lipids (Chen, Oyarzabal & Hong, 2016; Mavragani et al., 2016). Ionization events occur from many types of radiation including, X-rays, gamma-rays, alpha particles, beta particles, heavy ions, and neutrons. X-rays and gamma rays induce sparse ionization events and energy is exponentially absorbed by tissues. Conversely, energetic charged particles can cause dense ionization events, leading to clustered damage and secondary ionization events (Niemantsverdriet et al., 2012).

When sufficient energy is deposited it can damage the cellular environment; this releases danger signals either passively when the ionization events induce cell death, or actively by cells undergoing life threatening stress (Denning et al., 2019; Vénéreau, Ceriotti & Bianchi, 2015). These signaling molecules, such as alarmins or damage-associated molecular pattern molecules (DAMPs), promote an inflammatory and regenerative environment by activating tissue resident cells (Chen, Oyarzabal & Hong, 2016; Vénéreau, Ceriotti & Bianchi, 2015). Resident immune cells, such as macrophages and dendritic cells, use pattern recognition receptors on their surfaces to detect alarmins and DAMPs which initiate their activation and proliferation (Chen, Oyarzabal & Hong, 2016; Mavragani et al., 2016). Activated cells can then regulate the recruitment of circulating immune cells and initiate inflammation

to remove damaged cells, eliminate harmful stimuli, and promote tissue repair (Schaue et al., 2015; Roh & Sohn, 2018). However, uncontrolled inflammation can then lead to a state of disease progression.

Evidence Supporting this KER

Overall Weight of Evidence: Moderate

Biological Plausibility

There is strong biological evidence and mechanistic understanding linking deposition of energy to tissue resident activation. It is widely accepted that deposition of energy can cause the activation of resident tissue cells (Di Maggio et al., 2015; Frey et al., 2015; Mavragani et al., 2016; Multhoff & Radons, 2012; Pinto et al., 2016; Rodel et al., 2012; Schaue et al., 2015; Yahyapour et al., 2018; Zhao & Robbins, 2009; Rienecker et al., 2021). Ionization of local tissue leads to direct tissue damage, reduced cellular homeostasis, genotoxic stress, and oxidative stress (Mavragani et al., 2016; Yahyapour et al., 2018). This damage can initiate tissue resident cell activation (Davies et al., 2013; Langston, Shibata & Horng, 2017; Rienecker et al., 2021). Primary damage and follow-on free-radical events typically occur within microseconds, but the inflammatory response carries on the damage through waves of reactive oxygen species generation as well as cytokine and chemokine release (Schaue et al., 2015). The resultant loss of cellular homeostasis, as well as primary and secondary cellular damage leads to the release of DAMPs (Mavragani et al., 2016; Yahyapour et al., 2018). Resident cells then use pattern recognition receptors to detect DAMPs resulting in their activation through a series of intracellular signaling cascades (Mavragani et al., 2016; Yahyapour et al., 2018).

There are many resident cells that become activated in response to radiation damage including lymphocytes, neutrophils, endothelial cells, and dendritic cells. Among the resident cells, macrophages are present in virtually all tissues and are the first line of defense against foreign pathogens and stressors. Resident macrophages have a ramified morphology with long, dynamic processes and are constantly surveying for signals of injury or infection (Betlazar et al., 2016; Paladini et al., 2021). They are also scavenger cells which engulf metabolites and debris from surrounding apoptotic cells to maintain healthy organs and tissues. When damage is detected, local macrophages become activated and move to the site of injury, where they signal other immune cells and release cytokines, chemokines, and other soluble molecules to mediate wound healing and initiate an inflammatory response (Hladik & Tapio, 2016; Paladini et al., 2021; Yahyapour et al., 2016; Rienecker et al., 2021). Resident macrophages detect endogenous cellular components released from damaged, stressed, or dying cells through pattern recognition receptors such as toll-like receptors (TLRs) (Chen, Oyarzabal & Hong, 2016; Yahyapour et al., 2016). TLRs can detect a wide variety of DAMPs including those potentially formed by deposition of energy (i.e., oxidized DNA, uric acid, ATP and high-mobility group box 1 protein) (Yahyapour et al., 2016). When TLRs detect DAMPs in the extracellular environment, they initiate intracellular signaling cascades that lead to the nuclear translocation of transcription factors, such as nuclear factor-κB (NF-κB), to induce the production of proinflammatory cytokines and chemokines (Chen, Oyarzabal & Hong, 2016; Yahyapour et al., 2018). The resident macrophages also initiate granulocyte-macrophage colony formation and recruitment of early myeloid progenitors to the site of injury (Schaue et al., 2015).

This response has been shown to occur across organs and tissue types using the same underlying mechanisms (Chen, Oyarzabal & Hong, 2016, Mavragani et al., 2016, Schaue et al., 2015). However, tissues are distinct in the types of activated cells and the resulting inflammatory responses. For example, the liver hosts the largest population of macrophages (Kupper cells) and is enriched with T lymphocytes or natural killer cells (Szabo, Mandrekar & Dolganiuc, 2007). Local Kupper cells use pattern recognition receptors to detect local radiation damage which leads to their activation (Szabo, Mandrekar & Dolganiuc, 2007). Activated cells secrete proinflammatory mediators, recruit macrophages and regulate the response of local T lymphocytes (Szabo, Mandrekar & Dolganiuc, 2007). In the lungs, radiation damage is first detected by local epithelial cells that produce pro-inflammatory mediators including cytokines and reactive oxygen species (Chen et al., 2018). These mediators stimulate mucus secretion by goblet cells and recruit macrophages and dendritic cells to initiate inflammation (Moldoveanu et al., 2009). In some organs, such as the brain, resident immune cells are abundant because the organ is separated from the immune system by the blood brain barrier to protect it from infection by foreign cells (Banks & Erickson, 2010). It has been shown that brain exposure to ionizing radiation can initiate activation of other types of resident immune cells, such as microglia and astrocytes (Betlazar et al., 2016). Microglial cells are the first line of defense in response to radiation damage and become activated in response to DAMPs released from local damaged cells (Betlazar et al., 2016). Microglia cells release pro-inflammatory mediators to regulate an inflammatory response and recruit additional immune cells to the site of injury (Betlazar et al., 2016). Microglia can subsequently induce astrocyte activation via the COX-2 pathway in the presence of a stressor (Betlazar et al., 2016; Cucinotta et al., 2014; Paladini et al., 2021). When damage is detected, astrocytes proliferate and form scar tissue via reactive gliosis (Makale et al., 2017).

Empirical Evidence

The empirical evidence surrounding this KER comes from research using in vitro and in vivo models. All organ systems are vulnerable to tissue resident activation from deposition of energy, however, provided below are consistent example of evidence from brain studies. Tissue resident cell activation is typically determined in the brain through the observation of the activation or proliferation of brain-resident immune cells, microglia and astrocytes.

The data consistently shows that direct deposition of energy can elicit damage to tissues and induce resident immune cell activation. The literature space is populated with studies examining effects of high doses (>2 Gy) of radiation with sparse studies examining effects for lower dose exposures (<1 Gy). Much of the high dose evidence is from work exposing rodent models to doses between 0 and 200 cGy of heavy ions and/or protons via whole body irradiation (Allen et al., 2020; Krukowski et al., 2018a; Parihar et al., 2020; Parihar et al., 2018; Parihar et al., 2016; Poulose et al., 2011; Raber et al., 2019; Sumam et al., 2013). Some studies

exposing rodents to high energy particles use high dose ranges (up to 4 Gy) (Cummings et al., 2007; Rola et al., 2008). Also included are studies using high doses (1-10 Gy) of X-rays or gamma rays used in a clinical setting (Acharya et al., 2016; Casciati et al., 2016; Chen et al., 2016; Hua et al., 2012; Hwang et al., 2006; Mizumatsu et al., 2003; Monje et al., 2002; Rola et al., 2007; Rola et al., 2004). In addition, very high-dose studies, using doses up to 25-45 Gy were included which showed consistent tissue resident activation following deposition of energy (Chiang, McBride & Withers, 1993; Dey et al., 2020; Kyrkanides et al., 1999; Moravan et al., 2011).

Dose Concordance

The literature supports the dose-concordance of the relationship between energy deposition and tissue resident cell activation, specifically glial cells, following exposure to ionizing radiation. Some studies, using exposures involving 16O, 48Ti, 4He and protons, observed significant increases in activation at doses of 5, 15, 30 or 50 cGy (Allen et al., 2020; Krukowski et al., 2018a; Parihar et al., 2016; Parihar et al., 2018; Parihar et al., 2020). These studies report an approximate 1.25- to 5-fold increase in microglia markers post-irradiation. Astrocyte activation was not reported in these studies. Other lower dose studies observed a radiation dose-dependent 1.3- to 14-fold increase in markers indicating activation of astrocytes and/or microglia (Casiati et al., 2016; Cummings et al., 2007; Poulose et al., 2011; Raber et al., 2019; Rola et al., 2008; Suman et al., 2013). These studies used 56Fe, protons, 16O or 28 Si, gamma rays and X-rays at doses ranging from 1-4 Gy. Various stressors at moderate doses further support the dose concordance of energy deposition and activation of tissue resident cells (Acharya et al., 2016; Dey et al., 2020; Hua et al., 2012; Monje et al., 2002; Rola et al., 2007; Rola et al., 2004). Consistency in the dose-response relationship was mostly exhibited at the higher doses (2-10 Gy), with reports showing a steady dose-dependent increase in resident tissue activation (Chen et al., 2016; Casciati et al., 2016; Hwang et al., 2006; Rola et al., 2008). With very high doses of radiation (up to 45 Gy), significant increases of GFAP and Mac-I levels in glia are observed (Chiang, McBride & Withers, 1993; Kyrkanides et al., 1999; Mizumatsu et al., 2003; Moravan et al., 2011). Additionally, increase in CD68+ cells have been shown following a total dose of 26 Gy (Dey et al., 2020). Further studies using mouse primary microglial cultures irradiated with X-rays at 10 Gy have shown a 2.5-fold increase in tissue resident cell activation. In vivo mice irradiated with 30 Gy also show a 9-fold increase in microglial activation (Xu et al., 2015). In general, these studies highlight that with an increase in deposited energy larger amounts of primary and secondary tissue damage occurs, which leads to increased proliferation and activation of resident immune cells.

Time Concordance

Many long-term and a few short-term studies find tissue-resident cell activation after deposition of energy. Mice irradiated with 35 Gy of gamma rays show activated astrocytes and microglia 4 h after irradiation (Kyrkanides et al., 1999). Rats irradiated with X-rays at 15 Gy show activation of astrocytes at 6 h (Hwang et al., 2006). Many studies show 1.2- to 3-fold increased activation one or a few days after irradiation in rats and mice (Casciati et al., 2016; Hwang et al., 2006; Kyrkanides et al., 1999; Moravan et al., 2011; Poulose et al., 2011). Furthermore, it has also been shown that activation continues until 1 year, measured after weeks and months, with a maximum 14-fold increase in marker levels shown after 2 months post-irradiation (Acharya et al., 2016; Allen et al., 2020; Casciati et al., 2016; Chiang, McBride & Withers, 1993; Chen et al., 2016; Cummings et al., 2007; Dey et al., 2020; Hua et al., 2012; Kyrkanides et al., 1999; Mizumatsu et al., 2003; Monje et al., 2002; Moravan et al., 2011; Parihar et al., 2020; Parihar et al., 2018; Parihar et al., 2016; Poulose et al., 2011; Raber et al., 2019; Rola et al., 2008; Rola et al., 2004; Suman et al., 2013).

Incidence Concordance

No available data.

Essentiality

Since deposition of energy is a physical stressor, it can be shielded, but chemicals cannot effectively block or decrease it. Thus further research is required to determine the effect of shielding radiation on the activation of tissue resident cells. Since deposited energy initiates events immediately, the removal of deposited energy, a physical stressor, also supports the essentiality of the key event. Studies that do not deposit energy are observed to have no downstream effects.

Uncertainties and Inconsistencies

- There is no consensus about sex-related responses to radiation exposure and the resulting activation of tissue resident cells. Krukowski et al. (2018a) and Parihar et al. (2020) found that female mice were immune to the effects of 0.3 and 0.5 Gy radiation on cell activation, while Raber et al. (2019) found that only female mice showed increased activated cells after 2 Gy.
- A large amount of uncertainty surrounds the impact of low-dose ionizing radiation on tissue resident cell activation. More evidence is required to determine the relationship between ionizing radiation at doses < 1 Gy and tissue-resident cell activation.

Quantitative Understanding of the Linkage

Dose Concordance

The table below provides some representative examples of quantitative linkages between the two key events. It was difficult to identify a general trend across all the studies due to differences in experimental design and reporting of the data. All data is statistically significant unless otherwise stated.

Reference	Experiment description	Result

Suman et al., 2013	In vivo. 6- to 8-week-old female C57BL/6J mice were irradiated with either 1.6 Gy 56Fe ions or 2 Gy gamma rays (137Cs source) both at 1 Gy/min. GFAP levels in the cerebral cortex measured by immunoblotting were used to indicate astrocyte activation.	GFAP levels increased 2.2-fold in the gamma ray irradiated group and 4.3-fold in the 56Fe ion irradiated group.
Poulose et al., 2011	In vivo. 2-month-old male Sprague-Dawley rats were irradiated with 5, 50 and 100 cGy 16O particles. GFAP was measured by western blot in the hippocampus.	At maximum, GFAP increased 1.2-fold after 5 and 50 cGy and 1.3-fold after 100 cGy.
Parihar et al., 2016	In vivo. Male Thy1-EGFP transgenic mice were irradiated with 600 MeV/amu charged particles (16O and 48Ti) (0.05 to 0.25 Gy/min) at 0.05 and 0.3 Gy. Activated glial cells were indicated by ED1 markers through immunostaining.	Number of activated microglia increased with dose, with a greater fold difference following 48Ti radiation than 16O. A maximum 1.9-fold change was observed at 30 cGy 48Ti at 27 weeks.
Parihar et al., 2018	In vivo. Male C57BL/6J mice were irradiated with He ions at 5 and 30 cGy (5 cGy/min). ED1 cells were used as markers for activated microglia by immunostaining and DAPI counterstaining.	ED1+ cells increased 3.5-fold after 5 cGy and 3.8-fold after 30 cGy, indicating microglial activation.
Parihar et al., 2020	In vivo. Mice were irradiated with low doses (≤≤ 30 cGy) of helium ions. Brain tissue sections were stained to identify microglia activation by CD68+ cells.	A 2.5-fold increase in CD68+ cells was observed in the male irradiated group following 30 cGy irradiation, indicating microglia activation. No increase in CD68+ was seen in the female mice.
Krukowski et al., 2018a	In vivo. C57B16/J mice were exposed to GCR at 0, 15, 50 cGy (252 MeV/amu protons, 249.3 MeV/amu helium ions, and 594.4 MeV/amu oxygen ions). Microglia were stained and levels were measured by Iba-1.	50 cGy male cohorts showed a significant 3- to 5-fold increase in Iba-1 + cells compared to the controls, indicating activated microglia in the dorsal hippocampus. No change was observed in the females.
Allen et al., 2020	In vivo. Mice were exposed to 4He irradiation (400 MeV/amu) at 30 cGy. CD68+ cells and Iba-1 immunochemistry were used to measure activated microglia. GFAP was measured to determine astrogliosis.	1.25-fold change in CD68+ cells was observed in the 30 cGy group compared to the controls. Iba-1+ microglia cells did not change significantly. No change in GFAP expression, a marker indicative of astrogliosis.
Cummings et al., 2007	In vivo. Sprague-Dawley rats were irradiated with 56Fe ions (600 MeV/amu) with 4 Gy dose. GFAP immunochemistry was used to identify astrogliosis.	There was a significant increase in GFAP+ cells 6 and 12 months post irradiation with 4 Gy.
Rola et al., 2008	In vivo. Male mice were irradiated with 0.5-4 Gy 56Fe ions. CD68+ cells determined microglia activation and BrdU identified neurogenesis.	Dose dependent increase was observed in BrudU+/CD68+ cells indicating newly born activated microglia. Significant increases of 3.4, 4.4 and 14-fold were observed at 1 Gy, 2 Gy and 4 Gy, respectively.
Raber et al., 2019	In vivo. Mice were irradiated with 1 GeV protons, 16O or 28Si (0, 25, 50, or 200 cGy). ELISA was used to detect levels of CD68 for activated microglia.	Cortical CD68 levels were increased by 1.7-fold in females irradiated with 200 cGy. This effect was not seen in males.
Hwang et al., 2006	In vivo and in vitro. Sprague-Dawley rats were irradiated with X-rays at 2-10 Gy and 15 Gy. Immunostaining, RT-PCR and western blot were used to analyze GFAP protein levels.	A dose dependent fold increase of cells with processed morphology was found. A 12- to 29.5-fold increase in activated morphology was observed in an astrocyte mixed-culture irradiated with 0-10 Gy.
Mizumatsu et al., 2003	In vivo. 2-month-old male C57BL/J6 mice were irradiated with X-rays at 175 cGy/min. New activated microglia in the hippocampus were determined with BrdU and CD68 staining.	A dose-dependent increase in BrdU/CD68+ cells was observed. No cells were activated without irradiation, 14% were after 2 Gy, 38% were after 5 Gy and 54% were after 10 Gy.
Hua et al., 2012	In vivo. Male FxBN rats were irradiated with 10 Gy of 137Cs gamma rays. CD68 was labelled with ED-1 in the hippocampus to show activated microglia.	The density of ED-1+ microglia increased 2- to 3-fold after 10 Gy.
Rola et al., 2007	In vivo. 8-week-old C57BL/6J mice were irradiated with 5 Gy X-rays. Microglial generation and activation in the hippocampus was determined by BrdU and CD68 staining.	The number of BrdU/CD68+ cells increased 1.3-fold.
Chen et al., 2016	In vitro. Human CHME5 microglia were irradiated with 137Cs gamma rays (LET 0.9 keV/µm) delivered over 1-3 minutes. Activated cells were determined by morphology as well as western blot for CR3/43 and Glut-5 activation markers.	CR3/43 and Glut-5 were both observed after 8 Gy, but just slightly or not at all after 0.5 Gy. At 8 Gy, microglia demonstrated an activated morphology.
Monie et	In vivo. Adult female Fischer 344 rats were irradiated with X-rays at 175 cGy/min with two fractions of 5 Gy. Activated	The percent of GFAP+ cells increased from 5.4% to 7.4% after 10 Gy. The percent of ED-1+ cells

al., 2002	astrocytes and microglia were determined in the hippocampus through GFAP and ED-1 staining, respectively.	increased from 0% to 22% after 10 Gy.
Casciati et al., 2016	In vivo. Female and male C57BL/6 mice were irradiated with X-rays. Activated astrocytes and microglia were determined in the hippocampus through GFAP and Iba-1 staining, respectively.	Iba-1+ cells increased 1.5-fold after 2 Gy, while GFAP+ cells increased 1.3-fold after 2 Gy. No changes in GFAP were seen after 0.1 Gy.
Acharya et al., 2016	In vivo. 6-month-old male C57Bl/6J mice were irradiated with 9 Gy X-rays. Microglia activation was determined by CD68 staining.	In the hippocampus, CD68+ cells increased 1.75-fold, while in the medial prefrontal cortex, they increased 1.25-fold.
Rola et al., 2004	In vivo. 21-day-old male C57BL/J6 mice were irradiated with 5 Gy X-rays at 1.75 Gy/min. Microglial and astrocyte activation was determined by CD68 and GFAP staining, respectively, double-stained with BrdU for gliogenesis in the subgranular zone.	CD68+ cells increased 2.5-fold, while GFAP+ cells increased 2-fold.
Dey et al., 2020	In vivo. 6-month-old male C57BL/6J mice received X-ray irradiation in fractions of 8.67 Gy/day (1.10 Gy/min) on alternating days for a total dose of 26 Gy. Activated microglia were determined through CD68 staining in the hippocampus.	In the CA1 region, CD68+ cells increased 3-fold, while in the CA3 region they increased 5-fold.
Chiang, McBride & Withers, 1993	In vivo. 12-week-old male C3Hf/Sed/Kam mice were irradiated with X-rays (238 cGy/min). Activated astrocytes and microglia were determined through GFAP and Mac-1 immunohistochemistry, respectively.	GFAP+ cells in the hippocampus and corpus callosum increased 1.5-fold after 30 and 36 Gy, and 2-fold after 45 Gy. Mac-1+ cells in the corpus callosum increased after 2 (1.2-fold), 20 (1.9-fold), 30 (2-fold), 36 (1.8-fold) and 45 Gy (2.8-fold).
Kyrkanides et al., 1999	In vivo. Male C3H/HeN mice were irradiated with 60Co gamma rays (35 Gy, 0.9 Gy/min). Activated astrocytes and microglia were determined through GFAP and Mac-1 immunohistochemistry, respectively.	Mac-1 and GFAP levels both showed greatly increased expression after 35 Gy.
Moravan et al., 2011	In vivo. 8- to 10-week-old male C57BL/6J mice were irradiated with 137Cs gamma rays at 1.25 Gy/min. GFAP expression was measured by RT-qPCR.	GFAP increased 2- to 3-fold after 25 and 35 Gy, but not significantly after 5 and 15 Gy.
Xu et al., 2015	In vivo and in vitro. Primary microglia from male BALB/c mice were irradiated with 30 Gy using a 6 MV β-ionizing-ray linear accelerator. Male BALB/c mice were irradiated with 10 Gy X-rays. Microglial cell activation was determined through morphology and Iba-1 immunohistochemistry.	In vitro, 10 Gy resulted in a 2.5-fold increase in activated microglia. In vivo, 30 Gy resulted in a 9-fold increase in activated microglia.

Time Concordance

Reference	Experiment description	Result
Suman et al., 2013	In vivo. 6- to 8-week-old female C57BL/6J mice were irradiated with either 1.6 Gy 56Fe or 2 Gy 137Cs gamma rays both at 1 Gy/min. GFAP levels in the cerebral cortex measured by immunoblotting were used to indicate astrocyte activation.	GFAP levels were increased 2.2-fold in the gamma irradiated group and 4.3-fold in the 56Fe irradiated group 12 months after exposure.
Poulose et al., 2011	In vivo. 2-month-old male Sprague-Dawley rats were irradiated with 5, 50 and 100 cGy 16O particles. GFAP was measured by western blot in the hippocampus.	After 36 h, GFAP was increased 1.2-fold after 100 cGy. After 75 days, GFAP increased 1.2-fold after 5 and 50 cGy and 1.3-fold after 100 cGy.
Parihar et al., 2016	In vivo. Male Thy1-EGFP transgenic mice were irradiated with 600 MeV/amu charged particles (16O and 48Ti) (0.05 to 0.25 Gy/min) at 0.05 and 0.3 Gy. Activated glial cells were indicated by ED1 markers through immunostaining.	ED1+ cells increased ~1.2- to 1.6-fold 15 weeks post 16O irradiation and ~2-fold 27 weeks post irradiation in all 48Ti irradiated groups.
Parihar et al., 2018	In vivo. Male C57BL/6J mice were irradiated with He ions at 5 and 30 cGy (5 cGy/min). ED1 cells were used as markers for activated microglia by immunostaining and DAPI counterstaining.	52 weeks after radiation, ED1+ cells increased 3.5-fold and 3.8-fold, indicating microglial activation.
Parihar et al., 2020	In vivo. Mice were irradiated with low doses (≤≤ 30 cGy) of helium ions. Brain tissue sections were stained to identify microglia activation by CD68+ cells.	The number of activated microglia increased by 2.5-fold in the male irradiated group 15 weeks after 30 cGy 4He irradiation.
Allen et al., 2020	In vivo. Mice were exposed to 4He irradiation (400 MeV/amu) at 30 cGy. CD68+ cells and Iba-1 immunochemistry were used to measure activated microglia. GFAP was measured to	An increase in CD68+ cells was observed 7-8 weeks post-irradiation.

	determine astrogliosis.	
Rola et al., 2008	In vivo. Male mice were irradiated with 0.5-4 Gy 56Fe ions. CD68+ cells determined microglia activation and BrdU identified neurogenesis.	2 months post-irradiation, BrdU/CD68+ cells increased up to 14-fold.
Cummings et al., 2007	In vivo. Sprague-Dawley rats were irradiated with 56Fe ions (600 MeV/amu) with 4 Gy dose. GFAP immunochemistry was used to identify astrogliosis.	There was a significant increase in GFAP+ cells 6 and 12 months post irradiation. A maximum 1.7-fold change was observed 12 months post irradiation compared to the control.
Raber et al., 2019	In vivo. Mice were irradiated with 1 GeV protons, 16O or 28Si (0, 25, 50, or 200 cGy). ELISA was used to detect levels of CD68 for activated microglia.	1.7-fold increase in CD68 levels in female mice was seen 3 months following 200 cGy exposure.
Hwang et al., 2006	In vivo. Sprague-Dawley rats were irradiated with X-rays at 2-10 Gy and 15 Gy. Immunostaining, RT-PCR and western blot were used to analyze GFAP protein levels.	GFAP levels were slightly higher at 6 h post irradiation compared to the initial levels and significantly increased 24 h post-irradiation.
Mizumatsu et al., 2003	In vivo. 2-month-old male C57BL/J6 mice were irradiated with 10 Gy X-rays at 175 cGy/min. New activated microglia in the hippocampus were determined with BrdU and CD68 staining.	No cells were activated without irradiation or 48 h after irradiation, while up to 50% of cells were activated 2 months after irradiation.
Hua et al., 2012	In vivo. Male FxBN rats were irradiated with 10 Gy of 137Cs gamma rays. CD68 was labelled with ED-1 in the hippocampus to show activated microglia.	The density of ED-1+ microglia increased 2- to 3-fold after 1 week, and was just slightly increased after 10 weeks.
Chen et al., 2016	In vitro. Human CHME5 microglia were irradiated with 8 Gy gamma rays (LET 0.9 keV/µm) delivered over 1-3 minutes. Activated cells were determined by morphology as well as western blot for CR3/43 and Glut-5 activation markers.	Cells demonstrated a normal morphology until 6 days then an activated morphology starting 7 days post-irradiation. Glut-5 was observed after 7,10 and 14 days , while CR3/43 was observed after 2 weeks.
Monje et al., 2002	In vivo. Adult female Fischer 344 rats were irradiated with X-rays at 175 cGy/min with two fractions of 5 Gy. Activated astrocytes and microglia were determined in the hippocampus through GFAP and ED-1 (labels CD68) staining, respectively.	The percent of GFAP+ cells increased from 5.4% to 7.4% after 2 months. The percent of ED-1+ cells increased from 0% to 22% after 2 months.
Casciati et al., 2016	In vivo. Female and male C57BL/6 mice were irradiated with 2 Gy X-rays. Activated astrocytes and microglia were determined in the hippocampus through GFAP and Iba-1 staining, respectively.	After 1 day, Iba-1+ cells increased 1.5-fold, while after 6 months, GFAP+ cells increased 1.3-fold.
Acharya et al., 2016	In vivo. 6-month-old male C57Bl/6J mice were irradiated with 9 Gy X-rays. Microglia activation was determined by CD68 staining.	In the hippocampus, CD68+ cells increased 1.75-fold after 2 and 6 weeks, while in the medial prefrontal cortex they increased 1.25-fold after 6 weeks.
Rola et al., 2004	In vivo. 21-day-old male C57BL/6J mice were irradiated with 5 Gy X-rays at 1.75 Gy/min. Microglial and astrocyte activation was determined by CD68 and GFAP staining, respectively, double-stained with BrdU for gliogenesis in the subgranular zone.	Both 1 and 3 months post-irradiation, CD68+ cells increased 2.5-fold, while GFAP+ cells increased 2-fold 3 months post-irradiation.
Dey et al., 2020	In vivo. 6-month-old male C57BL/6J mice received X-ray irradiation in fractions of 8.67 Gy/day at a dose rate of 1.10 Gy/min on alternating days for a total dose of 26 Gy. Activated microglia were determined through CD68 staining in the hippocampus.	Measured 5 weeks post-irradiation, in the CA1 region, CD68+ cells increased 3-fold, while in the CA3 region they increased 5-fold. No significant changes in these areas were observed 15 weeks post-irradiation.
Chiang, McBride & Withers, 1993	In vivo. 12-week-old male C3Hf/Sed/Kam mice were irradiated with X-rays (238 cGy/min). Activated astrocytes and microglia were determined through GFAP and Mac-1 immunohistochemistry, respectively. ELISA was also used to measure GFAP.	From 30-45 Gy, GFAP was significantly increased 1.2-fold 15 days after irradiation, as well as 120-180 days after irradiation. Similarly, 150 days after irradiation, Mac-1 was increased 1.2- to 3-fold from 2 to 45 Gy.
Kyrkanides et al., 1999	In vivo. Male C3H/HeN mice were irradiated with 60Co gamma rays (35 Gy, 0.9 Gy/min). Activated astrocytes and microglia were determined through GFAP and Mac-1 immunohistochemistry, respectively.	Mac-1 was first seen increased after 4 h, but peaked at 24 h. GFAP was also first increased after 4 h, and increased throughout the 7 days measured.
Moravan et al., 2011	In vivo. 8- to 10-week-old male C57BL/6J mice were irradiated with 137Cs gamma rays at 1.25 Gy/min. GFAP expression was measured by RT-qPCR.	GFAP increased 2- to 3-fold after 25 and 35 Gy, but not significantly after 5 and 15 Gy. The significant increases were observed after 1, 30 and 180 days.

Known modulating factors

Modulating	Details	Effects on the KER	References

factor	Details	Effects on the KER	References
Sex	Male and female mice had different responses in tissue resident cell activation following irradiation.	Male mice typically showed an increase in microglia activation, while female mice showed no significant changes. However, not all studies found this trend.	Krukowski et al., 2018a; Parihar et al., 2020; Raber et al., 2019
Drug	Colony stimulating factor 1 receptor inhibitor PLX5622 (eliminates microglia).	PLX5622 reduced the number of activated microglia.	Acharya et al., 2016; Allen et al., 2020; Krukowski et al., 2018b
Drug	P2X7 receptor (associated with microglial activation) inhibitor Brilliant Blue G.	Treatment attenuated the increase in microglial activation both in vivo and in vitro after irradiation.	Xu et al., 2015
Age	10-day-old and 10-week-old mice.	At 10 days old, irradiated mice showed increased glial activation, while at 10 weeks old they did not show significant changes in activation.	Casciati et al., 2016
	7-, 17- and 27-month-old mice.	Activation of microglia after irradiation decreased as age was increased.	Hua et al., 2012
Genetics	Extracellular SOD knockout mice.	Microglial activation was increased more in SOD knockout mice than wild-type mice after 5 Gy gamma rays.	Rola et al., 2007

Known Feedforward/Feedback loops influencing this KER

N/A

References

Acharya, M. M. et al. (2016), "Elimination of microglia improves cognitive function following cranial irradiation", Scientific Reports, Vol. 6/1, Nature Publishing Group, https://doi.org/10.1038/srep31545.

Allen, B. D. et al. (2020), "Mitigation of helium irradiation-induced brain injury by microglia depletion", Journal of Neuroinflammation, Vol. 17/1, Nature, https://doi.org/10.1186/s12974-020-01790-9.

Al Zaman, M. A. and Q. M. R. Nizam. (2022), "Study on Shielding Effectiveness of a Combined Radiation Shield for Manned Long Termed Interplanetary Expeditions", Journal of Space Safety Engineering, Vol. 9/1, Elsevier, Amsterdam, https://doi.org/10.1016/j.jsse.2021.12.003.

Banks, W. A. and M. A. Erickson. (2010), "The blood–brain barrier and immune function and dysfunction", Neurobiology of Disease, Vol. 37/1, Elsevier, Amsterdam, https://doi.org/10.1016/j.nbd.2009.07.031.

Beck, G. and G. S. Habicht. (1996), "Immunity and the Invertebrates", Scientific American, Vol. 275/5, Nature, https://doi.org/10.1038/scientificamerican1196-60.

Betlazar, C. et al. (2016), "The impact of high and low dose ionising radiation on the central nervous system", Redox Biology, Vol. 9, Elsevier, Amsterdam, https://doi.org/10.1016/j.redox.2016.08.002.

Capri, M. et al. (2019), "Recovery from 6-month spaceflight at the International Space Station: muscle-related stress into a proinflammatory setting", The FASEB Journal, Vol. 33/4, Wiley, https://doi.org/10.1096/fj.201801625R.

Casciati, A. et al. (2016), "Age-related effects of X-ray irradiation on mouse hippocampus", Oncotarget, Vol. 7/19, https://doi.org/10.18632/oncotarget.8575.

Chen, H. et al. (2016), "Delayed activation of human microglial cells by high dose ionizing radiation", Brain Research, Vol. 1646, Elsevier, Amsterdam, https://doi.org/10.1016/j.brainres.2016.06.002.

Chen, L. et al. (2018), "Inflammatory responses and inflammation-associated diseases in organs", Oncotarget, Vol. 9/6, https://doi.org/10.18632/oncotarget.23208.

Chen, S.-H., E. A. Oyarzabal and J.-S. Hong. (2016), "Critical role of the Mac1/NOX2 pathway in mediating reactive microgliosis-generated chronic neuroinflammation and progressive neurodegeneration", Current Opinion in Pharmacology, Vol. 26, Elsevier, Amsterdam, https://doi.org/10.1016/j.coph.2015.10.001.

Chiang, C. S., W. H. McBride and H. R. Withers. (1993), "Radiation-induced astrocytic and microglial responses in mouse brain", Radiotherapy and Oncology, Vol. 29/1, Elsevier, Amsterdam, https://doi.org/10.1016/0167-8140(93)90174-7.

Cucinotta, F. A. et al. (2014), "Space radiation risks to the central nervous system", Life Sciences in Space Research, Vol. 2,

Elsevier, Amsterdam, https://doi.org/10.1016/j.lssr.2014.06.003.

Cummings, P. et al. (2007), "High-energy (hze) radiation exposure causes delayed axonal degeneration and astrogliosis in the central nervous system of rats", Gravitational and Space Research, Vol. 20/2.

Davies, L. C. et al. (2013), "Tissue-resident macrophages", Nature Immunology, Vol. 14/10, Nature, https://doi.org/10.1038/ni.2705.

Denning, N.-L. et al. (2019), "DAMPs and NETs in Sepsis", Frontiers in Immunology, Vol. 10, Frontiers, https://doi.org/10.3389/fimmu.2019.02536.

Dey, D. et al. (2020), "Neurological Impairments in Mice Subjected to Irradiation and Chemotherapy", Radiation Research, Vol. 193/5, BioOne, https://doi.org/10.1667/RR15540.1.

Di Maggio, F. M. et al. (2015), "Portrait of inflammatory response to ionizing radiation treatment", Journal of Inflammation, Vol. 12/1, Nature, https://doi.org/10.1186/s12950-015-0058-3.

Frey, B. et al. (2015), "Modulation of inflammation by low and high doses of ionizing radiation: Implications for benign and malign diseases", Cancer Letters, Vol. 368/2, Elsevier, Amsterdam, https://doi.org/10.1016/j.canlet.2015.04.010.

Heiervang, K. S. et al. (2010), "Effect of low dose ionizing radiation exposure in utero on cognitive function in adolescence", Scandinavian Journal of Psychology, Vol. 51/3, Wiley, https://doi.org/10.1111/j.1467-9450.2010.00814.x.

Hladik, D. and S. Tapio. (2016), "Effects of ionizing radiation on the mammalian brain", Mutation Research - Reviews in Mutation Research, Vol. 770, Elsevier, Amsterdam, https://doi.org/10.1016/j.mrrev.2016.08.003.

Hua, K. et al. (2012), "Regionally Distinct Responses of Microglia and Glial Progenitor Cells to Whole Brain Irradiation in Adult and Aging Rats", PLoS ONE, Vol. 7/12, PLOS, San Francisco, https://doi.org/10.1371/journal.pone.0052728.

Hwang, S. Y. et al. (2006), "Ionizing radiation induces astrocyte gliosis through microglia activation", Neurobiology of Disease, Vol. 21/3, Academic Press, https://doi.org/10.1016/j.nbd.2005.08.006.

Kannan, S. et al. (2007), "Microglial Activation in Perinatal Rabbit Brain Induced by Intrauterine Inflammation: Detection with 11C-(R)-PK11195 and Small-Animal PET", Journal of Nuclear Medicine, Vol. 48/6, https://doi.org/10.2967/jnumed.106.038539.

Krukowski, K. et al. (2018a), "Female mice are protected from space radiation-induced maladaptive responses", Brain, Behavior, and Immunity, Vol. 74, Academic Press Inc., https://doi.org/10.1016/j.bbi.2018.08.008.

Krukowski, K. et al. (2018b), "Temporary microglia-depletion after cosmic radiation modifies phagocytic activity and prevents cognitive deficits", Scientific Reports 2018 8:1, Vol. 8/1, Nature Publishing Group, https://doi.org/10.1038/s41598-018-26039-7.

Kyrkanides, S. et al. (1999), "TNFα and IL-1β mediate intercellular adhesion molecule-1 induction via microglia-astrocyte interaction in CNS radiation injury", Journal of Neuroimmunology, Vol. 95/1–2, Elsevier, Amsterdam, https://doi.org/10.1016/S0165-5728(98)00270-7.

Langston, P. K., M. Shibata and T. Horng. (2017), "Metabolism Supports Macrophage Activation", Frontiers in Immunology, Vol. 8, Frontiers, https://doi.org/10.3389/fimmu.2017.00061.

Makale, M. T. et al. (2017), "Mechanisms of radiotherapy-associated cognitive disability in patients with brain tumours", Nature Reviews Neurology, Vol. 13/1, Nature, https://doi.org/10.1038/nrneurol.2016.185.

Mavragani, I. V. et al. (2016), "Key mechanisms involved in ionizing radiation-induced systemic effects. A current review", Toxicology Research, Vol. 5/1, Oxford University Press, Oxford, https://doi.org/10.1039/c5tx00222b.

McCollough, C. H. et al. (2007), "Radiation Exposure and Pregnancy: When Should We Be Concerned?", RadioGraphics, Vol. 27/4, Radiological Society of North America, Oak Brook, https://doi.org/10.1148/rg.274065149.

Mizumatsu, S. et al. (2003), "Extreme sensitivity of adult neurogenesis to low doses of X-irradiation", Cancer Research, Vol. 63/14.

Moldoveanu, B. et al. (2009), "Inflammatory mechanisms in the lung.", Journal of inflammation research, Vol. 2, pp. 4021–4027, American Association for Cancer Research.

Monje, M. L. et al. (2002), "Irradiation induces neural precursor-cell dysfunction", Nature Medicine, Vol. 8/9, Nature, https://doi.org/10.1038/nm749.

Moravan, M. J. et al. (2011), "Cranial irradiation leads to acute and persistent neuroinflammation with delayed increases in T-cell infiltration and CD11c expression in C57BL/6 mouse brain", Radiation Research, Vol. 176/4, BioOne, https://doi.org/10.1667/RR2587.1.

Multhoff, G. and J. Radons. (2012), "Radiation, Inflammation, and Immune Responses in Cancer", Frontiers in Oncology, Vol. 2, Frontiers, https://doi.org/10.3389/fonc.2012.00058.

Niemantsverdriet, M. et al. (2012), "High and Low LET Radiation Differentially Induce Normal Tissue Damage Signals", International Journal of Radiation Oncology*Biology*Physics, Vol. 83/4, Elsevier, Amsterdam, https://doi.org/10.1016/j.ijrobp.2011.09.057.

Paladini, M. S. et al. (2021), "Microglia depletion and cognitive functions after brain injury: From trauma to galactic cosmic ray", Neuroscience Letters, Vol. 741, Elsevier, Amsterdam, https://doi.org/10.1016/j.neulet.2020.135462.

Parihar, V. K. et al. (2016), "Cosmic radiation exposure and persistent cognitive dysfunction", Scientific Reports, Vol. 6/June, Nature Publishing Group, https://doi.org/10.1038/srep34774.

Parihar, V. K. et al. (2018), "Persistent nature of alterations in cognition and neuronal circuit excitability after exposure to simulated cosmic radiation in mice", Experimental Neurology, Vol. 305, Academic Press Inc., https://doi.org/10.1016/j.expneurol.2018.03.009.

Parihar, V. K. et al. (2020), "Sex-Specific Cognitive Deficits Following Space Radiation Exposure", Frontiers in behavioral neuroscience, Vol. 14, Frontiers, https://doi.org/10.3389/fnbeh.2020.535885.

Patel, R. et al. (2020), "Protons and High-Linear Energy Transfer Radiation Induce Genetically Similar Lymphomas With High Penetrance in a Mouse Model of the Aging Human Hematopoietic System.", International journal of radiation oncology*biology*physics, Vol. 108/4, Elsevier, Amsterdam, https://doi.org/10.1016/j.ijrobp.2020.06.070.

Pinto, A. et al. (2016), "Ionizing radiation modulates human macrophages towards a pro-inflammatory phenotype preserving their pro-invasive and pro-angiogenic capacities", Scientific Reports, Vol. 6/1, Nature, https://doi.org/10.1038/srep18765.

Poulose, S. M. et al. (2011), "Exposure to 16O-particle radiation causes aging-like decrements in rats through increased oxidative stress, inflammation and loss of autophagy", Radiation Research, Vol. 176/6, BioOne, https://doi.org/10.1667/RR2605.1.

Raber, J. et al. (2019), "Combined Effects of Three High-Energy Charged Particle Beams Important for Space Flight on Brain, Behavioral and Cognitive Endpoints in B6D2F1 Female and Male Mice", Frontiers in physiology, Vol. 10, Frontiers, https://doi.org/10.3389/fphys.2019.00179.

Rienecker, K. D. A. et al. (2021), "Microglia: Ally and Enemy in Deep Space", Neuroscience & Biobehavioral Reviews, Vol. 126, https://doi.org/10.1016/j.neubiorev.2021.03.036.

Rodel, F. et al. (2012), "Modulation of Inflammatory Immune Reactions by Low-Dose Ionizing Radiation: Molecular Mechanisms and Clinical Application", Current Medicinal Chemistry, Vol. 19/12, Bentham Science Publishers, https://doi.org/10.2174/092986712800099866.

Roh, J. S. and D. H. Sohn. (2018), "Damage-Associated Molecular Patterns in Inflammatory Diseases.", Immune network, Vol. 18/4, https://doi.org/10.4110/in.2018.18.e27.

Rola, R. et al. (2008), "Hippocampal Neurogenesis and Neuroinflammation after Cranial Irradiation with 56 Fe Particles", Radiation Research, Vol. 169/6, BioOne, https://doi.org/10.1667/RR1263.1.

Rola, R. et al. (2004), "Radiation-induced impairment of hippocampal neurogenesis is associated with cognitive deficits in young mice", Experimental Neurology, Vol. 188/2, Elsevier, Amsterdam, https://doi.org/10.1016/j.expneurol.2004.05.005.

Rola, R. et al. (2007), "Lack of extracellular superoxide dismutase (EC-SOD) in the microenvironment impacts radiation-induced changes in neurogenesis", Free radical biology & medicine, Vol. 42/8, Elsevier, Amsterdam, https://doi.org/10.1016/j.freeradbiomed.2007.01.020.

Rowley, A. F. (1996), "The evolution of inflammatory mediators", Mediators of inflammation, Vol. 5/1, Hindawi, https://doi.org/10.1155/S0962935196000014.

Schaue, D. et al. (2015), "Radiation and inflammation", Seminars in radiation oncology, Vol. 25/1, Elsevier, Amsterdam, https://doi.org/10.1016/j.semradonc.2014.07.007.

Sonetti, D. et al. (1994), "Microglia in invertebrate ganglia", Proceedings of the National Academy of Sciences of the United States of America, Vol. 91/19, National Academy of Science, https://doi.org/10.1073/pnas.91.19.9180.

Suman, S. et al. (2013), "Therapeutic and space radiation exposure of mouse brain causes impaired dna repair response and premature senescence by chronic oxidant production", Aging, Vol. 5/8, https://doi.org/10.18632/aging.100587.

Szabo, G., P. Mandrekar and A. Dolganiuc. (2007), "Innate immune response and hepatic inflammation", Seminars in liver disease, Vol. 27/4, Thieme, https://doi.org/10.1055/s-2007-991511.

Vénéreau, E., C. Ceriotti and M. E. Bianchi. (2015), "DAMPs from Cell Death to New Life", Frontiers in immunology, Vol. 6, Frontiers, https://doi.org/10.3389/fimmu.2015.00422.

Xu, P. et al. (2015), "Extracellular ATP enhances radiation-induced brain injury through microglial activation and paracrine signaling via P2X7 receptor", Brain, Behavior, and Immunity, Vol. 50, Elsevier, Amsterdam, https://doi.org/10.1016/j.bbi.2015.06.020.

Yahyapour, R. et al. (2018), "Radiation-induced inflammation and autoimmune diseases", Military Medical Research, Vol. 5/1, Nature, https://doi.org/10.1186/s40779-018-0156-7.

Zhao, W. and M. Robbins. (2009), "Inflammation and Chronic Oxidative Stress in Radiation-Induced Late Normal Tissue Injury: Therapeutic Implications", Current Medicinal Chemistry, Vol. 16/2, Bentham Science, https://doi.org/10.2174/092986709787002790.

Relationship: 2771: Oxidative Stress leads to Altered Signaling

AOPs Referencing Relationship

AOP Name	Adjacency	Weight of Evidence	Quantitative Understanding
Deposition of energy leads to vascular remodeling	adjacent	High	Low
Deposition of Energy Leading to Learning and Memory Impairment	adjacent	High	Low
Deposition of energy leading to occurrence of bone loss	adjacent	High	Low

Evidence Supporting Applicability of this Relationship

Taxonomic Applicability

Term	Scientific Term	Evidence	Links
human	Homo sapiens	Low	NCBI
mouse	Mus musculus	High	NCBI
rat	Rattus norvegicus	High	NCBI
Pig	Pig	Moderate	NCBI

Life Stage Applicability

Life Stage	Evidence
Adult	Moderate
Juvenile	Moderate

Sex Applicability

Sex	Evidence
Male	High
Female	Low
Unspecific	Low

Based on the prioritized studies presented here, the evidence of taxonomic applicability is low for humans despite there being strong plausibility as the evidence only includes *in vitro* human cell-derived models. The taxonomic applicability for mice and rats is considered high as there is much available data using *in vivo* rodent models that demonstrate the concordance of the relationship. The taxonomic applicability was determined to be moderate for pigs as only one *in vivo* study provided meaningful support to the relationship. In terms of sex applicability, all *in vivo* studies that indicated the sex of the animals used male animals, therefore, the evidence for males is high and females is considered to be low for this KER. The majority of studies used adolescent animals, with a few using adult animals. Preadolescent animals were not used to support the KER; however, the relationship in preadolescent animals is still plausible.

Key Event Relationship Description

Oxidative stress occurs when the production of free radicals exceeds the capacity of cellular antioxidant defenses (Cabrera & Chihuailaf, 2011). Reactive oxygen species (ROS) and reactive nitrogen species (RNS) are both free radicals that can contribute to oxidative stress (Ping et al., 2020); however, ROS are more commonly studied than RNS (Nagane et al., 2021). ROS can mediate oxidative damage to biomacromolecules as they react with DNA, proteins and lipids, resulting in functional changes to these molecules (Ping et al., 2020). For example, ROS acting on lipids creates lipid peroxidation (Cabrera & Chihuailaf, 2011).

Many signaling pathways control and maintain physiological balance within a living organism, and these can be impacted by oxidative stress. Excessive reactive oxygen and nitrogen species (RONS) during oxidative stress can modify biological molecules and directly cause DNA damage, which can lead to altered signal transduction pathways (Hughson, Helm & Durante, 2018; Lehtinen & Bonni, 2006; Nagane et al., 2021; Ping et al., 2020; Ramadan et al., 2021; Schmidt-Ullrich et al., 2000; Soloviev & Kizub, 2019; Wang, Boerma & Zhou, 2016; Venkatesulu et al., 2018; Zhang et al., 2016). Different cell types can express distinct cellular pathways that can have varied response to an increase in oxidative stress. For example, oxidative stress in endothelial cells has been shown to inhibit the insulin-like growth factor 1 receptor (IGF-1R) and phosphatidylinositol-3-kinase/protein kinase B (PI3K/Akt) pathway and to activate the mitogen-activated protein kinase (MAPK) pathway, which can then have downstream detrimental effects (Ping et al., 2020). The MAPK family pathway is also activated in the central nervous system (CNS) in response

to oxidative stress through calcium-induced phosphorylation of several kinases. These include phosphoinositide 3-kinase (PI3K), protein kinase A (PKA) and protein kinase C (PKC) and calcium/calmodulin-dependent protein kinase II (CaMKII) (Lehtinen & Bonni, 2006; Li et al., 2013; Ramalingam & Kim, 2012). Oxidative stress in bone cells can lead to increased expression of the receptor activator of nuclear factor kappa B ligand (RANKL) and Nrf2 activation (Tahimic & Globus, 2017; Tian et al., 2017). Following activation, Nrf2 then interferes with the activation of runt-related transcription factor 2 (Runx2), and depending on the level of oxidative stress, this may result in altered bone cell function (Kook et al., 2015).

Evidence Supporting this KER

Overall weight of evidence: High

Biological Plausibility

Many reviews describe the role of oxidative stress in altered signaling. The mechanisms through which oxidative stress can contribute to changes in various signaling pathways are well-described. For example, oxidative stress can directly alter signaling pathways through protein oxidation (Ping et al., 2020; Schmidt-Ullrich et al., 2000; Valerie et al., 2007). Oxidation of cysteine and methionine residues, which are particularly sensitive to oxidation, can cause conformational change, protein expansion, and degradation, leading to changes in the protein levels of signaling pathways (Ping et al., 2020). Furthermore, oxidation of key residues in signaling proteins can alter their function, resulting in altered signaling. For example, oxidation of methionine 281 and 282 in the Ca^{2+}/calmodulin binding domain of Ca^{2+}/calmodulin-dependent protein kinase II (CaMKII) leads to constitutive activation of its kinase activity and subsequent downstream alterations in signaling pathways (Li et al., 2013; Ping et al., 2020). Similarly, during oxidative stress, tyrosine phosphatases can be inhibited by oxidation of a catalytic cysteine residue, resulting in increased phosphorylation of proteins in various signaling pathways (Schmidt-Ullrich et al., 2000; Valerie et al., 2007). Particularly relevant to this are the MAPK pathways. For example, the extracellular signal-regulated kinase (ERK) pathway is activated by upstream tyrosine kinases and relies on tyrosine phosphatases for deactivation (Lehtinen & Bonni, 2006; Valerie et al., 2007).

Furthermore, oxidative stress can indirectly influence signaling pathways through oxidative DNA damage which can lead to mutations or changes in the gene expression of proteins in signaling pathways (Ping et al., 2020; Schmidt-Ullrich et al., 2000; Valerie et al., 2007). DNA damage surveillance proteins like ataxia telangiectasia mutated (ATM) kinase and ATM/Rad3-related (ATR) protein kinase phosphorylate over 700 proteins, leading to changes in downstream signaling (Nagane et al., 2021; Schmidt-Ullrich et al., 2000; Valerie et al., 2007). For example, ATM, activated by oxidative DNA damage, phosphorylates many proteins in the ERK, p38, and Jun N-terminal kinase (JNK) MAPK pathways, leading to various downstream effects (Nagane et al., 2021; Schmidt-Ullrich et al., 2000).

The response of oxidative stress on signaling pathways has been studied extensively in various diseases. Herein presented are examples relevant to a few cell types related to vascular disease, impaired learning and memory, and bone loss. Many other pathways are plausible but available research has highlighted these to be critical to disease.

Endothelial cells: Endothelial cells can normally produce ROS. Antioxidant enzymes and the glutathione redox buffer control the redox state of vascular tissues. However, the dysregulation of signaling pathways can occur in the endothelium when oxidative stress is favored (Soloviev & Kizub, 2019). Oxidative stress can activate the acidic sphingomyelinase (ASMase)/ceramide pathway, the MAPK pathways, the p53/p21 pathway, and the signaling proteins p16 and p21, as well as inhibit the PI3K/Akt pathway (Hughson, Helm & Durante, 2018; Nagane et al., 2021; Ping et al., 2020; Ramadan et al., 2021; Soloviev & Kizub, 2019; Wang, Boerma & Zhou, 2016).

Bone cells: oxidative stress can induce signaling changes in the Wnt/β-catenin pathway, the RANK/RANKL pathway, the Nrf2/HO-1 pathway, and the MAPK pathways (Domazetovic et al., 2017; Manolagas & Almeida, 2007; Tian et al., 2017).

Brain cells: oxidative stress can induce alterations to various pathways such as the PI3K/Akt pathway, cAMP response element-binding protein (CREB) pathway, the p53/p21 pathway, as well as the MAPK family pathways, including JNK, ERK and p38 (Lehtinen & Bonni, 2006; Ramalingam & Kim, 2012).

Additionally, the electron transport chain in the mitochondria is an important source of ROS, which can damage mitochondria by inducing mutations in mitochondrial DNA. These mutations lead to mitochondrial dysfunction due to alterations in cellular respiration mechanisms that perpetuates oxidative stress and can then induce the release of signaling molecules related to apoptosis from the mitochondria. Pro-apoptotic markers (Bax, Bak and Bad) and anti-apoptotic markers (Bcl-2 and Bcl-xL) can regulate the caspase pathway that ultimately mediate apoptosis (Annunziato et al., 2003; Wang & Michaelis, 2010; Wu et al., 2019).

The mechanisms of oxidative stress leading to altered signaling may be different for each pathway. For example, although both the PI3K/Akt and MAPK pathways can be regulated by insulin-like growth factor (IGF)-1, ROS results in selective inhibition of the IGF-1R/PI3K/Akt pathway by inhibiting the IGF-1 receptor (IGF-1R) activation of IRS1 (Ping et al., 2020). Additionally, ROS-induced MAPK activation can be done through Ras-dependent signaling. Firstly, oxygen radicals mediate the phosphorylation of upstream epidermal growth factor receptors (EGFRs) on tyrosine residues, resulting in increased binding of growth factor receptor-bound protein 2 (Grb2) and subsequent activation of Ras signaling (Lehtinen & Bonni, 2006). Direct inhibition of MAPK phosphatases with hydroxyl radicals also activates this pathway (Li et al., 2013). In another mechanism, ROS competitively inhibit the Wnt/β-catenin pathway through the activation of forkhead box O (FoxO), which are involved in the antioxidant response and require binding of β-catenin for transcriptional activity (Tian et al., 2017).

Empirical Evidence

Evidence for this relationship was collected from studies using *in vivo* mouse, rat, and pig models, as well as *in vitro* mouse-derived, rat-derived, bovine-derived, and human-derived models. The stressors used to support this relationship include gamma rays, X rays, microgravity, hydrogen peroxide, chronic cold stress, heavy ion radiation, simulated ischemic stroke and growth differentiation factor (GDF) 15 overexpression. These stressors were shown to increase levels of oxidative stress and induce changes within relevant signaling pathways (Azimzadeh et al., 2021; Azimzadeh et al., 2015; Fan et al., 2017; Xu et al., 2019; Suman et al., 2013; Limoli et al., 2004; Tian et al., 2020; Hladik et al., 2020; Diao et al., 2018; Hasan, Radwan & Galal, 2019; Xin et al., 2015; El-Missiry et al., 2018; Kenchegowda et al., 2018; Kook et al., 2015; Sun et al., 2013; Yoo, Han & Kim, 2016, Zhao et al., 2013; Bai et al., 2020; Chen et al., 2009; Carvour et al., 2008; Wortel et al., 2019; Azimzadeh et al., 2017; Park et al., 2016; Sakata et al., 2015; Ruffels et al., 2004; Crossthwaite et al., 2002).

Incidence concordance

A few studies demonstrate greater changes to oxidative stress than to altered signaling. Human umbilical vein endothelial cells (HUVECs) irradiated with 10 Gy of X-rays showed a 20-fold increase in ROS and a 0.5-fold decrease in the ratio of p-Akt/Akt (Sakata et al., 2015). Microgravity exposure to preosteoblast cells showed a 0.24-fold decrease to the antioxidant Cu/Zn-superoxide dismutase (SOD) and a 0.36-fold decrease to p-Akt (Yoo, Han & Kim, 2016). It was also shown in rats that MDA levels increased by 1.5-fold while angiotensin and aldosterone increased by 1.4-fold after 6 Gy of gamma rays (Hasan, Radwan & Galal, 2020). Bai et al. (2020) demonstrated with multiple endpoints that ROS levels increased, and antioxidant enzyme levels decreased more than signaling pathways were altered.

Dose Concordance

Many studies demonstrate dose concordance for this relationship, at the same doses. Low-dose (0.5 Gy) X-ray irradiation of human coronary artery endothelial cells (HCAECs) show increased protein carbonylation with decreased glutathione S-transferase omega-1 (GSTO1) antioxidant levels and a simultaneous alteration of signaling proteins Rho GDP-dissociation inhibitor (RhoGDI), p16, and p21 (Azimzadeh et al., 2017). A dose of about 2 Gy of gamma rays showed decreased antioxidants as well as decreased protein levels and activation of the PI3K/Akt pathway in pig cardiac tissue (Kenchegowda et al., 2018). Similarly, gamma irradiation at 6 Gy resulted in reduced levels of the antioxidant glutathione (GSH) and increased levels of the lipid peroxidation marker MDA as well as an increase in the renin angiotensin aldosterone system (RAAS) measured in rat heart tissue and blood serum, respectively (Hasan, Radwan & Galal, 2020). HUVECs irradiated with 10 Gy of X-rays demonstrated increased ROS while p-Akt decreased and p-ERK1/2 increased (Sakata et al., 2015). Gamma radiation at 15 Gy led to both increased ROS as well as attenuated p38 MAPK and Nrf2 signaling pathways in murine cardiac tissue (Fan et al., 2017). In contrast, 16 Gy X-ray exposure led to decreased levels of the antioxidant SOD, increased MDA as well as increased MAPK signaling in murine heart tissue (Azimzadeh et al., 2021). After simulated microgravity, changes to signaling pathways, increased ROS and MDA, and decreased antioxidants were found both in *in vitro* mouse-derived bone cells and in *in vivo* rat femurs. Increased ROS levels and decreased antioxidants were found with changes in the RANK/RANKL pathway, Wnt/β-catenin pathway, Runx2, PI3K/Akt pathway, and MAPK pathways (Diao et al., 2018; Sun et al., 2013; Xin et al., 2015; Yoo, Han & Kim, 2016).

A few studies also find that oxidative stress often occurs at lower doses than altered signaling pathways. Bai et al. (2020) measured oxidative stress, shown by increased ROS and decreased antioxidant expression, at 2, 5, and 10 Gy of gamma rays. They also found Runx2 increased at the same doses, but the p53/p21 pathway was only significantly altered at 5 and 10 Gy (Bai et al., 2020). At similar doses, X-ray irradiated mouse osteoblast-like cell line MC3T3-E1 cells showed increased ROS and decreased antioxidants both 4 and 8 Gy (Kook et al., 2015). While HO-1 also increased at both 4 and 8 Gy, Nrf2 and Runx2 were measured altered at 8 Gy (Kook et al., 2015). In another study, X-ray irradiation at 16 Gy resulted in decreased SOD and increased MDA and protein carbonylation, which were associated with decreased PI3K/Akt pathway activity and protein levels, decreased ERK activity and protein levels, increased p38 activity, and increased p16 and p21 protein levels in heart tissue (Azimzadeh et al., 2015). Azimzadeh et al. (2015) also showed that at 8 Gy oxidative stress was still observed, but fewer signaling molecule levels and activity were altered at this. Particularly, no changes to MAPK pathways were observed.

Within the rat hippocampus, El-Missiry et al. (2018) demonstrated that exposure to 4 Gy of X-irradiation results in increased 4-HNE (oxidative stress marker) levels, reduced antioxidant activity and an increase in p53 expression. In the cerebral cortex of mice, Suman et al. (2013) reported that 1.6 Gy of ^{56}Fe and 2 Gy of gamma rays increased ROS levels, consequently increased p21 and

p53 levels. Limoli et al. (2004) also reported increased ROS levels in mice and rat neural precursor cells after exposure to X-irradiation (1-10 Gy), accompanied by increased expression of p21 and p53. Hladik et al. (2020) exposed female mice to 0.063, 0.125 or 0.5 Gy of gamma-radiation, which resulted in increases of protein carbonylation, as well as increased phosphorylation of CREB, ERK1/2 and p38. Radiation-induced changes in apoptotic markers were also reported. More specifically, there was a significant rise in pro-apoptotic markers Bax and caspase 3, with significant reduction in anti-apoptotic marker Bcl-xL (Hladik et al., 2020). Furthermore, middle cerebral artery occlusion (MCAO) surgery known to simulate ischemic stroke in C57BL/6J mice was shown to increase ROS levels, as well as the phosphorylation of ERK1/2, p38 and JNK (Tian et al., 2020).

Other studies that have used hydrogen peroxide (H_2O_2) to induce oxidative stress within cell cultures, have also observed alterations in signaling pathways. Zhao et al. (2013) exposed mouse hippocampal-derived HT22 cells to varying concentrations of H_2O_2 and found a dose-dependent increase in ROS production from 250-1000 µM. Additionally, treating the cells to H_2O_2 resulted in a concentration-dependent increase of ERK1/2, JNK1/2 and p38 phosphorylation. Ruffels et al. (2004) incubated human neuroblastoma cells (SH-SY5Y) to varying concentrations of H_2O_2 that ranged from 0.5-1.25 mM and found a dose-dependent increase in JNK1/2, ERK1/2 and Akt phosphorylation. Another study exposed SH-SY5Y and rat pheochromocytoma (PC12) cells to 0.05-2 mM H_2O_2 and found a dose-dependent increase in ROS from 0-1 mM in SH-SY5Y cells, and from 0-2 mM in PC12 cells with a concentration-dependent increase in ERK1/2, p38 and JNK phosphorylation (Chen et al., 2009). Furthermore, Crossthwaite et al. (2002) incubated neuronal cultures from 15- to 16-day-old Swiss mice to 100, 300 and 1000 µm H_2O_2 and showed increased levels of ROS. A corresponding increase in ERK1/2 and Akt activation was observed at 100-300 µm, and for JNK1/2 the observation was observed at 1000 µm. Carvour et al. (2008) treated N27 cells (rat dopaminergic cell line) to 3-30 µM H_2O_2 and measured increased ROS levels, as well as increased apoptotic signaling molecules caspase 3 and proapoptotic kinase protein kinase C-δ (PKCδ) cleavage.

Time Concordance

Limited evidence shows that oxidative stress leads to altered signaling pathways in a time concordant manner. When irradiated with X-rays, HCAECs, BAECs and MCT3T3-E1 osteoblast-like cells show increase in ROS or levels of protein carbonylation, or a decrease in the levels of superoxide dismutase (SOD), catalase (CAT), GSTO1 or GSH at earlier timepoints than alterations in the signaling molecules p16, p21, Ceramide, Runx2, and HO-1 (Azimzadeh et al., 2017; Kook et al., 2015; Wortel et al., 2019). As the key events are both molecular-level changes, both can occur quickly after irradiation. Wortel et al. (2019) found that increased hydrogen peroxide levels could be observed *in vitro* as early as 2 minutes post-irradiation, while ASMase activity and ceramide levels were only increased 5 minutes post-irradiation.

When exposed to H_2O_2, PC12 cells show an increase production of ROS with a corresponding increase in phosphorylation of MAPK proteins in a time-dependent fashion. An increase in ERK1/2, JNK and p38 phosphorylation was observed within 5-15 minutes and sustained for over 2 hours (Chen et al., 2009). When exposed to cold stress for 1, 2 and 3 weeks, MDA levels increased in a time-dependent manner from 1-3 weeks within the brain tissue isolated from C57BL/6 mice. The expressions of JNK, ERK and p38 phosphorylation levels were all also significantly upregulated in chronic cold-stressed groups for all time-points (Xu et al., 2019). After gamma irradiation (2 Gy), ROS increased 2 months post-irradiation, while increased p21 and decreased Bcl-2 were only observed at 12 months (Suman et al., 2013). However, other signaling molecules were increased at both times.

Essentiality

Several studies have investigated the essentiality of the relationship, where the blocking or attenuation of the upstream KE causes a change in frequency of the downstream KE. The increase in oxidative stress can be modulated by certain drugs, antioxidants and media. L-carnitine injections decreased ROS and increased p-p38/p38 and p-Nrf2/Nrf2 signaling (Fan et al., 2017). Fenofibrate was found to return SOD, phosphorylated MAPK signaling proteins and increase Nrf2 levels (Azimzadeh et al., 2021). Antioxidants (N-acetyl cysteine, curcumin) were shown to restore or reduce ROS levels closer to control levels following radiation or microgravity exposure, respectively. Signaling proteins in the Nrf2/HO-1 pathway and the RANKL/osteoprotegerin (OPG) ratio were decreased and brought closer to control levels (Kook et al., 2015; Xin et al., 2015). Hydrogen rich medium showed reduced ROS with restoration of OPG and RANKL signaling levels to controls (Sun et al., 2013). Polyphenol S3 (60 mg/kg/d) treatment was found to reverse the effect of microgravity on CAT, SOD and MDA, returning the levels to near control values. Meanwhile, Runx2 mRNA levels and β-catenin/β-actin levels increased following treatment (Diao et al., 2018). Sildenafil is another drug that was found to reduce ROS generation by inhibiting O_2^- production and intracellular peroxynitrite levels in bovine aortic endothelial cells (BAECs) after gamma irradiation. As well, ASMase activity and ceramide levels were inhibited by sildenafil (Wortel et al., 2019).

Within brain cells, several antioxidants have been found to attenuate oxidative stress-induced alterations in signaling pathways. These antioxidants include Melandrii Herba extract, N-acetyl-L-cysteine (NAC), gallocatechin gallate/epigallocatechin-3-gallate, Cornus officinalis (CC) and fermented CC (FCC), L-165041, fucoxanthin, and edaravone. These antioxidants were shown to reduce ROS and subsequently decrease phosphorylation of MAPKs such as ERK1/2, JNK1/2 and p38 after exposure to radiation, H2O2 or

LPS (Lee et al., 2017; Deng et al., 2012; Park et al., 2021; Tian et al., 2020; Schnegg et al., 2012; Zhao et al., 2017; Zhao et al., 2013; El-Missiry et al., 2018). Another documented modulator is mesenchymal stem-cell conditioned medium (MSC-CM), which was able to alleviate oxidative stress in HT22 cells and restore levels of p53 (Huang et al., 2021).

Uncertainties and Inconsistencies

- MAPK pathways can exhibit varied responses after exposure to oxidative stress. The expected response is an increase in the activity of the ERK, JNK, and p38 pathways as protein phosphatases, involved in the inactivation of MAPK pathways, are deactivated by oxidative stress (Valerie et al., 2007). Although some studies observe this (Azimzadeh et al., 2021; Sakata et al., 2015), others show a decrease (Fan et al., 2017; Yoo, Han & Kim, 2016) or varying changes (Azimzadeh et al., 2015) in the MAPK pathways.

Quantitative Understanding of the Linkage

The tables below provide representative examples of quantitative linkages between the two key events. It was difficult to identify a general trend across all the studies due to differences in experimental design and reporting of the data. All data that is represented is statistically significant unless otherwise indicated.

Response-response relationship

Dose/Incidence Concordance

Reference	Experiment Description	Result
Azimzadeh et al., 2017	*In vitro*. HCAECs were irradiated with 0.5 Gy of X-rays (0.5 Gy/min). Protein carbonylation and GSTO1 antioxidant levels were measured with a carbonylation assay and immunoblotting, respectively. Proteins from various signaling pathways including RhoGDI, p16, and p21 were measured with immunoblotting.	After 0.5 Gy, carbonyl content increased a maximum of 1.2-fold and GSTO1 decreased a maximum of 0.78-fold. After 0.5 Gy, p-RhoGDI decreased a maximum of 0.7-fold, p16 increased a maximum of 1.5-fold, and p21 increased a maximum of 1.2-fold.
Kenchegowda et al., 2018	*In vivo*. Male 3- to 5-month-old Gottingen minipigs and Sinclair minipigs were whole-body irradiated with 1.7-2.3 Gy of ^{60}Co gamma rays (0.6 Gy/min). Both survivors (n=23) and euthanized moribund animals (n=17) had measurements taken for oxidative stress and altered signaling taken from the heart. SOD, CAT, and p67 (subunit of NADPH oxidase/NOX, involved in producing superoxide) levels were determined with western blot. ELISA and western blot were used to measure altered signaling in the IGF/PI3K/Akt pathway.	Compared to survivors, radiation induced a 2.1-fold increase in p67, 0.87-fold decrease in SOD, and a 0.83-fold decrease in CAT (non-significant, ns) in the deceased group. Compared to survivors, the ratio of activated (phosphorylated) to total IGF-1R and the ratio of activated (phosphorylated) to total Akt both decreased 0.5-fold in the deceased group.
Kook et al., 2015	*In vitro*. MC3T3-E1 osteoblast-like cells were irradiated with 2, 4, and 8 Gy of X-rays (1.5 Gy/min). ROS were measured with a fluorescent probe, and SOD, CAT, and GSH antioxidant activities were determined with assay kits. Protein levels in the Nrf2/HO-1 signaling pathway were determined by either western blot or RT-PCR.	ROS increased linearly at 2 and 4 Gy up to 1.4-fold at 8 Gy (significant changes at 4 Gy and 8 Gy). GSH and SOD were decreased 0.7-fold at 4 Gy and 0.5-fold at 8 Gy (insignificant increases at 2 Gy). CAT was also decreased but not significantly. HO-1 increased 3.3-fold after 4 Gy and 4.9-fold after 8 Gy (insignificant increase at 2 Gy). Nrf2 increased 2.3-fold after 8 Gy. Runx2 mRNA was decreased 0.5-fold after 8 Gy.
Bai et al., 2020	*In vitro*. Rat-derived bone marrow-derived mesenchymal stem cells (bmMSCs) were irradiated with 2, 5, and 10 Gy of ^{137}Cs gamma rays. Mitochondrial and cellular ROS levels were determined with fluorescent probes. RT-qPCR was performed to measure antioxidant enzyme expression. Protein expression in various signaling pathways was measured by western blot.	Mitochondrial ROS increased 1.6-fold at 2 Gy (non-significant), 2-fold at 5 Gy, and 2.3-fold at 10 Gy. Cellular ROS increased 1.2-fold at 2 Gy, 1.5-fold at 5 Gy, and 2.1-fold at 10 Gy. Antioxidants SOD1, SOD2, and CAT all decreased about 0.9-fold (ns for SOD2) after 2 Gy, 0.8- to 0.7-fold at 5 Gy, and 0.7- to 0.4-fold at 10 Gy. Runx2 decreased 0.9-fold at 2 and 5 Gy and 0.6-fold at 10 Gy. p21 increased 1.6-fold at 5 Gy and 2.5-fold at 10 Gy. p53 increased 1.6-fold at 5 Gy and 1.7-fold at 10 Gy. p16 remained unchanged.
Fan et al., 2017	*In vivo*. 10-week-old male C57BL/6J mice were irradiated with ^{60}Co gamma rays at 3 Gy/day for 5 days. Left ventricular cardiac tissue was harvested for analysis. ROS was detected by dihydroethidium (DHE) staining. MAPK and Nrf2 signaling molecules were measured by western blot.	Following irradiation, ROS production increased by 3.6-fold. p-p38/p38 decreased by 0.36-fold and p-Nrf2/Nrf2 decreased by 0.14-fold.
Hasan,	*In vivo*. 6-week-old male Wistar rats were irradiated with 6 Gy ^{137}Cs gamma rays. Oxidative stress was	Following irradiation, MDA levels increased by 1.5-fold and GSH levels decreased by 0.5-fold. AngII and aldosterone

Radwan & Galal, 2020	measured by MDA and GSH in heart tissue. Angiotensin II (AngII) and aldosterone, key molecules in the RAAS pathway, were measured with ELISA kits in serum.	increased 1.4-fold compared to control.
Azimzadeh et al., 2015	*In vivo*. Male 10-week-old C57BL/6 mice were irradiated with 8 and 16 Gy of X-rays. SOD, MDA, and protein carbonylation levels were determined with immunoblotting, lipid peroxidation, and protein carbonylation assays, respectively, in heart tissue. Proteins in various signaling pathways were measured with immunoblotting in heart tissue.	SOD decreased 0.7-fold at both 8 and 16 Gy and MDA increased 1.4-fold after 8 Gy and 2.1-fold after 16 Gy. Protein carbonylation increased 1.4-fold after 16 Gy. Levels and activity of proteins in the PI3K/Akt pathway were decreased between 0.5- and 0.1-fold at both 8 and 16 Gy. The ERK/MAPK pathway was found decreased 0.5-fold at 16 Gy and the p38/MAPK pathway was found increased 1.3-fold at 16 Gy. p16 was increased 1.6-fold at both 8 and 16 Gy. p21 was increased 2.4-fold at both 8 and 16 Gy.
Sakata et al., 2015	*In vitro*. HUVECs were irradiated with 10 Gy X-rays at a dose rate of 5 Gy/min. Measurements were performed 0-72 h post-irradiation. ROS were detected by fluorescence microscopy. MAPK, Akt, p-p38, JNK and ERK1/2 signaling molecules were measured by western blot.	Following 10 Gy irradiation, the intensity representing ROS generation increased 20- and 30-fold at the 24 and 72 h timepoints, respectively. MAPK, p38 and JNK remained unchanged for the 72 h measured following 10 Gy irradiation. p-Akt/Akt in HUVECs after 10 Gy irradiation showed an initial decrease at 5 min and a delayed decrease of 0.5-fold at 6-24 h. p-ERK1/2 decreased at 5 min then increased to a maximum 1.75-fold change.
Wortel et al., 2019	*In vitro*. BAECs were irradiated with 10 Gy ^{137}Cs gamma rays at a rate of 1.66 Gy/min. Extracellular H2O2 was measured by Amplex Red Assay, intracellular H_2O_2 levels were determined by HyPer sensor and peroxynitrite was quantified by chemiluminescence assay. Superoxide levels were quantified by luminescence after treatment with Diogenes Complete Enhancer Solution. The activation of the ASMase enzyme and the levels of ceramide were quantified by radioenzymatic assay to deter mine the changes on the ASMase/ceramide pathway.	Following 10 Gy irradiation, intracellular H_2O_2 increased to a maximum 1.35-fold. Extracellular H_2O_2 increased by 1.75-fold. Peroxynitrite increased by 2.86-fold after 10 Gy (Fig 5). Superoxide levels increased over 350% at 2 minutes after 10 Gy irradiation. ASMase activity increased to a maximum 5.6-fold at 5 min after irradiation, then decreased and remained unchanged until the 30 min time-point. Ceramide increased from -500 to over 3000 pmol/106 cells. The significance of these changes was not indicated against a control.
Azimzadeh et al., 2021	*In vivo*. Male C57BL/6J mice 8 weeks of age were irradiated with 16 Gy of X-rays to the heart. SOD antioxidant activity and MDA in heart tissue were determined with an assay kit and lipid peroxidation assay, respectively. The level of proteins in MAPK pathways were determined by ELISA in heart tissue.	After 16 Gy, SOD decreased 0.8-fold and MDA increased 1.3-fold. After 16 Gy, p-ERK increased 1.5-fold, p-p38 increased 1.3-fold, and p-JNK increased 1.3-fold.
Xin et al., 2015	*In vitro* and *in vivo*. *In vitro*. MC3T3-E1 osteoblast-like cells were exposed to microgravity for 96 hours. ROS were determined with a fluorescent probe and the RANK/RANKL pathway was measured using RANKL and OPG assay kits. *In vivo*. Male 8-week-old Sprague-Dawley rats were exposed to hind-limb suspension for 6 weeks. Femur and plasma MDA and femur sulfhydryl levels were measured with assay kits and the RANK/RANKL pathway was measured in the femur using RANKL and OPG assay kits.	*In vitro*. ROS increased 1.5-fold and the RANKL/OPG ratio increased 1.6-fold. *In vivo*. Serum and femur MDA increased 1.4-fold and femur sulfhydryl decreased 0.6-fold. The RANKL/OPG ratio increased 3.5-fold.
Sun et al., 2013	*In vitro*. MC3T3-E1 osteoblast-like cells were exposed to microgravity (0.01G) for 96 hours. ROS production was measured by a fluorescent probe. The RANKL/OPG ratio was determined by assay kit	ROS increased 1.5-fold. The RANKL/OPG ratio increased 1.6-fold. Runx2 expression decreased 0.4-fold.

	and Runx2 mRNA expression was determined by RT-qPCR	
Yoo, Han & Kim, 2016	*In vitro*. Preosteoblast MC3T3-E1 cells were exposed to microgravity conditions by a 3D clinostat at a speed from 1-10 rpm. Oxidative stress was measured by Cu/Zn-SOD, Mn-SOD and catalase activity. Signaling molecules, p-Akt, phosphorylation of the mechanistic target of rapamycin p-(mTOR), and p-ERK were measured by western blot.	Following microgravity exposure, Cu/Zn-SOD and Mn-SOD levels decreased by 0.24 and 0.65-fold, respectively. Signaling molecules p-Akt decreased by 0.36-fold. p-mTOR and p-ERK decreased by 0.58-fold.
Diao et al., 2018	*In vivo*. The left femur of rats was studied after exposure to simulated microgravity. Oxidative stress was measured by MDA, SOD, and CAT levels. RANK/RANKL signaling pathway was measured in rat femur by enzyme-linked immunoassay detection of OPG/RANKL molecules. Signaling molecule, Runx2, mRNA levels were measured by quantitative real time PCR. The Wnt/β-catenin pathway was measured by western blot for β-catenin protein levels.	MDA increased by 1.4-fold. SOD and CAT levels decreased by 0.4-fold. OPG/RANKL decreased by 0.6-fold. Runx2 mRNA levels decreased 0.04-fold (Fig 8d). β-catenin decreased 0.6-fold.
El-Missiry et al., 2018	*In vivo*. Male Wistar rats were irradiated with gamma rays (^{137}Cs source, 4 Gy, 0.695 cGy/s) and measurements were taken from the hippocampus. Assay kits were used to assess levels of oxidative stress for marker 4-HNE (4-hydroxy-2-nonenal) and antioxidant markers GSH, glutathione peroxidase (GPx) and glutathione reductase (GR). Levels of p53 were determined using an assay kit.	After 4 Gy, 4-HNE increased 2.4-fold, protein carbonylation increased 3.2-fold, GSH decreased 0.4-fold, GPx decreased 0.3-fold, GR decreased 0.2-fold, and p53 increased 2.7-fold.
Suman et al., 2013	*In vivo*. Female adult C57BL/6J mice were irradiated with 1.6 Gy of ^{56}Fe or 2 Gy of ^{137}Cs gamma irradiation at 1 Gy/min, then measurements were taken from the cerebral cortex. ROS levels were determined with flow cytometry and 4-HNE levels were assessed with immunohistochemical staining. p21 and p53 levels were determined with immunoblotting.	ROS increased a maximum of 1.2-fold after gamma rays and 1.4-fold after ^{56}Fe radiation. The number of 4-HNE+ cells increased a maximum of 4.4-fold after gamma radiation and 14-fold after ^{56}Fe radiation. p21 increased a maximum of 1.5-fold after gamma rays and 3-fold after ^{56}Fe radiation. p53 increased a maximum of 8.4-fold after gamma rays and 9-fold after ^{56}Fe radiation.
Limoli et al., 2004	*In vivo*. Adult male C57BL/6J mice were irradiated with 1-10 Gy of X-ray at 1.75 Gy/min. MDA levels in the hippocampus were measured using an assay kit and western blot was used to determine p53 and p21 levels. *In vitro*. Neural precursor cells from the rat hippocampus were irradiated with 1-10 Gy of X-ray at 4.5 Gy/min. ROS levels were measured using CM-H2DCFDA dye and Western blot was used to measure p53 and p21 levels.	MDA levels increased about 30% at 10 Gy. ROS increased a maximum of 31% at 1 Gy and 35% at 5 Gy, after 24 and 12 hours, respectively. At 5 Gy, p53 levels increased a maximum of 4-fold, while p- p21 also increased at this dose.
Tian et al., 2020	*In vivo*. C57BL/6J mice (including miR-137-/- and Src-/- models) underwent middle cerebral artery occlusion (MCAO) to simulate ischemic stroke and measurements were taken 7 days later in the cerebral cortex. ROS levels were measured with DCFH-DA fluorescent dye. Signaling molecules were measured with western blotting or RT-qPCR.	ROS increased 1.8-fold. ERK1/2, p38 and JNK mRNA increased 2- to 3- fold. The ratios of phosphorylated to total ERK1/2, p38 and JNK increased 2- to 3- fold as well.
Hladik et al., 2020	*In vivo*. Female B6C3F1 mice were exposed to total body ^{60}Co gamma irradiation at 0.063, 0.125, or 0.5 Gy and at a dose rate of 0.063 Gy/min. Measurements from the hippocampus were taken up to 24 months post-irradiation. Protein levels in various signaling pathways (CREB, p38, ERK1/2, pro-apoptotic Bax and cleaved caspase 3, anti-apoptotic Bcl-xL) were determined with	Carbonylated proteins (indicative of ROS levels) were elevated in the 0.125 and 0.5 Gy group by approximately 25% and 30%, respectively. CREB phosphorylation increased by approximately 20% and 25% at 0.063 and 0.125 Gy, respectively. Phosphorylated p38 increased by approximately 100% and 80% at 0.063 and 0.125 Gy, respectively. Phosphorylated ERK1/2 increased by approximately 100% and 90% at 0.063 and 0.125 Gy, respectively. Anti-apoptotic BCL-xL decreased by 1.7-fold at 0.5 Gy,

	immunoblotting.	whereas pro-apoptotic Bax increased by approximately 2-fold at this dose. Caspase 3 also increased by approximately 2-fold at 0.5 Gy.
Carvour et al., 2008	*In vitro*. Mesencephalic dopaminergic neuronal cell line (N27) derived from rat mesencephalon were exposed to 3, 10, or 30 µM of H_2O_2. ROS levels were detected using dihydroethidine dye and flow cytometry. Western blot was used to detect cleaved PKCδ and Sytox fluorescence was used to measure caspase-3 enzyme activity.	Exposure to 10 and 30 µM of H_2O_2 resulted in 34 and 58% increases in ROS production, respectively, compared to untreated N27 cells. Exposure to 3, 10, and 30 µM hydrogen peroxide resulted in 2-, 10-, and 9-fold increases in caspase-3 enzyme activity. Lastly, exposure to 10 and 30 µM of H_2O_2 dose-dependently induced proteolytic cleavage of PKCδ.
Chen et al., 2009	*In vitro*. PC12 and SH-SY5Y human cells were incubated with H_2O_2. The production of ROS was measured by detecting the fluorescent intensity of oxidant-sensitive probe CM-H2DCFDA. Western blot analysis was used to assess activation of MAPKs.	Treatment with H_2O_2 for 24 h resulted in a concentration-dependent increase of ROS production at the concentrations of 0–1 mM in PC12 and SH-SY5Y cells. In comparison with PC12, SH-SY5Y cells appeared to be more sensitive to H_2O_2, thereby showing a decreased ROS production at 2 mM. Additionally, treatment of PC12 cells with H_2O_2 for 2 h increased phosphorylation of Erk1/2 and p38 in a concentration-dependent manner. Noticeably, H_2O_2-activation of JNK resulted in a robust (5–10-fold) increase of protein expression and phosphorylation of c-Jun at 0.3–1 mM. Similar results were also seen in SH-SY5Y cells (data not shown).

Time-scale

Time Concordance

Reference	Experiment Description	Result
Azimzadeh et al., 2017	*In vitro*. HCAECs were irradiated with 0.5 Gy of X-rays (0.5 Gy/min). Protein carbonylation and GSTO1 antioxidant level were measured with a carbonylation assay and immunoblotting, respectively. Proteins from various signaling pathways including RhoGDI, p16 and p21 were measured with immunoblotting. Measurements were taken at 1, 7, and 14 days after irradiation.	After 7 and 14 days, carbonyl content increased 1.2-fold (insignificant increase at 1 day post-irradiation). After 1-14 days, GSTO1 decreased 0.78-fold (significant decreases at all timepoints). After 1 and 7 days, p-RhoGDI decreased 0.7-fold (non-significant decrease at 14 days post-irradiation). p16 increased 1.2-fold after 7 days and 1.5-fold after 14 days (non-significant increase at 1 day post-irradiation). p21 increased 1.2-fold after 7 and 14 days (insignificant increase at 1 day post-irradiation).
Wortel et al., 2019	*In vitro*. BAECs were irradiated with 10 Gy ^{137}Cs gamma rays at a rate of 1.66 Gy/min. Superoxide levels were quantified by luminescence after treatment with Diogenes Complete Enhancer Solution. The activation of the ASMase enzyme and the levels of ceramide were quantified by radioenzymatic assay to deter mine the changes on the ASMase/ceramide pathway.	Superoxide increased by over 350% at 2 minutes post-irradiation. ASMase activity increased to a maximum 5.6-fold at 5 min post-irradiation. Ceramide increased from -500 to over 3000 pmol/106 cells at 5 minutes post-irradiation. The significance of these changes was not indicated against a control.
Kook et al., 2015	*In vitro*. MC3T3-E1 osteoblast-like cells were irradiated with X-rays (1.5 Gy/min). ROS were measured with a fluorescent probe, and SOD, CAT, and GSH antioxidant activities were determined with assay kits. Protein levels in the Nrf2/HO-1 signaling pathway were determined by either western blot or RT-PCR.	After 1 day and 8 Gy, ROS increased 1.4-fold, GSH decreased 0.5-fold, and SOD decreased 0.5-fold. CAT was also decreased but not significantly. After 1 day and 8 Gy, Nrf2 increased 2.3-fold. After 2 days and 8 Gy, HO-1 increased 4.9-fold. After 3 days and 8 Gy, Runx2 mRNA was decreased 0.5-fold.
Suman et al., 2013	*In vivo*. Female adult C57BL/6J mice were irradiated with 1.6 Gy of ^{56}Fe or 2 Gy of 137Cs gamma irradiation at 1 Gy/min, then measurements were taken from the cerebral cortex until up to 12 months. ROS levels were determined with flow cytometry and 4-HNE levels were determined with immunohistochemical staining. p21 and p53 levels were determined with immunoblotting.	All changes after ^{56}Fe radiation were found after both 2 and 12 months post-irradiation. Most endpoints were also increased at both time points following gamma irradiation, however, p21 only increased at 12 months by 3-fold, but not 2 months, while oxidative stress was shown at 2 months (0.2-fold increase).
Xu et al.	*In vitro*. Adult male C57BL/6 mice experienced chronic cold stress for various lengths (1, 2 and	MDA levels increased in a time-dependent manner. At 1 week, there was an approximate 3-fold increase, at 2 weeks was an approx. 4-fold increase and for 3 weeks, there was an approx. 5-fold increase in response to cold stress. Phosphorylated JNK increased by ~10%

Xu et al., 2019	3 weeks). Brain tissue was then collected, and Western blot was used to measure MDA and proteins of MAPK (JNK, ERK and p38).	(1 week) and ~30% at 2 and 3 weeks compared to room temperature control. Phosphorylated ERK increased by ~60% at 1 week, ~150% at 2 weeks and ~140% at 3 weeks. Phosphorylated p38 increased by ~50% at 1 week, ~100% at 2 weeks and ~150% at 3 weeks.
Chen et al., 2009	*In vitro*. PC12 and SH-SY5Y human cells were incubated with hydrogen peroxide. The production of ROS was measured by detecting the fluorescent intensity of oxidant-sensitive probe CM-H2DCFDA. Western blot analysis was used to assess activation of MAPKs.	They observed that H_2O_2 induced phosphorylation of MAPKs in a time-dependent fashion. Within 5–15 min, H_2O_2 increased phosphorylation of Erk1/2, JNK and p38, and such phosphorylation was sustained for over 2 h. Consistently, high levels of c-Jun and phospho-c-Jun were induced.

Known modulating factors

Modulating factor	Details	Effects on the KER	References
Drug	Fenofibrate (PPARα activator, PPARα is a transcription factor that can activate antioxidant response)	Treatment of mice with 100 mg/kg of body weight daily for 2 weeks before and 2 weeks after radiation restored SOD activity, returned the level of phosphorylated MAPK proteins and increased Nrf2 levels.	Azimzadeh et al., 2021
Drug	L-carnitine (antioxidant)	L-carnitine injections (100 mg/kg) following irradiation resulted in decreased DHE staining, indicating ROS, and increased p-p38/p38 and p-Nrf2/Nrf2.	Fan et al., 2017
Drug	N-acetyl cysteine (antioxidant)	Treatment of osteoblast-like cells with 5 mM restored ROS levels, SOD activity, and the level of proteins in the Nrf2/HO-1 pathway.	Kook et al., 2015
Drug	Curcumin (antioxidant)	Treatment of osteoblast-like cells with 4 μM reduced ROS levels and the RANKL/OPG ratio. Treatment of rats with 40 mg/kg of body weight reduced oxidative stress and the RANKL/OPG ratio.	Xin et al., 2015
Drug	Bradykinin potentiating factor (BFP) (antioxidant)	Treatment with BFP (1ug/g) after irradiation showed decreased AngII and aldosterone levels compared to irradiation alone.	Hasan, Radwan & Galal, 2020
Media	Hydrogen-rich (antioxidant)	Osteoblasts in a medium consisting of 75% H2, 20% O2, and 5% CO_2 (vol/vol/vol) showed a reduction in ROS production and restoration of normal signaling.	Sun et al., 2013
Drug	Melatonin (antioxidant)	Treatment with 200 nM melatonin reversed the effect of microgravity on Cu/Zn-SOD and Mn-SOD to control levels.	Yoo, Han & Kim, 2016
Drug	Polyphenol S3	Polyphenol S3 treatment reverses the effect of microgravity on CAT, SOD and MDA, returning the levels to near control values when S3 is used at high dose (60mg/kg/d). Runx2 mRNA levels and β-catenin/β-actin levels increased following treatment and simulated microgravity.	Diao et al., 2018
Drug	Sildenafil	Sildenafil (5 uM) inhibits O2- production and attenuates intracellular peroxynitrite in BAECs after 10 Gy irradiation. As well, ASMase activity and ceramide generation was inhibited.	Wortel et al., 2019
Drug	DPI (NOX-inhibitor)	Inhibits O_2^- production and intracellular H_2O_2 in BAECs after 10 Gy irradiation.	Wortel et al., 2019
Drug	Edaravone (EDA) which acts as a free radical scavenger	EDA treatment was able to reduce the levels of ROS and consequently decrease the expression levels of phosphorylated JNK, p38 and ERK1/2.	Zhao et al., 2013
Drug	Melandrii Herba extract (antioxidant)	The extract was able to reduce the H_2O_2-induced phosphorylation of ERK1/2, JNK1/2 and p38 in human neuroblastoma SH-SY5Y cells.	Lee et al., 2017
Drug	N-acetyl-L-cysteine (NAC) (antioxidant)	Attenuated the effects of H_2O_2 in BV-2 murine microglial cells as treatment with NAC reduced c-Jun and ERK1/2 phosphorylation.	Deng et al., 2012
Drug	Gallocatechin gallate (GCG) or epigallocatechin-3-gallate (EGCG), both of which have antioxidant properties	GCG and EGCG inhibits ROS accumulation in mouse hippocampal-derived HT22 cells and Wistar rats, respectively. This consequently reduced glutamate-induced phosphorylation of MAPKs (ERK and JNK) and returned p53 to control levels.	Park et al., 2021; El-Missiry et al., 2018
Drug	Cornus officinalis (CC) and fermented CC (FCC), both of which have antioxidant properties	Both CC and FCC were able to reduce intracellular ROS generation in H2O2-induced neurotoxicity in SH-SY5Y human neuroblastoma cells. This was accompanied with a decrease in ERK1/2, JNK and p38 phosphorylation.	Tian et al., 2020
Drug	L-165041, a PPARδ agonist (PPARα is a transcription	10 Gy of ^{137}Cs irradiation resulted in an increase in intracellular ROS and c-Jun, MEK1/2 and ERK1/2 phosphorylation in BV-2 cells, all of which	Schnegg et

	factor that can activate antioxidant response).	were attenuated with L-165041 treatment.	al., 2012
Drug	Fucoxanthin (antioxidant)	Fucoxanthin was able to inhibit the LPS-induced increase in intracellular ROS and phosphorylation of JNK, ERK and p38.	Zhao et al., 2017
Media	Mesenchymal stem-cell conditioned medium (MSC-CM)	MSC-CM was able to inhibit the X-ray-induced increase in ROS and MDA levels and decrease in SOD and GSH levels, resulting in activation of PI3/Akt.	Huang et al., 2021

Known Feedforward/Feedback loops influencing this KER

ROS can upregulate protein kinase C, which stimulates the production of ceramide from sphingomyelinase. Ceramide activates NADPH oxidase, which can then produce more ROS (Soloviev & Kizub, 2019). Another feedback loop exists between the Nrf2/HO-1 signaling pathway and oxidative stress. The Nrf2/HO-1 signaling pathway is involved in negative feedback of oxidative stress, activating transcription of anti-oxidative enzymes to regulate cellular ROS and maintain a redox balance (Tahimic & Globus, 2017; Tian et al., 2017). Lastly, the MAPK pathway also exhibits a feedback loop. ERK can regulate ROS levels indirectly through p22phox, which increases ROS and upregulates antioxidants by Nrf2 activation. JNK activation can lead to FoxO activation, thereby resulting in antioxidant production (Arfin et al., 2021; Essers et al., 2004).

References

Annunziato, L. (2003), "Apoptosis induced in neuronal cells by oxidative stress: role played by caspases and intracellular calcium ions", *Toxicology Letters*, Vol. 139/2–3, https://doi.org/10.1016/S0378-4274(02)00427-7.

Arfin, S. et al. (2021), “Oxidative Stress in Cancer Cell Metabolism”, *Antioxidants 2021*, Vol. 10/5, MDPI, Basel, https://doi.org/10.3390/ANTIOX10050642

Azimzadeh, O. et al. (2021), "Activation of pparα by fenofibrate attenuates the effect of local heart high dose irradiation on the mouse cardiac proteome", *Biomedicines*, Vol. 9/12, MDPI, Basel, https://doi.org/10.3390/biomedicines9121845

Azimzadeh, O. et al. (2017), "Proteome analysis of irradiated endothelial cells reveals persistent alteration in protein degradation and the RhoGDI and NO signalling pathways", *International Journal of Radiation Biology*, Vol. 93/9, Informa, London, https://doi.org/10.1080/09553002.2017.1339332

Azimzadeh, O. et al. (2015), "Integrative proteomics and targeted transcriptomics analyses in cardiac endothelial cells unravel mechanisms of long-term radiation-induced vascular dysfunction", *Journal of Proteome Research*, Vol. 14/2, American Chemical Society, Washington, https://doi.org/10.1021/pr501141b

Bai, J. et al. (2020), "Irradiation-induced senescence of bone marrow mesenchymal stem cells aggravates osteogenic differentiation dysfunction via paracrine signaling", *American Journal of Physiology - Cell Physiology*, Vol. 318/5, American Physiological Society, https://doi.org/10.1152/ajpcell.00520.2019

Boyce, B. F. and L. Xing. (2007), "The RANKL/RANK/OPG pathway", *Current Osteoporosis Reports*, Vol. 5/3, https://doi.org/10.1007/s11914-007-0024-y

Cabrera, M. P. and R. H. Chihuailaf. (2011), "Antioxidants and the Integrity of Ocular Tissues", *Veterinary Medicine International*, Vol. 2011, Hindawi, London, https://doi.org/10.4061/2011/905153

Carvour, M. et al. (2008), "Chronic Low-Dose Oxidative Stress Induces Caspase-3-Dependent PKCδ Proteolytic Activation and Apoptosis in a Cell Culture Model of Dopaminergic Neurodegeneration", *Annals of the New York Academy of Sciences*, Vol. 1139/1, https://doi.org/10.1196/annals.1432.020.

Chen, L. et al. (2009), "Hydrogen peroxide-induced neuronal apoptosis is associated with inhibition of protein phosphatase 2A and 5, leading to activation of MAPK pathway", *The International Journal of Biochemistry & Cell Biology*, Vol. 41/6, Elsevier, Amsterdam, https://doi.org/10.1016/j.biocel.2008.10.029.

Crossthwaite, A. J., S. Hasan and R. J. Williams. (2002), "Hydrogen peroxide-mediated phosphorylation of ERK1/2, Akt/PKB and JNK in cortical neurones: dependence on Ca2+ and PI3-kinase", *Journal of Neurochemistry*, Vol. 80/1, John Wiley & Sons, Hoboken, https://doi.org/10.1046/j.0022-3042.2001.00637.x.

Deng, Z. et al. (2012), "Radiation-Induced c-Jun Activation Depends on MEK1-ERK1/2 Signaling Pathway in Microglial Cells", (I. Ulasov, Ed.) *PLoS ONE*, Vol. 7/5, https://doi.org/10.1371/journal.pone.0036739.

Diao, Y. et al. (2018), "Polyphenols (S3) Isolated from Cone Scales of Pinus koraiensis Alleviate Decreased Bone Formation in Rat under Simulated Microgravity", *Scientific Reports*, Vol. 8/1, Nature, https://doi.org/10.1038/s41598-018-30992-8

Domazetovic, V. et al. (2017), "Oxidative stress in bone remodeling: role of antioxidants", *Clinical cases in mineral and bone metabolism*, Vol. 14/2, pp. 209-216

El-Missiry, M. A. et al. (2018), "Neuroprotective effect of epigallocatechin-3-gallate (EGCG) on radiation-induced damage and apoptosis in the rat hippocampus", *International Journal of Radiation Biology*, Vol. 94/9, https://doi.org/10.1080/09553002.2018.1492755.

Fan, Z. et al. (2017), "L-carnitine preserves cardiac function by activating p38 MAPK/Nrf2 signalling in hearts exposed to irradiation", *European Journal of Pharmacology*, Vol. 804, Elsevier, Amsterdam, https://doi.org/10.1016/j.ejphar.2017.04.003

Hasan, H. F., R. R. Radwan and S. M. Galal. (2020), "Bradykinin-potentiating factor isolated from Leiurus quinquestriatus scorpion venom alleviates cardiomyopathy in irradiated rats via remodelling of the RAAS pathway", *Clinical and Experimental Pharmacology and Physiology*, Vol. 47/2, Wiley, https://doi.org/10.1111/1440-1681.13202

Hladik, D. et al. (2020), "CREB Signaling Mediates Dose-Dependent Radiation Response in the Murine Hippocampus Two Years after Total Body Exposure", *Journal of Proteome Research*, Vol. 19/1, https://doi.org/10.1021/acs.jproteome.9b00552.

Huang, Y. et al. (2021), "Mesenchymal Stem Cell-Conditioned Medium Protects Hippocampal Neurons From Radiation Damage by Suppressing Oxidative Stress and Apoptosis", *Dose-Response*, Vol. 19/1, https://doi.org/10.1177/1559325820984944.

Hughson, R. L., A. Helm and M. Durante. (2018), "Heart in space: Effect of the extraterrestrial environment on the cardiovascular system", *Nature Reviews Cardiology*, Vol. 15/3, Nature, https://doi.org/10.1038/nrcardio.2017.157

Kenchegowda, D. et al. (2018), "Selective Insulin-like Growth Factor Resistance Associated with Heart Hemorrhages and Poor Prognosis in a Novel Preclinical Model of the Hematopoietic Acute Radiation Syndrome", *Radiation Research*, Vol. 190/2, BioOne, https://doi.org/10.1667/RR14993.1

Kook, S. H. et al. (2015), "Irradiation inhibits the maturation and mineralization of osteoblasts via the activation of Nrf2/HO-1 pathway", *Molecular and Cellular Biochemistry*, Vol. 410/1–2, Nature, https://doi.org/10.1007/s11010-015-2559-z

Kozbenko, T. et al. (2022), “Deploying elements of scoping review methods for adverse outcome pathway development: a space travel case example”, *International Journal of Radiation Biology*, Vol. 98/12. https://doi.org/10.1080/09553002.2022.2110306

Lee, K., A. Lee and I. Choi. (2017), "Melandrii Herba Extract Attenuates H2O2-Induced Neurotoxicity in Human Neuroblastoma SH-SY5Y Cells and Scopolamine-Induced Memory Impairment in Mice", *Molecules*, Vol. 22/10, MDPI, Basel, https://doi.org/10.3390/molecules22101646.

Lehtinen, M. and A. Bonni. (2006), "Modeling Oxidative Stress in the Central Nervous System", *Current Molecular Medicine*, Vol. 6/8, https://doi.org/10.2174/156652406779010786.

Li, J. et al. (2013), "Oxidative Stress and Neurodegenerative Disorders", *International Journal of Molecular Sciences*, Vol. 14/12, https://doi.org/10.3390/ijms141224438.

Limoli, C. L. et al. (2004), "Radiation Response of Neural Precursor Cells: Linking Cellular Sensitivity to Cell Cycle Checkpoints, Apoptosis and Oxidative Stress", *Radiation Research*, Vol. 161/1, https://doi.org/10.1667/RR3112.

Manolagas, S. C. and M. Almeida. (2007), "Gone with the Wnts: β-Catenin, T-Cell Factor, Forkhead Box O, and Oxidative Stress in Age-Dependent Diseases of Bone, Lipid, and Glucose Metabolism", *Molecular Endocrinology*, Vol. 21/11, Oxford University Press, Oxford, https://doi.org/10.1210/me.2007-0259

Essers, M. A. et al. (2004), “FOXO transcription factor activation by oxidative stress mediated by the small GTPase Ral and JNK”. *The EMBO journal*, Vol. 23/24, EMBO, https://doi.org/10.1038/sj.emboj.7600476

Nagane, M. et al. (2021), "DNA damage response in vascular endothelial senescence: Implication for radiation-induced cardiovascular diseases", *Journal of Radiation Research*, Vol. 62/4, Oxford University Press, Oxford, https://doi.org/10.1093/jrr/rrab032

Park, H. et al. (2016), "GDF15 contributes to radiation-induced senescence through the ROS-mediated p16 pathway in human endothelial cells", *Oncotarget*, Vol. 7/9, https://doi.org/10.18632/oncotarget.7457

Park, D. H. et al. (2021), "Neuroprotective Effect of Gallocatechin Gallate on Glutamate-Induced Oxidative Stress in Hippocampal HT22 Cells", *Molecules*, Vol. 26/5, MDPI, Basel, https://doi.org/10.3390/molecules26051387.

Ping, Z. et al. (2020), "Oxidative Stress in Radiation-Induced Cardiotoxicity", *Oxidative Medicine and Cellular Longevity*, Vol. 2020, Hindawi, London, https://doi.org/10.1155/2020/3579143

Ramadan, R. et al. (2021), "The role of connexin proteins and their channels in radiation-induced atherosclerosis", *Cellular and Molecular Life Sciences*, Vol. 78, Nature, https://doi.org/10.1007/s00018-020-03716-3

Ramalingam, M. and S.-J. Kim. (2012), "Reactive oxygen/nitrogen species and their functional correlations in neurodegenerative diseases", *Journal of Neural Transmission*, Vol. 119/8, Springer Nature, Berlin, https://doi.org/10.1007/s00702-011-0758-7.

Ruffels, J., M. Griffin and J. M. Dickenson. (2004), "Activation of ERK1/2, JNK and PKB by hydrogen peroxide in human SH-SY5Y neuroblastoma cells: role of ERK1/2 in H2O2-induced cell death", *European Journal of Pharmacology*, Vol. 483/2–3, Elsevier, Amsterdam https://doi.org/10.1016/j.ejphar.2003.10.032.

Sakata, K. et al. (2015), "Roles of ROS and PKC-βII in ionizing radiation-induced eNOS activation in human vascular endothelial cells", *Vascular Pharmacology*, Vol. 70, Elsevier, Amsterdam, https://doi.org/10.1016/j.vph.2015.03.016

Schmidt-Ullrich, R. K. et al. (2000), "Signal transduction and cellular radiation responses.", *Radiation research*, Vol. 153/3, BioOne,

https://doi.org/10.1667/0033-7587(2000)153[0245:stacrr]2.0.co;2

Schnegg, C. I. et al. (2012), "PPARδ prevents radiation-induced proinflammatory responses in microglia via transrepression of NF-κB and inhibition of the PKCα/MEK1/2/ERK1/2/AP-1 pathway", *Free Radical Biology and Medicine*, Vol. 52/9, https://doi.org/10.1016/j.freeradbiomed.2012.02.032.

Soloviev, A. I. and I. V. Kizub. (2019), "Mechanisms of vascular dysfunction evoked by ionizing radiation and possible targets for its pharmacological correction", *Biochemical Pharmacology*, Vol. 159, Elsevier, Amsterdam, https://doi.org/10.1016/j.bcp.2018.11.019

Suman, S. et al. (2013), "Therapeutic and space radiation exposure of mouse brain causes impaired DNA repair response and premature senescence by chronic oxidant production", *Aging*, Vol. 5/8, https://doi.org/10.18632/aging.100587.

Sun, Y. et al. (2013), "Treatment of hydrogen molecule abates oxidative stress and alleviates bone loss induced by modeled microgravity in rats", *Osteoporosis International*, Vol. 24/3, Nature, https://doi.org/10.1007/s00198-012-2028-4

Tahimic, C. G. T. and R. K. Globus. (2017), “Redox Signaling and Its Impact on Skeletal and Vascular Responses to Spaceflight”, *International Journal of Molecular Sciences*, Vol. 18/10, MDPI, Basel, https://doi.org/10.3390/IJMS18102153

Tian, Y. et al. (2017), "The impact of oxidative stress on the bone system in response to the space special environment", *International Journal of Molecular Sciences*, Vol. 18/10, MDPI, Basel, https://doi.org/10.3390/ijms18102132

Tian, W. et al. (2019), "Neuroprotective Effects of Cornus officinalis on Stress-Induced Hippocampal Deficits in Rats and H2O2-Induced Neurotoxicity in SH-SY5Y Neuroblastoma Cells", *Antioxidants*, Vol. 9/1, MDPI, Basel, https://doi.org/10.3390/antiox9010027.

Tian, R. et al. (2020), "miR-137 prevents inflammatory response, oxidative stress, neuronal injury and cognitive impairment via blockade of Src-mediated MAPK signaling pathway in ischemic stroke", *Aging*, Vol. 12/11, https://doi.org/10.18632/aging.103301.

Valerie, K. et al. (2007), "Radiation-induced cell signaling: inside-out and outside-in", *Molecular Cancer Therapeutics*, Vol. 6/3, American Association for Cancer Research, https://doi.org/10.1158/1535-7163.MCT-06-0596

Venkatesulu, B. P. et al. (2018), “Radiation-Induced Endothelial Vascular Injury: A Review of Possible Mechanisms”, *JACC: Basic to translational science*, Vol. 3/4, Elsevier, Amsterdam, https://doi.org/10.1016/j.jacbts.2018.01.014.

Wang. (2010), "Selective neuronal vulnerability to oxidative stress in the brain", *Frontiers in Aging Neuroscience*, https://doi.org/10.3389/fnagi.2010.00012.

Wang, Y., M. Boerma and D. Zhou. (2016), "Ionizing Radiation-Induced Endothelial Cell Senescence and Cardiovascular Diseases", *Radiation Research*, Vol. 186/2, BioOne, https://doi.org/10.1667/RR14445.1

Wortel, R. C. et al. (2019), "Sildenafil Protects Endothelial Cells From Radiation-Induced Oxidative Stress", *The Journal of Sexual Medicine*, Vol. 16/11, Elsevier, Amsterdam, https://doi.org/10.1016/j.jsxm.2019.08.015

Wu, Y., M. Chen and J. Jiang. (2019), "Mitochondrial dysfunction in neurodegenerative diseases and drug targets via apoptotic signaling", *Mitochondrion*, Vol. 49, https://doi.org/10.1016/j.mito.2019.07.003.

Xin, M. et al. (2015), "Attenuation of hind-limb suspension-induced bone loss by curcumin is associated with reduced oxidative stress and increased vitamin D receptor expression", *Osteoporosis International*, Vol. 26/11, Nature, https://doi.org/10.1007/s00198-015-3153-7

Xu, B. et al. (2019), "Oxidation Stress-Mediated MAPK Signaling Pathway Activation Induces Neuronal Loss in the CA1 and CA3 Regions of the Hippocampus of Mice Following Chronic Cold Exposure", *Brain Sciences*, Vol. 9/10, MDPI, Basel, https://doi.org/10.3390/brainsci9100273.

Yoo, Y. M., T. Y. Han and H. S. Kim. (2016), "Melatonin suppresses autophagy induced by clinostat in preosteoblast MC3T3-E1 cells", *International Journal of Molecular Sciences*, Vol. 17/4, MDPI, Basel, https://doi.org/10.3390/ijms17040526

Zhao, Z.-Y. et al. (2013), "Edaravone Protects HT22 Neurons from H 2 O 2 -induced Apoptosis by Inhibiting the MAPK Signaling Pathway", *CNS Neuroscience & Therapeutics*, Vol. 19/3, John Wiley & Sons, Hoboken, https://doi.org/10.1111/cns.12044.

Zhao, D. et al. (2017), "Anti-Neuroinflammatory Effects of Fucoxanthin via Inhibition of Akt/NF-κB and MAPKs/AP-1 Pathways and Activation of PKA/CREB Pathway in Lipopolysaccharide-Activated BV-2 Microglial Cells", *Neurochemical Research*, Vol. 42/2, Springer Nature, Berlin, https://doi.org/10.1007/s11064-016-2123-6.

Relationship: 2833: Oxidative Stress leads to Tissue resident cell activation

AOPs Referencing Relationship

AOP Name	Adjacency	Weight of Evidence	Quantitative Understanding

AOP Name	Adjacency	Weight of Evidence	Quantitative Understanding
Deposition of Energy Leading to Learning and Memory Impairment	adjacent	Moderate	Low

Evidence Supporting Applicability of this Relationship

Taxonomic Applicability

Term	Scientific Term	Evidence	Links
human	Homo sapiens	Low	NCBI
mouse	Mus musculus	Low	NCBI
rat	Rattus norvegicus	Moderate	NCBI

Life Stage Applicability

Life Stage	Evidence
Adult	Moderate
Not Otherwise Specified	Low

Sex Applicability

Sex	Evidence
Male	Moderate
Female	Not Specified
Unspecific	Low

Evidence for this relationship comes from in vitro human- and mouse-derived models, as well as in vivo rat models. Most of the evidence are in male adult and male models, although sex and age are not always specified.

Key Event Relationship Description

Oxidative stress encompasses an increase in the production of free radicals (e.g., superoxide, hydrogen peroxide and hydroxyl radicals) and a loss of antioxidant mechanisms (e.g., superoxide dismutase (SOD), glutathione peroxidase (GSH-Px) and catalase (CAT)). This imbalance can lead to damaging by-products that can activate tissue resident cells. Reactive oxygen and nitrogen species (RONS) are examples of free radicals that may promote oxidative injury (Simpson & Oliver, 2020). In addition, excess free radicals can promote a reduced capacity of the cells to maintain redox balance and prevent ongoing oxidative damage (Huang, Zou & Corniola, 2012; Rojo et al., 2014). Depending on the organ/tissue, different resident cell types may become activated by oxidative stress. For example, in the brain, oxidative stress will specifically activate microglial cells and astrocytes (Lee, Cha & Lee, 2021). Microglia cells are macrophages in the brain that respond to tissue injury, provide surveillance to neurons, and maintain synaptic homeostasis (Zhu et al., 2022). Astrocytes are critical regulators of neurogenesis and synaptogenesis, blood brain barrier permeability, and responsible for maintenance of cellular homeostasis (Zhu et al., 2022). Both microglial cells and astrocytes can change from resting to reactive states, termed gliosis, in response to excess RONS (Lee, Cha & Lee, 2021). In response to RONS, Toll like receptors (TLRs) located on microglia become activated to mediate the immune response (Gill et al., 2010; Mehdipour et al., 2021). These receptors then initiate a cascade of signaling pathways that contribute to the production of pro-inflammatory cytokines and free radicals, resulting in neuroinflammation (Heidari et al., 2022).

Reactive microglia cells increase in size and number, display a reduction in the length and density of their processes, and upregulate their macrophagic processes, marked by expression of proteins related to phagocytic activity such as cluster of differentiation 68 (CD68) (Hol & Pekny, 2015). Astrocytes undergoing astrogliosis exhibit cellular hypertrophy and an upregulation of glial fibrillary acidic protein (GFAP), an intermediate filament expressed exclusively in astrocytes that plays a critical role in astroglia cell activation (Hol & Pekny, 2015). Activation of both microglial cells and astrocytes can accelerate neuroinflammatory pathways that can ultimately promote further formation of ROS creating a feedforward loop (Lee, Cha & Lee, 2021; Simpson & Oliver, 2020; Zhu et al., 2022).

Evidence Supporting this KER

Overall Weight of Evidence: Moderate

Biological Plausibility

Biological Plausibility is Moderate. RONS can activate some inflammatory and anti-inflammatory pathways (TLR, TGF-β, NF-kB), and RONS are an essential part of multiple inflammatory and anti-inflammatory pathways (TLR4, TNF-a, TGF-β, NF-kB).

RONS activates or is essential to many inflammatory pathways including TGF-β (Barcellos-Hoff and Dix 1996; Jobling, Mott et al. 2006), TNF (Blaser, Dostert et al. 2016), Toll-like receptor (TLR) (Park, Jung et al. 2004; Nakahira, Kim et al. 2006; Powers, Szaszi et al. 2006; Miller, Goodson et al. 2017; Cavaillon 2018), and NF-kB signaling (Gloire, Legrand-Poels et al. 2006; Morgan and Liu 2011). These interactions principally involve ROS, but RNS can indirectly activate TLRs and possibly NF-kB. Since inflammatory

signaling and activated immune cells can also increase the production of RONS, positive feedback and feedforward loops can occur (Zhao and Robbins 2009; Ratikan, Micewicz et al. 2015; Blaser, Dostert et al. 2016).

Damage inflicted by RONS on cells activate TLRs and other receptors to promote release of cytokines (Ratikan, Micewicz et al. 2015). For example, oxidized lipids or oxidative stress-induced heat shock proteins can activate TLR4 (Miller, Goodson et al. 2017; Cavaillon 2018).

ROS is essential to TLR4 activation of downstream signals including NF-kB. Activation of TLR4 promotes the surface expression and movement of TLR4 into signal-promoting lipid rafts (Nakahira, Kim et al. 2006; Powers, Szaszi et al. 2006). This signal promotion requires NADPH-oxidase and ROS (Park, Jung et al. 2004; Nakahira, Kim et al. 2006; Powers, Szaszi et al. 2006). ROS is also required for the TLR4/TRAF6/ASK-1/p38 dependent activation of inflammatory cytokines (Matsuzawa, Saegusa et al. 2005). ROS therefore amplifies the inflammatory process.

RONS can also fail to activate or actively inhibit inflammatory pathways, and the circumstances determining response to RONS are not well known (Gloire, Legrand-Poels et al. 2006).

Responses to oxidative stress can vary depending on the organ system. In the central nervous system (CNS), biological plausibility supporting the connection between increased oxidative stress to tissue resident cell activation is moderately supported by evidence compiled from studies using animal and in vitro models. Multiple studies have shown that microglial cells and astrocytes are activated in response to RONS, meaning they change from resting to reactive states by secreting pro-inflammatory mediators and initiating antioxidant defenses mediated through TLRs (Simpson & Oliver, 2020; Heidari et al., 2022). Literature reviews describing the role of oxidative stress imbalances and glial cell activation in the context of general oxidative injury (Lee, Cha & Lee, 2021), stroke (Zhu et al., 2022) and neurodegenerative diseases (Reynolds et al., 2007; Simpson & Oliver, 2020) also suggest a relationship between increased oxidative stress and increased tissue resident cell activation in the CNS.

Empirical Evidence

Empirical Evidence is Moderate. Both RONS and inflammation increase in response to agents that increase RONS or inflammation, and antioxidants reduce inflammation. Multiple studies show dose-dependent changes in both RONS and inflammation in response to stressors including ionizing radiation and antioxidants. RONS have been measured at the same or earlier time points as inflammatory markers, but additional studies are needed to characterize the inflammatory response at the earliest time points to support causation. Uncertainties come from the positive feedback from inflammation to RONS potentially interfering with attempts to establish causality, and from the large number of inflammation-related endpoints with differing responses to stressors and experimental variation.

Oxidative activity is required for or promotes the response to multiple inflammatory stressors, including ionizing radiation, UV radiation (particularly UVB), the endotoxin LPS and other pathogen associated immune activators, and hemorrhagic shock (Park, Jung et al. 2004; Nakahira, Kim et al. 2006; Powers, Szaszi et al. 2006; Zhao and Robbins 2009; Ha, Chung et al. 2010; Hiramoto, Kobayashi et al. 2012; Straub, New et al. 2015).

Both intracellular concentrations of RONS and a wide range of inflammatory markers increase in response to RONS stressors. This paired increase was observed in vivo in rodents in tissue from multiple internal organs following exposure to whole body or abdominal ionizing radiation (Berruyer, Martin et al. 2004; Ha, Chung et al. 2010; Sinha, Das et al. 2011; Sinha, Das et al. 2012; Das, Manna et al. 2014; Ozyurt, Cevik et al. 2014; Khan, Manna et al. 2015; Zetner, Andersen et al. 2016; Haddadi, Rezaeyan et al. 2017; Ezz, Ibrahim et al. 2018) or following UV skin irradiation (Sharma, Meeran et al. 2007; Hiramoto, Kobayashi et al. 2012; Martinez, Pinho-Ribeiro et al. 2016). In vitro, the relationship has been reported in response to IR and UV in keratinocytes (Park, Ju et al. 2006; Kang, Kim et al. 2007; Martin, Sur et al. 2008; Lee, Jeon et al. 2010; Ren, Shi et al. 2016; Hung, Tang et al. 2017; Zhang, Zhu et al. 2017), immune cells (Matsuzawa, Saegusa et al. 2005; Nakahira, Kim et al. 2006; Manna, Das et al. 2015; Soltani, Ghaemi et al. 2016), as well as corneal and conjunctival epithelia, HEK cells, and vocal cord and foreskin fibroblasts (Narayanan, LaRue et al. 1999; Park, Jung et al. 2004; Saltman, Kraus et al. 2010; Black, Gordon et al. 2011; Han, Min et al. 2015). Direct application of micromolar concentrations of H_2O_2 in vitro also increases inflammatory markers in immune cells (Matsuzawa, Saegusa et al. 2005; Nakao, Kurokawa et al. 2008) and keratinocytes (Zhang, Zhu et al. 2017).

Interventions to reduce oxidative activity also reduce inflammation, further implicating RONS in the inflammatory process. Reduction of inflammation by these interventions has been documented in animals in response to IR (Berruyer, Martin et al. 2004; Sinha, Das et al. 2011; Sinha, Das et al. 2012; Das, Manna et al. 2014; Ozyurt, Cevik et al. 2014; Khan, Manna et al. 2015; Zetner, Andersen et al. 2016; Haddadi, Rezaeyan et al. 2017; Ezz, Ibrahim et al. 2018), UV (Sharma, Meeran et al. 2007; Lee, Jeon et al. 2010; Hiramoto, Kobayashi et al. 2012; Han, Min et al. 2015; Martinez, Pinho-Ribeiro et al. 2016; Ren, Shi et al. 2016; Hung, Tang et al. 2017) and hemorrhagic shock (Powers, Szaszi et al. 2006). In vitro, multiple studies in immune cells (Matsuzawa, Saegusa et al. 2005; Nakahira, Kim et al. 2006; Manna, Das et al. 2015; Soltani, Ghaemi et al. 2016)and keratinocytes (Park, Ju et al. 2006; Kang, Kim et al. 2007; Martin, Sur et al. 2008; Lee, Jeon et al. 2010; Ren, Shi et al. 2016; Hung, Tang et al. 2017; Zhang, Zhu et al. 2017) as well as HEK293, fibroblasts, and epithelial cells (Lee, Dimtchev et al. 1998; Narayanan, LaRue et al. 1999; Park, Jung et al. 2004; Han, Min et al. 2015) provide further evidence for reduction in various inflammatory markers with interventions to reduce RONS. Interventions include antioxidants such as propyl gallate, n-acetylcysteine, or naringin, as well as reduction in the function of NADPH oxidases (NOX/DUOX) via DPI or knockdown of gene expression. In studies using multiple doses of antioxidant, inflammation was reduced dose-dependently with the antioxidant dose (Nakahira, Kim et al. 2006; Manna, Das et al. 2015; Ren, Shi et al. 2016). Interventions reducing nitric oxide were not common, but in one study inhibiting iNOS did not reduce activation of NF-kB by IR (Lee, Dimtchev et al. 1998). The treatment to reduce RONS is administered before, or occasionally immediately after the inflammatory stressor, but experiments often continue treatment or don't explicitly report changing media in vitro, so the exact time point at which RONS are required is difficult to pinpoint.

IR and RONS decrease endogenous antioxidant activity (glutathione, superoxide dismutase, and catalase), and antioxidants rescue this suppression in antioxidant activity (Sharma, Meeran et al. 2007; Das, Manna et al. 2014). Mice with more endogenous glutathione have a lower inflammatory response to IR (Berruyer, Martin et al. 2004), suggesting that IR increases inflammation in part by decreasing antioxidants.

In response to inflammatory stressors, RONS has been measured at the same (Nakao, Kurokawa et al. 2008; Ha, Chung et al. 2010; Saltman, Kraus et al. 2010; Azimzadeh, Scherthan et al. 2011; Ameziane-El-Hassani, Talbot et al. 2015; Azimzadeh, Sievert et al. 2015; Zhang, Zhu et al. 2017) or earlier time points as inflammatory markers (Nakahira, Kim et al. 2006; Black, Gordon et al. 2011), This suggests that RONS precedes the generation of inflammatory markers, consistent with a role for RONS in promoting inflammation. However, inflammatory markers are not typically measured at the earliest time points, and a more comprehensive survey of the appearance of these events at early time points would help to clarify the timeline and confirm the temporal evidence for causation.

A relatively small number of studies in a variety of cell types have examined both RONS and inflammatory markers across multiple doses. Three of these report dose-dependent increases in both RONS and inflammatory markers; one in which the key events are evaluated immediately after H2O2 application (Nakao, Kurokawa et al. 2008), and two others evaluating them 24 hours or 8-16 weeks after IR (Ha, Chung et al. 2010; Azimzadeh, Sievert et al. 2015). A fourth study reports a dose-dependent reduction in inflammation in response to treatment with antioxidants (Nakahira, Kim et al. 2006). In three other studies, some or all markers of inflammation increase at lower doses but decrease at higher doses (Saltman, Kraus et al. 2010; Black, Gordon et al. 2011; Zhang, Zhu et al. 2017). In two of these studies, RONS is also not consistently increasing with dose (Saltman, Kraus et al. 2010; Zhang, Zhu et al. 2017), however, this finding is consistent with findings from other studies about lack of dose-dependence of ROS measured at intermediate time points after IR. Similarly, 30 minutes after low dose, IR IL8 increases with dose while ROS does not (Narayanan, LaRue et al. 1999). The mixed inflammatory response at higher doses suggests that additional factors such as negative and positive feedback and crosstalk between pathways are also involved in the relationship between RONS and IR.

Dose Concordance

Evidence to support this relationship in the brain is derived from studies using gamma rays (Schnegg et al., 2012), 6-OHDA (Wang et al., 2017), or H2O2 (Daverey & Agrawal, 2016) as the stressor. Oxidative stress and tissue resident cell activation was then assessed within the brain or glial cell cultures (Davery & Agrawal, 2016; Schnegg et al., 2012; Wang, 2017; Daverey & Agrawal, 2016; Schnegg et al., 2012; Wang et al., 2017). Few studies show that oxidative stress occurs at lower or the same dose of a stressor than tissue-resident cell activation. Treatment with 4 µg/µL of the neurotoxin 6-hydroxydopamine caused decreased antioxidant levels as well as increased glial fibrillary acidic protein (GFAP) levels in rats (Wang et al., 2017). In another study, astrocyte activation showed a slight linear increase in response to 50 µM, 100 µM and 200 µM of H2O2 (Daverey & Agrawal, 2016).

Time Concordance

Few studies show that oxidative stress occurs before or at the same time as tissue-resident cell activation in a time course. BV-2 microglia irradiated with 10 Gy gamma rays showed an increase in ROS 1h post-irradiation, while an increase in NF-κB and AP-1 DNA binding was also observed 1h post-irradiation (Schnegg et al., 2012). Treatment of human glioblastoma astrocytes (A172 cell) with 50 µM of H2O2 for various times, showed a small linear increase in GFAP levels from 2h to 24h of treatment (Daverey & Agrawal, 2016).

Incidence Concordance

Schnegg et al. (2012) irradiated BV-2 microglia with gamma rays and showed increased ROS as well as increased NF-κB and AP-1 DNA binding, indicating activated glial cells, at the same dose of 10 Gy.

Essentiality

Studies examining the use of antioxidants to inhibit free radicals demonstrate the essentiality of oxidative stress and tissue resident cell activation. This has been observed in microglial cells using multiple types of inhibitors. In BV-2 microglia, activation of PPARδ (involved in anti-inflammatory responses) with the agonist L-16504, reduced formation of reactive oxygen species and microglial activation (Schnegg et al., 2012). Treatment with multiple doses of an antioxidant Kukoamine A (KuA) elicited a dose-dependent partial attenuation of radiation-induced markers of microglial cell activation in rats (Zhang et al. 2017). After administration of another antioxidant, curcumin, levels of SOD and GSH-Px were restored and GFAP levels were decreased (Daverey & Agrawal, 2016; Wang et al., 2017). Furthermore, a knockout model of mitochondrial SOD (SOD2) resulted in an increase in reactivity of microglial cells post-irradiation (Fishman et. al 2009).

Uncertainties and Inconsistencies

Although ROS can activate NF-KB (Gloire, Legrand-Poels et al. 2006), not all studies consistently show NF-kB activation after RONs stressor IR. It is possible that the link between ROS and NF-kB depends on the local environmental context, with different studies not adequately controlling all influential variables. One study offers a possible explanation based on temporal response: in macrophages, NF-kB was activated by shorter exposures to H2O2 (30 min), but the response disappeared with longer exposures (Nakao, Kurokawa et al. 2008).

While many models in vivo and in vitro showed a decreased inflammatory response to RONS stressors IR in combination with antioxidants, in endothelial cells in culture the increase in IL6 and IL8 after IR was not reduced by antioxidants, although a synergistic increase in those cytokines occurring with combined TNF-a and IR treatment was reduced by antioxidants (Meeren,

Bertho et al. 1997). This is a reminder that multiple mechanisms can increase inflammation, that inflammatory factors participate in positive feedback loops, and that responses to stimuli vary between cells.

Many studies do not report direct measures of RONS. As RONS are quickly scavenged, the quantitative understanding of this relationship can be inconsistent, due to varied response of antioxidant enzymes across experimental conditions and time measurements.

Quantitative Understanding of the Linkage

The table below provides some representative examples of quantitative linkages between the two key events. It was difficult to identify a general trend across all the studies due to differences in experimental design and reporting of the data. All data is statistically significant unless otherwise stated.

Dose Concordance

Reference	Experiment description	Result
Wang, 2017	In vivo. Adult male Sprague-Dawley rats were treated with 4 µg/µL of the neurotoxin 6-hydroxydopamine. Oxidative stress was measured by SOD and GSH-Px levels through a bicinchoninic acid protein assay kit. GFAP was used as a marker of astrocytes and was detected using immunohistochemistry.	SOD decreased 0.64-fold and GSH-Px decreased 0.34-fold. GFAP increased 1.7-fold.
Daverey & Agrawal, 2016	In vitro. Human A172 (glioblastoma astrocytes) and HA-sp (spinal cord astrocytes) cell lines were treated with H2O2. GFAP expression was detected through immunofluorescence.	After 50 µM of H2O2, both cell types showed increased GFAP expression about 1.5-fold. GFAP was also increased 1.5- to 2-fold after 100 and 200 µM of H2O2.

Time Concordance

Reference	Experiment description	Result
Schnegg et al., 2012	In vitro. BV-2 immortalized microglia were irradiated with 10 Gy of 137Cs gamma raysat 3.56 Gy/min. Measured 1h after irradiation, intracellular ROS generation was measured by the fluorescent DCFH-DA probe, and activation of NF-κB and AP-1 was determined by immunoblotting as a measure of cell activation.	Both measured 1h after irradiation, ROS increased about 7-fold while NF-κB and AP-1 DNA binding was increased 2.5- and 2-fold, respectively.
Daverey & Agrawal, 2016	In vitro. Human A172 (glioblastoma astrocytes) and HA-sp (spinal cord astrocytes) cell lines were treated with 50 µM of the ROS H2O2. GFAP expression was detected through immunofluorescence after various durations of H2O2 treatment.	Both cell types showed increased GFAP about 1.5-fold, measured after treatment with H2O2. H2O2 administered for 2, 6 and 12h showed slight increases at each timepoint, while after 24h of H2O2 treatment, GFAP was only increased in A172 cells.

Incidence Concordance

Reference	Experimental description	Result
Schnegg et al., 2012	In vitro. BV-2 immortalized microglia were irradiated with 10 Gy of 137Cs gamma rays at 3.56 Gy/min. Intracellular ROS generation was measured by the fluorescent DCFH-DA probe, and activation of NF-κB and AP-1 was determined by immunoblotting as a measure of cell activation.	ROS increased about 7-fold while NF-κB and AP-1 DNA binding was increased 2.5- and 2-fold, respectively.

Known modulating factors

Modulating factor	Details	Effects on the KER	References
Drug	KuA (antioxidant)	After 30 Gy X-ray whole-brain irradiation of rats, activated microglia increased to over 320% of control. KuA at 5 mg/kg decreased this to 240%, at 10 mg/kg decreased it to 180% and at 20 mg/kg decreased it to 170%.	Zhang et al., 2017
Drug	L-16504 (PPARδ agonist, involved in anti-inflammatory responses)	Treatment prevented the increase in ROS and reduced NF-κB and AP-1 DNA binding.	Schnegg et al., 2012
Drug	Curcumin	Treatment increased SOD and GSH-Px levels and decreased the number	Wang et al., 2017; Daverey &

	(antioxidant)	of GFAP-positive cells.	Agrawal, 2016
Age	Increased age	Increased age can cause susceptibility to ROS accumulation and tissue-resident cell activation.	Liguori et al., 2018; Hanslik, Marino & Ulland, 2021
Diet	High antioxidant diet	Increased antioxidants in diet can lead to reduced oxidative stress.	Ávila-Escalante et al., 2020
Diet	Hypocaloric diet	Caloric restriction has been shown to lead to reduced markers of oxidative stress.	Ávila-Escalante et al., 2020
Smoking	Active smokers	Active smokers show reduced GSH-Px activity compared to non-smokers (measured in patients with coronary artery disease).	Kamceva et al., 2016
Prior Disease	Neurodegenerative diseases like Alzheimer's and Parkinson's	These diseases can generate an environment of increased oxidative stress and promotes the activation of glial cells.	Hanslik, Marino & Ulland, 2021
Genotype	SOD knockout mice	SOD2 knockout mice experienced increased microglia activation following irradiation, indicating an impact of genotype on tissue resident cell activation.	Fishman et al., 2009

Known Feedforward/Feedback loops influencing this KER

Since inflammatory signaling and activated immune cells can also increase the production of RONS, positive feedback and feedforward loops can occur (Zhao and Robbins 2009; Ratikan, Micewicz et al. 2015; Blaser, Dostert et al. 2016). Similarly, positive feedforward and feedback loops regarding RONS, cellular activation, and inflammation also occur in the CNS. Both RONS and microglial cell activation can accelerate neuroinflammatory pathways that can ultimately promote further formation of RONS (Lee, Cha & Lee, 2021; Simpson & Oliver, 2020; Zhu et al., 2022).

References

Ávila-Escalante, M. L. et al. (2020), "The effect of diet on oxidative stress and metabolic diseases—Clinically controlled trials", Journal of Food Biochemistry, Vol. 44/5, https://doi.org/10.1111/jfbc.13191.

Daverey, A. and S. K. Agrawal. (2016), "Curcumin alleviates oxidative stress and mitochondrial dysfunction in astrocytes", Neuroscience, Vol. 333, https://doi.org/10.1016/j.neuroscience.2016.07.012.

Fishman, K. et al. (2009), "Radiation-induced reductions in neurogenesis are ameliorated in mice deficient in CuZnSOD or MnSOD", Free Radical Biology and Medicine, Vol. 47/10, https://doi.org/10.1016/j.freeradbiomed.2009.08.016.

Gill, R., A. Tsung and T. Billiar. (2010), "Linking oxidative stress to inflammation: Toll-like receptors", Free Radical Biology and Medicine, Vol. 48/9, https://doi.org/10.1016/j.freeradbiomed.2010.01.006.

Hanslik, K. L., K. M. Marino and T. K. Ulland. (2021), "Modulation of Glial Function in Health, Aging, and Neurodegenerative Disease", Frontiers in Cellular Neuroscience, Vol. 15, https://doi.org/10.3389/fncel.2021.718324.

Heidari, A., N. Yazdanpanah and N. Rezaei. (2022), "The role of Toll-like receptors and neuroinflammation in Parkinson's disease", Journal of Neuroinflammation, Vol. 19/1, https://doi.org/10.1186/s12974-022-02496-w.

Hol, E. M. and M. Pekny. (2015), "Glial fibrillary acidic protein (GFAP) and the astrocyte intermediate filament system in diseases of the central nervous system", Current Opinion in Cell Biology, Vol. 32, https://doi.org/10.1016/j.ceb.2015.02.004.

Huang, T. T., Y. Zou and R. Corniola. (2012), "Oxidative stress and adult neurogenesis—Effects of radiation and superoxide dismutase deficiency", Seminars in Cell & Developmental Biology, Vol. 23/7, https://doi.org/10.1016/j.semcdb.2012.04.003.

Kamceva, G. et al. (2016), "Cigarette Smoking and Oxidative Stress in Patients with Coronary Artery Disease", Open Access Macedonian Journal of Medical Sciences, Vol. 4/4, https://doi.org/10.3889/oamjms.2016.117.

Lee, K. H., M. Cha and B. H. Lee. (2021), "Crosstalk between Neuron and Glial Cells in Oxidative Injury and Neuroprotection", International Journal of Molecular Sciences, Vol. 22/24, https://doi.org/10.3390/ijms222413315.

Liguori, I. et al. (2018), "Oxidative stress, aging, and diseases", Clinical Interventions in Aging, Vol.13, https://doi.org/10.2147/CIA.S158513.

Mehdipour, A. et al. (2021), "Ionizing radiation and toll like receptors: A systematic review article", Human Immunology, Vol. 82/6, https://doi.org/10.1016/j.humimm.2021.03.008.

Reynolds, A. et al. (2007), "Oxidative Stress and the Pathogenesis of Neurodegenerative Disorders", International Review of Neurobiology, Vol. 82, https://doi.org/10.1016/S0074-7742(07)82016-2.

Rojo, A. I. et al. (2014), "Redox Control of Microglial Function: Molecular Mechanisms and Functional Significance", Antioxidants & Redox Signaling, Vol. 21/12, https://doi.org/10.1089/ars.2013.5745.

Schnegg, C. I. et al. (2012), "PPARδ prevents radiation-induced proinflammatory responses in microglia via transrepression of NF-κB and inhibition of the PKCα/MEK1/2/ERK1/2/AP-1 pathway", Free Radical Biology and Medicine, Vol. 52/9, Pergamon, https://doi.org/10.1016/J.FREERADBIOMED.2012.02.032.

Simpson, D. S. A. and P. L. Oliver. (2020), "ROS Generation in Microglia: Understanding Oxidative Stress and Inflammation in Neurodegenerative Disease", Antioxidants, Vol. 9/8, https://doi.org/10.3390/antiox9080743.

Wang, Y. L. et al. (2017), "Protective Effect of Curcumin Against Oxidative Stress-Induced Injury in Rats with Parkinson's Disease Through the Wnt/ β-Catenin Signaling Pathway", Cellular Physiology and Biochemistry, Vol. 43/6, https://doi.org/10.1159/000484302.

Zhang, Y. et al. (2017), "Kukoamine A Prevents Radiation-Induced Neuroinflammation and Preserves Hippocampal Neurogenesis in Rats by Inhibiting Activation of NF-κB and AP-1", Neurotoxicity Research, Vol. 31/2, https://doi.org/10.1007/s12640-016-9679-4.

Zhu, G. et al. (2022), "Crosstalk Between the Oxidative Stress and Glia Cells After Stroke: From Mechanism to Therapies", Frontiers in Immunology, Vol. 13, https://doi.org/10.3389/fimmu.2022.852416.

Relationship: 2834: Tissue resident cell activation leads to Increase, Pro-Inflammatory Mediators

AOPs Referencing Relationship

AOP Name	Adjacency	Weight of Evidence	Quantitative Understanding
Deposition of Energy Leading to Learning and Memory Impairment	adjacent	Moderate	Low

Evidence Supporting Applicability of this Relationship

Taxonomic Applicability

Term	Scientific Term	Evidence	Links
human	Homo sapiens	Low	NCBI
mouse	Mus musculus	Moderate	NCBI
rat	Rattus norvegicus	Moderate	NCBI

Life Stage Applicability

Life Stage	Evidence
All life stages	Moderate

Sex Applicability

Sex	Evidence
Unspecific	Moderate

Evidence for this relationship comes from *in vitro* mouse- and human-derived models, as well as *in vivo* mouse and rat models. The relationship is not sex or life stage specific.

Key Event Relationship Description

Tissue-resident cell activation refers to the stimulation of resident cells in organ systems. Tissue-resident immune cells can be found throughout the body, each tissue and organ containing specific resident immune cells (Chen et al., 2018; Gray & Farber, 2022). Monocytes, found in the blood, and macrophages, found in all tissues in the body, are the main components of the immune system (Ivanova & Orekhov, 2016). In the brain, the primary tissue-resident macrophages are microglia, while astrocytes are also important cells found in the brain (Bourgognon & Cavanagh, 2020; Greene-Schloesser et al., 2012; Wang et al., 2020). Activated tissue-resident cells can undergo gliosis, whereby they adopt a hypertrophic morphology and proliferate, exhibiting rounding of the cell body and retraction of cell processes (Greene-Schloesser et al., 2012; Phatnani & Maniatis, 2015). It is well-characterized that activated tissue-resident cells can increase expression of pro-inflammatory mediators (Hladik & Tapio, 2016; Lumniczky, Szatmari & Safrany, 2017; Kaur et al., 2019). Acute inflammation from controlled biosynthesis of pro-inflammatory mediators protects tissue and promotes healing (Kim & Joh, 2006; Vezzani & Viviani, 2015). Prolonged tissue-resident cell activation leads to dysregulation in production or secretion of pro-inflammatory mediators, which results in chronic inflammation and damage to tissue (Kim & Joh, 2006; Vezzani & Viviani, 2015). Additionally, activated tissue-resident cells can show increased levels of transcription factor nuclear factor κB (NF-κB) and activated protein 1 (AP-1) DNA binding due to increased oxidative stress or DNA damage (Betlazar et al., 2016; Lumniczky, Szatmari & Safrany, 2017). Through the activity of NF-κB, AP-1 and other signaling pathways, activated immune cells can together produce/secrete a variety of cytokines and chemokines (Betlazar et al., 2016; Chen et al., 2018; Greene-

Schloesser et al., 2012; Kim & Joh, 2006; Phatnani & Maniatis, 2015; Smith et al., 2012; Wang et al., 2020). Chronic secretion of these inflammatory proteins can lead to downstream detriments, such as in the brain, altering blood-brain barrier permeability (Lumniczky, Szatmari & Safrany, 2017).

Evidence Supporting this KER

Overall Weight of Evidence: Moderate

Biological Plausibility

Tissue-resident cells recognize pathogens or molecules released by injured or activated cells (Vezzani & Viviani, 2015). In response, resident cells become activated and release various pro-inflammatory mediators (Chen et al., 2018; Gray & Farber, 2022). There is an abundance of studies which explore this relationship using the brain microenvironment, where astrocytes and microglia are the primary tissue-resident cells. After activation, these cells increase in number (whether through proliferation or recruitment), undergo morphological changes and release cytokines release (Greene-Schloesser et al., 2012; Kim & Joh, 2006).

Several pathways and molecules are involved in the inflammatory response to activate tissue-resident cells. These molecules include certain pro-inflammatory cytokines and various inflammatory stimuli, such as lipopolysaccharide (LPS), thrombin (a protease), β-amyloid (Aβ), interferon (IFN)-γ, CD40 and gangliosides (Dheen, Kaur & Ling, 2007; Kim & Joh, 2006). For example, LPS can diffuse into brain parenchyma and activate microglia, which then expresses inflammatory mediators and ROS to initiate inflammation (Dheen, Kaur & Ling, 2007; Kim & Joh, 2006). As well, pattern recognition receptor activation, through molecules such as damage-associated molecular pattern molecules (DAMPs), can activate tissue-resident cells and, in turn, lead to pro-inflammatory mediator secretion (Chen et al., 2018).

Once resident cells become activated, various pathways, including the NF-κB transcription factor pathway and the mitogen-activated protein kinase (MAPK)-AP-1 signaling pathway, can result in pro-inflammatory mediator production (Chen et al., 2018; Vezzani & Viviani, 2015; Wang et al., 2020). When activated, microglia and astrocytes are sources of cytokines in the central nervous system (CNS) (Bourgognon & Cavanagh, 2020; Kim & Joh, 2006; Smith et al., 2012; Vezzani & Viviani, 2015; Boyd et al., 2021). Furthermore, uniquely in the brain, astrocyte activation can lead to blood-brain barrier permeability through decreased astrocyte function, which can allow pro-inflammatory mediators to enter from the blood (Lumniczky, Szatmari & Safrany, 2017).

An abundance of studies supports the connectivity of the two key events using activated glial cells in the brain microenvironment. Activated astrocytes express high levels of glial fibrillary acidic protein (GFAP) (Greene-Schloesser et al., 2012), while microglia activation results in the expression of OX-42, Iba1 (activated and non-activated), Mac-1, CD68, F4-80, Glut-5 and CR3/43. These markers play an important role in the phagocytic activity and morphological changes of activated microglia (Jurga, Paleczna & Kuter, 2020). Upon expression of these markers, cells release pro-inflammatory mediators, these can further activate other glial cells (Bourgognon & Cavanagh, 2020). This results in an inflammatory state, that initiates the further release of cytokines including IL-1 and TNF-α, IL-6, Cox-2 (Betlazar et al., 2016; Kim & Joh, 2006; Smith et al., 2012) and chemokines MCP-1 and ICAM-1 (Greene-Schloesser et al., 2012; Kyrkanides et al., 2002). Chronic activation of these cells can result in neurodegenerative disease due to their continuous release and the overexpression of potentially cytotoxic molecules, which may eventually lead to cognitive decline (Dheen, Kaur & Ling, 2007; Kaur et al., 2019; Smith et al., 2012). To suppress this activity, anti-inflammatory proteins need to be released such as tumor growth factor (TGF)-β and IL-10; these act to reduce neuron activity (Kim & Joh, 2006; Phatnani & Maniatis, 2015). In a state of chronic inflammation, the production of pro-inflammatory proteins increases, while anti-inflammatory proteins decrease, and this imbalance results in a reduced stress response (Jeon & Kim, 2016).

Empirical Evidence

The evidence supporting the relationship between tissue-resident cell activation leading to increased pro-inflammatory mediators was gathered from studies using human (Chen et al., 2016; Lodermann et al., 2012) and mouse (Dong et al., 2015; Komatsu et al., 2017; Liu et al., 2010; Ramanan et al., 2008; Scharpfenecker et al., 2012; van Neerven et al., 2010; Welser-Alves & Milner, 2013) in vitro cell cultures as well as rat (Lee et al., 2010; Liu et al., 2010; Zhou et al., 2017) and mouse (Dong et al., 2015; Kyrkanides et al. 2002; Parihar et al., 2018) in vivo models. The stressors used were gamma rays (Kyrkanides et al., 2002; Lee et al., 2010), X-rays (Liu et al., 2010; Lodermann et al., 2012; Scharpfenecker et al., 2012), 4He ions (Parihar et al., 2018), nominal photon energy (Zhou et al., 2017) and LPS treatment (Komatsu et al., 2017; van Neerven et al., 2010; Welser-Alves & Milner, 2013). Tissue-resident cell activation is assessed by examining the morphology of activated cells (Dong et al., 2015; Zhou et al., 2017) and the detection of activation markers (Chen et al., 2016; Dong et al., 2015; Liu et al., 2010; Parihar et al., 2018; Scharpfenecker et al., 2012; van Neerven et al., 2010; Welser-Alves & Milner, 2013; Zhou et al., 2017) and AP-1 and NF-κB DNA binding (Komatsu et al., 2017; Lee et al., 2010; Lodermann et al., 2012; Ramanan et al., 2008). Pro-inflammatory mediators, including cytokines, adhesion markers, and inflammatory enzymes were assessed at both the protein and mRNA level although transcriptional responses may not necessarily translate to changes in active signaling molecules. Such studies provide indirect evidence to support the relationship.

Dose Concordance

Many studies demonstrate that activation of tissue-resident cells occurs at lower or the same doses as increased pro-inflammatory mediators. Although, at doses of ionizing radiation less than 1 Gy, evidence suggests anti-inflammatory activation of macrophages instead of towards inflammation (Wu et al., 2017). This was shown after irradiation of human monocytes from 0.1 to 0.7 Gy which resulted in decreased NF-κB nuclear translocation and decreased IL-1β levels (Lodermann et al., 2012). Dong et al. (2015) used various models and endpoints to study this relationship. In vitro mouse microglia showed an activated morphology, increased F4-80

(activated macrophage indicator), and increased levels and expression of TNF-α and IL-1β all after 16 Gy X-rays (Dong et al., 2015). With the same stressor and dose but in mice kidneys, F4-80 and various pro-inflammatory cytokines were increased (Scharpfenecker et al., 2012). In vivo mice with 10 Gy cranial X-ray irradiation showed a similar response (Dong et al., 2015). Activation of glial cells in rat brains as well as levels of IL-1β and TNF-α in BV2 murine microglial cells increased linearly after 2, 4, 6, 8 and 10 Gy X-rays (Liu et al., 2010). Multiple studies found that LPS treatment at 1 µg/mL resulted in both macrophage activation and TNF-α production (Lodermann et al., 2012; Welser-Alves & Milner, 2013). Rats with 10 Gy gamma ray irradiation showed increases in both NF-κB and AP-1 DNA binding activity, indicators of activated microglia. At the same dose, pro-inflammatory mediators TNF-α, IL-1β and MCP-1 also increased (Lee et al., 2010). When human microglia were irradiated with gamma rays, they showed a characteristic activated morphology after 8 Gy, while CR3/43 and Glut-5 (microglial activation markers) showed increased expression after 8 Gy, and IL-1α and TNF-α also showed increased expression after 8 Gy (Chen et al., 2016).

Time Concordance

Many studies observed that tissue-resident cell activation occurs earlier or at the same time as increased pro-inflammatory mediators. Mice irradiated with 4He particles showed increases in both activated microglia and pro-inflammatory chemokine CCL-3 after 1 year (Parihar et al., 2018). In vitro murine microglial cells and in vivo rat brains were irradiated with X-rays and showed increases in activated glial cells, as well as IL-1β and TNF-α pro-inflammatory mediators 24h post-irradiation (Liu et al., 2010). After mouse cranial X-ray irradiation, the number of F4-80 positive cells/mm2 was significantly increased from 3h to 2 weeks with a maximum after 24h, while TNF-α and IL-1β both showed significantly increased levels and expression at many times from 3h to 6 weeks post-irradiation, with maximum levels occurring after 24h (Dong et al., 2015). Gamma ray irradiation of rats showed increased NF-κB and AP-1 DNA binding at 4 and 8h after irradiation, with levels reduced to control after 24h, and mRNA and protein levels of pro-inflammatory mediators TNF-α, IL-1β and MCP-1 in the hippocampus and cerebellum showed a similar trend (Lee et al., 2010). Juvenile rats irradiated with 4MV photon energy showed that microglial density increased at 6 and 24 h post-irradiation in the external germinal layer of the cerebellum, while IL-1α, IL-1β, IL-6, IL-18, GRO/KC and CCL-2 were all significantly increased after 24h (Zhou et al., 2017). Human microglia irradiated with gamma rays showed a characteristic activated morphology after 7 days (Chen et al., 2016). In addition, activation markers CR3/43 and Glut-5 were expressed after 2 weeks and Glut-5 continued expression after 1 week and 10 days. IL-1α and TNF-α showed increased expression after 7 days, which was slightly lower after 2 weeks, but still significant (Chen et al., 2016).

Incidence Concordance

Two studies identified an incidence-concordant relationship between tissue resident cell activation and increase in pro-inflammatory mediators. Parihar et al. (2018) found increased microglial activation after mice were irradiated with 5 and 30 cGy 4He particles. Chemokine CCL-3 was increased slightly after both 5 and 30 cGy. Zhou et al. (2017) irradiated juvenile rats with a single dose of 6 Gy nominal photon energy (4MV) and showed microglial proliferation in the external germinal layer of the cerebellum, while cytokines (IL-6, IL-18) and chemokines (CCL-2, GRO/KC) increased significantly.

Essentiality

In the absence of tissue-resident cell activation, an increase in pro-inflammatory mediators is not expected. The activation of tissue-resident cells can be attenuated by tamoxifen. Tamoxifen, an estrogen receptor modulator that can serve as a radiosensitizer, attenuated microglial activation and significantly decreased inflammatory cytokine production, including IL-1β and TNF-α, compared to the X-ray irradiated samples (4, 6, 8, 10 Gy) in absence of tamoxifen (Liu et al., 2010). A study by van Neerven et al. (2010) pretreated cells of mice cerebral cortices with a transcriptional activator, retinoic acid (RA) containing anti-inflammatory effects, for 12 h, and then exposed the cells for another 12 h to RA and LPS, an endotoxin which induces production of IL-1β, IL-6, TNFα in astrocytes. RA, when used with LPS, led to a significant reduction of the LPS-induced release of IL-1β, IL-6, TNF-α (van Neerven et al., 2010). Similarly, N-acetyl-L-cysteine (NAC) at 40 and 80 µM was able to reduce the LPS-induced levels of IL-6, TNF-α while preventing NF-κB nuclear translocation (Komatsu et al., 2017). NF-κB and AP-1 transcription factors binding to DNA indicate activated microglia, which was observed post-irradiation in the study by Ramanan et al. (2008). Radiation led to an increase in TNFα and IL-1β expression in microglia cultures, as well as an increase in Cox-2 protein levels. Treatment with SP 600125 (SP), a specific c-jun kinase inhibitor, which prevented AP-1 binding to DNA, was found to inhibit the radiation-induced increase in TNF-α, IL-1β, and Cox-2 expression. In contrast, treating BV-2 cells with 6-amino-4-(4-phenoxyphenylethylamino) quinazoline (Q), NF-κB activation inhibitor, prevented the increase in NF-κB binding to DNA, thus blocking the activation of tissue-resident cells, which then inhibited the radiation-induced increase in IL-1β expression but allowed the radiation-induced increases in Cox-2 and TNF-α. (Ramanan et al., 2008). Proinflammatory marker, ICAM-1, increased by 2.2-fold 72 h following 35 Gy irradiation (Kyrkanides et al. 2002). However, inhibition of Cox-2, a microglial activator, by NS-398 led to a 0.6-fold decrease in ICAM-1 levels induced by radiation in the brain. (Kyrkanides et al. 2002).

Uncertainties and Inconsistencies

More work could be done to observe this relationship in human models.

Quantitative Understanding of the Linkage

The table below provides some representative examples of quantitative linkages between the two key events. It was difficult to identify a general trend across all the studies due to differences in experimental design and reporting of the data. All data is statistically significant unless otherwise stated.

Dose Concordance

Reference	Experiment Description	Result
Liu et al., 2010	In vivo. BV2 murine microglia were irradiated with 0, 2, 4, 6, 8 or 10 Gy X-rays to measure microglial activation, and OX-42 and GFAP staining was performed on 15 Gy irradiated rat brains to measure microglial and astrocyte activation, respectively. In vitro. BV-2 murine microglia were irradiated with 0, 2, 4, 6, 8 or 10 Gy X-rays to determine cytokines IL-1β and TNF-α production. Glial activation was identified by light microscopy and immunohistochemistry. ELISA was used to assess cytokine levels of IL-1β and TNF-α.	Irradiation of in vitro microglia cultures caused a dose-dependent increase in microglial activation from 0 to 10 Gy. At 15 Gy, in vivo astrocyte activation increased 5-fold, while microglial activation increased 3-fold. Levels of IL-1β and TNF-α production were also dose-dependently increased following 0 to 10 Gy irradiated microglia, resulting in an 8.6-fold increase for IL-1β and a 6.8-fold increase for TNF-α after 10 Gy.
Welser-Alves & Milner, 2013	In vitro. Cultures of microglia and astrocytes from postnatal mouse central nervous system were stimulated with 1 µg/mL LPS. ELISA and immunocytochemistry were used to measure glial cytokine (TNF-α) production with Mac-1 as a microglial marker.	Microglia activation with 1 µg/mL LPS led to increased TNF-α production from 40.6 pg/ml to 1875.0 pg/ml, and TNF-α showed co-localization with Mac-1 positive microglia. TNF-α was not present in astrocytes.
Lee et al., 2010	In vivo. Rats received whole-brain gamma ray irradiation at 10 Gy. Levels of AP-1 and NF-κB (microglial activation) as well as pro-inflammatory mediators TNF-α, IL-1β, IL-6, and MCP-1 were determined in the hippocampus and cortex. AP-1 and NF-κB DNA binding was determined through electrophoretic mobility shift assay (EMSA), and pro-inflammatory mediator levels were determined using enzyme-linked immunosorbent assay (ELISA).	After 10 Gy, DNA binding of NF-κB and AP-1 increased a maximum of 3.6-fold and 2.8-fold, respectively. Hippocampus: After 10 Gy at maximum, TNF-α was increased 23-fold, IL-1β increased 10-fold, IL-6 did not significantly change, and MCP-1 increased 1.6-fold. Cortex: After 10 Gy at maximum, TNF-α increased 30-fold, IL-1β increased 7-fold. IL-6 did not significantly change, and MCP-1 increased 2.2-fold.
Chen et al., 2016	In vitro. Human CHME5 microglia were irradiated with various doses of 137Cs gamma radiation delivered acutely over 1-3 minutes. Microglial activation markers CR3/43 and Glut-5 were determined by Western blot, morphology of microglia was determined through fluorescence microscopy, and expression of cytokines IL-1α and TNF-α were determined through RT-PCR.	After 8 Gy, microglia showed a characteristic activated morphology, but not after 0.5 Gy. CR3/43 and Glut-5 were both expressed after 8 Gy, but not 0.5 Gy. mRNA levels measured at 8 Gy were found to increase a maximum of 7.8-fold for IL-1α and 5.8-fold for TNF-α.
Dong et al., 2015	In vivo and in vitro. BV2 mouse microglial cells and C57BL/6J mice brains were irradiated with various doses of X-rays. Iba1 staining was performed to determine cell morphology, while anti-F4-80 antibodies were used to determine microglial activation. TNF-α and IL-1β levels were determined through RT-PCR, ELISA (in vitro), and Western blot (in vivo).	In vitro: At 16 Gy, microglia adopted a characteristic activated morphology while F4-80 was greatly upregulated. Also at 16 Gy, IL-1β expression increased a maximum of 23-fold, TNF-α expression increased a maximum of 13-fold, IL-1β increased from 0 to a maximum of 530 pg/mL, and TNF-α increased from almost 0 to a maximum of 115 pg/mL. In vivo: The number of F4-80 positive cells/mm2 increased from 9 to a maximum of 40 after 10 Gy. Also at 10 Gy, IL-1β expression increased a maximum of 7-fold, TNF-α expression increased a maximum of 5-fold, IL-1β levels increased a maximum of 10-fold, and TNF-α levels increased a maximum of 5-fold compared to controls.
Komatsu et al.,	In vitro. Murine macrophage RAW264 cell line activation was induced by 1 µg/mL LPS treatment. Activation was determined through NF-κB nuclear translocation	After LPS treatment, cytosolic NF-κB decreased 0.64-fold, nuclear NF-κB increased 7.2-fold and IκB (NF-κB inhibitor) decreased 0.21-fold. Both TNF-α and IL-6

2017	measured by western blot. Pro-inflammatory mediators TNF-α and IL-6 were measured by ELISA.	were increased from around 0 ng/mL to about 70 and 30 ng/mL, respectively.
Lodermann et al., 2012	In vitro. Human monocytic leukaemia cell lines were irradiated with X-rays at 0.1, 0.3, 0.5, 0.7 and 1 Gy. Activation was determined through NF-κB nuclear translocation by western blot. IL-1β was measured by ELISA.	NF-κB and IL-1β both showed linear decreases from 0.1 to 0.7 Gy, resulting in maximum decreases of 0.6- to 0.7-fold. Although, the decrease for NF-κB was nonsignificant. No changes were observed at 1 Gy.
Scharpfenecker et al., 2012	In vitro. Mice kidneys were irradiated with 16 Gy of X-rays. Immunofluorescence stainings were performed for IL-6, IL-1β and macrophage marker F4-80.	F4-80 positive area increased by 6.7 and 3.8-fold in Eng+/+ and Eng+/- irradiated mice respectively. Macrophages in irradiated mouse kidney led to IL-6 and IL-1β production.

Time Concordance

Reference	Experiment Description	Result
Parihar et al., 2018	In vivo. C57BL/6 J mice were irradiated with 4He particles 1 year after irradiation. The level of CCL-3 was determined in the brain, and microglial activation was determined by immunohistochemistry in the perirhinal cortex.	At maximum, there was a 3.8-fold increase in activated microglia, CCL-3 increased 2.2-fold.
Liu et al., 2010	In vitro. BV2 murine microglia were irradiated with X-rays to measure microglial activation after 24h, and OX-42 and GFAP staining was performed on irradiated rat brains to measure microglial and astrocyte activation, respectively, after 3 days. BV-2 murine microglia were irradiated with X-rays to determine cytokines IL-1β and TNF-α production after 24h. Glial activation was identified by light microscopy and immunohistochemistry. ELISA was used to assess cytokine levels of IL-1β and TNF-α.	10 Gy irradiation of microglia cultures caused an increase in microglial activation after 24h. At 15 Gy after 3 days, astrocyte activation increased 5-fold, while microglial activation increased 3-fold. Levels of IL-1β and TNF-α were also increased in 10 Gy irradiated microglia, resulting in an 8.6-fold increase for IL-1β and a 6.8-fold increase for TNF-α after 24h.
Lee et al., 2010	In vivo. Rats received whole-brain gamma ray irradiation at 10 Gy. Levels of AP-1 and NF-κB (microglial activation) as well as pro-inflammatory mediators TNF-α, IL-1β, IL-6, and MCP-1 were determined 4, 8, and 24h after irradiation in the hippocampus and cortex. AP-1 and NF-κB DNA binding was determined through electrophoretic mobility shift assay (EMSA), and pro-inflammatory mediator levels were determined using enzyme-linked immunosorbent assay (ELISA).	DNA binding of NF-κB and AP-1 increased a maximum of 3.6-fold and 2.8-fold, respectively, after 8h. Binding activity returned to control levels after 24h. Hippocampus: At control, TNF-α was 3.6 pg/mg protein, which increased 23-fold after 4 hours, 8.3-fold after 8h, and 3.6-fold after 24h. IL-1β increased linearly from 4 to 24h, reaching a 10-fold maximum increase. IL-6 did not significantly change other than a non-significant decrease over 24h, even though an increase in IL-6 mRNA was observed at 4h with RT-qPCR. MCP-1 showed a maximum increase of 1.6-fold after 8h. Cortex: At control, TNF-α was 4.4 pg/mg protein, which increased 30-fold after 4 hours, 13-fold after 8h, and 4.1-fold after 24h. IL-1β showed a maximum increase of 7-fold after 4h. IL-6 did not significantly change other than a non-significant decrease over 24h, even though an increase in IL-6 mRNA was observed at 4h with RT-qPCR. MCP-1 showed a maximum increase of 2.2-fold after 8h.
Chen et al., 2016	In vitro. Human CHME5 microglia were irradiated with 8 Gy gamma radiation (137Cs source) delivered acutely over 1-3 minutes. Microglial activation markers CR3/43 and Glut-5 were determined by Western blot, morphology of microglia was determined through fluorescence microscopy, and expression of cytokines IL-1α and TNF-α were determined through RT-PCR.	Beginning after 7 days, microglia showed a characteristic activated morphology. CR3/43 was expressed after 2 weeks, while Glut-5 was expressed after 1 week, 10 days, and 2 weeks. After 7 days, mRNA levels were found to increase a maximum of 7.8-fold for IL-1α and 5.8-fold for TNF-α. mRNA levels dropped slightly but were still above controls after 2 weeks.

Zhou et al., 2017	In vivo. Juvenile rats were irradiated with 4MV nominal photon energy and a single dose of 6 Gy (2.3 Gy/min). At 6 or 24h, the molecular and cellular changes in the EGL of the cerebellum was studied. Immunohistochemistry staining was used to measure Iba1 (microglia marker) with morphometry analysis performed on microglia. Luminex assay measured cytokines, chemokines and growth factors for the inflammatory response.	Microglia density increased by 2.3-fold after 6 h and 6.77-fold 24 h post-irradiation. Most of the iba1-positive cells had a bushy or amoeboid morphology, signifying an activated state. At 6 h of irradiation, IL-1α and CCL-2 increased by 2-2.8-fold. IL-1β decreased at 6 h then slightly increased at 24 h post-irradiation. IL-6, IL-18, GRO/KC, VEGF, and GM-CSF all increased significantly at 24 h compared to the control group.
Dong et al., 2015	In vivo and in vitro. BV2 mouse microglial cells and C57BL/6J mice brains were irradiated with X-rays. Iba1 staining was performed to determine cell morphology, while anti-F4-80 antibodies were used to determine microglial activation. TNF-α and IL-1β levels were determined through RT-PCR, ELISA (in vitro), and Western blot (in vivo) from 3h to 6 weeks after irradiation.	In vivo, the number of F4-80 positive cells/mm2 increased from 9 to a maximum of 40 after 24h, decreased over 2 weeks, and returned to control levels at 4 and 6 weeks. IL-1β expression increased to a maximum after 72h and was significantly increased from 6h to 6 weeks. TNF-α expression was a maximum after 3 and 6h, was at controls from 24h to 1 week, and was increased again from 2 to 6 weeks. IL-1β levels were high after 3h, lower at 6h, increased to a maximum at 2 weeks, then decreased at 4 and 6 weeks. TNF-α levels increased to a maximum after 72h, then decreased until 4 weeks, where they increased again after 6 weeks. In vitro. IL-1β levels reached a maximum at 3h, but then decreased at 6h, before rising again at 12h. TNF-α levels remained elevated up to 24h, although its peak was at 6h.

Incidence Concordance

Reference	Experimental Description	Result
Parihar et al., 2018	In vivo. C57BL/6 J mice were irradiated with 4He particles at either 5 or 30 cGy (5 cGy/min). The level of CCL-3 was determined in the brain, and microglial activation was determined by ED-1 immunohistochemistry in the perirhinal cortex.	Microglial activation increased 3.5-fold after 5 cGy and 3.8-fold after 30 cGy. CCL-3 increased 1.4-fold (non-significant, ns) after 5 cGy and 2.2-fold after 30 cGy.
Zhou et al., 2017	In vivo. Juvenile rats were irradiated with 4 MV nominal photon energy and a single dose of 6 Gy (2.3 Gy/min). At 6 or 24h, the molecular and cellular changes in the EGL of the cerebellum was studied. Immunohistochemistry staining was used to measure Iba1 (microglia marker) with morphometry analysis performed on microglia. Luminex assay measured cytokines, chemokines and growth factors for the inflammatory response.	Microglia density increased by 2.3-fold after 6 h.and 6.77-fold 24 h post-irradiation. Most of the iba1-positive cells had a bushy or amoeboid morphology, signifying an activated state. At 6 h of irradiation, IL-1α and CCL-2 increased by 2-2.8-fold. IL-1β decreased at 6 h then slightly increased at 24 h post-irradiation. IL-6, IL-18, GRO/KC, VEGF, and GM-CSF all increased significantly at 24 h compared to the control group.

Known modulating factors

Modulating factor	Details	Effects on the KER	References
Drug	Flavonoids	Flavonoids can inhibit NF-κB, preventing transcription of pro-inflammatory mediators in active glial cells.	Wang et al., 2020
Drug	Tamoxifen (estrogen receptor modulator commonly used in breast cancer treatment)	Treatment with Tamoxifen decreased the radiation-induced activation of glial cells. It also consistently decreased the amount of TNF-α and IL-1β and blood-brain barrier permeability after irradiation at various doses.	Liu et al., 2010
Drug	RA (modulates inflammatory effects in different cell types)	RA treatment completely inhibited the increase in pro-inflammatory mediators after LPS-induced glial activation.	van Neerven et al., 2010
Drug	SP (JNK, c-jun N-terminal kinase, inhibitor)	AP-1 DNA binding (glial activation) was reduced by SP treatment after irradiation. TNF-α, Cox-2 and IL-1β were reduced by SP treatment after irradiation or viral infection.	Ramanan et al., 2008
Drug	Q (NF-κB inhibitor)	NF-κB DNA binding (glial activation) was reduced by Q treatment after irradiation. IL-1β was also reduced by Q treatment after irradiation.	Ramanan et al., 2008

Drug	NS-398 (Cox-2 inhibitor)	Treatment with NS-398 reduced TNF-α, IL-1β, IL-6, ICAM-1 and MCP-1 expression after irradiation.	Kyrkanides et al., 2002
Age	Increased age	Aging tissue becomes more sensitive to immune signals and increases inflammation. In the aging brain, microglia will produce more pro-inflammatory mediators.	Patterson, 2015
Drug	NAC	NAC treatment inhibited pro-inflammatory mediator production in macrophages.	Komatsu et al., 2017

Known Feedforward/Feedback loops influencing this KER

It is well-characterized that activated tissue-resident cells can increase expression of pro-inflammatory mediators (Hladik & Tapio, 2016; Lumniczky, Szatmari & Safrany, 2017; Kaur et al., 2019). However, there exists a feedforward loop for this key event relationship as pro-inflammatory mediators can also activate tissue-resident cells within the brain and perpetuate the inflammatory response (Kim & Joh, 2006; Vezzani & Viviani, 2015). Thus, after stimulation by cytokines, chemokines or inflammogens such as from damaged neurons, microglia and astrocytes activate inflammatory signaling pathways, which result in increased expression and/or release of inflammatory mediators such as cytokines, eicosanoids, and metalloproteinases (Dong & Benveniste, 2001; Bourgognon & Cavanagh, 2020). Various studies have shown that overexpression of IL-1β in moues models resulted in the appearance of inflammatory markers including activated glial cells and increased pro-inflammatory cytokine and chemokine mRNAs (Hein et al., 2010; Moore et al., 2009). Additionally, IL-6 plays a role in activating glial cells as mouse models with IL-6 knocked out showed reduced astrocytic population, as well as a reduced ability in activating microglia (Klein et al., 1997). Cytokines and chemokines can also increase the permeability of the blood-brain barrier, further increasing pro-inflammatory mediator levels (Lumniczky, Szatmari & Safrany, 2017).

References

Betlazar, C. et al. (2016), "The impact of high and low dose ionising radiation on the central nervous system", Redox Biology, Vol. 9, Elsevier B.V., https://doi.org/10.1016/j.redox.2016.08.002.

Bourgognon, J. M. and J. Cavanagh. (2020), "The role of cytokines in modulating learning and memory and brain plasticity", Brain and Neuroscience Advances, Vol. 4, SAGE Publications, https://doi.org/10.1177/2398212820979802.

Boyd, A. et al. (2021), "Control of Neuroinflammation through Radiation-Induced Microglial Changes", Cells, Vol. 10/9, Multi-Disciplinary Digital Publishing Institute (MDPI), Basel, https://doi.org/10.3390/cells10092381.

Chen, H. et al. (2016), "Delayed activation of human microglial cells by high dose ionizing radiation", Brain Research, Vol. 1646, Elsevier B.V., https://doi.org/10.1016/j.brainres.2016.06.002.

Chen, L. et al. (2018). “Inflammatory responses and inflammation-associated diseases in organs”, Oncotarget, Vol.9/6, Oncotarger, Orchard Park, https://doi.org/10.18632/oncotarget.23208

Dheen, S. T., C. Kaur and E. Ling. (2007), "Microglial Activation and its Implications in the Brain Diseases", Current Medicinal Chemistry, Vol. 14/11, Bentham Science Publishers https://doi.org/10.2174/092986707780597961.

Dong, Y. and E. N. Benveniste. (2001), "Immune function of astrocytes", Glia, Vol. 36/2, John Wiley & Sons, Hoboken, https://doi.org/10.1002/glia.1107.

Dong, X. et al. (2015), "Relationship between irradiation-induced neuro-inflammatory environments and impaired cognitive function in the developing brain of mice", International Journal of Radiation Biology, Vol. 91/3, Informa Healthcare, London, https://doi.org/10.3109/09553002.2014.988895.

Gray, J. I., & D. L. Farber (2022). “Tissue-Resident Immune Cells in Humans”, Annual Review of Immunology, Vol. 40/1, Annual Reviews, San Mateo, https://doi.org/10.1146/annurev-immunol-093019-112809

Greene-Schloesser, D. et al. (2012), "Radiation-induced brain injury: A review", Frontiers in Oncology, Frontiers Media, Lausanne, https://doi.org/10.3389/fonc.2012.00073.

Hein, A. M. et al. (2010), "Sustained hippocampal IL-1β overexpression impairs contextual and spatial memory in transgenic mice", Brain, Behavior, and Immunity, Vol. 24/2, https://doi.org/10.1016/j.bbi.2009.10.002.

Hladik, D. and S. Tapio. (2016), "Effects of ionizing radiation on the mammalian brain", Mutation Research, Vol. 770, Elsevier B.V., https://doi.org/10.1016/j.mrrev.2016.08.003.

Ivanova, E. A., & A. N. Orekhov. (2016), “Monocyte Activation in Immunopathology: Cellular Test for Development of Diagnostics and Therapy”, Journal of Immunology Research, Vol. 2016, Hindawi, https://doi.org/10.1155/2016/4789279

Jeon, S. W. and Y. K. Kim. (2016), "Neuroinflammation and cytokine abnormality in major depression: Cause or consequence in that illness?", World Journal of Psychiatry, Vol. 6/3, https://doi.org/10.5498/wjp.v6.i3.283.

Jurga, A. M., M. Paleczna and K. Z. Kuter et al. (2020), "Overview of General and Discriminating Markers of Differential Microglia Phenotypes", Frontiers in Cellular Neuroscience, Vol. 14, Frontiers Media S.A., Lausanne, https://doi.org/10.3389/fncel.2020.00198.

Kaur, D., V. Sharma and R. Deshmukh. (2019), "Activation of microglia and astrocytes: a roadway to neuroinflammation and Alzheimer's disease", Inflammopharmacology, Vol. 27/4, Springer Nature, Berlin, https://doi.org/10.1007/s10787-019-00580-x.

Kim, Y. S. and T. H. Joh. (2006), "Microglia, major player in the brain inflammation: their roles in the pathogenesis of Parkinson's disease", Experimental & Molecular Medicine, Vol. 38/4, Springer Nature, Seoul, https://doi.org/10.1038/emm.2006.40.

Klein, M. A. et al. (1997), "Impaired neuroglial activation in interleukin-6 deficient mice", Glia, Vol. 19/3, https://doi.org/10.1002/(SICI)1098-1136(199703)19:3<227::AID-GLIA5>3.0.CO;2-W.

Komatsu, W. et al. (2017), "Nasunin inhibits the lipopolysaccharide-induced pro-inflammatory mediator production in RAW264 mouse macrophages by suppressing ROS-mediated activation of PI3 K/Akt/NF-κB and p38 signaling pathways", Bioscience, Biotechnology, and Biochemistry, Vol. 81/10, Elsevier, https://doi.org/10.1080/09168451.2017.1362973

Kyrkanides, S. et al. (2002), "Cyclooxygenase-2 modulates brain inflammation-related gene expression in central nervous system radiation injury", Molecular Brain Research, Vol. 104/2, Elsevier, https://doi.org/10.1016/S0169-328X(02)00353-4.

Lee, W. H. et al. (2010), "Irradiation induces regionally specific alterations in pro-inflammatory environments in rat brain", International Journal of Radiation Biology, Vol. 86/2, Informa, London, https://doi.org/10.3109/09553000903419346.

Liu, J. L. et al. (2010), "Tamoxifen alleviates irradiation-induced brain injury by attenuating microglial inflammatory response in vitro and in vivo", Brain Research, Vol. 1316, Elsevier B.V., https://doi.org/10.1016/j.brainres.2009.12.055.

Lodermann, B. et al. (2012), "Low dose ionising radiation leads to a NF-κB dependent decreased secretion of active IL-1β by activated macrophages with a discontinuous dose-dependency", International Journal of Radiation Biology, Vol. 88/10, Informa, London, https://doi.org/10.3109/09553002.2012.689464

Lumniczky, K., T. Szatmári and G. Sáfrány. (2017), "Ionizing Radiation-Induced Immune and Inflammatory Reactions in the Brain", Frontiers in Immunology, Vol. 8, Frontiers Media S.A., Lausanne, https://doi.org/10.3389/fimmu.2017.00517.

Moore, A. H. et al. (2009), "Sustained expression of interleukin-1β in mouse hippocampus impairs spatial memory", Neuroscience, Vol. 164/4, https://doi.org/10.1016/j.neuroscience.2009.08.073.

Parihar, V. K. et al. (2018), "Persistent nature of alterations in cognition and neuronal circuit excitability after exposure to simulated cosmic radiation in mice", Experimental Neurology, Vol. 305, Elsevier B.V., https://doi.org/10.1016/j.expneurol.2018.03.009.

Patterson, S. L. (2015), "Immune dysregulation and cognitive vulnerability in the aging brain: Interactions of microglia, IL-1β, BDNF and synaptic plasticity", Neuropharmacology, Vol. 96, Elsevier B.V., https://doi.org/10.1016/j.neuropharm.2014.12.020.

Phatnani, H. and T. Maniatis. (2015), "Astrocytes in Neurodegenerative Disease: Table 1.", Cold Spring Harbor Perspectives in Biology, Vol. 7/6, Cold Spring Harbor Laboratory Press, https://doi.org/10.1101/cshperspect.a020628.

Ramanan, S. et al. (2008), "PPARα ligands inhibit radiation-induced microglial inflammatory responses by negatively regulating NF-κB and AP-1 pathways", Free Radical Biology and Medicine, Vol. 45/12, Elsevier B.V., https://doi.org/10.1016/j.freeradbiomed.2008.09.002.

Scharpfenecker, M. et al. (2012), "The TGF-β co-receptor endoglin regulates macrophage infiltration and cytokine production in the irradiated mouse kidney", Radiotherapy and Oncology, Vol. 105/3, Elsevier B.V., https://doi.org/10.1016/J.RADONC.2012.08.021

Smith, J. A. et al. (2012), "Role of pro-inflammatory cytokines released from microglia in neurodegenerative diseases", Brain Research Bulletin, Vol. 87/1, Elsevier B.V., https://doi.org/10.1016/j.brainresbull.2011.10.004.

van Neerven, S. et al. (2010), "Inflammatory cytokine release of astrocytes in vitro is reduced by all-trans retinoic acid", Journal of Neuroimmunology, Vol. 229/1–2, Elsevier B.V., https://doi.org/10.1016/j.jneuroim.2010.08.005.

Vezzani, A. and B. Viviani. (2015), "Neuromodulatory properties of inflammatory cytokines and their impact on neuronal excitability", Neuropharmacology, Elsevier B.V., https://doi.org/10.1016/j.neuropharm.2014.10.027.

Wang, Q. et al. (2020), "Radioprotective effect of flavonoids on ionizing radiation-induced brain damage", Molecules, MDPI AG, Basel, https://doi.org/10.3390/molecules25235719.

Welser-Alves, J. V. and R. Milner. (2013), "Microglia are the major source of TNF-α and TGF-β1 in postnatal glial cultures; Regulation by cytokines, lipopolysaccharide, and vitronectin", Neurochemistry International, Vol. 63/1, Elsevier B.V., https://doi.org/10.1016/j.neuint.2013.04.007.

Wu, Q. et al. (2017), "Macrophage biology plays a central role during ionizing radiation-elicited tumor response", Biomedical Journal, Vol. 40/4, Elsevier, https://doi.org/10.1016/j.bj.2017.06.003

Zhou, K. et al. (2017), "Radiation induces progenitor cell death, microglia activation, and blood-brain barrier damage in the juvenile rat cerebellum", Scientific Reports, Vol. 7, Springer Nature, London, https://doi.org/10.1038/srep46181.

Relationship: 2835: Increase, Pro-Inflammatory Mediators leads to Increase, Neural Remodeling

AOPs Referencing Relationship

AOP Name	Adjacency	Weight of Evidence	Quantitative Understanding
Deposition of Energy Leading to Learning and Memory Impairment	adjacent	Moderate	Low

Evidence Supporting Applicability of this Relationship

Taxonomic Applicability

Term	Scientific Term	Evidence	Links
mouse	Mus musculus	Moderate	NCBI
rat	Rattus norvegicus	Moderate	NCBI

Life Stage Applicability

Life Stage	Evidence
Adult	Moderate
Not Otherwise Specified	Low
Juvenile	Low

Sex Applicability

Sex	Evidence
Male	Moderate
Female	Low
Mixed	Moderate
Unspecific	Low

Evidence for this relationship comes from rat and mouse models. There is in vivo evidence in both male and female animals, with more evidence in males. Animal age is occasionally not indicated in studies, but most evidence is in adult rodent models.

Key Event Relationship Description

Inflammatory mediators such as IL-1β, TNF-α, and IL-6 can affect the normal behavior of neuronal cells through alterations in: (a) the neuronal architecture and (b) synaptic activity. Overexpression of these pro-inflammatory mediators can disrupt the integrity of neurons through increased necrosis and demyelination, decreased neurogenesis, neural stem cell proliferation and synaptic complexity (Cekanaviciute et al., 2018; Fan & Pang, 2017). Structurally, the neuron is comprised of the cell body, dendrites, axon, and axon terminals, all of which are critical in the normal functioning of the central nervous system. Another important component of the neuron is its signaling properties, which uses chemical neurotransmitters to transfer messages in the synaptic cleft (Cekanaviciute et al., 2018; Hladik & Tapio, 2016). Disruption to these structures or signalling properties results in neural remodeling.

Under physiological conditions, cytokine levels are low, but these can increase in response to various insults. Cytokines mediate immune response through ligand binding to cell surface receptors, which activate signaling cascades such as the JAK-STAT or MAPK pathways to produce or recruit more cytokines. Once organs initiate inflammatory reactions, the cytokines are capable of impairing neuronal function through direct effects on neurons or by indirect mechanisms mediated by microglia, astrocytes or vascular endothelial cells (Mousa & Bakhiet, 2013; Prieto & Cotman, 2018).

Evidence Supporting this KER

Overall Weight of Evidence: Moderate

Biological Plausibility

Various studies provide support for the biological plausibility of the link between an increase in pro-inflammatory mediators and neural remodeling. It is known that cytokines and their receptors are constitutively expressed by neurons in the central nervous system, and even in normal or pathological states, these cytokines act on neurons (Kishimoto et al., 1994). One important factor in the pathogenesis of neurotoxicity is the overexpression of pro-inflammatory mediators, or Th1-type, cytokines. These cytokines bind to their receptors to induce a conformational change, which triggers the activation of intracellular signaling pathways that alter cell structure and function (Mousa and Bakhiet, 2013). Several sources have reported a change in physical and electrophysiological properties of neurons in either whole-brain samples, specific brain regions such as the hippocampus or dentate gyrus, or neuronal

cell cultures in response to increased expression of cytokines (Jenrow et al., 2013; Fan and Pang, 2017; Wong et al., 2004). The main cytokines presenting detrimental effects are IL-1β, TNF-α, and IL-6, which can cause alterations in neuronal architecture such as morphological changes in dendrites and synapses (Tang et al., 2017; Cekanaviciute et al., 2018; Shi et al., 2017). Many studies have also reported decreased proliferation and differentiation in progenitor cells, inhibited neural stem cell differentiation and decreased neurogenesis following increases in cytokines (Zonis et al., 2015; Wong et al., 2004; Tang et al., 2017). IL-6 can affect neurogenesis through various distinct mechanisms. One mechanism is through the stimulation of hypothalamic-pituitary-adrenal axis, which then increases circulating glucocorticoids. These steroids can then inhibit cell proliferation and neurogenesis in the dentate gyrus (Turnbull and Rivier, 1999; Gould et al., 1992; Cameron and Gould, 1994). Decreased neurogenesis in the hippocampus is also well documented as a result of pro-inflammatory mediators, and one possible mechanism for this detrimental effect is through the interaction of IL-1β and orphan nuclear receptor, TLX. This receptor is required to maintain the neural precursor cell pool in neurogenic brain regions, and it has been shown that IL-1β can reduce the expression of TLX and consequently cell proliferation (Ryan et al., 2013). TNF-α affects neuronal fate by interacting with its receptor, TNFR1, which is expressed on neural stem cells. It has been reported that TNFR1-mediated signaling pathway inhibits growth therefore, a reduction in neuron production after TNF-α injection (Chen and Palmer, 2013). A clear mechanistic relationship has not yet been established, although it is accepted that pro-inflammatory mediators can alter the structure and function of neurons.

Empirical Evidence

The empirical evidence collected for this KER comes from both in vitro and in vivo studies. Neural remodeling can be defined by changes to the physical, functional and/or electrophysiological properties of neurons. Most of the evidence examines effects of inflammation induced by either dextran sodium sulfate (DSS) treatment, seizure induction, heavy ion or X-ray irradiation at higher doses (>5 Gy) and varying dose-rates from 78.0 cGy/min to 3.2 Gy/min, or lipopolysaccharide injection on both in vivo and in vitro rodent models. Injections or treatments with pro-inflammatory cytokines were also used. These studies provide evidence to support a causal association between an increase in pro-inflammatory mediators and decreased neurogenesis, but also provide evidence of reduced neuronal signaling, neural stem cell and progenitor cell proliferation, as well as a change in overall neuronal shape (Zonis et al., 2015; Vallieres et al., 2002; Green et al., 2012; Wu et al., 2012; Chen and Palmer, 2013; Saraiva et al., 2019; Zhang et al., 2017; Dong et al., 2015; Kalm et al., 2013; Wong et al., 2004; Jenrow et al., 2013; Liu et al, 2010).

Time Concordance

Multiple studies suggest time-concordant relationship between increases in pro-inflammatory mediators leading to neural remodeling. The proliferation and survival of stem and progenitor cells, collectively known as neural precursor cells, was decreased or inhibited in response to increase pro-inflammatory cytokines at 4 days, 7 days and 1-month post-treatment (Zonis et al., 2015; Wong et al., 2004, Green et al., 2012; Ryan et al., 2013; Vallieres et al., 2002). Various studies also report a reduction in neurogenesis in the hippocampus and dentate gyrus 1-month post-treatment that was well-correlated with increased IL-1β, TNF-α, and IL-6 levels (Zonis et al., 2015; Vallieres et al., 2002; Wu et al., 2012; Chen and Palmer, 2013). In addition to a significant decrease in neurogenesis 1-month post-treatment, a study found that sustained IL-1β expression caused a significant reduction in neurogenesis that persisted for 3 months (Wu et al., 2012). Another study observed that X ray-induced increases in IL-1β and TNF-α at three and six hours resulted in a time-dependent decrease in DCX+ cells, a marker for neurogenesis, which persisted for 2 weeks. This was seen after a single dose of 10 Gy (Dong et al., 2015). Thus, these studies provide evidence to support time concordance of the relationship using both in vivo and in vitro models.

Dose Concordance

No available data.

Incidence Concordance

No available data.

Essentiality

Several treatments that directly alter pro-inflammatory mediators preserve neuronal integrity in the dentate gyrus and positively modulate hippocampal neurogenesis. The treatments included MW-151, a selective inhibitor of pro-inflammatory cytokine production and kukoamine A, an alkaloid that inhibits neuronal oxidative stress and hippocampal apoptosis (Jenrow et al., 2013; Zhang et al., 2017). Another treatment used was histamine, which has been shown to ameliorate the loss of neuronal complexity and synaptic plasticity (Saraiva et al., 2019). Multiple studies use cytokine receptor antagonists or knock-out key receptors to block the effects of IL-1β, TNF-α, and CCL2, which have preserves neuron survival (Green et al., 2012; Ryan et al., 2013; Wu et al., 2012; Chen and Palmer, 2013). Another knockout model of complement component 3 (C3) have also been used to demonstrate essentiality. C3 is a central molecule in the complement cascade, and its roles include microglia-mediated synapse elimination. C3 knockout models have been shown to cause reduced pro-inflammatory cytokines, increased synaptic number, reduced neuron loss and synaptic morphology impairment (Shi et al., 2017).

Uncertainties and Inconsistencies

- Various in vitro studies have reported a stimulation of neural precursor cell proliferation and differentiation or increased neurogenesis by different cytokines such as IL-6 and IFN-γ (Islam et al., 2009; Wong et al., 2004). Another study found increased proliferation within the hippocampus after repeated IL-6 and IL-1β infusion (Seguin et al., 2009). Although a clear mechanism has not yet been elucidated, it is thought that these cytokines have contradictory effects from the differential activation of various signaling cascades (Borsini et al., 2015). For example, hyper-IL-6, a fusion of IL-6 and IL-6 receptor, was found to increase neurogenesis through the activation of MAPK/CREB (mitogen-activated protein kinase/cAMP response

element binding protein) cascade (Islam et al., 2009).

- Kalm et al. (2013) found a higher inflammatory response in lipopolysaccharide (LPS) treated females compared with males after irradiation. Specifically, increased levels of pro-inflammatory cytokines IL-1β, IL-12, and IL-17, as well as pro-inflammatory chemokines CCL4, CCL3 and CCL2 were detected relative to vehicle-treated animals and LPS-treated males. This was associated with a 32% decrease in DCX+ cells, a marker for neurogenesis, in females. However, in LPS-treated males, a 64% reduction in DCX+ cells compared to vehicle-treated males following irradiation was reported (Kalm et al., 2013). Further research is required to elucidate the exact effects of increased pro-inflammatory mediators on neuronal integrity between males and females.

Quantitative Understanding of the Linkage

The table below provides some representative examples of quantitative linkages between the two key events as presented in the paper. It was difficult to identify a general trend across all the studies due to differences in experimental design and reporting of the data. All data is statistically significant unless otherwise stated.

Time Concordance

Reference	Experiment Description	Results
Zonis et al., 2015	In vitro. Adult female C57Bl/6 mice were treated with 3% wt/vol dextran sodium sulfate (DSS) using a multiple-cycle administration for up to 26 days. ELISA and qRT-PCR were used to measure cytokine levels in neural precursor cells and neural progenitor cell cultures. Western blot and immunostaining were used to measure Ki67 (neuronal cell proliferation marker), DCX (marker for neurogenesis), BLBP (marker for stem/early progenitor cells) and nestin (neural stem cell marker and involved in radial growth of axons). p21 (regulator of cell cycle progression at G1 and S phase) was also measured using these methods.	Neural precursor cells (NPCs) treated with 50 ng/mL of IL-6 led to a decline in the % of neuroblasts, with declines from 41% ± 6.4% in untreated cells to 22.39% ± 5.2% in IL-6-treated cells). Thus, decreasing neurogenesis was observed in in NPCs after DSS treatment. Chronic intestinal inflammation (29 days post-treatment) reduced hippocampal neurogenesis. Evidence has highlighted that IL-1β and TNF-α mRNA levels were increased more than 2-fold, as well as a fourfold increase in p21 mRNA levels, which were accompanied by an approximate 2-fold down-regulation of progenitor cell proliferation and neurogenesis. Protein levels of IL-1β and TNF-α were not assessed.
Jenrow et al., 2013	In vivo. Adult male Fischer 344 rats were exposed to 10 Gy of whole-brain irradiation (WBI) using a 137Cs irradiator at a dose rate of 3.2 Gy/min. Rats also underwent mitigating therapy with MW01-2-151SRM (MW-151), a selective inhibitor of β amyloid-induced glial pro-inflammatory cytokine production that was initiated 24 h post-WBI and was continued for 28 days post-WBI by daily injection. Immunofluorescence assays for cell proliferation and neurogenesis were performed at 2 months and for neuroinflammation at 2 and 9 months post-WBI.	MW-151 mitigated radiation-induced neuroinflammation, measured by OX-6+ cell densities, an indicator of pro-inflammatory level of activation, at 2- and 9-months post-irradiation. The 10 Gy group had mean OX-6+ cell densities of 1,966 (±218) and 1,493 (±270) cells/mm3, respectively. In the 10 Gy MW-151 group, the mean OX-6+ cell densities were significantly reduced to 849 (±350) and 437 (±119) cells/mm3, respectively. In addition to this, 2 months post-irradiation, the mean DCX+ cell density, a marker for neurogenesis, was 1,375 (±535) cells/mm3 in the 10 Gy group, but was significantly increased to 4,702 (±622) cells/mm3 after MW-151 therapy.
Vallieres et al., 2002	In vitro. Seizure was induced in transgenic mice expressing IL-6 under control of the glial fibrillary acidic protein (GFAP) promoter. Bromodeoxyuridine (BrdU) assay and immunofluorescence was used to detect proliferating neural progenitor cells and fluoro-jade staining was used to detect degenerating neurons.	IL-6 compromised proliferation, survival, and differentiation of hippocampal progenitor cells when expressed over the long term (31 days) in young adult transgenic mice expressing the IL-6 transgene, causing a 63% decrease in the production rate of new neurons. The BrdU assay revealed a 27% reduction in progenitor cell proliferation, 53% reduction in progenitor cell survival in the dorsal hippocampus.
Wong et al., 2004	In vitro. Neural stem cell lines derived from adult C57BL/6 mice were allowed to proliferate and differentiate for 1 h to 3 days in the presence of IFN-γ and TNF-α. Proliferation and cytotoxicity assays were used to assess neural stem cell survival and their ability to differentiate and proliferate.	IFN-γ (100 U/mL) and TNF-α (10 ng/mL) inhibited neural stem cell proliferation. The reduction was first significant at 4 days when control cells began to proliferate rapidly, and until day 6, control cells continued to proliferate while IFN-γ and TNF-α inhibited proliferation.
Green et al., 2012	In vitro. Rat hippocampal NPC cultures were treated with IL-1β (10 ng/mL) in the presence or absence of IL-1 receptor antagonist (IL-1RA), which prevents the interaction of IL-1β with IL-1R1. Cell proliferation analysis was performed, and RT-PCR and immunoblotting was used to measure DCX and cytokines. MTT assay was used to assess cell viability.	Treatment with 10 ng/mL of IL-1β significantly decreased neurosphere circumference in a time-dependent manner. Compared to untreated cultures, a difference was seen at day 4, which continued until day 7. Neural integrity was assessed by examining the neural cell viability and proliferation IL-1β treatment for 24 hours after 4 days in vitro significantly decreased cell proliferation. IL-1β treatment for 7 days in vitro caused a significant decrease in cell viability compared to untreated cultures.
Wu et al.	In vitro. Wild-type and IL-1βXAT C57BL/6 mice were exposed to Cre recombinase to induce IL-1β	There was a significant effect of sustained IL-1β overexpression on adult neurogenesis one month after

Wu et al., 2012	overexpression. Immunohistochemistry was used to measure IL-1β and DCX, a marker for migrating neuroblasts and neurogenesis.	injection. A 94% decrease in migrating neuroblasts and neurogenesis was found, mirroring the pattern of neuroinflammation. 3 months post-injection, there was also an 87% reduction in neurogenesis.
Chen and Palmer, 2013	In vitro. Microglial cultures isolated from neonatal pups of C57BL/6 mice were treated with 1 µg/mL LPS, then incubated in neural stem cell (NSC) differentiation medium. The conditioned medium was then collected and applied to NSCs. Immunohistochemistry was used to measure cytokine levels and DCX, a marker for neurogenesis.	After 72 h, neurogenesis significantly reduced in the differentiation culture after TNF-α injection of 20 ng/mL. One month after injection, proliferation and survival of endogenous neural stem cells decreased, as well as a reduction in neurogenesis.
Saraiva et al., 2019	In vitro. C57BL/6J male mice were injected with 1 or 2 mg/kg LPS. Histamine was also injected in the hippocampal dentate gyrus. The BrdU assay was used to quantify proliferating cells, while immunohistochemical analysis and western blot was used to measure IL-1β and DCX.	In mice exposed to LPS, histamine significantly increased the total amount of proliferative cells. Mice exposed to 1 mg/kg of LPS had 98.8 ± 4.7 BrdU+ cells, a marker for proliferating cells, whereas 1 mg/kg of LPS + His had 197.6 ± 28.2 BrdU+ cells. 2 mg/kg of LPS yielded 96.7 ± 9.7 BrdU+ cells and 2 mg/kg of LPS + Histamine had 154.1 ± 23.8 BrdU+ cells. Histamine was also able to revert the LPS-induced loss of neuronal volume from 238.6 ± 19.7 (1 mg/kg LPS) to 331.1 ± 33.4 (1 mg/kg LPS + His) µm3. And 248.7 ± 18.8 (2 mg/kg LPS) to 334.3 ± 24.8 (2 mg/kg LPS + His) µm3. Postsynaptic density protein 95 (PSD-95) levels were also elevated due to histamine treatment (2 mg/kg LPS, 55.8 ± 9.9; 2 mg/kg LPS + His, 110.1 ± 12.9).
Ryan et al., 2013	In vitro. Adult Sprague Dawley rat dentate gyrus NPC cultures were prepared and treated with IL-1β (100 ng/mL) for 7 days. Immunohistochemistry was used to detect NPCs, proliferating cells and newly born cells.	24 h after IL-1β treatment (100 ng/mL), there was no difference in proliferating neural cells relative to untreated cells. However, at 7 days post-treatment, there was a significant reduction in proliferating neural cells. There was also a decrease in neurogenesis.
Dong et al., 2015	In vitro. The mouse microglial cell line, BV-2, were irradiated with a single 16 Gy dose of X-rays, then assessed at various time points up to 6 weeks. ELISA was used to measure levels of IL-1β and TNFα, whereas immunohistochemical staining was used to detect DCX+ cells.	DCX+ cells, a marker of neurogenesis, were significantly reduced at 6 h until 2 weeks post-irradiation, which was accompanied by increased levels of IL-1β and TNF-α. TNF-α levels peaked at 3 h post-irradiation, decreased at 6 h, then increased in a time-dependent manner until 2 weeks. IL-1β levels increased in a time-dependent manner until peaking at 72 h, then spiked again at 6 weeks.

Known modulating factors

Modulating Factor	Details	Effects on the KER	References
Drug Therapy	MW01-2-151SRM (MW-151) – water soluble, nontoxic, bioavailable compound that mitigates pro-inflammatory cytokine production, glial activation and inflammation in rat hippocampus.	MW-151 reduced the neuroinflammation caused by 10 Gy of heavy ion exposure, thus preserving the integrity of neurogenic signaling in the dentate gyrus.	Jenrow et al., 2013
Genetic Manipulation	IL-1 receptor antagonist to prevent the interaction between IL-1β with IL-1R1.	After 7 days in vitro, IL-1β significantly decreased the percentage of DCX-positive neurons, but pre-treatment and subsequent co-treatment with IL-1RA abolished this anti-neurogenic effect of IL-1β.	Green et al., 2012
Hormone	Histamine – an endogenous amine that can regulate both brain inflammation and neurogenesis.	Histamine treatment significantly increased the total number cells, positively modulates hippocampal neurogenesis, ameliorates the loss of neuronal complexity of hippocampal neuroblasts and reverts synaptic plasticity loss caused by LPS.	Saraiva et al., 2019
Drug	Tamoxifen – synthetic, non-steroidal estrogen receptor modulator with anti-inflammatory and neuroprotective properties.	Tamoxifen decreased the production of inflammatory cytokines released from irradiated microglia, attenuating glial activation and decreasing neuronal apoptosis.	Liu et al., 2010
Drug	Kukoamine A (KuA) – alkaloid extracted from traditional Chinese herb cortex lycii radicis that has been previously reported to have antioxidant properties.	KuA inhibited radiation-induced increases in pro-inflammatory cytokines, alleviated the activation of hippocampal microglia and ameliorated the suppression of hippocampal neurogenesis.	Zhang et al., 2017
Genetics	Polymorphism that increases the expression of APOE4 increases the risk of developing Alzheimer's diseases, which generally consists of a decline in memory, thinking and language.	In homozygous human APOE4 knock-in mice, a dramatic increase in pro-inflammatory cytokines TNF-α, IL-1β and IL-6 was seen after LPS injection compared to the APOE2 and APOE3 alleles, suggesting that APOE4 is implicated in a greater inflammatory response.	Hunsberger et al., 2019; Zhu et al., 2012

Known Feedforward/Feedback loops influencing this KER

NA

References

Borsini, A. et al. (2015), "The role of inflammatory cytokines as key modulators of neurogenesis", Trends in Neurosciences, Vol. 38/3, Elsevier, Amsterdam, https://doi.org/10.1016/j.tins.2014.12.006.

Cameron, H. A. and E. Gould. (1994), "Adult neurogenesis is regulated by adrenal steroids in the dentate gyrus", Neuroscience, Vol. 61/2, Elsevier, Amsterdam, https://doi.org/10.1016/0306-4522(94)90224-0.

Cekanaviciute, E., S. Rosi and S. V. Costes. (2018), "Central nervous system responses to simulated galactic cosmic rays", International Journal of Molecular Sciences, Vol. 19/11, Multi-Disciplinary Digital Publishing Institute, Basel, https://doi.org/10.3390/ijms19113669.

Chen, Z. and T. D. Palmer. (2013), "Differential roles of TNFR1 and TNFR2 signaling in adult hippocampal neurogenesis", Brain, Behavior, and Immunity, Vol. 30, Elsevier Inc., Amsterdam, https://doi.org/10.1016/j.bbi.2013.01.083.

Dong, X. et al. (2015), "Relationship between irradiation-induced neuro-inflammatory environments and impaired cognitive function in the developing brain of mice", International Journal of Radiation Biology, Vol. 91/3, Taylor & Francis Group, London, https://doi.org/10.3109/09553002.2014.988895.

Fan, L. W. and Y. Pang. (2017), "Dysregulation of neurogenesis by neuroinflammation: Key differences in neurodevelopmental and neurological disorders", Neural Regeneration Research, Vol. 12/3, Wolters Kluwer, Alphen aan den Rijn, https://doi.org/10.4103/1673-5374.202926.

Gould, E. et al. (1992), "Adrenal hormones suppress cell division in the adult rat dentate gyrus", The Journal of Neuroscience, Vol. 12/9, Society for Neuroscience, Washington, https://doi.org/10.1523/JNEUROSCI.12-09-03642.1992.

Green, H. F. et al. (2012), "A role for interleukin-1β in determining the lineage fate of embryonic rat hippocampal neural precursor cells", Molecular and Cellular Neuroscience, Vol. 49/3, Elsevier Inc., Amsterdam, https://doi.org/10.1016/j.mcn.2012.01.001.

Hladik, D. and S. Tapio. (2016), "Effects of ionizing radiation on the mammalian brain", Mutation Research - Reviews in Mutation Research, Vol. 770, Elsevier B.V., Amsterdam, https://doi.org/10.1016/j.mrrev.2016.08.003.

Hunsberger, H. C. et al. (2019), "The role of APOE4 in Alzheimer's disease: strategies for future therapeutic interventions", Neuronal Signaling, Vol. 3/2, Portland Press, London, https://doi.org/10.1042/NS20180203.

Islam, O. et al. (2009), "Interleukin-6 and Neural Stem Cells: More Than Gliogenesis", (C.-H. Heldin, Ed.)Molecular Biology of the Cell, Vol. 20/1, The American Society for Cell Biology, Rockville, https://doi.org/10.1091/mbc.e08-05-0463.

Jenrow, K. A. et al. (2013), "Selective Inhibition of Microglia-Mediated Neuroinflammation Mitigates Radiation-Induced Cognitive Impairment", Radiation Research, Vol. 179/5, Bio One, Washington, https://doi.org/10.1667/RR3026.1.

Kalm, M., K. Roughton and K. Blomgren. (2013), "Lipopolysaccharide sensitized male and female juvenile brains to ionizing radiation", Cell Death & Disease, Vol. 4/12, https://doi.org/10.1038/cddis.2013.482.

Kishimoto, T., T. Taga and S. Akira. (1994), "Cytokine signal transduction", Cell, Vol. 76/2, Elsevier, Amsterdam, https://doi.org/10.1016/0092-8674(94)90333-6.

Liu, J.-L. et al. (2010), "Tamoxifen alleviates irradiation-induced brain injury by attenuating microglial inflammatory response in vitro and in vivo", Brain Research, Vol. 1316, Elsevier, Amsterdam, https://doi.org/10.1016/j.brainres.2009.12.055.

Mousa, A. and M. Bakhiet. (2013), "Role of Cytokine Signaling during Nervous System Development", International Journal of Molecular Sciences, Vol. 14/7, Multi-Disciplinary Digital Publishing Institute, Basel, https://doi.org/10.3390/ijms140713931.

Prieto, G. A. and C. W. Cotman. (2017), "Cytokines and cytokine networks target neurons to modulate long-term potentiation", Cytokine & Growth Factor Reviews, Vol. 34, Elsevier, Amsterdam, https://doi.org/10.1016/j.cytogfr.2017.03.005.

Ryan, S. M. et al. (2013), "Negative regulation of TLX by IL-1β correlates with an inhibition of adult hippocampal neural precursor cell proliferation", Brain, Behavior, and Immunity, Vol. 33, Elsevier, Amsterdam, https://doi.org/10.1016/j.bbi.2013.03.005.

Saraiva, C. et al. (2019), "Histamine modulates hippocampal inflammation and neurogenesis in adult mice", Scientific Reports, Vol. 9/1, Springer Nature, Berlin, https://doi.org/10.1038/s41598-019-44816-w.

Seguin, J. A. et al. (2009), "Proinflammatory cytokines differentially influence adult hippocampal cell proliferation depending upon the route and chronicity of administration.", Neuropsychiatric disease and treatment, Vol. 5, Dove Press Ltd., Macclesfield, http://www.ncbi.nlm.nih.gov/pubmed/19557094.

Shi, Q. et al. (2017), "Complement C3 deficiency protects against neurodegeneration in aged plaque-rich APP/PS1 mice", Science Translational Medicine, Vol. 9/392, American Association for the Advancement of Science, Washington,

https://doi.org/10.1126/scitranslmed.aaf6295.

Tang, F. R., W. K. Loke and B. C. Khoo. (2017), "Postnatal irradiation-induced hippocampal neuropathology, cognitive impairment and aging", Brain and Development, Vol. 39/4, Elsevier, Amsterdam, https://doi.org/10.1016/j.braindev.2016.11.001.

Turnbull, A. V. and C. L. Rivier. (1999), "Regulation of the Hypothalamic-Pituitary-Adrenal Axis by Cytokines: Actions and Mechanisms of Action", Physiological Reviews, Vol. 79/1, American Physiology Society, Rockville, https://doi.org/10.1152/physrev.1999.79.1.1.

Valliéres, L. et al. (2002), "Reduced hippocampal neurogenesis in adult transgenic mice with chronic astrocytic production of interleukin-6", Journal of Neuroscience, Vol. 22/2, Society for Neuroscience, Washington, https://doi.org/10.1523/jneurosci.22-02-00486.2002.

Wong, G., Y. Goldshmit and A. M. Turnley. (2004), "Interferon-γ but not TNFα promotes neuronal differentiation and neurite outgrowth of murine adult neural stem cells", Experimental Neurology, Vol. 187/1, Elsevier, Amsterdam, https://doi.org/10.1016/j.expneurol.2004.01.009.

Wu, M. D. et al. (2012), "Adult murine hippocampal neurogenesis is inhibited by sustained IL-1β and not rescued by voluntary running", Brain, Behavior, and Immunity, Vol. 26/2, Elsevier Inc., Amsterdam, https://doi.org/10.1016/j.bbi.2011.09.012.

Zhang, Y. et al. (2017), "Kukoamine A Prevents Radiation-Induced Neuroinflammation and Preserves Hippocampal Neurogenesis in Rats by Inhibiting Activation of NF-κB and AP-1", Neurotoxicity Research, Vol. 31/2, Springer Nature, Berlin, https://doi.org/10.1007/s12640-016-9679-4.

Zhu, Y. et al. (2012), "APOE genotype alters glial activation and loss of synaptic markers in mice", Glia, Vol. 60/4, John Wiley & Sons, Inc., Hoboken, https://doi.org/10.1002/glia.22289.

Zonis, S. et al. (2015), "Chronic intestinal inflammation alters hippocampal neurogenesis", Journal of Neuroinflammation, Vol. 12/1, Springer Nature, Berlin, https://doi.org/10.1186/s12974-015-0281-0.

Relationship: 2836: Increase, Neural Remodeling leads to Impairment, Learning and memory

AOPs Referencing Relationship

AOP Name	Adjacency	Weight of Evidence	Quantitative Understanding
Deposition of Energy Leading to Learning and Memory Impairment	adjacent	Moderate	Low

Evidence Supporting Applicability of this Relationship

Taxonomic Applicability

Term	Scientific Term	Evidence	Links
mouse	Mus musculus	Moderate	NCBI
rat	Rattus norvegicus	Moderate	NCBI

Life Stage Applicability

Life Stage	Evidence
Adult	Moderate
Not Otherwise Specified	Low
Juvenile	Low

Sex Applicability

Sex	Evidence
Male	Moderate
Female	Low

Evidence for this relationship comes from rat and mouse models. There is in vivo evidence in both male and female animals, with more evidence in males. Animal age is occasionally not indicated in studies, but most evidence is in adult rodent models.

Key Event Relationship Description

Neural stem cells (NSCs) come from different sources, such as the subgranular zone (SGZ) located in the dentate gyrus (DG) of the hippocampal formation, and the subventricular zone (SVZ) region of the brain. NSCs give rise to mature neurons that are then able to receive signals from other neurons (Bálentová & Adamkov, 2020; Hladik & Tapio, 2016; Monje & Palmer, 2003; Romanella et al., 2020; Tomé et al., 2015). Changes in neuronal architecture can lead to altered synaptic activity, necrosis, demyelination, neurogenesis, neurodegeneration, and dendrite morphology, all of which encompass neural remodeling (Hladik & Tapio, 2016; Monje & Palmer, 2003; Tomé et al., 2015). These alterations can then cause cognitive deficits in the form of impaired learning and memory (Barker & Warburton, 2011; Hladik & Tapio, 2016; Monje & Palmer, 2003; Tomé et al., 2015). Impaired learning consists reduced ability to create new associative or non-associative relationships, whereas impaired memory consists of decreased ability to establish sensory, short-term or long-term memories (Desai et al., 2022; Kiffer et al., 2019). Multiple brain areas are involved these processes, such as the hippocampal region, amygdala, prefrontal cortex, basal ganglia, and other areas of the neocortex (Cucinotta et al., 2014; Desai et al., 2022; NCRP Commentary, 2016).

Evidence Supporting this KER

Overall Weight of Evidence: Moderate

Biological Plausibility

Several reviews provide support for the biological plausibility of the link between neural remodeling and impaired learning and memory. It is generally accepted that neural remodeling can disrupt learning and memory through changes to neurogenesis, neurodegeneration, neuronal excitability and synaptic plasticity, demyelination and dendritic spine density (Hladik & Tapio, 2016; Bálentová & Adamkov, 2020; Tomé et al., 2015; Monje & Palmer, 2003; Romanella et al., 2020).

Neurogenesis in the DG creates new neurons in the hippocampus that can make connections to Cornu Ammonis (CA) neurons involved in learning and memory (Monje & Palmer, 2003; Tomé et al., 2015). Accordingly, learning and memory can be impaired through reduced neurogenesis in the neurogenic SGZ of the DG (Bálentová & Adamkov, 2020; Monje & Palmer, 2003). Many studies also associate decreased neurogenesis to impaired hippocampal-dependent cognitive function, indicating that it is a common mechanism for the relationship (Tomé et al., 2015). Similarly, apoptosis and neurodegeneration impair cognitive function (Bálentová & Adamkov, 2020; Hladik & Tapio, 2016). In the hippocampus, the degree of atrophy corresponds to the degree of impaired learning and memory (Tomé et al., 2015).

Synaptic strength and neuronal excitability are important components of learning and memory. Decreased hippocampal excitability and disrupted long-term potentiation (LTP), a form of long-term synaptic plasticity, are associated with reduced learning and memory (Romanella et al., 2020). Changes in the expression of synaptic receptors and other synaptic proteins may also result in impaired learning and memory (Hladik & Tapio, 2016).

Demyelination correlates with decreased long-term memory formation (Tomé et al., 2015) and along with white matter necrosis, these lead to impaired learning and memory (Bálentová & Adamkov, 2020). Although demyelination is a factor in learning and memory, sub-threshold demyelination may still cause impaired learning and memory (Monje & Palmer, 2003).

Reduced dendritic complexity and spine density are also associated with impaired learning and memory (Bálentová & Adamkov, 2020; Hladik & Tapio, 2016; Romanella et al., 2020). The complexity of signal processing in the hippocampus can be reduced by a loss in dendritic spines, which results in impaired learning and memory (Romanella et al., 2020). In addition, various studies show reduced dendritic branching, length and area in hippocampal neurons associated with learning and memory (Hladik & Tapio, 2016).

Empirical Evidence

The empirical evidence surrounding this KER stems from research using in vivo models. When compared to the control, irradiated subjects demonstrated significant changes in neuronal integrity and cognitive deficits (Achanta, Fuss & Martinez, 2009; Acharya et al., 2019; Akiyama et al., 2001; Hodges et al., 1998; Howe et al., 2019; Krukowski et al., 2018; Madsen et al., 2003; Miry et al., 2021; Parihar et al., 2015, 2016; Raber et al., 2004; Rola et al., 2004; Simmons et al., 2019; Sorokina et al., 2021; Whoolery et al., 2017; Winocur et al., 2006).

Dose Concordance

There is strong evidence suggesting dose-concordance between neural remodeling and impaired learning and memory. Dose-dependent changes in dendritic complexity are correlated with behavioral deficits at doses from 0.05 to 30 Gy (Bálentová & Adamkov, 2020; Howe et al., 2019; Parihar et al., 2015, 2016; Simmons et al., 2019; Whoolery et al., 2017). Mice exposed to 0.05 and 0.3 Gy of 48Ti showed dose-dependent decreases in total dendritic length and number of dendritic branch points. When subjected to cognitive testing, mice exposed to 0.3 Gy demonstrated greater impairment in the novel object recognition (NOR) and object in place (OiP) tests compared to 0.05 Gy exposed mice (Parihar et al., 2016). These results for OiP were correlated positively to the number of dendritic spines and negatively to the number of postsynaptic density protein 95, also a marker for neural remodeling. Similarly, another study identified a correlation between the total number of dendritic spines and the performance of mice in the OiP task (Parihar et al., 2015). This study also demonstrated dose-dependent decreases in the total number of spines, total dendritic length, number of branch points, number of dendritic branches, and DI in both the NOR and OiP tasks when exposed to 0.05 and 0.3 Gy of 16O and 48Ti.

Changes in the levels of neurogenesis also exhibit dose-concordance with cognitive deficits. Whoolery et al. (2017) identified a 0.8- and 0.4-fold decrease in the number of Ki-67+ cells in male mice exposed to 0.2 and 1 Gy of 28Si particles, respectively. The mice

also demonstrated a decrease in percentage freezing by 0.4-fold in contextual FC, indicative of impaired learning and memory, when exposed to 0.2 Gy, although no significant changes in learning and memory were seen at 1 Gy. Another study identified dose-dependent decreases in the numbers of Ki67+ and BrdU+ cells in three age groups (postnatal day (PD) 21, PD 50, and PD 70) in rats exposed to 0.3, 3, and 10 Gy of ionizing radiation (Achanta, Fuss & Martinez, 2009). In PD 21 rats, dose-dependent decreases in freezing response were observed at doses of 0.3 and 10 Gy during the trace fear conditioning/testing. These results show that higher doses of irradiation lead to greater alterations in neuronal integrity, correlated with greater cognitive impairments. Many other studies showed decreased neurogenesis or increased neurodegeneration and impaired learning and memory at doses from 0.3 to 25 Gy, with stressors like X-rays, gamma rays, carbon ions and iron ions (Achanta, Fuss & Martinez, 2009; Akiyama et al., 2001; Hodges et al., 1998; Madsen et al., 2003; Miry et al., 2021; Raber et al., 2004; Rola et al., 2004; Sorokina et al., 2021; Winocur et al., 2006).

Neuron excitation has also been measured to assess neuron integrity. After 0.18 Gy of 252Cf neutron, with an activity of 1.6 GBq, excitatory signaling in CA1 neurons of mice was reduced and both NOR and OiP showed decreased learning and memory (Acharya et al., 2019).

Synaptic composition in hippocampal neurons was assessed as well to determine neuron integrity. GluR1, involved in hippocampal-dependent working memory, and recognition memory were both reduced after 0.5 Gy of simulated galactic cosmic radiation (GCR) (Krukowski et al., 2018).

Time Concordance

Evidence supporting time concordance between neural remodeling and impaired learning and memory come from several studies. Whoolery et al. (2017) found that the number of Ki-67+ cells decreased 24 hours after 0.2 Gy of 28Si radiation of mice, while contextual FC 3 months after radiation showed impaired memory. Similarly, after 10 Gy X-rays, cell proliferation and the number of immature neurons decreased by 95% in mice after 3 months, and a Barnes maze showed impaired hippocampal-dependent spatial learning and memory measured after proliferation at 3 months as well (Raber et al., 2004). After mice were irradiated with 16O and 48Ti particles at 0.05 and 0.30 Gy, dendritic complexity and spine density were reduced and synaptic spine puncta were increased 15 weeks post-irradiation while learning and memory was impaired 15 and 24 weeks post-irradiation (Parihar et al., 2016). Neurogenesis was reduced immediately after 3 Gy 300 kVp X-ray radiation in rats and remained low 2 and 6 weeks later, and memory was impaired 1, 3 and non-significantly at 7 weeks post-irradiation (Madsen et al., 2003). Rats irradiated with gamma rays showed decreased neurogenesis and impaired performance during FC both 4 weeks post-irradiation (Winocur et al., 2006). In a longer-term study, neurogenesis was impaired 1 and 3 months after 5 Gy X-ray radiation in mice, while the Morris Water Maze (MWM) demonstrated impaired learning and memory also at 3 months (Rola et al., 2004). This trend continued after 9 months where both learning and memory through NOR testing and neural remodeling through mushroom and thin spine density were reduced after mice were irradiated with 0.05 Gy 16O particles (Howe et al., 2019). Hodges et al. (1998) showed neural remodeling at 41 weeks after 250 kVp X-ray irradiation and impaired learning and memory from 35 to 44 weeks post-irradiation.

Incidence Concordance

No available data.

Essentiality

No identified studies applied countermeasures to support the causal relationship between neural remodeling and impaired learning and memory.

Uncertainties and Inconsistencies

- One study observed cognitive deficits in the one- and two-way avoidance, press-lever avoidance, and water maze tests, but through pathological examination, no abnormalities were seen in the brains (white matter and axons were normal with no inflammation or glial response) (Lamproglou et al., 1995). This is indicative of impaired cognition without any changes in neuron integrity.
- At 25 Gy of X-irradiation, Hodges et al. (1998) observed both neural remodeling and impaired learning and memory. However, at 20 Gy in the same study, neural remodeling was not observed.
- Whoolery et al. (2017) found that neural remodeling was high at 1 Gy and low and 0.2 Gy but found impaired learning and memory at 0.2 Gy and not at 1 Gy.
- Miry et al. (2021) found that 1 Gy of 56Fe particles led to increased learning and memory 20 months after exposure, although this is part of the compensatory or repair mechanisms following early suppressive changes.

Quantitative Understanding of the Linkage

The table below provides some representative examples of quantitative linkages between the two key events. It was difficult to identify a general trend across all the studies due to differences in experimental design and reporting of the data. All data is statistically significant unless otherwise stated.

Dose Concordance

Reference	Experiment Design	Summary

Acharya et al., 2019	In vivo. Mice were irradiated with neutrons from a 252Cf source over 180 days at 1 mGy/day. Electrophysiological measurements were taken from CA1 pyramidal neurons to assess neuron integrity. NOR, OiP and FE were used to assess learning and memory.	Spontaneous excitatory postsynaptic current (sEPSC) frequency decreased with a mean difference of approximately –0.81 Hz. Field excitatory postsynaptic potential (fEPSP) slopes also decreased in the dorsal hippocampus and cortical layer. Avoidance behavior was increased by 20 sec, time spent interacting was decreased by 10 sec, and the discrimination index in both NOR and object in place OiP were decreased by 19.
Parihar et al., 2016	In vivo. Male Thy1-EGFP transgenic mice were irradiated with charged particles (16O and 48Ti) at 600 MeV/amu (0.05 to 0.25 Gy/min). In the medial prefrontal cortex, neuron integrity was measured through spine density, dendritic complexity and postsynaptic density protein 95 synaptic puncta, while NOR, OiP, TO and FE tests were done to assess learning and memory. Wistar rats were used in an attentional set-shifting (ATSET) test.	Dendritic complexity and spine density were both decreased about 0.7-fold, while synaptic puncta were increased about 1.5-fold after both types of radiation at 0.05 and 0.3 Gy. Impairment in cognitive ability was observed at both 0.05 and 0.3 Gy. The impairment was typically greater in 48Ti than 16O. The correlation between the OiP DI and number of synaptic puncta was significant at 0.05 Gy 48Ti and 0.3 Gy 48Ti and 16O. The correlation between the OiP DI and number of dendritic spines was significant at 0.05 Gy 48Ti and 16O and 0.3 Gy 48Ti.
Parihar et al., 2015	In vivo. Thy1- EGFP transgenic mice were irradiated with 600 MeV/amu 16O and 48Ti particles (0.5-1 Gy/min). In the medial prefrontal cortex, neuron integrity was measured through spine density, dendritic complexity and postsynaptic density protein 95 synaptic puncta, while learning and memory was assessed with NOR and OiP.	Dendritic complexity was decreased 0.6-fold, spine density decreased 0.5-fold and synaptic puncta increased 1.4-fold for both radiation types at 0.05 and 0.3 Gy. The DI for NOR and OiP was reduced dose- and particle size-dependently, decreasing from a control DI of 30-40 to DI < 0 after 0.3 Gy of 48Ti. The correlation between OiP DI and number of dendritic spines was significant with 0.3 Gy 48Ti.
Krukowski et al., 2018	In vivo. Male and female C57Bl/6J mice were irradiated with GCR (60% 252 MeV/n protons, 20% 249.3 MeV/n helium and 20% 594.4 MeV/n oxygen) at various doses. Neuronal integrity was measured through synaptic composition and number of synaptosomes. Memory was assessed through NOR.	No changes were observed in female mice. Male mice showed a 0.9-fold decrease in the number of synaptosomes after 0.5 Gy. GluR1 (associated with hippocampal-dependent working memory) levels were decreased 0.8-fold. No changes in synapsin 1 and postsynaptic density protein 95 were observed. Recognition memory was reduced after 0.15 and 0.5 Gy irradiation in male mice, as irradiated mice did not spend significantly more time with the novel object.
Raber et al., 2004	In vivo. Male C57BL/6J mice were irradiated with 10 Gy of X-rays. Ki-67 positive (proliferating) and DCx positive (immature) cells were measured to assess neuron integrity. NOR, MWM and Barnes maze were used to assess learning and memory.	Before cognitive testing, the number of Ki-67 and DCx positive cells each decreased by 95% after irradiation. In the Barnes maze, irradiated mice took a longer path to reach the escape tunnel and also made more errors than control mice. Irradiated mice showed no impairment during NOR and the MWM.
Madsen et al., 2003	In vivo. Adult male Wistar rats were irradiated with 3 Gy of 300 kVp X-rays (4.58 Gy/min). Neuron integrity was assessed using BrdU (thymidine analog) staining to show neurogenesis in the DG. Learning and memory was assessed using NOR, novel location recognition (NLR) and a water maze.	At a dose of 3 Gy, BrdU-positive cells decreased from approximately 1750 to values too small to be observed when injected during the second block of irradiation. The place recognition test showed reduced time spent in the novel location to almost 50% in irradiated rats. NOR and the water maze did not show any changes in cognitive function.
Akiyama et al., 2001	In vivo. Male Fischer 344 rats were irradiated with 25 Gy of 10 MeV X-rays. Bodian and neurofilament (NF) staining were used to identify axons in the corpus callosum. MWM and a passive avoidance test were used to assess learning and memory.	Rats irradiated with 25 Gy had fewer axons and took longer in each trial to reach the platform in the MWM, although not significantly. When the platform was removed, irradiated rats crossed the area where the platform was 0.6-fold fewer times than control rats. During passive avoidance, the retention time after a shock was also decreased 0.6-fold in irradiated rats.
Hodges et al., 1998	In vivo. Male Sprague–Dawley rats were irradiated with 250 kVp X-rays at 1.4 Gy/min. Histological analysis was performed to measure damage and necrosis in the fimbria-fornix, hippocampus and corpus callosum. Learning and memory were measured through a T-maze and water maze.	At 20 Gy, there was no histological evidence of neural remodeling, while learning and memory were impaired. At 25 Gy, various necrotic areas were observed in the brain, while learning and memory were impaired. For example, irradiated rats at both 20 and 25 Gy showed 2-fold more errors in the T-maze.
Rola et al., 2004	In vivo. Male C57BL/6J mice were irradiated with X-rays at 1.75 Gy/min). Ki-67 positive (proliferating) and DCx positive (immature) cells were measured along with BrdU staining to assess neuron integrity in the subgranular zone.	The number of Ki-67-positive and DCx-positive cells decreased linearly at 0, 2 and 5 Gy, then leveled off at 10 Gy, reaching reductions of 0.1-fold for Ki-67 and 0.3-fold for DCx. The number of BrdU-positive cells decreased by 70% after 5 Gy. Also, after 5 Gy in the MWM, irradiated mice spent 30% less time in the target

	NOR, NLR, MWM, Barnes maze and passive avoidance learning were used to assess learning and memory.	quadrant compared to control mice, indicative of reduced memory retention. No changes were observed in NOR, NLR, Barnes maze and passive avoidance tests.
Whoolery et al., 2017	In vivo. Nestin-GFP male and female mice (C57BL/6J background) were irradiated with 300 MeV/n 28Si particles (linear energy transfer = 67 keV/µm) at 1 Gy/min. Stereological immunopositive cell counts were determined for BrdU, Ki-67 and DCx in the DG granule cell layer. FC was used to assess learning and memory.	Ki-67-positive cells decreased 0.8-fold at 0.2 Gy and 0.4-fold at 1 Gy, which occurred in both males and females. BrdU-positive cells decreased by 0.8- and 0.7-fold at 1 Gy in males and females, respectively. DCx-positive cells decreased by 0.5-fold at 1 Gy in both sex groups. Small and nonsignificant decreases in BrdU- and DCx-positive cells occurred at 0.2 Gy. Mice exhibited a decrease in percentage freezing of 0.4-fold at 0.2 Gy in contextual FC. No changes in learning and memory were observed at 1 Gy.
Howe et al., 2019	In vivo. C57BL/6 mice were irradiated with heavy ions 16O (600 MeV/n) at 0.05 Gy. NOR was used to assess non-spatial declarative memory. Y-maze assessed short-term spatial memory of mice. Sholl analysis was performed to quantify the neurons in the hippocampus. The morphology and density of dendritic spines from the DG and dorsal CA1 and CA3 pyramidal neurons. Behaviour was evaluated 9 months after irradiation.	Overall dendritic complexity in the DG decreased 0.59-fold, while overall dendrite density in the DG decreased 0.94-fold. Irradiated animals exhibited a 0.11-fold change in the discrimination ratio in NOR, as the irradiated group was unable to discriminate between the familiar and novel object, indicating cognitive impairment. Irradiated mice spent more time exploring the novel object than the familiar object in the Y-maze, indicating no impairment on short-term spatial memory.
Achanta, Fuss & Martinez, 2009	In vivo. Male Sprague Dawley rats were irradiated with 0.3, 3 or 10 Gy of X-rays. BrdU staining was used to assess neuronal proliferation. Changes in cognitive behavior was evaluated by FC/testing. Fear testing was performed at 90 days post-irradiation.	At 3-months post-irradiation, total number of Ki67+ cells (proliferative marker for cells) decreased by 0.8-, 0.7-, and 0.3-fold in the PD 21 group; 0.8-, 0.7-, and 0.3-fold in the PD 50 group; and 0.9-, 0.083-, and 0.3-fold in the PD 70 group, at 0.3, 3, and 10 Gy, respectively. Total number of BrdU+ cells decreased by 0.7-, 0.4-, and 0.1-fold in the PD 21 group; 0.6-, 0.48-, and 0.03-fold in the PD 50 group; and 0.9-, 0.6-, and 0.04-fold in the PD 70 group, at 0.3, 3, and 10 Gy, respectively. % mean freezing in the PD 21 group in response to a conditioned stimulus (CS) decreased by 0.7- and 0.6-fold in the trace fear conditioning after 3 Gy and 10 Gy, respectively, and 0.7- and 0.6-fold with an intertrial interval (ITI) after 3 Gy and 10 Gy, respectively. % mean freezing in the PD 50 group in response to a CS decreased by 0.6-fold in trace fear conditioning after 10 Gy, and 0.6-fold with an ITI after both 0.3 and 10 Gy. % mean freezing in the PD 70 group in response to a CS decreased by 0.6-fold in trace fear conditioning and 0.6-fold with an ITI after 10 Gy.
Winocur et al., 2006	In vivo. Long-Evans rats were irradiated with 7.5 or 10 Gy of 60Co gamma rays. BrdU staining was used to label the DNA of proliferating cells. DCX as an immature neuron marker and NeuN for mature neuron staining were used. Cognitive impairment was identified by contextual FC in the studied rats 4 weeks after irradiation.	Numbers of BrdU+ cells decreased by 0.2- and 0.2-fold after 10 and 7.5 Gy, respectively. Total number of DCX+ cells decreased by 0.03- and 0.10-fold, for 10 and 7.5 Gy, respectively. Times spent freezing in the irradiated context-only group were decreased by 0.1- and 0.4-fold at the short and long delays, respectively.
Simmons et al., 2019	In vivo. C57BL/6J mice were irradiated with 30 Gy electrons (16 and 20 MeV). Spatial and non-spatial object recognition was studied by object location and NOR 10 weeks after irradiation. Spine density was measured by Golgi-stained hippocampal neuron tracing using Neurolucida neuron tracing software and Neurolucida Explorer software (MBF Bioscience).	Apical dendritic spine density decreased 0.8-fold in 30 Gy conventional irradiated (given over 240 s) mice. The discrimination index for NOR decreased from 23% to 8% after 30 Gy given conventionally. The discrimination index for NOL decreased from 12% to -8% after 30 Gy given conventionally. Conventionally irradiated mice spent significantly less time with the object in a new location, indicating impairment to hippocampus learning and memory. Irradiated mice spent less time exploring a novel object than control mice. No significant changes were observed when the 30 Gy was given over 0.1-0.16 s.
Sorokina et	In vivo. Male mice were irradiated with accelerated carbon ions at 0.7 Gy (450 MeV/n). Spatial learning, short-term and long-term hippocampus-dependent memory were studied using Barnes Maze and NOR 2 months after	Neuronal quantification revealed a decrease in the number of cells in irradiated mice by 0.9-fold in the DG. The length of the CA3c field of the dorsal hippocampus decreased by 0.89-fold. In the Barnes maze, the latency to the goal box was 3.1-fold higher

al., 2021	irradiation. Nissl staining was performed 1 month after cognitive evaluations to quantify neuronal cells.	in the irradiated mice than control on the 9th day after learning, indicating long-term decreased learning. NOR did not show any changes to learning and memory, shown through the 0.7 Gy irradiated mice spending significantly longer with the novel object.
Miry et al., 2021	In vivo. C57BL/6J mice were irradiated with 0.1, 0.5 and 1 Gy 56Fe. Active avoidance was used to study spatial learning and discrimination. Immunohistological analysis of proliferating neural cells were performed using DCX, an immature neural marker. Other tests performed included the Barnes Maze for spatial learning. Mice were studied at multiple time-points (2, 6, 12, and 20 months) post-exposure.	2 months post-exposure, levels of DCX+ cells decreased by 0.7- (0.1 Gy), 0.4- (0.5 Gy) and 0.6-fold (1 Gy) in male mice, and 0.7- (0.1 Gy), 0.6- (0.5 Gy) and 0.4-fold (1 Gy) in female mice. 12 months post-exposure, levels of DCX+ cells increased by 2.6- (0.1 Gy), 2.4- (0.5 Gy), and 2.3-fold (1 Gy) in male mice, and 2.2- (0.1 Gy), 1.1- (0.5 Gy), and 2-fold (1 Gy) in female mice. In the active avoidance task, the normalized error entries significantly increased in both male and female 0.5 Gy irradiated mice compared to the 0 Gy group. In Barnes maze, male mice 20 months post-exposure to 1 Gy 56Fe showed a significant decrease in latency to escape. The most profound change was measured on day 2 with a 0.6-fold decrease in latency to escape, as the irradiated mice learned the location of the escape box faster than the control group over the 5-day training period.

Time Concordance

Reference	Experiment Design	Summary
Parihar et al., 2016	In vivo. Male Thy1-EGFP transgenic mice were irradiated with 600 MeV/amu charged particles (16O and 48Ti) (0.05 to 0.25 Gy/min) at 0.05 and 0.3 Gy. In the medial prefrontal cortex, neuron integrity was measured through spine density, dendritic complexity and postsynaptic density protein 95 synaptic puncta, while NOR, OiP, TO and fear extinction (FE) tests were done to assess learning and memory. Wistar rats were used in an ATSET test.	Dendritic complexity and spine density were reduced 0.7-fold 15 weeks post-irradiation, while synaptic puncta were increased 1.3-fold 15 weeks post-irradiation and 1.5-fold 27 weeks post-irradiation. Learning and memory were impaired 15 weeks post-irradiation, and even further impaired 24 weeks post-irradiation.
Raber et al., 2004	In vivo. Male C57BL/6J mice were irradiated with 10 Gy of X-rays. Ki-67 positive (proliferating) and DCx positive (immature) cells were measured to assess neuron integrity. NOR, MWM and Barnes maze were used to assess learning and memory.	Before cognitive testing (3 months post-irradiation), the number of Ki-67 and DCx positive cells each decreased by 95% after irradiation. In the Barnes maze, irradiated mice took a longer path to reach the escape tunnel and also made more errors than control mice 3 months after irradiation. Irradiated mice showed no impairment during NOR and the MWM.
Madsen et al., 2003	In vivo. Adult male Wistar rats were irradiated with 3 Gy of 300 kVp X-rays (4.58 Gy/min). Neuron integrity was assessed using BrdU (thymidine analog) staining to show neurogenesis in the DG. Learning and memory was assessed using NOR, NLR and a water maze.	At a dose of 3 Gy, numbers of BrdU-positive cells (neurogenesis) decreased from approximately 1750 to values too low to be observed when injected during the second block of irradiation. BrdU-positive cells decreased from 1300 to 300 when injected 2 weeks after end of irradiation. BrdU-positive cells decreased from 1300 to 250 when injected 6 weeks after end of irradiation. The place recognition test showed impairments in irradiated animals as time in the new arm decreased from 72% to 62% at 1 week post-irradiation; and 67% to 54% at 3 weeks post-irradiation. After 7 weeks, rats showed impaired location memory but not significantly.
Hodges et al., 1998	In vivo. Male Sprague–Dawley rats were irradiated with 250 kVp X-rays at 1.4 Gy/min and 20 or 25 Gy. Histological analysis was performed to measure damage and necrosis in the fimbria-fornix, hippocampus and corpus callosum. Learning and memory were measured through a T-maze and water maze.	Neural remodeling, only measured at 41 weeks after radiation, was observed. Impaired learning and memory wereobserved from 35 to 44 weeks after radiation.
Rola et al., 2004	In vivo. Male C57BL/6J mice were irradiated with X-rays at 1.75 Gy/min). Ki-67 positive and DCx positive cells were measured along with BrdU staining to assess neuron integrity in the subgranular zone. NOR, NLR, MWM, Barnes maze and passive avoidance learning were used to assess learning and memory.	The number of Ki-67-positive and DCx-positive cells decreased 0.1-fold and 0.3-fold, respectively, 48h after 5 Gy. The number of BrdU-positive cells decreased by 70% at both 1 and 3 months after 5 Gy. Also, after 3 months, in the MWM, irradiated mice spent 30% less time in the target quadrant after 5 Gy compared to control mice. No changes were observed in NOR, NLR, Barnes maze and passive avoidance tests.
		24 h post-irradiation, BrdU-positive cells decreased by 0.75- and 0.65-

Whoolery et al., 2017	In vivo. Nestin-GFP male and female mice (C57BL/6J background) were irradiated with 300 MeV/n 28Si particles (linear energy transfer = 67 keV/µm) at 1 Gy/min. Stereological immunopositive cell counts were determined for BrdU, Ki-67 and DCx in the DG granule cell layer. FC was used to assess learning and memory.	24 h post-irradiation, BrdU-positive cells decreased by 0.5- and 0.6-fold at 1 Gy in the male and female groups, respectively, DCx-positive cells decreased by 0.5-fold at 1 Gy in both sex groups and Ki-67-positive cells decreased by 0.8-fold at 0.2 Gy and 0.4-fold at 1 Gy in both males and females. At 3 months post-irradiation, BrdU-positive cells decreased by 0.83- and 0.31-fold in male mice only at 0.2 and 1 Gy, respectively, Ki-67 was not significantly changed and DCx was reduced at 1 Gy but only when both sexes were combined. 3 months post-irradiation, male mice exhibited a decrease in percentage freezing of 0.43-fold at 0.2 Gy in contextual FC.
Howe et al., 2019	In vivo. C57BL/6 mice were irradiated with heavy ions 16O (600 MeV/n) at 0.05 Gy. NOR was used to assess non-spatial declarative memory. Y-maze assessed short-term spatial memory of mice. Sholl analysis was performed to quantify the neurons in the hippocampus. The morphology and density of dendritic spines from the DG and dorsal CA1 and CA3 pyramidal neurons. Behavior was evaluated 9 months after irradiation.	9 months after irradiation, mice exhibited a 0.1-fold change in discrimination ratio in NOR indicating cognitive impairment. Dendritic spine density at 9 months post-irradiation was found to be reduced in the DG.
Achanta, Fuss & Martinez, 2009	In vivo. Male Sprague Dawley rats were irradiated with 0.3, 3 or 10 Gy. BrdU staining was used to assess neuronal proliferation. Changes in cognitive behavior were evaluated by FC/testing. Fear testing was performed at 90 days post-irradiation.	Total number of BrdU+ cells and total number of Ki67+ cells (proliferative marker for cells) 3-months post-irradiation decreased in PD 21, PD50 and PD 70 groups. Fear conditioning/testing at 90 days post-irradiation showed a decrease in % mean freezing in response to a CS in PD21, PD50 and PD 70. As well, ITI decreased in the studied groups.
Winocur et al., 2006	In vivo. Long-Evans rats were irradiated with 7.5 or 10 Gy of 60Co gamma rays. BrdU staining was used to label the DNA of proliferating cells. DCX as an immature neuron marker and NeuN for mature neuron staining were used. Cognitive impairment was identified by contextual fear conditioning in the studied rats 4 weeks after irradiation.	Numbers of BrdU+ cells decreased by 0.22- and 0.23-fold 4 weeks after irradiation. Fear conditioning took place 4 weeks post-irradiation. The time spent freezing in the irradiated context-only group was decreased by 0.1- and 0.4-fold at the short and long delays, respectively.
Sorokina et al., 2021	In vivo. Male mice were irradiated with accelerated carbon ions at 0.7 Gy (450 meV/n). Spatial learning, short-term and long-term hippocampus-dependent memory were studied using Barnes Maze and NOR 2 months after irradiation. Nissl staining was performed 1 month after cognitive evaluations to quantify neuronal cells.	1 month after cognitive evaluations, neuronal quantification revealed a decrease in the number of cells by 0.9-fold in the DG. The length of the CA3c field of the dorsal hippocampus decreased by 0.5-fold. In the Barnes maze 2 months after irradiation, the latency to the goal box was 3.1-fold higher in the irradiated mice than control on the 9th day after learning. Meanwhile no significant changes in latency to the goal box were observed on the second day of learning. NOR did not show any changes to memory.
Miry et al., 2021	In vivo. C57BL/6J mice were irradiated with 0.1, 0.5 and 1 Gy of 56Fe ions. Active avoidance was used to study spatial learning and discrimination. Immunohistological analysis of proliferating neural cells were performed using DCX, an immature neural marker. Other tests performed included the Barnes maze for spatial learning. Mice were studied at multiple time-points (2, 6, 12, and 20 months) post-exposure.	2 months post-exposure, levels of DCX+ cells decreased by 0.4- to 0.7- fold in both male and female mice. 12 months post-exposure, DCX+ cells were increased in irradiated mice compared to control mice and levels of DCX+ cells increased by 1.1- to 2.6-fold in male and female mice. 20 months after exposure, learning was found to be improved.

Known modulating factors

Modulating factor	Details	Effects on the KER	References
Sex	Female mice	Female mice were protected from the GCR-induced deficits in learning and memory and did not show changes in synapse levels	Krukowski et al., 2018
Antioxidant	α-tocopherol	Improved global cognitive ability, memory and executive function	Hladik & Tapio, 2016
Stem cells	Human neural stem cell	Increased neurogenesis in the brain after radiation and	Hladik & Tapio, 2016

	treatment	improved learning and memory	
Drug	Ramipril (Angiotensin converting enzyme inhibitor)	Mitigated neurodegeneration and prevented cognitive impairment	Hladik & Tapio, 2016
Drug	Memantine (NMDA receptor antagonist)	Reduced rate of memory decline after radiotherapy	Bálentová & Adamkov, 2020
Hypoxia	Systemic hypoxia	Systemic hypoxia reversed the effects of radiation on learning and memory	Bálentová & Adamkov, 2020; Hladik & Tapio, 2016

Known Feedforward/Feedback loops influencing this KER

NA

References

Achanta, P., M. Fuss and J. L. Martinez. (2009), "Ionizing Radiation Impairs the Formation of Trace Fear Memories and Reduces Hippocampal Neurogenesis", Behavioral Neuroscience, Vol. 123/5, https://doi.org/10.1037/a0016870.

Acharya, M. M. et al. (2019), "New concerns for neurocognitive function during deep space exposures to chronic, low dose-rate, neutron radiation", eNeuro, Vol. 6/4, Society for Neuroscience, https://doi.org/10.1523/ENEURO.0094-19.2019.

Akiyama, K. et al. (2001), "Cognitive Dysfunction and Histological Findings in Adult Rats One Year After Whole Brain Irradiation.", Neurologia medico-chirurgica, Vol. 41/12, Japan Neurological Society, https://doi.org/10.2176/nmc.41.590.

Bálentová, S. and M. Adamkov. (2020), "Pathological changes in the central nervous system following exposure to ionizing radiation", Physiological Research, Czech Academy of Sciences, https://doi.org/10.33549/PHYSIOLRES.934309.

Burgess, N. (2002), "The hippocampus, space, and viewpoints in episodic memory", The Quarterly Journal of Experimental Psychology, Vol. 55/4, Experimental Psychology Society, https://doi.org/10.1080/02724980244000224.

Cucinotta, F. A. et al. (2014), "Space radiation risks to the central nervous system", Life Sciences in Space Research, Vol. 2, Elsevier Ltd, Amsterdam, https://doi.org/10.1016/j.lssr.2014.06.003.

Desai, R. I. et al. (2022), "Impact of spaceflight stressors on behavior and cognition: A molecular, neurochemical, and neurobiological perspective", Neuroscience & Biobehavioral Reviews, Vol. 138, Elsevier, Amsterdam, https://doi.org/10.1016/j.neubiorev.2022.104676.

D'Hooge, R. and P. P. De Deyn. (2001), "Applications of the Morris water maze in the study of learning and memory", Brain Research Reviews, Vol. 36/1, Elsevier B.V., https://doi.org/10.1016/S0165-0173(01)00067-4.

Hladik, D. and S. Tapio. (2016), "Effects of ionizing radiation on the mammalian brain", Mutation Research - Reviews in Mutation Research, Vol. 770, Elsevier B.V., https://doi.org/10.1016/j.mrrev.2016.08.003.

Hodges, H. et al. (1998), "Late behavioural and neuropathological effects of local brain irradiation in the rat", Behavioural Brain Research, Vol. 91/1–2, Elsevier, https://doi.org/10.1016/S0166-4328(97)00108-3.

Howe, A. et al. (2019), "Long-term changes in cognition and physiology after low-dose 16 O irradiation", International Journal of Molecular Sciences, Vol. 20/1, MDPI AG, https://doi.org/10.3390/ijms20010188.

Kiffer, F., M. Boerma and A. Allen. (2019b), "Behavioral effects of space radiation: A comprehensive review of animal studies", Life Sciences in Space Research, Vol. 21, Elsevier, Amsterdam, https://doi.org/10.1016/j.lssr.2019.02.004.

Krukowski, K. et al. (2018), "Female mice are protected from space radiation-induced maladaptive responses", Brain, Behavior, and Immunity, Vol. 74, Academic Press Inc., https://doi.org/10.1016/j.bbi.2018.08.008.

Lamproglou, I. et al. (1995), "Radiation-induced cognitive dysfunction: An experimental model in the old rat", International Journal of Radiation Oncology, Biology, Physics, Vol. 31/1, Elsevier, https://doi.org/10.1016/0360-3016(94)00332-F.

Madsen, T. M. et al. (2003), "Arrested neuronal proliferation and impaired hippocampal function following fractionated brain irradiation in the adult rat", Neuroscience, Vol. 119/3, Elsevier Ltd, https://doi.org/10.1016/S0306-4522(03)00199-4.

Miry, O. et al. (2021), "Life-long brain compensatory responses to galactic cosmic radiation exposure", Scientific Reports 2021 11:1, Vol. 11/1, Nature Publishing Group, https://doi.org/10.1038/s41598-021-83447-y.

Monje, M. L. and T. Palmer. (2003), "Radiation injury and neurogenesis", Current Opinion in Neurology, Vol. 16/2, Ovid Technologies (Wolters Kluwer Health), https://doi.org/10.1097/01.wco.0000063772.81810.b7.

National Council on Radiation Protection and Measures (NCRP). (2016). Commentary No. 25 – Potential for central nervous system effects from radiation exposure during space activities phase I: Overview.

Parihar, V. K. et al. (2016), "Cosmic radiation exposure and persistent cognitive dysfunction", Scientific Reports, Vol. 6/1, Nature

Publishing Group, https://doi.org/10.1038/srep34774.

Parihar, V. K. et al. (2015), "What happens to your brain on the way to Mars", Science Advances, Vol. 1/4, American Association for the Advancement of Science, https://doi.org/10.1126/SCIADV.1400256.

Raber, J. et al. (2004), "Radiation-induced cognitive impairments are associated with changes in indicators of hippocampal neurogenesis", Radiation Research, Vol. 162/1, Allen Press, https://doi.org/10.1667/RR3206.

Rola, R. et al. (2004), "Radiation-induced impairment of hippocampal neurogenesis is associated with cognitive deficits in young mice", Experimental Neurology, Vol. 188/2, Academic Press Inc., https://doi.org/10.1016/j.expneurol.2004.05.005.

Romanella, S. M. et al. (2020), "Noninvasive Brain Stimulation & Space Exploration: Opportunities and Challenges", Neuroscience & Biobehavioral Reviews, Vol. 119, https://doi.org/10.1016/j.neubiorev.2020.09.005.

Simmons, D. A. et al. (2019), "Reduced cognitive deficits after FLASH irradiation of whole mouse brain are associated with less hippocampal dendritic spine loss and neuroinflammation", Radiotherapy and Oncology, Vol. 139, https://doi.org/10.1016/j.radonc.2019.06.006.

Sorokina, S. S. et al. (2021), "Low dose of carbon ion irradiation induces early delayed cognitive impairments in mice", Radiation and Environmental Biophysics, Vol. 60, Nature, https://doi.org/10.1007/s00411-020-00889-0.

Tomé, W. A. et al. (2015), "Hippocampal-dependent neurocognitive impairment following cranial irradiation observed in pre-clinical models: current knowledge and possible future directions", The British Journal of Radiobiology, Vol. 89/1057, British Institute of Radiology, https://doi.org/10.1259/bjr.20150762.

Vorhees, C. V. and M. T. Williams. (2014), "Assessing Spatial Learning and Memory in Rodents", ILAR Journal, Vol. 55/2, Oxford University Press, Oxford, https://doi.org/10.1093/ilar/ilu013.

Whoolery, C. W. et al. (2017), "Whole-body exposure to 28Si-radiation dose-dependently disrupts dentate gyrus neurogenesis and proliferation in the short term and new neuron survival and contextual fear conditioning in the long term", Radiation Research, Vol. 188/5, Radiation Research Society, https://doi.org/10.1667/RR14797.1.

Winocur, G. et al. (2006), "Inhibition of neurogenesis interferes with hippocampus-dependent memory function", Hippocampus, Vol. 16/3, https://doi.org/10.1002/HIPO.20163.

Relationship: 2840: Altered Signaling leads to Increase, Neural Remodeling

AOPs Referencing Relationship

AOP Name	Adjacency	Weight of Evidence	Quantitative Understanding
Deposition of Energy Leading to Learning and Memory Impairment	adjacent	Moderate	Low

Evidence Supporting Applicability of this Relationship

Taxonomic Applicability

Term	Scientific Term	Evidence	Links
human	Homo sapiens	Low	NCBI
mouse	Mus musculus	Moderate	NCBI
rat	Rattus norvegicus	Low	NCBI

Life Stage Applicability

Life Stage	Evidence
Juvenile	Moderate
Adult	Low

Sex Applicability

Sex	Evidence
Male	Moderate
Female	Low
Unspecific	Moderate

Evidence for this relationship comes from human-derived cells, rat, and mouse models, with most of the evidence in mice. There is in vivo evidence in both male and female animals, with more evidence in males. Animal age is occasionally not indicated in studies, but most evidence is in adolescent rodent models with a few studies using adult animals.

Key Event Relationship Description

Alterations in signaling pathways can trigger disruption to neuronal structures, which can lead to altered morphology, changes in neurogenesis, neurodegeneration, apoptotic activity and synaptic activity, collectively known as neural remodeling (Cekanaviciute et al., 2018; Chakraborti et al., 2012; Hladik & Tapio, 2016). These intracellular pathways are key processes to control various cell functions such as cell growth, death or communication. Within the neuron, multiple signaling pathways influence its structure and function. For example, the phosphatidylinositol 3-kinase (PI3K)/Akt and mitogen-activated protein kinase (MAPK) family pathways are involved in neuronal survival, proliferation, morphology, and synaptic plasticity (Davis and Laroche, 2006; Long et al., 2021; Mazzucchelli and Brambilla, 2000). The senescence pathway induces cell cycle arrest and can restrict neurogenesis (McHugh and Gil, 2018). The apoptotic pathway can be initiated within the mitochondria due to dysfunction within the respiratory chain and induces various signaling proteins such as p53, BAX, caspases and cytochrome C (Betlazar et al., 2016; Mielke and Herdegen, 2000; Wang et al., 2020). Apoptosis of neurons results in a reduction in neuron numbers, demonstrating neural remodeling. A few studies also measure high apoptosis levels over time, indicating sustained neuron loss contributing to reduced neural activity (Chow, Li, and Wong, 2000; Limoli et al., 2004; Pius-Sadowska et al., 2016). Additionally, the brain-derived neurotrophic factor (BDNF)-cAMP-calcium response element binding protein (CREB) pathway is involved in the regulation of excitatory transmission as CREB-dependent transcription allows for persistent pre- and post-synaptic neurotransmitter release at excitatory synapses (Ran et al., 2012).

Evidence Supporting this KER

Overall Weight of Evidence: Moderate

Biological Plausibility

Neural remodeling can be induced by changes in multiple signaling pathways, including MAPK signaling, PI3K/Akt signaling, senescence signaling, and apoptotic signaling. These pathways are involved in the homeostatic regulation of neuron numbers, morphology, proliferation, differentiation, and synaptic activity.

Like many signaling pathways, MAPK pathways help maintain the biological functions in neurons, and changes to the expression or activity of signaling molecules in MAPK pathways can result in neural remodeling. The extracellular signal-regulated protein kinase (ERK)1/2 MAPK pathway is crucial for modulating synaptic function and alteration in expression of critical proteins in this pathway will result in long-term potentiation (LTP) deficits (Davis and Laroche, 2006; Mazzucchelli and Brambilla, 2000). Research shows that modulations in ERK1/2 expression and activity can decrease cell proliferation in the hippocampus (Betlazar et al., 2016). The p38 MAPK pathway is also involved in maintaining neuronal plasticity and synaptic function, by inducing metabotropic glutamate receptor (mGluR)-dependent long-term depression (LTD) in hippocampal neurons (Falcicchia et al., 2020). However, p38 demonstrates variable effects in neuronal survival and proliferation. Although p38 signaling is required for the survival of developing neurons, p38 can also be involved in the induction of apoptosis, and subsequent inhibition of p38 promotes cell survival (Mielke and Herdegen, 2000; Nebreda and Porras, 2000). The role of p38 is often dependant on the cell type and stimulus and will determine whether p38 has a positive or negative role on neural cell proliferation (Nebreda and Porras, 2000). The c-Jun NH2-terminal kinase (JNK) MAPK pathway plays a similar role to the p38 pathway, and its function is also dependant on the cell type and context of the cellular environment. JNK can induce apoptosis as well as regulate proteins like tau and microtubule-associated protein (MAP)2 involved in altering cytoskeletal dynamics and cell morphology (Mielke and Herdegen, 2000; Sherrin, Blank, and Todorovic, 2011). JNK is also involved in both pre- and post-synaptic function through the phosphorylation of AMPA receptors and postsynaptic density protein (PSD)95 (Sherrin, Blank, and Todorovic, 2011).

The PI3K/Akt pathway is involved in many neuronal functions. Activation of the PI3K/Akt pathway promotes transcription of survival genes and inhibits death genes, while also regulating the activity of various death pathways (Long et al., 2021; Rai et al., 2019). Alterations in Akt expression and activity can decrease cell proliferation in the hippocampus (Betlazar et al., 2016). The pathway can also regulate neuron morphology, as neurite outgrowth can be induced by activation of the pathway (Rodgers and Theibert, 2002). Synaptic plasticity and LTP, which is induced by the activation of NMDA receptors and the subsequent insertion of AMPA receptors to the membrane, can additionally be regulated by the PI3K/Akt pathway. It has been shown that the mammalian target of rapamycin (mTOR), downstream of Akt, increases the expression of LTP-related proteins while PI3K guides AMPA insertion on the membrane (Long et al., 2021). Therefore, maintaining the appropriate expression levels of signaling molecules is critical for proper neural development and function.

The signaling molecules p53/p21 and p16 as part of the cellular senescence pathway can induce cell cycle arrest. For example in neural stem cells (NSCs), reduced functionality and limited neurogenesis is associated with increased senescence markers (McHugh and Gil, 2018).

The apoptosis pathway, consisting of the pro-apoptotic tumor necrosis factor-related apoptosis-inducing ligand (TRAIL) receptor, caspases, cytochrome C, and Bcl-2-associated X protein (BAX) as well as the anti-apoptotic B-cell lymphoma (Bcl)-2 protein, contributes to a reduction in neuron numbers through cell death when activated (Betlazar et al., 2016; Wang et al., 2020). This pathway may be induced by perturbations to other signaling pathways, including MAPK, PI3K/Akt, and senescent pathways (Hladik and Tapio, 2016; Mielke and Herdegen, 2000). For example, JNK and p53 can both antagonise the anti-apoptotic Bcl-2, while JNK

can stabilize p53 and p53 enhances BAX (Mielke and Herdegen, 2000).

Signaling pathways not just in neurons, but also in astrocytes and microglia, can influence neural remodeling. For example, it was previously mentioned that p38 signaling in neurons contribute to hippocampal mGluR-dependent LTD. In astrocytes, p38 signaling is necessary for NMDA-dependent LTD during astrocyte-to-neuron communication (Falcicchia et al., 2020). In addition, BDNF signaling in both neurons and astrocytes prevents cell death in the respective cells through activation of the ERK and PI3K/Akt pathways. Neuronal death can be prevented by BDNF signaling in both cell types because astrocytes release factors that prevent neuronal death (Rai et al., 2019).

Synergistic and antagonistic interactions between signaling pathways can also occur, contributing to the complexity and context-dependence of the neural remodeling response to various signaling pathways. For example, nuclear factor of activated T-cells (NFATc) nuclear translocation and transcriptional activation can be encouraged by the PI3K/Akt pathway and the ERK pathway and inhibited by p38 and JNK (Macian, 2005; Mielke and Herdegen, 2000). Activation of NFATc promotes neuronal survival, synaptic plasticity, and neurite outgrowth through the transcription of multiple target genes (Zhang et al., 2018). BDNF activation of the ERK, PI3K/Akt, and Ca2+/calmodulin-dependent protein kinase II (CaMKII) pathways through tropomyosin receptor kinase (Trk) activation results in the activation of CREB transcriptional activity (Cunha, Brambilla, and Thomas, 2010). CREB is essential for the regulation of excitatory transmission, and exogenous stressors can induce hippocampal neuronal damage through the inhibition of this pathway (Hladik and Tapio, 2016; Wang et al., 2020).

Empirical Evidence

The empirical evidence for this KER comes from in vivo mouse and rat models as well as in vitro rat-, mouse-, and human-derived cell models. Stressors used included gamma ray radiation (El-Missiry et al., 2018; Eom et al., 2015; Ivanov and Hei, 2014; Kanzawa et al., 2006; Pius-Sadowska et al., 2016; Suman et al., 2013), X-ray radiation (Chow, Li and Wong, 2000; Huang et al., 2021; Limoli et al., 2004; Silasi et al., 2004), electron radiation (Ji et al., 2014; Zhang et al., 2018), iron-56 ion radiation (Suman et al., 2013), simulated ischemic stroke (Tian et al., 2020), and pharmacological modulation of signaling molecules (Kumar et al., 2005). Neural remodeling can be determined through various endpoints, including neuronal apoptosis, morphology, proliferation, differentiation, and synaptic activity.

Dose Concordance

Several studies demonstrate dose concordance for this relationship. Studies have observed that altered signaling can occur at the same stressor doses as neural remodelling. X-irradiation at doses ranging from 0.5 Gy to 10 Gy resulted in changes in protein levels and phosphorylated proteins in key signaling pathways, as well as increased apoptotic activity and decreased number of neurons. Silasi et al. (2004) irradiated male and female mice with either acute (single 0.5 Gy dose) or chronic (0.05 Gy/day for 10 days) X-ray radiation at 0.002 Gy/s and found that chronic radiation decreased the levels of phosphorylated Akt, ERK1/2, CREB and CaMKII in males. Female mice showed a 1.3-fold increase in ERK1/2. A decrease in DCx+ cells was also observed in both sexes. At 2 Gy, Chow, Li and Wong (2000) reported an increase in p53+ cells and apoptosis within the brain. 10 Gy of X-irradiation resulted in an increase in BAX/Bcl-2 ratio, p53 and cleaved caspase 3 levels, as well as apoptosis within hippocampal neurons (Huang et al., 2021). Another radiation source is electrons, and doses from 2 to 20 Gy also affect protein levels and phosphorylated proteins in key signaling pathways, as well as neuronal structure and number. Zhang et al. (2018) reported a dose-dependent decrease in dephosphorylated (active) NFATc4/3 after 2 and 8 Gy, as well as an increase in phosphorylated (inactive) NFATc4/3 at these doses within the brains of rats. Total neurite length and branching points dose-dependently decreased at 2 and 8 Gy, whereas total dendritic length decreased at only 2 Gy. Whole-brain irradiation of rats at 20 Gy decreased p-ERK1/2, p-Akt, BDNF, p-TrkB, p-CaMKII, and p-CREB. Irradiation at 20 Gy also reduced the number of DCx+ cells and the number of BrdU+/NeuN+ cells (Ji et al., 2014).

Furthermore, studies using gamma irradiation as a stressor have also shown changes within this KER. Doses ranged from 2-10 Gy and resulted in altered levels of phosphorylated and dephosphorylated proteins in the MAPK family, apoptotic pathway, senescence pathway and BDNF-pCREB pathway (El-Missiry et al., 2018; Ivanov & Hei, 2014; Kanzawa et al., 2006; Pius-Sadowska et al., 2016; Suman et al., 2013). In another study, Kumar et al. (2005) utilized pharmacological inhibition of various signaling proteins such as those associated with the PI3K-Akt and MAPK family pathway. The results elicited changes in hippocampal neuron morphology as defined by a reduction in dendritic branch length, number of terminal tips, soma area, spine density and filopodia density.

Time Concordance

Multiple studies demonstrate that signaling pathways are altered before neural remodeling is observed in a time-course. Altered signaling pathways are often found as early as hours post-irradiation, while neural remodeling is first measured after days. NSCs isolated from rats showed an increase in p-JNK as early as 1h post-irradiation (10 Gy of gamma rays), while apoptosis was measured 48h post-irradiation (Kanzawa et al., 2006). After 5 Gy X-ray irradiation of rat neural precursor cells, p53 and p21 signaling was increased after 2h, while the first significant increase in apoptosis was observed after 24h (Limoli et al., 2004). In mice exposed to gamma ray irradiation at 10 Gy, multiple signaling molecules were increased as early as 3h post-irradiation, while measurements of apoptosis and neuronal morphological changes occurred 48h post-irradiation (Pius-Sadowska et al., 2016). Neuron levels were found decreased 24h post-irradiation in this study, although this was in an in vivo mouse model. Human NSCs irradiated with 5 Gy of gamma rays showed many signaling molecules were dysregulated after 6h, apoptosis was first increased after 24h, and the differentiation of NSCs was decreased after 10-12 days (Ivanov and Hei, 2014).

A few studies also demonstrated time concordance when altered signaling was measured after days or longer. Rat neurons irradiated with electrons at 2 Gy showed higher inactive and lower active levels of NFATc4/3 after both 1 and 3 days (Zhang et al., 2018). The number of branching points were subsequently decreased after only 3 days. However, total neurite length was decreased after 1 day. Furthermore, total dendritic length decreased after both 14 and 28 days, although this was in an in vivo rat model (Zhang et al., 2018). In a longer-term study using both gamma ray (2 Gy) and 56Fe ion (1.6 Gy) irradiation of mice, Suman et al. (2013) found changes in apoptotic and senescent signaling pathways at both 2 and 12 months post-irradiation, while increased apoptosis and decreased cortical thickness were only measured after 12 months.

Incidence Concordance

Several studies reported an incident-concordant relationship between altered signaling pathways and neural remodeling. In the study conducted by Suman et al. (2013), female mice were irradiated with either gamma rays (2 Gy) or 1 GeV/n 56Fe ions (1.6 Gy) and at both doses, an increase in p16, p21, p53, BAX and apoptosis was observed. A decrease in Bcl-2 and cortical thickness was also seen after both gamma and 56Fe irradiation. Another study irradiated neural stem cells with 6 Gy of gamma rays and found increased p-Akt, p-p53, p-STAT3, and mGluR1, with decreased neural stem cells (Eom et al., 2015). At 5 Gy of X-irradiation, Limoli et al. (2004) also found increased levels of p53 and phosphorylated p53 with increased apoptosis and decreased DCx+ cells.

Through the use of middle cerebral artery occlusion, a technique to simulate an ischemic stroke, alteration in signaling pathways were shown. Following the administration of this procedure in male mice, the ratios of phosphorylated to total ERK1/2, p38 and JNK increased, as well as levels of BAX, cleaved caspase-3 and the percent of apoptosis. Anti-apoptotic marker Bcl-2 also decreased after surgery (Tian et al., 2020).

Essentiality

Attenuation of altered signaling consistently results in a reduction in neural remodeling. Multiple studies showed this using genetic knockout of signaling molecules. For example, genetic knockout of Src, an upstream activator of multiple signaling pathways, or a combination of p38 and ERK1/2 in mice with a simulated ischemic stroke led to the inhibition of signaling in the MAPK pathways, decreased apoptosis, and increased neuron levels compared to wild-type mice (Tian et al., 2020). In accordance, activation of Src led to increased MAPK signaling and apoptosis compared to wild-type mice after simulated ischemic stroke (Tian et al., 2020). Two studies showing that neurons decreased following 1-5 Gy irradiation of mice found that knockout of p53 decreased apoptosis and slightly restored neuron numbers (Chow, Li and Wong, 2000; Limoli et al., 2004).

Inhibition of various signaling molecules after irradiation also led to reduced neural remodeling. The mGluR1 inhibitor LY367385 restored NSC numbers after irradiation of neural-like stem cells with 6 Gy of gamma rays (Eom et al., 2015). Similarly, the JNK inhibitor SP600125 restored neuronal differentiation after 2 Gy gamma ray irradiation of NSCs (Kanzawa et al., 2006). Zhang et al. (2018) found that activation of NFATc4/3 nuclear translocation with BDNF was able to restore neurite length and the number of total branching points in rats and rat-derived neurons after 2 Gy electron irradiation, while inactivation of NFATc4/3 nuclear translocation with CsA produced the opposite effect in rat-derived neurons after irradiation.

Uncertainties and Inconsistencies

- The changes to a signaling pathway may provide inconsistent outcomes in neural remodeling. For example, the p38 pathway is involved in many, often opposing, biological processes (Nebreda and Porras, 2000). Different cell types and exposures can be associated with the expression of different receptors of the p38 pathway, resulting in different biological changes. In addition, signaling pathways that synergize or antagonize with each other may be influenced at the same time resulting in cumulative effects across different pathways (Nebreda and Porras, 2000).
- Eom et al., 2015: Irradiation of C17.2 mouse neural stem-like cells with 6 Gy of gamma rays resulted in an increase in β-III tubulin expression, indicating a rise in neurons post-irradiation. However, all other studies observed a decrease in neuron numbers post-irradiation.

Quantitative Understanding of the Linkage

The table below provides some representative examples of quantitative linkages between the two key events. It was difficult to identify a general trend across all the studies due to differences in experimental design and reporting of the data. All data is statistically significant unless otherwise stated.

Dose Concordance

Reference	Experiment Description	Result
		The PI3K inhibitor LY294002, at a dose of 50 μM, resulted in a 0.4-fold decrease in p-Akt (activated Akt) and a decrease in p-S6 (activated S6, downstream in the PI3K/Akt pathway) to less than 0.1-fold. The mTOR inhibitor rapamycin, at a dose of 1

Kumar et al., 2005	In vitro. Hippocampal cornu ammonis (CA)3/CA1 pyramidal neurons extracted from rats were subjected to pharmacological inhibition of various signaling molecules. The level of various signaling molecules was determined with western blot. Confocal microscopy was used to assess hippocampal neuron morphology, including total dendritic branch length, number of terminal tips, soma area, spine density, and filopodia density.	μM, resulted in a decrease in p-S6 to less than 0.1-fold. The MAPK/ERK kinase (MEK) (kinase upstream of ERK) inhibitor U0126, at a dose of 10 μM, resulted in a decrease in p-ERK to less than 0.1-fold. LY294002 decreased total dendritic branch length 0.7-fold, the number of terminal tips 0.7-fold, soma area 0.6-fold, spine density 0.8-fold, and filopodia density 0.7-fold. Rapamycin decreased total dendritic branch length 0.5-fold, the number of terminal tips 0.6-fold, soma area 0.6-fold, spine density 0.7-fold, and filopodia density 0.5-fold. U0126 alone did not show any changes to neural remodeling, but U0126 with overexpression of RasL61 (activates the signaling pathway) decreased the total dendritic branch length 0.8-fold, decreased the number of terminal tips 0.4-fold, increased spine density 1.4-fold, and decreased filopodia density 0.5-fold compared to just RasL61 alone.
Kanzawa et al., 2006	In vitro. NSCs isolated from the frontal cortex of embryonic Fisher 344 rats were irradiated with a maximum of 10 Gy 137Cs gamma rays at 3.4 Gy/min. Signaling was determined by western blot. Apoptotic morphology of cells was determined with Hoechst 33258 staining. Apoptosis of just neurons was measured by a TUNEL assay.	p-JNK (activated) increased a maximum of 60% after 10 Gy. No changes in p38 or ERK1/2 activation were observed. Cytochrome C and BAX were increased, and Bcl-2 was decreased after 10 Gy. The percent of apoptotic cells increased from 40 to 65% after 10 Gy. The percent of apoptotic neurons increased from 15 to 42% after 10 Gy. The percent of TUNEL+ cells that were p-JNK+ increased from 33 to 82% after 10 Gy as well.
Silasi et al., 2004	In vivo. Male and female C57/Bl6 mice were whole-body irradiated with either acute (single 0.5 Gy dose) or chronic/fractionated (0.05 Gy/day for 10 days) X-ray radiation, both at 0.002 Gy/s. Western blot was used to assess the levels of proteins in various signaling pathways in the hippocampus. DCx staining (immature neurons) was performed to determine hippocampal neurogenesis.	After chronic radiation, male mice showed a 1.2-fold increase in Akt, a 0.95-fold decrease in p-Akt, a 0.6-fold decrease in p-ERK1/2, a 0.8-fold decrease in CaMKII, and a 0.9-fold decrease in p-CREB. Female mice showed a 1.3-fold increase in ERK1/2. After chronic radiation, DCx+ cells decreased 0.5-fold in both males and females. After acute radiation, a 0.6-fold decrease in p-ERK1/2 and a 0.7-fold decrease in CaMKII in males was observed, and DCx+ cells decreased 0.8-fold in males (non-significant) and 0.9-fold in females (non-significant).
Ivanov & Hei, 2014	In vitro. Human NSCs or neuroblastoma SK-N-SH cells were irradiated with 2.5, 5 or 10 Gy of 137Cs gamma rays (0.82 Gy/min). Western blot analysis was used to assess the levels of various signaling proteins. The percentage of hypodiploid nuclei was analyzed using flow cytometry to quantify apoptotic cells. Survival of differentiated cells was assessed with staining for Nestin (NSCs) and DCx (immature neurons).	NSCs: p53 and TRAIL were increased at 2.5 and 5 Gy. Akt, p-Akt, p-p38, p-JNK, and pro-caspase-8 and -3 (inactive) were decreased at 5 Gy. The percent of NSCs that were apoptotic increased at 2.5 and 5 Gy, with a 5-fold increase at 10 Gy. At 5 Gy, just 11% of NSCs survived after differentiation compared to the unirradiated control. Neuroblastoma cells: p53, BAX, and p-ERK1/2 were increased at 2.5, 5, and 10 Gy. p-p38 was increased at 5 and 10 Gy. p-JNK2 and p-Akt were decreased at 10 Gy. Differentiation of NSCs cultured with non-irradiated SK-N-SH cells led to a survival rate of 19%, while NSCs cultured with 5 Gy irradiated SK-N-SH cells had a survival rate of 5%.
Zhang et al., 2018	In vivo and in vitro. Male 1-month-old Sprague-Dawley rats were whole-brain irradiated with electrons (4 MeV) at 2 Gy. Primary cultured hippocampal neurons from 18-day-old Sprague-Dawley rat embryos were irradiated with electrons at 2 or 8 Gy. Western blot was used to assess phosphorylated (inactive) and dephosphorylated (active) NFATc4/3 levels in vitro. Neurite growth in vitro was determined by immunofluorescence of β-tubulin+ neurons. In vivo dendritic growth was determined in the dentate gyrus with a retrovirus labeling newborn neurons with green fluorescent protein.	In vitro: Dephosphorylated NFATc4/3 decreased by 20% at 2 Gy and 30% at 8 Gy. p-NFATc4/3 increased by 60% at 2 Gy and 90% at 8 Gy. Total neurite length decreased after 3 days by 24% at 2 Gy and 32% at 8 Gy. Branching points decreased by 29% at 2 Gy and 36% at 8 Gy after 3 days. In vivo: Total dendritic length in the dentate gyrus decreased about 30% after 2 Gy.
Chow, Li and Wong,	In vivo. Female C57BL6/J mice (57 to 123 days old) were irradiated with X-rays to the entire brain (2 Gy). p53 levels were determined through immunohistochemistry. Apoptosis levels were	In the subependymal region of the brain, 2 Gy resulted in the identification of many p53+ cells while none were found in the control. Specifically in glial cells, 2 Gy in the subependyma

2000	quantified through morphological assessment after hematoxylin and eosin staining.	increased the p53+ cells from 0.23 to 15.7%. Apoptosis in the subependyma increased from 0.33 to 11.5% at 2 Gy.
Huang et al., 2021	In vitro. HT22 hippocampal neuronal cells were irradiated with 10 Gy of X-rays (6 Gy/min). Levels of proteins in the PI3K/Akt, p53, and apoptotic signaling pathways were determined by western blot. Apoptosis was measured by flow cytometry with annexin V (marker for apoptotic cells) and propidium iodide staining.	The ratio of p-PI3K/PI3K increased 5-fold (non-significant), the ratio of p-Akt/Akt increased 2-fold (non-significant), the ratio of BAX/Bcl-2 increased 5-fold, p53 increased 2-fold, cleaved caspase-3 increased 2.7-fold, and apoptosis increased 9-fold all at 10 Gy.
El-Missiry et al., 2018	In vivo. Adult male albino Wistar rats were whole-body irradiated with 137Cs gamma rays at 4 Gy (0.695 cGy/s). Levels of signaling proteins in the hippocampus were determined with respective assay kits. Hematoxylin and eosin staining in the hippocampal dentate gyrus was used for histopathological analysis. Apoptosis levels in the hippocampus were determined by flow cytometry with annexin V (marker for apoptotic cells) and propidium iodide staining. Radiation was delivered to the animal's entire body.	Radiation at 4 Gy resulted in 2- to 4-fold increases in p53, cytochrome C, BAX, and caspase-3, -8, and -9 levels. Radiation at 4 Gy also resulted in a 0.2-fold decrease in Bcl-2. The percent of live cells decreased 0.6-fold, the frequency of apoptosis increased 3- to 4-fold, and the frequency of necrosis increased 7-fold. In addition, 4 Gy resulted in extensive damage to the dentate gyrus.
Pius-Sadowska et al., 2016	In vivo. Female 6- to 8-week-old BALB/c mice were whole-brain irradiated with 60Co gamma rays at 10 Gy. After whole-brain irradiation, the levels of various signaling molecules were assessed with western blot in the brain. Apoptosis was measured with a TUNEL assay in the hippocampus. Nissl staining was used to assess neuron morphology in the hippocampus.	Irradiation at 10 Gy resulted in a maximum 1.8-fold increase in caspase-3, a 1.7-fold increase in BDNF, a 1.8-fold increase in TrkA, a 3.8-fold increase in TrkB, a 1.7-fold increase in TrkC, a 4.1-fold increase in p-ERK1/2, and a 2.9-fold increase in p-Akt. Without irradiation, no TUNEL+ cells were found in the brain, while 10 Gy resulted in the detection of apoptotic nuclei in the dentate gyrus. Also, degenerative morphological changes were observed in the hippocampus after 10 Gy.
Ji et al., 2014	In vivo. Male 1-month-old Sprague-Dawley rats were whole-brain irradiated with electrons (4 MeV) at 20 Gy. Western blot was performed to assess the levels and activity of proteins in the BDNF-pCREB pathway in the hippocampus. Neurogenesis in the dentate gyrus was assessed using DCx (immature neurons) or BrdU/NeuN (new neurons) staining.	Irradiation at 20 Gy decreased p-ERK1/2 by 15%, p-Akt by 34% BDNF by 38%, p-TrkB by 54%, p-CaMKII by 30%, and p-CREB by 29%. Irradiation at 20 Gy also reduced the number of DCx+ cells by 92% and the number of BrdU+/NeuN+ cells by 82%.

Time Concordance

Reference	Experiment Description	Result
Kanzawa et al., 2006	In vitro. NSCs isolated from the frontal cortex of embryonic Fisher 344 rats were irradiated with 137Cs gamma rays at 10 Gy (3.4 Gy/min). Signaling was determined by western blot. Apoptotic morphology of cells was determined with Hoechst 33258 staining. Apoptosis of just neurons was measured by a TUNEL assay.	p-JNK increased 30% after 1h and 60% after 2h post-irradiation. Starting 24h post-irradiation, BAX and cytochrome C were increased, and Bcl-2 was decreased. Apoptosis increased 48h post-irradiation.
Suman et al., 2013	In vivo. Female 6- to 8-week-old C57BL/6J mice were irradiated with either 137Cs gamma rays (2 Gy) or 1 GeV/n 56Fe ions (1.6 Gy) both at 1 Gy/min. p16, p21, p53, BAX, and Bcl-2 levels were determined in the cerebral cortex with immunoblotting. Hematoxylin and eosin staining was used to measure cerebral cortex thickness, and a TUNEL assay was used to measure apoptosis.	Altered signaling through p16, p21, p53, BAX, and Bcl-2 protein levels was observed as early as 2 months post-irradiation, while increased apoptosis and decreased cortical thickness were only shown at 12 months.
Limoli et al., 2004	In vivo and in vitro. Male 2-month-old C57BL/J6 mice (1.75 Gy/min) and neural precursor cells (4.5 Gy/min) isolated from rats were irradiated with X-rays at 5 Gy. Mice were irradiated cranially. Western blot analysis was done in vitro to measure levels of p53 and p21 proteins. An antibody against DCx was used to detect immature neurons in the dentate gyrus in vivo. FACS analysis of propidium iodide fluorescence was used to assess apoptosis in vitro.	In vitro: At 2h post-irradiation, p53 protein levels increased 2-fold compared to unirradiated controls. At 6h post-irradiation, p53 protein levels increased 4-fold compared to unirradiated controls. At the same timepoints increases in p21 and p-p53 were observed. Apoptosis showed a maximum increase 12h post-irradiation. In vivo: DCx+ cells were decreased at 24h post-irradiation.
	In vitro. Human NSCs or neuroblastoma SK-N-SH cells were irradiated	Altered signaling in both cell types was

Ivanov & Hei, 2014	with 5 Gy of 137Cs gamma rays (0.82 Gy/min). Western blot analysis was used to assess the levels of various signaling proteins. The percentage of hypodiploid nuclei was analyzed using flow cytometry to quantify apoptotic cells. Survival of differentiated cells was assessed with staining for Nestin (neuroprogenitors) and DCx (immature neurons).	observed 6h post-irradiation. Apoptosis of NSCs was observed only 24h post-irradiation. NSC differentiation was reduced 10-12 days post-irradiation.
Zhang et al., 2018	In vivo and in vitro. Male 1-month-old Sprague-Dawley rats were whole-brain irradiated with electrons (4 MeV) at 2 Gy. Primary cultured hippocampal neurons from 18-day-old Sprague-Dawley rat embryos were irradiated with electrons at 2 or 8 Gy. Western blot was used to assess phosphorylated (inactive) and dephosphorylated (active) NFATc4/3 levels in vitro. Neurite growth in vitro was determined by immunofluorescence of β-tubulin+ neurons. In vivo dendritic growth was determined with a retrovirus labeling newborn neurons with green fluorescent protein.	In vitro: Dephosphorylated NFATc4/3 was decreased and p-NFATc4/3 was increased at both 1- and 3-days post-irradiation. Although total neurite length was decreased at both 1 and 3 days as well, the number of branching points was only decreased at 3 days post-irradiation. In vivo: Total dendritic length decreased at both 14- and 28-days post-irradiation.
Pius-Sadowska et al., 2016	In vivo. Female 6- to 8-week-old BALB/c mice were whole-brain irradiated with 60Co gamma rays at 10 Gy. The levels of various signaling molecules were assessed with western blot in the brain. Apoptosis was measured with a TUNEL assay in the hippocampus. Nissl staining was used to assess neuron morphology in the hippocampus.	Following 10 Gy, the various signaling molecules were increased as early as 3h, while apoptosis and morphological changes were found 48h post-irradiation.

Incidence Concordance

Reference	Experimental Description	Results
Tian et al., 2020	In vivo. Male 8- to 10-week-old C57BL/6J mice were subjected to middle cerebral artery occlusion to simulate an ischemic stroke. MAPK signaling molecules and BAX/Bcl-2 apoptotic markers were measured with western blotting in ischemic brain tissues. Apoptosis was determined using a TUNEL assay in the ischemic cerebral cortex. Endpoints were measured 7 days after surgery.	After surgery, ERK1/2, p38 and JNK mRNA increased 2- to 3- fold. The ratios of phosphorylated to total ERK1/2, p38 and JNK increased 2- to 3- fold as well. BAX increased 2.5-fold, Bcl-2 decreased 0.15-fold, and cleaved caspase-3 increased 1.5-fold. The % of TUNEL+ cells increased 2-fold.
Eom et al., 2015	In vitro. C17.2 mouse neural stem-like cells were irradiated with 6 Gy of 137Cs gamma rays at 0.95 Gy/min. Protein levels in signaling pathways were determined by western blot. The number of cells expressing nestin (NSC marker) were quantified with immunocytochemistry. Endpoints were measured 72h post-irradiation.	Radiation at 6 Gy led to increased p-Akt, p-p53, p-STAT3, and mGluR1 at least 2-fold. NSCs decreased 0.4-fold.
Suman et al., 2013	In vivo. Female 6- to 8-week-old C57BL/6J mice were irradiated with either 137Cs gamma rays (2 Gy) or 1 GeV/n 56Fe ions (1.6 Gy) both at 1 Gy/min. p16, p21, p53, BAX, and Bcl-2 levels were determined in the cerebral cortex with immunoblotting. Hematoxylin and eosin staining was used to measure cerebral cortex thickness, and a TUNEL assay was used to measure apoptosis.	p16 increased a maximum of 3.4-fold after gamma rays and 5-fold after 56Fe radiation. p21 increased a maximum of 1.5-fold after gamma rays and 3-fold after 56Fe radiation. p53 increased a maximum of 8.4-fold after gamma rays and 9-fold after 56Fe radiation. BAX increased a maximum of 2.3-fold after gamma rays and 6.7-fold after 56Fe radiation. Bcl-2 decreased a maximum of 0.6-fold after gamma rays and 0.4-fold after 56Fe radiation. Gamma rays increased apoptosis 1.8-fold and 56Fe ions increased apoptosis 3.6-fold. Gamma rays decreased cortical thickness 0.9-fold and 56Fe ions decreased cortical thickness 0.7-fold.
Limoli et al., 2004	In vivo and in vitro. Male 2-month-old C57BL/J6 mice (1.75 Gy/min) and neural precursor cells (4.5 Gy/min) isolated from rats were irradiated with X-rays. Mice were irradiated cranially. Western blot analysis was done in vitro to measure levels of p53 and p21 proteins. An antibody against DCx was used to detect immature neurons in the dentate gyrus in vivo. FACS analysis of propidium iodide fluorescence	In vitro: At 5 Gy, p53 levels increased a maximum of 4-fold, while p-p53 and p21 were also increased at this dose. Apoptosis was increased a maximum of 1.4-fold after 5 Gy. In vivo: The number of DCx+ cells decreased 0.4-fold after 5 Gy.

	was used to assess apoptosis in vitro.	

Known modulating factors

Modulating factor	Details	Effects on the KER	References
Genetic	Src (regulates the activation of MAPK pathways) knockout	Src knockout in mice inactivated MAPK and apoptotic signaling and reduced apoptosis in the brain after middle cerebral artery occlusion.	Tian et al., 2020
	miR-137 (silences Src) knockout	miR-137 knockout in mice increased MAPK and apoptotic signaling and further increased apoptosis after middle cerebral artery occlusion.	Tian et al., 2020
	p38 and ERK1/2 knockout	p38 and ERK1/2 knockout in mice inactivated MAPK and apoptotic signaling and reduced apoptosis in the brain after middle cerebral artery occlusion.	Tian et al., 2020
	p53 knockout	Irradiation (1-5 Gy) of p53 knockout mice led to a higher number of neurons and decreased apoptosis compared to irradiation of wild-type mice.	Chow, Li and Wong, 2000; Limoli et al., 2004
Drug	LY367385 (mGluR1 inhibitor). mGluR1 is involved in neuronal differentiation.	LY367385 (25 M) increased the number of NSCs after 6 Gy radiation of C17.2 neural stem-like cells.	Eom et al., 2015
	SP600125 (JNK inhibitor)	SP600125 (5 µM) restored neuronal differentiation after it was reduced by 2 Gy radiation of rat NSCs.	Kanzawa et al., 2006
	Cyclosporin (CsA, prevents NFATc4/3 nuclear translocation)	CsA (1 µg/mL) further reduced the levels of dephosphorylated NFATc4/3 as well as total neurite length and branching points after both 2 and 8 Gy irradiation of rat neurons.	Zhang et al., 2018
	BDNF (induces NFATc4/3 nuclear translocation)	BDNF (100 ng/mL in vitro, 0.75 µg/1.5 µL in vivo) slightly restored the levels of dephosphorylated NFATc4/3 after 2 Gy irradiation and completely restored neurite length and total branching points both in vitro and in vivo.	Zhang et al., 2018
Sex	Female mice	Male mice showed many changes in Akt and ERK1/2 activity following acute and chronic irradiation at 0.5 Gy. However, female mice showed only few changes. In addition, male mice showed a trend of fewer immature neurons after 0.5 Gy radiation.	Silasi et al., 2004
Exercise	Forced running in 30-minute intervals twice per day, 5 times per week for 3 weeks.	Forced running after irradiation completely restored the levels of the signaling molecules in the BDNF-pCREB pathway and slightly restored neurogenesis.	Ji et al., 2014

Known Feedforward/Feedback loops influencing this KER

NA

References

Betlazar, C. et al. (2016), "The impact of high and low dose ionising radiation on the central nervous system", Redox Biology, Vol. 9, Elsevier, Amsterdam, https://doi.org/10.1016/j.redox.2016.08.002.

Cekanaviciute, E., S. Rosi and S. V. Costes. (2018), "Central Nervous System Responses to Simulated Galactic Cosmic Rays", International Journal of Molecular Sciences, Vol. 19/11, Multidisciplinary Digital Publishing Institute (MDPI), Basel, https://doi.org/10.3390/IJMS19113669.

Chakraborti, A. et al. (2012), "Cranial Irradiation Alters Dendritic Spine Density and Morphology in the Hippocampus", PLOS ONE, Vol. 7/7, Public Library of Science, San Francisco, https://doi.org/10.1371/JOURNAL.PONE.0040844.

Chow, B. M., Y.-Q. Li and C. S. Wong. (2000), "Radiation-induced apoptosis in the adult central nervous system is p53-dependent", Cell Death & Differentiation, Vol. 7/8, Springer Nature, https://doi.org/10.1038/sj.cdd.4400704.

Cunha, C., R. Brambilla and K. L. Thomas. (2010), "A simple role for BDNF in learning and memory?", Frontiers in Molecular Neuroscience, Vol. 3/1, Frontiers, https://doi.org/10.3389/neuro.02.001.2010.

Davis, S. and S. Laroche. (2006), "Mitogen-activated protein kinase/extracellular regulated kinase signalling and memory stabilization: a review", Genes, Brain and Behavior, Vol. 5, Wiley, https://doi.org/10.1111/j.1601-183X.2006.00230.x.

El-Missiry, M. A. et al. (2018), "Neuroprotective effect of epigallocatechin-3-gallate (EGCG) on radiation-induced damage and apoptosis in the rat hippocampus", International Journal of Radiation Biology, Vol. 94/9, Informa, London, https://doi.org/10.1080/09553002.2018.1492755.

Eom, H. S. et al. (2015), "Ionizing radiation induces neuronal differentiation of Neuro-2a cells via PI3-kinase and p53-dependent pathways", International Journal of Radiation Biology, Vol. 91/7, Informa, London, https://doi.org/10.3109/09553002.2015.1029595.

Falcicchia, C. et al. (2020), "Involvement of p38 MAPK in Synaptic Function and Dysfunction", International Journal of Molecular Sciences, Vol. 21/16, MDPI, Basel, https://doi.org/10.3390/ijms21165624.

Hladik, D. and S. Tapio. (2016), "Effects of ionizing radiation on the mammalian brain", Mutation Research - Reviews in Mutation Research, Vol. 770, Elsevier, Amsterdam, https://doi.org/10.1016/j.mrrev.2016.08.003.

Huang, Y. et al. (2021), "Mesenchymal Stem Cell-Conditioned Medium Protects Hippocampal Neurons From Radiation Damage by Suppressing Oxidative Stress and Apoptosis", Dose-Response, Vol. 19/1, SAGE publications, https://doi.org/10.1177/1559325820984944.

Ivanov, V. N. and T. K. Hei. (2014), "A role for TRAIL/TRAIL-R2 in radiation-induced apoptosis and radiation-induced bystander response of human neural stem cells", Apoptosis, Vol. 19/3, Springer Nature, https://doi.org/10.1007/s10495-013-0925-4.

Ji, J. et al. (2014), "Forced running exercise attenuates hippocampal neurogenesis impairment and the neurocognitive deficits induced by whole-brain irradiation via the BDNF-mediated pathway", Biochemical and Biophysical Research Communications, Vol. 443/2, Elsevier, Amsterdam, https://doi.org/10.1016/j.bbrc.2013.12.031.

Kanzawa, T. et al. (2006), "Ionizing radiation induces apoptosis and inhibits neuronal differentiation in rat neural stem cells via the c-Jun NH2-terminal kinase (JNK) pathway", Oncogene, Vol. 25/26, Springer Nature, https://doi.org/10.1038/sj.onc.1209414.

Kumar, V. et al. (2005), “Regulation of Dendritic Morphogenesis by Ras-PI3K-Akt-mTOR and Ras-MAPK Signaling Pathways”, Journal of Neuroscience, Vol. 25/49, Society for Neuroscience, https://doi.org/10.1523/JNEUROSCI.2284-05.2005.

Limoli, C. L. et al. (2004), "Radiation Response of Neural Precursor Cells: Linking Cellular Sensitivity to Cell Cycle Checkpoints, Apoptosis and Oxidative Stress", Radiation Research, Vol. 161/1, BioOne, https://doi.org/10.1667/RR3112.

Long, H.-Z. et al. (2021), "PI3K/AKT Signal Pathway: A Target of Natural Products in the Prevention and Treatment of Alzheimer’s Disease and Parkinson’s Disease", Frontiers in Pharmacology, Vol. 12, Frontiers, https://doi.org/10.3389/fphar.2021.648636.

Macian, F. (2005), "NFAT proteins: key regulators of T-cell development and function", Nature Reviews Immunology, Vol. 5/6, Springer Nature, https://doi.org/10.1038/nri1632.

Mazzucchelli, C. and R. Brambilla. (2000), "Ras-related and MAPK signalling in neuronal plasticity and memory formation", Cellular and Molecular Life Sciences, Vol. 57/4, Springer Nature, https://doi.org/10.1007/PL00000722.

McHugh, D. and J. Gil. (2018), "Senescence and aging: Causes, consequences, and therapeutic avenues", Journal of Cell Biology, Vol. 217/1, Rockefeller University Press, New York, https://doi.org/10.1083/jcb.201708092.

Mielke, K. and T. Herdegen. (2000), "JNK and p38 stresskinases — degenerative effectors of signal-transduction-cascades in the nervous system", Progress in Neurobiology, Vol. 61/1, Elsevier, Amsterdam, https://doi.org/10.1016/S0301-0082(99)00042-8.

Nebreda, A. R. and A. Porras. (2000), "p38 MAP kinases: beyond the stress response", Trends in Biochemical Sciences, Vol. 25/6, Elsevier, Amsterdam, https://doi.org/10.1016/S0968-0004(00)01595-4.

Pius-Sadowska, E. et al. (2016), "Alteration of Selected Neurotrophic Factors and their Receptor Expression in Mouse Brain Response to Whole-Brain Irradiation", Radiation Research, Vol. 186/5, BioOne, https://doi.org/10.1667/RR14457.1.

Rai, S. N. et al. (2019), "The Role of PI3K/Akt and ERK in Neurodegenerative Disorders", Neurotoxicity Research, Vol. 35/3, Elsevier, Amsterdam, https://doi.org/10.1007/s12640-019-0003-y.

Ran, I., I. Laplante and J.-C. Lacaille. (2012), "CREB-Dependent Transcriptional Control and Quantal Changes in Persistent Long-Term Potentiation in Hippocampal Interneurons", Journal of Neuroscience, Vol. 32/18, Society for Neuroscience, https://doi.org/10.1523/JNEUROSCI.5463-11.2012.

Rodgers, E. E. and A. B. Theibert. (2002), "Functions of PI 3-kinase in development of the nervous system", International Journal of Developmental Neuroscience, Vol. 20/3–5, Wiley, https://doi.org/10.1016/S0736-5748(02)00047-3.

Sherrin, T., T. Blank and C. Todorovic. (2011), "c-Jun N-terminal kinases in memory and synaptic plasticity", Reviews in the Neurosciences, Vol. 22/4, De Gruyter, https://doi.org/10.1515/rns.2011.032.

Silasi, G. et al. (2004), "Selective brain responses to acute and chronic low-dose X-ray irradiation in males and females", Biochemical and Biophysical Research Communications, Vol. 325/4, Elsevier, Amsterdam, https://doi.org/10.1016/j.bbrc.2004.10.166.

Suman, S. et al. (2013), "Therapeutic and space radiation exposure of mouse brain causes impaired DNA repair response and premature senescence by chronic oxidant production", Aging, Vol. 5/8, https://doi.org/10.18632/aging.100587.

Tian, R. et al. (2020), "miR-137 prevents inflammatory response, oxidative stress, neuronal injury and cognitive impairment via blockade of Src-mediated MAPK signaling pathway in ischemic stroke", Aging, Vol. 12/11, https://doi.org/10.18632/aging.103301.

Wang, Q. et al. (2020), "Radioprotective Effect of Flavonoids on Ionizing Radiation-Induced Brain Damage", Molecules, Vol. 25/23, MDPI, Basel, https://doi.org/10.3390/molecules25235719.

Zhang, Q. et al. (2018), "The effect of brain-derived neurotrophic factor on radiation-induced neuron architecture impairment is associated with the NFATc4/3 pathway", Brain Research, Vol. 1681, Elsevier, Amsterdam, https://doi.org/10.1016/j.brainres.2017.12.032.

Relationship: 2841: Increase, DNA strand breaks leads to Increase, Neural Remodeling

AOPs Referencing Relationship

AOP Name	Adjacency	Weight of Evidence	Quantitative Understanding
Deposition of Energy Leading to Learning and Memory Impairment	adjacent	Moderate	Low

Evidence Supporting Applicability of this Relationship

Taxonomic Applicability

Term	Scientific Term	Evidence	Links
human	Homo sapiens	Low	NCBI
mouse	Mus musculus	Moderate	NCBI
rat	Rattus norvegicus	Low	NCBI

Life Stage Applicability

Life Stage	Evidence
Juvenile	Low
Adult	Moderate

Sex Applicability

Sex	Evidence
Male	Moderate
Female	Low

Evidence for this relationship is derived from studies that use human-derived cells and mouse models, with most of the evidence in mice. There is in vivo evidence in male animals. Most evidence is from adult models.

Key Event Relationship Description

DNA single strand breaks (SSBs) and double strand breaks (DSBs) can lead to cell cycle arrest and apoptosis (Madabhushi, Pan and Tsai, 2014; Michaelidesova et al., 2019). In proliferative cells like neural stem/progenitor cells this will reduce neurogenesis within the brain (Alt and Schwer, 2018; Lee and McKinnon, 2007; Michaelidesova et al., 2019). Although the role of DSBs is less well-characterized in mature neurons (Lee and McKinnon, 2007; Thadathil fsylet al., 2019), some evidence suggests that unrepaired DNA strand breaks could also have deleterious effects in these neurons (Wang et al., 2017). Furthermore, there is evidence that DNA strand breaks can induce changes to neural plasticity and synaptic activity through changes in gene expression (Konopka and Atkin, 2022; Thadathil et al., 2019). This can occur via changes in N-methyl-D-aspartate (NMDA) and α-amino-3-hydroxy-5-methyl-isoxazole-4-propionate (AMPA) receptor activity or changes in the expression of early response genes (ERGs) that encode transcription factors controlling processes like neurite outgrowth, synapse development and maturation and the balance between excitatory and inhibitory synapses (Konopka and Atkin, 2022).

Evidence Supporting this KER

Overall Weight of Evidence: Moderate

Biological Plausibility

The biological plausibility between DNA strand breaks leading to neural remodeling is supported by literature.

Neural remodeling due to DNA strand breaks can occur through apoptosis (Abner and McKinnon, 2004; Desai et al., 2022; Madabhushi, Pan and Tsai, 2014; Michaelidesova et al., 2019; Wang et al., 2017; Zhu et al., 2019). Newly post-mitotic neurons with DSBs may undergo checkpoint mediated apoptosis as a mechanism to prevent their incorporation into the nervous system as

mature neurons (Alt and Schwer, 2018; Lee and McKinnon, 2007). In response to DSBs, developing neural progenitor cells and a trace number of neural stem cells will undergo cell cycle arrest at critical stages. In the mammalian genome, DNA strand breaks can regulate checkpoint activation through the activation of phosphoinositide 3-kinase (PI3K)-related family of serine/threonine kinases (PIKK), ataxia telangiectasia mutated (ATM) and ATM/RAD3-related (ATR), that can phosphorylate many downstream proteins (Wang et al., 2017). Specifically, DSBs can activate ATM which phosphorylates p53, which can then act on apoptosis factors, p53-upregulated modulator of apoptosis (PUMA), CD95 (Fas/APO1) and apoptotic peptidase activating factor 1 (Apaf1) (Zhu et al., 2019). Activation of this pathway in proliferating cells like neuronal precursors can reduce neurogenesis (Wang et al., 2017; Michaelidesova et al., 2019).

DNA strand breaks can also lead to changes in synaptic activity, neural plasticity, proliferation, and differentiation. Neurons communicate electrically and chemically through synaptic contacts. Neural plasticity refers to the ability of the nervous system to modify its structure, function or connections in response to stimuli. DNA damage can modulate the activity and expression of glutamate receptors, including NMDA/AMPA, which are involved in synaptic activity, plasticity and neuronal activation in the central nervous system. The changes in receptor activity and expression modulate neuronal gene expression and lead to changes in plasticity (Konopka and Atkin, 2022). Additionally, changes in ERG expression following DNA damage can lead to certain neural remodeling changes, such as neurite outgrowth, synapse development and maturation (Konopka and Atkin, 2022). As well, inhibition of the cell cycle by DNA strand breaks can impair neurogenesis through decreased differentiation and proliferation of neural stem cells (NSCs) (Michaelidesova et al., 2019).

Empirical Evidence

The empirical evidence for this KER comes from in vivo mouse models as well as in vitro mouse- and human-derived cell models. Stressors used included X-ray radiation (Barazzuol, Ju and Jeggo, 2017; Barazzuol et al., 2015; Huang et al., 2021; Zhang et al., 2017), 60Co gamma ray radiation (Zanni et al., 2015), 137Cs gamma rays (Acharya et al., 2010), and 6 MV photon radiation (Schmal et al., 2019). Neural remodeling can be determined through various endpoints, including neuronal apoptosis, morphology, proliferation, differentiation and altered synaptic activity. Markers of DNA strand breaks in this KER include p53 binding protein 1 (53BP1), phosphorylation of H2AX (γ-H2AX), and phosphorylation of ATM (p-ATM).

Dose Concordance

Several studies demonstrate dose concordance for the relationship between DNA strand breaks leading to neural remodeling. Adult mice irradiated with X-rays showed increased 53BP1 foci in the lateral ventricle at doses as low as 0.1 Gy, while neuronal apoptosis and impaired neurogenesis were observed as low as 1 Gy (Barazzuol, Ju and Jeggo, 2017). Juvenile and adult male mice irradiated with 0.5 to 2 Gy of 6 MV photons showed increased DSBs in neurons at the same doses as impaired neurogenesis (Schmal et al., 2019). X-ray irradiation of mice aged 2 to 4 months with 50 mGy, 100 mGy and 200 mGy showed increased DSBs in the cerebellum, as well as apoptosis in the subventricular zone (SVZ) (Barazzuol et al., 2015).

Time Concordance

Many studies demonstrate that DNA strand breaks occur prior to neural remodeling. Studies frequently measure increased DNA DSBs through γ-H2AX foci or 53BP1 foci within 1 h post-irradiation and increased neuronal apoptosis 4 to 6 h post-irradiation (Acharya et al., 2010; Barazzuol, Ju and Jeggo, 2017; Barazzuol et al., 2015; Zhang et al., 2017). Studies have also measured neural remodeling at later timepoints than this. For example, Zhang et al. (2017) showed increased apoptosis at 2 days after 12 Gy of X-ray irradiation in HT22 hippocampal neurons, and Acharya et al. (2010) demonstrated decreased human NSC (hNSC) differentiation at 2 days and decreased cell numbers at 3 days following 5 Gy of 137Cs gamma rays.

Incidence Concordance

Few studies show greater levels of DNA strand breaks than neural remodeling. In hNSCs irradiated with 5 Gy of 137Cs gamma rays, γ-H2AX foci increased 30-fold, while apoptosis increased 2- to 3-fold and hNSC differentiation decreased 0.5-fold (Acharya et al., 2010). A study using multiple doses of X-rays (50, 100 and 200 mGy) demonstrated greater increases to DNA strand breaks than to apoptosis. At 200 mGy, 53BP1 foci increased 30-fold and terminal deoxynucleotidyl transferase dUTP nick end labeling (TUNEL)+ cells increased 10-fold (Barazzuol et al., 2015).

Essentiality

Multiple studies show that inhibition of DNA strand breaks can reduce neural remodeling. Treatment of HT22 hippocampal neuronal cells with minocycline inhibited the expression of γ-H2AX and the p-ATM/ATM ratio as well as reduced apoptosis following X-ray exposure (Zhang et al., 2017). Similarly, mesenchymal stem cell conditioned media (MSC-CM) reduced the expression of γ-H2AX and reduced apoptosis, reversing the changes induced by X-ray radiation (Huang et al., 2021). Lithium chloride was also shown to

reduce γ-H2AX levels and increase proliferation in neural stem cells irradiated with 60Co gamma rays (Zanni et al., 2015).

Uncertainties and Inconsistencies

None identified.

Quantitative Understanding of the Linkage

The table below provides some representative examples of quantitative linkages between the two key events. All data is statistically significant unless otherwise stated.

Dose Concordance

Reference	Experiment Description	Result
Schmal et al., 2019	In vivo. Juvenile and adult male mice were whole-body irradiated with various doses (5, 10, 15 or 20 fractions of 0.1 Gy) of 6 MV photons. DNA DSBs were determined by 53BP1 immunofluorescence in mature neurons. Neural remodeling was assessed by the level of DCX+ neuroprogenitor cells and transcription factor SRY (sex-determining-region-Y) box 2 (SOX2)+ stem/progenitor cells in the subgranular zone (SGZ) of the hippocampal dentate gyrus.	At 72h post-irradiation of juvenile mice, 53BP1 foci increased 1.5-fold at 0.5 Gy and 2.7-fold at 2 Gy, while DCX+ cells decreased 0.9-fold at 0.5 Gy and 0.7-fold at 2 Gy. At 72h post-irradiation of adult mice, 53BP1 foci increased 1.2-fold (non-significant) at 0.5 Gy and 2-fold at 2 Gy, while DCX+ cells decreased 0.9-fold at 0.5 Gy and 0.8-fold at 2 Gy. SOX2+ cells did not change at 72 h post-irradiation, but decreased 0.6-fold in juvenile mice and 0.8-fold in adult mice at 2 Gy after 1 month.
Barazzuol et al., 2015	In vivo. C57BL/6 mice aged 2-4 months were irradiated with 50 mGy, 100 mGy and 200 mGy of X-rays. Apoptosis in the SVZ was determined with a TUNEL assay. DSBs in the cerebellum were quantified with 53BP1 immunofluorescence.	53BP1 foci increased linearly from 0.05 foci/cell at 0 Gy to 1.3 foci per cell at 200 mGy. The number of TUNEL+ cells increased linearly from 5 cells/section at 0 Gy to about 50 cells/section at 200 mGy.
Barazzuol, Ju and Jeggo, 2017	In vivo. C57BL/6 mice were irradiated with various doses of X-rays (0.5 Gy/min). Immunofluorescence was used to detect TUNEL+ cells (apoptotic), Ki67+ cells (proliferating) and DCX+ cells (neuron progenitors). 53BP1 was also detected by immunofluorescence.	53BP1 foci increased over 10-fold at 0.1 Gy and about 80-fold at 2 Gy in the lateral ventricle. At 1, 2, and 3 Gy, Ki67+ cells in the lateral ventricle decreased 0.2-fold, and TUNEL+ cells were increased in the lateral ventricle. At 2 Gy, DCX+ cells decreased to less than 0.1-fold.

Time Concordance

Reference	Experiment Description	Result
Acharya et al., 2010	In vitro. hNSCs were irradiated with 5 Gy of 137Cs gamma rays (2.2 Gy/min. γ-H2AX foci for DSBs were quantified with immunofluorescence. Apoptosis of hNSCs was measured using fluorescence-activated cell sorting (FACS) for poly (ADP-ribose) polymerase (PARP) cleavage (early marker) and annexin V binding (late marker). Differentiation of hNSCs was measured by β-III-Tubulin staining and cell numbers were measured by SYBR green fluorescence.	γ-H2AX foci were increased from 5% to 95% as early as 0.3 h post-irradiation. PARP+ cells were increased 3-fold at 6 h post-irradiation, while annexin V+ cells were increased 2-fold 48 h post-irradiation. hNSC differentiation was decreased 0.5-fold 2 days post-irradiation. hNSC cell numbers were decreased 0.3-fold 3 days post-irradiation.
Barazzuol et al., 2015	In vivo. C57BL/6 mice aged 2-4 months were irradiated with 50 mGy, 100 mGy and 200 mGy of X-rays. Apoptosis in the SVZ was determined with a TUNEL assay. DSBs in the cerebellum were quantified with 53BP1 immunofluorescence.	The earliest increase in 53BP1 foci was observed at 0.25 h post-irradiation. The earliest increase in TUNEL+ cells was observed at 6 h post-irradiation.
Zhang et al., 2017	In vitro. Cells from the HT22 mouse hippocampal neuronal cell line were irradiated with 12 Gy of X-rays (4 Gy/min). γ-H2AX and p-ATM protein expression were determined with western blot. Apoptosis was determined with flow cytometry using annexin V and propidium iodide staining.	At 30 minutes post-irradiation, γ-H2AX increased 3.2-fold and the ratio of p-ATM/ATM increased 4.4-fold. Apoptosis increased over 10-fold at 48 h post-irradiation.
Barazzuol, Ju and Jeggo, 2017	In vivo. C57BL/6 mice were irradiated with various doses of X-rays (0.5 Gy/min). Immunofluorescence was used to detect TUNEL+ cells (apoptotic), Ki67+ cells (proliferating) and DCX+ cells (neuron progenitors). 53BP1 was also detected by immunofluorescence.	A peak in 53BP1 foci occurred at 0.5 h post-irradiation. Changes to TUNEL+ cells, Ki67+ cells and DCX+ cells were observed at 6 h post-irradiation.

Incidence Concordance

Reference	Experimental Description	Results
Acharya et al., 2010	In vitro. hNSCs were irradiated with 5 Gy of 137Cs gamma rays (2.2 Gy/min. γ-H2AX foci for DSBs were quantified with immunofluorescence. Apoptosis of hNSCs was measured using FACS for PARP cleavage (early marker) and annexin V binding (late marker). Differentiation of hNSCs was measured by β-III-Tubulin staining and cell numbers were measured by SYBR green fluorescence.	γ-H2AX foci were increased about 20-fold. PARP+ cells were increased 3-fold and annexin V+ cells were increased 2-fold. hNSC differentiation was decreased by 0.5-fold. hNSC cell numbers were decreased 0.3-fold.
Barazzuol et al., 2015	In vivo. C57BL/6 mice aged 2-4 months were irradiated with 50 mGy, 100 mGy and 200 mGy of X-rays. Apoptosis in the SVZ was determined with a TUNEL assay. DSBs in the cerebellum were quantified with 53BP1 immunofluorescence.	53BP1 foci increased almost 30-fold between 0 Gy and 200 mGy. The number of TUNEL+ cells increased about 10-fold between 0 Gy and 200 mGy.

Known modulating factors

Modulating factor	Details	Effects on the KER	References
Drug	MSC-CM	Treatment reduced the expression of γ-H2AX and reduced apoptosis	Huang et al., 2021
	Lithium chloride	Reduced the level of γ-H2AX and increased proliferation of neural stem cells.	Zanni et al., 2015
	Minocycline (an antibiotic shown to reduce radiation-induced memory loss)	Treatment inhibited the increase in γ-H2AX and p-ATM and reduced apoptosis.	Zhang et al., 2017
Genetics	DNA ligase IV-null mutation	Mice with this mutation show greatly increased levels of apoptosis compared to wild-type mice due to reduced DNA repair following irradiation.	Barazzuol et al., 2015
Age	Hippocampal neurogenesis is more pronounced in younger mice.	Proliferative potential of neuronal precursors in the hippocampus, determined by Ki-67 immunostaining, was significantly reduced in juvenile mice but not significantly affected in adult mice after irradiation.	Schmal et al., 2019

Known Feedforward/Feedback loops influencing this KER

Some studies suggest that neuron activity can generate DNA DSBs. Specifically, it has been shown that γ-H2AX foci can be formed by the activation of NMDA a https://www.canada.ca/en/public-health/services/laboratory-biosafety-biosecurity/pathogen-safety-data-sheets-risk-assessment/epstein-barr-virus.html nd AMPA glutamate receptors (reviewed by Konopka and Atkin, 2022). Activity induced DSBs in mature neurons subsequently influence gene expression and neuronal activity (Alt and Schwer, 2018).

References

Abner, C. W. and P. J. McKinnon. (2004), "The DNA double-strand break response in the nervous system", DNA Repair, Vol. 3/8–9, Elsevier, Amsterdam, https://doi.org/10.1016/j.dnarep.2004.03.009.

Acharya, M. M. et al. (2010), "Consequences of ionizing radiation-induced damage in human neural stem cells", Free Radical Biology and Medicine, Vol. 49/12, Elsevier, Amsterdam, https://doi.org/10.1016/j.freeradbiomed.2010.08.021.

Alt, F. W. and B. Schwer. (2018), "DNA double-strand breaks as drivers of neural genomic change, function, and disease", DNA Repair, Vol. 71, Elsevier, Amsterdam, https://doi.org/10.1016/j.dnarep.2018.08.019.

Barazzuol, L., L. Ju, and P. A. Jeggo. (2017), “A coordinated DNA damage response promotes adult quiescent neural stem cell activation”, PLoS biology, 15(5), PLOS, San Francisco, https://doi.org/10.1371/journal.pbio.2001264

Barazzuol, L. et al. (2015), "Endogenous and X-ray-induced DNA double strand breaks sensitively activate apoptosis in adult neural stem cells", Journal of Cell Science, Vol. 128/19, The Company of Biologists, Cambridge, https://doi.org/10.1242/jcs.171223.

Desai, R. I. et al. (2022), "Impact of spaceflight stressors on behavior and cognition: A molecular, neurochemical, and neurobiological perspective", Neuroscience & Biobehavioral Reviews, Vol. 138, Elsevier, Amsterdam, https://doi.org/10.1016/j.neubiorev.2022.104676.

Huang, Y. et al. (2021), "Mesenchymal Stem Cell-Conditioned Medium Protects Hippocampal Neurons From Radiation Damage by Suppressing Oxidative Stress and Apoptosis", Dose-Response, Vol. 19/1, SAGE Publications https://doi.org/10.1177/1559325820984944.

Konopka, A. and J. D. Atkin. (2022), "The Role of DNA Damage in Neural Plasticity in Physiology and Neurodegeneration", Frontiers in Cellular Neuroscience, Vol. 16, Frontiers, https://doi.org/10.3389/fncel.2022.836885.

Lee, Y. and P. J. McKinnon. (2007), "Responding to DNA double strand breaks in the nervous system", Neuroscience, Vol. 145/4, Elsevier, Amsterdam, https://doi.org/10.1016/j.neuroscience.2006.07.026.

Madabhushi, R., L. Pan and L.-H. Tsai. (2014), "DNA Damage and Its Links to Neurodegeneration", Neuron, Vol. 83/2, Elsevier, Amsterdam, https://doi.org/10.1016/j.neuron.2014.06.034.

Michaelidesova, A. et al. (2019), "Effects of Radiation Therapy on Neural Stem Cells", Genes, Vol. 10/9, MDPI, Basel, https://doi.org/10.3390/genes10090640.

Schmal, Z. et al. (2019), "DNA damage accumulation during fractionated low-dose radiation compromises hippocampal neurogenesis", Radiotherapy and Oncology, Vol. 137, Elsevier, Amsterdam, https://doi.org/10.1016/j.radonc.2019.04.021.

Thadathil, N. et al. (2019), "DNA double-strand breaks: a potential therapeutic target for neurodegenerative diseases", Chromosome Research, Vol. 27/4, Springer Nature, https://doi.org/10.1007/s10577-019-09617-x.

Wang, H. et al. (2017), "Chronic oxidative damage together with genome repair deficiency in the neurons is a double whammy for neurodegeneration: Is damage response signaling a potential therapeutic target?", Mechanisms of Ageing and Development, Vol. 161, Elsevier, Amsterdam, https://doi.org/10.1016/j.mad.2016.09.005.

Zanni, G. et al. (2015), "Lithium increases proliferation of hippocampal neural stem/progenitor cells and rescues irradiation-induced cell cycle arrest in vitro", Oncotarget, Vol. 6/35, https://doi.org/10.18632/oncotarget.5191.

Zhang, L. et al. (2017), "The inhibitory effect of minocycline on radiation-induced neuronal apoptosis via AMPKα1 signaling-mediated autophagy", Scientific Reports, Vol. 7/1, Springer Nature, https://doi.org/10.1038/s41598-017-16693-8.

Zhu, L.-S. et al. (2019), "Emerging Perspectives on DNA Double-strand Breaks in Neurodegenerative Diseases", Current Neuropharmacology, Vol. 17/12, Bentham Science Publishers, https://doi.org/10.2174/1570159X17666190726115623.

Relationship: 2811: Oxidative Stress leads to Increase, DNA strand breaks

AOPs Referencing Relationship

AOP Name	Adjacency	Weight of Evidence	Quantitative Understanding
Deposition of energy leading to occurrence of cataracts	adjacent	Moderate	Low
Deposition of Energy Leading to Learning and Memory Impairment	adjacent	Moderate	Moderate
Deposition of energy leads to vascular remodeling	adjacent	High	Moderate

Evidence Supporting Applicability of this Relationship

Taxonomic Applicability

Term	Scientific Term	Evidence	Links
human	Homo sapiens	Low	NCBI
rat	Rattus norvegicus	Low	NCBI
rabbit	Oryctolagus cuniculus	Low	NCBI
bovine	Bos taurus	Low	NCBI
mouse	Mus musculus	Low	NCBI

Life Stage Applicability

Life Stage	Evidence
Adult	Low
Not Otherwise Specified	Low

Sex Applicability

Sex	Evidence
Unspecific	Low
Male	Low

This KER is plausible in all life stages, sexes, and organisms with DNA. The evidence is from human, rodent, rabbit and bovine in vitro studies that do not specify the sex, as well as an adult rat in vivo study.

Key Event Relationship Description

Oxidative stress is an event that involves both a reduction in free radical scavengers and enzymes, and an increase in free radicals (Brennan et al., 2012). Oxidative stress needs to be maintained within an organism to avoid an excess of damage to biological structures, such as DNA. A redox homeostasis between the radicals and the scavengers is necessary. Between reactive oxygen species (ROS) and reactive nitrogen species (RNS), collectively known as RONS, ROS is particularly significant to oxidative damage and disease states. Radicals such as singlet oxygen and hydroxyl radical are highly unstable and will react with molecules near their generation point, while radicals such as H_2O_2 are more stable and membrane permeable, meaning they can travel further to find electrons (Spector, 1990). Since DNA is mainly found in nucleus, ROS needs to reach the nucleus to induce breaks. Hydroxyl radicals, in addition to being highly reactive, are capable of causing DNA damage (Halliwell et al., 2021; Engwa et al., 2020). The regulation of these radicals is achieved by the antioxidant defense response (ADR), which includes enzymatic and non-enzymatic processes. The ADR is recruited to manage RONS levels, with antioxidants such as superoxide dismutase (SOD) functioning as the first line of defense (Engwa et al., 2020). These antioxidants act as scavengers to oxidants, reacting with them before reaching other structures within the cell such as DNA strands (Cabrera et al., 2011; Engwa et al., 2020). The backbone of DNA can fragment upon sustained exposure to ROS (Uwineza et al., 2019; Cannan et al., 2016). Due to low oxidation potentials, adenine and guanine are the DNA bases more prone to oxidation, with oxidation potentials (normal hydrogen electrode) at pH 7 of 1.3 eV and 1.42 eV compared to the 1.6 eV and 1.7 eV of cytosine and thymine (Fong, 2016; Halliwell et al., 2021; Poetsch, 2020). In fact, certain radicals even target guanine in a selective fashion, including carbonate anion radical ($CO_3^{\bullet-}$) and singlet oxygen ($^1O_2$) (Halliwell et al., 2021).

Evidence Supporting this KER

Overall Weight of Evidence: Moderate

Biological Plausibility

The biological plausibility of the relationship between increased oxidative stress leading to increased DNA double strand breaks (DSBs) is highly supported by the literature. Evidence was collected from studies conducted using in vitro lens epithelial cell models and derived from humans, bovine and germ line cells (Spector, 1990; Stohs, 1995; Aitken et al., 2001; Spector, 1995). As this evidence is derived from studies using a human cell model it limits the ability to compare between different taxonomies (Ahmadi et al., 2022; Cencer et al., 2018; Liu et al., 2013; Meng et al., 2021; Smith et al., 2015; Zhou et al., 2016). Other evidence comes from human-derived and rodent models of neuronal and endothelial cells (Cervelli et al., 2014; El-Missiry et al., 2018; Huang et al., 2021; Sakai et al., 2017; Ungvari et al., 2013; Zhang et al., 2017).

ROS that are generated specifically as a result of radiation are highly localized, increasing the likelihood of clustered regions of damage. Naturally generated ROS are more widespread and as a result less capable of generating clusters of damage. ROS will act on DNA bases to oxidize or delete them from the sequence, which create nicks on the strand (Cannan et al., 2016). This damage can occur to any DNA base but bases such as guanine and adenine are most vulnerable due to their low oxidation potentials (Fong, 2016). The mechanism through which the strand break occurs is a result of base excision repair (BER) happening at multiple sites that are too close together, resulting in the spontaneous conversion to DSBs prior to completion of repair. ROS damage to bases clustered together means that multiple sites of BER are happening very close together and while the strand may be able to support the damaged area for one repair, concurrent repairs make surrounding areas more fragile and the strand breaks at the nick sites are under added strain (Cannan et al., 2016). Endogenous damage to DNA as a result of radicals appears over time and mainly as isolated lesions, a pattern understood to be due to the diffusion of the radicals resulting in homogenous distribution patterns. This differs from the specific situations where radiation acts as the stressor to increase oxidative stress, as the radiation track will be highly localized and form radicals within that hit space. This leads to non-homologous lesions and clustered damage to the DNA (Ward et al., 1985).

Empirical Evidence

This relationship is well supported through empirical evidence from studies using stressors such as H_2O_2, photons, γ- and X-ray, which cause an increase in markers of oxidative stress such as ROS-generating enzymes (lactate dehydrogenase, LDH), and a decrease in free radical scavengers, resulting in DNA strand fragmentation. These studies include both in vivo and in vitro human lens epithelial cells (LECs), mouse, rat and rabbit models, including neuronal cells lines and endothelial cells (Ahmadi et al., 2022; Cencer et al., 2018; Cervelli et al., 2014; El-Missiry et al., 2018; Huang et al., 2021; Liu et al., 2013; Meng et al., 2021; Spector et al., 1997; Ungvari et al., 2013; Zhang et al., 2017; Zhou et al., 2016; Sakai et al., 2017).

Dose/Incidence Concordance

There is high evidence to support a dose concordance between oxidative stress and DNA strand breaks. One in vitro study demonstrated that when ROS levels in LECs are 10% above control following 0.5 Gy gamma ray exposure, DNA strand breaks increased 15-20% above control (Ahmadi et al., 2021). Another study with ultraviolet (UV)B radiation demonstrated higher ROS levels after exposure to 0.14 J/cm^2 on in vitro LECs as compared to a lower dose exposure (0.014 J/cm^2) for the same time. This corresponded to DNA strand break levels also increasing following high dose rate exposure, but not with the low dose exposure (Cencer et al., 2018).

A 30 µM of H_2O_2 treatment of in vitro LECs is associated with a 1.4x increase in lactate dehydrogenase (LDH) and 55% more DNA strand breaks (Liu et al., 2013; Smith et al., 2015). Following exposure of in vitro LECs to 50 µM H_2O_2, increased ROS levels, 4x for LDH, and decreased antioxidant levels, 2x control for GSH-Px and SOD, are associated with a 3x increase in γ-H2AX, a marker of DNA strand breaks (Meng et al., 2021). SOD and GSH decreased by 2-fold following 100 µM H_2O_2 exposure on LECs with an in vitro model (Zhou et al., 2016). At 125 µM H_2O_2 intact DNA can be reduced to near 1% of pre-treatment levels for in vitro LECs (Spector et al., 1997). Following 400 µM H_2O_2 LDH increased to 1200% of control in neuroblastoma cells (Feng et al., 2016) and DNA strand breaks increased to over 150% of control in in vitro LECs (Li et al., 1998).

Exposure of in vitro mouse hippocampal neuronal cells (HT22 cell line) to 10 Gy of X-irradiation resulted in a 5x increase in ROS generation and 3x increase in γ-H2AX (Huang et al., 2021). Another study exposed the same cell line to 8 and 12 Gy of X-irradiation and found a ~2x increase in ROS at 8 Gy and a 4.4x and 3.2x increase in phosphorylation of ataxia telangiectasia mutated (ATM) and γ-H2AX, respectively, 30 minutes after 12 Gy (Zhang et al., 2017). A separate study exposed adult male rats to 4 Gy of γ-irradiation and found 2x increase in 4-hydroxy-2-nonenal (4-HNE) (lipid peroxidation marker) and 3x increase in protein carbonylation. Glutathione reductase decreased by approximately 5x, whereas glutathione and glutathione peroxidase levels decreased by approximately 3x each. Tail DNA %, tail length and tail moment (DNA strand break parameters) increased by approximately 2x, 3x and 6x, respectively (El-Missiry et al., 2018).

Endothelial cells exposed to irradiation also demonstrated the relation between oxidative stress and DNA strand breaks. Rat cerebromicrovascular endothelial cells (CMVECs) exposed to 8 Gy ^{137}Cs gamma rays showed increased cellular peroxide production and mitochondrial oxidative stress. Tail DNA content indicating DNA damage was also increased from 0 to 45% (Ungvari et al., 2013). Human umbilical vein endothelial cells (HUVECs) were irradiated with single (0.125, 0.25, 0.5 Gy), or fractionated (2 × 0.125 Gy, 2 × 0.250 Gy) doses of X-rays. Intracellular ROS production increased in a dose-dependent manner following 0.125, 0.25, 0.5 Gy, and γ-H2AX foci positive cells were observed at all doses (Cervelli et al., 2014). Human aortic endothelial cells (HAECs) exposed to 100µM H_2O_2 showed 3.7-fold increase in intracellular ROS and a 3.4- and 4.7-fold increase in γ-H2AX and p-ATM, respectively (Sakai et al., 2017).

Time Concordance

There is low evidence to support a time concordance between oxidative stress to strand breaks on DNA. Non-protein-thiol levels, an antioxidant, in in vitro LECs decreased to near zero by 30 min post-exposure to 300 μM H_2O_2, before recovering to 70% of control by 120 min. At 60 min post-exposure to 125 μM H_2O_2 there was a start to a divergence from control level DNA fragmentation, one that increased logarithmically, with the treated group having a 14~18% reduction in intact DNA by 9 h post-exposure (Yang et al., 1998). Time response information is difficult to monitor for DNA strand breaks because repair will occur, reducing the number of breaks over time. At 0 minutes post in vitro exposure to 40 μM H_2O_2 LECs had ~145% of control level DNA strand breaks but that number dropped to ~105% by 30 minutes post-exposure (Li et al., 1998).

Essentiality

Oxidative stress has been found to increase levels of DNA strand breaks above background levels (Li et al., 1998; Liu et al., 2013; Cencer et al., 2018; Ahmadi et al., 2022; El-Missiry et al., 2018; Huang et al., 2021; Cervelli et al., 2017; Sakai et al., 2017). It has been shown that inhibition of oxidative stress leads to a reduction in DNA strand breaks. Sulforaphane (SFN) is an isothiocyanate, which provides chemical protection against ROS by activating the release of enzymatic scavengers. When SFN was added to in vitro LECs exposed to 30 μM H_2O_2, LDH decreased to near unexposed cell levels from the 1.4x control level without SFN. This LDH drop was associated with reducing the levels of DNA strand breaks induced by oxidative stress almost 3-fold as compared to cells without SFN (Liu et al., 2013). In another study, intact DNA levels were returned to control when treated with μPx-11 (peroxidase that breaks down H_2O_2), following exposure to 125 μM H_2O_2. This was a near 100% recovery compared to the drop seen in LECs that did not contain μPx-11 (Spector et al., 1997).

Within the brain of Wistar rats, epigallocatechin-3-gallate (EGCG) ameliorated radiation-induced increases in lipid peroxidation and protein carbonylation, as well as decreases in glutathione (GSH), glutathione peroxidase (GPx) and glutathione reductase (GR) and reverted the levels back to those similar to controls. DNA strand break parameters also returned to those similar to controls after treatment with EGCG (El-Missiry et al., 2018). Similar effects were also shown in another study using treatment mesenchymal stem cell-conditioned medium in mouse hippocampal cells exposed to 10 Gy of X-irradiation (Huang et al., 2021).

HUVECs pretreated with the antioxidant mixture RiduROS blunted ROS generation in a concentration-dependent manner by 65% ± 5.6% and 98% ± 2%, at 0.1 and 1 μg/mL, respectively, compared with cells irradiated without pretreatment. Low-dose irradiation also increased DSB-induced γ-H2AX foci compared with control cells and 24 h of RiduROS pretreatment reduced the γ-H2AX foci number by 41% (Cervelli et al., 2017). Additionally, HAECs treated with eicosapentaenoic acid (EPA) and docosahexaenoic acid (DHA) found significantly reduced intracellular ROS at 100μM, as well as reduced γ-H2AX foci formation by 47% and 48% following EPA and DHA treatment respectively. (Sakai et al., 2017).

Uncertainties and Inconsistencies

N/A

Quantitative Understanding of the Linkage

The following tables provide representative examples of the relationship, unless otherwise indicated, all data is significantly significant.

Dose Concordance

Reference	Experiment Description	Result
Cencer et al., 2018	In vitro, human LECs exposed to UVB and tested for 120 min post exposure with fluorescent probes to detect ROS production and mitochondrial superoxide, and tetramethylrhodamine-dUTP (TMR) red assay to detect strand breaks.	Both ROS and DNA strand breaks were increased by both 0.014 J/cm^2 and 0.14 J/cm^2 UVB radiation. At 0.014 J/cm^2, cellular ROS increased a maximum of 15 fluorescence units above the control at 5 minutes post-UVB, while DNA strand breaks increased about 115 fluorescence units above the control at this time. At 0.14 J/cm^2, cellular ROS increased a maximum of about 35 fluorescence units above the control at 90 minutes post-UVB, while mitochondrial superoxide increased about 30 fluorescence units above the control and DNA strand breaks increased about 125 fluorescence units above the control at this time.
Ahmadi et al., 2021	In vitro, human LECs exposed to 0.065-0.3 Gy/min gamma radiation, with dihydroethdium (DHE) fluorescent probes to measure ROS levels and comet assay to measure strand breaks.	Human LECs exposed in vitro to 0.1 - 0.5 Gy gamma rays showed a gradual increase in ROS levels and a corresponding gradual increase in DNA in the tail from the comet assay (indicative of increased DNA strand breaks) with the maximum dose displaying a 10% increase in ROS levels and a 17% increase in DNA strand damage.
Li et al., 1998	In vitro, bovine LECs were exposed to 40 and 400 μM H_2O_2 with an alkaline unwinding assay to determine strand break levels.	Immediately after LECs were exposed to 40 μM and 400 μM H_2O_2, there were ~145% and ~150% DNA strand breaks compared to the unexposed control level, respectively. The amounts of DNA strand breaks in cells exposed to both concentrations were reduced to ~105% of the unexposed control level after 30 mins. After 400 μM H_2O_2, oxidative stress as measured by LDH was 1200% of control in neuroblastoma cells.
Spector et al., 1997	In vitro, rat LECs exposed to 100 and 125 μM H_2O_2 with alkaline elution assay to determine single strand break level.	Exposure to 125 μM of H_2O_2 to lens epithelial cells resulted in reduction of intact DNA to near 1% by 9 hr post-exposure. Exposure to 100 μM H_2O_2 reduced SOD and GSH levels by 2-fold.
El-Missiry et al., 2018	In vivo, albino Wistar rats were exposed to 4 Gy of γ radiation (^{137}Cs source) at 0.695 rad/s. Kits were used to measure 4-HNE (secondary product of lipid peroxidation) and protein carbonyl group levels as markers of oxidative stress. Antioxidants including GSH, GPx and GR were also assessed. The comet assay was used to analyze DNA strand breaks by visualizing DNA tail %, tail length and tail moment.	4-HNE and protein carbonyl levels increased by approximately 2- and 3-fold after radiation exposure. GSH and GPx levels decreased by approximately 3-fold each, whereas GR levels decreased by approximately 5-fold. Tail DNA %, tail length and tail moment increased by approximately 2-, 3- and 6-fold after exposure to 4 Gy.
Hosseini et	In vitro. CMVECs and rat hippocampal neurons were irradiated with 2-8 Gy ^{137}Cs gamma rays. 5(and 6)-chloromethyl-2′,7′-dichlorodihydrofluorescein diacetate	Day 1 post-irradiation showed increased cellular peroxide production and increased mitochondrial oxidative stress in CMVECs in a dose-dependent manner, increasing a maximum

Ungvari et al., 2013	acetyl ester (CM-H2DCFDA) staining, and flow cytometry were used to measure ROS production. DNA damage was quantified by measuring the tail DNA content (as a percentage of total DNA) using the Comet Assay-IV software.	of ~3-fold at 8 Gy. Tail DNA content also increased in a dose-dependent manner with an approximate increase from 0 to 45% at 8 Gy.
Huang et al., 2021	In vitro, HT22 cells (mouse hippocampal neuronal cell line) were exposed to 10 Gy of X-irradiation at 6 Gy/min. ROS levels were measured using H2-DCFDA staining and fluorescence microscope analysis, whereas western blotting was used to detect γ-H2AX.	At 10 Gy, intracellular ROS generation increased by 5-fold and γ-H2AX increased by 3-fold.
Zhang et al., 2017	In vitro. HT22 cells were exposed to 8 and 12 Gy X-rays. Relative intracellular ROS levels were determined by DCFDA. p-ATM, γ-H2AX were measured with Western blot.	Following 8 Gy irradiation, intracellular ROS levels increased ~1.8-fold. Phosphorylation of ATM and γ-H2AX were increased 4.4-fold and 3.2-fold, respectively, 30 minutes after 12 Gy.
Cervelli et al., 2014	In vitro. HUVECs were irradiated with single doses (0.125, 0.25, 0.5 Gy), or fractionated doses (2 × 0.125 Gy, 2 × 0.250 Gy) of X-rays. Intracellular ROS generation was measured with a fluorescent dye, C-DCFDA, using a spectrofluorometer. Immunofluorescence microscopy was used to measure γ-H2AX foci.	Intracellular ROS production was significantly increased in a dose-dependent manner (1.6-, 2- and 2.8-fold at 0.125, 0.25, 0.5 Gy, respectively). When HUVECs were exposed to fractionated doses, no increase in ROS generation was observed, compared with respective single doses. 24h post-irradiation the percentage of foci-positive cells exposed to 0.125 Gy, 2 × 0.125 Gy, 0.250 Gy, 2 × 0.250 Gy and 0.5 Gy, was 1.68, 1.48, 3.53, 2.59, 8.74-fold over the control, respectively.
Sakai et al., 2017	In vitro. HAECs were exposed to 100uM H_2O_2. Intracellular ROS was measured by CM-H2DCFDA. DNA DSBs were detected by immunofluorescent analysis with γ-H2AX as a marker.	Intracellular ROS increased by ~3.7-fold p-ATM increased by ~4.7-fold. γ-H2AX increased by ~3.4-fold.

Incidence Concordance

Reference	Experiment Description	Result
Meng et al., 2021	In vitro, human LECs exposed to 50 µM H_2O_2 with DCFH-DA fluorescent probe to detect ROS levels and immunofluorescence and western blot assay to detect γ-H2AX.	50 µM H_2O_2 exposure to lens epithelial cells increased oxidative stress, with ROS measured by LDH, by 4-fold and decreased the level of antioxidants by 2-fold as measured by SOD and GSH-PX. This resulted in 3-fold increase in γ-H2AX.
Smith et al., 2015	In vitro, human LECs exposed to 30 µM H_2O_2 with alkaline comet assay to determine amount of strand breaks.	Treatment of lens epithelial cells to 30 µM H_2O_2 induced DNA strand breaks by 55% at 0.5 hr after exposure and increased the level of LDH by ~1.4 fold at 24 hr post-exposure.
Liu et al. 2013	In vitro, human LECs exposed to 30 µM H_2O_2 with alkaline comet assay determination of strand breaks.	LDH increased by ~1.4 fold at 24 hr post-exposure, with a 5x increase from control levels in DNA strand breaks.

Time Concordance

Reference	Experiment Description	Result
Yang et al., 1998	In vitro, rabbit LECs exposed to H_2O_2 with TCA addition and thiol assay to determine non-protein thiol (NP-SH) level and alkaline elusion assay to determine strand breaks.	In rabbit LECs exposed in vitro to 125 µM H_2O_2, non-protein thiol levels decreased to <5% control (indicates oxidative stress) 30 min post-irradiation, and % DNA retained using alkaline elution decreased by 1.6 log (indicates increased DNA fragmentation) within the next 8.5 h.

Known modulating factors

There is limited evidence demonstrating this relationship across different life stages/ages or sexes (Cencer et al., 2018; Li et al., 1998).

Modulating Factors	MF Details	Effects on the KER	References
Age	Reduced antioxidant capacities have been linked to aged lenses (in humans >30 years old). The development of a chemical barrier between the cortex and the nucleus is partially responsible, as it prevents GSH from protecting aged lens cells from ROS.	Prevention of RONS-mediated damage is primarily achieved by antioxidants, so a lowered capacity would likely lead to reduced damage mitigation abilities. 78% of lens over 30 had a low level of GSH in the center compared to 14% of lens under 30. Lens epithelial cells have an associated 3-fold increase in γ-H2AX (marker of DNA damage) when GSH-PX decreases by 2-fold.	Taylor & Davies, 1987; Cabrera & Chihuailaf, 2011; Quinlan & Hogg, 2018; Sweeney & Truscott, 1998; Meng & Fang, 2021
Free radical scavengers	ROS-scavengers are essential components of the body's natural defense against oxidative damage. Increased ROS production leads to increased incidence of electron donation by scavengers, thus reducing the overall level of free radical scavengers available to deal with ROS.	Isothiocyanates, such as sulforaphane (SFN), activate the release of more enzymatic scavengers. When SFN was added to in vitro LECs, LDH decreased to near unexposed cell levels and was associated with 3.3x less DNA strand breaks compared to the non-SFN cells following stressor exposure. Epigallocatechin-3-gallate (EGCG) also has antioxidant properties and was shown to alleviate radiation-induced increases in oxidative stress and DNA strand breaks within rat hippocampi.	Taylor et al., 1987; Cabrera et al., 2011; Liu et al., 2013; El-Missiry et al., 2018
Media	Mesenchymal stem cell-conditioned medium (MSC-CM), which has self-renewal, differential and proliferation capacities.	MSC-CM treatment has also been shown to improve ROS levels and decrease radiation-induced DNA strand breaks within mouse hippocampal neuronal cells.	Huang et al., 2021

Known Feedforward/Feedback loops influencing this KER

N/A

References

Ahmadi, M. et al. (2021), “Early Responses to Low-Dose Ionizing Radiation in Cellular Lens Epithelial Models”, Radiation Research, Vol.197, Radiation Research Society, Indianapolis, https://doi.org/10.1667/RADE-20-00284.1.

Aitken, R.J. and C. Krausz. (2001), “Oxidative stress, DNA damage and the Y chromosome”, Reproduction, Vol.122/2001, Bioscientifica, Bristol, https://doi.org/10.1530/rep.0.1220497.

Annesley, S.J. and P.R. Fisher. (2019), “Mitochondria in Health and Disease”, Cells, Vol.8/7, MDPI, Basel, https://doi.org/10.3390/cells8070680.

Brennan, L., R. McGreal and M. Kantorow. (2012), “Oxidative stress defense and repair systems of the ocular lens”, Frontiers in Bioscience – Elite, Vol.4/E(1), Frontiers in Bioscience, Singapore, https://doi.org/10.2741/365.

Britton, S. et al. (2020), “ATM antagonizes NHEJ proteins assembly and DNA-ends synapsis at single-ended DNA double strand breaks”, Nucleic Acids Research, Vol.48/17, Oxford University Press, Oxford, https://doi.org/10.1093/nar/gkaa723.

Cabrera, M. and R. Chihuailaf. (2011), “Antioxidants and the integrity of ocular tissues”, Veterinary Medicine International, Vol.2011, Hindawi Limited, London, https://doi.org/10.4061/2011/905153.

Cannan, W. and D. Pederson. (2016), “Mechanisms and consequences of double-strand DNA break formation in chromatin”, Journal of Cell Physiology, Vol.231/1, Wiley, Hoboken, https://doi.org/10.1002/jcp.25048.

Cencer, C. et al. (2018), “PARP-1/PAR Activity in Cultured Human Lens Epithelial Cells Exposed to Two Levels of UVB Light”, Photochemistry and Photobiology, Vol.94/1, Wiley-Blackwell, Hoboken, https://doi.org/10.1111/php.12814.

Cervelli, T.et al. (2014), “Effects of single and fractionated low-dose irradiation on vascular endothelial cells”, Atherosclerosis, Vol.235/2, Elsevier, Amsterdam, https://doi.org/10.1016/j.atherosclerosis.2014.05.932.

Cervelli, T. et al. (2017), “A New Natural Antioxidant Mixture Protects against Oxidative and DNA Damage in Endothelial Cell Exposed to Low-Dose Irradiation”, Oxidative medicine and cellular longevity, Vol. 2017, Hindawi, London, https://doi.org/10.1155/2017/9085947.

Climent, M. et al. (2020), “MicroRNA and ROS Crosstalk in Cardiac and Pulmonary Diseases”, International Journal of Molecular Science, Vol.21/12, MDPI, Basel, https://doi.org/10.3390/ijms21124370.

Dahm-Daphie, J., C. Sass, and W. Alberti. (2000), “Comparison of biological effects of DNA damage induced by ionizing radiation and hydrogen peroxide in CHO cells”, International Journal Radiation Biology, Vol.76/1, Informa, London, https://doi.org/10.1080/095530000139023.

El-Missiry, M. A. et al. (2018), "Neuroprotective effect of epigallocatechin-3-gallate (EGCG) on radiation-induced damage and apoptosis in the rat hippocampus", International Journal of Radiation Biology, Vol. 94/9, https://doi.org/10.1080/09553002.2018.1492755.

Engwa, G.A., F.N. Nweke and B.N. Nkeh-Chungag. (2020), “Free Radicals, Oxidative Stress-Related Diseases and Antioxidant Supplementation”, Alternative therapies in health and medicine, Vol.28/1, InnoVision Health Media, Eagan, pp.114-128.

Feng, C. et al. (2016), “Lycopene protects human SH-SY5Y neuroblastoma cells against hydrogen peroxide-induced death via inhibition of oxidative stress and mitochondria-associated apoptotic pathways”, Molecular Medicine Reports, Vol.13/5, Spandidos Publications, Athens, https://doi.org/10.3892/mmr.2016.5056.

Fong, C.W. (2016), “Platinum anti-cancer drugs: Free radical mechanism of Pt-DNA adduct formation and anti-neoplastic effect”, Free Radical Biology and Medicine, Vol.95/June 2016, Elsevier, Amsterdam, https://doi.org/10.1016/j.freeradbiomed.2016.03.006.

Halliwell, B. et al. (2021), “Hydroxyl radical is a significant player in oxidative DNA damage in vivo”, Chemical Society Reviews, Vol.50, Royal Society of Chemistry, London, https://doi.org/10.1039/d1cs00044f.

Huang, Y. et al. (2021), "Mesenchymal Stem Cell-Conditioned Medium Protects Hippocampal Neurons From Radiation Damage by Suppressing Oxidative Stress and Apoptosis", Dose-Response, Vol. 19/1, https://doi.org/10.1177/1559325820984944.

Kay, J. et al. (2019), “Inflammation-induced DNA damage, mutations and cancer”, DNA Repair, Vol.83, Elsevier, Amsterdam, https://doi.org/10.1016/j.dnarep.2019.102673.

Jeggo, P.A., V. Geuting and M. Löbrich. (2011), “The role of homologous recombination in radiation-induced double-strand break repair”, Radiotherapy and Oncology, Vol.101/1, Elsevier, Amsterdam, https://doi.org/10.1016/j.radonc.2011.06.019.

Kurutas E. B. (2016), “The importance of antioxidants which play the role in cellular response against oxidative/nitrosative stress: current state”, Nutrition journal, Vol.15/1, Biomed Central, London, https://doi.org/10.1186/s12937-016-0186-5.

Kruk, J., K. Kubasik-Kladna and H. Aboul-Enein. (2016), “The Role Oxidative Stress in the Pathogenesis of Eye Diseases: Current Status and a Dual Role of Physical Activity”, Mini-Review in Medicinal Chemistry, Vol.16/3, Bentham Science Publishers, Sharjah, https://doi.org/10.2174/1389557516666151120114605.

Li, Y. et al. (1998), “Response of lens epithelial cells to hydrogen peroxide stress and the protective effect of caloric restriction”, Experimental Cell Research, Vol.239/2, Elsevier, Amsterdam, https://doi.org/10.1006/excr.1997.3870.

Liu, H. et al. (2013), “Sulforaphane can protect lens cells against oxidative stress: Implications for cataract prevention”, Investigative Ophthalmology and Visual Science, Vol.54/8, Association for Research in Vision and Ophthalmology, Rockville, https://doi.org/10.1167/iovs.13-11664.

Meng, K. and C. Fang. (2021), “Knockdown of Tripartite motif-containing 22 (TRIM22) relieved the apoptosis of lens epithelial cells by suppressing the expression of TNF receptor-associated factor 6 (TRAF6)”, Bioengineered, Vol.12/1, Taylor & Francis, Oxfordshire, https://doi.org/10.1080/21655979.2021.1980645.

Nishida, M. et al. (2005), “Ga12/13- and Reactive Oxygen Species-dependent Activation of c-Jun NH2-terminal Kinase and p38 Mitogen-activated Protein Kinase by Angiotensin Receptor Stimulation in Rat Neonatal Cardiomyocytes”, Journal of Biological Chemistry, Vol.280/18, American Society for Biochemistry and Molecular Biology, Rockville, https://doi.org/10.1074/jbc.M409710200.

Poetsch, A.R. (2020), “The genomics of oxidative DNA damage, repair, and resulting mutagenesis”, Computational and Structural Biotechnology Journal, Vol.18, Elsevier,

Amsterdam, https://doi.org/10.1016/j.csbj.2019.12.013.

Quinlan, R.A., and P.J. Hogg. (2018), “γ-Crystallin redox–detox in the lens”, Journal of Biological Chemistry, Vol.293/46, American Society for Biochemistry and Molecular Biology, Rockville, https://doi.org/10.1074/jbc.H118.006240.

Sakai, C. et al. (2017), “Fish oil omega-3 polyunsaturated fatty acids attenuate oxidative stress-induced DNA damage in vascular endothelial cells”, PloS one, Vol.12/11, https://doi.org/10.1371/journal.pone.0187934.

Scully, R. and A. Xie. (2013), “Double strand break repair functions of histone H2AX”, Mutation Research, Vol.750/1-2, Elsevier, Amsterdam, https://doi.org/10.1016/j.mrfmmm.2013.07.007.

Smith, A. et al. (2015), “Ku80 counters oxidative stress-induced DNA damage and cataract formation in the human lens”, Investigative Ophthalmology and Visual Science, Vol.56/13, Association for Research in Vision and Ophthalmology, Rockville, https://doi.org/10.1167/iovs.15-18309.

Spector, A. et al. (1997), “Microperoxidases catalytically degrade reactive oxygen species and may be anti-cataract agents”, Experimental Eye Research, Vol.65/4, Academic Press Inc, Cambridge, https://doi.org/10.1006/exer.1997.0336.

Spector, A. et al. (1996), “Variation in cellular glutathione peroxidase activity in lens epithelial cells, transgenics and knockouts does not significantly change the response to H2O2 stress”, Experimental Eye Research, Vol.62/5, Academic Press Inc, Cambridge, https://doi.org/10.1006/exer.1996.0063.

Spector, A. (1995), “Oxidative stress-induced cataract: mechanism of action”, The FASEB Journal, Vol.9/12, Federation of American Societies for Experimental Biology, Bethesda, https://doi.org/10.1096/fasebj.9.12.7672510.

Spector, A. (1990), “Oxidation and Aspects of Ocular Pathology”, CLAO Journal, Vol.16/1, Lippincott, Williams and Wilkins Ltd, Philadelphia, S8-S10.

Stohs, S. (1995), “The role of free radicals in toxicity and disease”, Journal of Basic Clinical Physiology and Pharmacology, Vol.6/3-4, Walter de Gruyter GmbH, Berlin, https://doi.org/10.1515/jbcpp.1995.6.3-4.205.

Sweeney, M.H.J. and R.J.W. Truscott. (1998), “An Impediment to Glutathione Diffusion in Older Normal Human Lenses: a Possible Precondition for Nuclear Cataract”, Experimental Eye Research, Vol.67, Academic Press Inc, Cambridge, https://doi.org/10.1006/exer.1998.0549.

Taylor, A. and K. J. A. Davies (1987), “Protein oxidation and loss of protease activity may lead to cataract formation in the aged lens”, Free Radical Biology & Medicine, Vol. 3, Pergamon Journals Ltd, United States of America, pp. 371-377

Ungvari, Z. et al. (2013), "Ionizing Radiation Promotes the Acquisition of a Senescence-Associated Secretory Phenotype and Impairs Angiogenic Capacity in Cerebromicrovascular Endothelial Cells: Role of Increased DNA Damage and Decreased DNA Repair Capacity in Microvascular Radiosens", The Journals of Gerontology Series A: Biological Sciences and Medical Sciences, Vol. 68/12, https://doi.org/10.1093/gerona/glt057.

Uwineza, A. et al. (2019), “Cataractogenic load – A concept to study the contribution of ionizing radiation to accelerated aging in the eye lens”, Mutation Research - Reviews in Mutation Research, Vol.779, Elsevier, Amsterdam, https://doi.org/10.1016/j.mrrev.2019.02.004.

Ward, J.F., W.F. Blakely & E.I. Joner. (1985), “Mammalian Cells Are Not Killed by DNA Single-Strand Breaks Caused by Hydroxyl Radicals from Hydrogen Peroxide”, Radiation Research, Vol.103/3, Radiation Research Society, Indianapolis, hptts://doi.org/10.2307/3576760.

Wu, H. et al. (2021), “Lactate dehydrogenases amplify reactive oxygen species in cancer cells in response to oxidative stimuli”, Signal Transduction and Targeted Therapy, Vol.6/1, Nature Portfolio, Berlin, https://doi.org/10.1038/s41392-021-00595-3.

Yang, Y. et al. (1998), “The effect of catalase amplification on immortal lens epithelial cell lines”, Experimental Eye Research, Vol.67/6, Academic Press Inc, Cambridge, https://doi.org/10.1006/exer.1998.0560.

Yuan, J., R. Adamski and J. Chen. (2010), “Focus on histone variant H2AX: To be or not to be”, FEBS Letters, Vol.584/17, Wiley, Hoboken, https://doi.org/10.1016/j.febslet.2010.05.021.

Zhang, L. et al. (2017), "The inhibitory effect of minocycline on radiation-induced neuronal apoptosis via AMPKα1 signaling-mediated autophagy", Scientific Reports, Vol. 7/1, https://doi.org/10.1038/s41598-017-16693-8.

Zhou, Y. et al. (2016), “Protective Effect of Rutin Against H2O2-Induced Oxidative Stress and Apoptosis in Human Lens Epithelial Cells”, Current Eye Research, Vol.41/7, Taylor & Francis, Oxfordshire, https://doi.org/10.3109/02713683.2015.1082186.

Relationship: 1977: Energy Deposition leads to Increase, DNA strand breaks

AOPs Referencing Relationship

AOP Name	Adjacency	Weight of Evidence	Quantitative Understanding
Deposition of energy leading to lung cancer	adjacent	High	High
Deposition of energy leading to population decline via DNA strand breaks and follicular atresia	adjacent	High	
Deposition of energy leading to population decline via DNA strand breaks and oocyte apoptosis	adjacent		
Deposition of energy leading to occurrence of cataracts	adjacent	High	High
Deposition of energy leads to vascular remodeling	adjacent	High	High

AOP Name	Adjacency	Weight of Evidence	Quantitative Understanding
Deposition of Energy Leading to Learning and Memory Impairment	adjacent	High	High

Evidence Supporting Applicability of this Relationship

Taxonomic Applicability

Term	Scientific Term	Evidence	Links
mouse	Mus musculus	High	NCBI
human	Homo sapiens	High	NCBI
rat	Rattus norvegicus	High	NCBI
bovine	Bos taurus	Low	NCBI
rabbit	Oryctolagus cuniculus	Low	NCBI
Pig	Pig	Low	NCBI

Life Stage Applicability

Life Stage	Evidence
All life stages	High

Sex Applicability

Sex	Evidence
Unspecific	High

This KER is plausible in all life stages, sexes, and organisms with DNA. The majority of the evidence is from In vivo adult mice and human In vitro models that do not specify the sex.

Key Event Relationship Description

Direct deposition of ionizing energy refers to imparted energy interacting directly with the DNA double helix and producing randomized damage. This can be in the form of double strand breaks (DSBs), single-strand breaks, base damage, or the crosslinking of DNA to other molecules (Smith et al., 2003; Joiner, 2009; Christensen, 2014; Sage and Shikazono, 2017). Among these, the most detrimental type of DNA damage to a cell is DSBs. They are caused by the breaking of the sugar-phosphate backbone on both strands of the DNA double helix molecule, either directly across from each other or several nucleotides apart (Ward, 1988; Iliakis et al., 2015). This occurs when high-energy subatomic particles interact with the orbital electrons of the DNA causing ionization (where electrons are ejected from atoms) and excitation (where electrons are raised to higher energy levels) (Joiner, 2009). The number of DSBs produced and the complexity of the breaks is highly dependent on the amount of energy deposited on and absorbed by the cell. This can vary as a function of the dose-rate (Brooks et al., 2016) and the radiation quality which is a function of its linear energy transfer (LET) (Sutherland et al., 2000; Nikjoo et al., 2001; Jorge et al., 2012). LET describes the amount of energy that an ionizing particle transfers to media per unit distance (Smith et al., 2003; Okayasu, 2012a; Christensen et al., 2014). High LET radiation, such as alpha particles, heavy ion particles, and neutrons can deposit larger quantities of energy within a single track than low LET radiation, such as γ-rays, X-rays, electrons, and protons (Kadhim et al., 2006; Franken et al., 2012; Frankenberg et al., 1999; Rydberg et al., 2002; Belli et al., 2000; Antonelli et al., 2015). As such, radiation with higher LETs tends to produce more complex, dense structural damage, particularly in the form of clustered damage, in comparison to lower LET radiation (Nikjoo et al., 2001; Terato and Ide, 2005; Hada and Georgakilas, 2008; Okayasu, 2012a; Lorat et al., 2015; Nikitaki et al., 2016). Thus, the complexity and yield of clustered DNA damage increases with ionizing density (Ward, 1988; Goodhead, 2006). However, clustered damage can also be induced even by a single radiation track through a cell.

While the amount of DSBs produced depends on the radiation dose (see dose concordance), it also depends on several other factors. As the LET increases, the complexity of DNA damage increases, decreasing the repair rate, and increasing toxicity (Franken et al., 2012; Antonelli et al., 2015).

Evidence Supporting this KER

Overall Weight of Evidence for this KER: High

Biological Plausibility

The biological rationale linking the direct deposition of energy on DNA with an increase in DSB formation is strongly supported by numerous literature reviews that are available on this topic (J .F. Ward, 1988; Lipman, 1988; Hightower, 1995; Terato & Ide, 2005; Goodhead, 2006; Kim & Lee, 2007; Asaithamby et al., 2008; Hada & Georgakilas, 2008; Jeggo, 2009; Clement, 2012; Okayasu, 2012b; Stewart, 2012; M. E. Lomax et al., 2013; EPRI, 2014; Hamada, 2014; Moore et al., 2014; Desouky et al., 2015; Ainsbury, 2016; Foray et al., 2016; Hamada & Sato, 2016; Hamada, 2017a; Sage & Shikazono, 2017; Chadwick, 2017; Wang et al., 2021; Nagane et al., 2021; Sylvester et al., 2018; Baselet et al., 2019). Ionizing radiation can be in the form of high energy particles (such as alpha particles, beta particles, or charged ions) or high energy photons (such as gamma-rays or X-rays). Ionizing radiation can break the DNA within chromosomes both directly and indirectly, as shown through using velocity sedimentation of DNA through neutral and alkaline sucrose gradients. The most direct path entails a collision between a high-energy particle or photon and a strand of DNA.

Additionally, excitation of secondary electrons in the DNA allows for a cascade of ionization events to occur, which can lead to the formation of multiple damage sites (Joiner, 2009). As an example, high-energy electrons will traverse a DNA molecule in a mammalian cell within 10^{-18} s and 10^{-14} s, resulting in 100,000 ionizing events per 1 Gy dose in a 10 µm cell (Joiner, 2009). The amount of damage can be influenced by factors such as the cell cycle stage and chromatin structure. It has been shown that in more condensed, packed chromatin structures such as those present in intact cells and heterochromatin, it is more difficult for the DNA to be damaged (Radulescu et al., 2006; Agrawala et al., 2008; Falk et al., 2008; Venkatesh et al., 2016). In contrast, DNA damage is more easily induced in lightly-packed chromatin such as euchromatin and nucleoids, (Radulescu et al., 2006; Falk et al., 2008; Venkatesh et al., 2016).

Of the possible radiation-induced DNA damage types, DSB is considered to be the most harmful to the cell, as there may be severe consequences if this damage is not adequately repaired (Khanna & Jackson, 2001; Smith et al., 2003; Okayasu, 2012a; M. E. Lomax et al., 2013; Rothkamm et al., 2015).

A considerable fraction of DSBs can also be formed in cells through indirect mechanisms. In this case, deposited energy can split water molecules near DNA, which can

generate a significant quantity of reactive oxygen species in the form of hydroxyl free radicals (Ward, 1988; Wolf, 2008; Desouky et al., 2015; Maier et al., 2016, Cencer et al., 2018; Bains, 2019; Ahmadi et al., 2021). Estimates using models and experimental results suggest that hydroxyl radicals may be present within nanoseconds of energy deposition by radiation (Yamaguchi et al., 2005). These short-lived but highly reactive hydroxyl radicals may react with nearby DNA. This will produce DNA damage, including single-strand breaks and DSBs (Ward, 1988; Sasaki, 1998; Desouky et al., 2015; Maier et al., 2016). DNA breaks are especially likely to be produced if the sugar moiety is damaged, and DSBs occur when two single-strand breaks are in close proximity to each other (Ward, 1988).

Empirical Evidence

Empirical data strongly supports this KER. The evidence presented below is summarized in table 1. The types of DNA damage produced by ionizing radiation and the associated mechanisms, including the induction of DSBs, are reviewed by Lomax et al. (2013) and documents produced by international radiation governing frameworks (Valentin, 1998; UNSCEAR, 2000). Other reviews also highlight the relationship between the deposition of energy by radiation and DSB induction, and discuss the various methods available to detect these DSBs (Terato & Ide, 2005; Rothkamm et al., 2015; Sage & Shikazono, 2017). A visual representation of the time frames and dose ranges probed by the dedicated studies discussed here is shown in Figures 1 & 2 below.

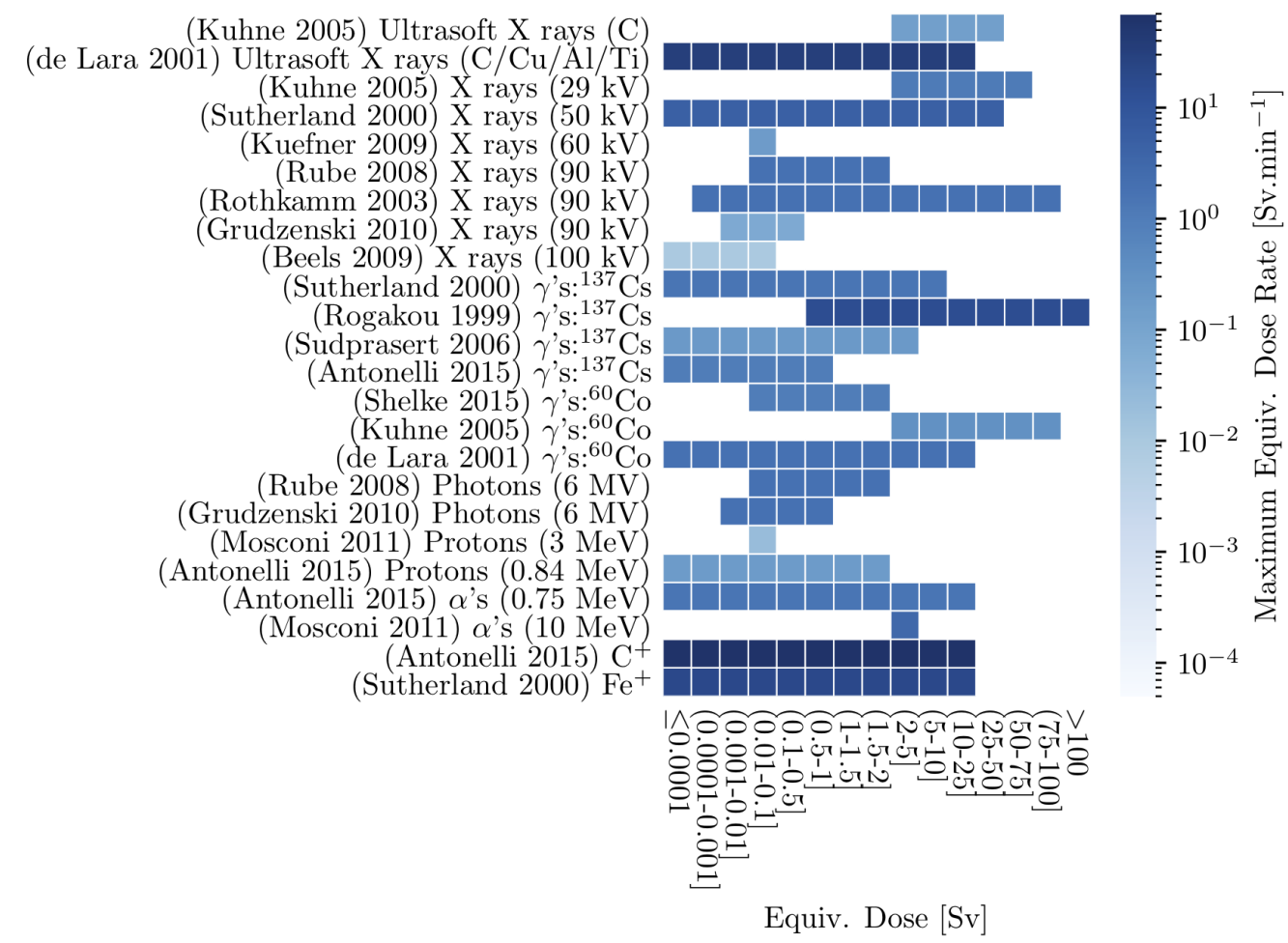

Figure 1: Plot of example studies (y-axis) against equivalent dose (Sv) used to determine the empirical link between direct deposition of energy and DSBs. The z-axis denotes the equivalent dose rate used in each study. The y-axis is ordered from low LET to high LET from top to bottom.

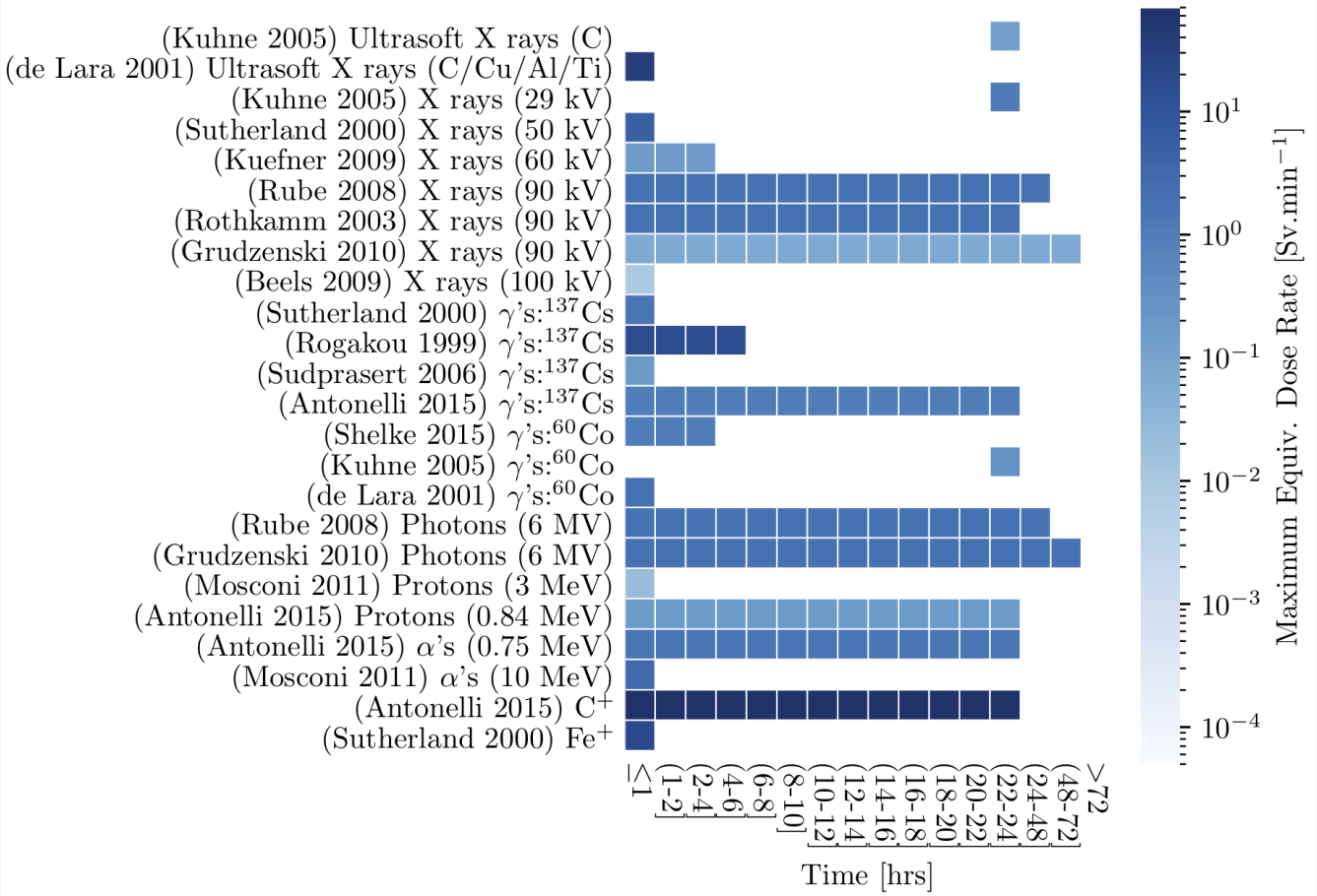

Figure 2: Plot of example studies (y-axis) against time scales used to determine the empirical link between direct deposition of energy and DSBs. The z-axis denotes the equivalent dose rate used in each study. The y-axis is ordered from low LET to high LET from top to bottom.

Dose Concordance

There is evidence in the literature suggesting a dose concordance between the direct deposition of energy by ionizing radiation and the incidence (Grudzenski et al., 2010) of DNA DSBs. Results from in vitro (Aufderheide et al., 1987; Sidjanin, 1993; Bucolo, 1994; Frankenberg et al., 1999; Rogakou et al., 1999; Belli et al., 2000; Sutherland et al., 2000; Lara et al., 2001; Rydberg et al., 2002; Baumstark-Kham et al., 2003; Rothkamm and Lo, 2003; Long, 2004; Kuhne et al., 2005; Sudprasert et al., 2006; Beels et al., 2009; Grudzenski et al., 2010; Liao, 2011; Franken et al., 2012; Bannik et al., 2013; Shelke & Das, 2015; Antonelli et al., 2015; Markiewicz et al., 2015; Allen, 2018; Dalke, 2018; Bains, 2019; Ahmadi et al., 2021; Sabirzhanov et al., 2020; Ungvari et al., 2013; Rombouts et al., 2013; Baselet et al., 2017), in vivo (Reddy, 1998; Sutherland et al., 2000; Rube et al., 2008; Beels et al., 2009; Grudzenski et al., 2010; Markiewicz et al., 2015; Barnard, 2018; Barnard, 2019; Barnard, 2022; Schmal et al., 2019; Barazzuol et al., 2017; Geisel et al., 2012), ex vivo (Rube et al., 2008; Flegal et al., 2015) and simulation studies (Charlton et al., 1989) suggest that there is a positive, linear, dose-dependent increase in DSBs with increasing deposition of energy across a wide range of radiation types (iron ions, X-rays, ultrasoft X-rays, gamma-rays, photons, UV light, and alpha particles) and radiation doses (1 mGy - 100 Gy) (Aufderheide et al., 1987; Sidjanin, 1993; Frankenberg et al., 1999; Sutherland et al., 2000; de Lara et al., 2001; Baumstark-Khan et al., 2003; Rothkamm & Lo, 2003; Kuhne et al., 2005; Rube et al., 2008; Grudzenski et al., 2010; Bannik et al., 2013; Shelke & Das, 2015; Antonelli et al., 2015; Dalke, 2018; Barazzuol et al., 2017; Ungvari et al., 2013; Rombouts et al., 2013; Baselet et al., 2017; Geisel et al., 2012). DSBs have been predicted to occur at energy deposition levels as low as 75 eV (Charlton et al., 1989).

Time Concordance

There is evidence suggesting a time concordance between the direct deposition of energy and the incidence of DSBs. A number of different models and experiments have provided evidence of ionizing radiation-induced foci (IRIF), which can be used to infer DSB formation seconds (Mosconi et al., 2011) or minutes after radiation exposure (Rogakou et al., 1999; Rothkamm and Lo, 2003; Rube et al., 2008; Beels et al., 2009; Kuefner et al., 2009; Grudzenski et al., 2010; Antonelli et al., 2015; Acharya et al., 2010; Sabirzhanov et al., 2020; Rombouts et al., 2013; Nübel et al., 2006; Baselet et al., 2017; Zhang et al., 2017).

Essentiality

Deposition of energy is essential for DNA strand breaks. They can also be caused through other routes, such as oxidative stress (Cadet et al., 2012), but under normal physiological conditions deposition of energy is necessary. This was tested through many studies using various indicators such as 53BP1 foci/cell, γH2AX foci/cell, DNA

migration, and the amount of DNA in tails for the comet assay. Various organisms such as humans, mice, rabbits, guinea pigs, and cattle were used. They showed that without the deposition of energy, there was only a negligible amount of DNA strand breaks (Aufderheide et al., 1987; Sidjanin, 1993; Bucolo, 1994; Reddy, 1998; Rogers, 2004; Bannik et al., 2013; Dalke, 2018; Bains, 2019; Barnard, 2019; Barnard, 2021).

Uncertainties and Inconsistencies

Uncertainties and inconsistencies in this KER are as follows:

- Studies have shown that dose-rates (Brooks et al., 2016) and radiation quality (Sutherland et al., 2000; Nikjoo et al., 2001; Jorge et al., 2012) are factors that can influence the dose-response relationship.
- Low-dose radiation has been observed to have beneficial effects and may even invoke protection against spontaneous genomic damage (Feinendegen, 2005; Day et al., 2007; Feinendegen et al., 2007; Shah et al., 2012; Nenoi et al., 2015; Dalke, 2018). This protective effect has been documented in in vivo and in vitro, as reviewed by ICRP (2007) and UNSCEAR (2008) and can vary depending on the cell type, the tissue, the organ, or the entire organism (Brooks et al., 2016).
- Depositing ionizing energy is a stochastic event; as such this can influence the location, degree and type of DNA damage imparted on a cell. As an example, studies have shown that mitochondrial DNA may also be an important target for genotoxic effects of ionizing radiation (Wu et al., 1999).

Quantitative Understanding of the Linkage

Quantitative understanding of this linkage suggests that DSBs can be predicted upon exposure to ionizing radiation. This is dependent on the biological model, the type of radiation and the radiation dose. In general, 1 Gy of radiation is thought to result in 3000 damaged bases (Maier et al., 2016), 1000 single-strand breaks, and 40 DSBs (Ward, 1988; Foray et al., 2016; Maier et al., 2016) . The table below provides representative examples of the calculated DNA damage rates across different model systems, most of which are examining DNA DSBs.

Dose Concordance

The following tables provide representative examples of the relationship, unless otherwise indicated, all data is significantly significant.

Reference	Experiment Description	Result
Ward, 1988	In vitro. Cells containing approximately 6 pg of DNA were exposed to 1 Gy.	Under the assumption of 6 pg of DNA per cell. 60 eV of energy deposited per event over a total of 1 Gy. Deoxyribose (2.3 pg/cell): 14,000 eV deposited, 235 events. Bases (2.4 pg/cell): 14.7 keV deposited, 245 events. Phosphate (1.2 pg/cell): 7,300 eV deposited, 120 events. Bound water (3.1 pg/cell): 19 keV deposited, 315 events. Inner hydration shell (4.2 pg/cell): 25,000 eV deposited 415 events.
Charlton, 1989	In-silico. A computer simulation/model was used to test various types of radiation with doses from 0 to 400 eV (energy deposited) on the amount of DNA damage produced.	Simulated dose-concordance prediction of increase in number of DSBs/54 nucleotide pairs as direct deposition of energy increases in the range 75-400 eV. In the range 100 - 150 eV: 0.38 DSBs/54 nucleotide pairs and at 400 eV: ~0.80 DSBs per 64 nucleotide pairs.
Sutherland, 2000	In vitro. Human cells were exposed to ^{137}Cs γ-rays (0 – 100 Gy, 0.16 – 1.6 Gy/min). The frequency of DSBs was determined using gel electrophoresis.	Using isolated bacteriophage T7 DNA and 0-100 Gy of γ radiations, observed a response of 2.4 DSBs per megabase pair per Gy.
Rogakou et al., 1999	In vitro. Normal human fibroblasts (IMR90) and human breast cancer cells (MCF7 were exposed to 0.6 and 2 Gy ^{137}Cs γ-rays delivered at 15.7 Gy/min. The number of DSBs were determined by immunoblotting for γ-H2AX.	Radiation doses of 0.6 Gy & 2 Gy to normal human fibroblasts (IMR90) and MCF7 cells resulted in 10.1 & 12.2 DSBs per nucleus on average (0.6 Gy), respectively; increasing to 24 & 27.1 DSBs per nucleus (2 Gy).
Kuhne et al., 2005	In vitro. Primary human skin fibroblasts (HSF2) were exposed to 0 – 70 Gy ^{60}Co γ-rays (0.33 Gy/min), X-rays (29 kVp, 1.13 Gy/min), and CKX-rays (0.14 Gy/min). The number of DSBs were determined with pulsed-field gel electrophoresis.	γ-ray and X-ray irradiation of primary human skin fibroblasts (HSF2) at 0 - 70 Gy. γ-rays: (6.1 ± 0.2) x 10-9 DSBs per base pair per Gy, X-rays: (7.0 ± 0.2) x 10-9 DSBs per base pair per Gy. CKX -rays: (12.1 ± 1.9) x 10-9 DSBs per base pair per Gy.
Rothkamm, 2003	In vitro. Primary human fibroblast cell lines MRC-5 (lung), HSF1 and HSF2 (skin), and180BR (deficient in DNA ligase IV) were exposed to 1 mGy – 100 Gy X-rays (90 kV). Low doses were delivered at 6 – 60 mGy/min and high doses were delivered at 2 Gy/min. The number of DSBs were determined with pulsed-field gel electrophoresis.	X-ray irradiation of primary human fibroblasts (MRC-5) in the range 1 mGy - 100 Gy, 35 DSBs per cell per Gy.
Grudzenski et al, 2010	In vitro. Primary human fibroblasts (HSF1) and C57BL/6NCrl adult mice were exposed to X-rays (2.5 – 200 mGy, 70 mGy/min), and photons (10 mGy – 1 Gy, 2 Gy/min (100 mGy and 1 Gy), and 0.35 Gy/min (10 mGy)). γ-H2AX immunofluorescence was observed to determine DSBs.	X-rays irradiating primary human fibroblasts (HSF1) in the range 2.5 - 100 mGy yielded a response of 21 foci per Gy. When irradiating adult C57BL/6NCrl mice with photons a response of 0.07 foci per cell at 10 mGy was found. At 100 mGy the response was 0.6 foci per cell and finally, at 1 Gy; 8 foci per cell.
de Lara, 2001	In vitro. Chinese hamster cells (V79-4) were exposed to 0 – 20 Gy of ^{60}Co γ-rays (2 Gy/min), and ultrasoft X-rays (0.7 – 35 Gy/min): carbon-K shell (0.28 keV), copper L-shell (0.96 keV), aluminum K-shell (1.49 keV), and titanium K-shell (4.55 keV). The number of DSBs were determined with pulsed-field gel electrophoresis.	V79-4 cells irradiated with γ-rays and ultrasoft X-rays (carbon K-shell, copper L-shell, aluminium K-shell and titanum K-shell) in the range 0 - 20 Gy. Response (DSBs per Gy per cell): γ-rays: 41, carbon K-shell: 112, copper L-shell: 94, aluminum K-shell: 77, titanium K-shell: 56.
Rübe et al., 2008	In vivo. Brain, lung, heart and small intestine tissue from adult SCID, A-T, BALB/c and C57BL/6NCrl mice; Whole blood and isolated lymphocytes from BALB/c and C57BL/6NCrl mice were exposed to 0.1 – 2 Gy of photons (whole body irradiation, 6 MV, 2 Gy/min) and X-rays (whole body irradiation, 90 kV, 2 Gy/min). γ-H2AX foci were determined with immunochemistry to measure DSBs.	Linear dose-dependent increase in DSBs in the brain, small intestine, lung and heart of C57BL/6CNrl mice after whole-body irradiation with 0.1 - 1.0 Gy of radiation. 0.8 foci per cell (0.1 Gy) and 8 foci per cell (1 Gy).
	In vitro. Primary human foreskin fibroblasts (AG01522) were exposed to 0 –	

Antonelli et al., 2015	1 Gy of ^{136}Cs γ-rays (1 Gy/min), protons (0.84 MeV, 28.5 keV/um), carbon ions (58 MeV/u, 39.4 keV/um), and alpha particles (americium-241, 0.75 MeV/u, 0.08 Gy/min, 125.2 keV/um). γ-H2AX foci were determined with immunochemistry to measure DSBs.	Linear dose-dependent increase in the number of DSBs from 0 - 1 Gy for γ-rays and alpha particles as follows: γ-rays: 24.1 foci per Gy per cell nucleus, alpha particles: 8.8 foci per Gy per cell nucleus.
Barnard et al., 2019	In vivo. 10-week-old female C57BL/6 mice were whole-body exposed to 0.5, 1, and 2 Gy of 60Co γ-rays at 0.3, 0.063, and 0.014 Gy/min. p53 binding protein 1 (53BP1) foci were determined via immunofluorescence.	Central LECs showed a linear increase in mean 53BP1 foci/cell with the maximum dose and dose-rate displaying a 78x increase compared to control. Peripheral LECs and lower dose rates displayed similar results, with slightly fewer foci.
Ahmadi et al., 2021	In vitro. Human LEC cells were exposed to 137Cs γ-rays at doses of 0, 0.1, 0.25, and 0.5 Gy and dose rates of 0.065 and 0.3 Gy/min. DNA strand breaks were measured using the comet assay.	Human LECs showed a gradual increase in the tail from the comet assay with the maximum dose and dose-rate displaying a 3.7x increase compared to control. Lower dose-rates followed a similar pattern with a lower amount of strand breaks.
Hamada et al., 2006	In vitro. Primary normal human diploid fibroblast (HE49) cells were exposed to 0.1, 0.5, and 4 Gy X-rays at 240 kV with a dose rate of 0.5 Gy/min. The number of H2AX foci/cell, which represented DNA strand breaks, was determined 6 – 7 minutes after irradiation through fluorescence microscopy.	Cells displayed a linear increase in the number of H2AX foci/cell, with the maximum dose displaying a 125x increase compared to control.
Dubrova & Plumb, 2002		At 1 Gy observe 70 DSBs, 1000 single-strange breaks and 2000 damaged DNA bases per cell per Gy.
Sabirzhanov et al., 2020	In vitro. Rat cortical neurons were exposed to 2, 8 or 32 Gy of X rays (320 kV) at a dose rate of 1.25 Gy/min. Western blot was used to measure γ-H2AX, p-ataxia telangiectasia mutated (ATM) and p- ATM/RAD3-related (ATR) levels.	In rat cortical neurons, p-ATM increased at 2, 8, and 32 Gy, with a 15-fold increase at 8 and 32 Gy. γ-H2AX levels increased at 8 and 32 Gy.
Geisel et al., 2012	In vivo. Patients with suspected coronary artery disease receiving X-rays from computed tomography or conventional coronary angiography had levels of DSBs assessed in blood lymphocytes by γ-H2AX fluorescence.	There was a correlation between effective dose (in mSv) and DSBs. For both conventional coronary angiography and computed tomography, a dose of 10 mSv produced about 2-fold more DNA DSBs than a dose of 5 mSv.
Ungvari et al., 2013	In vitro. Rat cerebromicrovascular endothelial cells and hippocampal neurons were irradiated with 2-10 Gy of ^{137}Cs gamma rays. DNA strand breaks were assessed with the comet assay.	DNA damage increased at all doses (2-10 Gy). In the control, less than 5% of DNA was in the tail, while by 6 Gy, 35% of the DNA was in the tail in cerebromicrovascular endothelial cells and 25% was in the tail in neurons.
Rombouts et al., 2013	In vitro. EA.hy926 cells and human umbilical vein endothelial cells were irradiated with various doses of X-rays (0.25 Gy/min). γ-H2AX foci were assessed with immunofluorescence.	More γ-H2AX foci were observed at higher doses in both cell types. In human umbilical vein endothelial cells, few foci/nucleus were observed at 0.05 Gy, with about 23 at 2 Gy. In EA.hy926 cells, few foci/nucleus were observed at 0.05 Gy, with about 37 at 2 Gy.
Baselet et al., 2017	In vitro. Human telomerase-immortalized coronary artery endothelial cells were irradiated with various doses of X-rays (0.5 Gy/min). Immunocytochemical staining was performed for γ-H2AX and 53BP1 foci.	Doses of 0.05 and 0.1 Gy did not increase the number of γ-H2AX foci, but 0.5 Gy increased foci number by 5-fold and 2 Gy by 15-fold. A dose of 0.05 Gy did not increase the number of 53BP1 foci, but 0.1 Gy, 0.5 Gy and 2 Gy increased levels by 3-fold, 7-fold and 8-fold, respectively.

Time Concordance

Reference	Experiment Description	Result
Rogakou et al., 1999	In vitro. Normal human fibroblasts (IMR90), human breast cancer cells (MCF7), human astrocytoma cells (SF268), Indian muntjac Muntiacus muntjak normal skin fibroblasts, Xenopus laevisA6 normal kidney cells, Drosophila melanogaster epithelial cells, and Saccharomyces cerevisiae were exposed to 0.6, 2, 20, 22, 100, and 200 Gy 137Cs γ-rays. Doses below 20 Gy were delivered at 15.7 Gy/min and other doses were delivered in 1 minute. DNA breaks were visualized using γ-H2AX antibodies and microscopy.	DSBs were present at 3 min and persisted from 15 - 60 min.
Hamada & Woloschak, 2017	In vitro. human LECs were exposed to 0.025 Gy X-rays at 0.42 – 0.45 Gy/min. 53BP1 foci were measured via indirect immunofluorescence.	In cells immediately exposed to 0.025 Gy, the level of 53BP1 foci/cell increased to 3.3x relative to control 0.5 h post-irradiation.
Hamada et al., 2006	In vitro. Primary normal human diploid fibroblast (HE49) cells were exposed to 0.1, 0.5, and 4 Gy (deposition of energy) at 240 kV with a dose rate of 0.5 Gy/min. The number of H2AX foci/cell, which represented DNA strand breaks, was determined through fluorescence microscopy.	In cells immediately exposed to 0.5 Gy, 11% of cells had 18 foci six min post-irradiation, compared to 90% of controls having 0 foci.
Acharya et al., 2010	In vitro. Human neural stem cells were exposed to 1, 2 and 5 Gy of γ-rays at a dose rate of 2.2 Gy/min. The levels of γ-H2AX phosphorylation post irradiation were assessed by immunocytochemistry, fluorescence-activated cell sorting (FACS) analysis and γ-H2AX foci enumeration.	The number of cells positive for nuclear γ-H2AX foci peaked at 20 min post-irradiation. After 1h, this level quickly declined.
Schmal et al., 2019	In vivo. Juvenile and adult C57BL/6 mice were exposed to whole body 6-MV photons at 2 Gy/min. Irradiations were done in 5x, 10x, 15x and 20x fractions of 0.1 Gy. Double staining for NeuN and 53BP1 was used to quantify DNA damage foci and the possible accumulation in the hippocampal dentate gyrus.	To assess possible accumulation of persisting 53BP1-foci during fractionated radiation, juvenile and adult mice were examined 72 h after exposure to 5×, 10×, 15×, or 20× fractions of 0.1 Gy, compared to controls. The number of persisting 53BP1-foci increased significantly in both juvenile and adult mice during fractionated irradiation (maximum at 1 m post-IR).
Dong et al., 2015	In vivo. C57BL/6J mice were exposed to 2 Gy of X-rays at 2 Gy/min using a 6 MV source. γ-H2AX foci were assessed with immunofluorescence in the brain.	At 0.5 h, about 14 γ-H2AX foci/cell were present. This decreased linearly to about 2 foci/cell at 24 h, with no foci/cell from 48 h to 6 weeks.
Barazzuol et al., 2017	In vivo. C57BL/6 mice were exposed to 0.1 or 2 Gy of X-rays (250 kV) at a rate of 0.5 Gy/min. 53BP1 foci were quantified with immunofluorescence in neural stem cells and neuron progenitors in the lateral ventricle.	At both 0.5 and 6 h post-irradiation, increased 53BP1 foci were observed, with the highest level at 0.5 h.
Sabirzhanov et al., 2020	In vitro. Rat cortical neurons were exposed to 2, 8 or 32 Gy of X rays (320 kV) at a dose rate of 1.25 Gy/min. Western blot was used to measure γ-H2AX, p-ATM and p-ATR levels.	In rat cortical neurons, γ-H2AX, p-ATM and p-ATR all increased at 30 minutes post-irradiation, with a sustained increase until 6 h.

Zhang et al., 2017	In vitro. HT22 hippocampal neuronal cellsT were irradiated with X-rays (320 kVp) at 8 or 12 Gy at a dose rate of 4 Gy/min. The comet assay was preformed to assess the DNA double strand breaks in HT22 cells. Western blot was used to measure γ-H2AX and p-ATM.	At 8 Gy, the comet assay showed an increased tail moment at both 30 minutes and 24 h post-irradiation. At 12 Gy, p-ATM was increased over 4-fold at both 30 minutes and 1 h post-irradiation. γ-H2AX was increased over 3-fold at 30 minutes post-irradiation and almost 2-fold at 1 and 24 h.
Geisel et al., 2012	In vivo. Patients with suspected coronary artery disease receiving X-rays from computed tomography or conventional coronary angiography had levels of DSBs assessed in blood lymphocytes by γ-H2AX fluorescence.	DSBs were increased at 1 h post-irradiation and returned to pre-irradiation levels by 24 h.
Park et al., 2022	In vitro. Human aortic endothelial cells were irradiated with 137Cs gamma rays at 4 Gy (3.5 Gy/min). γ-H2AX was measured with western blot. p-ATM and 53BP1 were determined with immunofluorescence.	γ-H2AX, p-ATM, and 53BP1 were shown increased at 1 h post-irradiation and slightly decreased for the rest of the 6 h but remained elevated above the control.
Kim et al., 2014	In vitro. Human umbilical vein endothelial cells were irradiated with 4 Gy of 137Cs gamma rays. γ-H2AX levels were determined with immunofluorescence.	γ-H2AX foci greatly increased at 1 and 6 h post-irradiation, with the greatest increase at 1 h.
Dong et al., 2014	In vitro. Human umbilical vein endothelial cells were irradiated with 2 Gy of 137Cs gamma rays. γ-H2AX levels were determined with immunofluorescence.	γ-H2AX foci increased 8-fold at 3 h, 7-fold at 6 h, and 2-fold at 12 and 24 h post-irradiation.
Rombouts et al., 2013	In vitro. EA.hy926 cells and human umbilical vein endothelial cells were irradiated with X-rays (0.25 Gy/min). γ-H2AX foci were assessed with immunofluorescence.	The greatest increase in γ-H2AX foci was observed 30 minutes post-irradiation, while levels were still slightly elevated at 24 h.
Nübel et al., 2006	In vitro. Human umbilical vein endothelial cells were irradiated with gamma rays at 20 Gy. DNA strand breaks were assessed with the comet assay and western blot for γ-H2AX.	The olive tail moment increased 5-fold immediately after irradiation and returned to control levels by 4 h. A large increase in γ-H2AX was observed at 0.5 h post-irradiation, with lower levels at 4 h but still above the control.
Baselet et al., 2017	In vitro. Human telomerase-immortalized coronary artery endothelial cells were irradiated with various doses of X-rays (0.5 Gy/min). Immunocytochemical staining was performed for γ-H2AX and 53BP1 foci.	Increased γ-H2AX and 53BP1 foci were observed at 0.5 h post-irradiation, remaining elevated at 4 h but returning to control levels at 24 h.
Gionchiglia et al., 2021	In vivo. Male CD1 and B6/129 mice were irradiated with X-rays at 10 Gy. Brain sections were single or double-stained with antibodies against γ-H2AX and p53BP1.	In the forebrain, cerebral cortex, hippocampus and subventricular zone (SVZ)/ rostral migratory stream (RMS)/ olfactory bulb (OB), γH2AX and p53BP1 positive cells increased at both 15 and 30 minutes post-irradiation, with the greatest increase at 30 minutes.

Response-response relationship

There is evidence of a response-response relationship between the deposition of energy and the frequency of DSBs. In studies encompassing a variety of biological models, radiation types and radiation doses, a positive, linear relationship was found between the radiation dose and the number of DSBs (Aufderheide et al., 1987; Sidjanin, 1993; Frankenberg et al., 1999; Sutherland et al., 2000; de Lara et al., 2001; Baumstark-Khan et al., 2003; Rothkamm & Lo, 2003; Kuhne et al., 2005; Rube et al., 2008; Grudzenski et al., 2010; Bannik et al., 2013; Shelke & Das, 2015; Antonelli et al., 2015; Hamada, 2017b; Dalke, 2018; Barazzuol et al., 2017; Geisel et al., 2012; Ungvari et al., 2013; Rombouts et al., 2013; Baselet et al., 2017). There were, however, at least four exceptions reported. When human blood lymphocytes were irradiated with X-rays in vitro, a linear relationship was only found for doses ranging from 6 - 500 mGy; at low doses from 0 - 6 mGy, there was a quadratic relationship reported (Beels et al., 2009). Secondly, simulation studies predicted that there would be a non-linear increase in DSBs as energy deposition increased, with a saturation point at higher LETs (Charlton et al., 1989). Furthermore, primary normal human fibroblasts exposed to 1.2 – 5 mGy X-rays at 5.67 mGy/min showed a supralinear relationship, indicating at low doses, the DSBs are mostly due to radiation-induced bystander effects. Doses above 10 mGy showed a positive linear relationship (Ojima et al., 2008). Finally, in the human lens epithelial cell line SRA01/04, DNA strand breaks appeared immediately after exposure to UVB (0.14 J/cm2) and were repaired after 30 minutes. They then reappeared after 60 and 90 minutes. Both were once again repaired within 30 minutes. However, the two subsequent stages of DNA strand breaks did not occur when exposed to a lower dose of UVB (0.014 J/cm2) (Cencer et al., 2018).

Time-scale

Data from temporal response studies suggests that DSBs likely occur within seconds to minutes of energy deposition by ionizing radiation. In a variety of biological models, the presence of DSBs has been well documented within 10 - 30 minutes of radiation exposure (Rogakou et al., 1999; Rube et al., 2008; Beels et al., 2009; Kuefner et al., 2009; Grudzenski et al., 2010; Antonelli et al., 2015; Acharya et al., 2010; Dong et al., 2015; Barazzuol et al., 2017; Sabirzhanov et al., 2020; Rombouts et al., 2013; Nübel et al., 2006; Baselet et al., 2017; Zhang et al., 2017; Gionchiglia et al., 2021); there is also evidence that DSBs may actually be present within 3 - 5 minutes of irradiation (Kleiman, 1990; Rogakou et al., 1999; Rothkamm & Lo, 2003; Rube et al., 2008; Grudzenski et al., 2010; Cencer et al., 2018). Interestingly, one study that focussed on monitoring the cells before, during and after irradiation by taking photos every 5, 10 or 15 seconds found that foci indicative of DSBs were present 25 and 40 seconds after collision of the alpha particles and protons with the cell, respectively. The number of foci were found to increase over time until plateauing at approximately 200 seconds after alpha particle exposure and 800 seconds after proton exposure (Mosconi et al., 2011).

After the 30 minute mark, DSBs have been shown to rapidly decline in number. By 24 hours post-irradiation, DSB numbers had declined substantially in systems exposed to radiation doses between 40 mGy and 80 Gy (Aufderheide et al., 1987; Baumstark-Khan et al., 2003; Rothkamm & Lo, 2003; Rube et al., 2008; Grudzenski et al., 2010; Bannik et al., 2013; Markiewicz et al., 2015; Russo et al., 2015; Antonelli et al., 2015; Dalke, 2018; Bains, 2019; Barnard, 2019; Ahmadi et al., 2021; Dong et al., 2015; Dong et al., 2014; Sabirzhanov et al., 2020; Rombouts et al., 2013; Baselet et al., 2017; Gionchiglia et al., 2021), with the sharpest decrease documented within the first 5 h (Kleiman, 1990; Sidjanin, 1993; Rogakou et al., 1999; Rube et al., 2008; Kuefner et al., 2009; Grudzenski et al., 2010; Bannik, 2013; Markiewicz et al., 2015; Shelke and Das, 2015; Cencer et al., 2018; Acharya et al., 2010; Park et al., 2022; Kim et al., 2014; Nübel et al., 2006). Interestingly, DSBs were found to be more persistent when they were induced by higher LET radiation (Aufderheide et al., 1987, Baumstark-Khan et al., 2003; Antonelli et al., 2015).

Known modulating factors

Modulating Factor	Details	Effects on the KER	References
Nitroxides	Increased concentration	Decreased DNA strand breaks.	DeGraff et al., 1992; Citrin & Mitchel, 2014
5-fluorouracil	Increased concentration	Increased DNA strand breaks.	De Angelis et al., 2006; Citrin & Mitchel, 2014
Thiols	Increased concentration	Decreased DNA strand breaks.	Milligan et al., 1995; Citrin & Mitchel, 2014
Cisplatin	Increased concentration	Decreased DNA break repair.	Sears & Turchi; Citrin & Mitchel, 2014

Known Feedforward/Feedback loops influencing this KER

Not identified.

References

Agrawala, P.K. et al. (2008), "Induction and repairability of DNA damage caused by ultrasoft X-rays: Role of core events.", Int. J. Radiat. Biol., 84(12):1093–1103. doi:10.1080/09553000802478083.

Ahmadi, M. et al. (2021), “Early responses to low-dose ionizing radiation in cellular lens epithelial models”, Radiation research, Vol.197/1, *Radiation Research Society*, United States, https://doi.org/10.1667/RADE-20-00284.1

Ainsbury, E. A. et al. (2016), “Ionizing radiation induced cataracts: Recent biological and mechanistic developments and perspectives for future research”, *Mutation research. Reviews in mutation research*, Vol. 770, Elsevier B.V., Amsterdam, https://doi.org/10.1016/j.mrrev.2016.07.010

Alexander, J. L. and Orr-Weaver, T. L. (2016), “Replication fork instability and the consequences of fork collisions from replication”, *Genes & Development*, Vol. 30/20, Cold Spring Harbor Laboratory Press, https://doi.org/ 10.1101/gad.288142.116

Allen, C. H. et al. (2018), “Raman micro-spectroscopy analysis of human lens epithelial cells exposed to a low-dose-range of ionizing radiation”, *Physics in medicine & biology*, Vol. 63/2, IOP Publishing, Bristol, https://doi.org/10.1088/1361-6560/aaa176

Antonelli, A.F. et al. (2015), "Induction and Repair of DNA DSB as Revealed by H2AX Phosphorylation Foci in Human Fibroblasts Exposed to Low- and High-LET Radiation: Relationship with Early and Delayed Reproductive Cell Death", Radiat. Res. 183(4):417-31, doi:10.1667/RR13855.1.

Acharya, M. et al. (2010), “Consequences of ionizing radiation-induced damage in human neural stem cells”, Free Radical Biology and Medicine. 49(12):1846-1855, doi:10.1016/j.freeradbiomed.2010.08.021.

Asaithamby, A. et al. (2008), "Repair of HZE-Particle-Induced DNA Double-Strand Breaks in Normal Human Fibroblasts.", Radiat Res. 169(4):437–446. doi:10.1667/RR1165.1.

Aufderheide, E. et al. (1987), “Heavy ion effects on cellular DNA: Strand break induction and repair in cultured diploid lens epithelial cells”, *International journal of radiation biology and related studies in physics, chemistry and medicin*e, Vol. 51/5, Taylor & Francis, London, https://doi.org/10.1080/09553008714551071

Bannik, K. et al. (2013), “Are mouse lens epithelial cells more sensitive to γ-irradiation than lymphocytes?”, *Radiation and environmental biophysics*, Vol. 52/2, Springer-Verlag, Berlin/Heidelberg, https://doi.org/10.1007/s00411-012-0451-8

Bains, S. K. et al. (2019), “Effects of ionizing radiation on telomere length and telomerase activity in cultured human lens epithelium cells”, I*nternational journal of radiation biology*, Vol. 95/1, Taylor & Francis, Abingdon, https://doi.org/10.1080/09553002.2018.1466066

Barazzuol, L et al. (2017), “A coordinated DNA damage response promotes adult quiescent neural stem cell activation. PLOS Biology, 15(5). https://doi.org/10.1371/journal.pbio.2001264

Barnard, S. G. R. et al. (2018), “Dotting the eyes: mouse strain dependency of the lens epithelium to low dose radiation-induced DNA damage”, *International journal of radiation biology*, Vol. 94/12, Taylor & Francis, Abingdon, https://doi.org/10.1080/09553002.2018.1532609

Barnard, S. G. R. et al. (2019), “Inverse dose-rate effect of ionising radiation on residual 53BP1 foci in the eye lens”, *Scientific Reports*, Vol. 9/1, Nature Publishing Group, England, https://doi.org/10.1038/s41598-019-46893-3

Barnard, S. G. R. et al. (2022), “Radiation-induced DNA damage and repair in lens epithelial cells of both Ptch1 (+/-) and Ercc2 (+/-) mutated mice”, *Radiation Research*, Vol. 197/1, Radiation Research Society, United States, https://doi.org/10.1667/RADE-20-00264.1

Baselet, B. et al. (2019), “Pathological effects of ionizing radiation: endothelial activation and dysfunction”, Cellular and molecular life sciences, Vol. 76/4, Springer Nature, https://doi.org/10.1007/s00018-018-2956-z

Baselet, B. et al. (2017), “Functional Gene Analysis Reveals Cell Cycle Changes and Inflammation in Endothelial Cells Irradiated with a Single X-ray Dose”, Frontiers in pharmacology, Vol. 8, Frontiers, https://doi.org/10.3389/fphar.2017.00213

Baumstark-Khan, C., J. Heilmann, and H. Rink (2003), ‘Induction and repair of DNA strand breaks in bovine lens epithelial cells after high LET irradiation”, *Advances in space research*, Vol. 31/6, Elsevier Ltd, England, https://doi.org/10.1016/S0273-1177(03)00095-4

Beels, L. et al. (2009), "g-H2AX Foci as a Biomarker for Patient X-Ray Exposure in Pediatric Cardiac Catheterization", Are We Underestimating Radiation Risks?":1903–1909. doi:10.1161/CIRCULATIONAHA.109.880385.

Belli M, Cherunbini R, Vecchia MD, Dini V, Moschini G, Signoretti C, Simon G, Tabocchini MA, Tiveron P. 2000. DNA DSB induction and rejoining in V79 cells irradiated with light ions: a constant field gel electrophoresis study. Int J Radiat Biol. 76(8):1095-1104.

Brooks, A.L., D.G. Hoel & R.J. Preston (2016), "The role of dose rate in radiation cancer risk: evaluating the effect of dose rate at the molecular, cellular and tissue levels using key events in critical pathways following exposure to low LET radiation.", Int. J. Radiat. Biol. 92(8):405–426. doi:10.1080/09553002.2016.1186301.

Bucolo, C. et al. (1994), “The effect of ganglioside on oxidation-induced permeability changes in lens and in epithelial cells of lens and retina”, *Experimental eye research,* Vol. 58/6, Elsevier Ltd, London, https://doi.org/10.1006/exer.1994.1067

Cabrera et al. (2011), “Antioxidants and the integrity of ocular tissues”, in Veterinary medicine international, SAGE-Hindawi Access to Research, United States. DOI: 10.4061/2011/905153

Cadet, J. et al. (2012), “Oxidatively generated complex DNA damage: tandem and clustered lesions”, Cancer letters, Vol. 327/1, Elsevier Ireland Ltd, Ireland. https://doi.org/10.1016/j.canlet.2012.04.005

Cannan, W.J. & D.S. Pederson (2016), "Mechanisms and Consequences of Double-Strand DNA Break Formation in Chromatin.", J. Cell Physiol. 231(1):3–14. doi:10.1002/jcp.25048.

Cencer, C. S. et al. (2018), “PARP-1/PAR activity in cultured human lens epithelial cells exposed to two levels of UVB light”, Photochemistry and photobiology, Vol. 94/1, Wiley, Hoboken, https://doi.org/10.1111/php.12814

Chadwick, K.H., (2017), Towards a new dose and dose-rate effectiveness factor (DDREF)? Some comments., J Radiol Prot., 37:422-433. doi: 10.1088/1361-6498/aa6722.

Charlton, D.E., H. Nikjoo & J.L. Humm (1989), "Calculation of initial yields of single- and double-strand breaks in cell nuclei from electrons, protons and alpha particles.", Int. J. Rad. Biol., 53(3):353-365, DOI: 10.1080/09553008814552501

Christensen, D.M. (2014), "Management of Ionizing Radiation Injuries and Illnesses, Part 3: Radiobiology and Health Effects of Ionizing Radiation.", 114(7):556–565. doi:10.7556/jaoa.2014.109.

Citrin, D.E. & J.B. Mitchel (2014), "Public Access NIH Public Access.", 71(2):233–236. doi:10.1038/mp.2011.182.doi.

Dalke, C. et al. (2018), “Lifetime study in mice after acute low-dose ionizing radiation: a multifactorial study with special focus on cataract risk”, Radiation and environmental biophysics, Vol. 57/2, Springer Berlin Heidelberg, Berling/Heidelberg, https://doi.org/10.1007/s00411-017-0728-z

Day, T.K. et al. (2007), "Adaptive Response for Chromosomal Inversions in pKZ1 Mouse Prostate Induced by Low Doses of X Radiation Delivered after a High Dose.", Radiat Res. 167(6):682–692. doi:10.1667/rr0764.1.

De Angelis, P. M. et al. (2006), “Cellular response to 5-fluorouracil (5-FU) in 5-FU-resistant colon cancer cell lines during treatment and recovery”, Molecular Cancer, Vol. 5/20, BioMed Central, https://doi.org/10.1186/1476-4598-5-20

DeGraff, W. G. et al. (1992), “Nitroxide-mediated protection against X-ray- and neocarzinostatin-induced DNA damage”, Free Radical Biology and Medicine, Vol. 13/5, Elsevier, https://doi.org/10.1016/0891-5849(92)90142-4

Desouky, O., N. Ding & G. Zhou (2015), "ScienceDirect Targeted and non-targeted effects of ionizing radiation.", J. Radiat. Res. Appl. Sci. 8(2):247–254. doi:10.1016/j.jrras.2015.03.003.

Dong et al. (2015), “Relationship between irradiation-induced neuro-inflammatory environments and impaired cognitive function in the developing brain of Mice. International Journal of Radiation Biology, 91(3):224–239. https://doi.org/10.3109/09553002.2014.988895

Dong, X. et al. (2014), “NEMO modulates radiation-induced endothelial senescence of human umbilical veins through NF-κB signal pathway”, Radiation Research, Vol. 183/1, BioOne, https://doi.org/10.1667/RR13682.1

Dubrova, Y.E. & M.A. Plumb (2002), "Ionising radiation and mutation induction at mouse minisatellite loci The story of the two generations", Mutat. Res. 499(2):143–150.

EPRI (2014), Epidemiology and mechanistic effects of radiation on the lens of the eye: Review and scientific appraisal of the literature, EPRI, California

Falk, M., E. Lukášová & S. Kozubek (2008), "Chromatin structure influences the sensitivity of DNA to γ-radiation.", Biochim. Biophys. Acta. - Mol. Cell. Res. 1783(12):2398–2414. doi:10.1016/j.bbamcr.2008.07.010.

Feinendegen, L.E. (2005), "UKRC 2004 debate Evidence for beneficial low level radiation effects and radiation hormesis. Radiology.", 78:3–7. doi:10.1259/bjr/63353075.

Feinendegen, L.E., M. Pollycove & R.D. Neumann (2007), "Whole-body responses to low-level radiation exposure: New concepts in mammalian radiobiology.", Exp. Hematol. 35(4 SUPPL.):37–46. doi:10.1016/j.exphem.2007.01.011.

Flegal, M. et al. (2015), "Measuring DNA Damage and Repair in Mouse Splenocytes After Chronic In Vivo Exposure to Very Low Doses of Beta- and γ-Radiation.", (July):1–9. doi:10.3791/52912.

Foray, N., M. Bourguignon and N. Hamada (2016), “Individual response to ionizing radiation”, Mutation research. Reviews in mutation research, Vol. 770, Elsevier B.V., Amsterdam, https://doi.org/10.1016/j.mrrev.2016.09.001

Franken NAP, Hovingh S, Cate RT, Krawczyk P, Stap J, Hoebe R, Aten J, Barendsen GW. 2012. Relative biological effectiveness of high linear energy transfer alpha-particles for the induction of DNA-double-strand breaks, chromosome aberrations and reproductive cell death in SW-1573 lung tumour cells. Oncol reports. 27:769-774.

Frankenberg D, Brede HJ, Schrewe UJ, Steinmetz C, Frankenberg-Scwager M, Kasten G, Pralle E. 1999. Induction of DNA Double-Strand Breaks by 1H and 4He Ions in Primary Human Skin Fibroblasts in the LET range of 8 to 124 keV/µm. Radiat Res. 151:540-549.

Geisel, D. et al. (2012), “DNA double-strand breaks as potential indicators for the biological effects of ionising radiation exposure from cardiac CT and conventional coronary angiography: a randomised, controlled study”, European Radiology, Vol. 22/8, Springer Nature, https://doi.org/10.1007/s00330-012-2426-1

Gionchiglia, N. et al. (2021), “Association of Caspase 3 Activation and H2AX γ Phosphorylation in the Aging Brain: Studies on Untreated and Irradiated Mice,” Biomedicines. 9(9):1166. doi: 10.3390/biomedicines9091166.

Goodhead, D.T. (2006), "Energy deposition stochastics and track structure: What about the target?", Radiat. Prot. Dosimetry. 122(1–4):3–15. doi:10.1093/rpd/ncl498.

Grudzenski, S. et al. (2010), "Inducible response required for repair of low-dose radiation damage in human fibroblasts.", Proc. Natl. Acad. Sci. USA. 107(32): 14205-14210, doi:10.1073/pnas.1002213107.

Hada, M. & A.G. Georgakilas (2008), "Formation of Clustered DNA Damage after High-LET Irradiation: A Review.", J. Radiat. Res., 49(3):203–210. doi:10.1269/jrr.07123.

Hamada, N. et al. (2006), “Histone H2AX phosphorylation in normal human cells irradiated with focused ultrasoft X rays: evidence for chromatin movement during repair”, Radiation Research, Vol. 166/1, Radiation Research Society, United States, https://doi.org/10.1667/RR3577.1

Hamada, N. (2014), “What are the intracellular targets and intratissue target cells for radiation effects?”, Radiation research, Vol. 181/1, The Radiation Research Society, Lawrence, https://doi.org/10.1667/RR13505.1

Hamada, N. and T. Sato (2016), “Cataractogenesis following high-LET radiation exposure”, Mutation Research. Reviews in mutation research, Vol. 770, Elsevier B.V., Amsterdam, https://doi.org/10.1016/j.mrrev.2016.08.005

Hamada, N. (2017a), “Ionizing radiation sensitivity of the ocular lens and its dose rate dependence”, International journal of radiation biology, Vol. 93/10, Taylor & Francis, Abingdon, https://doi.org/10.1080/09553002.2016.1266407

Hamada, N. and G. E. Woloschak (2017), “Ionizing radiation response of primary normal human lens epithelial cells”, PloS ONE, Vol. 12/7, Public Library Science, San Francisco, https://doi.org/10.1371/journal.pone.0181530

Havas, M. (2017), “When theory and observation collide: Can non-ionizing radiation cause cancer?”, Environmental pollution, Vol. 221, Elsevier Ltd, England. https://doi.org/10.1016/j.envpol.2016.10.018

Hightower, K. R. (1995), “The role of the lens epithelium in development of UV cataract”, Current eye research, Vol. 14/1, Informal UK Ltd, Philadelphia, https://doi.org/10.3109/02713689508999916

Iliakis, G., T. Murmann & A. Soni (2015), "Alternative end-joining repair pathways are the ultimate backup for abrogated classical non-homologous end-joining and homologous recombination repair: Implications for the formation of chromosome translocations.", Mutat. Res. - Genet. Toxicol. Environ. Mutagen. 793:166–175. doi:10.1016/j.mrgentox.2015.07.001.

Joiner, M. (2009), "Basic Clinical Radiobiology", Edited by. [1] P.J. Sadler, Next-Generation Met Anticancer Complexes Multitargeting via Redox Modul Inorg Chem 52 21.:375. doi:10.1201/b13224.

Jorge, S.-G. et al. (2012), "Evidence of DNA double strand breaks formation in Escherichia coli bacteria exposed to alpha particles of different LET assessed by the SOS response.", Appl. Radiat. Isot. 71(SUPPL.):66–70. doi:10.1016/j.apradiso.2012.05.007.

Kadhim, M.A., M.A. Hill & S.R. Moore, (2006), "Genomic instability and the role of radiation quality.", Radiat. Prot. Dosimetry. 122(1–4):221–227. doi:10.1093/rpd/ncl445.

Khanna, K.K. & S.P. Jackson (2001), "DNA double-strand breaks: signaling, repair and the cancer connection.", Nature Genetics. 27(3):247-54. doi:10.1038/85798.

Kim, K. S. et al. (2014), “Characterization of DNA damage-induced cellular senescence by ionizing radiation in endothelial cells”, International Journal of Radiation Biology, Vol. 90/1, Informa, London, https://doi.org/10.3109/09553002.2014.859763

Kim, J. N. and B. M. Lee (2007), “Risk factors, health risks, and risk management for aircraft personnel and frequent flyers”, Journal of toxicology and environmental health. Part B, Critical reviews, Vol. 10/3, Taylor & Francis Group, Philadelphia, https://doi.org/10.1080/10937400600882103

Kleiman, N. J., R. Wang and A. Spector (1990), “Ultraviolet light induced DNA damage and repair in bovine lens epithelial cells”, Current eye research, Vol. 9/12, Informa UK Ltd, Oxford, https://doi.org/10.3109/02713689009003475

Kozbenko, T. et al. (2022), “Deploying elements of scoping review methods for adverse outcome pathway development: a space travel case example”, International Journal of Radiation Biology, 1–12. https://doi.org/10.1080/09553002.2022.2110306

Kuefner, M.A. et al. (2009), "DNA Double-Strand Breaks and Their Repair in Blood Lymphocytes of Patients Undergoing Angiographic Procedures.", Investigative radiology. 44(8):440-6. doi:10.1097/RLI.0b013e3181a654a5.

Kuefner, M.A. et al. (2015), "Chemoprevention of Radiation-Induced DNA Double-Strand Breaks with Antioxidants.", Curr Radiol Rep (2015) 3: 81. https://doi.org/10.1007/s40134-014-0081-9

Kuhne, M., G. Urban & M. Lo, (2005), "DNA Double-Strand Break Misrejoining after Exposure of Primary Human Fibroblasts to CK Characteristic X Rays, 29 kVp X Rays and Co γ-Rays.", Radiation Research. 164(5):669-676. doi:10.1667/RR3461.1.

de Lara, C.M. et al. (2001), "Dependence of the Yield of DNA Double-Strand Breaks in Chinese Hamster V79-4 Cells on the Photon Energy of Ultrasoft X Rays.", Radiation Research. 155(3):440-8. doi:10.1667/0033-7587(2001)155[0440:DOTYOD]2.0.CO;2.

Liao, J. et al. (2011), “Anti-UVC irradiation and metal chelation properties of 6-benzoyl-5,7-dihydroxy-4-phenyl-chromen-2-one: An implications for anti-cataract agent”, International journal of molecular sciences, Vol. 12/10, MDPI, Basel. https://doi.org/10.3390/ijms12107059

Lipman, R. M., B. J. Tripathi, R. C. Tripathi (1998), “Cataracts induced by microwave and ionizing radiation”, Survey of ophthalmology, Vol. 33/3, Elsevier Inc, United States, https://doi.org/10.1016/0039-6257(88)90088-4

Lomax, M.E., L.K. Folkes & P.O. Neill (2013). "Biological Consequences of Radiation-induced DNA Damage: Relevance to Radiotherapy", Statement of Search Strategies Used and Sources of Information Why Radiation Damage is More Effective than Endogenous Damage at Killing Cells Ionising Radiation-induced Do. 25:578–585. doi:10.1016/j.clon.2013.06.007.

Long, A. C., C. M. H. Colitz, and J. A. Bomser (2001), “Apoptotic and necrotic mechanisms of stress-induced human lens epithelial cell death”, Experimental biology and medicine, SAGE Publications, London, https://doi.org/10.1177/153537020422901012

Lorat, Y. et al. (2015), "Nanoscale analysis of clustered DNA damage after high-LET irradiation by quantitative electron microscopy – The heavy burden to repair.", DNA Repair (Amst). 28:93–106. doi:10.1016/j.dnarep.2015.01.007.

Maier, P. et al. (2016), "Cellular Pathways in Response to Ionizing Radiation and Their Targetability for Tumor Radiosensitization.", Int. J. Mol. Sci., 14;17(1), pii:E102, doi:10.3390/ijms17010102.

Markiewicz, E. et al. (2015), “Nonlinear ionizing radiation-induced changes in eye lens cell proliferation, cyclin D1 expression and lens shape”, Open biology, Vol. 5/4, Royal society, London, https://doi.org/10.1098/rsob.150011

Milligan, J. R. et al. (1995), « DNA repair by thiols in air shows two radicals make a double-strand break”, Radiation Research, Vol 143/3, pp. 273-280

Moore, S., F.K.T. Stanley & A.A. Goodarzi (2014), "The repair of environmentally relevant DNA double strand breaks caused by high linear energy transfer irradiation – No simple task.", DNA repair (Amst), 17:64–73. doi: 10.1016/j.dnarep.2014.01.014.

Mosconi, M., U. Giesen & F. Langner (2011), "53BP1 and MDC1 foci formation in HT-1080 cells for low- and high-LET microbeam irradiations.", Radiat. Envrion. Biophys. 50(3):345–352. doi:10.1007/s00411-011-0366-9.

Nagane, M. et al. (2021), “DNA damage response in vascular endothelial senescence: Implication for radiation-induced cardiovascular disease”, Journal of Radiation Research, Vol. 62/4, https://doi.org/10.1093/jrr/rrab032

Nenoi, M., B. Wang & G. Vares (2015), "In vivo radioadaptive response: A review of studies relevant to radiation-induced cancer risk.", Hum. Exp. Toxicol. 34(3):272–283.

doi:10.1177/0960327114537537.

Nikitaki, Z. et al. (2016), "Measurement of complex DNA damage induction and repair in human cellular systems after exposure to ionizing radiations of varying linear energy transfer (LET).", Free Radiac. Res. 50(sup1):S64-S78, doi:10.1080/10715762.2016.1232484.

Nikjoo, H. et al. (2001), "Computational approach for determining the spectrum of DNA damage induced by ionizing radiation.", Radiat. Res. 156(5 Pt 2):577–83.

Nübel, T. et al. (2006), "Lovastatin protects human endothelial cells from killing by ionizing radiation without impairing induction and repair of DNA double-strand breaks", Clinical Cancer Research, Vol. 12/3, American Association for Cancer Research, https://doi.org/10.1158/1078-0432.CCR-05-1903

Ojima, M., N. Ban, and M. Kai (2008), "DNA double-strand breaks induced by very low X-ray doses are largely due to bystander effects", Radiation Research, Vol. 170/3, Radiation Research Society, United States, https://doi.org/10.1667/RR1255.1

Okayasu, R. (2012a), "Repair of DNA damage induced by accelerated heavy ions-A mini review.", Int. J. Cancer. 130(5):991–1000. doi:10.1002/ijc.26445.

Okayasu, R. (2012b), "Heavy ions — a mini review.", 1000:991–1000. doi:10.1002/ijc.26445.

Park, J. W. et al. (2022), "Metformin alleviates ionizing radiation-induced senescence by restoring BARD1-mediated DNA repair in human aortic endothelial cells", Experimental Gerontology, Vol. 160, Elsevier, Amsterdam, https://doi.org/10.1016/j.exger.2022.111706

Parris, C.N. et al. (2015), "Enhanced γ-H2AX DNA damage foci detection using multimagnification and extended depth of field in imaging flow cytometry.", Cytom. Part A. 87(8):717–723. doi:10.1002/cyto.a.22697.

Radulescu I., K. Elmroth & B. Stenerlöw (2006), "Chromatin Organization Contributes to Non-randomly Distributed Double-Strand Breaks after Exposure to High-LET Radiation.", Radiat. Res. 161(1):1–8. doi:10.1667/rr3094.

Rastogi, R. P. et al. (2010), "Molecular mechanisms of ultraviolet radiation-induced DNA damage and repair", Journal of nucleic acids, Hindawi Ltd, United States. https://doi.org/10.4061/2010/592980

Reddy, V. N. et al. (1998), "The effect of aqueous humor ascorbate on ultraviolet-B-induced DNA damage in lens epithelium", Investigative ophthalmology & visual science, Vol. 39/2, Arvo, pp. 344-350

Rogakou, E.P. et al. (1999), "Megabase Chromatin Domains Involved in DNA Double-Strand Breaks In Vivo.", J. Cell Biol, 146(5):905-16. doi: 10.1083/jcb.146.5.905.

Rogers, C. S. et al. (2004), "The effects of sub-solar levels of UV-A and UV-B on rabbit corneal and lens epithelial cells", Experimental eye research, Vol. 78/5, Elsevier Ltd, London, https://doi.org/10.1016/j.exer.2003.12.011

Rombouts, C. et al. (2013), "Differential response to acute low dose radiation in primary and immortalized endothelial cells", International Journal of Radiation Biology, Vol. 89/10, Informa, London, https://doi.org/10.3109/09553002.2013.806831

Rothkamm, K. et al. (2015), "Review DNA Damage Foci: Meaning and Significance.", Environ. Mol. Mutagen., 56(6):491-504, doi: 10.1002/em.21944.

Rothkamm, K. & M. Lo (2003), "Evidence for a lack of DNA double-strand break repair in human cells exposed to very low x-ray doses.", PNAS, 100(9):5057-62. doi:10.1073/pnas.0830918100.

Rübe, C.E. et al. (2008), "Cancer Therapy: Preclinical DNA Double-Strand Break Repair of Blood Lymphocytes and Normal Tissues Analysed in a Preclinical Mouse Model: Implications for Radiosensitivity Testing.", Clin. Cancer Res., 14(20):6546–6556. doi:10.1158/1078-0432.CCR-07-5147.

Russo, A. et al. (2015), "Review Article Genomic Instability: Crossing Pathways at the Origin of Structural and Numerical Chromosome Changes.", Envrion. Mol. Mutagen. 56(7):563-580. doi:10.1002/em.

Rydberg B, Heilbronn L, Holley WR, Lobrich M, Zeitlin C et al. 2002. Spatial Distribution and Yield of DNA Double-Strand Breaks Induced by 3-7 MeV Helium Ions in Human Fibroblasts. Radiat Res. 158(1):32-42.

Sabirzhanov, et al. (2020), "Irradiation-Induced Upregulation of miR-711 Inhibits DNA Repair and Promotes Neurodegeneration Pathways.", Int J Mol Sci. 21(15):5239. doi: 10.3390/ijms21155239.

Sage, E. & N. Shikazono (2017), "Free Radical Biology and Medicine Radiation-induced clustered DNA lesions: Repair and mutagenesis.", Free Radic. Biol. Med. 107(December 2016):125–135. doi:10.1016/j.freeradbiomed.2016.12.008.

Sasaki, H. et al. (1998), "TEMPOL protects against lens DNA strand breaks and cataract in the x-rayed rabbit", Investigative ophthalmology & visual sciences, Vol. 39/3, Arvo, Rockville, pp. 544-552

Schmal, Z. et al. (2019), "DNA damage accumulation during fractionated low-dose radiation compromises hippocampal neurogenesis", Radiotherapy and Oncology. 137:45-54. doi:10.1016/j.radonc.2019.04.021.

Sears, C. R. and J. J. Turchi (2012), "Complex cisplatin-double strand break (DSB) lesions directly impair cellular non-homologous end-joining (NHEJ) independent of downstream damage response (DDR) pathways", Journal of biological chemistry, Vol 287/29, The American Society for Biochemistry and Molecular Biology, Inc, USA, https://doi.org/ 10.1074/jbc.M112.344911

Shah, D.J., R.K. Sachs & D.J. Wilson (2012), "Radiation-induced cancer: A modern view." Br. J. Radiol. 85(1020):1166–1173. doi:10.1259/bjr/25026140.

Shelke, S. & B. Das (2015), "Dose response and adaptive response of non- homologous end joining repair genes and proteins in resting human peripheral blood mononuclear cells exposed to γ radiation.", (December 2014):365–379. doi:10.1093/mutage/geu081.

Sidjanin, D., S. Zigman and J. Reddan (1993), "DNA damage and repair in rabbitlens epithelial cells following UVA radiation", Current eye research, Vol. 12/9, Informa UK Ltd, Oxford, https://doi.org/10.3109/02713689309020382

Smith, J. et al. (2003), "Impact of DNA ligase IV on the delity of end joining in human cells.", Nucleic Acids Research. 31(8):2157-2167.doi:10.1093/nar/gkg317.

Smith, T.A. et al. (2017), "Radioprotective agents to prevent cellular damage due to ionizing radiation." Journal of Translational Medicine.15(1).doi:10.1186/s12967-017-1338-x.

Stewart, F. A. et al. (2012), "ICRP publication 118: ICRP statement on tissue reactions and early and late effects of radiation in normal tissues and organs – threshold doses

for tissue reactions in a radiation protection context", Annals of the ICRP, Vol, 41/1-2, Elsevier Ltd, London, https://doi.org/10.1016/j.icrp.2012.02.001

Sudprasert, W., P. Navasumrit & M. Ruchirawat (2006), "Effects of low-dose γ radiation on DNA damage, chromosomal aberration and expression of repair genes in human blood cells.", Int. J. Hyg. Envrion. Health, 209:503–511. doi:10.1016/j.ijheh.2006.06.004.

Sutherland, B.M. et al. (2000), "Clustered DNA damages induced in isolated DNA and in human cells by low doses of ionizing radiation.", J. of Rad. Res. 43 Suppl(S):S149-52. doi: 10.1269/jrr.43.S149

Sylvester, C. B. et al. (2018), "Radiation-Induced Cardiovascular Disease: Mechanisms and Importance of Linear Energy Transfer", Frontiers in cardiovascular medicine, Vol. 5, Frontiers, https://doi.org/10.3389/fcvm.2018.00005

Terato, H. & H. Ide (2005), "Clustered DNA damage induced by heavy ion particles.", Biol. Sci. Sp. 18(4):206–215. doi:10.2187/bss.18.206.

Ungvari, Z. et al. (2013), "Ionizing radiation promotes the acquisition of a senescence-associated secretory phenotype and impairs angiogenic capacity in cerebromicrovascular endothelial cells: role of increased DNA damage and decreased DNA repair capacity in microvascular radiosensitivity", The journals of gerontology. Series A, Biological sciences and medical sciences, Vol. 68/12, Oxford University Press, Oxford, https://doi.org/10.1093/gerona/glt057

Valentin, J.D.J (1998), "Chapter 1. Ann ICRP.", 28(4):5–7. doi:10.1016/S0146-6453(00)00002-6. http://www.ncbi.nlm.nih.gov/pubmed/10882804.

Venkatesh, P. et al. (2016), "Effect of chromatin structure on the extent and distribution of DNA double strand breaks produced by ionizing radiation; comparative study of hESC and differentiated cells lines.", Int J. Mol. Sci. 17(1). doi:10.3390/ijms17010058.

Wang, et al. (2021), "Ionizing Radiation-Induced Brain Cell Aging and the Potential Underlying Molecular Mechanisms.", Cells. 10(12):3570. doi: 10.3390/cells10123570

Ward, J. F. (1988), "DNA Damage Produced by Ionizing Radiation in Mammalian Cells: Identities, Mechanisms of Formation, and Reparability.", Prog. Nucleic Acid Res. Mol. Biol. 35(C):95–125. doi:10.1016/S0079-6603(08)60611-X.

Wolf, N. et al. (2008), "Radiation cataracts: Mechanisms involved in their long delayed occurrence but then rapid progression", Molecular vision, Vol. 14/34-35, Molecular Vision, Atlanta, pp. 274-285

Wu, L.J. et al. (1999), "Targeted cytoplasmic irradiation with alpha particles induces mutations in mammalian cells.", Proc. Natl. Acad. Sci. 96(9):4959–4964. doi:10.1073/pnas.96.9.4959.

Yamaguchi, H. et al. (2005), "Estimation of Yields of OH Radicals in Water Irradiated by Ionizing Radiation.", J. of Rad. Res. 46(3):333-41. doi: 10.1269/jrr.46.333.

Zhang, L. et al. (2017), "The inhibitory effect of minocycline on radiation-induced neuronal apoptosis via AMPKα1 signaling-mediated autophagy.", Sci Rep.7(1):16373. doi: 10.1038/s41598-017-16693-8.

Relationship: 2856: Increase, DNA strand breaks leads to Altered Signaling

AOPs Referencing Relationship

AOP Name	Adjacency	Weight of Evidence	Quantitative Understanding
Deposition of energy leads to vascular remodeling	adjacent	High	Moderate
Deposition of Energy Leading to Learning and Memory Impairment	adjacent	Moderate	Low

Evidence Supporting Applicability of this Relationship

Taxonomic Applicability

Term	Scientific Term	Evidence	Links
human	Homo sapiens	Low	NCBI
mouse	Mus musculus	Moderate	NCBI
rat	Rattus norvegicus	Moderate	NCBI

Life Stage Applicability

Life Stage	Evidence
Juvenile	Low
Adult	Moderate

Sex Applicability

Sex	Evidence
Male	Moderate
Female	Low

Evidence for this relationship is predominantly from studies using rat- and mouse-derived cells, with some in vivo evidence in mice

and rats. There is in vivo evidence in male animals, but no in vivo studies specify the use of female animals. In vivo evidence is from adult models.

Key Event Relationship Description

DNA strand breaks can lead to altered signaling of various pathways through the DNA damage response. DNA strand breaks, which are a form of DNA damage, can induce ataxia telangiectasia mutated (ATM) and ATM/RAD3-related (ATR), two phosphoinositide 3-kinase (PI3K)-related serine/threonine kinases (PIKKs) (Abner and McKinnon, 2004; Lee and McKinnon, 2007; Nagane et al., 2021; Sylvester et al., 2018; Thadathil et al., 2019; Wang et al., 2020; Wang et al., 2017). Following DNA strand breaks, DNA damage response cellular signaling can phosphorylate downstream proteins and activate several transcription factors and pathways (Wang et al., 2017). Spontaneous DNA strand breaks from endogenous sources will induce signaling as a normal response to facilitate DNA repair. However, excessive DNA damage induced by a stressor will result in increased activation of these pathways and subsequent harmful downstream effects. Signaling pathways induced by DNA strand breaks include p53/p21 (Abner and McKinnon, 2004; Baselet et al., 2018; Lee and McKinnon, 2007; Nagane et al., 2021; Sylvester et al., 2018; Thadathil et al., 2019; Wang et al., 2020; Wang et al., 2017), caspase (Abner and McKinnon, 2004; Baselet et al., 2019; Wang et al., 2020; Wang et al., 2016) and mitogen-activated protein kinase (MAPK) family pathways (Ghahremani et al., 2002; Nagane et al., 2021).

Evidence Supporting this KER

Overall weight of evidence: Moderate

Biological Plausibility

There is strong evidence supporting the link between DNA strand breaks leading to altered signaling pathways. Single strand breaks (SSBs) or double strand breaks (DSBs) in DNA from both endogenous and exogenous sources can induce the DNA damage response, which can result in the induction of various signaling pathways (Baselet et al., 2019). DNA strand breaks are well known to lead to the activation of ATM and ATR as part of the normal DNA damage response (Abner and McKinnon, 2004; Baselet et al., 2019; Lee and McKinnon, 2007; Nagane et al., 2021; Sylvester et al., 2018; Thadathil et al., 2019; Wang et al., 2020; Wang et al., 2017; Wang et al., 2016). While ATM tends to be recruited to DSBs, ATR is recruited by many types of DNA damage including both DSBs and SSBs (Maréchal and Zou, 2013; Wang et al., 2017). Following a DNA DSB, the Mre11-Rad50-Nbs1 (MRN) complex senses and directly binds to the DNA ends at the site of the break, which subsequently activates ATM (Lee and McKinnon, 2007; Maréchal and Zou, 2013). Following a DNA SSB, resection of the damaged strand by apurinic/apyrimidinic endonuclease (APE)1/APE2 is followed by coating the single-stranded DNA with replication protein A (RPA), where the recruitment of the ATR-ATR interacting protein (ATRIP) complex and the activation of ATR occurs (Caldecott, 2022; Maréchal and Zou, 2013).

ATM and ATR can phosphorylate over 700 proteins (Nagane et al., 2021), and phosphorylation of key signaling proteins by ATM/ATR will alter signaling in their respective pathways. High levels of DNA strand breaks induced by exogenous stressors will enhance ATM/ATR activation and subsequently further activate downstream signaling, leading to downstream consequences. The extracellular signal-regulated kinase (ERK), c-Jun N-terminal kinase (JNK) and p38 MAPK subfamily pathways can be phosphorylated and activated by ATM/ATR (Ghahremani et al., 2002; Nagane et al., 2021). Additionally, ATM/ATR can phosphorylate p53 on serine 15 to enhance the stability of p53, leading to activation of the p53 pathway and changes in the transcriptional activity of p53 (Abner and McKinnon, 2004; Baselet et al., 2019; Lee and McKinnon, 2007; Nagane et al., 2021; Sylvester et al., 2018; Thadathil et al., 2019; Wang et al., 2020; Wang et al., 2017; Wang et al., 2016). The apoptosis pathway downstream of p53 can also be activated by DNA strand breaks (Abner and McKinnon, 2004; Baselet et al., 2019; Lee and McKinnon, 2007; Thadathil et al., 2019; Wang et al., 2020).

Empirical Evidence

Evidence for this relationship was collected from studies using in vivo mouse and rat models as well as in vitro mouse-derived, rat-derived and human-derived cell models. The stressors used to support this relationship include ^{137}Cs gamma rays and X rays. Markers of DNA strand breaks in this KER include p53 binding protein 1 (53BP1), phosphorylation of H2AX (γ-H2AX), phosphorylation of ATR (p-ATR) and phosphorylation of ATM (p-ATM). Altered signaling was measured mostly by the protein expression of the p53/p21 and apoptosis pathways.

Dose Concordance

A few studies have indicated a dose concordance between the increase in DNA strand breaks and altered signaling pathways. X-ray irradiation of rat cortical neurons showed increased DNA damage markers, γ-H2AX, p-ATM and p-ATR and increased levels of signaling proteins, including p21, p-p53 and cleaved caspase 3 at both doses of 8 and 32 Gy (Sabirzhanov et al., 2020). ^{137}Cs gamma irradiated cerebromicrovascular endothelial cells (CMVECs) and rat hippocampal neurons showed increased DNA strand breaks, measured by comet assay, at 2-10 Gy, and increased caspase 3/7 activity at 2, 4 and 6 Gy (Ungvari et al., 2013).

Time Concordance

Many studies demonstrate that DNA strand breaks occur before altered signaling in a time course. Although both KEs can occur

quickly, Gionchiglia et al. (2021) showed in mice that γ-H2AX and p53BP1 foci were increased as early as 15 minutes after 10 Gy of X-ray irradiation while cleaved caspase 3 did not increase until 30 minutes after irradiation. In HT22 hippocampal neurons irradiated with 12 Gy of X-rays, γ-H2AX and p-ATM were increased at 30 minutes post-irradiation while p53 was increased after 1 h and caspase 3 was increased after 48 h (Zhang et al., 2017). Similarly, rat cortical neurons irradiated with 8 Gy of X-rays showed increased p-ATM, γ-H2AX and p-ATR after 30 minutes, while p-p53, p21 and cleaved caspase 3 did not increase until 3 or 6 h post-irradiation (Sabirzhanov et al., 2020). Multiple studies using human- and rat-derived endothelial cells irradiated with 4 Gy of ^{137}Cs gamma rays show increased DNA strand breaks at 1 h post-irradiation, with altered signaling to p53 and p21 at 6 h and to caspase 3/7 at 18 h post-irradiation (Kim et al., 2014; Park et al., 2022; Ungvari et al., 2013). In a longer-term study irradiating human lung microvascular endothelial cells (HMVEC-L) with 15 Gy of X-rays, increased DNA strand breaks were observed at 14 days post-irradiation, while altered signaling in the p53 pathway was observed at 21 days post-irradiation (Lafargue et al., 2017).

Incidence concordance

A few studies have demonstrated an incidence concordance between DNA strand breaks and altered signaling at equivalent doses. Following X-ray irradiation of mice, DNA damage markers, γ-H2AX and p53BP1, increased by 10, 15 and 5-fold in different region of the brain, while cleaved caspase 3 signaling molecule increased by 1.4 and 2.6-fold (Gionchiglia et al., 2021). Gamma ray irradiation of Wistar rats showed a 6-fold increase in DNA damage marker compared to a 0.2-fold decrease in (B-cell lymphoma 2) Bcl-2 and a 2- to 4-fold increase in signaling proteins p53, Bcl-2-associated protein X (Bax) and caspase 3/8/9 (El-Missiry et al., 2018).

Essentiality

Some studies show that preventing an increase in DNA strand breaks will restore signaling. Treatment with mesenchymal stem cell-conditioned medium (MSC-CM) reduced γ-H2AX, decreased the levels of p53, Bax, cleaved caspase 3 and increased the levels of Bcl-2 in HT22 cells irradiated with 10 Gy of X-rays (Huang et al., 2021). The inhibition of microRNA (miR)-711 decreased levels of DNA damage markers, p-ATM, p-ATR and γ-H2AX, and decreased signaling molecules including p-p53, p21 and cleaved caspase 3 (Sabirzhanov et al., 2020).

Uncertainties and Inconsistencies

None identified

Quantitative Understanding of the Linkage

The tables below provide some representative examples of quantitative linkages between the two key events. All data that is represented is statistically significant unless otherwise indicated.

Response-response relationship

Dose Concordance

Reference	Experiment Description	Result
Sabirzhanov et al., 2020	*In vitro*. Rat cortical neurons were exposed to 2, 8 and 32 Gy X-rays. DNA damage was determined by γ-H2AX staining and western blot analysis of p-ATM and p-ATR. Altered signaling was determined by levels of p-p53, p21, cleaved caspase 3, measured by Western blot.	Irradiated primary cortical neurons showed increased γ-H2AX by 30-fold at both 8 and 32 Gy but not at 2 Gy. p-ATM was increased at all doses, increasing about 15-fold at 8 and 32 Gy. Signaling molecules including p-p53, p21, and cleaved caspase 3 were increased at all doses.
Ungvari et al., 2013	*In vitro*. CMVECs and rat hippocampal neurons were irradiated with ^{137}Cs gamma rays. DNA strand breaks were assessed with the comet assay. Caspase 3/7 activity was determined by an assay kit.	DNA damage increased at all doses (2-10 Gy). In the control, less than 5% of DNA was in the tail while by 6 Gy 35% of the DNA was in the tail in CMVECs and 25% was in the tail in neurons. In CMVECs, 2, 4, and 6 Gy increased caspase 3/7 activity 5- to 6-fold.

Incidence Concordance

Reference	Experiment Description	Result
El-Missiry et al., 2018	*In vivo*. Wistar rats were irradiated with 4 Gy of ^{137}Cs gamma rays (0.695 cGy/s). DNA damage was assessed with a comet assay. Multiple signaling proteins were assessed with assay kits.	The tail moment increased 6-fold while signaling proteins including p53, Bax, and caspases 3/8/9 increased 2- to 4-fold, and Bcl-2 decreased 0.2-fold.
Gionchiglia	*In vivo*. CD1 and B6/129 mice were irradiated with 10 Gy of X-rays. γ-H2AX and 53BP1 foci were quantified with	γ-H2AX and p53BP1 foci increased about 10-fold in the forebrain and cerebral cortex, about 15-fold in the hippocampus and about 5-fold in

et al., 2021	immunofluorescence. Cleaved caspase 3 positive cells were measured with immunofluorescence.	the subventricular zone (SVZ)/ rostral migratory stream (RMS)/ olfactory bulb (OB). Cleaved caspase 3 increased 1.4-fold in the cerebral cortex and hippocampus and 2.6-fold in the SVZ/RMS/OB.

Time-scale

Time Concordance

Reference	Experiment Description	Result
Zhang et al., 2017	*In vitro*. HT22 cells were irradiated with 12 Gy of X-rays (1.16 Gy/min). p-ATM, γ-H2AX, cleaved caspase 3 and p53 were measured with Western blot.	p-ATM and γ-H2AX were increased 4.4-fold and 3.2-fold, respectively, 30 minutes after 12 Gy. p53 was increased 4.6-fold at 1 h post-irradiation. A 9-fold increase in cleaved caspase 3 was observed 48 h post-irradiation.
Gionchiglia et al., 2021	*In vivo*. CD1 and B6/129 mice were irradiated with 10 Gy of X-rays. γ-H2AX and 53BP1 foci were quantified with immunofluorescence in neurons. Cleaved caspase 3 positive neurons were measured with immunofluorescence.	At both 15 and 30 minutes post-irradiation, γ-H2AX and p53BP1 foci increased. However, cleaved caspase 3 increased at 30 minutes but not at 15 minutes.
Sabirzhanov et al., 2020	*In vitro*. Rat cortical neurons were exposed to 2, 8 and 32 Gy X-rays. DNA damage was determined by γ-H2AX staining and western blot analysis of p-ATM and p-ATR. Altered signaling was determined by levels of p-p53, p21, cleaved caspase 3, measured by Western blot.	DNA damage occurred as early as 30 min post 8 Gy irradiation, indicated by increased p-ATM, γ-H2AX and p-ATR. Signaling molecules p-p53, p21 and cleaved caspase 3 increased at 3 or 6h post-irradiation.
Park et al., 2022	*In vitro*. Human aortic endothelial cells (HAECs) were irradiated with 4 Gy of ^{137}Cs gamma rays (3.5 Gy/min). γ-H2AX was measured with western blot. p-ATM and 53BP1 were determined with immunofluorescence. p-p53 and p21 were measured with Western blot.	γ-H2AX, p-ATM, and 53BP1 were shown increased at 1 h post-irradiation, while p-p53 and p21 were increased at 6 h post-irradiation.
Kim et al., 2014	*In vitro*. Human umbilical vein endothelial cells (HUVECs) were irradiated with 4 Gy ^{137}Cs gamma rays. DNA damage was determined by γ-H2AX. p21 and p53 were measured by Western blot.	γ-H2AX foci greatly increased at 1 and 6 h post-irradiation, while p-p53 and p21 were increased at 6 h post-irradiation.
Ungvari et al., 2013	*In vitro*. CMVECs and rat hippocampal neurons were irradiated with 2-6 Gy of ^{137}Cs gamma rays. DNA strand breaks were assessed with the comment assay. Caspase 3/7 activity was determined by an assay kit.	DNA damage in neurons and CMVECs increased at 1 h post-irradiation, while caspase 3/7 activity increased the greatest at 18 h post-irradiation in CMVECs.
Lafargue et al., 2017	*In vitro*. HMVEC-L were irradiated with 15 Gy of X-rays. γ-H2AX foci were assessed with immunofluorescence. p-ATM and ATM were assessed with Western blot. Signaling proteins including p53, p21 and p16 were assessed with western blot.	Without irradiation, most cells had 0 or 1 γ-H2AX foci, while 14 days after 15 Gy, most cells had 2-6 γ-H2AX foci. The ratio of p-ATM/ATM was also increased 14 days after 15 Gy. p53, p21, and p16 were all increased at 21 days after 15 Gy.

Known modulating factors

Modulating factor	Details	Effects on the KER	References
Media	MSC-CM	Treatment decreased γ-H2AX, p53, the Bax/Bcl-2 ratio and cleaved caspase 3 in irradiated neurons.	Huang et al., 2021
Genetic	miR-711	miR-711 inhibition reduced the DNA damage response including p-ATM, p-ATR, and γ-H2AX. It also decreased signaling molecules including p-p53, p21, and cleaved caspase 3.	Sabirzhanov et al., 2020
Drug	Minocycline	Treatment with minocycline in irradiated neurons reduced the DNA damage response through reduced γ-H2AX and p-ATM. Caspase 3 was also inhibited by minocycline, but p53 was not changed.	Zhang et al., 2017
Drug	Metformin	Treatment reduced p-ATM, p-p53 and p21 levels, but did not change the level of 53BP1 in irradiated HAECs.	Park et al., 2022

Known Feedforward/Feedback loops influencing this KER

None identified

References

Abner, C. W. and P. J. McKinnon. (2004), "The DNA double-strand break response in the nervous system", *DNA Repair*, Vol. 3/8–9,

Elsevier, Amsterdam, https://doi.org/10.1016/j.dnarep.2004.03.009.

Baselet, B. et al. (2019), "Pathological effects of ionizing radiation: endothelial activation and dysfunction", *Cellular and Molecular Life Sciences*, Vol. 76/4, Springer Nature, https://doi.org/10.1007/s00018-018-2956-z.

Caldecott, K. W. (2022), "DNA single-strand break repair and human genetic disease", *Trends in Cell Biology*, 32(9), Elsevier, Amsterdam, https://doi.org/10.1016/j.tcb.2022.04.010

El-Missiry, M. A. et al. (2018), "Neuroprotective effect of epigallocatechin-3-gallate (EGCG) on radiation-induced damage and apoptosis in the rat hippocampus", *International Journal of Radiation Biology*, Vol. 94/9, Informa, London, https://doi.org/10.1080/09553002.2018.1492755.

Ghahremani, H. et al. (2002), "Interaction of the c-Jun/JNK Pathway and Cyclin-dependent Kinases in Death of Embryonic Cortical Neurons Evoked by DNA Damage", *Journal of Biological Chemistry*, Vol. 277/38, Elsevier, Amsterdam, https://doi.org/10.1074/jbc.M204362200

Gionchiglia, N. et al. (2021), "Association of Caspase 3 Activation and H2AX γ Phosphorylation in the Aging Brain: Studies on Untreated and Irradiated Mice", *Biomedicines*, Vol. 9/9, MDPI, Basel, https://doi.org/10.3390/biomedicines9091166.

Huang, Y. et al. (2021), "Mesenchymal Stem Cell-Conditioned Medium Protects Hippocampal Neurons From Radiation Damage by Suppressing Oxidative Stress and Apoptosis", *Dose-Response*, Vol. 19/1, SAGE publications, https://doi.org/10.1177/1559325820984944.

Kozbenko, T. et al. (2022), "Deploying elements of scoping review methods for adverse outcome pathway development: a space travel case example", *International Journal of Radiation Biology*, Vol. 98/12. https://doi.org/10.1080/09553002.2022.2110306

Kim, K. S. et al. (2014), "Characterization of DNA damage-induced cellular senescence by ionizing radiation in endothelial cells", *International Journal of Radiation* Biology, Vol. 90/1, Informa, London, https://doi.org/10.3109/09553002.2014.859763.

Lafargue, A. et al. (2017), "Ionizing radiation induces long-term senescence in endothelial cells through mitochondrial respiratory complex II dysfunction and superoxide generation", *Free Radical Biology and Medicine*, Vol. 108, Elsevier, Amsterdam, https://doi.org/10.1016/j.freeradbiomed.2017.04.019.

Lee, Y. and P. J. McKinnon. (2007), "Responding to DNA double strand breaks in the nervous system", *Neuroscience*, Vol. 145/4, Elsevier, Amsterdam, https://doi.org/10.1016/j.neuroscience.2006.07.026.

Maréchal, A. and L. Zou. "DNA damage sensing by the ATM and ATR kinases", *Cold Spring Harbor Perspectives in Biology*, 5(9), Cold Spring Harbor Laboratory Press, https://doi.org/10.1101/cshperspect.a012716

Nagane, M. et al. (2021), "DNA damage response in vascular endothelial senescence: Implication for radiation-induced cardiovascular diseases", *Journal of Radiation Researc*h, Vol. 62/4, Oxford University Press, Oxford, https://doi.org/10.1093/jrr/rrab032.

Park, J.-W. et al. (2022), "Metformin alleviates ionizing radiation-induced senescence by restoring BARD1-mediated DNA repair in human aortic endothelial cells", *Experimental Gerontology*, Vol. 160, Elsevier, Amsterdam, https://doi.org/10.1016/j.exger.2022.111706.

Sabirzhanov, B. et al. (2020), "Irradiation-Induced Upregulation of miR-711 Inhibits DNA Repair and Promotes Neurodegeneration Pathways", *International Journal of Molecular Sciences*, Vol. 21/15, MDPI, Basel, https://doi.org/10.3390/ijms21155239.

Sylvester, C. B. et al. (2018), "Radiation-Induced Cardiovascular Disease: Mechanisms and Importance of Linear Energy Transfer", *Frontiers in Cardiovascular Medicine*, Vol. 5, Fronteirs, https://doi.org/10.3389/fcvm.2018.00005.

Thadathil, N. et al. (2019), "DNA double-strand breaks: a potential therapeutic target for neurodegenerative diseases", *Chromosome Research*, Vol. 27/4, Springer Nature, https://doi.org/10.1007/s10577-019-09617-x.

Ungvari, Z. et al. (2013), "Ionizing Radiation Promotes the Acquisition of a Senescence-Associated Secretory Phenotype and Impairs Angiogenic Capacity in Cerebromicrovascular Endothelial Cells: Role of Increased DNA Damage and Decreased DNA Repair Capacity in Microvascular Radiosensitivity", *The journals of gerontology. Series A, Biological sciences and medical sciences*, Vol. 68/12, Oxford University Press, Oxford, https://doi.org/10.1093/gerona/glt057.

Wang, Q. et al. (2020), "Radioprotective Effect of Flavonoids on Ionizing Radiation-Induced Brain Damage", *Molecules*, Vol. 25/23, MDPI, Basel, https://doi.org/10.3390/molecules25235719.

Wang, H. et al. (2017), "Chronic oxidative damage together with genome repair deficiency in the neurons is a double whammy for neurodegeneration: Is damage response signaling a potential therapeutic target?", *Mechanisms of Ageing and Development*, Vol. 161, Elsevier, Amsterdam, https://doi.org/10.1016/j.mad.2016.09.005.

Wang, Y., M. Boerma and D. Zhou. (2016), "Ionizing Radiation-Induced Endothelial Cell Senescence and Cardiovascular Diseases", *Radiation Research*, Vol. 186/2, BioOne, https://doi.org/10.1667/RR14445.1.

Zhang, L. et al. (2017), "The inhibitory effect of minocycline on radiation-induced neuronal apoptosis via AMPKα1 signaling-mediated autophagy", *Scientific Reports*, Vol. 7/1, Springer Nature, https://doi.org/10.1038/s41598-017-16693-8.

List of Non Adjacent Key Event Relationships

Relationship: 2837: Energy Deposition leads to Increase, Neural Remodeling

AOPs Referencing Relationship

AOP Name	Adjacency	Weight of Evidence	Quantitative Understanding
Deposition of Energy Leading to Learning and Memory Impairment	non-adjacent	Moderate	Low

Evidence Supporting Applicability of this Relationship

Taxonomic Applicability

Term	Scientific Term	Evidence	Links
mouse	Mus musculus	High	NCBI
rat	Rattus norvegicus	Low	NCBI
dog	Canis lupus familiaris	Low	NCBI

Life Stage Applicability

Life Stage	Evidence
Adult	Moderate
Not Otherwise Specified	Low
Juvenile	Low

Sex Applicability

Sex	Evidence
Male	High
Female	Low
Unspecific	Low

Evidence for this relationship comes from dog, rat, and mouse models, with a lot of evidence in mice. There is in vivo evidence in both male and female animals, a large amount of evidence in males. Animal age is occasionally not indicated in studies, but most evidence is in adult rodent models.

Key Event Relationship Description

Energy deposition through ionizing radiation can lead to chemical changes including bond breakages and the generation of by-products, such as free radicals from water hydrolysis, which can change cellular homeostasis (Einor et al., 2016; Martinez-López & Hande, 2020; Reisz et al., 2014). This energy can come in many forms (i.e., gamma rays, X-rays, alpha particles, heavy ions, protons), to produce a range in complexity of damage (Drobny, 2013). When deposited onto neurons, oxidative stress can affect neuronal signaling through the induction of alterations to the neuronal architecture and synaptic activity. The energy can further cause necrosis and demyelination, and decrease neurogenesis and synaptic complexity; these together are important to maintain the integrity of the neurons (Cekanaviciute et al., 2018; J. R. Fike et al., 1984; Hladik & Tapio, 2016). Furthermore, there can also be disruptions in neuronal signaling, as well as changes to drebrin cluster and postsynaptic density proteins (PSD), which are known to regulate dendritic spine morphogenesis. Together these can lead to neural remodeling (Takahashi et al., 2003).

Evidence Supporting this KER

Overall Weight of Evidence: Moderate

Biological Plausibility

Multiple reviews provide support of biological plausibility between deposition of energy and neuron remodeling. Numerous studies examine the effects of multiple radiation sources including gamma rays, X-rays, protons, heavy ions, alpha particles, and neutrons, on both in vivo and in vitro model systems. The collected data demonstrate changes in the physical and electrophysiological properties of neurons in response to ionizing radiation exposure (Cekanaviciute et al., 2018; Hladik & Tapio, 2016). Irradiation of the brain induces oxidative stress and inflammation, which is linked to the occurrence of neuronal alterations within the hippocampus, an important structure in the process of learning and memory (Jarrard, 1993; Monje et al., 2003; Rola et al., 2007:

Lalkovičová et al., 2022). There is no clear understanding on how deposited energy directly affects neuron integrity; however, immature neurons are found to be more radiosensitive and exhibit significant changes in spine density, dendritic spine length, protein clustering, and decreased cell proliferation, leading to reduced dendritic complexity (Manda et al., 2008a ; Mizumatsu et al., 2003; Okamoto et al., 2009; Rola et al., 2005; Shirai et al., 2013). Many neurodegenerative conditions are related to changes in synaptic plasticity, including changes in neuronal connectivity, action potential, and synaptic protein levels (Vipan Kumar Parihar & Limoli, 2013). These alterations occur primarily within the hippocampus and dentate gyrus, two regions of the mammalian brain where adult neurogenesis can occur (Ming & Song, 2011) following ionizing radiation exposure.

Empirical Evidence

The empirical evidence collected for this KER stems from research using both in vitro and in vivo models. Neural remodeling encompasses changes to the physical and/or electrophysiological properties of neurons (Acharya et al., 2019; Klein et al., 2021). Most of the evidence examines the effects of moderate (0.1-0.5 Gy) or high (>2 Gy) dose irradiation on both in vivo and in vitro rodent models. Studies using X-ray and/or heavy ion irradiation ranging from 0.05 – 30 Gy identify similar alterations in dendritic spine structure, neurogenesis, and apoptosis (Allen et al., 2015; Cekanaviciute et al., 2018; J. R. Fike et al., 1984; Hladik & Tapio, 2016; Kiffer et al., 2020; Manda et al., 2008a; Mizumatsu et al., 2003; Okamoto et al., 2009; Vipan K. Parihar et al., 2016; Vipan K. Parihar; Rola et al., 2005; Tiller-Borcich et al., 1987; Panagiotakos et al., 2007). The low dose evidence (<0.1 Gy) stems from studies from heavy ion or alpha particle irradiation of hippocampal mouse tissue (Krukowski et al., 2018b; Vipan K. Parihar et al., 2016; Vipan K. Parihar, Allen, et al., 2015). High dose studies (2 Gy up to 90 Gy) show more extreme changes in neuron integrity through decreased CNPase levels, increased necrosis and reduced cytoskeleton proteins (Chiang et al., 1993; Jiang et al., 2014; Shirai et al., 2013).

Dose Concordance

Several studies support a dose-concordant relationship between energy deposition and neural remodeling. Dose-dependent increases in neuronal apoptosis/necrosis and decreases in F-actin, drebrin and synapsin I protein clusters are observed in a range of doses from 0.5 Gy to 10 Gy (Mizumatsu et al., 2003; Okamoto et al., 2009). Studies that examine changes in dendritic spines exhibit dose-dependent decreases in filopodia spines at 0.1 Gy to 10 Gy (Vipan K. Parihar, Pasha, et al., 2015; Vipan Kumar Parihar & Limoli, 2013). High-dose irradiation resulted in more severe damage in the white matter, including edema, demyelination, and necrosis at 15 Gy (Tiller-Borcich et al., 1987), as well as significant decreases in protein clusters at doses greater than 30 Gy (Shirai et al., 2013).

Across different types of radiation stressors, the data exhibits consistent dose-dependent changes to neuron integrity but of different magnitudes. A study examining the effects of 56Fe and 12C ions observed dose-dependent decreases in neurogenesis within each age group and type of irradiation. Overall, 56Fe irradiation of 9-month-old mice revealed a greater decrease in proliferating cells and immature neurons compared to 12C ions, except at 3 Gy, where there was a slightly greater number of proliferating cells (Rola et al., 2005). Similarly, compared to 16O particles, Parihar et al. found greater decreases in the numbers of dendritic branches and branch points when exposed to 48Ti particles; however, 16O particles led to a greater decrease in spine density (Parihar et al., 2015).

Time Concordance

Multiple studies support time concordance between deposition of energy and neural remodeling. Most of these studies identify persistent, time-dependent deterioration of the neuronal structure up to 4 months post-irradiation at doses ranging from 0.05 – 30 Gy and using radiation types of gamma rays, protons, X-rays, and heavy ions (Chakraborti et al., 2012; Vipan K. Parihar et al., 2016; Vipan K. Parihar, Allen, et al., 2015; Vipan K. Parihar, Pasha, et al., 2015; Vipan Kumar Parihar & Limoli, 2013). At 9 months post-irradiation (0.5 Gy of protons), Bellone et al. (2015) observed enhanced synaptic excitability, indicative of increases in synaptic density, and Rola et al., (2005) found that the number of proliferating neural precursor cells was lower than that at 3 months (1 and 3 Gy of 56Fe ions). At 24 h to 15 months post-irradiation (25 Gy of X-rays), Panagiotakos et al. (2007) showed unrepairable damage to both the subventricular zone and neural stem cell compartment in the female rat model. A study at 30 months (15 Gy of X-rays) revealed a reduction in computed tomography (CT) density, indicative of edema, demyelination, axonal swelling, and/or necrosis(J. R. Fike et al., 1984). In examining different radiation types, the time-response relationship could not be clearly identified due to differences in experimental design across studies. However, two studies analyzing PSD-95 expression, a protein involved in regulating synaptic plasticity, at 10- and 30-days post-irradiation found that 1 Gy of gamma ray irradiation led to similar time-dependent increases in PSD-95 compared to 1 Gy of proton irradiation (Vipan K. Parihar, Pasha, et al., 2015; Vipan Kumar Parihar & Limoli, 2013).

Incidence Concordance

No available data.

Essentiality

As deposition of energy is a physical stressor, it cannot be blocked by chemicals, however, it can be shielded. (Al Zaman & Nizam, 2022). Further research is required to determine the effects of shielding radiation on neural remodeling. Since deposited energy initiates events immediately, the removal of deposited energy, a physical stressor, also supports the essentiality of the key event. Studies that do not deposit energy are observed to have no downstream effects.

Uncertainties and Inconsistencies

- One study shows that at a high dose of 90 Gy (X-rays), hippocampal dendritic spine length is increased compared to the

control (Shirai et al., 2013). Kiffer et al. found a decrease in spine length in the CA1 subregion of the hippocampus; however, there was an increase in spine length and dendritic complexity in the dorsal dentate gyrus after exposure to 0.5 Gy 1H and 0.1 Gy 16O (Kiffer et al., 2020). Further research involving different regions of the brain is required to identify the effects of deposition of energy on the dentate gyrus.

- The study by Krukowski et al. (2018a), as highlighted in a review by Cekanaviciute et al. (2018), found a lack of cellular changes in hippocampal synapse loss and microgliosis in females subjected to low dose ionizing radiation. Another study highlighted in this review showed greater reduction in new neuronal survival in male than female mice in response to 28Si irradiation (Whoolery et al., 2017). Additional data is required to determine if these differences are sex-related or due to other factors. There is a lack of studies performed on female subjects to identify specific sex-related effects of deposited energy on neuron integrity.
- Previous studies have found transient changes in neurogenesis after exposure to 56Fe ions at varying doses ranging from 10 cGy to 1 Gy (DeCarolis et al., 2014; Miry et al., 2021https://pubmed.ncbi.nlm.nih.gov/25170435/https://pubmed.ncbi.nlm.nih.gov/33619310/). These studies found early decreases in neurogenesis, although DeCarolis et al. reported that this reduction returned to normal as early as 7 days post-irradiation. In a separate study, Miry et al. (2021) found that at 12 months post-exposure, neurogenesis levels significantly exceeded controls. Other inconsistent studies include Acharya et al. (2019) and Bellone et al. (2015); the former reported decreases in CA1 pyramidal neuron excitability after exposure to 18 cGy of neutron radiation, whereas the latter study reported increases in post-synaptic excitability within CA1 neurons after 0.5 Gy of proton irradiation.

Quantitative Understanding of the Linkage

The table below provides some representative examples of quantitative linkages between the two key events. It was difficult to identify a general trend across all the studies due to differences in experimental design and reporting of the data. All data is statistically significant unless otherwise stated.

Dose Concordance

Reference	Experimental Description	Results
Acharya et al., 2019	In vivo. Male mice were irradiated with 252Cf neutrons at a dose rate of 1 mGy per day for 180 days. The mice were then sacrificed, and brains were removed to conduct whole-cell electrophysiology on the pyramidal neurons in the dorsal hippocampus.	18 cGy of neutron radiation caused pyramidal neurons to be more hyperpolarized with a mean difference score (Mdiff) of -2.56 mV. CA1 pyramidal neurons exhibited a decrease in excitability (Mdiff = 30.8 pA) at 18 cGy.
Vipan Kumar Parihar & Limoli, 2013	In vivo. Male transgenic mice were exposed to cranial gamma irradiation at a dose of 1 or 10 Gy. This was done using a 137Cs irradiator at a dose rate of 2.07 Gy/min. After tissue harvesting, fluorescent imaging was performed on hippocampal neurons expressing the enhanced green fluorescent protein (EGFP) transgene to analyze changes in dendritic tree.	Dose-dependent reductions in the number of dendritic branch points, length, and area at both 10 and 30 days after gamma irradiation. Significant increase in PSD-95 (postsynaptic scaffolding protein) expression of 2.7-fold at 10 Gy at both time-points, and 1.7- and 2.2-fold increases for 1 Gy at 10 and 30 days, respectively. 1.8- and 3.7-fold decrease in filopodia at 1 and 10 Gy.
Vipan K. Parihar, Pasha et al., 2015	In vitro. Male transgenic mice were exposed to whole body proton irradiation at a dose of 0.1 or 1 Gy. This was done using 250 MeV plateau phase protons at a dose rate of 0.25 Gy/min. Mice were sacrificed 10 or 30 days post-irradiation, then fluorescent imaging was performed on hippocampal neurons expressing the EGFP transgene to analyze changes in dendritic tree. Immunohistochemistry was also performed to measure synaptic proteins.	Dose-dependent increases in postsynaptic density protein 95 (PSD-95) expression of 1.8- (0.1 Gy) and 2.1-fold (1 Gy) at 30 days in the dentate gyrus after proton irradiation. Dose-dependent reduction in synaptophysin expression of 1.3- (0.1 Gy) and 1.9-fold (1 Gy) in the dentate hilus. Dose-dependent and time-dependent decreases in number of filopodia spines (2.9- and 3.7-fold decreases at 10 and 30 days at 1 Gy).
Mizumatsu et al., 2003	In vivo. Male mice were exposed to cranial X-irradiation at 1, 2, 5 and 10 Gy (rate of 175 cGy/min). Confocal microscopy was then used to assess changes in neurogenesis and neuronal proliferation.	Numbers of immature neurons in the subgranular zone reduced by 36, 51, 56, and 67% at 1, 2, 5, and 10 Gy, respectively, indicative of decreased neurogenesis. Decrease in number of neural cells by 41, 53, and 61% at 2, 5, and 10 Gy, indicative of increased apoptosis.
Rola et al., 2005	In vivo. Male mice received whole-body irradiation with iron or carbon ions at doses of 1, 2 or 3 Gy. These were delivered at dose rates of 0.87 ± 0.16 Gy/min and 1.23 ± 0.07 Gy/min for iron and carbon ions, respectively. Confocal microscopy and immunohistochemistry were then performed to	56Fe irradiation led to 48% (1 Gy, 3 months old), 76% (3 Gy, 3 months), 81% (1 Gy, 9 months old), and 65% (3 Gy, 9 months) decreases in proliferating (Ki67-positive) cells in the dentate subgranular zone and 34% (1 Gy, 3 months), 71% (3 Gy, 3 months), 59% (1 Gy, 9 months), and 89% (3 Gy, 9 months) decreases in immature neurons (DCx-positive cells). 12C irradiation led to 25% (1 Gy, 9 months) and 72% (3 Gy, 9 months) decreases in Ki67-positive

	analyze proliferating neurons and neurogenesis.	cells and 20% (1 Gy, 9 months) and 62% (3 Gy, 9 months) decreases in DCx-positive cells.
Chiang et al., 1993	In vivo. Male mice were exposed to 2, 8, 20, 30, 36 and 45 Gy of X-irradiation at a dose rate of 238 cGy/min. ELISA was performed to analyze CNPase levels.	CNPase (myelin-associated enzyme) levels were decreased to approximately 85% after 20, 30, and 45 Gy before increasing to normal values at 15 days. At 60 days, 20 Gy CNPase levels peaked with an approximate increase to 110% before decreasing to 84% at 180 days. At 30 Gy, CNPase levels peaked after 120 days at 86% before decreasing to 64% after 270 days. At 45 Gy, CNPase levels continued to decrease to 73% 180 days post-irradiation.
Allen et al., 2015	In vitro. Male mice received whole-body iron irradiation at 0.5 Gy (dose rate was not indicated). Golgi staining was performed for spine analysis and Sholl analysis for dendritic morphology quantification.	Dentate gyrus spine density 34% decreased after 0.5 Gy 56Fe irradiation. Dentate gyrus dendritic length decreased by 20% at 79.0 and 100.8 µm from soma and 27% at 120.9 and 130.2 µm from soma. CA1 basal spine density decreased by 32%. A peak decrease of 49% in CA1 dendritic length was observed at 77 µm from soma. CA3 apical spine density decreased by 20%.
Vipan K. Pariar et al., 2016	In vitro. Male transgenic mice and male rats were exposed to charged particles (16O and 48Ti at 600 MeV/n) at dose rates between 0.05 and 0.25 Gy/min. After tissue harvesting, confocal imaging was used for EGFP expressing neurons to assess neuronal morphometry 15 weeks post exposure.	Total dendritic length was decreased by 25%, 28%, 33%, and 34%; number of dendritic branch points decreased by 25%, 27%, 25%, and 27% respectively; and number of dendritic branches by 15%, 83%, 32%, and 28%, for 16O – 5 cGy, 16O – 30 cGy, 48Ti – 5 cGy, and 48Ti – 30 cGy, respectively.
Shirai et al., 2013	In vitro. Hippocampal cultures were exposed to 30, 60 and 90 Gy of X-irradiation at a rate of 86.7 cGy/min. Green fluorescent protein (GFP) transfection was used to analyze the effects of X-ray irradiation on dendritic spine morphology and density. Fluorescent immunohistochemistry was used to evaluate cytoskeletal proteins within dendritic spines.	Significant increase in dendritic spine length at 90 Gy by 1.2-fold. No change in width of dendritic spines. Number of F-actin clusters decreased by 1.4- (30 Gy), 1.57- (60 Gy), and 1.4-fold (90 Gy). Number of drebrin clusters decreased by 1.3- (30 and 60 Gy) and 1.4-fold (90 Gy).
Okamoto et al., 2009	In vitro. Primary neurons from the hippocampi of fetal rats were exposed to 0.5, 4 and 10 Gy of X-irradiation. Immunofluorescence was performed to analyze synaptic proteins and TUNEL staining was performed to identify neuronal apoptosis.	Significant increase in apoptosis of neurons of 1.3- (0.5 Gy), 1.9- (4 Gy), and 2.5-fold (10 Gy) at 7 days post-irradiation and 1.4- (0.5 Gy), 2.3- (4 Gy), and 2.6-fold (10 Gy) at 14 days post-irradiation. Significant decrease in F-actin clusters of 1.4-fold (10 Gy) at 7 days, and 1.4- (4 Gy) and 1.5-fold (10 Gy) at 14 days. Significant decrease in drebrin of 1.8-fold (10 Gy) at 7 days, and 1.7- (4 Gy) and 1.5-fold (10 Gy) at 14 days. Significant decrease in Synapsin-I of 1.1-fold (10 Gy) at 14 days.
Vipan K. Parihar, Allen, et al., 2015	In vivo. Male transgenic mice (with EGFP transgene) were exposed to 5-30 cGy of charged particles (16O and 48Ti) at dose rates between 0.5 and 1.0 Gy/min. After tissue harvesting, confocal microscopy, imaging and neuronal morphometry were performed to evaluate dendritic complexity and spine density 8 weeks post radiation exposure.	Significant reductions in number of dendritic branches by 1.5- (16O – 30 cGy), 1.8- (48Ti – 5 cGy), and 1.7-fold (48Ti – 30 cGy), number of branch points by 1.5- (16O – 30 cGy), 1.4- (48Ti – 5 cGy), and 1.8-fold (48Ti – 30 cGy), total dendritic length by 1.5- (16O – 5 cGy), 1.8- (16O – 30 cGy), 1.5- (48Ti – 5 cGy), and 1.7-fold (48Ti – 30 cGy), number of spines by 1.5- (16O – 5 cGy), 1.8- (16O – 30 cGy), 1.7- (48Ti – 5 cGy), 1.9-fold (48Ti – 30 cGy), and spine density by 1.7- (16O – 5 cGy), 1.6- (16O – 30 cGy), 1and 1.5-fold (48Ti – 5 and 30 cGy). Significant increase in PSD-95 puncta by 1.5-fold (all doses and radiation types) 8 weeks post-irradiation.
Kiffer et al., 2020	In vivo. Male mice received whole-body 1H and 16O irradiation at 0.5 and 0.1 Gy, respectively. The dose rates were 18-19 cGy/min (1H irradiation) and 18-33 cGy/min (16O irradiation). Golgi staining was performed for dendritic morphology quantification and spine analyses.	Dentate gyrus dendritic complexity increased by 1.4-fold after 0.5 Gy (1H) and 0.1 Gy (16O) combined irradiation.
Klein et al., 2021	In vivo. Male mice received whole-body simulated galactic cosmic irradiation (1H, 16O, 4He, 28Si, 56Fe) at 5 and 30 cGy. The dose rate was 5 cGy/min for the mixed-ion simulated galactic cosmic radiation (GCR). Electrophysiological measurements were then taken to assess changes in synaptic signaling within the CA1 region of the hippocampus.	30 cGy of mixed-ion GCR causes CA1 pyramidal neurons to have elevated amplitudes in the spontaneous inhibitory postsynaptic currents (sIPSC) with a mean difference score (Mdiff) of 5.54 pA. There was also a decrease in the sIPSC rise times (Mdiff = -0.45 ms). These results show that GCR leads to enhanced inhibitory synaptic signaling.

Time Concordance

References	Experimental Description	Results
Vipan K. Parihar, Pasha, et al., 2015	In vitro. Male transgenic mice were exposed to whole body proton irradiation at a dose of 0.1 or 1 Gy. This was done using 250 MeV plateau phase protons at a dose rate of 0.25 Gy/min. Mice were sacrificed at 10 or 30 days post-irradiation, then fluorescent imaging was performed on hippocampal neurons expressing the EGFP transgene to analyze changes in dendritic tree. Immunohistochemistry was also performed to measure synaptic proteins.	Time-dependent increase in PSD-95 of 1.6- (10 days) and 2.1-fold (30 days). Time-dependent decrease in synaptophysin of 1.4- (10 days) and 1.9-fold (30 days) in the dentate hilus.
Bellone et al., 2015	In vivo. Male mice received whole-body irradiation with 0.5 Gy of 150 MeV protons at a rate of 1.5-2.5 Gy/min. Electrophysiological experiments were conducted to measure synaptic response changes.	After 9 months, exposure to 0.5 Gy of proton irradiation resulted in an increase in postsynaptic excitability by 53% at 1.50 mA stimulation. Synaptic efficacy was increased by 118%. fEPSP (excitatory postsynaptic potential) slopes increased approximately 15 – 46% at least 60 minutes post-stimulation. There were no changes in presynaptic ability.
J. R. Fike et al., 1984	In vivo. Male beagle dogs were exposed to 10, 15, 30 Gy of X-irradiation at a rate of 3 Gy/min. Computed tomography (CT) scan and histological examination were performed to identify differences in tissue density within the cerebrum.	Animals receiving 10 Gy had no response up to 12 months. Time to maximum computed tomography (CT) response was 6.3 months for 15 Gy and 5.2 months for 30 Gy.
Chakraborti et al., 2012	In vitro. Male mice were irradiated with a single dose of 10 Gy from a 137Cs source at a rate of 1.67 Gy/min. After harvesting, neurons underwent Golgi staining to analyze changes in spine density and morphology.	10 Gy of gamma irradiation led to a time-dependent decrease in spine density in the dentate gyrus by 11.9% (1 week) and 26.9% (1 month), a significant reduction in proportion of mushroom spines by 24.3% (1 week) and 15.7% (1 month), a significant decrease in the number of thin spines by 11.49% (1 week) and 13.2% (1 month), and a significant increase in number of mushroom spines by 12.1% (1 week) and 25.3% (1 month).
Okamoto et al., 2009	In vitro. Primary neurons from the hippocampi of fetal rats were exposed to 0.5, 4 and 10 Gy of X-rays. Immunofluorescence was performed to analyze synaptic proteins and TUNEL staining was performed to identify neuronal apoptosis.	Significant increase in apoptosis of neurons of 1.3- (0.5 Gy), 1.9- (4 Gy), and 2.5-fold (10 Gy) at 7 days post-irradiation and 1.4- (0.5 Gy), 2.3- (4 Gy), and 2.6-fold (10 Gy) at 14 days post-irradiation. Significant decrease in F-actin clusters of 1.4-fold (10 Gy) at 7 days, and 1.4- (4 Gy) and 1.5-fold (10 Gy) at 14 days. Significant decrease in drebrin of 1.8-fold (10 Gy) at 7 days, and 1.7- (4 Gy) and 1.5-fold (10 Gy) at 14 days. Significant decrease in Synapsin-I of 1.1-fold (10 Gy) at 14 days.
Panagiotakos et al., 2007	In vitro. Female Sprague Dawley rat brains were irradiated with X-rays at 25 Gy (117.5 cGy/min) while shielding the olfactory bulb. Immunohistochemistry, stereological analysis, fluorescence intensity quantification, electron microscopy and magnetic resonance imaging were preformed to assess long term radiation damage 24 h to 15 months post irradiation.	The number of BrdU+ cells in the subventricular zone (SVZ) decreased significantly 15 months post irradiation (average number of BrdU+cells was 5,541+/–624 compared to the control group of 34,680+/–9,413). Doublecortin (DCX)-expressing neuroblasts were lost permanently immediately post irradiation.

Known modulating factors

Modulating Factor	Details	Effects on the KER	References
Drug	SB415286 – a potent and selective cell-permeable, ATP-competitive GSK-3β inhibitor, as GSK-3β induces apoptosis in response to various conditions	Treatment with SB415286 provided significant neuroprotection against radiation necrosis within the brain at 45 Gy.	Jiang et al., 2014
Diet	N1-acetyl-N2-formyl-5-methoxykynuramine (AFMK) – a melatonin metabolite which has antioxidant properties.	AMFK treatment ameliorated levels of reactive oxygen species, and increased number of immature neurons and proliferating cells post-irradiation in vivo. Without the treatment, exposure to radiation led to a significant decrease in DCX positive cells by 81% and Ki-67 positive cells by 86%. (AMFK) treatment provided protection to immature neurons by 45.38% and proliferating cells by 52.35%.	Manda et al., 2008b
	PLX5622-1200 ppm (PLX)		

Drug	PLX3397 1200 ppm (PLX) diet that contains CSF1-R (colony stimulating factor 1 receptor) inhibitor that induces depletion of microglia within 3 days.	The PLX diet was able to significantly increase the levels of the presynaptic protein, synapsin 1 after exposure to helium irradiation.	Krukowski et al., 2018b

Known Feedforward/Feedback loops influencing this KER

NA

References

Acharya, M. M. et al. (2019), "New concerns for neurocognitive function during deep space exposures to chronic, low dose-rate, neutron radiation", eNeuro, Vol. 6/4, Society for Neuroscience, Washington, https://doi.org/10.1523/ENEURO.0094-19.2019.

Allen, A. R. et al. (2015), "56Fe Irradiation Alters Spine Density and Dendritic Complexity in the Mouse Hippocampus", Radiation Research, Vol. 184/6, BioOne, Washington, https://doi.org/10.1667/RR14103.1.

Al Zaman, M. A. and Q. M. R. Nizam. (2022), "Study on Shielding Effectiveness of a Combined Radiation Shield for Manned Long Termed Interplanetary Expeditions", Journal of Space Safety Engineering, Vol. 9/1, Elsevier, Amsterdam, https://doi.org/10.1016/j.jsse.2021.12.003.

Bellone, J. A. et al. (2015), "A single low dose of proton radiation induces long-term behavioral and electrophysiological changes in mice", Radiation Research, Vol. 184/2, BioOne, Washington, https://doi.org/10.1667/RR13903.1.

Cekanaviciute, E., S. Rosi and S. V. Costes. (2018), "Central Nervous System Responses to Simulated Galactic Cosmic Rays", International Journal of Molecular Sciences, Vol. 19/11, Multidisciplinary Digital Publishing Institute (MDPI), Basel, https://doi.org/10.3390/IJMS19113669.

Chakraborti, A. et al. (2012), "Cranial Irradiation Alters Dendritic Spine Density and Morphology in the Hippocampus", PLOS ONE, Vol. 7/7, Public Library of Science, San Francisco, https://doi.org/10.1371/JOURNAL.PONE.0040844.

Chiang, C. S., W. H. McBride and H. Rodney Withers. (1993), "Myelin-associated changes in mouse brain following irradiation", Radiotherapy and Oncology, Vol. 27/3, Elsevier, Amsterdam, https://doi.org/10.1016/0167-8140(93)90079-N.

DeCarolis, N. A. et al. (2014), "56Fe particle exposure results in a long-lasting increase in a cellular index of genomic instability and transiently suppresses adult hippocampal neurogenesis in vivo", Life Sciences in Space Research, Vol. 2, https://doi.org/10.1016/j.lssr.2014.06.004.

Dhikav, V. and K. Anand. (2012), "Hippocampus in health and disease: An overview", Annals of Indian Academy of Neurology, Vol. 15/4, Wolters Kluwer, Alphen aan den Rijn, https://doi.org/10.4103/0972-2327.104323.

Drobny, J. G. (2013), "Introduction", Ionizing Radiation and Polymers (pp. 1–10), Elsevier, Amsterdam, https://doi.org/10.1016/B978-1-4557-7881-2.00001-8.

Einor, D. et al. (2016), "Ionizing radiation, antioxidant response and oxidative damage: A meta-analysis", Science of The Total Environment, Vols. 548–549, Elsevier, Amsterdam, https://doi.org/10.1016/j.scitotenv.2016.01.027.

Fike, J. R. et al. (1984), "Computed Tomography Analysis of the Canine Brain: Effects of Hemibrain X Irradiation", Radiation Research, Vol. 99/2, Allen Press, Lawrence, https://doi.org/10.2307/3576373.

Hainmueller, T. and M. Bartos. (2020), "Dentate gyrus circuits for encoding, retrieval and discrimination of episodic memories", Nature Reviews Neuroscience, Vol. 21/3, Springer Nature, Berlin, https://doi.org/10.1038/s41583-019-0260-z.

Harris, K. M. and J. K. Stevens. (1989), "Dendritic spines of CA 1 pyramidal cells in the rat hippocampus: serial electron microscopy with reference to their biophysical characteristics", Journal of Neuroscience, Vol. 9/8, Society for Neuroscience, Washington, https://doi.org/10.1523/JNEUROSCI.09-08-02982.1989.

Hladik, D. and S. Tapio. (2016), "Effects of ionizing radiation on the mammalian brain", Mutation Research - Reviews in Mutation Research, Vol. 770, Elsevier B.V., Amsterdam, https://doi.org/10.1016/j.mrrev.2016.08.003.

HR, C. C. M. W. W. (1993), "Radiation-induced astrocytic and microglial response in mouse brain", papers3://publication/uuid/729C572E-9A43-4EF4-A184-8A9DAD8CBC38.

Jarrard, L. E. (1993), "On the role of the hippocampus in learning and memory in the rat", Behavioral and Neural Biology, Vol. 60/1, Academic Press, Cambridge, https://doi.org/10.1016/0163-1047(93)90664-4.

Jiang, X. et al. (2014), "A GSK-3β Inhibitor Protects Against Radiation Necrosis in Mouse Brain", International Journal of Radiation Oncology*Biology*Physics, Vol. 89/4, Elsevier, Amsterdam, https://doi.org/10.1016/J.IJROBP.2014.04.018.

Kiffer, F. et al. (2020), "Late Effects of 1H + 16O on Short-Term and Object Memory, Hippocampal Dendritic Morphology and Mutagenesis", Frontiers in Behavioral Neuroscience, Vol. 14, Frontiers Media S.A., https://doi.org/10.3389/fnbeh.2020.00096.

Klein, P. M. et al. (2021), "Detrimental impacts of mixed-ion radiation on nervous system function", Neurobiology of Disease, Vol. 151, Elsevier, https://doi.org/10.1016/j.nbd.2021.105252.

Krukowski, K. et al. (2018a), "Female mice are protected from space radiation-induced maladaptive responses", Brain, Behavior, and Immunity, Vol. 74, Academic Press Inc., https://doi.org/10.1016/j.bbi.2018.08.008.

Krukowski, K. et al. (2018b), "Temporary microglia-depletion after cosmic radiation modifies phagocytic activity and prevents cognitive deficits", Scientific Reports 2018 8:1, Vol. 8/1, Nature Publishing Group, Berlin, https://doi.org/10.1038/s41598-018-26039-7.

Lalkovičová, M. (2022), "Neuroprotective agents effective against radiation damage of central nervous system", Neural Regeneration Research, Vol. 17/9, https://doi.org/10.4103/1673-5374.335137.

Manda, K., M. Ueno and K. Anzai. (2008a), "Memory impairment, oxidative damage and apoptosis induced by space radiation: Ameliorative potential of α-lipoic acid", Behavioural Brain Research, Vol. 187/2, Elsevier, Amsterdam, https://doi.org/10.1016/j.bbr.2007.09.033.

Manda, K., M. Ueno and K. Anzai. (2008b), "Space radiation-induced inhibition of neurogenesis in the hippocampal dentate gyrus and memory impairment in mice: ameliorative potential of the melatonin metabolite, AFMK", Journal of Pineal Research, Vol. 45/4, John Wiley & Sons, Inc., Hoboken, https://doi.org/10.1111/j.1600-079X.2008.00611.x.

Martinez-López, W. and M. P. Hande. (2020), "Health effects of exposure to ionizing radiation", Advanced Security and Safeguarding in the Nuclear Power Industry (pp. 81–97), Elsevier, Amsterdam, https://doi.org/10.1016/B978-0-12-818256-7.00004-0.

Ming, G. and H. Song. (2011), "Adult Neurogenesis in the Mammalian Brain: Significant Answers and Significant Questions", Neuron, Vol. 70/4, NIH Public Access, https://doi.org/10.1016/J.NEURON.2011.05.001.

Miry, O. et al. (2021), "Life-long brain compensatory responses to galactic cosmic radiation exposure", Scientific Reports, Vol. 11/1, https://doi.org/10.1038/s41598-021-83447-y.

Mizumatsu, S. et al. (2003), "Extreme sensitivity of adult neurogenesis to low doses of X-irradiation", Cancer Research, Vol. 63/14.

Monje, M. L., H. Toda and T. D. Palmer. (2003), "Inflammatory Blockade Restores Adult Hippocampal Neurogenesis", Science, Vol. 302/5651, American Association for the Advancement of Science, Washington, https://doi.org/10.1126/SCIENCE.1088417.

Okamoto, M. et al. (2009), "Effect of radiation on the development of immature hippocampal neurons in vitro", Radiation Research, Vol. 172/6, BioOne, Washington, https://doi.org/10.1667/RR1741.1.

Panagiotakos, G. et al. (2007), "Long-Term Impact of Radiation on the Stem Cell and Oligodendrocyte Precursors in the Brain", (S. Akbarian, Ed.)PLoS ONE, Vol. 2/7, https://doi.org/10.1371/journal.pone.0000588.

Parihar, V. K. et al. (2016), "Cosmic radiation exposure and persistent cognitive dysfunction", Scientific Reports, Vol. 6/June, Nature Publishing Group, Berlin, https://doi.org/10.1038/srep34774.

Parihar, V. K. et al. (2015), "What happens to your brain on the way to Mars", Science Advances, Vol. 1/4, American Association for the Advancement of Science, Washington, https://doi.org/10.1126/SCIADV.1400256.

Parihar, V. K. et al. (2014), "Persistent changes in neuronal structure and synaptic plasticity caused by proton irradiation", Brain Structure and Function 2014 220:2, Vol. 220/2, Springer Nature, Berlin, https://doi.org/10.1007/S00429-014-0709-9.

Parihar, V. K. and C. L. Limoli. (2013), "Cranial irradiation compromises neuronal architecture in the hippocampus", Proceedings of the National Academy of Sciences of the United States of America, Vol. 110/31, National Academy of Sciences, Washingtonhttps://doi.org/10.1073/pnas.1307301110.

Reisz, J. A. et al. (2014), "Effects of Ionizing Radiation on Biological Molecules—Mechanisms of Damage and Emerging Methods of Detection", Antioxidants & Redox Signaling, Vol. 21/2, Mary Ann Liebert, Inc., New Rochelle, https://doi.org/10.1089/ars.2013.5489.

Rola, R. et al. (2005), "High-LET radiation induces inflammation and persistent changes in markers of hippocampal neurogenesis", Radiation Research (Volume 164, pp. 556–560), BioOne, Washington, https://doi.org/10.1667/RR3412.1.

Rola, R. et al. (2007), "Lack of extracellular superoxide dismutase (EC-SOD) in the microenvironment impacts radiation-induced changes in neurogenesis", Free Radical Biology and Medicine, Vol. 42/8, Pergamon, Bergama, https://doi.org/10.1016/J.FREERADBIOMED.2007.01.020.

Shirai, K. et al. (2006), "Differential effects of x-irradiation on immature and mature hippocampal neurons in vitro", Neuroscience Letters, Vol. 399/1–2, Elsevier, Amsterdam, https://doi.org/10.1016/j.neulet.2006.01.048.

Shirai, K. et al. (2013), "X Irradiation Changes Dendritic Spine Morphology and Density through Reduction of Cytoskeletal Proteins in Mature Neurons", Radiation Research, Vol. 179/6, Allen Press, Lawrence, https://doi.org/10.1667/RR3098.1.

Takahashi, H. et al. (2003), "Drebrin-Dependent Actin Clustering in Dendritic Filopodia Governs Synaptic Targeting of Postsynaptic Density-95 and Dendritic Spine Morphogenesis", The Journal of Neuroscience, Vol. 23/16, Society for Neuroscience, Washington,

https://doi.org/10.1523/JNEUROSCI.23-16-06586.2003.

Tiller-Borcich, J. K. et al. (1987), "Pathology of Delayed Radiation Brain Damage: An Experimental Canine Model", Radiation Research, Vol. 110/2, Allen Press, Lawrence, https://doi.org/10.2307/3576896.

Whoolery, C. W. et al. (2017), "Whole-body exposure to 28Si-radiation dose-dependently disrupts dentate gyrus neurogenesis and proliferation in the short term and new neuron survival and contextual fear conditioning in the long term", Radiation Research, Vol. 188/5, Radiation Research Society, https://doi.org/10.1667/RR14797.1.

Relationship: 2838: Energy Deposition leads to Impairment, Learning and memory

AOPs Referencing Relationship

AOP Name	Adjacency	Weight of Evidence	Quantitative Understanding
Deposition of Energy Leading to Learning and Memory Impairment	non-adjacent	Moderate	Low

Evidence Supporting Applicability of this Relationship

Taxonomic Applicability

Term	Scientific Term	Evidence	Links
human	Homo sapiens	Low	NCBI
mouse	Mus musculus	High	NCBI
rat	Rattus norvegicus	High	NCBI

Life Stage Applicability

Life Stage	Evidence
Adult	High
Old Age	Low
Juvenile	Low

Sex Applicability

Sex	Evidence
Male	High
Female	Low

Evidence for this relationship comes from human, rat, and mouse models, with a large amount of evidence in mice and rats. There is in vivo evidence in both male and female animals, with a lot of evidence in males. This relationship has been shown in adult animals in many studies.

Key Event Relationship Description

Deposition of energy from ionizing radiation (IR) can induce biological changes within living systems (UNSCEAR, 1982). The amount of IR absorbed and consequently the amount of damage ensued is quantified by the linear energy transfer (LET) of the radiation. Low-LET radiation consists of electromagnetic ionizing radiation such as X- and gamma rays, as well as protons that deposit smaller amounts of energy, whereas high-LET radiation deposits large amounts of energy and includes heavy ions, alpha particles and high-energy and neutrons. Therefore, high-LET radiation produces dense ionization while low-LET radiation induces sparse ionization events where energy is exponentially absorbed by tissues.

Deposition of energy can lead to reduced cognitive function related to learning and memory. Impaired learning can be seen as diminished ability to create new associative or non-associative relationships, whereas impaired memory consists of reduced ability to establish sensory, short-term or long-term memories (Desai et al., 2022; Kiffer et al., 2019b). Multiple brain areas are involved in learning and memory processes, with the most well-known occurring in the hippocampal region, as well as the amygdala, the prefrontal cortex, the basal ganglia, and other areas of the neocortex. These regions of the brain have been shown to be affected by deposition of energy (Cucinotta et al., 2014; Desai et al., 2022; NCRP Commentary, 2016).

Following deposition of energy, the process begins at the macromolecular level from direct damage to neurons and glial cells and via the generation of oxidative stress and promotion of neuroinflammatory environments in the central nervous system (CNS)

(Mhatre et al., 2022; Lalkovičová et al., 2022). The altered cellular environment caused by a deposition of energy can impact the functions of both neurons and glial cells, which can promote a persistent pro-inflammatory response, reduced neurogenesis, reduced dendritic spine lengths and density, and the inhibition of neuronal connectivity and synaptic activity (Hladik & Tapio, 2016; Cekanaviciute et al., 2018). In vivo studies link structural and functional changes in neurons and glial cells to a decreased ability to complete cognitive assessments that test various domains of learning and memory.

Evidence Supporting this KER

Overall Weight of Evidence: Moderate

Biological Plausibility

The biological rationale linking deposition of energy to impaired learning and memory is strongly supported in the literature, as reported by several review articles published on the subject (Desai et al., 2022; Kiffer et al., 2019b; Pasqual et al., 2021; NCRP, 2016; Collett et al., 2020; Cucinotta et al., 2014; Hladik & Tapio, 2016; Cekanaviciute et al., 2018; Mhatre et al., 2022; Lalkovičová et al., 2022; Greene-Schloesser et al., 2012; Turnquist et al., 2020; Katsura et al., 2021). It is well established that radiation exposure leads to both acute and chronic elevation in reactive oxygen species (ROS), and this subsequently mediates cell signaling within mature neurons, neural stem cells and glial cells (NCRP, 2016; Mhatre et al., 2022). ROS acts as a second messenger to activate microglia and astrocytes via redox-responsive transcription factor-mediated molecular signaling pathways, and once these glial cells are activated, they can adopt a pro-inflammatory morphology and thus release pro-inflammatory mediators (Hladik & Tapio, 2016; Cucinotta et al., 2014; Collett et al., 2020). Pro-inflammatory mediators such as cytokines mediate the immune response through ligand binding to cell surface receptors that can activate signaling cascades such as JAK-STAT or MAPK pathways to produce or recruit more cytokines (Mousa & Bakhiet, 2013; Prieto & Cotman, 2018).

Once these inflammatory reactions are initiated, the radiation-activated microglia can alter the functions of neurons. Structurally, the neuron is comprised of the cell body, dendrites, axon, and axon terminals (Lodish et al., 2000). Neurons communicate by electrical and chemical signaling via synapses, where axons from the presynaptic neuron interface with the dendritic arms of the postsynaptic neuron. Deposition of energy inhibits neuronal connectivity and synaptic activity through the loss of dendritic spines as well as dendrite length and branching (Cekanaviciute et al., 2018; Jandial et al., 2018). Overexpression of pro-inflammatory mediators disrupts the integrity of neurons through increased necrosis and demyelination, decreased neurogenesis, decreased neural stem cell proliferation and decreased synaptic complexity (Hladik & Tapio, 2016; Cekanaviciute et al., 2018; Lalkovičová et al., 2022). Together, these radiation-induced neuronal damage and persistent neuroinflammation alter learning and memory capabilities as evidenced by behavioral changes from in vivo studies.

Empirical Evidence

There is strong evidence supporting the connection between the deposition of energy leading to impaired learning and memory. The evidence was gathered from studies using in vivo rodent models and human studies. The applied stressors ranged from 0.5 cGy to 40 Gy and included heavy ions (e.g.,28Si, 16O, 56Fe, 48Ti), X-rays, gamma rays, protons, and alpha particles. Impaired learning and memory in rodents were measured through various behavioural tests that assessed several cognitive aspects such as short-term memory, long-term memory, recognition memory, spatial memory, working memory, declarative memory, associative learning, discrimination, and reversal learning (Britten et al., 2018; Rabin et al., 2014; Lonart et al., 2012; Britten et al., 2012; Bellone et al., 2015; Parihar et al., 2016; Rabin et al., 2012; Krukowski et al., 2018a; Forbes et al., 2014; Gan et al., 2019; Manda et al., 2007a; Acharya et al., 2016; Impey et al., 2016; Parihar et al., 2018; Belarbi et al., 2013; Krukowski et al., 2018b; Jewell et al., 2018; Rabin et al., 2015; Parihar et al., 2015; Kiffer et al., 2019a ; Hodges et al., 1998). Additionally in humans, cognitive test scores from the Swedish military enlistment exam of 18-year-old men, which evaluates general instruction, concept discrimination, technical comprehension, and spatial recognition, were used to evaluate the potential impact of beta ray, gamma ray, or X-ray exposures from radiotherapy treatment for cutaneous haemangioma when they were infants (18 months old or earlier) (Hall et al., 2004).

Dose Concordance

Many studies demonstrate dose concordance relating to deposition of emerging and impaired learning and memory. NOR is a behavioral assay that is used to evaluate recognition memory by measuring the time spent with a novel object instead of a familiar one after habituation and training with the familiar object (Cekanaviciute et al., 2018Mice irradiated with 9 Gy X-rays showed a DI (discrimination index; tendency to explore novel instead of familiar objects/locations) of -13 compared to the control of 23, demonstrating impaired memory after irradiation (Acharya et al., 2016). Another study in rats reported a reduction in the discrimination ratio (DR) from 0.5 to 0.2 after 40 Gy X-rays, also suggesting reduced learning and memory after radiation exposure (Forbes et al., 2014). However, this was only observed in 3-month-old rats. Mice irradiated with 0.05 or 0.3 Gy of either 16O and 48Ti particles showed a dose- and particle size-dependent decrease in the DI for NOR (Parihar et al., 2015; Parihar et al., 2016). Another study with heavy ions also reported impairments in novel object recognition after 0.1 Gy and 0.4 Gy of 56Fe ion irradiation, but not after 0.2 Gy of 56Fe ion irradiation (Impey et al., 2016). Memory was also inhibited in mice after 4He particle irradiation at 0.5 Gy, but not after 4He particle irradiation at 0.15 Gy or 1 Gy after being tested using NOR (Krukowski et al., 2018b). In a mixed ion beam study using the galactic cosmic ray (GCR) simulator, NOR was impaired after 0.15 Gy and 0.5 Gy of irradiation in males only, with no reduction in performance reported in female mice (Krukowski et al., 2018a). In contrast, results from a separate study suggest that there is an impact on female mice, as female mice irradiated with 16O particles showed dose-dependent decreases in the DR from 22 (control) to -2 (0.1 Gy) and -5 (0.25 Gy) for NOR (Kiffer et al., 2019a). Memory assessed with NOR was also

impaired in rats exposed to various particles (protons, carbon, oxygen, silicon, titanium and iron ions) with doses from 0.1 to 2 Gy (Rabin et al., 2014). Rats irradiated with 0.25 Gy 56Fe or 0.05 Gy 16O particles showed attenuated memory, but not learning, measured with NOR (Rabin et al., 2015).

Object in Place (OiP), a similar test to NOR where the same objects are used but the locations of one or more of the objects is changed, is also used to assess memory (Cekanaviciute et al., 2018). Mice irradiated with 9 Gy X-rays showed a DI of -3 compared to the control of 38 suggesting impaired memory (Acharya et al., 2016). Mice irradiated with 16O particles showed a dose-dependent decrease in the DI for NOR at 0.05 or 0.3 Gy, while 48Ti irradiation also resulted in significantly decreased DI at both 0.05 and 0.3 Gy (Parihar et al., 2015; Parihar et al., 2016). After 0.05 and 0.3 Gy 4He irradiation, mice also showed reduced performance in the OiP test suggesting impaired memory (Parihar et al., 2018).

A few studies used the multistage attentional set shifting (ATSET) test, which measures the ability to relearn cues over various schedules of reinforcement (Heisler et al., 2015). During ATSET, simple discrimination (SD) was inhibited by 0.05, 0.15 and 0.2 Gy of 28Si particles in rats, shown by increased latency to complete the task and a 20 to 30 percentage point decrease in completion of various stages (Britten et al., 2018). Of rats irradiated with 0.2 Gy 56Fe particles, 2 of 11 completed all stages, while 8 of 11 control rats completed all stages (Lonart et al., 2012). In addition, the same study (Lonart et al., (2012) demonstrated that irradiated rats required significantly more attempts to complete the SD stage. The number of attempts for compound discrimination (CD) was increased about 2-fold from 0.01 to 0.15 Gy in rats irradiated with 56Fe particles (Jewell et al., 2018). There was also a dose-dependent decrease in the percent of rats that failed at least 1 stage. Similarly, rats took more trial (2X) to complete the CD stage after 5 cGy of 48Ti (Parihar et al., 2016).

Fear conditioning (FC) and fear extinction (FE) are used to assess learning and memory. FC measures the learned fear response to an adverse event, while FE measures the dissociation of this response to the adverse event (Parihar et al., 2016). Mice tested with fear conditioning after 9 Gy X-rays spent 19% of the time frozen, while control mice spent 43% of the time frozen during the context test (Acharya et al., 2016). Mice irradiated with 0.3 Gy 48Ti showed similar levels of FC to controls, but FE was inhibited in irradiated mice as they were unable to abolish fear memory (Parihar et al., 2016). This also occurred for 0.05 Gy 4He particles (Parihar et al., 2018).

Various maze tests were performed to assess learning and memory. During an MWM test, control mice took 246 cm to reach the hidden platform, while 10 Gy-irradiated mice took 392 cm (Belarbi et al., 2013). A water maze did not show initial differences in learning and memory after 0.5 Gy protons, but reversal learning, where mice had to forget what they had previously learned, showed 1.6-fold increased swim distance to the hidden platform in irradiated mice (Bellone et al., 2015). Rats irradiated with X-rays (13 Gy) and 56Fe particles (0.2, 0.4 and 0.6 Gy) showed increased escape latency compared to controls (Britten et al., 2012). A Hebb-Williams maze after rats were irradiated with 6 Gy gamma rays showed significant decreases in learning and memory as well (Manda et al., 2007a). After irradiation, rats exposed to 25 Gy had significant impairments in both the T-maze, a measure of spatial working memory,and water maze tests, while rats exposed to lower dose of 20 Gy, had significant impairment of working memory in the T-maze (Hodges et al., 1998).

A Swedish cohort study by Hall et al. (2004) showed that exposure to β-rays, gamma rays and X-ray doses of 1 to 250 mGy for treatment of cutaneous hemangioma during infancy was related to reduced test scores approximately 18 years later, including tests of concept discrimination (P=0.03), general instruction (P=0.03) and technical comprehension (P=0.003). In mice, reduced performance on temporal order (TO) tasks, where short-term memory is assessed through the animals' preference to two sets of objects, was reported after 0.05 and 0.3 Gy of 16O, 48Ti and 4He particle irradiation (Parihar et al., 2016; Parihar et al., 2018). A three-chamber social approach task, which assesses social memory, was impaired in male mice after 0.5 Gy of exposure to the GCR simulator compared with animals exposed to 0.15 Gy of GCR simulator. However, there were no significant differences in TO in the exposed animals compared to unexposed controls (Krukowski et al., 2018a). Performance on operant responding, which reflects the cortex' ability to organize processes was assessed in rats. Performance on this test was reduced after 0.25, 0.5, 1 and 2 Gy 56Fe ion exposure, suggesting alterations in learning and memory (Rabin et al., 2012). However, there was no consistent trend across doses (Rabin et al., 2012).

Furthermore, a meta-analysis identified several studies that showed a risk of developing central nervous diseases such as Alzheimer's and dementia after exposure to low-to-moderate doses of ionizing radiation in adulthood. The various studies investigated CNS diseases in relation to occupational exposure, environmental exposure, those exposed for medical purposes, Chernobyl cleanup workers and Japanese Atomic Bomb Survivors with dose ranges <1 Gy. Results from the meta-analysis suggest that there is no increase in standardized mortality ratio (SMR) from diseases of the nervous system when comparing the radiation exposed cohorts to the general population. However, there was a positive and significant excess relative risk from ionizing radiation for Parkinson's disease (Azizova et al., 2020; Lopes et al., 2022).

Time Concordance

Novel object recognition (NOR) was used in multiple studies to assess recognition memory at varying time points following energy deposition. In many cases, the deposition of energy by radiation led to impaired recognition memory in the animal models studied. A decrease in DI indicates a reduction in recognition memory. At 5 to 6 weeks after 9 Gy irradiation, mice had decreased DI for NOR (Acharya et al., 2016). Similarly, at 6 weeks after 48Ti (0.05 and 0.30 Gy) and 16O (0.30 Gy) irradiation, the DI for NOR decreased significantly in male mice (Parihar et al., 2015). After exposure to 5 and 30 cGy of 48Ti, cognitive impairment was greater after 24 weeks than 12 weeks as evidenced by reduced NOR DI for both doses of 48Ti (Parihar et al., 2016). Mice at 90 days post helium exposure or 45 days post GCR simulator radiation (0.15 or 0.50 Gy) both demonstrated memory impairments as mice were unable to distinguish novel and familiar objects (Krukowski et al., 2018a; Krukowski et al., 2018b). After 2 weeks of

exploring, mice previously irradiated with 0.1 or 0.4 Gy showed impaired object recognition; however, at the 20-week time-point, no impairment was indicated following 0.1, 0.2 or 0.4 Gy of 56Fe (Impey et al., 2016). NOR performance was impaired in mice at 2- and 4-months post 16O irradiation, 11 months post 12C irradiation, at 3- and 12-months post 56Fe exposure and at 7- and 17-months post 48Ti irradiation. As well, NOR was impaired 4, 5, 9, 10 and 13 months after 28Si exposure, with the lowest performance occurring at 9 months (Rabin et al., 2014). Mice demonstrated impaired memory 270 days after 16O radiation at 0.01 Gy or 0.25 Gy (Kiffer et al., 2019a). Four and 13 months after proton exposure, NOR was impaired in rats (Rabin et al., 2014). Also in rats, memory ability decreased 18 h after 56Fe and 16O exposure but no significant changes in learning ability by NOR were found after 48 h (Rabin et al., 2015). Months after 40 Gy X-ray irradiation, rats showed differences in NOR results by age. Rats that were 3 months old at the time of irradiation, showed a decrease in NOR 3 months post irradiation, while no changes were observed in older ages and later timepoints (Forbes et al., 2014). No changes in novel object location (NOL) were observed for rats between 6 and 15 months of age (Forbes et al., 2014).

To study spatial learning and memory, mice and rat models were subjected to various maze tests. Proton-irradiated mice tested with Barnes maze and water maze did not show impairment 3 months after irradiation (Bellone et al., 2015). However, 3 months after exposure to 13 Gy of X-rays, rats became less capable of escaping the Barnes maze and demonstrated increased escape latency (Britten et al., 2012). After 6 months, mice reached the platform with a longer distance during the reversal learning test (Bellone et al., 2015). Rats exposed to 0, 8 and 10 Gy of X-rays experienced no impairments in spatial memory, while those exposed to 0.2, 0.4 and 0.6 Gy 56Fe demonstrated increased relative escape latency over the 3-day testing periods (Britten et al., 2012). Cognitive changes in spatial learning or memory were observed in the water maze after 2 weeks, but not at 20 weeks (Impey et al., 2016). Mice studied in a water maze 1 year following 4He irradiation (0.05 and 0.30 Gy) showed impaired cognitive flexibility and memory retrieval (Parihar et al., 2018). Mice previously irradiated with 6 Gy gamma rays needed a 1.7-fold increase in time to reach the goal of the Hebb-William maze by day 30 post-irradiation, while in the control, the time required decreased 0.2-fold by day 30 (Manda et al., 2007a). Irradiated mice 9 months after 16O irradiation at 0.1 and 0.25 Gy had no difference in positive discrimination ratio during a Y-maze test, a measure spatial working memory, compared with control mice, indicating that radiation had no effect on memory 9 months post-irradiation (Kiffer et al., 2019a). Rats irradiated at 20 Gy and 25 Gy experienced deficits in T-maze testing 35 weeks post irradiation and at 44 weeks, rats exposed to 25 Gy reflected working memory deficits assessed by the water maze test (Hodges et al., 1998).

OiP used in multiple studies showed impairment in discrimination of objects after irradiation. Mice 5 to 6 weeks after 9 Gy irradiation showed decreased OiP DI (Acharya et al., 2016). Similarly, 6 weeks after charged particle exposure, the DI for OiP in male mice decreased to a greater extent following 48Ti irradiation compared to 16O irradiation (Parihar et al., 2015). As well, a greater change was observed after 0.30 Gy of 16O irradiation compared with 0.05 Gy of 16O irradiation after 6 weeks, indicating higher impairment at the higher dose (Parihar et al., 2015). In a similar experiment to Parihar et al. (2015), the OiP DI decreased after 0.30 Gy of 48Ti irradiation at week 12, in addition to DI decrease at 24 weeks after 0.30 Gy of 16O irradiation and 0.05 Gy of 48Ti irradiation. Hence, cognitive impairment was greater after 24 weeks than 12 weeks (Parihar et al., 2016). 4He particle irradiation of mice led to long-term recognition memory impairments at 6, 15 and 52 weeks post-radiation (Parihar et al., 2018).

Fear conditioning and fear extinction of previously irradiated mice were studied at different timepoints after irradiation. Mice irradiated with 0.3 Gy and 0.05 Gy spent more time freezing their motion than the control mice at 24 weeks and 1 year, respectively, following irradiation (Parihar et al., 2016; Parihar et al., 2018). Mice irradiated with 9 Gy X-rays spent less time frozen during FC, measured after 5-6 weeks (Acharya et al., 2016). FE was attenuated in mice after 0.3 Gy of 48Ti irradiation after 24 weeks post-irradiation (Parihar et al., 2016). The same was found after 0.05 Gy of 4He exposure 1-year post-irradiation (Parihar et al., 2018).

ATSET was used to assess simple and compound discrimination, reversal learning and set shifting, among others. Only 2 out of 11 of the irradiated rats (0.20 Gy of 56Fe) completed all the paradigms 90 days after radiation compared to 8 out 11 unirradiated rats that completed all paradigms (Lonart et al., 2012). At 90-days post-irradiation, irradiated rats required more trial attempts to complete the simple discrimination stage compared to the control rats (Lonart et al., 2012). Rats took 2-fold more tries to complete the CD stage 12 weeks after radiation (Parihar et al., 2016).

In irradiated mice, temporal order DI decreased at 12 and 24 weeks for all tested doses (0.05 or 0.30 Gy of 16O or 48Ti), demonstrating cognitive impairment (Parihar et al., 2016). Meanwhile, Parihar et al. (2018) found impaired TO memory for 6-, 15- and 52-weeks post 4He particle irradiation (Parihar et al., 2018). Male mice had significantly impaired social memory in the three-chamber social approach task at day 45 following exposure to 0.50 Gy of the GCR simulator (Krukowski et al., 2018a). Operant responding as a cognitive function test was used on 56Fe irradiated rats who showed decreased cognitive function at 2, 4-8, 10-, and 15-months post-irradiation (Rabin et al., 2012). Swedish men who were irradiated under 18 months of age were found to have cognitive impairments following reduced test scores for technical comprehension, concept discrimination and general instruction at 18 and 19 years old (Hall et al., 2004).

Incidence Concordance

No available data.

Essentiality

As deposition of energy is a physical stressor, it cannot be blocked by chemicals although it can be shielded. Further research is required to determine the effect of shielding radiation on learning and memory. Since deposited energy initiates events immediately, the removal of deposited energy also supports the essentiality of the key event. Studies that do not deposit energy are observed to

have no downstream effects. However, impaired learning and memory can occur in response to ionizing radiation, although in the absence of this energy deposition, compromised cognitive abilities would occur with aging, or if predisposed to neurodegenerative diseases such as Alzheimer's (Lindsay et al., 2002).

Uncertainties and Inconsistencies

- Most of the evidence for this KER is supported using in vivo rodent models; therefore, there is still a knowledge gap on how radiation exposure realistically alters the brains of other species, such as humans, to lead to impaired learning and memory (Desai et al., 2022). Additionally, further research is needed to gain a better understanding on the sex differences in behavioral effects after radiation exposure (Kiffer et al., 2019b).
- Belarbi et al. (2013) did not find any changes in NOR performance after 10 Gy gamma rays.
- Forbes et al. (2014) showed impaired ability during NOR tests, but not during NOL tests after 40 Gy X-rays.
- Kiffer et al. (2019a) showed impaired ability during NOR tests, but not during Y-maze tests after 0.1 and 0.25 Gy 16O particles.
- Miry et al. (2021) showed impaired hippocampal-dependent learning and memory 2 months after 10, 50 and 100 cGy 56Fe exposure, but by 6 months post-exposure, deficits in spatial learning were no longer observed in irradiated mice. Instead, enhanced spatial learning was observed at 12- and 20-months post-exposure.

Quantitative Understanding of the Linkage

The table below provides some representative examples of quantitative linkages between the two key events. It was difficult to identify a general trend across all the studies due to differences in experimental design and reporting of the data. All data is statistically significant unless otherwise stated.

Dose Concordance

Reference	Experiment Description	Result
Hodges et al., 1998	In vivo. Male Sprague-Dawley Rats were irradiated with X-rays at 0, 20 Gy or 25 Gy at 1.4 Gy/min. Rats were tested from 26 weeks to 44 weeks after irradiation using the T maze and water maze to assess working memory and brain damage induced by radiation.	Rats irradiated with 25 Gy, showed impairments in all tests and rats irradiated with 20 Gy were not as impaired in the water maze learning and had no impairment in water maze working memory. Rats irradiated with 20 Gy had significant impairment of working memory in the T-maze.
Hall et al., 2004	In vivo. A Swedish cohort study that analyzed military tests of learning ability, logical reasoning and spatial recognition of 2211 men 17-18 years after β-ray, 26Ra gamma ray or X-ray radiation for cutaneous hemangioma before the age of 18 months from 1930-1959.	Test scores for concept discrimination and general instruction as well as technical comprehension decreased in a dose-dependent manner from 0 to 250 mGy. Spatial recognition did not significantly change.
Acharya et al., 2016	In vivo. C57Bl/6J mice were irradiated with 9 Gy X-rays and novel object recognition (NOR), OiP and FC were measured. The DI was calculated from exploration times in familiar and novel locations. Percent of time spent freezing was used to determine FC.	The DI for NOR was 23 without irradiation and -13 with 9 Gy. The DI for OiP was 38 without irradiation and -3 with 9 Gy. Mice without irradiation spent 43% of the time frozen and mice with 9 Gy spent 19% of the time frozen during the context test.
Belarbi et al., 2013	In vivo. C57Bl/6J mice were irradiated with 10 Gy 137Cs gamma rays. NOR and MWM were used to determine learning and memory impairment.	NOR did not show any significant differences between control and 10 Gy irradiated groups. In MWM, control mice traveled 246 cm to the hidden platform, while 10 Gy irradiated mice traveled 392 cm to the hidden platform.
Bellone et al., 2015	In vivo. Male B6C3F1/J mice were irradiated with 150 MeV protons at 0.5 Gy (1.5-2.5 Gy/min). A water maze was used to assess learning and memory.	No changes were found initially during the water maze test, but irradiated mice took a 1.6-fold longer swim distance to reach the platform during the reversal learning phase.
Britten et al., 2012	In vivo. Wistar rats were irradiated with 125 kVp X-rays or 1 GeV/u 56Fe ions to study the effect of low dose exposure in the spatial learning ability of rats. Rats were tested 3 months after irradiation using the Barnes maze.	13 Gy X-ray irradiated rats and rats exposed to all doses of 56Fe ions studied (0.2, 0.4 and 0.6 Gy) demonstrated a higher relative escape latency of 1.8-fold and ~2.5-fold, respectively, compared to the control group.
Britten et al., 2018	In vivo. Wistar rats were exposed to heavy ions, 600 MeV/n 28Si. Attentional set shifting (ATSET) was used to assess various cognitive	28Si irradiation of rats significantly reduced their ability to complete simple discrimination. Rats exposed to 0.05 Gy, 0.15 Gy and 0.20 Gy had a lower percentage stage completion of simple discrimination compared to 0 Gy rats (60-70% completion compared to 90%). 0.15

	processes.	Gy irradiated rats also had a lower completion rate of compound discrimination compared to 0 Gy rats.
Lonart et al., 2012	In vivo. Male Wistar rats were irradiated with 56Fe ions. ATSET test was used to assess simple and compound discrimination, reversal learning and set-shifting, among others.	8 of 11 unirradiated rats completed all the paradigms, while only 2 of 11 irradiated rats (0.20 Gy) completed all the paradigms. Irradiated rats required more trial attempts to complete the simple discrimination stage compared to unirradiated rats.
Forbes et al., 2014	In vivo. Male FxBN rats were irradiated with X-rays at 40 Gy from 2 fractions of 5 Gy per week over 4 weeks (each fraction at 1.25 Gy/min). Learning and memory were assessed using NOR and NOL.	40 Gy significantly reduced the DR of 3-month-old rats during NOR from 0.5 to 0.2. No changes in NOL were observed, and no changes at other ages were observed.
Parihar et al., 2015	In vivo. Male Thy1-EGFP transgenic mice were irradiated with charged particles (16O and 48Ti) at 600 MeV/amu (0.5 to 1.0 Gy/min). NOR and OiP tests were done to assess learning and memory.	NOR: The control group DI was 39. The DI was 25 after 5 cGy 16O, 10 after 30 cGy 16O, 2 after 5 cGy 48Ti and -4 after 30 cGy 48Ti. OiP: The control group DI was 32. The DI was 29 after 5 cGy 16O, -4 after 30 cGy 16O, -8 after 5 cGy 48Ti and -3 after 30 cGy 48Ti.
Parihar et al., 2016	In vivo. Male Thy1-EGFP transgenic mice were irradiated with charged particles (16O and 48Ti) at 600 MeV/amu (0.05 to 0.25 Gy/min). NOR, OiP, TO and FE tests were done to assess learning and memory. Wistar rats were used in the ATSET test.	Impairment in cognitive ability was observed at both 5 and 30 cGy. The impairment was typically greater in 48Ti than 16O. The DI was between 20 and 40 for all controls and was reduced to less than 0 after many of the different radiation treatments.
Parihar et al., 2018	In vivo. Male C57BL/6J mice were irradiated with 4He particles (400 MeV/n) at 5 cGy/min. Learning and memory were assessed using OiP, TO and FE.	Cognitive tests showed impaired learning and memory at both 5 and 30 cGy (except FE which was only tested at 5 cGy). For example, control mice spent 2-fold more time exploring novel objects than familiar objects, while irradiated rats did not spend significantly different time exploring novel objects. Impairment at 30 cGy was not significantly different than at 5 cGy.
Impey et al., 2016	In vivo. Male C57BL/6J mice were irradiated with 600 MeV 56Fe ions at 0.1, 0.2 or 0.4 Gy and various dose rates from 0.25 to 0.36 Gy/min. NOR and a water maze were used to determine learning and memory ability.	Transiently, mice with 0.1 and 0.4 Gy spent more time exploring the familiar object and less exploring the novel object. No differences were observed in the water maze test.
Jewell et al., 2018	In vivo. Male Wistar rats were irradiated with 56Fe particles (600 MeV/n) at 1 and 3 cGy (2 cGy/min), or 5, 10 and 15 cGy (5 cGy/min). ATSET was performed to assess various cognitive processes.	At every dose, the number of attempts for CD was significantly increased, with a maximum of 2-fold. Various doses were also able to significantly increase the number of attempts for SD, CD reversal and intra-dimensional shifting (IDS). Significant increases in time to complete the test were sparse. However, doses of 3 cGy and above showed nonsignificant increases in latency in almost all tests.
Krukowski et al., 2018b	In vivo. C57BL/6J wild type mice were exposed to alpha particles at 0, 15, 50 or 100 cGy (16.37 cGy/min). NOR was used as an assay for behavioral analysis at 90 days post-irradiation.	After 50 cGy exposure, animals spent similar time exploring the familiar and novel object, indicating memory impairment.
Krukowski et al., 2018a	In vivo. Male and female C57BL/6J wild type mice were exposed to 0, 15 or 50 cGy of GCR simulator (2.54 cGy/min). NOR assay was used to study recognition memory. A three-chamber social approach task determined social behavior and social memory.	NOR: Male mice demonstrated memory impairment when exposed to 15 or 50 cGy. Three-chamber social approach task: Male mice exposed to 50 cGy showed impairments in social memory compared to the 15 cGy group.
Kiffer et al., 2019a	In vivo. Female C57BL/6 mice were irradiated with 16O particles (600 MeV/n) at 0.1 or 0.25 Gy (18 to 33 cGy/min). A Y-maze was performed to measure spatial memory and NOR was performed to measure non-spatial declarative memory.	Y-maze: No changes were observed in irradiated mice. NOR: The DR was 22 for the control, -2 for 0.1 Gy and -5 for 0.25 Gy. Both changes were significant.
Manda et	In vivo. Male Swiss albino mice were irradiated with 6 Gy 60Co gamma rays. Hebb-Williams	Irradiated mice took approximately 8 times longer to reach their goals

al., 2007a	maze was used to measure learning ability and spatial working memory continuously for 30 days after radiation exposure.	and their learning ability declined after radiation exposure compared to controls and mice pre-treated with melatonin.
Rabin et al., 2012	In vivo. Male Fischer 344 rats were irradiated with various doses (50 to 100 cGy/min) of 56Fe particles (1000 MeV/n). Operant responding was used to test cognitive function. Rats were trained to press a lever to receive food at various reinforcement schedules.	Doses of 25, 50, 150 and 200 cGy influenced cognitive function. However, there was no significant trend related to dose.
Rabin et al., 2014	In vivo. Male Sprague-Dawley rats were irradiated with various types of ionizing radiation (5 to 100 cGy/min so the time did not exceed 3 to 4 mins). LET ranged from 0.22 (protons) to 181 (56Fe) keV/µM. The dose ranged from 0.1 to 200 cGy. The radiation types used were 16O (600 and 1000 MeV/n), 12C (290 MeV/n), 28Si (380, 600 and 1000 MeV/n), 48Ti (1100 MeV/n), 56Fe (600 MeV/n) and protons (1000 MeV/n). NOR was performed to assess learning and memory.	In most particles studied, a lower or equal dose to that of younger rats was needed to disrupt NOR and cognitive performance in older rat subjects. Recognition memory performance was disrupted by a dose 10% - 50% less in older rats than younger rats. Older rats irradiated with 380 MeV/n 28Si particles showed a recognition memory disruption at a lower dose (0.005 Gy in older rats compared to 0.1 Gy in younger rats). Whereas higher dose was necessary to disrupt recognition memory in older rats exposed to 1000 MeV/n 28Si particles compared to the younger rats (0.5 Gy in older rats compared to 0.25 Gy in younger rats). Following 28Si radiation, memory was impaired at every dose from 0.1 to 2 Gy.
Rabin et al., 2015	In vivo. Male Sprague-Dawley rats were irradiated with 56Fe particles (600 MeV/n, 12 keV/µm) at 25 cGy (25 cGy/min) or 16O particles (600 MeV/n, 189 keV/µm) at 5 cGy (5 cGy/min). NOR was performed to determine recognition learning and memory.	56Fe and 16O both resulted in an equal time spent with the novel object during the memory NOR test. The NOR test did not show significant changes in learning ability.

Time Concordance

Reference	Experiment Description	Result
Hall et al., 2004	In vivo. A Swedish cohort study that analyzed military tests of learning ability, logical reasoning and spatial recognition of 2211 men 17- 18 years after β-ray, 6Ra gamma ray or X-ray radiation for cutaneous hemangioma before the age of 18 months from 1930-1959.	Irradiation at 18 months old or less resulted in significantly reduced concept discrimination and general instruction as well as technical comprehension test scores at 18 and 19 years of age.
Hodges et al., 1998	In vivo. Male Sprague-Dawley Rats were irradiated with X-rays at 0, 20 Gy or 25 Gy at 1.4 Gy/min. Rats were tested from 26 weeks to 44 weeks after irradiation using the T maze and water maze to assess working memory and brain damage induced by radiation.	At 29 weeks post irradiation, no learning impairments were observed in the irradiated groups during the T-maze forced alteration task. At 35 weeks post irradiation, the mean percentage of correct responses changed from 80% to 65% in both groups during the T-maze testing. At 44 weeks after irradiation, rats exposed to 25 Gy showed working memory deficits assessed by the water maze test.
Bellone et al., 2015	In vivo. Male B6C3F1/J mice were irradiated with 150 MeV protons at 0.5 Gy (1.5-2.5 Gy/min). A water maze was used to assess learning and memory 3 and 6 months post-irradiation.	No changes were observed in either test after 3 months. After 6 months, mice took a 1.6-fold longer distance to reach the platform.
Britten et al., 2012	In vivo. Wistar rats were irradiated with 125 kVp X-rays or 1 GeV/u 56Fe ions to study the effect of low dose exposure in the spatial learning ability of rats. Rats were tested for 3 days 3 months after irradiation using the Barnes maze.	3 months after exposure to 13 Gy of X-rays, rats demonstrated increased escape latency. Rats exposed to 8 and 10 Gy of X-rays experienced similar escape latency as the 0 Gy group over 3 days. Rats exposed to 56Fe ion irradiation demonstrated increased relative escape latency throughout the 3-day testing periods at all doses (0.2, 0.4 and 0.6 Gy).
Acharya et al., 2016	In vivo. C57Bl/6J mice were irradiated with 9 Gy of X-rays and NOR, OiP and FC were measured 5 and 6 weeks post-irradiation. The discrimination index (DI) was calculated from exploration times in familiar and novel locations. Percent of time spent freezing was used to determine FC.	5 to 6 weeks after irradiation, the DI for NOR and OiP were significantly reduced, and mice spent significantly less time frozen.
Forbes et al., 2014	In vivo. Male FxBN rats were irradiated with X-rays at 40 Gy from 2 fractions of 5 Gy per week over 4 weeks (each fraction at 1.25 Gy/min). Learning and memory were assessed using NOR and NOL at 3 and 18 months post-	Irradiation significantly reduced the DR of 3-month-old rats during NOR, from 0.5 to 0.2, 3 months after irradiation. No changes in NOL were observed, and no

	irradiation.	changes at other ages and timepoints were observed.
Parihar et al., 2015	In vivo. Male Thy1-EGFP transgenic mice were irradiated with charged particles (16O and 48Ti) at 600 MeV/amu (0.5 to 1.0 Gy/min). NOR and OiP tests were done to assess learning and memory 6 weeks after irradiation.	After 6 weeks, impairment in cognitive ability was observed. The impairment was greater in 48Ti than 16O and greater in 30 cGy than 5 cGy.
Parihar et al., 2016	In vivo. Male Thy1-EGFP transgenic mice were irradiated with charged particles (16O and 48Ti) at 600 MeV/amu (0.05 to 0.25 Gy/min). NOR, OiP, TO and FE tests were done to assess learning and memory after 12 and 24 weeks. Wistar rats were used in the ATSET test.	Cognitive ability was lower after 24 weeks than 12 weeks in mice, but radiation was able to reduce the DI in tests at both time points.
Parihar et al., 2018	In vivo. Male C57BL/6 J mice were irradiated with 4He particles (400 MeV/n) at 5 cGy/min. Learning and memory were assessed using OiP and TO 6, 15 and 52 weeks after irradiation. FE was assessed 1 year after irradiation. Water maze was performed 1 year following radiation.	Learning and memory were significantly attenuated at all time points tested using all tests.
Impey et al., 2016	In vivo. Male C57BL/6J mice were irradiated with 600 MeV 56Fe at 0.1, 0.2 and 0.4 Gy and various dose rates from 0.25 to 0.36 Gy/min. NOR and a water maze were used to determine learning and memory ability 2 and 20 weeks post-irradiation.	Some mice at 2 weeks spent more time exploring the familiar object and less exploring the novel object. No differences were observed after 20 weeks in NOR or in the water maze test after either time point.
Krukowski et al., 2018b	In vivo. C57BL/6J wild type mice were exposed to alpha particles at 0, 15, 50 or 100 cGy (16.37 cGy/min). NOR was used as an assay for behavioural analysis at 90 days post-irradiation.	At late time points (90 + days post alpha exposure) mice exposed to either 15 or 50 cGy of alpha particles exhibited deficits in recognition memory as they were unable to distinguish the novel and familiar objects.
Krukowski et al., 2018a	In vivo. Male and female C57BL/6J wild type mice were exposed to 0, 15 or 50 cGy of GCR simulator (2.54 cGy/min). NOR assay was used to study recognition memory. A three-chamber social approach task determined social behavior and social memory.	At 45 days post-exposure, male mice exposed to 50 cGy of GCR showed significant impairments in social memory in the three-chamber social approach task compared to the 15 cGy group. NOR test revealed that radiation-induced recognition memory impairments in male cohorts only at 15 and 50 cGy.
Kiffer et al., 2019a	In vivo. Female C57BL/6 mice were irradiated with 16O particles (600 MeV/n) at 0.1 or 0.25 Gy (18 to 33 cGy/min). A Y-maze was performed to measure spatial memory and NOR was performed to measure non-spatial declarative memory.	After 270 days, NOR showed impaired memory. Irradiated mice at 0.1 and 0.25 Gy spent significantly more time exploring the novel object in the Y-maze, indicating no radiation-induced memory impairment.
Lonart et al., 2012	In vivo. Male Wistar rats were irradiated with 56Fe particles. ATSET test was used to assess simple and compound discrimination, reversal learning and set-shifting among others.	8 of 11 unirradiated rats completed all the paradigms, while only 2 of 11 irradiated rats (0.2 Gy) completed all the paradigms 90 days post-irradiation. Irradiated rats required more trial attempts to complete the simple discrimination stage compared to unirradiated rats 90 days post-irradiation.
Manda et al., 2007a	In vivo. Male Swiss albino mice were irradiated with 6 Gy 60Co gamma rays. Hebb-Williams maze was used to measure learning ability and spatial working memory continuously for 30 days after radiation exposure.	Time needed to reach the goal increased by 1.7-fold by day 30 after radiation, while in sham-irradiated control mice it decreased 0.2-fold in this time.
Rabin et al., 2012	In vivo. Male Fischer 344 rats were irradiated with various doses (50 to 100 cGy/min) of 56Fe particles (1000 MeV/n). Operant responding was used to test cognitive function. Rats were trained to press a lever to receive food at various reinforcement schedules.	Tests done 2, 4, 5, 6, 7, 8, 10 and 15 months after irradiation showed decreased cognitive function compared to controls. However, no consistent changes across time points were shown.
Rabin et al., 2014	In vivo. Male Sprague-Dawley rats were irradiated with various types of ionizing radiation (5 to 100 cGy/min so the time did not exceed 3 to 4 mins). LET ranged from 0.22 (protons) to 181 (56Fe) keV/µM. The dose ranged from 0.1 to 200 cGy. The radiation types used were 16O (600 and 1000 MeV/n), 12C (290 MeV/n), 28Si (380, 600 and 1000 MeV/n), 48Ti (1100 MeV/n), 56Fe (600 MeV/n) and protons (1000 MeV/n). NOR was performed to assess learning and memory at various times.	16O impaired NOR performance after 2 and 4 months, but not after 10 and 12 months. 12C showed impaired NOR performance after 11 months but not 1 month. 28Si radiation showed significantly impaired NOR performance at a few doses after 4, 5, 9, 10 and 13 months, with the lowest performance occurring at 9 months. 48Ti showed impairment at 7 and 17 months. 56Fe showed impairment at 3 and 12 months. Protons showed impairment at 4 and 13 months.
Rabin et	In vivo. Male Sprague-Dawley rats were irradiated with 56Fe particles (600 MeV/n, 12 keV/µm) at 25 cGy (25 cGy/min) or 16O particles (600 MeV/n, 189 keV/µm) at 5	56Fe and 16O both resulted in a 0.8-fold decrease in memory ability about 18 h after radiation. The NOR test did not show significant changes in learning ability measured about 48 h after radiation.

al., 2015	cGy (5 cGy/min). NOR was performed within 48 h to determine recognition learning and memory.	

Known modulating factors

Modulating Factor	Details	Effects on the KER	References
Drug	PLX5622-1200ppm (PLX) diet that contains a CSF1-R (colony stimulating factor 1 receptor) inhibitor that induces depletion of microglia within 3 days.	The PLX diet was able to rescue the short and long-term memory impairments due to radiation exposure.	Krukowski et al., 2018b; Acharya et al., 2016
Drug	Fluoxetine treatment – an antidepressant that belongs to the selective serotonin reuptake inhibitor (SSRI) class.	Fluoxetine was able to attenuate the learning and memory defects in mice that were subjected to radiation.	Gan et al., 2019
Genotype	CCR2 (chemokine C-C motif receptor 2) knockout. CCR2 is involved in peripheral macrophage infiltration at the sites of injury in the CNS.	CCR2 deficiency was able to prevent the cognitive impairments induced by cranial radiation as shown by improvements in the MWM test.	Belarbi et al., 2013
Drug	Treatment with α-lipoic acid (LA) as it has antioxidant properties.	LA-treated mice did not show any significant decline in spatial memory post-irradiation.	Manda et al., 2007b
Sex	Male and female mice responded differently to NOR, three chamber social approach and open field task following irradiation.	Male animals generally demonstrated memory impairment after irradiation.	Krukowski et al., 2018a
Drug	Treatment with melatonin as it is involved in many physiological processes and has antioxidant properties.	Pre-treatment with melatonin showed significant protection against impairment in learning ability. Melatonin was found to reduce the time taken to reach the goal in a Hebb-Williams maze compared to irradiation.	Manda et al., 2007a
Various modulating factors	Commonly applied countermeasures include: • Those targeting the reduction of oxidative stress (ie. Pharmaceutical antioxidants, nutritional antioxidants) • Decreasing DNA damage (ie. Overexpression of BMI1 gene to accelerate DNA repair) • Enhancing cell survival (ie. Inhibition of p53-induced apoptosis) • Reducing inflammation (ie. Pharmaceutically blocking pro-inflammatory cytokine/chemokine signaling) • Limiting tissue damage and increasing repair (ie. Cell transplants)	Various approaches to CNS radioprotection have been utilized as either primarily protective (administered prior to irradiation) or mitigative (administered after irradiation). These countermeasures have been found to limit the harmful effects of radiation exposure.	Pariset et al., 2021

Known Feedforward/Feedback loops influencing this KER

TNF is a key cytokine that can initiate and promote inflammation through the activation of the NFκB pathway in glia cells. In uncontrolled conditions, TNF can lead to the development of neurodegenerative diseases as it can increase the production of pro-inflammatory cytokines and can also lead to elevated levels of iNOS, COX-2, and NOX subunits. These can then activate NADPH oxidases to produce ROS, which can activate the NFκB pathway to amplify the overall TNF/ROS/NFκB responses to promote neuroinflammation. This process ultimately results in a feed-forward loop of chronic neurodegeneration and consequently, impaired learning and memory (Fischer and Maier, 2015).

References

Acharya, M. M. et al. (2016), "Elimination of microglia improves cognitive function following cranial irradiation", Scientific Reports, Vol. 6/1, Nature Publishing Group, Berlin, https://doi.org/10.1038/srep31545.

Azizova, T. V et al. (2020), "Occupational exposure to chronic ionizing radiation increases risk of Parkinson's disease incidence in Russian Mayak workers", International Journal of Epidemiology, Vol. 49/2, Oxford University Press, Oxford, https://doi.org/10.1093/ije/dyz230.

Belarbi, K. et al. (2013), "CCR2 deficiency prevents neuronal dysfunction and cognitive impairments induced by cranial irradiation", Cancer Research, Vol. 73/3, American Association for Cancer Research, California, https://doi.org/10.1158/0008-5472.CAN-12-2989.https://doi.org/10.1158/0008-5472.CAN-12-2989

Bellone, J. A. et al. (2015), "A single low dose of proton radiation induces long-term behavioral and electrophysiological changes in mice", Radiation Research, Vol. 184/2, BioOne, Washington, https://doi.org/10.1667/RR13903.1.

Britten, R. A. et al. (2012), "Low (20 cGy) doses of 1 GeV/u 56Fe-particle radiation lead to a persistent reduction in the spatial learning ability of rats", Radiation Research, Vol. 177/2, BioOne, Washington, https://doi.org/10.1667/RR2637.1.

Britten, R. A. et al. (2018), "Impaired Attentional Set-Shifting Performance after Exposure to 5 cGy of 600 MeV/n 28 Si Particles", Radiation Research, Vol. 189/3, BioOne, Washington, https://doi.org/10.1667/RR14627.1.

Cekanaviciute, E., S. Rosi and S. V. Costes. (2018), "Central nervous system responses to simulated galactic cosmic rays", International Journal of Molecular Sciences, Multidisciplinary Digital Publishing Institute (MDPI) AG, Basel, https://doi.org/10.3390/ijms19113669.

Collett, G. et al. (2020), "The psychological consequences of (perceived) ionizing radiation exposure: a review on its role in radiation-induced cognitive dysfunction", International journal of radiation biology, Vol. 96/9, Taylor & Francis Group, London, https://doi.org/10.1080/09553002.2020.1793017.

Cucinotta, F. A. et al. (2014), "Space radiation risks to the central nervous system", Life Sciences in Space Research, Vol. 2, Elsevier Ltd, Amsterdam, https://doi.org/10.1016/j.lssr.2014.06.003.

Desai, R. I. et al. (2022), "Impact of spaceflight stressors on behavior and cognition: A molecular, neurochemical, and neurobiological perspective", Neuroscience & Biobehavioral Reviews, Vol. 138, Elsevier, Amsterdam, https://doi.org/10.1016/j.neubiorev.2022.104676.

Fischer, R. and O. Maier. (2015), "Interrelation of Oxidative Stress and Inflammation in Neurodegenerative Disease: Role of TNF", Oxidative Medicine and Cellular Longevity, Vol. 2015, Hindawi, London, https://doi.org/10.1155/2015/610813.

Forbes, M. E. et al. (2014), "Early-delayed, radiation-induced cognitive deficits in adult rats are heterogeneous and age-dependent", Radiation Research, Vol. 182/1, BioOne, Washington, https://doi.org/10.1667/RR13662.1.

Gan, H. et al. (2019), "Fluoxetine reverses brain radiation and temozolomide-induced anxiety and spatial learning and memory defect in mice", J Neurophysiol, Vol. 121, American Physiology Society, Rockville, https://doi.org/10.1152/jn.00581.2018.-Ra.

Greene-Schloesser, D. et al. (2012), "Radiation-induced brain injury: A review", Frontiers in Oncology, Vol. 2, Frontiers, Lausanne, https://doi.org/10.3389/fonc.2012.00073.

Hall, P. et al. (2004), "Effect of low doses of ionising radiation in infancy on cognitive function in adulthood: Swedish population based cohort study", British Medical Journal, Vol. 328/7430, British Medical Journal Publishing Group, London, https://doi.org/10.1136/bmj.328.7430.19.

Heisler, J. M. et al. (2015), "The Attentional Set Shifting Task: A Measure of Cognitive Flexibility in Mice", Journal of Visualized Experiments, 96, JoVe, Cambridge, https://doi.org/10.3791/51944.

Hladik, D. and S. Tapio. (2016), "Effects of ionizing radiation on the mammalian brain", Mutation Research - Reviews in Mutation Research, Vol. 770, Elsevier B.V., Amsterdam, https://doi.org/10.1016/j.mrrev.2016.08.003.

Hodges, H. et al. (1998), "Late behavioural and neuropathological effects of local brain irradiation in the rat", Behavioural Brain Research, Vol. 91/1–2, Elsevier, Amsterdam, https://doi.org/10.1016/S0166-4328(97)00108-3.

Impey, S. et al. (2016), "Short- and long-term effects of 56Fe irradiation on cognition and hippocampal DNA methylation and gene expression", BMC Genomics, Vol. 17/1, Springer Nature, Berlin, https://doi.org/10.1186/s12864-016-3110-7.

Jandial, R. et al. (2018), "Space–brain: The negative effects of space exposure on the central nervous system", Surgical Neurology International, Vol. 9/1, MedKnow Publications, Mumbai, https://doi.org/10.4103/sni.sni_250_17.

Jewell, J. S. et al. (2018), "Exposure to ≤15 cgy of 600 mev/n 56 fe particles impairs rule acquisition but not long-term memory in the attentional set-shifting assay", Radiation Research, Vol. 190/6, BioOne, Washington, https://doi.org/10.1667/RR15085.1.

Katsura, M. et al. (2021), "Recognizing Radiation-induced Changes in the Central Nervous System: Where to Look and What to Look For", RadioGraphics, Vol. 41/1, https://doi.org/10.1148/rg.2021200064.

Kiffer, F. et al. (2019a), "Late Effects of 16O-Particle Radiation on Female Social and Cognitive Behavior and Hippocampal

Physiology", Radiation Research, Vol. 191/3, BioOne, Washington, https://doi.org/10.1667/RR15092.1.

Kiffer, F., M. Boerma and A. Allen. (2019b), "Behavioral effects of space radiation: A comprehensive review of animal studies", Life Sciences in Space Research, Vol. 21, Elsevier, Amsterdam, https://doi.org/10.1016/j.lssr.2019.02.004.

Krukowski, K. et al. (2018b), "Temporary microglia-depletion after cosmic radiation modifies phagocytic activity and prevents cognitive deficits", Scientific Reports, Vol. 8/1, Nature Publishing Group, Berlin, https://doi.org/10.1038/s41598-018-26039-7.

Krukowski, K. et al. (2018a), "Female mice are protected from space radiation-induced maladaptive responses", Brain, Behavior, and Immunity, Vol. 74, Academic Press Inc., Cambridge, https://doi.org/10.1016/j.bbi.2018.08.008.

Lalkovičová, M. (2022), "Neuroprotective agents effective against radiation damage of central nervous system", Neural Regeneration Research, Vol. 17/9, https://doi.org/10.4103/1673-5374.335137.

Lindsay, J. (2002), "Risk Factors for Alzheimer's Disease: A Prospective Analysis from the Canadian Study of Health and Aging", American Journal of Epidemiology, Vol. 156/5, https://doi.org/10.1093/aje/kwf074.

Lodish, H. et al. (2000), "Overview of Neuron Structure and Function", W. H. Freeman, https://www.ncbi.nlm.nih.gov/books/NBK21535/ (accessed October 27, 2021).

Lonart, G. et al. (2012), "Executive function in rats is impaired by low (20 cGy) doses of 1 GeV/u 56Fe particles", Radiation Research, Vol. 178/4, BioOne, Washington, https://doi.org/10.1667/RR2862.1.

Lopes, J. et al. (2022), "Risk of Developing Non-Cancerous Central Nervous System Diseases Due to Ionizing Radiation Exposure during Adulthood: Systematic Review and Meta-Analyses", Brain Sciences, Vol. 12/8, Multi-Disciplinary Digital Publishing Institute (MDPI), Basel, https://doi.org/10.3390/brainsci12080984.

Manda, K. et al. (2007a), "Melatonin attenuates radiation-induced learning deficit and brain oxidative stress in mice", Acta Neurobiologiae Experimentalis, Vol. 67/1.

Manda, K. et al. (2007b), "Radiation-induced cognitive dysfunction and cerebellar oxidative stress in mice: Protective effect of α-lipoic acid", Behavioural Brain Research, Vol. 177/1, Elsevier, Amsterdam, https://doi.org/10.1016/j.bbr.2006.11.013.

Mhatre, S. D. et al. (2022), "Neuro-consequences of the spaceflight environment", Neuroscience & Biobehavioral Reviews, Vol. 132, Elsevier, Amsterdam, https://doi.org/10.1016/j.neubiorev.2021.09.055.

Miry, O. et al. (2021), "Life-long brain compensatory responses to galactic cosmic radiation exposure", Scientific Reports 2021 11:1, Vol. 11/1, Nature Publishing Group, https://doi.org/10.1038/s41598-021-83447-y.

Mousa, A. and M. Bakhiet. (2013), "Role of Cytokine Signaling during Nervous System Development", International Journal of Molecular Sciences, Vol. 14/7, Multidisciplinary digital Publishing Institute (MDPI), Basel, https://doi.org/10.3390/ijms140713931.

National Council on Radiation Protection and Measures (NCRP). (2016). Commentary No. 25 – Potential for central nervous system effects from radiation exposure during space activities phase I: Overview.

Parihar, V. K. et al. (2016), "Cosmic radiation exposure and persistent cognitive dysfunction", Scientific Reports, Vol. 6/1, Nature Publishing Group, Berlin, https://doi.org/10.1038/srep34774.

Parihar, V. K. et al. (2015), "What happens to your brain on the way to Mars", Science Advances, Vol. 1/4, American Association for the Advancement of Science, Washington, https://doi.org/10.1126/sciadv.1400256.

Parihar, V. K. et al. (2018), "Persistent nature of alterations in cognition and neuronal circuit excitability after exposure to simulated cosmic radiation in mice", Experimental Neurology, Vol. 305, Academic Press Inc., Cambridge, https://doi.org/10.1016/j.expneurol.2018.03.009.

Pariset, E. et al. (2021), "Ionizing radiation-induced risks to the central nervous system and countermeasures in cellular and rodent models", International Journal of Radiation Biology, Vol. 97/sup1, Taylor & Francis Group, London, https://doi.org/10.1080/09553002.2020.1820598.

Pasqual, E. et al. (2021), "Cognitive effects of low dose of ionizing radiation – Lessons learned and research gaps from epidemiological and biological studies", Environment International, Vol. 147, Elsevier, Amsterdam, https://doi.org/10.1016/j.envint.2020.106295.

Prieto, G. A. and C. W. Cotman. (2017), "Cytokines and cytokine networks target neurons to modulate long-term potentiation", Cytokine & Growth Factor Reviews, Vol. 34, Elsevier, Amsterdam, https://doi.org/10.1016/j.cytogfr.2017.03.005.

Rabin, B. M. et al. (2012), "Interaction between age of irradiation and age of testing in the disruption of operant performance using a ground-based model for exposure to cosmic rays", Age, Vol. 34/1, Springer Nature, Berlin, https://doi.org/10.1007/s11357-011-9226-4.

Rabin, B. M. et al. (2015), "Acute effects of exposure to 56Fe and 16O particles on learning and memory", Radiation Research, Vol.

184/2, BioOne, Washington, https://doi.org/10.1667/RR13935.1.

Rabin, B. M., B. Shukitt-Hale and K. L. Carrihill-Knoll. (2014), "Effects of Age on the Disruption of Cognitive Performance by Exposure to Space Radiation", Journal of Behavioral and Brain Science, Vol. 04/07, Scientific Research Publishing, Inc, Wuhan, https://doi.org/10.4236/jbbs.2014.47031.

Turnquist, C., B. T. Harris and C. C. Harris. (2020), "Radiation-induced brain injury: current concepts and therapeutic strategies targeting neuroinflammation", Neuro-Oncology Advances, Vol. 2/1, Oxford University Press, Oxford, https://doi.org/10.1093/noajnl/vdaa057.

Relationship: 2839: Increase, Pro-Inflammatory Mediators leads to Impairment, Learning and memory

AOPs Referencing Relationship

AOP Name	Adjacency	Weight of Evidence	Quantitative Understanding
Deposition of Energy Leading to Learning and Memory Impairment	non-adjacent	Moderate	Low

Evidence Supporting Applicability of this Relationship

Taxonomic Applicability

Term	Scientific Term	Evidence	Links
human	Homo sapiens	Low	NCBI
mouse	Mus musculus	Moderate	NCBI
rat	Rattus norvegicus	Low	NCBI

Life Stage Applicability

Life Stage	Evidence
All life stages	Moderate

Sex Applicability

Sex	Evidence
Unspecific	Moderate

Evidence for this relationship comes from human, rat, and mouse models, with most of the evidence in mice. The relationship is not sex or life stage specific.

Key Event Relationship Description

Inflammatory mediators such as IL-1β, TNF-α, and IL-6, can influence the normal behavior of neuronal cells and their functional connection. Overexpression of pro-inflammatory mediators disrupts the integrity and function of the neuronal network through decreased neurogenesis, synaptic complexity and increased necrosis and demyelination, ultimately impairing learning and memory (Cekanaviciute, Rosi, & Costes, 2018; Fan & Pang, 2017). Impaired short-term and long-term memory, as well as associative learning are consequences of the dysregulated expression of pro-inflammatory cytokines as reported in behavioural paradigms (Donzis & Tronson, 2014).

Under physiological conditions, cytokine levels are low but greatly increased in response to various insults. Cytokines mediate immune response through ligand binding to cell surface receptors, which activate signaling cascades such as the JAK-STAT or MAPK pathways to produce or recruit more cytokines. Once organs initiate inflammatory reactions, the cytokines can modulate different metabolic and molecular pathways that have direct effects on neurons or indirect effects mediated by microglia, astrocytes or vascular endothelial cells (Mousa & Bakhiet, 2013; Prieto & Cotman, 2018). Modulation of these pathways ultimately affects crucial neuronal networks such as that within the hippocampus, which is one of the main brain regions responsible for learning and memory (Barrientos et al., 2015; Bourgognon & Cavanagh, 2020).

Evidence Supporting this KER

Overall Weight of Evidence: Moderate

Biological Plausibility

Several reviews provide support of biological plausibility between increase in pro-inflammatory mediators and impaired learning and

memory. In the central nervous system, cytokines and their receptors are constitutively expressed and affect brain plasticity, which is the ability to modify its activity and connections in response to intrinsic or extrinsic stimuli. In a pathological state, pro-inflammatory, or Th-1 type cytokines become particularly relevant in the brain and these cytokines bind to their receptors to induce a conformational change and activate intracellular signaling pathways (Mousa & Bakhiet, 2013). The main cytokines presenting detrimental effects are IL-1β, TNF-α and IL-6, as these are the most studied.

The mechanism by which these cytokines modify learning and memory processes are not clearly understood due to the complexity of inflammatory signaling, although it involves alterations in the neural circuits that regulate these processes (Bourgognon & Cavanagh, 2020; Pugh et al., 2001). Multiple studies have demonstrated that IL-1β presents a critical role in the formation of hippocampal dependent memory, as IL-1β and its receptor are highly expressed in the hippocampus. Experimentally elevated levels of IL-1β in the hippocampus lead to impaired performance in behavioral paradigms such as spatial memory, contextual learning, and passive avoidance tasks (Donzis & Tronson, 2014; Pugh et al. 2001; Yirmiya & Goshen, 2011).

There are several possible mechanisms for this detrimental effect. One proposed mechanism is through reduced N-methyl-d-aspartate (NMDA) and α-amino-3-hydroxy-5-methyl-4-isoxazolepropionic acid (AMPA) receptor functions, both of which are involved in long-term potentiation, a process that strengthens synaptic connections between neurons. Other potential mechanisms for the effects of IL-1β on brain plasticity and memory can involve the activation of several pathways such as p38 mitogen-activated protein kinase (MAPK), c-jun NH2-terminal kinase (JNK), caspase 1, nuclear factor kappa B (NF-kB), and brain-derived neurotrophic factor (BDNF). These complex pathways have roles in neuronal health, long-term potentiation, brain plasticity and ultimately learning and memory (Patterson, 2015). The mechanisms of IL-6 and TNF-α in terms of impaired cognition also remain unclear, although the pathways that these cytokines activate are similar to those of IL-1β due to the network of cytokine interactions (Donzis & Tronson, 2014).

Empirical Evidence

The empirical evidence collected for this KER comes from in-vivo studies and various methods used to assess the impairment in learning and memory. The behavioral paradigms test associative learning, as well as long and short-term memory (Bourgognon & Cavanagh, 2020).

Various studies also examined the presence of pro-inflammatory mediators induced by lipopolysaccharide (LPS) injections (Sparkman et al., 2006), Escherichia coli (E. coli) injections (Barrientos et al., 2009), direct cytokine injections (Gonzalez et al., 2009; Goshen et al., 2007; Taepavarapruk & Song, 2010), ionizing radiation (Bhat et al., 2020; Jenrow et al., 2013), surgical procedures (Tan et al., 2014) and transgenic models with overexpressed pro-inflammatory cytokines (Hein et al., 2010; Heyser et al., 1997; Moore et al., 2009).

Dose Concordance

Dose concordance relating an increase in pro-inflammatory mediators leading to an impaired learning and memory was demonstrated using various stressors, including ionizing radiation, LPS, IL-1β, and E. coli injections.

A 10 Gy X-ray irradiation in mice led to an increase in IL-6 secretion compared to dimethyl sulfoxide (DMSO) control. Impaired learning and memory were assessed by a decrease in freezing time in fear conditioning tests and a decrease in novel object recognition and object in place discrimination index (DI) (Bhat et al., 2020). A 10 Gy gamma irradiation of rats' brains similarly indicated impaired cognitive function and an increase in OX-6+ cell density, indicative of inflammation (Jenrow et al., 2013).

Rats injected with 2.5x109 CFU of E. coli showed a significant increase in IL-1β in multiple regions of the brain, spleen and serum, along with impaired memory and learning as indicated by fear conditioning (Barrientos et al., 2009). Mice injected with 100 µg of LPS demonstrated an increase in IL-1β, TNF-α, IL-6 and IL-10 levels, while the performance in a Morris water maze was impaired, indicating impairments in spatial memory (Sparkman et al., 2006)..

Time Concordance

Various studies show that an increase in pro-inflammatory mediators is observed before or at the same time as impaired learning and memory. Some studies observe each event at the same time at specific timepoints. In mice injected with LPS, an increase in IL-1β, TNF-α, IL-6 and IL-10 was observed after 4 hours, while impaired learning and memory were also consistently observed 4 h after LPS injection (Sparkman et al., 2006). Both key events were also found in rats from 4 h to 8 days after E. coli injection (Barrientos et al., 2009). Cohort studies using age as a stressor in humans found increased pro-inflammatory mediators and decreased cognitive function over 6 months (Holmes et al., 2009) and 7 years (Alley et al., 2008). Many studies observe increased pro-inflammatory mediators occurring before impaired learning and memory. Rats with hippocampal injections of IL-1β showed impaired memory 24 h and 7 days later (Gonzalez et al., 2009). Rats showed increased hippocampal IL-1β and IL-6 levels 6 h after surgery to expose the right carotid artery, while learning and memory was impaired 2 weeks later (Tan et al., 2014). When mice were irradiated with X-rays, IL-6 was found to increase 24 h later, while learning and memory was impaired 5 weeks later (Bhat et al., 2020). Rats irradiated with gamma rays showed increased inflammation after 2 months, while memory was impaired after 6 months (Jenrow et al., 2013).

Incidence Concordance

Some evidence also shows that pro-inflammatory mediators increase equal to or greater than the amount that impairs learning and memory at the same stressor severity. Many of these studies were done with transgenic mice expressing IL-1β or IL6 as a stressor and showed increased levels of various pro-inflammatory mediators including ICAM-1, CCL2, IL-1α, COX-1 and MCP-1 from 2- to 147-fold, while learning and memory were decreased a maximum of 0.6-fold (Hein et al., 2010; Heyser et al., 1997; Moore et al.,

2009).

Other Evidence

Multiple longitudinal cohort studies followed hundreds to thousands of older adults over the course of several years ranging from four to sixteen years and examined the relationship between pro-inflammatory marker levels and the rate of cognitive change over time. These studies reported linear negative correlations between IL-6 and TNF-α levels and learning and memory ability as the populations aged (Alley et al., 2010; Holmes et al., 2009; Schram et al., 2007).

Essentiality

Studies show that overexpression of pro-inflammatory cytokines affect learning and memory, and several treatments that alter the effects/function of pro-inflammatory mediators preserve cognitive function. The treatments included MW-151, a selective inhibitor of pro-inflammatory cytokine production, lidocaine, an anesthetic with anti-inflammatory properties, ethyl-eicosapentaenoate (E-EPA) and 1-[(4-nitrophenyl)sulfonyl]-4-phenylpiperazine (NSPP), both of which are anti-inflammatory drugs and α-melanocyte stimulating hormone (α-MSH), which antagonizes the effects of pro-inflammatory cytokines through G protein coupled receptors (Bhat et al., 2020; Gonzalez et al., 2009; Jenrow et al., 2013; Taepavarapruk and Song, 2010; Tan et al., 2014). More details are provided in the Modulating Factors section below.

Uncertainties and Inconsistencies

- Due to the indirect linkage between the two key events, there is no clear understanding of how increases in pro-inflammatory mediators cause impaired learning and memory. (Donzis & Tronson, 2014).
- A previous prospective population-based cohort study found an association between antihistamine use and increased risk of dementia, which is the loss of cognitive functioning. Therefore, anti-inflammatory medications such as antihistamines could modulate the progression to impaired learning and memory (Gray et al., 2015).

Quantitative Understanding of the Linkage

The table below provides some representative examples of quantitative linkages between the two key events. It was difficult to identify a general trend across all the studies due to differences in experimental design and reporting of the data. All data is statistically significant unless otherwise stated.

Dose Concordance

Reference	Experiment Description	Result
Sparkman et al., 2006	In-vivo. Three-month-old male C57BL/6 mice were injected with 100 µg of LPS. Pro-inflammatory mediator levels were determined with immunohistochemical staining. Spatial working memory was evaluated through a Morris water maze.	IL-1β increased from 15 pg/mL (control) to 400 pg/mL. TNF-α increased from <5 pg/mL (control) to 360 pg/mL. IL-6 increased from undetectable levels (control) to 300 pg/mL. IL-10 increased from undetectable levels (control) to 260 pg/mL. Performance in the water maze was impaired in distance swam, latency and swim speed after LPS injection, with a maximum 2-fold increased swim distance.
Taepavarapruk & Song, 2010	In-vivo. Male Long-Evans rats were administered 15 ng/µL/day of IL-1β for either 1 or 7 days. IL-1 expression was determined, and memory was assessed with an eight-arm radial maze.	IL-1β administration of 105 ng/µL resulted in a 2.5-fold increase in IL-1 expression and a 1.5-fold increase in number of entries, indicating memory impairment.
Goshen et al., 2007	In-vivo. 2–4-month-old male mice were injected with IL-1β and IL-1ra (IL-1 receptor antagonist) at 1 or 10 ng (injected in 10 µL) doses. IL-1β was assessed by quantitative real time RT-PCR, and hippocampal IL-1ra was determined by ELISA. Contextual fear conditioning was used to assess associative learning and memory. Evaluations were taken after 3 weeks of recovery. Water maze was used for spatial memory testing.	Mice that were injected with a high dose of IL-1β (10 ng) had shorter freezing times, indicating impaired contextual fear conditioning, whereas mice injected with a low dose of IL-1β (1 ng) showed longer freezing times, indicating improved contextual fear conditioning. Spatial memory was impaired in IL-1raTG rats (astrocyte-directed overexpression of IL-1ra) as latency and path length was increased (non-significantly) in the majority of the trials compared to wild type rats.
Gonzalez et al., 2009	In-vivo. Adult male Wistar rats had hippocampal injections of 5 ng/0.25 µL of IL-1β post-conditioning and memory was assessed through freezing behavior.	Rats injected with 5 ng/0.25 µL IL-1β displayed impaired contextual fear memory, where injected rats spent 0.6-fold less time freezing.
Bhat et al., 2020	In-vivo. Female mice were exposed to X-ray irradiation at 0, 2, 4 and 10 Gy (5.519 Gy/min). Novel object recognition, object in place and fear conditioning evaluated memory. IL-6 levels were measured by ELISA.	There was a significant 2.97-fold increase in the secretion of IL-6 in cells irradiated with 10 Gy compared to DMSO control. DMSO was used as a control as treatment mice were also treated with NSPP solubilized in DMSO. Irradiated mice demonstrated a significant decrease in DI for novel object recognition and object in place. Irradiated

		mice also spent significantly less time freezing in context fear, context gen and pre-tone assessments of fear conditioning.
Jenrow et al., 2013	In-vivo. Adult male Fischer 344 rats' brains were irradiated with 10 Gy gamma rays. OX-6 levels (indicative of inflammation levels) were determined, and novel object recognition was performed to assess memory.	10 Gy increased OX-6+ cell density from 1493±270 to 1966±218 cells/mm3. Also, after 10 Gy, the discrimination ratio for novel object recognition decreased from 68.76±11.30% to 21.71±10.86%.
Barrientos et al., 2009	In-vivo. Male F344xBN F1 rats, either old (24 months) or young (3 months), received an injection of 2.5x109 CFU of E. coli. IL-1β levels were determined using ELISA and fear conditioning was performed to assess learning and memory.	Significant increases in IL-1β were observed in the hippocampus, hypothalamus, parietal cortex, serum and spleen after injection, with a maximum 4-fold increase. Injected mice also spent 0.6-fold less time freezing.

Time Concordance

Reference	Experiment Description	Result
Sparkman et al., 2006	In-vivo. Three-month-old male C57BL/6 mice were injected with 100 µg of LPS. Pro-inflammatory mediator levels were determined with immunohistochemical staining and measured 4 h after LPS injection. Spatial working memory was evaluated 4 h after LPS injection through a Morris water maze.	IL-1β increased from 15 pg/mL (control) to 400 pg/mL. TNF-α increased from <5 pg/mL (control) to 360 pg/mL. IL-6 increased from undetectable levels (control) to 300 pg/mL. IL-10 increased from undetectable levels (control) to 260 pg/mL. Performance in the water maze was found impaired in distance swam, latency and swim speed 4 h after LPS injection, with a maximum 2-fold increased swim distance.
Gonzalez et al., 2009	In-vivo. Adult male Wistar rats had hippocampal injections of 5 ng/0.25 µL of IL-1β post-conditioning and memory was assessed through freezing behavior.	Rats spent 0.6- to 0.7-fold less time freezing 24 h after injection with IL-1β. Rats also showed impaired long-term memory 7 days after injection when they spent 0.7-fold less time frozen.
Bhat et al., 2020	In-vivo. Female mice were exposed to X-ray irradiation at 0, 2, 4 and 10 Gy (5.519 Gy/min). Novel object recognition, object in place and fear conditioning evaluated memory. IL-6 levels were measured by ELISA.	24 hours after exposure to 10 Gy irradiation, mice showed a significant 2.97-fold increase in the secretion of IL-6 compared to DMSO control (DMSO was used as a control as mice were also treated with NSPP solubilized in DMSO). At week 5, irradiated mice demonstrated a significant decrease in DI for novel object recognition and object in place, and spent less time freezing in context fear, context gen and pre-tone assessments of fear conditioning.
Jenrow et al., 2013	Adult male Fischer 344 rats' brains were irradiated with 10 Gy 137Cs gamma rays. OX-6 levels (indicative of inflammation levels) were determined, and novel object recognition was performed to assess memory.	After 2 months, OX-6+ cell density increased from 1493±270) to 1966±218 cells/mm3. A similar but smaller increase was found after 9 months. Only measured after 6 months, the discrimination ratio for novel object recognition decreased from 68.76±11.30% to 21.71±10.86%.
Tan et al., 2014	In-vivo. Four-month-old male Fischer 344 rats had 1 cm of right carotid artery dissected free from surrounding tissue in a 15-minute surgery. IL-6 and IL-1β levels were determined by western blot and a Barnes maze was used to test spatial learning and memory.	Surgery increased IL-1β and IL-6 in the hippocampus by 2- to 3-fold compared to controls 6 h after surgery. Additionally, rats in the surgery group took 2- to 3-fold more time to identify the target in the Barnes maze task 2 weeks after surgery.
Barrientos et al., 2009	In-vivo. Male F344xBN F1 rats, either old (24 months) or young (3 months), received an injection of 2.5x109 CFU of E. coli. IL-1β levels were determined using ELISA and fear conditioning was performed to assess hippocampal-dependent learning and memory.	Significant increases in IL-1β were observed in the hippocampus, hypothalamus, parietal cortex, serum and spleen most frequently 4 h after injection, with a maximum 4-fold increase. IL-1β in the hypothalamus was also increased in old mice up to 8 days after injection. Old mice spent less time freezing 4 days after injection, while old injected mice also spent 0.6-fold less time freezing 8 days after injection.
	In-vivo. A cohort study of older adults aged 70-79 years that were tested in 1988, 1991 and 1995 to determine changes in cognitive functioning and IL-6 levels. ELISA was used to	As IL-6 levels increased, mean cognitive scores

Alley et al., 2008	measure IL-6 levels. Cognitive function was determined by various tests, including spatial recognition, spatial ability, verbal recall, language and abstraction. Short Portable Mental Status Questionnaire (SPMSQ) was used as a measure of cognitive performance. Participants were re-interviewed at 2.5 and 7 years.	decreased compared to baseline cognitive scores. A linear inverse association was found between inflammation and general cognitive scores, both measured at the end of the 7-year study.
Holmes et al., 2009	In-vivo. A cohort study of subjects with mild to severe Alzheimer's disease who were cognitively assessed and tested for inflammatory markers. Cognitive assessments were performed using the Alzheimer's Disease Assessment Scale (ADAS-COG) test. The sandwich immunoassay multiplex cytokine assay measured TNF-α at 2, 4 and 6 months	Subjects with high TNF-α levels (3.2 [standard error (SE) 0.6]) at baseline observed greater changes in ADAS-COG over 6-months compared to subjects with low TNF-α (0.8 [SE 0.8]). The mean change in ADAS-COG score was 2.6 (±7.0) points over the 6 months.

Incidence Concordance

Reference	Experiment Description	Result
Moore et al., 2009	In-vivo. Transgenic mice overexpressing IL-1β (activated by microinjection of FIV-Cre) for 2 weeks underwent spatial and non-spatial behavioral tasks using a Morris water maze. IL-1β, IL-1α and MCP-1 were measured by RT-PCR.	Measurement of IL-1β in hippocampal tissue revealed mRNA levels increased 22.9-fold. The pro-inflammatory mediators IL-1α and MCP-1 mRNA levels were also increased 3.1- and 147-fold, respectively. Overexpression of IL-1β in the hippocampus hindered acquisition and long-term memory retention on the spatial task but did not impact non-spatial learning.
Hein et al., 2010	In-vivo. Male and female IL-1βXAT mice on a C57BL/6 background (containing a dormant human IL-1β gene activated by a virus expressing Cre) were injected with 1.5x104 viral particles of the feline immunodeficiency virus (expresses Cre) in the hippocampus. Fear conditioning and a Morris water maze were performed to assess learning and memory.	IL-1β was increased 15-fold in the hippocampus, and the expression of other pro-inflammatory mediators CCL2, IL-1α and COX-1 were similarly increased. Mice spent 0.6-fold less time freezing and 0.8-fold less time in the target quadrant, indicating impaired learning and memory. No differences between males and females were observed.
Heyser et al., 1997	In-vivo. C57BL/6 x SJL hybrid mice with a GFAP-IL6 fusion gene were tested for avoidance learning and expression of ICAM-1.	Compared to non-transgenic (+/+) mice, ICAM-1 was increased 2-fold at 3 months old and 4-fold at 12 months old in both heterozygous (+/tg) and homozygous (tg/tg) transgenic mice. Also compared to +/+ mice, +/tg mice showed impaired avoidance response at 12 months old, where tg/tg mice showed impaired avoidance at 3, 6 and 12 months old.

Other Evidence

Reference	Experiment Description	Result
Alley et al., 2008	In-vivo. A cohort study of older adults aged 70 to 79 years that were tested in 1988, 1991 and 1995 to determine changes in cognitive functioning and IL-6 levels. ELISA was used to measure IL-6 levels. Cognitive function was determined by various tests, including spatial recognition, spatial ability, verbal recall, language and abstraction. Short Portable Mental Status Questionnaire (SPMSQ) was used as a measure of cognitive performance. Participants were re-interviewed at 2.5 and 7 years.	As IL-6 levels increased, mean cognitive scores decreased compared to baseline cognitive scores. A linear inverse association was found between inflammation and general cognitive scores, both measured over the course of 7 years. Participants in the top IL-6 tertile (IL-6 > 3.8 pg/mL) had 62% increased odds of declines in global cognitive function (Odds Ratio (OR) = 1.62, 95% Confidence Interval (CI), 1.07–2.45). They also had 88% increased odds of cognitive impairment, (OR = 1.88, 95% CI, 1.20–2.94), relative to those with lower levels of IL-6.

Holmes et al., 2009	In-vivo. A cohort study of subjects with mild to severe Alzheimer's disease were cognitively assessed and tested for inflammatory markers. Cognitive assessments were performed using the Alzheimer's Disease Assessment Scale (ADAS-COG) test. The sandwich immunoassay multiplex cytokine assay measured TNF-α at 2, 4 and 6 months	Subjects with high TNF-α levels (3.2 [SE 0.6]) at baseline observed greater changes in ADAS-COG over 6-months compared to subjects with low TNF-α (0.8 [SE 0.8]). The mean change in ADAS-COG score was 2.6 (SD 7.0) points over the 6 months.
Schram et al., 2007	In-vivo. The Leiden 85-plus Study, performed with participants aged 85 to 90 years (n= 705), assessed memory function and its association with inflammatory markers. IL-6 plasma levels were measured by ELISA. C-reactive protein (CRP) pro-inflammatory mediator was measured by Rate Near Infrared Particle Immunoassay. The 12-Picture Learning Test was used to evaluate memory function.	When levels of pro-inflammatory mediators were higher than baseline, delayed recall memory point estimate was negative, indicating impaired memory.

Known modulating factors

Modulating factor	Details	Effects on the KER	References
Drug	NSPP (anti-inflammatory drug)	There was a 0.35-fold decrease in IL-6 levels compared to controls when 10 Gy irradiated mice were treated with NSPP. Mice that were exposed to whole brain irradiation (10 Gy) and treated with NSPP (5 mg/kg) exhibited significantly improved performance in novel object recognition and object in place.	Bhat et al., 2020
Drug	α-MSH (modulator of action of pro-inflammatory cytokines)	α-MSH injected into the hippocampus prevented the IL-1β-induced decrease in contextual fear memory.	Gonzalez et al., 2009
Drug	MW-151 (inhibitor of pro-inflammatory microglial cytokine production)	Treatment decreased the OX-6+ cell density and restored memory.	Jenrow et al., 2013
Drug	Lidocaine (an anti-inflammatory local anesthetic)	Lidocaine treatment restored IL-6 levels and improved memory.	Tan et al., 2014
Age	Young age	Rats aged 3 months showed increased IL-1β levels in the hippocampus for less time than in mice aged 24 months. Hippocampal-dependent memory was impaired in the old mice. The inflammatory response is shorter and less severe in young individuals, leading to reduced cognitive impairment.	Barrientos et al., 2009; Barrientos et al., 2012
Drug	E-EPA (known to improve cognitive function through reducing inflammation)	E-EPA reduced the increase in IL-6 expression and improved memory to control levels.	Taepavarapruk & Song, 2010

Known Feedforward/Feedback loops influencing this KER

Not identified.

References

Alley, D. E. et al. (2008), "Inflammation and Rate of Cognitive Change in High-Functioning Older Adults", The Journals of Gerontology Series A: Biological Sciences and Medical Sciences, Vol. 63/1, Oxford University Press, Oxford, https://doi.org/10.1093/gerona/63.1.50.

Alley, D. E. et al. (2008), "Inflammation and Rate of Cognitive Change in High-Functioning Older Adults", The Journals of Gerontology Series A: Biological Sciences and Medical Sciences, Vol. 63/1, https://doi.org/10.1093/gerona/63.1.50.

Barrientos, R. M. et al. (2015), "Neuroinflammation in the normal aging hippocampus", Neuroscience, Vol. 309, Elsevier, Amsterdam, https://doi.org/10.1016/j.neuroscience.2015.03.007.

Barrientos, R. M. et al. (2009), "Time course of hippocampal IL-1 β and memory consolidation impairments in aging rats following peripheral infection", Brain, Behavior, and Immunity, Vol. 23/1, Elsevier, Amsterdam, https://doi.org/10.1016/j.bbi.2008.07.002.

Barrientos, R. M. et al. (2012), "Aging-related changes in neuroimmune-endocrine function: Implications for hippocampal-dependent cognition", Hormones and Behavior, Vol. 62/3, Elsevier, Amsterdam, https://doi.org/10.1016/j.yhbeh.2012.02.010.

Bhat, K. et al. (2020), "1-[(4-Nitrophenyl)sulfonyl]-4-phenylpiperazine treatment after brain irradiation preserves cognitive function in mice", Neuro-Oncology, Vol. 22/10, Oxford University Press, Oxford, https://doi.org/10.1093/neuonc/noaa095.

Bourgognon, J.-M. and J. Cavanagh. (2020), "The role of cytokines in modulating learning and memory and brain plasticity", Brain and Neuroscience Advances, Vol. 4, https://doi.org/10.1177/2398212820979802.

Cekanaviciute, E., S. Rosi and S. Costes. (2018), "Central Nervous System Responses to Simulated Galactic Cosmic Rays", International Journal of Molecular Sciences, Vol. 19/11, MDPI, Basel, https://doi.org/10.3390/ijms19113669.

Donzis, E. J. and N. C. Tronson. (2014), "Modulation of learning and memory by cytokines: Signaling mechanisms and long term consequences", Neurobiology of Learning and Memory, Vol. 115, Elsevier, Amsterdam, https://doi.org/10.1016/j.nlm.2014.08.008.

Fan, L. W. and Y. Pang. (2017), "Dysregulation of neurogenesis by neuroinflammation: key differences in neurodevelopmental and neurological disorders", Neural Regeneration Research, Vol. 12/3, Wolters Kluwer, https://doi.org/10.4103/1673-5374.202926.

Gonzalez, P. V. et al. (2009), "Memory impairment induced by IL-1β is reversed by α-MSH through central melanocortin-4 receptors", Brain, Behavior, and Immunity, Vol. 23/6, Elsevier, Amsterdam, https://doi.org/10.1016/j.bbi.2009.03.001.

Goshen, I. et al. (2007), "A dual role for interleukin-1 in hippocampal-dependent memory processes", Psychoneuroendocrinology, Vol. 32/8–10, Elsevier, Amsterdam, https://doi.org/10.1016/j.psyneuen.2007.09.004.

Gray, S. L. et al. (2015), "Cumulative Use of Strong Anticholinergics and Incident Dementia", JAMA Internal Medicine, Vol. 175/3, https://doi.org/10.1001/jamainternmed.2014.7663.

Hein, A. M. et al. (2010), "Sustained hippocampal IL-1β overexpression impairs contextual and spatial memory in transgenic mice", Brain, Behavior, and Immunity, Vol. 24/2, Elsevier, Amsterdam, https://doi.org/10.1016/j.bbi.2009.10.002.

Heyser, C. J. et al. (1997), "Progressive decline in avoidance learning paralleled by inflammatory neurodegeneration in transgenic mice expressing interleukin 6 in the brain", Proceedings of the National Academy of Sciences, Vol. 94/4, National Academy of Sciences, Washington, https://doi.org/10.1073/pnas.94.4.1500.

Holmes, C. et al. (2009), "Systemic inflammation and disease progression in Alzheimer disease", Neurology, Vol. 73/10, Wolters Kluwer, https://doi.org/10.1212/WNL.0b013e3181b6bb95.

Jenrow, K. A. et al. (2013), "Selective Inhibition of Microglia-Mediated Neuroinflammation Mitigates Radiation-Induced Cognitive Impairment", Radiation Research, Vol. 179/5, BioOne, https://doi.org/10.1667/RR3026.1.

Moore, A. H. et al. (2009), "Sustained expression of interleukin-1β in mouse hippocampus impairs spatial memory", Neuroscience, Vol. 164/4, Elsevier, Amsterdam, https://doi.org/10.1016/j.neuroscience.2009.08.073.

Mousa, A. and M. Bakhiet. (2013), "Role of Cytokine Signaling during Nervous System Development", International Journal of Molecular Sciences, Vol. 14/7, MDPI, Basel, https://doi.org/10.3390/ijms140713931.

Patterson, S. L. (2015), "Immune dysregulation and cognitive vulnerability in the aging brain: Interactions of microglia, IL-1β, BDNF and synaptic plasticity", Neuropharmacology, Vol. 96, Elsevier, Amsterdam, https://doi.org/10.1016/j.neuropharm.2014.12.020.

Prieto, G. A. and C. W. Cotman. (2017), "Cytokines and cytokine networks target neurons to modulate long-term potentiation", Cytokine & Growth Factor Reviews, Vol. 34, Elsevier, Amsterdam, https://doi.org/10.1016/j.cytogfr.2017.03.005.

Pugh, C. R. et al. (2001), "The immune system and memory consolidation: a role for the cytokine IL-1β", Neuroscience & Biobehavioral Reviews, Vol. 25/1, Elsevier, Amsterdam, https://doi.org/10.1016/S0149-7634(00)00048-8.

Schram, M. T. et al. (2007), "Systemic Markers of Inflammation and Cognitive Decline in Old Age", Journal of the American Geriatrics Society, Vol. 55/5, Wiley, https://doi.org/10.1111/j.1532-5415.2007.01159.x.

Sparkman, N. L. et al. (2006), "Interleukin-6 Facilitates Lipopolysaccharide-Induced Disruption in Working Memory and Expression of Other Proinflammatory Cytokines in Hippocampal Neuronal Cell Layers", Journal of Neuroscience, Vol. 26/42, Society for Neuroscience, https://doi.org/10.1523/JNEUROSCI.3376-06.2006.

Taepavarapruk, P. and C. Song. (2010), "Reductions of acetylcholine release and nerve growth factor expression are correlated with memory impairment induced by interleukin-1β administrations: effects of omega-3 fatty acid EPA treatment", Journal of Neurochemistry, Vol. 112/4, Wiley https://doi.org/10.1111/j.1471-4159.2009.06524.x.

Tan, H. et al. (2014), "Critical role of inflammatory cytokines in impairing biochemical processes for learning and memory after surgery in rats", Journal of Neuroinflammation, Vol. 11/1, Springer Nature, https://doi.org/10.1186/1742-2094-11-93.

Yirmiya, R. and I. Goshen. (2011), "Immune modulation of learning, memory, neural plasticity and neurogenesis", Brain, Behavior, and Immunity, Vol. 25/2, Elsevier, Amsterdam, https://doi.org/10.1016/j.bbi.2010.10.015.